IOSTC

SECOND INTERNATIONAL

OIL SANDS

TAILINGS CONFERENCE

Edmonton, Alberta
Canada

December 2010

Proceeding of the Second International Oil Sands Tailings Conference

5-8 December 2010, Edmonton, Alberta, Canada

Second International Oil Sands Tailings Conference

Edited by

David Sego & Nicholas Beier

University of Alberta, Geotechnical Center and
Oil Sands Tailing Research Facility (UofA)

University of Alberta Geotechnical Center Edmonton, Alberta, Canada

Published by: University of Alberta, Dept. of Civil & Environmental Engineering

Printed in Canada

Forward

The management of Oil Sands Tailings is beset with technical challenges and is an area of increasing public interest. Mature fine tailings (MFT) requires long term containment, and the appropriate management of capping waters represents the most visible of the challenges facing the industry. The vast quantities of tailings sand produced during bitumen extraction are used extensively to construct safe containment dykes that contain the MFT and capping water. Over the last 15 years, this sand has also been used to assist with the disposal of MFT in the form of consolidated/composite tailings (CT). Considerable technical work has been carried out over the last 40 years, but much of it is not easily accessible to the public hindering the proper recognition of these extensive efforts and major advancements. Much of the scientific and engineering advancements are published in diverse specialized conferences and journals making it a challenge to review this important literature. The Fine Tailing Fundamentals Consortium in 1995 synthesized many of these studies. This was followed by the **International Conference on Oil Sands Tailings 2008** at which an industrial and regulatory perspective on the needs for tailings research and management was presented in the theme lectures and by manuscripts.

The aim of the **International Conference on Oil Sands Tailings 2010** is to provide a further exchange of information between the people responsible for managing the oil sands tailings: researchers and providers of tailings management services who have experience with this industry. The presentations and conference proceedings will provide an update with a special focus on industry activities related to meeting ERCB's Directive 74 and will highlight the extensive research presently underway.

I want to personally thank the Oil Sands Tailings Research Facility (OSTRF) and the Canadian Oil Sands Network for Research and Development (CONRAD) for their encouragement and support for the conference. The conference would not have been possible without the dedication of Roy Ifill, Nicholas Beier, Vivian Giang and especially Sally Petaske who provided so much assistance and leadership.

The success of this conference is only possible due to the presentations and the quality of the research presented in the manuscripts contained in the Proceedings. I want to thank our professional colleagues who willingly shared their experiences and insight with us. To all the authors, thank you for contributing your technical knowledge and for your efforts in submitting your manuscripts, especially in these extremely busy days when time is our most precious commodity.

The Proceedings contain information representing hundreds of years of collective experience. I know you will find insight and answers that will assist you in a better understanding of oil sands tailings.

David C. Sego

Chair, Organizing Committee

Thank you to the following sponsors for their support in making the 2nd International Oil Sands Tailings Conference a success:

CONRAD
Canadian Oil Sands Network for Research and Development

OSTRF
Oil Sands Tailings Research Facility

UNIVERSITY OF ALBERTA
QUAECUMQUE VERA

PLATINUM SPONSORS

Syncrude

CONETEC

SRIN
Oil Sands Research and Information Network

GOLD SPONSORS

Canadian Natural

Alfa Laval Inc.

FLSmidth

BGC ENGINEERING INC.
AN APPLIED EARTH SCIENCES COMPANY

Esso Imperial Oil

Maxxam

SILVER SPONSORSHIP

Champion Technologies™

LAYFIELD

HB Wick Drains
A Division of Hayward Baker
formerly Nilex Construction NILEX

Geotech DRILLING

WEIR MINERALS

TABLE OF CONTENTS

KEYNOTE PRESENTATIONS

SESSION 1 - TAILINGS PROPERTIES

SESSION 2 - TAILINGS DEWATERING

SESSION 3 - NEW CONCEPTS

SESSION 4 - WATER/CHEMISTRY

SESSION 5 - SOFT TAILINGS STABILIZATION/RECLAMATION

SESSION 6 - WATER TREATMENT

SESSION 7 - NEW CONCEPTS

Keynote

Presentations

TAILINGS WATER IN THE SUBSURFACE ENVIRONMENT: STATUS AND WAYS FORWARD

J. Barker[1], A. Ulrich[2], J. Birks[3] and U. Mayer[4]
[1]Department of Earth & Environmental Sciences, University of Waterloo, Waterloo, Ontario, Canada
[2]Department of Civil & Environmental Engineering, University of Alberta, Edmonton, Alberta, Canada
[3]Sustainable Ecosystems, Alberta Innovates Technology Futures
[4]Department of Earth & Ocean Sciences, University of British Columbia, British Columbia, Canada

ABSTRACT

Currently, oil sands process water is retained in some of the largest tailings ponds in the world. Unfortunately, such structures leak to some degree, with process-affected water potentially impacting surface water and groundwater. Three occurrences of process-affected water in the subsurface outside of tailings structures are presented to illustrate the apparent behaviour of organic contaminants, salts, and some trace metals in the groundwater environment. There is little migration of petroleum hydrocarbons such as BTEX or PAHs of concern at conventional oil and gas operations. Naphthenic acids (NAs) are a complex and apparently difficult to characterize group of organic chemicals naturally occurring in oil sands, which become concentrated in tailings water. The apparent toxicity of NAs has raised concern about release of tailings water to aquatic ecosystems. Unfortunately, NAs appear to be mobile and persistent in shallow sand aquifers. The anoxic, process-affected groundwater plume does not appear to enhance significant trace metal mobilization from aquifer solids, however.

The current literature includes mainly laboratory experiments and retrospective field studies at existing tailings ponds. Researchers from the Universities of Alberta, British Columbia, and Waterloo, and the Alberta Innovates Technology Futures, supported by Suncor Energy and NSERC, have initiated research to evaluate the development of groundwater seepage and the fate of process-affected groundwater at a newly constructed tailings facility associated with a shallow sandy aquifer. This research is assessing the development of seepage, geochemical processes during seepage, and groundwater remediation strategies. An understanding of the processes controlling the inorganic chemistry of seepage water is being gained through laboratory experiments, field monitoring, controlled field experiments, and numerical modeling. A similar approach is being applied to assess groundwater remediation through in situ chemical oxidation of NAs, using persistent oxidants (persulfate and permanganate). An interesting technology combination is also being pursued: the potential for sulfate, the product of persulfate reaction, to further enhance subsequent anaerobic degradation of NAs. Initial lab and field findings suggest these oxidants may be capable of removing most NAs (as measured by FTIR), but the low in situ temperatures and hydrogeological heterogeneities will make practical application challenging.

RECENT ADVANCEMENTS IN THE GEOTECHNICAL CHARACTERIZATION OF OIL SANDS TAILINGS

James Sharp[1], David Woeller[1] and Mark Styler[2]
[1]ConeTec, Vancouver, British Columbia, Canada
[2]University of British Columbia, Vancouver, British Columbia, Canada

ABSTRACT

The in-situ geotechnical characterization of soft oil sands tailings is now a routine procedure in Alberta, Canada. These generally large tailings impoundments are deposited in either external dammed facilities or within previously mined open pits. When hydraulically discharged, the fines can accumulate as a thick fluid or soft solid material at the center of the deposit while coarse sand beaches form closer to the discharge points. The large volumes of soft fine grained tailings create challenges for reclamation and are an increasing concern for mine operators, environmental groups, and regulatory agencies. As such, there has been a focus in recent years to adequately characterize these deposits with the end goal of reclamation in mind. New tailings processes developed to improve fines capture and tailings strength are being implemented, and need to be properly characterized in order to evaluate their performance. Investigation techniques used in traditional geotechnical characterization of soils are not adequately sensitive to produce meaningful results in very soft deposits, which can exhibit both fluid and solid behaviour. Recent improvements of in-situ testing techniques now offer tools specific to very soft deposits. Tools discussed include low capacity cone penetrometers, full flow penetrometers, gamma radiation measurements, high resolution pore pressure dissipation testing, low capacity vane shear testing, and special sampling techniques. Interpretation methods to properly interpret the data are discussed, specifically as it relates to the strength and composition of the various tailings mixtures and physical states. Some recommendations on the best utilization of the various investigation and interpretation methods are made.

ENVIRONMENTAL DE-WATERING OF FLUID FINE TAILINGS

G. Ward Wilson
Geotechnical Research Center, University of Alberta

ABSTRACT

The Oil Sands Industry is currently investigating various methods of de-watering fluid fine tailings. One application of interest is de-watering mature fine tailings (MFT) by surface deposition. These tailings typically have solids contents in the range of 35%. Increasing the solids content of the MFT to values greater than 60% has been shown to produce desirable physical properties. Methods of de-watering include in-line flocculation with organic polymers followed by thin lift deposition, as well as flocculation and centrifugation of MFT to produce a paste like material that is placed in thicker layers using conveyors and trucks.

The present paper will focus on the mechanisms of de-watering that occur following deposition. De-watering can be thought of as a flux boundary problem. For example, de-watering a 1.0 m thick profile of MFT with an initial solids content of 35% to a solids content of 60% requires about 200 mm per 1 m^2 of water to exit the boundaries of the profile. Flux boundary conditions are driven by atmospheric forcing events associated with evaporative drying and freeze/thaw effects, as well as drainage of liquid water due to run-off and foundation seepage. The relative contributions of each these three primary mechanisms for de-watering within the climatic regime at Fort McMurray are discussed and quantified.

Session 1

Tailings Properties

SOME PROPERTIES OF SUNCOR OIL SANDS TAILINGS

Chengmai Guo, P.Eng. & Patrick Sean Wells, P.Eng.
Suncor Energy Inc., Fort McMurray, Alberta, Canada

ABSTRACT

Significant progress has been made in Mature Fine Tailing (MFT) management and CT technology development at Suncor during the past decades. While MFT drying technology has been rapidly developed in the recent years, wet tailings pond will continue to play important role in tailings storage. This paper introduces Suncor pond assessment program and Block Modeling technology, presents some properties of Suncor tailings including Dense MFT (DMFT) and CT.

INTRODUCTION OF SUNCOR TAILINGS PONDS AT WEST SIDE OF THE RIVER

Great Canadian Oil Sands (later Suncor Energy, Inc.) started its commercial operation in Fort McMurray in 1966 as the first oil sands facility. The operation currently includes open pit mining and in-situ bitumen recovery, with a daily production over 300,000 barrel per day.

The ore at the surface mine site is part of the Athabasca deposits within the lower McMurray formation. This ore is typically made up of 80% sand, 4% water, and 11% bitumen, with a fines content (<44 μm) of about 11% of the total solids. Early mining operation used bucket wheels, but was replaced in the mid 1990s by a more efficient truck and shovel method. The Clark Hot Water Extraction method is used with higher than 93% bitumen recovery. The remaining material, consisting of sand, fines, water, and residual bitumen, make up the tailings stream and are discharged into the containment ponds.

Figure 1 shows the tailings ponds on the west side of the Athabasca River. Pond 1 started as the first tailings pond in the industry, and has now been decommissioned, closed, and renamed to Wapisiw Lookout. The whole tailings stream from extraction operations (known as Regular Tailings, RT) was discharged into the pond with the sand used to construct the containment dyke known as Tar Island Dyke (TID), the excess sand and some fines settling to form a beach, and the remainder of the fine particles entering the water column as thin fine tailings. After 2-3 years time, this material settles to about 30% solids by weight and is known as Mature Fine Tailings (MFT). Operations continued until the mid 1990's when the pond was filled. In 2002 closure operations were started by discharging cyclone underflow material known as Densified Tailings (DT) coupled with the withdrawal of the MFT which was pumped out for use in other tailings processes or for temporary storage in ponds better suited to the long term treatment of the material. This infilling operation continued until the fall of 2009, and now Pond 1 has become the first reclaimed tailings pond in oil sands industry.

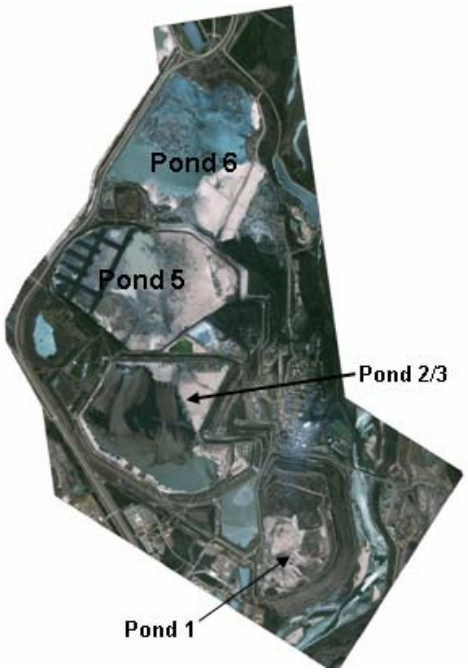

Figure 1. Suncor Tailing Ponds at West Side of the River

Pond 2/3 was initially a mine pit. It started in 1976 with RT deposition until 1996. From 1996 to late 2009, cyclone overflow mixed with CT released water and froth treatment tailings (known as BRFT deposition) was discharged into the pond. With the commissioning of a new extraction plant on the east side of the lease in late 2009, only froth tailings and recycle water are discharged into this pond. It continues to be a primary water recirculation pond for the plant operations.

One of the first tailings treatment technologies to see large, commercial scale implementation in the industry was pioneered by Suncor, followed rapidly by other oil sands operators, was known as Consolidated Tailings (CT) in the mid 1990s. CT is a mixture of coarse sand, MFT, and gypsum. The gypsum acts as coagulant and the mixture forms a non-segregating material which releases water and consolidates more rapidly than MFT. Pond 5 was the first CT pond at Suncor with deposition beginning in 1996. Deposition continued until June 2009, and now this pond is being capped by coke to provide trafficable surface for artificial dewatering and final reclamation. Pond 6 was opened in 2002 as a tailings pond and started CT deposition in 2005. Starting in 2007, with the pond near its maximum containment elevation, MFT was transferred to Pond 7 to allow continued CT deposition. Active CT deposition was completed in September, 2009, and pond will be capped over the next few years.

In the 40 years of continuous operation, the volumes of tailings material which have been deposited along with material transfers between ponds and the varied tailings material types (RT, DT, CT, MFT, etc) deposited have made the tailings properties within these ponds complex. To characterise these properties, a new technology and approach was required. This paper describes pond assessment methods and computer modeling technology used at Suncor, and presents some properties of the dense MFT (DMFT) in Pond 2/3 and the CT in Pond 5.

POND ASSESSMENT AND MODELING ANALYSIS IN SUNCOR

Suncor conducts annual pond assessment operations to provide basic information to tailings planning, process engineering, and reclamation teams. The field investigations include pond bottom and mudline soundings, profile sampling and vane shear testing, and cone penetration testing (CPT). The mudline surface, typically characterised as a solids content greater than 10%, is determined through the use of fish-finders which use sonar technology. The pond bottom sounding is conducted by spiked weights known as AK97 or CT09 probes. This typically determines the surface within the pond having undrained shear strengths greater than 2 kPa. A piston sampler is used to get samples above this pond bottom, with samples from drill cores used below the pond bottom. Field vane shear testing and ball CPT are used to determine the undrained shear strength and consolidation behaviour of the tailings material while laboratory tests, including bitumen/ mineral/water (BMW) analysis by the Dean and Stark method, fines content by wet sieve (passing 325 mesh), and clay content determination through a modified methylene blue analysis are used to characterise the tailings material properties. The test results are used to determine the material components, density, material tonnage, and strengths. By comparing the pump house production data with actual deposition data in tailings ponds, tailings deposition performance is analyzed annually.

Prior to 2006, tailings performance and volumetric analysis was conducted qualitatively and through spreadsheet-based volume estimation. Sampling data was used to analyze the segregation and density properties by observational methods. Spreadsheets generated simple representations of the tailings volume at different depth intervals (pond peels) and the average values of the parameters (solids content, sand to fines ratio, etc) with depth was used to evaluate the amounts of different components (sand, fines, water, bitumen) contained within the pond. There was no consideration of the spatial distribution of the tailings material across the pond.

Block Modeling was recently introduced at Suncor (Wells, et. al., 2008) to analyze the tailings material distribution and evaluate the material properties at different depths. This advancement has allowed the pond assessments to move from observational approximations to a more quantitative and defendable methodology. The application of the block model with fairly wide spaced sample sites is made possible due to the low viscosity and semi-fluid properties of the tailings material above the pond. In these regions the material has fairly extensive lateral continuity. Block modeling has become a useful tool for tailings management at Suncor.

DENSE MFT (DMFT) IN POND 2/3

Figure 2 shows the sampling sites at Pond 2/3 in 2009. The wet pond surface area, defined as the area within the shoreline, was 252 ha, with a large exposed beach in the NE corner. Since middle 1990s, a mixture of cyclone overflow, froth treatment tailings, and CT release water was

discharged at the NE corner, moving gradually westward as the beach built up and the tailings lines were relocated. Most of the sand and silts rapidly settled to form the beach, with the remaining fines transported into the water column and settling to form MFT. An east-west cross dyke, located in the middle of the pond with top elevation about 50' below pond surface, separated the original Pond 2 from Pond 3.

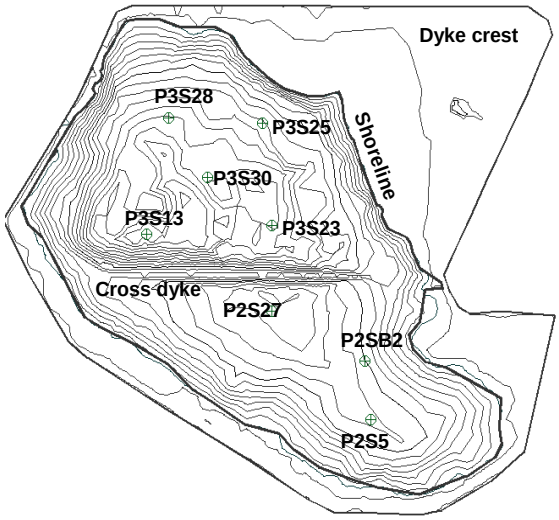

Figure 2. Sampling Sites at Pond 2/3 in 2009

Figure 3 shows the depth profiles of solids and fines contents at Site 30 (approximately in the middle of Pond 3) in different years. In 1993, the profile shows standard settling behaviour of the MFT, with solids content less than 50% and fines content greater than 90%. At the 1050' elevation, fines contents dropped with a corresponding increase in overall density. This transition zone appears to occur at or near the 40% solids mark, where increases in density of the MFT are associated with increasing sand content. In 1998 transition point moved up to 1100', and in 2009 to 1175'. In this type of active pond, as the viscosity and yield stress of the MFT increases along with settled densities, sand transported across the pond through mass beach flows and line deposition is hindered from settling to the bottom of the pond and may become entrained in the thicker MFT matrices. This sandy material, with solids contents greater than 50% and fines contents less than 70%, has been termed Dense MFT (DMFT) at Suncor, and represents a new classification of material with distinct implications for pond management.

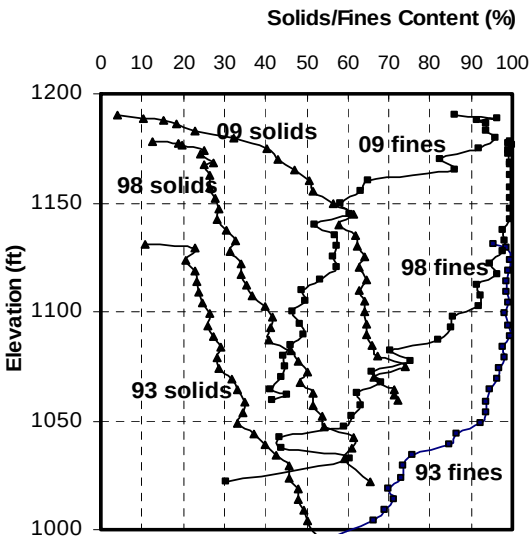

Figure 3. Depth Profiles of Solids and Fines Contents at Site 30 in Different Years

There were 7 sampling sites at Pond 2/3 in 2009, and these are shown in Figure 2. At each site, samples were obtained for BMW, fines and clay content analyses. The results were input into a modelling package known as Surpac to conduct surface and block modeling. Due to the presence of the cross dyke, below 1140' elevation (top of the dyke), the tailings properties have no lateral continuity between the Pond 2 and Pond 3 areas. Above the cross dyke, the material likely behaved as in a single pond. Based on this assumption, the whole pond space was modeled separately as three parts: Pond 2/3 above 1140', Pond 2 below 1140', and Pond 3 below 1140'.

Figure 4 shows fines contents in the cross section C-C from the 2009 block model. Fines content decreased with elevation in both Pond 2 and Pond 3, and with fines contents greater than 90% were found only above 1150'. Pond 3 material generally contained more sand relative to Pond 2 deposits, due likely to sand loading from tailings discharge at NE. Figure 5 shows the solids contents for the same cross section. The 50% solids content elevation was 1055' in Pond 3, and 1033' in Pond 2. High sand uptake at Pond 3 also lifted up the level of DMFT. The combination of the three pond models showed that only 35% of the total soft deposits in Pond 2/3 had fines content greater than 90%, 44% material had fines content less than 70%, and about 50% of the material had solids contents greater than 50%.

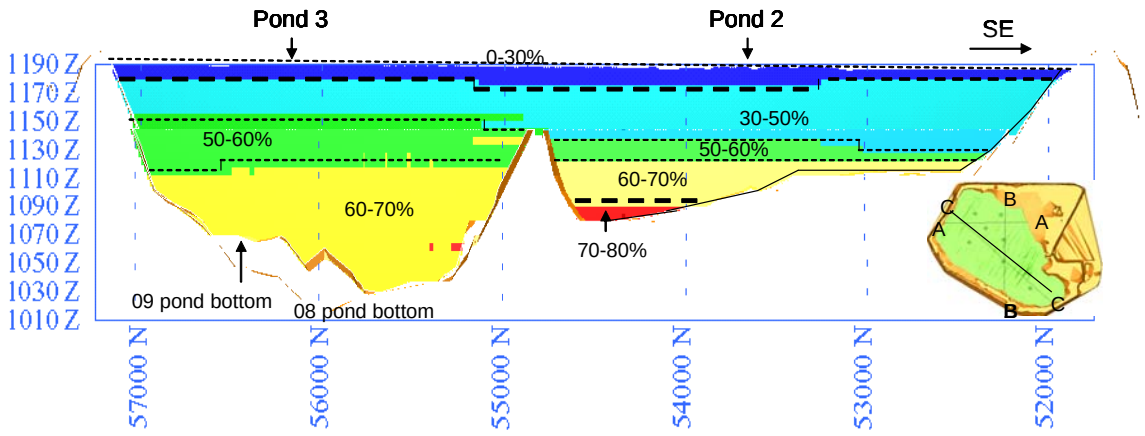

Figure 4. 2009 Pond 2/3 Fines Content Cross Section C-C by Block Modeling

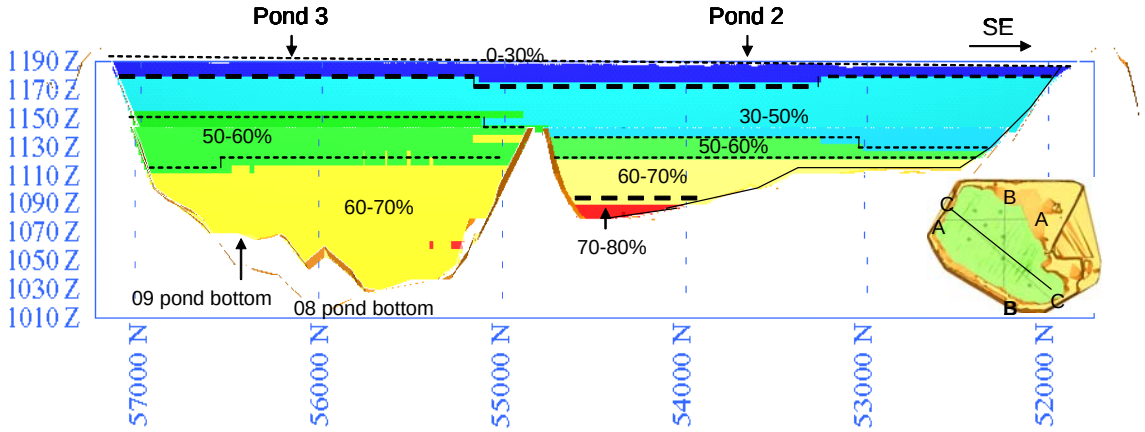

Figure 5. 2009 Pond 2/3 Solids Content Cross Section C-C by Block Modeling

Figure 6 shows the Ternary diagram of the soft material samples in Pond 2/3 from the 2009 testing. Most samples plot below the segregation boundary for MFT/cyclone underflow mixture and the boundary for raw tailings (FTFC, 1995), indicating non-segregating behaviour under static condition. Most of the sand particles in DMFT will likely stay non-segregating due to increased MFT density and viscosity. However, part of the sand may segregate under dynamic conditions which can occur during pond material movements, circulation currents, and tailings discharging.

In oil sands tailings, a measurement of the dewatering of material known as fines-over-fines-plus-water (f/(f+w)) is commonly used. “f” denotes mass fines content (<44um); “w” represents water content, percentage of water mass to solids mass. Great efforts have been made to theoretically model the consolidation of tailings material, with different theories introduced to attempt to describe the behaviour. However, to date no theory has provided a close match to actual data collected from an operational tailings pond. Two factors may have contributed to the challenge: lack of mature consolidation theory for this type of material and the complexity of the environment within the tailings ponds. Given the relatively poor description from theory, empirical analysis of historical pond assessment data may provide valuable information.

Historical sample data from 1990 to 2009 near Site 30 was used to analyze the changes of f/(f+w) for the tailings materials at different depth zones and in different years. The results are shown in Figure 7. The increases in f/(f+w) at 5 different depth zones follow similar trends, and indicates that MFT dewatering during the past two decades has not been effected by total stress. This is similar to the observation of the 10 m MFT standpipe at the University of Alberta (Scott, et. al., 2004) which

for more than 20 years has shown very little to no effective stress even while the total MFT volume decreased significantly.

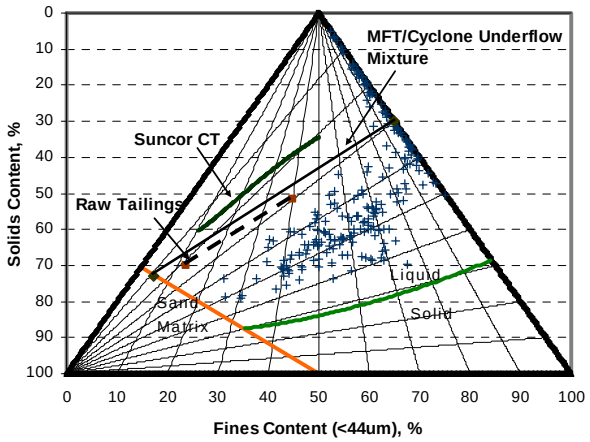

Figure 6. Ternary Diagram of 2009 Pond 2/3 Soft Deposits

Figure 8 shows the fitted curve from Pond 3 historical data along with the curve by MacKinnon and Sethi (1993), which was based on the historical data in the early years of Suncor ponds with most of the fines contents near or greater than 90%. The two curves are close during the first 3-4 years, but dewatering rates from the recent historical data (after 1993) were higher. One reason may be the increased sand content in the MFT as shown in Figure 3. Figure 8 also shows the average f/(f+w) of the 10 m standpipe at the University of Alberta at the 21 year point (Scott, et. al., 2004). The MFT in the standpipe was sourced from Sycrude's plant with an initial solids content 30.6% and a fines content of 90%. After 21 years the solids content increased to 40.6%. By assuming the final fines content the same as the initial sample, the final f/(f+w) (about 23 years from discharging into tailings pond), was about 39.2%, which was significantly below the prediction by empirical curves from Pond 3 MFT. Two reasons likely have contributed to the differences: 1). Increased sand content have accelerated dewatering of the MFT in the pond; 2). Biogas generation in the pond could have also increased the MFT densification (Guo, et. al, 2004). Released gas bubbles have been evident on the surface of the pond for a number of years.

Based on this apparently accelerated densification, there has been a reduced total MFT inventory, and increased process water available for recirculation. However, the undrained shear strength of DMFT is usually less than 1 kPa which is not sufficient to support direct capping, but is too thick to allow standard transfer systems to recover the material for processing. Further densification to trafficable ground will likely take decades under natural condition, which requires other methods of dealing with the material.

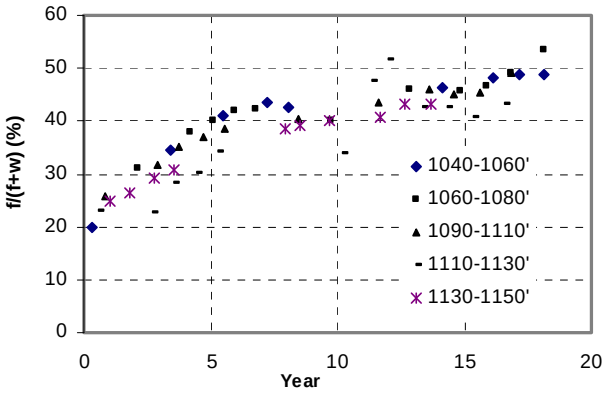

Figure 7. f/(f+w) Changes with Time at Different Depth Zones near Site 30 at Pond 3

There are two options for the treatment of the DMFT: removing and treating it outside the pond, and containing and treating in-situ. In-situ treatment could be achieved through capping and artificial dewatering, but requires waiting until the pond in decommissioned. In order to use the pond space to contain new tailings deposits, some of the DMFT has to be removed.

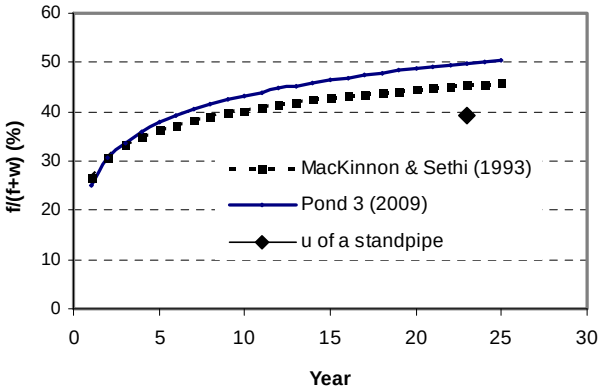

Figure 8. MFT Densification Curves by Different Sources

Due to high viscosity and yield stresses as well as the depths of the material, traditional submersible pumps have difficulty retrieving the material. Traditional methods of modifying the material properties to allow pumping often involve dilution of the DMFT, but will offset the benefits of the accelerated dewatering. More effective dredging/pumping technology is required to remove this type of material at in-situ density. Once removed, surface dewatering such as the TRO process is an option to achieve trafficability and reclamation targets.

CT/SOFT CT IN POND 5

Consolidated Tailings (CT) is a tailings treatment technology developed to reduce MFT inventories while creating trafficable surfaces suitable for reclamation. While significant progress has been made in this technology, some challenges have affected its efficiency. CT quality is impacted by process efficiencies and field deposition methods. In CT production, part of the mixture could be affected by the availability or quality of the components (MFT, sand, and gypsum). When the quality of one or more of these components deviates sufficiently from set standards, the final mixture will no longer respond as designed. These mixtures, known as off-spec CT can result in segregated deposits or become “soft CT” in the pond.

In terms of reclamation, trafficability of the material is a key parameter for CT performance. Figure 9 shows the foot and heavy equipment trafficable boundaries for Pond 5 as measured in 2009, determined through by vane shear tests.

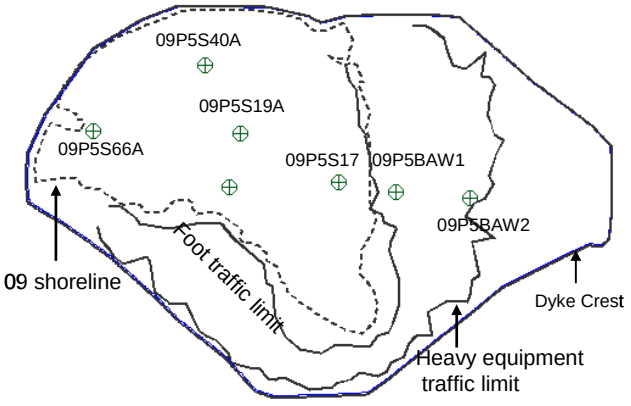

Figure 9. Pond 5 Beach Trafficability Boundaries in 2009

By November 2009, about 60% of the total surface area within the dyke crest had become foot trafficable. Areas trafficable by heavy equipment was limited to the upper portion of the beach near the dyke.

Figure 10 and Figure 11 shows SFR and solids content profiles at two sites, 09P5BAW1 and 09P5SBAW2 (as shown in Figure 9). Site BAW1 was in the lower beach and near the foot trafficable line, while BAW2 was located at the mid to upper part of the beach near the heavy equipment trafficable boundary. At BAW1, the SFR values ranged from 2 to 9 showing lower SFR CT (SFR 2-4) trapped below higher SFR CT and sand beach (with SFR 6-9). At Site BAW1, the SFR values widely ranged from 3.3 to 14. The deposits mainly consisted of high SFR CT (SFR 5-7) and densified tailings sand. The overall fines contents increased with distance from the dyke to the shoreline, which also corresponds roughly to distance from the discharge points.

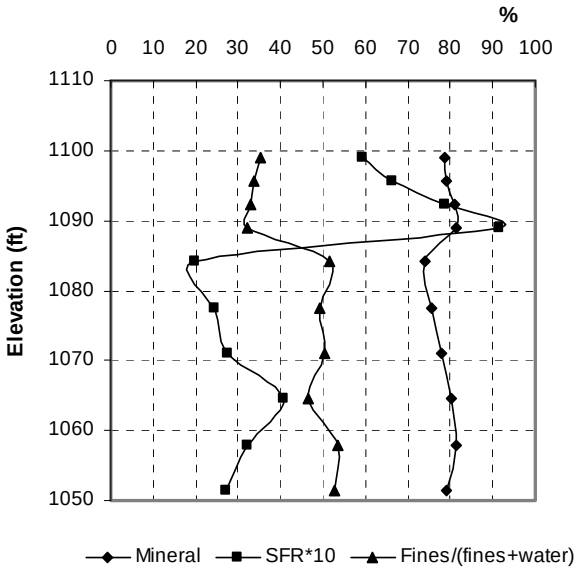

Figure 10. Sampling Profiles at 09P5BAW1

Figure 12 and Figure 13 show the profiles of SFR and solids content below pond bottom at two locations in 2008. Site 64 was near a horizontal tremie discharge line in the north part of the pond. The deposits formed between 2007 and 2008 had SFR values ranging from 3.2~5.9, which were similar to the on-spec CT from the plant. Site 46 was near site 09P5S17, with deposits mainly from spigot discharge. At Site 46, the SFR values below pond bottom ranged from 1 to 6, showing a wide range of SFRs and evident inter-layering of the varying sand contents. This indicates CT spigot

beaching has trapped high fines material (MFT and soft CT) below pond bottom. CT tremie systems are usually used when the pond is covered by a watercap since direct CT beaching into water will cause significant segregation. When the surface water is removed, CT beaching is the preferred deposition method as the deposits trap more fines below pond bottom, and minimise the surface area of the exposed soft deposits.

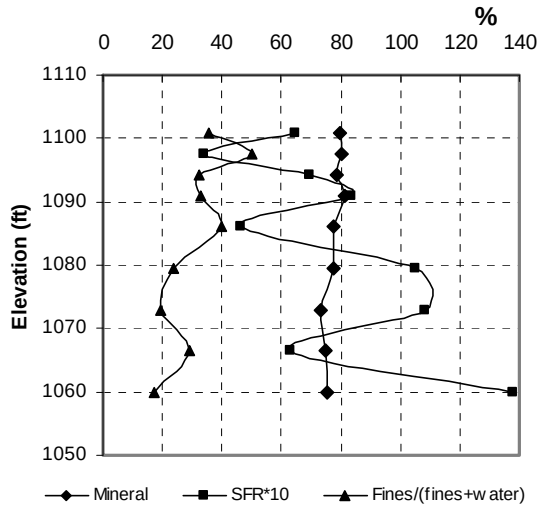

Figure 11. Sampling Profiles at 09P5BAW2

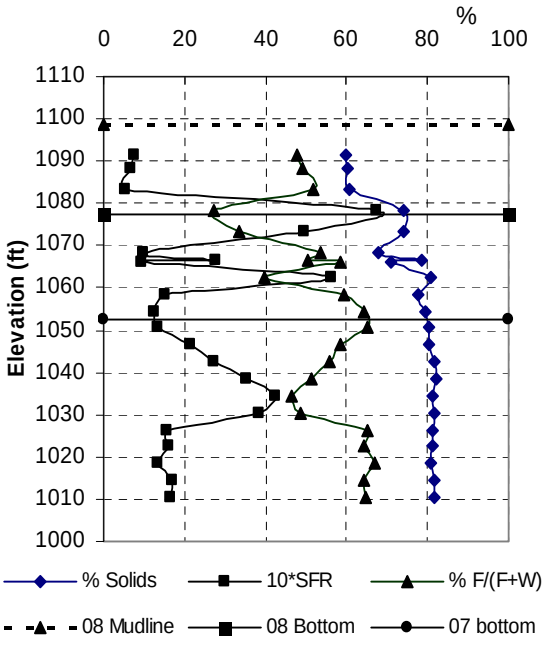

Figure 12. Sampling Profiles at Site 08P5S46A

Figure 14 and Figure 15 show cross sections of solids content and SFR from the 2009 block models of Pond 5. Most of the soft deposits above the pond bottom had SFR values less than 3 (only small portion was greater than 3), and the material near the east side generally contained more sand and had higher solids contents relative to the west side. There's a deep soft zone with low SFR (SFR<1) and low solids contents (<50%) in the west side. This was likely due to CT beaching operations primarily from the NE and SE, corralling the softer material.

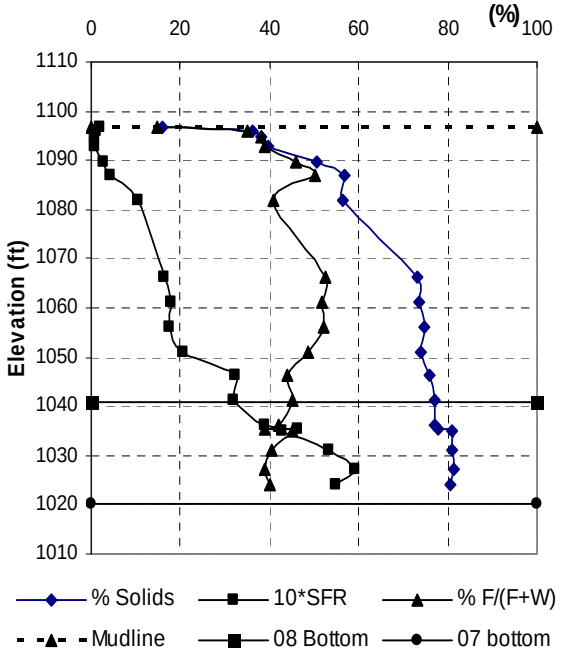

Figure 13. Sampling Profiles at Site 08P5S64

Of the sediments found above the pond bottom in 2009, 20.8% had solids contents less than 50%, 55.8% had solids contents greater than 70%, and 39.1% had solids contents greater than 75%. Typically in these types of deposits, a material with solids contents above 80% usually forms solid pond bottom with strengths in excess of 5kPa. While over a decade CT deposition in Pond 5 has transformed most of the pond surface (about 60%) into trafficable ground, the overall density of the soft material has also increased through self-weight consolidation and sand loading. Figure 16 shows the solids contents vs. SFR of the soft deposits for different years. For the deposits with SFR greater than 3, the solids contents in different years were similar and near 80%, indicating rapid consolidation. For the deposits with SFR less than 3, the solids contents increased over time, showing continuous dewatering of the soft deposits.

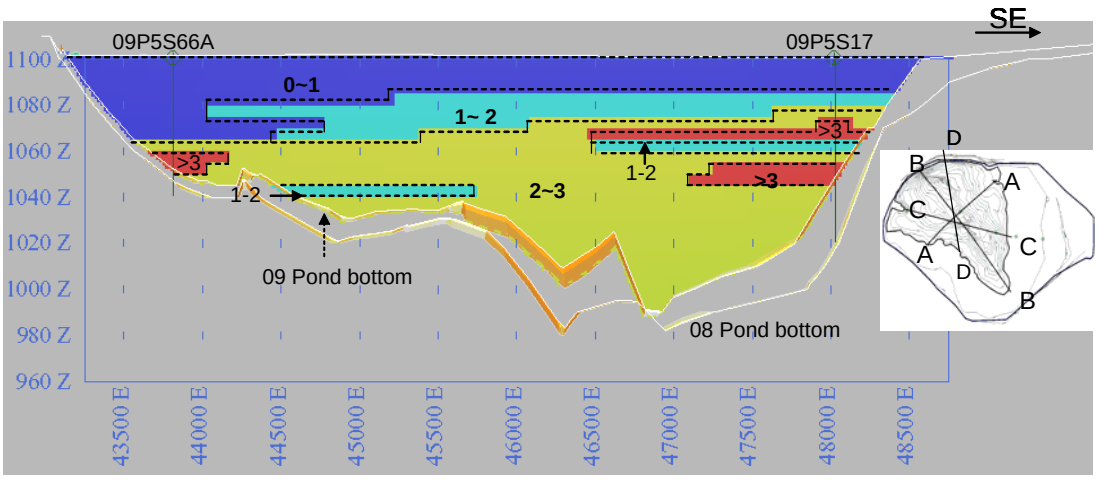

Figure 14. 2009 Pond 5 Solids Content Cross Section C by Block Modeling

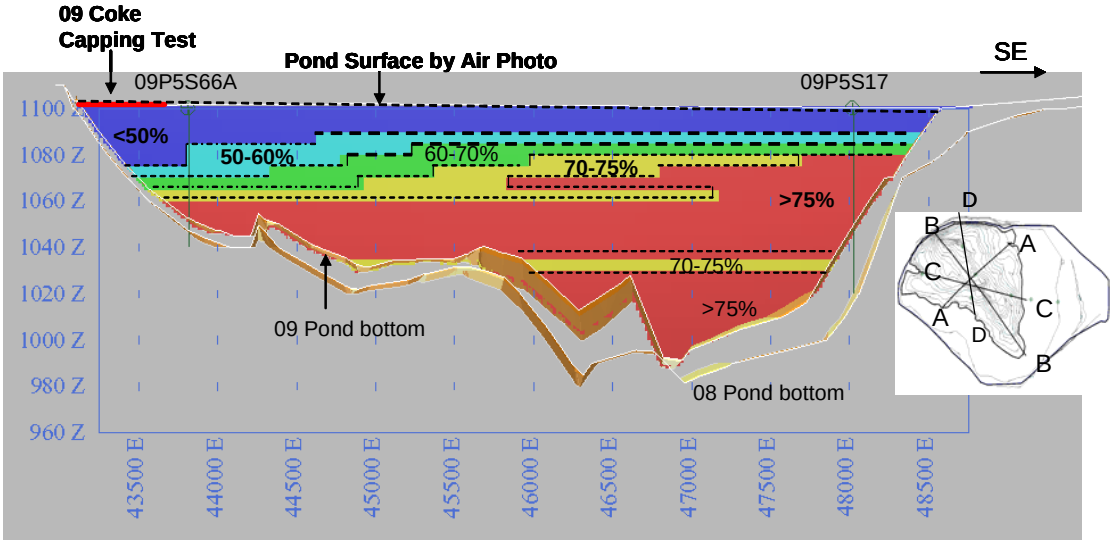

Figure 15. 2009 Pond 5 SFR Cross Section C by Block Modeling

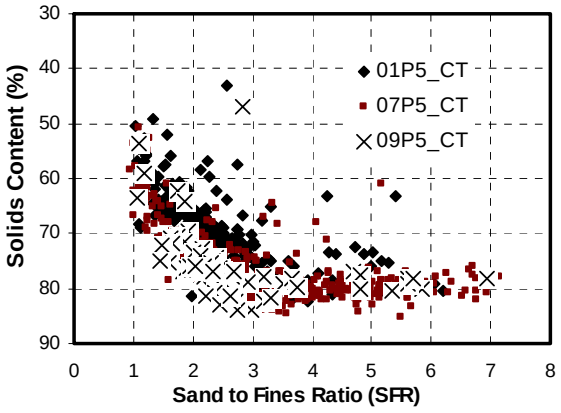

Figure 16. Solids Content vs. SFR of Pond 5 Deposits in Different Years

Figure 17 shows the depth profiles of undrained shear strength determined by field vane tests and ball penetration test at Site 19A in 2009. Above the pond bottom, the undrained shear strengths (peak) were less than 2 kPa, and the strengths at the top 20-30' were less than 1 kPa. Preliminary modeling by Suncor consultants indicates it may require many decades for the soft sediments to become trafficable under self-weight consolidation. In order to achieve a reclaimed surface within the timeframes dictated by operational approvals, surface capping and artificial dewatering is required. Large scale field tests, conducted since 2008, have resulted in a high confidence that creating a trafficable surface on Pond 5 by 2019 is achievable.

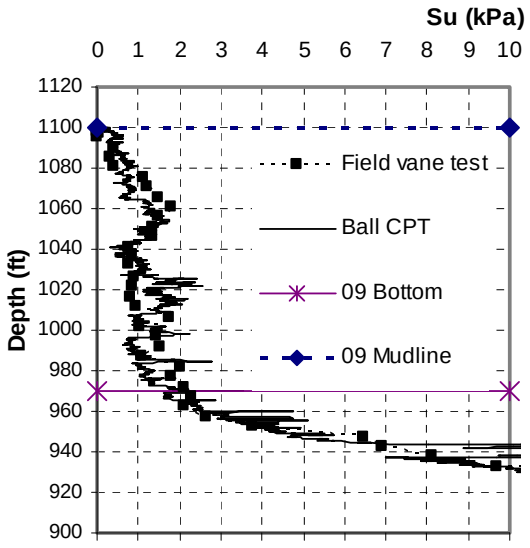

Figure 17. Undrained Shear Strength (peak) Profiles at 09P5S19A by Ball CPT and Vane Test

SUMMARY

- Block Modeling has greatly improved tailings pond assessment by shifting pond characterisation from observation/qualitative approaches to better quantitative methods. It has proven a useful tool for tailings pond management.
- Due to continuous, slow rate sand loading of the MFT, both sand and solids contents in Pond 2/3 (especially Pond 3) have significantly increased. The MFT dewatering rate has also increased.
- Sand loading and increased dewatering has led to the formation of dense MFT (DMFT) with solids contents greater than 50% and SFR less than 1.0.
- Large portion of Pond 2/3 soft sediments has become DMFT. Alternative technologies are required to transfer and treat this material.
- Over a decade CT deposition in Pond 5 has transformed the majority of the pond surface to trafficable ground, also has also increased the SFR and density of the soft sediments.
- The CT/soft CT properties in Pond 5 are related to the quality in the CT plant, and was also significantly affected by deposition methods and final deposition locations in the pond.
- Due to low strength and very slow self-weight consolidation of the soft sediments in Pond 5, surface capping and artificial dewatering is required to provide trafficable surface for final reclamation. Large scale testing has given us confidence to achieve the goal.

REFERENCES

FTFC (Fine Tailings Fundamentals Consortium), 1995. Advances in Oil Sands Tailings Research. Alberta Department of Energy. Oil Sands and Research Division. Edmonton. Alberta.

Guo, C., Chalaturnyk, R.J., Scott, J.D., MacKinnon, M., 2004. Densification of oil sands tailings by biological gas generation. 57th Canadian Geotechnical Conference, Quebec City, 8 pages on a CD.

MacKinnon, M. Sethi, A. 1993. A comparison of the physical and chemical properties of the tailings ponds at the Syncrude and Suncor Oil Sands Plants. Oil Sands – Our Petroleum Future Conference April 4-7, 1993, Edmonton, AB.

Scott, J. D., Chalaturnyk, R., Jeeravipoolvarn, S., Fine tailings decrease in volume by creep compression. 57th Canadian Geotechnical Conference, Quebec City, QC., Oct. 2004.

Wells, S., Guo, C. Application of Block Modeling to Suncor Tailings Characterisation. First International Oil Sands Tailings Conference, Dec 7-10, 2008, Edmonton, AB.

OIL SANDS TAILINGS SAND HYDRAULIC CONDUCTIVITY

Gord McKenna[1], Kevin Biggar[1], Soe Moe Kyaw Win[1], Jeff Journault[1]
Tim Eaton[2], Dave Sego[3], and Norbert Morgenstern[3]
[1]BGC Engineering,
[2]Shell Canada Energy,
[3]University of Alberta Geotechnical Centre

ABSTRACT

The saturated hydraulic conductivity of oil sands tailings sand is an important consideration in landform and dam design. To examine the role of uncertainty and variability in this parameter, a database of 843 saturated hydraulic conductivity measurements was generated from Syncrude tailings sand. Test volumes span 11 orders of magnitude (lab permeameter to entire dyke cross sections) and hydraulic conductivities span seven orders of magnitude. The average large-scale (dyke) horizontal hydraulic conductivity ranged from 10^{-4} to 10^{-3} cm/s (geometric mean of $5x10^{-4}$ cm/s). Statistical distributions for each test method are approximately lognormally distributed with coefficients of variations of 10 to 25 percent (for log-transformed data). Recognition of scale effects and asymptotically increasing hydraulic conductivity with increasing test volume are important in selecting design values.

A recent field test of tailings sand hydraulic conductivity was conducted at Shell's Muskeg River Mine to determine what design value should be used for tailings sand drainage elements of in-pit dykes. Two test pads were constructed with multiple lifts using equipment and methods similar to those used in dyke construction, and hydraulic conductivity and density performance was measured. These results were then evaluated in the context of the lessons learned from the analysis of the historical data to develop design values for the tailings sand drainage elements.

INTRODUCTION

Geotechnical engineers do not usually explicitly consider geostatistics of hydraulic conductivity in their designs. This paper describes the geostatistical nature of the hydraulic conductivity of oil sands tailings sand and uses this framework (based on McKenna, 2002), along with supporting field data, for the design of a tailings sand filter drain for an oil sands in-pit dyke.

Background

The hydraulic conductivity of oil sands tailings sand is an important factor in the design of dykes and landforms in the oil sands region. Most designs assume that tailings sand hydraulic conductivity has a unique deterministic value, however there are considerable spatial variability and scale effects. This paper provides an example of a simple geostatistical framework for tailings sand hydraulic conductivity (a fairly homogeneous artificial material). It demonstrates scale effects on means, variances, and coefficients of variation. It includes a large database of measured values from Syncrude, practical methods for choosing design hydraulic conductivities, and a design example from the Shell Muskeg River Mine.

The extremely large range of saturated hydraulic conductivities for soils is well known but the spatial variability and scale effects of a given material are underappreciated and seldom considered explicitly in routine seepage and hydrogeology practice. The geostatistics of hydraulic conductivity, however, is an area of ongoing, intense, sophisticated academic investigation and there is a vast literature, most of which is rather daunting for non-mathematicians. There is little accessible guidance for landform and dyke designers and other practitioners.

For tailings structures (dykes, dams and ponds), the state of practice implicitly compensates for this limited understanding. For example, practitioners predicting seepage discharge rates, tend to select among the highest hydraulic conductivity values from laboratory testing for most designs. Greater confidence is placed in larger scale tests and where practical, testing and back analysis is done at the same scale as the design. The underlying rationale is that there will be well-connected higher hydraulic conductivity zones (preferential flow zones) that will govern field performance that are often undetected in laboratory tests or small scale field tests. A combination of using upper-bound hydraulic conductivity and generous conservatism in seepage design, especially in use of generous

supply-to-demand ratios for internal drainage systems, has allowed reasonably good operational performance. For cases where fluxes and water table elevations need to be controlled to certain maximum operational values, these design practices have an accepted record of success and involve a modest effort in engineering and testing. To reduce residual uncertainty, monitoring is employed and remedial measures implemented if acceptable performance is not achieved. The state of practice does not include the explicit use of geostatistics but it is generally handled implicitly.

However when it comes to prediction of the behaviour of seepage plumes, and especially the performance of liners, covers and other aquitards meant to have low seepage rates, many predictions grossly underestimate seepage fluxes and contaminant transport velocities, mainly from small undetected high hydraulic conductivity zones or a poor understanding of groundwater flow mechanisms (e.g., Sarewitz et al 2000). It seems that some of the problems come from a failure to appreciate geostatistics – especially the variability, upscaling, and short autocorrelation distances of hydraulic conductivity (Benson, 1991). Of particular interest to the landform designer is the effect of spatial variability on deep percolation through unsaturated covers – small areas of undetected higher vertical hydraulic conductivity (often due to macropermeability) may govern performance of the cover (and the landform) as a whole.

The landform designer is not only interested in predicting maximum rates of seepage and controlling water tables through civil engineering means. They are also interested in the variability in water table location (as an element of performance, diversity, and risk), the ranges and temporal changes in seepage fluxes (as influent to, or effluent from, wetlands and other aquatic landscape elements), rates of ionic movements and dilution or concentration, prediction of deep percolation through covers, flushing mechanisms within vegetation root zones, and soil moisture availability to plants. In other words, they are both interested in the geographic (spatial) variation of performance on a landform (especially near surface) as well as the temporal fluxes of large and small watersheds to the rest of the landscape. This interest comes from the necessity of trying to achieve or balance often competing objectives and because it is often impractical (or impossible) to use a purely conservative or even deterministic approach. A probabilistic approach with ranges of possible outcomes will become a common feature of landform design as a part of risk-based approaches to evaluate various design options. Of all aspects of landscape performance relating to seepage, the most important issue is often the seepage water quantity and quality where it interacts with the biosphere.

For traditional tailings dyke design, when the design hydraulic conductivity is incorrectly selected, the design may be changed during construction. Based on analysis of performance during early construction, drainage schemes may be altered (additional drains may be installed or omitted), seepage cutoff walls may be installed, rates of dyke rise may be increased or decreased – it is common for a tailings dyke to go through several design phases during its life as experience is gained with the performance of the foundation and construction fills. Most of the design changes cost the mining company money, either in the form of additional construction costs, or lost savings in starting a non-optimal design. In the worst case, poor design and management can lead to dam failure. Managing these risks is a standard and accepted part of dyke design and construction. Risks are often managed early on by using conservative values for hydraulic conductivity and fluxes.

When the wrong hydraulic conductivity (or percolation) values are selected relative to long term landscape performance, common results are uncontrolled seepage plumes, water tables that are too high or too low (or waters too salty or contaminated) to support intended soils and vegetation (and land use), increased erosion, and reduced trafficability. Fluxes of seepage water reporting to water treatment facilities may be much higher than anticipated. Downstream land uses that require certain quantity and quality of water may be affected. In general, selection of the wrong design permeabilities results in high reclamation costs and extensive post-closure retrofits, or acceptance of reduced landscape performance and land use limitations may result. Because of the inherent uncertainty in any prediction of long term landscape performance, accommodation for this uncertainty, including some degree of retrofitting, is likely required in any case.

HISTORICAL DATA ANALYSIS

Methods

As detailed in McKenna (2002) a database of 843 Syncrude tailings sand hydraulic conductivities were compiled that included the following:

- Lab triaxial hydraulic conductivity tests on small intact beach cores sampled using ground freezing to maintain the original structure intact
- Lab reconstituted permeameter tests
- Field percolation "coffee-can" tests on tailings beaches
- Field infiltration tests from Guelph and double-ring infiltrometers
- Field falling head standpipe slug tests
- Laboratory model (flume) tests
- Field tailings sand cell construction pore pressure dissipation tests
- Field pump tests
- Field gradients between standpipes
- Dyke section seepage back analysis

Details of the analyses to determine hydraulic conductivities is presented in McKenna (2002). Figure 1 shows the range of grain size distributions. A representative volume for each test was estimated. Data was analyzed for simple geostatistical parameters and scale effects were investigated against a framework published by Schulze-Makuch et al. (1999).

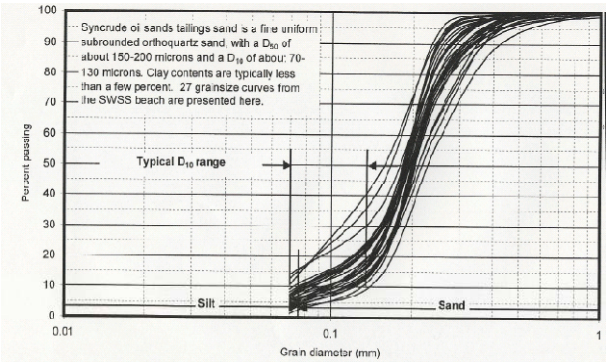

Figure 1. Typical range of grain size distributions for Syncrude oil sands tailings sand.

Results

Horizontal to vertical hydraulic conductivity ratios

It was originally hoped that results from this study would confirm the typically used horizontal to vertical hydraulic conductivity ratio (kh/kv) for dyke design of 16 for oil sands tailings sand. The lack of statistical difference between horizontal and vertical permeabilities from the frozen core samples suggests that the kh/kv ratio varies from sample to sample for small surface tests and may average about one. Back analyses of dyke sections is somewhat insensitive to kh/kv ratio (because they are dominated by horizontal flow), and values of 1 to 20 are common. For other test methods, the effects of vertical hydraulic conductivity are overwhelmed by other factors (model and field errors) and provide little insight into this ratio.

For sands within 2 m of the beach surface, an average kh/kv ratio of 1 is recommended with values between 0.1 and 10 considered in sensitivity analysis. For designs involving larger volumes, such as for pumping or other drainage schemes and for dyke design, an average ratio of 10 is recommended with average ratios from 1 to 20 considered in sensitivity analyses.

The remainder of the analysis discussed below focuses exclusively on kh.

Surface sample permeabilities

Data from the very shallow tests should be considered separately from the rest of the database. Recognized some twenty-five years ago (Alberta Department of the Environment, 1977), this conclusion seems to have been lost until the present study. In particular, the lab field frozen cores, field percolation, field Guelph permeameter, and field infiltration tend to produce higher hydraulic conductivity values than other methods. Values of 10^{-3} cm/s were common with kh/kv=1.

The reason for the hydraulic conductivity difference is not clear – surface materials generally have similar densities (measured by field nuclear densometers) as deep sands and have the same lithology and stratigraphy. The difference may lie with confining stress, near-surface macro-permeability, or subtle density effects. The percolation tests likely also suffer from significant experimental and model error – most of the comparisons of means and variances between the four surface test datasets indicates they are significantly different from each other ($\alpha = 0.05$).

Recognition of this surface layer as a distinct material (with respect to hydraulic conductivity) is

important to modelling and design of covers and percolation.

Scale effects on kh

Figure 2 plots the hydraulic conductivity as a function of volume. It is interesting to note that there appears to be an upper bound of hydraulic conductivity of 10^{-3} cm/s at all scales. The lower bound varies over five orders of magnitude at small scale and one order of magnitude at larger scales. It is concluded that at larger scales, there is preferential flow through the zones with the higher hydraulic conductivity, though even at this larger scale, there is still some variability. The mean value of hydraulic conductivity increases with increasing scale volume to a constant value. Scale effects are addressed in more detail below.

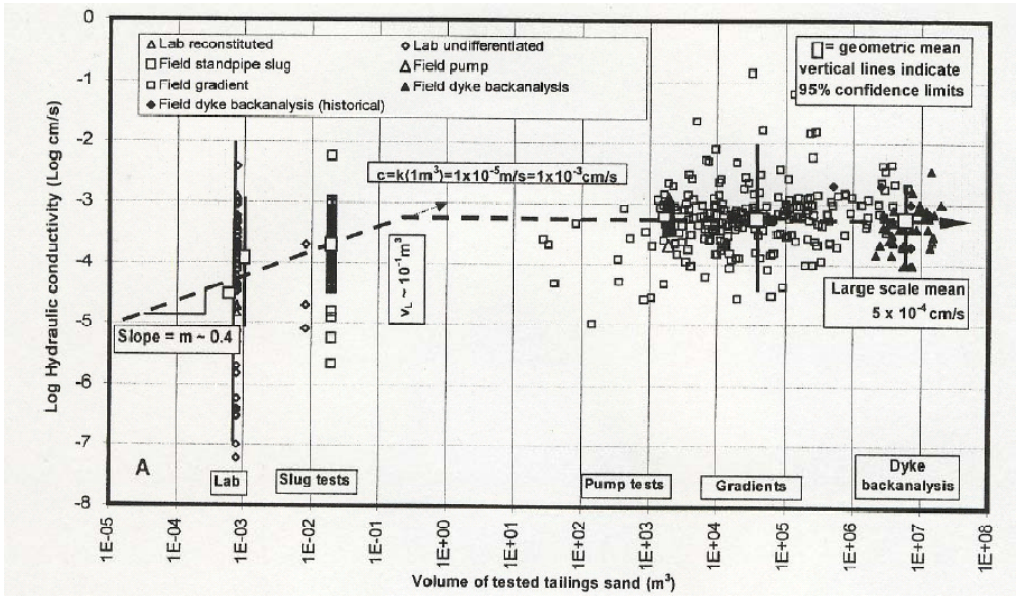

a)

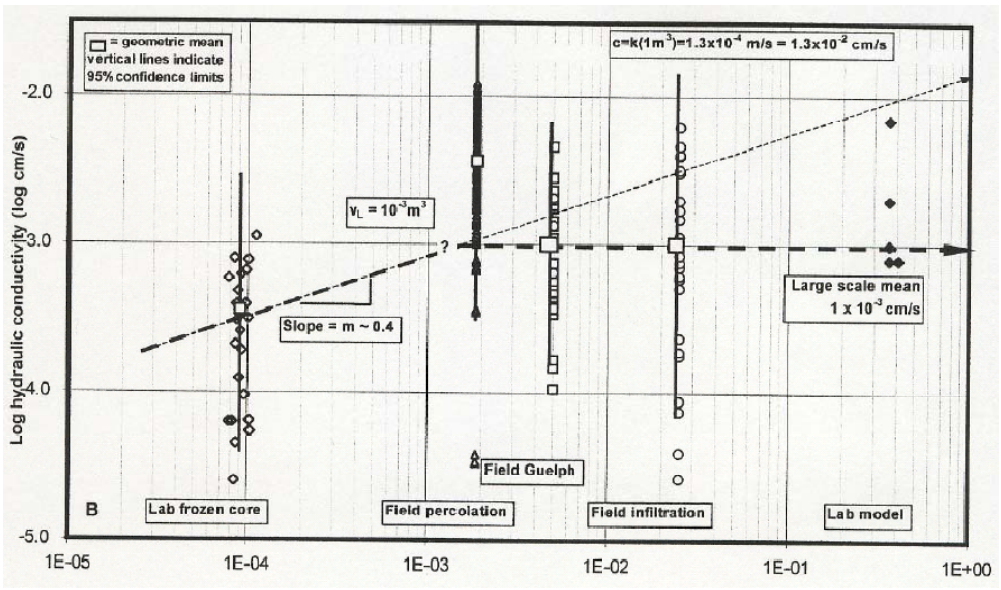

b)

Figure 2. Tailings sand hydraulic conductivity data from Mildred Lake tailings basin plotted based on: a) non-surface and b) surface material (after McKenna, 2000) Curve fitting follows the framework of Schulze-Makuch et al. (1999)

The distribution of hydraulic conductivity values from each test method generally has a strongly positive skewness – they are skewed towards the lower values of hydraulic conductivity. The distribution of the data can be approximated with several common statistical distributions, and like most geological data, have a lognormal distribution.

Coefficient of variation (CoV), which is the standard deviation divided by the mean, is a useful measure of variation of geotechnical properties (e.g., Phoon and Kulhawy, 1999a,1999b) for data (or transformed data) with a distribution that is approximately symmetric about the mean. The CoV for each dataset is listed in Table 1 and typically ranges from about 10 to 25% (for log transformed data with hydraulic conductivity units of cm/s) which is similar to that of other geotechnical properties of typical geotechnical materials as reported by Phoon and Kulhawy (1999a; 1999b). They are slightly greater than the CoV of 5 to 15% for log-transformed hydraulic conductivity of a wide variety of materials tests calculated from Schulze-Makuch et al. (1999) and 3 to 10 percent for unconsolidated materials by Bierkens (1996) and similar to those for fluvial sands by Rehfeldt et al. (1992). Thus CoV of log transformed hydraulic conductivity would appear to be independent of material type. Whether the effect of scale and test type on CoV is important will depend on the application.

Based on this study for large dykes, an average value for horizontal hydraulic conductivity (kh) is interpreted as $5x10^{-4}$ cm/s (Figure 2a) with a horizontal to vertical hydraulic conductivity ratio (kh/kv) of 1 to 20. Recognition of a range of values of about +/- one-half order of magnitude (a range of 10^{-4} to 10^{-3} cm/s) is needed in design.

While it is disappointing to only be able to predict design parameters and future performance within a range of one order of magnitude, this is a common outcome hydraulic conductivity, and more generally, for many environmental models. In many cases, coping with the uncertainty rather than trying to refine the parameters and models, is a preferable course (Sarewitz et al., 2000).

Figure 2b presents measured hydraulic conductivity as a function of test volume for non-surface tailings sand. The mean and variance are a function of the scale tested (Table 1). For small test volumes, the mean is low and the variance is high whereas the opposite is true for large test volumes. This reduction in variance with increasing test volume is common in geostatistics. The increase in the mean with increasing test volume is often observed for hydraulic conductivity data – one can rationalize that the calculated average hydraulic conductivity of larger samples will be dominated by more permeable zones within the deposit, especially for horizontal conductivities of layered systems. Whether it is true for vertical hydraulic conductivity will depend more on the degree of interconnectedness of higher hydraulic conductivity zones. In some cases, overall anisotropy may be due to the spatial relation of layers rather than (or in addition to) anisotropy within elements.

SUMMARY

Data from very shallow hydraulic conductivity tests indicates that tests on tailings sand in the upper 1 m have a value of about 10^{-3} cm/s with a kh/kv=1 and a CoV=15 to 20%.

For the testing of tailings sand at greater than 1m depth a large-scale horizontal hydraulic conductivity (kh) is interpreted as $5x10^{-4}$ cm/s, with a horizontal to vertical ratio (kh/kv) of 1 to 20 and a CoV=15%. For smaller scales recognition of a range of values of about +/- one-half order of magnitude (a range of 10^{-4} to 10^{-3} cm/s) is needed in design.

For smaller scale tests (such as lab and slug tests), expect a slightly lower hydraulic conductivity and more variation.

On a practical note, the 85^{th} percentile hydraulic conductivity of laboratory testing seems to correspond to the field scale hydraulic conductivity. So a laboratory strategy is to test 10 samples and select the 8^{th} or 9^{th} highest as an estimate of the large-scale field horizontal field value.

Perhaps the most important conclusion is that even with extensive testing and analytical efforts, large-scale hydraulic conductivity can only be estimated to within +/- one-half order of magnitude even for a rather homogenous, as-built, artificial material like oil sand tailings sand. Testing and designs need to account for local variability at small scale, and uncertainty at large scale, by employing conservatism in design, and where possible, the ability to modify designs if unacceptable performance is discovered.

DESIGN CASE HISTORY

Introduction

Due to the high costs associated with importing clean sand fill to use in chimney drains and sand drainage blankets for in-pit dykes constructed of lean oil sands at the Muskeg River Mine, it was desirable to investigate the viability of using tailings sand as a drainage media.

Table 1. Statistical summary of hydraulic conductivity tests

Test type	n	Test volume (m^3)	Generalized range k_h (cm/s)	Raw hydraulic conductive data (cm/s)				Log transform of permeability data (log cm/s)			
				Avg	σ^2	σ	CoV[a] %	Avg	σ^2	σ	CoV[a] %
All data	*829*	*10^{-4} to 10^{+7}*	*10^{-7} to 10^{-2}*	*$1.9x10^{-3}$*	*$3.6x10^{-5}$*	*$6.0x10^{-3}$*	*319*	*-3.30*	*0.71*	*0.85*	*26*
Lab frozen core	*23*	*10^{-4}*	*10^{-5} to 10^{-3}*	*$3.5x10^{-4}$*	*$8.6x10^{-8}$*	*$2.9x10^{-4}$*	*84*	*-3.65*	*0.21*	*0.46*	*13*
Field percolation	*199*	*10^{-3}*	*10^{-3} to 10^{-2}*	*$4.5x10^{-3}$*	*$8.0x10^{-6}$*	*$2.8x10^{-3}$*	*63*	*-2.48*	*0.16*	*0.41*	*16*
Field Guelph permea-meter	*26*	*5 x 10^{-3}*	*10^{-4} to 10^{-2}*	*$1.2x10^{-3}$*	*$1.0x10^{-6}$*	*$1.0x10^{-3}$*	*88*	*-3.11*	*0.16*	*0.41*	*13*
Field infiltration	*30*	*10^{-2}*	*10^{-4} to 10^{-2}*	*$1.7x10^{-3}$*	*$2.8x10^{-6}$*	*$1.7x10^{-3}$*	*99*	*-3.08*	*0.39*	*0.63*	*20*
Lab reconstituted	16	10^{-3}	10^{-5} to 10^{-3}	$2.2x10^{-4}$	$9.3x10^{-8}$	$3.0x10^{-4}$	136	-3.96	0.28	0.53	13
Lab undiff-erentiated	43	10^{-3}	10^{-7} to 10^{-3}	$2.7x10^{-4}$	$3.9x10^{-7}$	$6.2x10^{-4}$	232	-4.52	1.57	1.25	28
Field stand-pipe slug	172	10^{-2}	10^{-5} to 10^{-3}	$2.9x10^{-4}$	$2.3x10^{-7}$	$4.8x10^{-4}$	167	-3.72	0.16	0.40	11
Lab model	6	10^{-1}	10^{-3} to 10^{-2}	$2.3x10^{-3}$	$4.7x10^{-6}$	$2.2x10^{-3}$	96	-2.79	0.11	0.33	12
Field con-solidation	10	10^{+1}	10^{-6} to 10^{-4}	$3.8x10^{-5}$	$1.4x10^{-9}$	$3.8x10^{-5}$	101	-4.69	0.33	0.57	12
Field pump	26	10^{+3}	10^{-4} to 10^{-3}	$5.8x10^{-4}$	$4.8x10^{-8}$	$2.2x10^{-4}$	38	-3.27	0.02	0.16	5
Field gradient	229	10^{+2} to 10^{+7}	10^{-4} to 10^{-2}	$2.1x10^{-3}$	$1.2x10^{-4}$	$1.1x10^{-2}$	513	-3.23	0.29	0.54	17
Field dyke back analysis	37	10^{+6} to 10^{+7}	10^{-4} to 10^{-3}	$5.8x10^{-4}$	$3.3x10^{-7}$	$5.8x10^{-4}$	99	-3.36	0.10	0.32	10
Field dyke back analysis (historical)	7	10^{+6} to 10^{+7}	10^{-4} to 10^{-3}	$1.2x10^{-3}$	$6.0x10^{-7}$	$7.8x10^{-4}$	65	-3.11	0.24	0.49	16
All lab	82			$2.8x10^{-4}$	$2.5x10^{-7}$	$5.0x10^{-4}$	176	-4.17	1.08	1.04	25
All infiltration	56			$1.4x10^{-3}$	$2.0x10^{-6}$	$1.4x10^{-3}$	99	-3.09	0.29	0.54	17
All dyke back analysis	44			$6.8x10^{-4}$	$4.2x10^{-7}$	$6.5x10^{-4}$	96	-3.32	0.13	0.36	11

[a] CoV = Coefficient of variance = coefficient of variation = standard deviation / mean = σ / Avg. Coefficients of variation of log transformed distributions are sensitive to the units and base of the logarithm. In the case of the final column, base 10 logarithms are used to cover hydraulic conductivity data with units of cm/s.

Italicized text indicates surface beach samples (low confining stress)

The tailings sand is cycloned at the extraction plant to remove fines, then is placed in a sand farming area using cell construction. A field testing program was conducted using these farmed sands to determine the fines content distribution within the deposit, as well as the hydraulic conductivity and placed density using the same equipment and procedures that would be used in full scale operations.

Methodology

Two trial pads were constructed of tailings sand, and field and laboratory testing on the tailings sand was performed. The two pads were 50 m long by 40 m wide; Pad 1 had three 1.0 m thick lifts and Pad 2 had two 0.5 m lifts. Hauling and placement was performed using 40T articulated dump trucks, and spreading and compaction was performed with D8 or D9 dozers, similar to how the sand would be placed in the drainage elements of the in pit dykes. Portions of the pads were scarified with a grader equipped with ripper teeth prior to placement of the subsequent lifts to evaluate if low hydraulic conductivity resulted at the lift boundary interface due to compaction. Troxler Nuclear Density tests were performed at 12 locations on each lift (approximately 10 m apart) except the last lift on Test Pad 2, and Guelph Permeameter (GP) tests were conducted at a total of 13 locations and at various depths on the test pads. Bulk samples were collected for sieve analysis, moisture content and Standard Proctor compaction tests.

Results

The grain size distribution of the tailings sand tested is shown in Figure 3, and shows the sand to be a uniform medium to fine sand with 4% to 9% fines (<75um).

Table 2 summarizes the results of the density testing, Figure 4 shows the variation in Troxler density at the 12 different points tested on each pad, The densities varied between 1680 and 1910 kg/m^3, with a mean value of 1787 kg/m^3 for Pad 1 (1.0 m lifts) and ranged between 1670 and 1760 kg/m^3 with a mean of 1722 kg/m^3 for Pad 2 (0.5 m lifts). Due to high compactive effort of dozers (D8 or D9), measured dry density from test pads are close to 100% of the Standard Proctor maximum dry density (Table 2) though the moisture contents are 8% to 9% dry of Standard Proctor optimum moisture content.

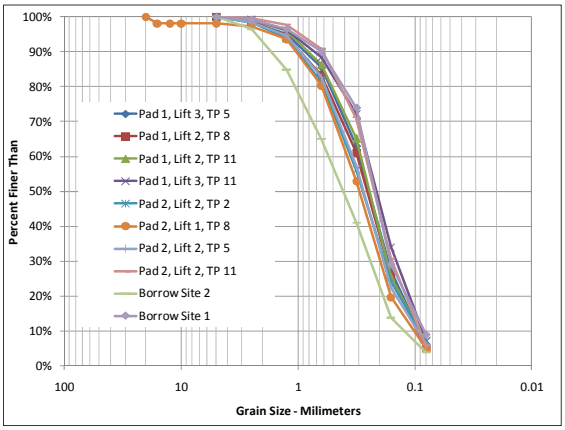

Figure 3. Grain size distribution of tailings sand from Muskeg River test program.

The results indicate that the Troxler measured dry densities of the 0.5 m thick lifts appear to be generally lower than the 1.0 m thick lifts, though the scatter is sufficient to render this inconclusive. This is contrary to what would be expected and cannot be explained at this time, except that the difference is likely insignificant.

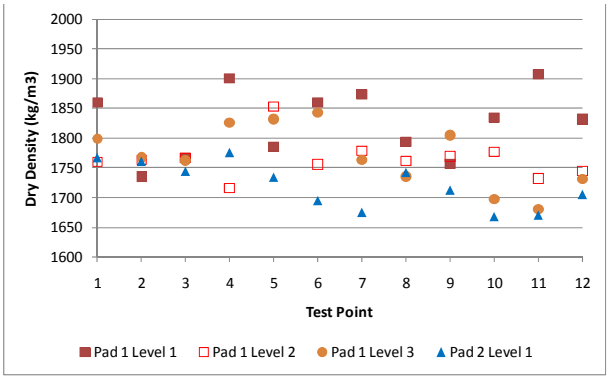

Figure 4. Troxler dry densities from Muskeg River Mine field test program.

Figure 5 shows the variation in hydraulic conductivity with test depth from the GP tests, with no distinct trends, and showing that the range of measured permeabilities varied over a relatively small range of 1.1×10^{-3} to 8.6×10^{-3} cm/s. The average hydraulic conductivity for Pad 1 was 5.3×10^{-3} cm/s (n=9), and for Pad 2 was 3.9×10^{-3} cm/s (n=4).

To examine the changes in hydraulic conductivity versus dry density, only the data from Test Pad 1 could be evaluated because no Troxler densities were obtained where GP testing was done on Test

Pad 2. Figure 6 shows this relationship. One might infer a decrease in hydraulic conductivity with increasing dry density, however due to the small variation in hydraulic conductivities, the relationship may not be significant.

Table 2. Density results from Muskeg River Mine tailings sand testing

Location	Lift	Troxler Dry Density (kg/m^3)			Moisture Content (%)		SPMDD
	Thickness (m)	Range	Average	n	Range	Average	(kg/m^3 @ %MC)
Test Pad 1	1.0	1680-1906	1787	36	2.7-4.2	3.1	1768 @ 11.0%
Test Pad 2	0.5	1671-1762	1722	12	3.2-4.5	3.8	1740 @ 11.6%

SPMDD = Standard Proctor Maximum Dry Density

Lastly, it was desired to evaluate if there would be reduced hydraulic conductivity at the lift interfaces due to the track packing by the dozers. No discernible increase in the hydraulic conductivity of the test points was observed where scarification took place compared to test points where no scarification took place (data not shown), indicating that no significant reduction in hydraulic conductivity should occur at the lift boundary due to track packing by dozers providing similar material and procedures are used.

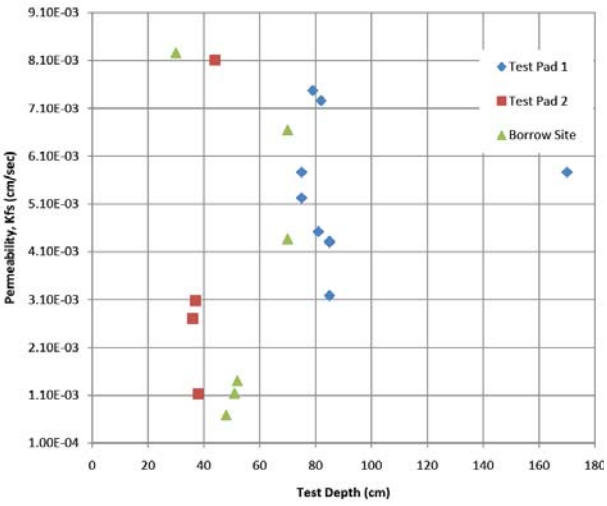

Figure 5. Hydraulic conductivity from Guelph Permeameter tests versus test depth for Muskeg River Mine field test program.

Based on all the tests, an average hydraulic conductivity value of 4.9x10^{-3} cm/s was observed from the GP tests on the test pads, with the range being 1.1x10^{-3} to 8.6x10^{-3} cm/s.

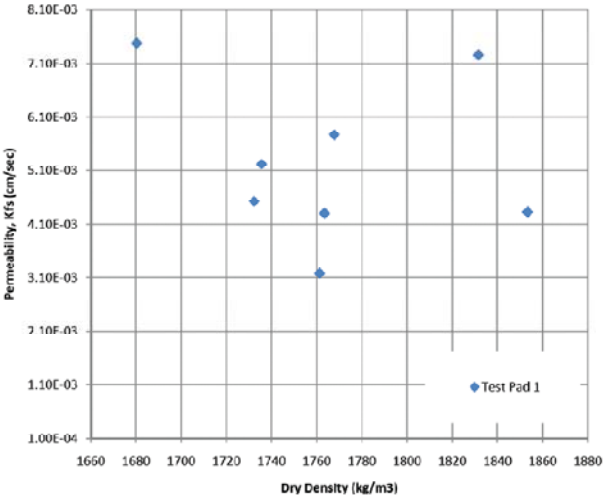

Figure 6. Hydraulic conductivity from Guelph Permeameter tests versus depth for Test Pad 1 (1.0 m lift thickness).

DISCUSSION

The work described in the first part of this paper from McKenna (2002) found that the hydraulic conductivity of surficial deposits of beaches and cell sand (measured using a variety of methods) is a separate population from deeper deposits, with higher and isotropic hydraulic conductivities, and obtained a value of approximately 1x10^{-3} cm/s. The work also observed that there was an increase in the hydraulic conductivity as the volume of the tested material increased up to a threshold value (Figure 2a) postulating that there is preferential flow through the zones with the higher hydraulic conductivity. The deeper and larger scale tests had a mean approximately one-half order of magnitude lower than the surficial material, with kh= 5x10^{-4} cm/s. The tests on the deeper and larger scale soils were in hydraulically placed

deposits (cell construction and beaches) which have anisotropic characteristics due to the deposition and placement techniques, and a recommended value of kh/kv = 10 appears to be appropriate.

The MRM test program intended to measure the vertical hydraulic conductivity accounting for the placement method that will be used in chimney drain construction using farmed tailings sand. It is not anticipated that there will be any anisotropy using this construction method compared to hydraulic placement of sand during cell and beach construction, as reported in McKenna (2000). Based upon the results obtained in the MRM test program, and considering the material presented in McKenna (2000) relating to scale and depth impacts, the actual hydraulic conductivity value for tailings sand in the drainage elements of the dams is anticipated to be approximately one-half order of magnitude lower than the average value obtained in the field tests, therefore should be approximately $1x10^{-3}$ cm/s, providing similar placement is used and that the tailings sand has a maximum fines content less than 9% and average fines of ~6%.

CONCLUSIONS

The hydraulic conductivity of oil sands tailings sand based on tests from the Syncrude Mildred Lake site appears to have a scale dependency. Smaller scale tests, and tests near surface deposits appear to be isotropic, and to have values approximately one–half order of magnitude higher than the horizontal hydraulic conductivity obtained from larger scale tests and back analysis. The average value of hydraulic conductivity for the shallow and small scale tests is approximately $1x10^{-3}$ cm/s, and the horizontal hydraulic conductivity value for larger scale tests and back analysis is approximately $5x10^{-4}$ cm/s, The deeper and larger scale values appear to be anisotropic with the ratio of kh/kv varying from 1 to 20, with a reasonable value of 10.

The hydraulic conductivity of tailings sand from Shell's Muskeg River Mine site determined in test plots where the placement and compaction was designed to mimic chimney drain construction was measured to be approximately 5×10^{-3} cm/s in deposits up to 3.0 m thick. Accounting for a much larger deposit in the actual tailings dyke and using the relationships observed in McKenna (2002), a reduction of one-half order of magnitude appears to be appropriate. Additionally, compaction at the lift boundary did not appear to reduce the vertical hydraulic conductivity of the deposit.

Thus, despite the large database of tailings sand hydraulic conductivity available, these results indicate that the end user of the data should perform appropriate testing to best simulate the application being considered, then also consider scale and anisotropy effects when selecting a design value.

REFERENCES

Alberta Department of the Environment, 1977. Great Canadian Oil Sands Tar Island tailings dyke: report of the GCOS Tar Island Tailings Dyke Design Review Panel. Alberta Environment, Edmonton, 192 pp.

Benson, C.H., 1991. Predicting excursions beyond regulatory thresholds of hydraulic conductivity from quality control measurements, First Canadian Conference on Environmental Geotechnics, Montreal, pp. 447-454.

Bierkens, M.F.P., 1996. Modeling hydraulic conductivity of a complex confining layer at various spatial scales. Water Resources Research, 32 (8): 2369-2382.

McKenna, G. 2002. Sustainable mine reclamation and landscape engineering. Ph.D. Thesis, Chapter 6. University of Alberta.

Phoon, K-K. and Kulhawy, F.H., 1999a. Characterization of geotechnical variability. Canadian Geotechnical Journal, 36 (4): 612-624.

Phoon, K-K. and Kulhawy, F.H., 1999b. Evaluation of geotechnical property variability. Canadian Geotechnical Journal, 36(4): 625-639.

Rehfeldt, K.R., Boggs, J.M. and Gelhar, L.W., 1992. Field-study of dispersion in a heterogeneous aquifer. 3: Geostatistical analysis of hydraulic conductivity. Water Resources Research, 28 (12): 3309-3324.

Sarewitz, D.R., Byerly, R. and Pielke, R.A., 2000. Prediction: science, decision making, and the future of nature. Island Press, Washington, DC, 405pp.

Schulze-Makuch, D., Carlson, D.A., Cherkauer, D.S. and Malik, P., 1999. Scale dependency of hydraulic conductivity in heterogeneous media. Ground Water, 37 (6): 904-919.

PREDICTING DEVELOPMENT OF UNDRAINED SHEAR STRENGTH IN SOFT OIL SANDS TAILINGS

Srboljub Masala[1] and Jonathan Matthews[2]
[1]Klohn Crippen Berger, Calgary, Alberta, Canada
[2]Shell Energy Canada, Calgary, Alberta, Canada

ABSTRACT

This paper presents a methodology that can be used to make projections of the rate of development of undrained shear strength in a hydraulically placed oil sands tailings deposit. The predictions are based on the assumption that tailings pond will be managed in a manner that leads to normal consolidation of the deposit, i.e. the tailings remains saturated at all times and there are no benefits attributed to desaturation, compaction, or freeze-thaw desiccation.

The method is based on the Critical State Soil Mechanics concept of the Undrained Strength Ratio (USR). Application of this method includes simulation of deposit settling behaviour using a finite strain consolidation theory. In the initial planning stages, the input parameters for the analysis may be estimated from literature or be based on laboratory tests. In later stages of research, at a pilot scale or in commercial production, the input values should be refined using field monitoring and characterization data from actual tailings deposits.

INTRODUCTION

Background

Recent legislation in Alberta (ERCB, 2009) requires oil sands operators to manage a portion of fine tailings solids such that these deposit created have minimum undrained shear strength of 5kPa within one year after deposition and an undrained shear strength of at least 10kPa five years after the end of deposition. Therefore, methods are required to predict the rate at which undrained shear strength will develop in tailings deposits so that the management techniques that support regulatory requirements may be identified and applied.

Representatives from various oil sands mine operators worked cooperatively to analyze the strength-in-time challenge and concluded a consistent methodology was required for the industry (KCB, 2010a). This paper presents the result of this work – a methodology for prediction of strength gain in a soft oil sands tailings deposit that has been placed hydraulically and remains saturated to surface for the duration of deposition. The method makes use of traditional geotechnical concepts and applies them in a structured and consistent manner. The method can be generally applied to any natural or artificial soil deposit in the normally consolidating (NC) conditions.

The paper first states the assumptions about the physical processes and material behavior in a tailings pond. A theoretical basis for tailings settling analysis and prediction of the undrained shear strength gain in an NC tailings deposit is then established in a deductive manner. Appropriate numerical tools are selected. Screening and selection of input data, as the most important aspect of the prediction process, are discussed in detail. The limits of applicability are stated, and directions for future research are identified. Finally, examples are presented for the illustration of the methodology.

METHODOLOGY

Assumptions

A. The Critical State Soil Mechanics (CSSM) is applicable to soft oil sand tailings.

The CSSM was developed considering two idealized soils: pure sand and pure clay. Most tailings are “non-standard soils” in geotechnical terms. For example, non-segregating tailings (NST) with typical sand-to-fines ratios SFR_{44}=3 to 5 are classified as silty sands, with fines content FC_{44}=20-25%. Similarly, thickened tailings (TT) often belong to sandy or silty clays in the geotechnical classifications. These “non-standard materials” are presently subject to increased scrutiny in the CSSM research. The focus is not on the applicability of the CSSM to the ‘non-standard soils’, but on the enhancement of predictive capability of the CSSM theories and generalizations of their constitutive parameters.

B. The tailings that have never been exposed to higher stresses than in the current state, i.e. have never been frozen and thawed, desaturated, eroded, or compacted by surface load or seepage, behave as normally consolidated (NC) soils.

C. Undrained strength of a saturated NC tailings deposit can be determined using a concept of the Undrained Strength Ratio (USR):

$$USR = \left\{ \frac{s_u}{p'} \right\} \left\{ \frac{s_u}{\sigma_v'} \right\}$$

where: s_u = undrained shear strength; p' = average effective stress p' = 1/3(σ_v' + 2 σ_h'), σ_v' = vertical effective stress; and σ_h' = horizontal effective stress.

The USR concept predates the CSSM and can be used independently for strength prediction as an empirical parameter. However, the USR concept finds its best explanation within the CSSM framework.

D. The USR concept is applicable to under-consolidated soils, i.e. soft tailings in the process of consolidation.

Tanaka and Sakagami (1989) reported CPT results on soft marine clays in under-consolidated and normally consolidated states. They showed that the relationship between the cone resistance and the s_u from the unconfined undrained test was the same, irrespective of the state of consolidation (incomplete or full). Towhata and Ryull (1990) performed undrained triaxial compression tests on Bangkok clay at various stages of consolidation and found nearly linear relationship between the undrained strength and the degree of consolidation. Both studies show that the magnitude of current effective stress directly controls the undrained shear strength of clay.

E. The USR may be reliably determined using the traditional geotechnical laboratory and field investigation methods:

- *laboratory strength testing methods, like the triaxial or direct or simple shear tests;*
- *field penetration methods like the field vane test (FVT), cone penetration test (CPT) or ball penetration test (BPT) for estimating shear strength;*
- *soil sampling with density profiling, and calculation of total vertical stresses via integration of a density profile;*
- *pore pressure measurements versus depth to determine pore-pressure profile.*

The emphasis is on the field methods as more representative. Increased uncertainty exists with sampling of sandy tailings, especially in the loose state, when more complex laboratory-field investigations may be needed, or existing extensive tailings databases may be consulted.

F Settling of an NC soil deposit can be simulated using the one-dimensional finite-strain consolidation theory (FSC) without time-dependent effects (e.g. creep, thixotropy, etc.).

Terzaghi's consolidation theory is not applicable. One-dimensionality is a simplification of the complexity of an actual tailings pond, but it is satisfactory for practical purposes. Major difficulties with consolidation simulations are related to selection of representative input data and their scale dependency rather than the geometry of a tailings pond.

G. Possible impacts of:

- *anisotropy (stratification);*
- *chemical bonding or cementation;*
- *time-dependent phenomena: thixotropy, creep (secondary compression), stress or strain rate; etc.*

on the consolidation process and strength properties are considered secondary effects and are neglected in the analysis.

Two important implications of the adopted assumptions are:

- the compressibility equation defines a unique relationship between the effective stress and void ratio; and
- the USR defines a unique relationship between the effective stress and undrained strength.

This means that the undrained strength is uniquely related to void ratio. Therefore, the strength gain is directly connected to the consolidation progress and resulting densification of the deposit (in the NC conditions). There is experimental evidence that electrochemical effect impact compressibility and undrained strength of very soft soils, with high void ratios and at low effective stresses (Sills, 1998; Bartholomeeusen, 2002). The working hypothesis

is that these influences fade with increasing effective stress and become of secondary importance at the stress levels of about 15-25 kPa, which are required for a 5 kPa undrained strength. An important task for future investigations will be validation of this assumption.

Procedure

The tailings strength gain prediction is envisaged as an iterative process over a mine lifetime. The results of an initial, planning stage should be understood as first predictions that will be improved as new field information becomes available.

Planning (pre-pilot) stage:

- Prepare input data for consolidation analyses;
- Simulate the consolidation process of a future tailings deposit;
- Adopt a representative USR value;
- Calculate shear strength evolution with time based on the consolidation analysis.

Pilot stage:

- Improve the consolidation parameters and the USR value based on a back-analysis of pilot test monitoring data;
- Repeat the four steps from the pre-pilot stage.

Commercial production:

- Regularly update the consolidation and strength input data based on pond monitoring and annual survey data;
- Refine the consolidation analysis and verify or update the strength gain prediction.

Input Data

Determination of input data is the most important aspect of this analysis. The input consists of the settling (consolidation) and the strength data.

Settling (Consolidation) Analysis

The input for settling analysis, which is an initial boundary value problem in mathematical terms, comprises material parameters and initial and boundary conditions. Material parameters consist of the compressibility and hydraulic conductivity equations, expressed as functions of void ratio and/or vertical effective stress. When a sedimentation stage is present, the sedimentation-consolidation threshold concentration is required as the third material parameter.

Discriminating Sedimentation and Consolidation

The main characteristic of the settling process of tailings as fluid-solid suspensions is large deformations – settlements. If the initial consistency of the suspension is solid-like, then it undergoes consolidation; if it is fluid-like, the settling process includes sedimentation as the first stage, followed by consolidation.

It is important to understand whether the tailings suspension undergoes sedimentation, which is a fluid dynamics process and does not involve effective stresses. Application of a pure consolidation model to a problem that includes an initial sedimentation stage may result in overestimating of the consolidation rate and shear strength of the deposit.

The most common mechanistic approach, which neglects time-dependent effects, adopts a single value of solids content (or an equivalent parameter like concentration or water content) as the transition between sedimentation and consolidation. A rough estimate of the transition point is relatively simple to obtain by calculating the soil's Liquidity Index (LI):

$$LI = \frac{w - PL}{LL - PL}$$

with w = water content, LL = Liquid Limit and PL = Plastic Limit. This approach may become inaccurate with highly active clays, when a suspension undergoes 'gelation', with particles developing a spatial solid network at very low concentrations. The oil sands fine tailings clays are comprised primarily of kaolinite and illite and risk of gelation is assumed to be low (but not negligible). Bitumen adsorbs on the surface of clay particles causing the clay to become less hydrophilic (Czarnecka and Gillott, 1980). This affects the soil Atterberg limits and its geotechnical 'activity' which further impacts the soil (tailings) strength (Ali Rahman et al, 2010). The quantification of these effects for Shell fine tailings has not been undertaken in a systematic manner. The author's practice is to perform the testing of Atterberg limits on bituminous samples and to use process (pond) water. Investigations are underway to clarify and quantify the influence of bitumen.

A rule of thumb for the sedimentation-consolidation threshold estimate is illustrated in Figure 1 for samples from Shell Albian Sands operations. The solid-liquid transition may be assumed as the geotechnical water content corresponding to minimum LI = 1.5. This is taken as the point where soil strength become measurable and serves as the point of demarcation between sedimentation and consolidation. For Shell paste thickener underflow (PTU) tailings produced using the overflow from hydrocycloning of whole tailings the transition occurs at solids content of 70-75% by weight. For mature fine tailings (MFT) it occurs at about 60wt% solids.

A number of programs exists for the simulation of 1D finite strain consolidation, however software that solves a simultaneous sedimentation-consolidation problem is scarce (Bartholomeeusen et al, 2000; Masala, 2010).

Material Parameters

Laboratory Tests

During early design and evaluation, tailings deposit material properties may be determined from published literature, pre-project studies or, preferably, from laboratory tests on representative tailings material. A frequently used laboratory test in oil sands research is the large-strain consolidation (LSC) test – essentially, an oedometer test conducted in an expanded size chamber; for a comprehensive review see Bo (2008). The LSC tests provide the compressibility functions through incremental loading, usually up to several hundred kilopascals. At selected increments, the values of hydraulic permeability are obtained by percolation (constant head or flow) tests with selected hydraulic gradients.

The compressibility equation from a LSC test is expressed in terms of void ratio versus vertical effective stress. Sills (1998) shows that, while the soil is extremely soft, the equation should include a creep-like factor, to be able to fully explain experimental evidence. The creep compression effect appears to reduce at higher effective stress levels. An international Class A prediction seminar, named Sidere, (Bartholomeeusen et al, 2000) provided evidence that the time-dependent phenomena are of importance at low effective stresses up to several kPa. This is far below the stress levels of 15-25 kPa that correlate with a shear strength of 5 kPa, so that neglecting time-dependent influences appears justified in our analysis.

The LSC test is actually performed on a small sample of about one litre in volume. The test is sensitive to details, which often result in irregularities and scatter in obtained test data. As the commercial operations are subject to a wide variation in tailings composition (especially variability in particle-size, mineralogy, and bitumen content), it is prudent to test a series of samples with changing physical properties to get information on sensitivity of the consolidation properties to variations in tailings density, gradation, etc. The input obtained from laboratory tests should always be expressed as ranges of values for the parameters, and the simulations should be able to bound the consolidation behavior within the 'best and worst case' limits (see Figures 4-5).

Back-Analyses of Field Tests

It is the experience of the authors that the compressibility from laboratory tests is usually reasonably consistent with the commercial-scale deposit behavior, while the hydraulic conductivities from laboratory tests often underestimate the field values. It is, therefore, advisable to improve the predictive capabilities of a tailings settling model by back-analyzing the monitoring data of deposition tests at an intermediate, or pilot, scale. The pilot test cells should be adequately instrumented. Instrumentation redundancy is highly recommended, based on the authors' experience.

For a given void ratio, hydraulic conductivities that are back-calculated from pilot tests may be an order of magnitude higher than those determined from the LSC tests, as shown in Figure 5 for Shell TT material. This may be explained by development of macro drainage features at the pilot scale. Features such as sand boils may serve as means for accelerating the dissipation of excess pore-pressures more rapidly in the field, especially when the deposits are in the early stages of consolidation.

Pilot scale deposition tests are usually limited to a fraction of the effective stresses achieved in the laboratory testing, as the depth of a pilot test vessel is much smaller than the depth of a commercial tailings pond. Therefore, the up-scaling of compressibility is not straightforward.

Moving from pilot tests to commercial operations may introduce another set of scale-dependent effects that can impact the representative material properties. Biogenic processes in tailings ponds may create a drainage structure that enhances consolidation; for example, the upward coalescence and migration of methane bubbles may leave drainage channels in fluid to very soft tailings that increase the effective vertical hydraulic conductivity (Guo et al, 2004).

The representative hydraulic conductivity may also become much lower than at a smaller scale in the case of segregation of tailings upon discharge. It will create distinctive heterogeneity in the deposit, with segregated tailings finer and more fluid than planned. This will result in retarded consolidation and slower undrained shear strength gain than expected.

Selection of appropriate compressibility and hydraulic conductivity functions for predicting commercial-scale performance from test data is not straightforward and requires diligent observation and monitoring, with specific experience and judgment in data interpretation. Determination of representative material properties should be understood as an iterative process, with continual improvement of predictive capacity as more commercial-scale experience is collected. When the commercial operations begin, the material parameters for consolidation analyses should be regularly updated using field monitoring and characterization data from the actual tailings deposit as part of on-going tailings management best practices.

Initial and Boundary Conditions

The initial conditions in the case of an existing deposit consist of the solids content profile. If the deposit is initially under-consolidated, the pore pressure profile is also needed. If the pond is empty, the filing schedule and tailings density variation during filling are also required as input.

The boundary conditions in consolidation analyses should specify stress and hydraulic values at the boundaries – the top and bottom of the pond.

Undrained Strength Ratio (USR)

Laboratory Determination

Undrained strength s_u is not a fundamental soil property. Instead, it is a measured soil response during undrained loading which assumes zero volume change. As such, s_u is affected by: deposition history, type of testing, boundary conditions, rate of loading, initial stress state, confining stress level, etc. As s_u is stress level dependent, normalization by vertical or mean effective stress has proven very useful in geotechnical analyses, with the ratio of s_u and effective stress named the Undrained Strength Ratio USR (Ladd et al, 1977).

Values of s_u determined by laboratory testing vary according to the type of test employed; therefore, USR values will be different for different tests. The highest s_u and USR values are obtained in triaxial compression tests, the lowest in triaxial extension, while direct and simple shear tests produce values between the triaxial test limits. The shear tests are reported to provide good agreement with case histories. A number of predictive USR equations have been developed from laboratory tests over the past 50 years (Mayne, 2001), and their values for Shell TT tailings cover the range from 0.17 to 0.33. These formulae can be used for preliminary analyses.

It is also possible to conduct laboratory testing on actual tailings and determine a site specific USR. However, all laboratory results depend on sampling quality. Soft oil sands tailings are difficult to sample with minimal disturbance and the sampling methods that have been shown to minimize sample disturbance, e.g. ground freezing, are used sparingly due to substantial sampling costs. Field tests are recommended to compensate for the difficulties with laboratory testing: field vane shear (FVT), cone penetration testing with pore pressure measurement (CPTu), and 'full-flow' penetrometers such as T-bar or ball penetration (BPT).

The authors wish to present a simple and inexpensive laboratory method to provide a rough estimate of the solids content required for certain low undrained strength, based on the relationship between s_u and LI. Figure 1 shows this relationship for the Shell fine tailings: paste thickener underflow (PTU) with two initial solids contents, and mature fine tailings (MFT). The plot was obtained as a by-product of fine tailings laboratory drying test. The strength is related to suction and not to compaction due to consolidation, but the data in the range of LI>0.5 can be useful for this purpose. A rough estimate of the solids contents needed for the undrained strength of 5 kPa is shown in Table 1. Some of the samples were soaked after drying and

re-tested, but are nevertheless well aligned with the others, indicating strength reversal (decrease) after re-wetting.

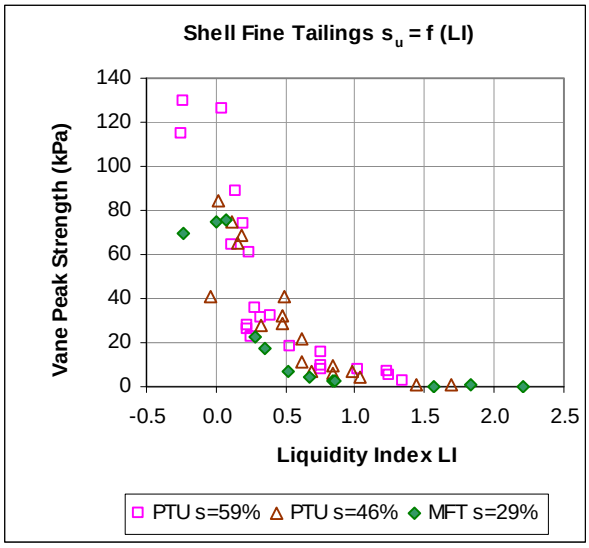

Figure 1. Shell Fine Tailings s_u = f (LI)

Field Tests

The vane is the commonly used field strength test. It is the only field method that measures strength directly, and both peak and remoulded (residual) values can be obtained. The penetration method strengths are indirect, based on correlations. Disadvantages of the VFT include:

- strength is obtained at discrete, well spaced points – no continuous profile;
- time constraints related to test duration;
- it is influenced by anisotropy and stratification (thin layers of stiffer material);
- it is rate sensitive;
- correction factors are needed to determine a representative strength for geotechnical analyses.

Table 1. Solids Contents for s_u=5 kPa

Tailings	LL / PL as geotechnical water content	LL / PL as solids content	Solids content for s_u = 5 kPa from Fig. 1
	(%)	(%)	(%)
PTU	30 / 14	77 / 88	74-78
MFT	50 / 21	67 / 83	73

It is the authors' opinion that the effects of anisotropy, stratification and rate-sensitivity are less important in oil sands soft tailings deposits. It is important, though, that the applied testing rates ensure undrained behavior of the material.

CPT is continuous and provides stratigraphy; however, it is not accurate in soft deposits due to low tip resistance with the standard 10 cm^2 area cone. When estimating undrained strength, a correction for overburden pressure is required. Estimation of an equivalent elastic stiffness G may be required as well.

T-bar and ball penetrometers do not require overburden corrections for conversion of tip resistance to undrained strength. The conversion factor is related to the soil stiffness and strength, surface roughness of the probe and the in situ stress state. The main potential for the BPT is testing of shallow very soft tailings where the measured cone resistance will be very small. However, the sedimentation stage of tailings slurries must be discriminated in the s_u calculation from penetration tests, when the buoyancy of heavy liquid is measured instead of the resistance of soft soil.

Figures 2 and 3 present the results of investigation of the correlation of VFT with CPT and BPT tests at Shell's pilot plant - the Tailings Testing Facility (TTF) at the Muskeg River Mine (MRM) site, see KCB (2010b). The tip-resistance-to-strength conversion factors N_{kt} and N_b were calculated from parallel VFT, CPT and BPT test in NST/CT and TT deposits. The Shell NST/CT specific values for N_{kt} and N_b are close to the widely used averages N_{kt} = 15 and N_b = 10.5, respectively. However, the TT conversion factors deviate from the average values. Even for NST, the scatter of data points suggests caution when estimating strengths from the penetration tests. Additional investigations are underway at the TTF site.

In authors' opinion, the field vane and ball penetration provide better accuracy relative to the standard cone penetrometer in measuring the in situ undrained strength of soft soils. The field vane is traditionally used as the reference method for field strength testing. Our research shows that the CPT and BPT correlations with vane may exhibit high uncertainties for oil sands tailings, especially for fine tailings (pastes and thickened tailings).

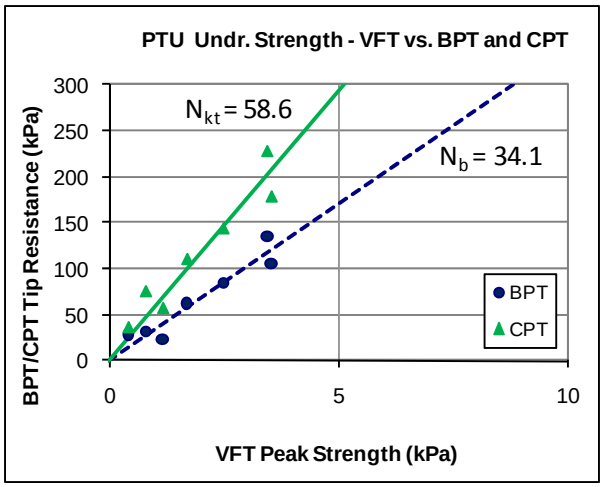

Figure 2. VFT-CPT s_u Correlation for Shell PTU

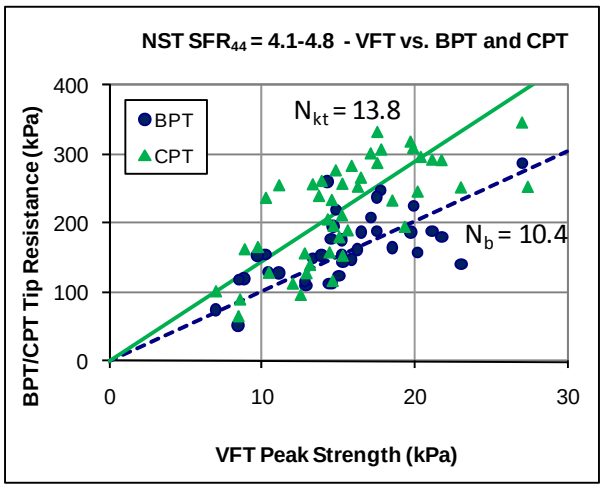

Figure 3. VFT-BPT s_u Correlation for Shell NST

EXAMPLE

The tailings considered in this example is Shell's Treated Thickened Tailings (TTT) with an average SFR_{44}=0.75. The filling schedule for the example is presented in Table 2. After ten years of TT deposition at a uniform rate and three years of self-weight consolidation, the pond is capped with coarse sandy tailings (CST). Different filling schedules were used in the actual tailings planning; the filling schedule was simplified for this example.

In consolidation analyses, the pond bottom was assumed impermeable and the phreatic surface was always at the top of the deposit, including the CST cap.

Table 2. Filling Schedule for Shell TTT Case

Year	Elapsed Time	Solids Content	Slurry Volume (without consolidation)	Tailings Type
	years	%	m^3/m^2/year	
2010 - 2020	10	45	3.6	TT
2023 - 2024	1	55	9.6	CST

Consolidation properties for a preliminary analysis were obtained from the LSC tests (Figures 4 and 5). The results of the preliminary analysis are not presented here.

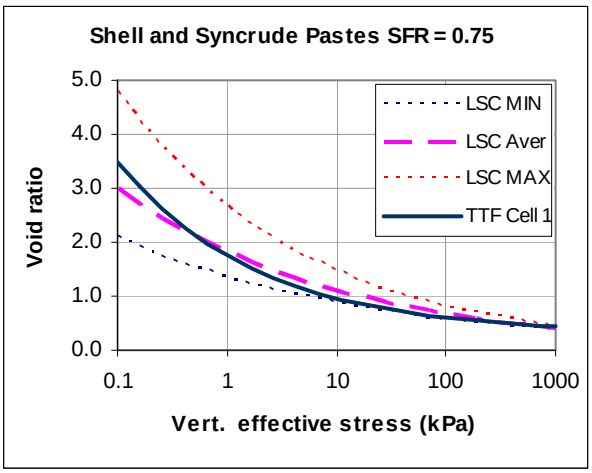

Figure 4. Compressibility, JPM TT

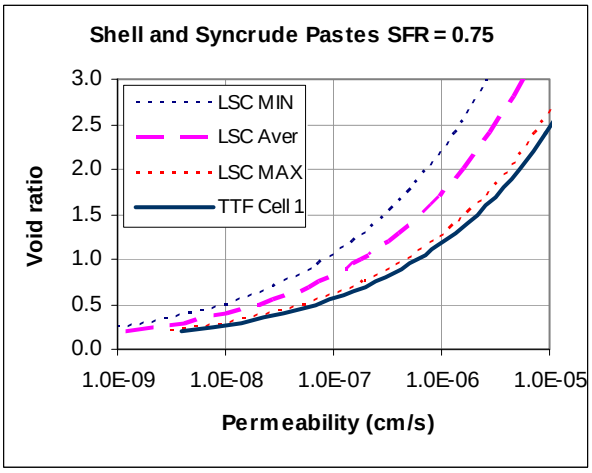

Figure 5. Hydraulic Conductivity, JPM TT

After the pilot stage of investigations at Shell's TTF at the MRM site, the consolidation properties were updated using back-analysis of monitoring data

from the pilot test in Cell 1. TTF Cell 1 was a 5 m deep pit, with the base area of 50x20 m^2. Two instrumented poles were placed along the longer axis, at the thirds of the length from the cell ends. The monitoring included: graduated stadia for tailings heights (two posts and 5 locations on the cell sides); standpipe piezometers for phreatic surface levels (two locations); total stress measurement at the cell bottom (one location); and pore pressure measurement every metre of depth on average (two locations, 8 instruments). In the back-analysis, it was essential to closely simulate not only the settlements (Figure 6), but also the pore pressure distribution variation over time, since dissipation of excess pore pressures determines effective stresses, which govern development of undrained strength. Figure 7 shows measured and simulated time responses of two piezometers; the piezometer data in the middle of the deposit are a little better best-fitted than the piezometer data near the bottom of the cell.

An order of magnitude higher hydraulic conductivity was obtained from the field data, see Figure 5.

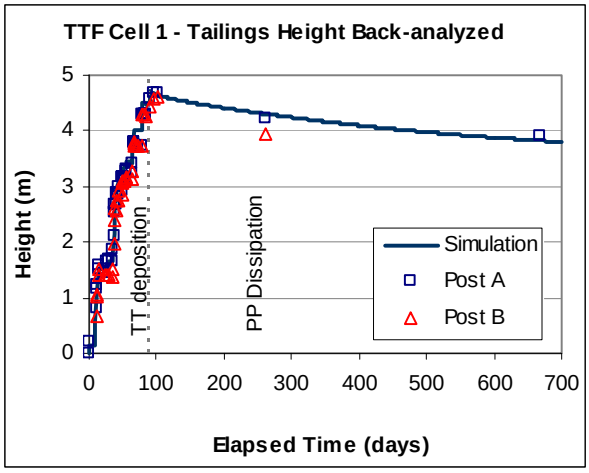

Figure 6. TT Pilot Test Back-Analysis, Settlements

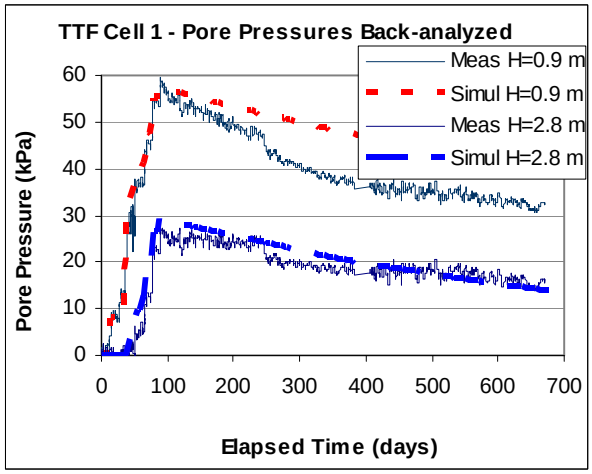

Figure 7. TT Pilot Test Back-Analysis, Pore Pressures

The analysis results are presented in Figures 8-12: the settlements over time and the profiles of excess pore pressure, effective stress and undrained strength. Figure 13 shows the variation of the s_u = 5 kPa level in the tailings deposit with time. A 'residual' layer with s_u < 5kPa always exists at the top of a saturated NC soil.

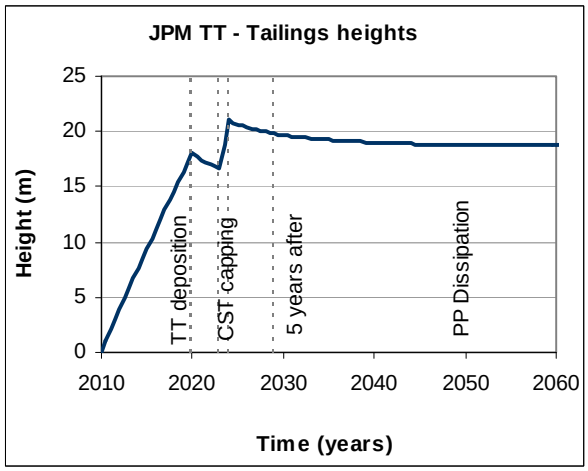

Figure 8. JPM TT Example - Settlements

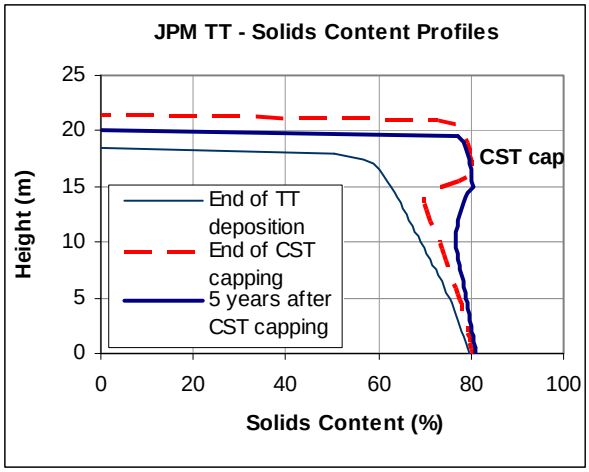

Figure 9. JPM TT Example - Solids Content Profiles

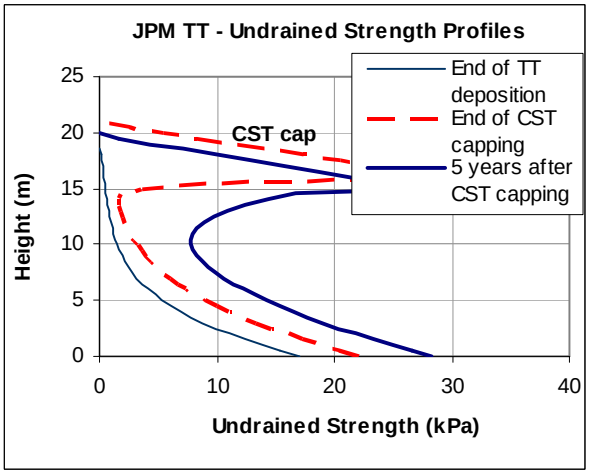

Figure 12. JPM TT Example - Undrained Strength Profiles

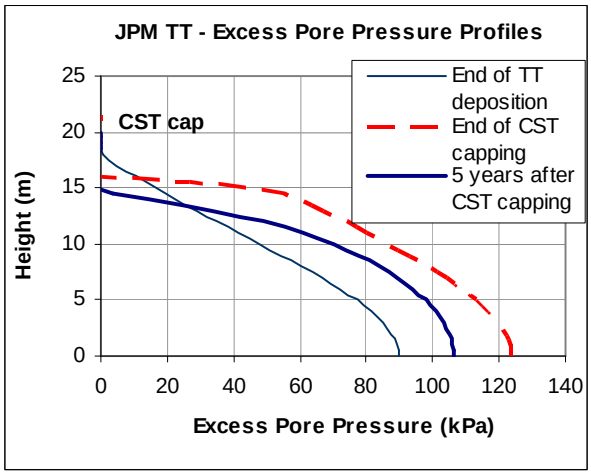

Figure 10. JPM TT Example - Excess Pore Pressure Profiles

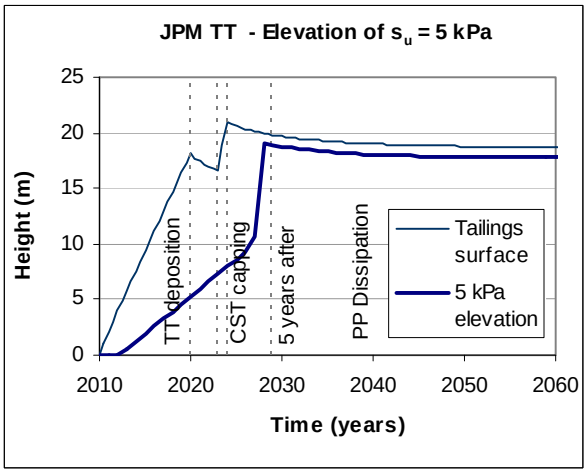

Figure 13. JPM TT - Elevation of s_u = 5 kPa

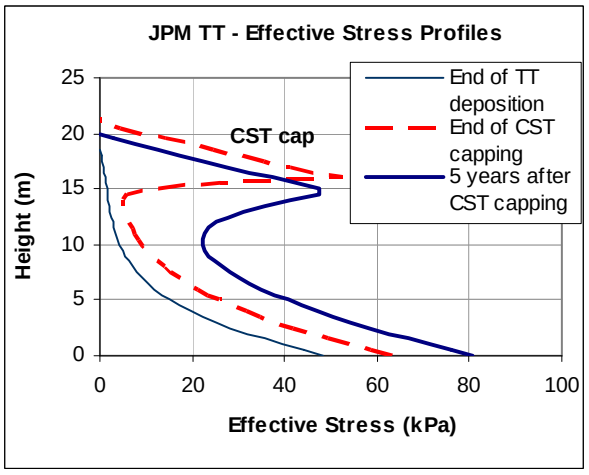

Figure 11. JPM TT - Effective Stress Profiles

The TT deposit in the example satisfies the 10 kPa strength requirement before reclamation (Directive 074), but cannot satisfy the 5 kPa strength criterion with the adopted filling rate.

The USR=0.35 was based on the results of vane and ball penetration tests in pilot test cell. Reference formulae, based on laboratory tests, produced lower USR values than 0.35 obtained by the field methods. There is no a satisfactory answer, but possible causes are considered in:

- TT composition and a relatively high percentage of bitumen;

- Air bubbles observed in deposit samples, that may result in partially drained behavior and

may render common CPT/BPT interpretations inadequate in this case;
- Low vertical effective stresses in the pilot test cell of max 50 kPa (strength envelopes are curved at low stresses);

CONCLUSIONS

The paper demonstrated the value of using the CSSM framework coupled with the large-strain consolidation and, optionally, sedimentation theories in the interpretation of shear strength development in soft oil sands tailings.

A method for prediction of undrained strength development in soft oil sands tailings was presented. The method is generally applicable to any normally consolidating soil.
The basic premise is that current effective stresses control undrained shear strength in the NC deposits. With time-dependent effects neglected, this leads to a unique relationship between strength and void ratio. This approach may be challenged when effective stresses are very low (several kilopascals).

Determination of input data is the critical aspect of presented methodology. The process of predicting deposit strength will benefit from iteration, with continual improvement of the prediction as new information becomes available. The emphasis is on selection of input data based on back-analyses of field tests and large-scale monitoring data.

REFERENCES

Ali Rahman, Z. et al. 2010. Influence of Oil Contamination on Geotechnical Properties of Basaltic Residual Soil. American Journal of Applied Sciences **7**(7): 954-961,

Bartholomeeusen, G. et al. Sidere: numerical prediction of large-strain consolidation. Geotechnique, 2002, **52**(9), 639-648.

Bo, M. W. 2008. Compressibility of Ultra-Soft Soils. World Scientific Publishing Co. Ltd., Singapore.

Czarnecka, e. and J. E. Gillott. 1980. Formation and Characterization of Clay Complexes with Bitumen from Athabasca Oil Sand. Clay and Clay minerals, **28**(3), 197-203.

Energy Resources Conservation Board (ERCB). 2009. Directive 074, Tailings Performance Criteria and Requirements for Oil Sands Mining Schemes, Calgary, February 2009.

Guo, C. et al. 2004. Densification of Oil Sands Tailings by Biological Activity. 57th Can. Geotech. Conf., Quebec. 30-37.

KCB. 2010a. Shell TT and CT Undrained Strength Predictive Framework. Presentation prepared for Shell Canada, March 05, 2010.

KCB. 2010b. Correlation of s_u Determined Using CPT, BPT and VFT Test in NST and TT Deposits in Shell's TTF at Muskeg River Mine. Memo prepared for Shell Canada, April 2010.
Ladd, C.C. et al. 1977. Stress-Deformation and Strength Characteristics. 9th Int. Conf. on Soil Mech. and Found. Eng., Tokyo, Vol. 2, 421-494.

Masala, S. 2010. Coupled sedimentation and consolidation modelling of fine tailings. Geo2010, 63rd Can. Geotech. Conf., Calgary, AB, Sept. 12-16, 2010.

Mayne, P.W. 2001. Stress-strain-strength-flow parameters from enhanced in-situ tests. Int. Conf. on In-Situ Measurement of Soil Properties & Case Histories, Bali, Indonesia, May 21-24, pp. 27-48.

Sills, G.C. 1998. Development of structure in sedimenting soils. Phil. Trans. Roy. Soc. Lond. A 356, 2515–2534.

Tanaka, Y. and T. Sakagami, 1989. Piezocone testing in underconsoliated clay. Canadian Geotechnical Journal, 26, 563-567.

Towhata, I. and K.S. Ryull. Undrained Strength of Underconsolidated Clays and Its Application to Stability Analysis of Submarine Slopes Under Rapid Sedimentation, Soils and Foundations, **30**(1), 100-114.

Session 2

Tailings Dewatering

TAILINGS DEWATERING IN THE OIL SANDS

Sue Longo[1], Ryan Francoeur[1], Mark Labelle[1], and Irwin Wislesky[2]
[1]Golder Paste Technology Ltd., Sudbury, Ontario, Canada
[2]Golder Associates Ltd., Mississauga, Ontario, Canada

ABSTRACT

With the advent of Directive 074, there has been increased pressure on oil sands operators to find practical, field proven solutions to deal with tailings management. While significant research and development has gone into understanding the characteristics of oil sands tailings materials and their subsequent behaviours in the field, there are still uncertainties. All operations will need to dewater their oil sands tailings in some manner to produce a material that will gain strength over time. There is great interest among oil sands companies to investigate and potentially apply different dewatering techniques for surface disposal of their waste materials. In addition to exploring the advantages and disadvantages of various dewatering methods that can be considered for oil sands tailings, this paper also presents the considerations, practical aspects, benefits and drawbacks of oil sands dewatering based on our experience over many years which includes the results from multiple test programs that we have carried out.

THE SETTING

The tailings "problem" in the oil sands industry in Alberta is the world's worst kept secret. Since the beginning of oil sands mining in the 1960s huge volumes of tailings have been produced and are continuing to be produced. These tailings and associated effluent (fluid fine tailings) must be contained and cannot be released directly to the environment. The tailings are composed of very fine particles that are piped out, generally as a slurry, to containment areas. As a result, vast surface areas are currently occupied with tailings and effluent. The tailings in these ponds settle and consolidate very slowly.

The accumulated volume and aerial expanse of these fluid fine tailings and the potential associated environmental concerns have received more and more public attention to the point where governments, public groups and aboriginal communities have voiced their concerns.

While millions of dollars have been spent in research and development and multiple tailings management techniques and field trials have been attempted to solve the "problem", as of 2010 there is still no practical field proven solution. With more applications to mine pending and no permanent solution available to oil sands operators, pressure from government and the public forced the Energy Resources Conservation Board of Alberta (ERCB) to institute some rules regarding tailings management.

WHY DEWATER?

Directive 074

The ERCB tailings Directive (074) Tailings Performance Criteria and Requirements for Oil Sands Mining Schemes was issued in February 2009 and includes phasing in the requirements over a three year period.

The main thrust of the Directive is to reduce the huge volume of accumulated fluid fine tailings and their associated water management and environmental issues. The Directive focuses on management and accountability of tailings and associated process water/effluent. Dedicated Disposal Areas (DDAs) are required to capture 50% by weight of the fines (defined as <44 µm) in the oil sands processed (or an equivalent amount from accumulated Mature Fine Tailings-MFT). The 50% fines capture requirement is in addition to the fines captured currently in hydraulically placed dykes and beaches.

DDAs must be formed in a manner that ensures trafficable deposits. The performance criteria are based on the strength of the deposit. In order to allow for auditing, the ERCB set the following criteria to be achieved annually:

- Minimum undrained shear strength of 5 kilopascals (kPa) for the material deposited in the previous year;
- Removal or remediation of material deposited in the previous year that does not meet the 5 kPa requirement;

- Deposit ready for reclamation within five years after active deposition has ceased. The deposit will have the strength, stability, and structure necessary to establish a trafficable surface. The surface must have minimum undrained shear strength of 10 kPa; and
- Reports are to be prepared annually detailing the tailings management process and the deposition results with respect to the Directive and agreed upon schedule and methodology.

In effect, the Directive indicates that both existing and newly formed tailings will need to be formed into dry land deposits. For this to occur, an effective means of separating the effluent/liquid from the tailings solids must be employed. Some form of dewatering will be required.

Sustainability

In this day and age, the overall goal with any mining project is to be a sustainable development with the intent for reclamation and closure in as progressive a manner as possible. As a part of Directive 074 it should be noted that the current regulation reduces the rate of MFT growth and at some point in the future it is anticipated that zero growth MFT and reduction in accumulated MFT will be required. This is a fundamental shift in the current operation of oil sands mines and mills and will require a fundamental shift in operating philosophy. Unlike normal mining operations which are very linear in thought and operation, the idea of tailings or waste management needs to begin at the end. What is meant by this is that once the end result is established i.e. what the deposit should look like upon closure, one can then work backwards to produce a material to meet those requirements and characteristics. Only by engineering your waste, so to speak, will the end results be achievable.

There are multiple factors to take into account when facing these kinds of long term issues which include:

- Material characteristics and behaviour;
- Storage capacity;
- Stability of stack (geotechnically and geochemically);
- Water management (collection, treatment, reuse and release);
- Seepage/leachate;
- Life of mine;
- Closure and reclamation systems; and
- Capital and operating costs.

As mentioned above, the driver has to be the deposition strategy and the process technology to achieve this will follow. There is no one size fits all and in order to reduce or eliminate the production of MFT, tailings management and, in particular, deposition planning needs to become a major area of focus for oil sands operators.

DEWATERING TECHNOLOGIES

General Dewatering Technologies and Associated Deposition Strategies

Although an operator can accomplish the Directive requirements with one technology, the ERCB has recommended the use of a suite of technologies to mitigate implementation risk factors and increase operational flexibility. The choice of process technology, of course, must be done in conjunction with the depositional strategy; otherwise, the risk is that the process will not be able to achieve the requirements of the deposition plan. The advantages of one methodology over another is dependent on many factors, including production rate, process type, location, distance from mill to disposal area, water management needs, operational constraints, cost, etc.

The following are the dewatering strategies that will be explored:

- Thickening (conventional and paste);
- In-line flocculation;
- Centrifuge;
- Co-mingling; and
- Other strategies such as electro-osmosis may be explored further in the future.

<u>Thickening</u>
Thickening generally involves a large thickener tank with a slow turning rake system into which the tailings slurry is placed after the extraction process, along with a flocculant. The turning process, shape of the tank and rake system, retention time and flocculant along with the basic

material properties controls the potential thickness of the product. The thickened material is extracted from the bottom of the tank and clarified water/effluent is decanted from the top of the tank.

The thickened material is pumped to a containment facility (or pit or back underground) and the decanted effluent can be reused directly in the extraction process or placed in a temporary separate facility for later reuse or treatment and release. Paste can be obtained from this process depending on the grain size of the material and may also require some modifications to the tank and the other control measures indicated above.

In-line Flocculation
This dewatering measure involves placement of a flocculant in the pipeline at a sufficient distance from the discharge point to allow the required mixing/contact to take place in the pipe. The tailings settle out and separate from the effluent upon discharge and deposit forming a beach with the effluent flowing away into a collection pond.

Centrifuge
A centrifuge is a device that spins, providing a gravitational force that causes the tailings to form against a porous side wall. The effluent passes through the wall and the solid tailings remains. These tailings are then collected and sent out to a tailings containment facility.

Co-Mingling
Co-mingling involves mixing coarser materials with fine materials to produce a product that is more amenable to dewatering and strength gain. In some processes the tailings go through a cyclone process to separate the finer fraction from the sands. These materials can be recombined in specific portions to form a uniform, non-segregating tailings (NST) with better dewatering characteristics. Additives that have been considered include waste rock, sand, fly ash, gypsum, CO_2, etc.

The deposition strategies to be considered are:

- Thick lift;
- Thin lift;
- Cell structure;
- Single end point discharge; and
- Multiple spigot discharge.

The use of supplementary measures to promote dewatering and consolidation has also been considered and these include toe drains, ditches, deposition slope, underdrains and the effect of freeze-thaw cycles. In all cases it is important to ensure that water readily drains away from the deposit and is not allowed to form a pond on or adjacent to the deposit.

Advantages/Disadvantages

Thick Lift
This would likely be the preferred deposition methodology if appropriate dewatering, consolidation and strength gain could occur. Unfortunately, the low permeability nature of the tailings means dewatering will be slow. It will be necessary to optimize the thickness of the material to ensure sufficient strength gain is occurring throughout. One means to allow for increased layer thickness would be to provide a number of lateral drains, but this would increase the cost and pose some operational difficulties. Co-mingling could also be considered to facilitate this method.

Thin Lift
Thin lift deposition of thickened tailings can generally be considered to be less than 0.5m per lift. A thin lift is placed and given time to consolidate prior to application of a subsequent lift. The thinner the lift, the faster it will drain. The effective drainage is influenced by the permeability of the layer and the underlying layer, as well as the moisture content of the underlying layer. Evaporation can also play a major role. This deposition method requires large areas and the ability to move from one area to another to allow sufficient drying time for each layer.

Cell Structure
Cells can be constructed in advance of deposition with a strong and permeable material (sand sizes to rockfill). These cells could then be filled in and allowed to dewater and consolidate while other cells are filled in. The cells could be filled in with thin lifts or thick lifts depending on the overall behaviour of the tailings. After sufficient strength gain is achieved, new cells can be constructed over top of the previously deposited cells.

Discharge Methods
Tailings are generally pumped through a pipeline to the tailings disposal area. Depending on the corresponding deposition strategy, either single point discharge or multiple spigot discharge options exist. The advantage with single point

discharge is that you can direct the flow in a straightforward way with minimal operational input. With multi point discharge you can direct the flow in a more systematic way to build the deposit without the hassle of repeated pipeline moves and more easily facilitate the uniformity of thin lift layers. In the case of cell structures, multi spigot discharge makes switching between cells more practical.

TEST RESULTS

Since 2006, there has been significant work done on a variety of tailings materials from the Alberta oil sands. The following sections will highlight the major findings and some of the performance indicators to date.

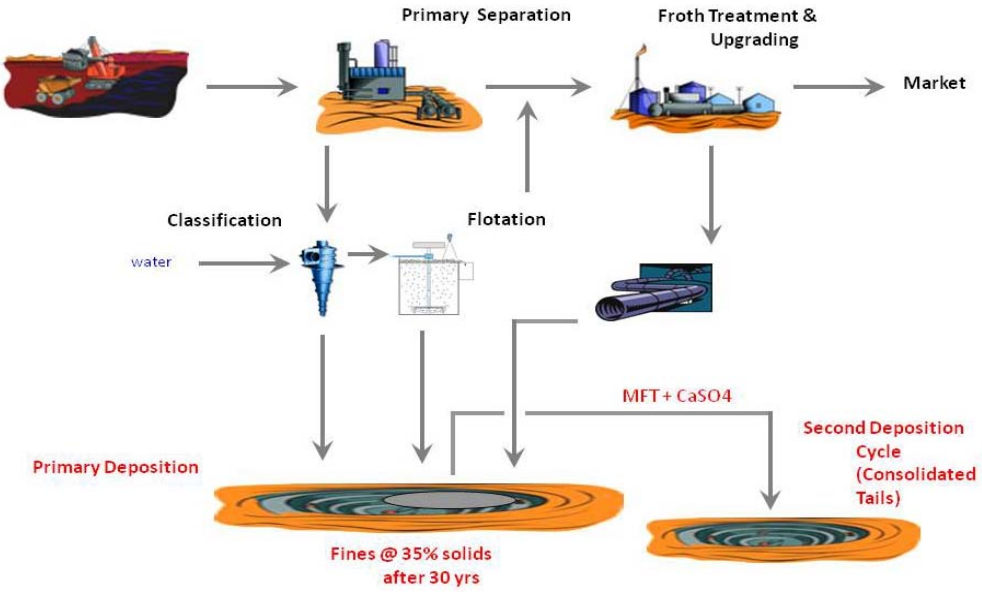

Figure 1. Typical Process

Lab Data

In the typical flowsheet shown (Figure 1) there are multiple tailings streams coming out of an oil sands production circuit. Each site or operation will have different quantities and mixes of these streams:

- Cyclone underflow and overflow;
- Flotation tailings;
- Recovery unit (RU) tailings; and
- MFT.

Laboratory testing results to date on the three different tailings streams include:

- Index tests;
- Primary stream thickening (settling columns and bench scale thickening units, mini-pilot plant testing)(underflow); and
- Secondary stream thickening or clarification (overflow).

For each of the three different tailings streams the following test parameters are presented:

- Feed wt% solids;
- Underflow density achieved;
- Maximum underflow density possible; and
- Overflow quality.

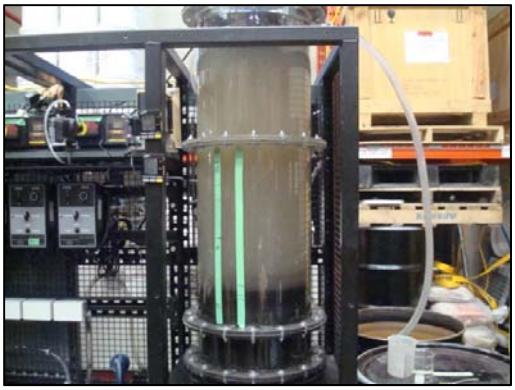

Photo 1. Mini Portable Thickener Plant

Table 1. Summary of Test Results from RU Samples

Sample	Characterization Tests	Feed wt% Solids	Flocculant Dosage	Underflow Density (24 hr mark)	Max Underflow Density	Overflow Quality
RU Sample #1	58% passing 20 µ; 1.57 S.G.	5% (diluted from ~20%)	300 g/tonne	58%	-	0.3-0.5%
RU Sample #2 (single floc)	35% passing 20 µ;1.87 S.G	5% (diluted from 10-15%)	75 g/tonne	46%	51.7	0.4%

Table 2. Summary of Test Results from Flotation Tailings Samples

Sample	Characterization Tests	Feed wt% Solids	Flocculant Dosage	Underflow Density (24 hr mark)	Max Underflow Density	Overflow Quality
Flotation Tailings Sample #1	15% passing 20 µ; 2.68 S.G	10% (diluted from 15%)	100 g/tonne	52%	-	0.03%

Table 3. Summary of Test Results from MFT Samples

Sample	Characterization Tests	Feed wt% Solids	Flocculant Dosage	Underflow Density (24 hr mark)	Max Underflow Density	Overflow Quality
MFT Sample #1	66% passing 20 µ; 2.28 S.G.	3% diluted from 30%	300-500 g/tonne	46-50%	-	0.06-0.08%
MFT Sample #2 (two stage floc addition)	87% passing 20 µ; 2.33 S.G.	3% diluted from 31%	250 g/tonne each (2 stage floc)	45%	44.9	0.4-0.6%

The important things to note out of the above results are as follows:

- The difference in RU samples underflow density is due to the asphaltines content;
- Generally speaking, the coarser the PSD the better the thickening results will be (blended streams are currently being looked at and have provided some promising results);

- Only at lower temperatures do the asphaltines cause the effect of reduced underflow and at elevated temperatures they are part of the slimes from the overflow and have little effect on the underflow;
- Feed density optimization is critical and the range of MFT feed densities is much lower (3-5%) than RU feeds (8-10%) or Flotation tailings feed (10-12%); and
- MFT using single flocculant dosage did not give good results – there was no apparent water release. Two stage MFT flocculation showed promising results.

Photo 2. Thickened Tailings

Dewatering Performance

The performance in each of the testing formats (1L, 4L, Bench Scale Paste Thickener and Mini-pilot Plant) for each of the materials tested showed consistent and increasing performance in terms of underflow density.

Table 4. Summary of Dewatering Performance through all FormatsSingle Flocculation

Type of Testing	RU Tailings	Flotation Tailings	MFT
1L	37	-	28
4L	39	52	31
Bench-scale Thickener	40-46	-	-
Mini-plant	42-47	-	46
Centrifuge	47.9	63	56

Table 5. Summary of Dewatering Performance through all FormatsTwo Stage Flocculation

Type of Testing	RU Tailings	MFT
1L	39	11
4L	45-46	18
Bench Scale Thickener	46.8	45.1
Mini-plant	-	-
Centrifuge	54.2	-

The increase in underflow density results or “scale up” between the various settling test procedures tends to depend very heavily on the material type (MFT has much greater increase then the RU tailings) and is indicative of the move from static bench scale testing to dynamic test methods. It is consistent with what would be expected from each stage, although it is substantially different from what would be seen in a similar comparison of base or precious metal tailings.

Major Effects

In the course of the testwork the five following major effects were noted:

- Temperature (room 17°C versus elevated process 90°C);
- Overflow recycling;
- Underflow recycling;
- Asphaltines; and
- Fine material content.

In the case of temperature, the highest underflow solids were highly dependent on feed % solids (at room or elevated temperatures). Also flocculant dosage and type were found to be highly dependent on temperature. There were many flocculants that worked well at room temperature but produced minimal underflow density at elevated temperatures. The switchover point between working and not working flocculants seemed to be at the 40°C mark.

In the case of overflow recycling, with all materials there was a significant reduction in underflow solids density (between 17 to 50%) with the RU sample, and solids content in overflow increased substantially even after the first recycle of overflow

and continued to increase over time/number of recycles. Interestingly, the settling velocity increased the more times the overflow was recycled. By treating or partially treating the overflow and then recycling, this effect was minimized, if not eliminated.

In a similar manner, recycling the underflow, which is a common practice in the metals industry, also appears to reduce the overall underflow solids density while increasing the settling velocity. More investigation into this aspect is required to know by how much it reduces the underflow solids density and if there is a practical limit of recycles before it manifests.

There is a need to investigate the underflow recycling issue in dynamic mode as opposed to static bench scale tests.

Asphaltines created issues in performing many of the standard characterization tests and during the mini-plant trials it was shown that as the flocculant dosage increased, more asphaltines were trapped in the bed, creating layers of "sponginess" that tended to decrease the underflow density. On the other hand when the flocculation dosage rate was decreased the underflow solids increased and the overflow solids increased as a result of the asphaltines "foaming" off of the top of the dewatering unit.

Photo 3. Asphaltines Foaming on Surface

Generally speaking, the amount of fines present in all samples as well as the presence of the asphaltine materials tends to blind any kind of filtering process leaving very little option in this regard for dewatering.

Overall, it was not unexpected that higher asphaltines content provided lower underflow density; however, the degree that flocculant dosage and temperature had an effect with the presence of the asphaltines was surprising.

Also a not unexpected result was the confirmation that any recirculation load of fines or flocculant is problematic for final underflow density.

Geotechnical Performance

In general there are four main mechanisms to promote consolidation and desiccation in a stack:

- Weight;
- Evaporation;
- Drainage; and
- Freeze/thaw.

Methods to enhance these can include acidification (CO_2 addition), reworking (ploughing), other additives, covers, etc.

Producing a non-segregating material is also considered to be a key to performance and site management. If segregation occurs, then one is effectively required to deal with different materials in a single disposal area which adds a level of complication. Fines removal in advance of deposition could be considered within the tolerances of Directive 74 as a means of improving the geotechnical and drainage characteristics of the deposit.

In testing done to date, with respect to the various dewatering and geotechnical techniques discussed earlier, some significant early findings are below:

- Some physical properties of oil sands tailings are not easy to determine;
- Some In-line flocculation tends to inhibit evaporation potential of the deposited tailings;
- Flocculants can be temperature dependent;
- The thickening process is dependent on the tailings production process (rate, water content, temperature, chemistry, etc.);
- The effects of freeze/thaw and evaporation are not readily quantifiable;
- The thickening process must continue after deposition to maintain pumpability;

- Overall there appears to be a need in the industry to create a set of standardized test procedures to evaluate both tailings materials and additive effectiveness;
- An acceptable lift thickness is dependent on the drainage characteristics of the material, the available area for tailings, the production rate, the surface slope, additional drainage measures in place and the meteorological conditions; and
- Effective means are required to maintain a deposit in a drained state and to promote drainage away from the tailings.

PRACTICAL CONSIDERATIONS

What to Watch out For

In the experience gained by the testwork performed over the last few years it is clear that all tailings streams can be dewatered to some extent and can make favourable deposition stacks.

The key is to understand the process, chemistry, site conditions, availability of potential additives, quantity, production rate and meteorological conditions. Each site will therefore have a unique solution.

There is no one size fits all to meet the thickening and deposition needs. It is important to note that fines capture, as well as strength requirements, must be in accordance with Directive 074.

What to Aim For

As discussed above, there needs to be a concerted effort to develop a set of standard test procedures to understand the behavioural characteristics of oil sands tailings. In addition, the dewatering that takes place after deposition requires more study and quantification.

Consideration could also be given to handling some of the fines separately to optimize the thickening process.

It is recommended that a holistic and systematic approach be applied to meeting the conditions presented in Directive 074. This could include, but not be limited to, the following:

- Understanding the site conditions (deposition area, location, meteorology, etc.);
- Understanding all the process characteristics (quantity, production rate, physical properties, chemical properties, etc.);
- Understanding the properties of the tailings based on standardized test methods;
- Additive screening tests;
- Thickening methodology testing;
- Small scale deposition tests;
- Large scale deposition tests;
- Field deposition tests/trials;
- Modeling;
- Implementation; and
- Instrumentation and monitoring.

Photo 4. Flocculant Screening Tests

Photo 5. Small Scale Deposition Test

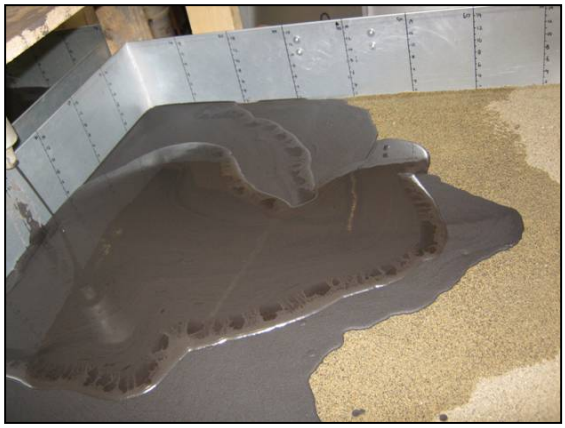

Photo 6. Small Scale Deposition Test with Sand Bottom

Photo 7. Larger Scale Deposition Test (Modified Flume)

There are potentially other dewatering methods that could be explored and an open mind is necessary to develop these technologies that may prove to be better at a given site. Electro-kinetics is one thickening method that has merit for consideration. There are also many additives that may be appropriate at one site over another such as polymers and local waste or overburden materials.

REFERENCES

Ahmed, M., Labelle, M., Brown, R. and Lahaie, R. "Paste Pumping and Deposition Field Trials and Concepts on Syncrude's Dewatered MFT (Centrifuge Cake). Tailings and Mine Waste '09, University of Alberta Geotechnical Centre, Proceedings of the Thirteenth International Conference on Tailings and Mine Waste, 1-4 November 2009, Banff, Alberta, Canada, pp 417-427.

Houlihan, R.H., Mian, M.H. and Lord, E.R., "Oil Sands Tailings – Technology Developments and Regulation. Paste 2010, Proceedings of the 13th International Seminar on Paste and Thickened Tailings, 3-6 May 2010, Toronto, Canada, Australian Centre for Geomechanics, Australia, pp 423-435.

EFFECTS OF WEATHER AND TAILINGS PROPERTIES ON TAILINGS DRYING RATES IN NORTHERN ALBERTA

Charles Gantzer, Todd Fasking, Michael Costello, and Jed Greenwood
Barr Engineering Company, Minneapolis, Minnesota, USA

ABSTRACT

Air drying of thickened oil sands tailings enables it to meet the Energy Resources Conservation Board strength requirements for fine tailings. Drying times are influenced by the potential evaporation rates associated with weather conditions, by the evaporative efficiency of the slurry, and by the mass of the water that must be removed to meet strength requirements. The evaporative efficiency is the ratio of the actual evaporative water-loss rate for a slurry divided by the potential evaporation rate; it can vary with potential evaporation. In this study, the limiting factor that defined drying time requirements for thin layers of theoretical mature fine tailings (MFT) varied seasonally and diurnally. In the summer, the evaporative efficiency of the tailings limited evaporative water loss rates, while the potential evaporation rates defined water-loss rates during cooler months and at night during all seasons.

INTRODUCTION

Directive 074 from the Energy Resources Conservation Board requires the reduction of fluid tailings through fines capture in dedicated disposal areas (DDA's). The DDA's must achieve a minimum undrained shear strength of 5 kPa. One drying approach being considered to reduce the amount of fluid oil sands tailings is the sequential atmospheric drying of thin layers or lifts of tailings. Once a lift has reached the target degree of dryness, another layer would be placed above the dried layer. The number of lifts that a drying bed can process during a drying season depends on the rate at which the tailings can be dried. The areal size requirements for the drying beds are also dependent on the drying rate. For slurries subject to desiccation and consolidation, drying rates are a function of the potential evaporation rate associated with local weather conditions, e.g., solar radiation, wind speed, air temperature, and relative humidity, and the resistance of the slurry to evaporative water loss, e.g., the potential for the drying tailings to form a crust and the salt content of the water (Simms et al., 2009). This resistance is often expressed in terms of an evaporative efficiency.

Potential evaporation can be described as the rate at which water from a shallow pan evaporates under local weather conditions. Evaporative efficiency is the ratio of the actual evaporative water loss rate for a slurry divided by the potential evaporation. The evaporation efficiency of a slurry can vary from 0.5 to 1.0 (Cargill, 1985) and can vary with the potential evaporation (GEO-SLOPE, 2010).

The drying of tailings is a two-stage process. As illustrated in Figure 1, the first stage of drying is characterized by a constant rate of water loss. During second-stage drying, the rate of water loss slows with time. The dividing point between first- and second-stage drying approximates the shrinkage limit. During first-stage drying, the interstitial pores of the tailings remain water-filled. Evaporative water loss results in the consolidation of the tailings. However, once the shrinkage limit is reached, additional evaporative water loss results in the interstitial pores becoming increasingly air-filled, and with time the water table and the air front migrate downward. First-stage drying is easier to characterize numerically than second-stage drying (Cargill, 1985).

Because the target undrained shear strengths for oil sands tailings (MFT) can be achieved before the tailings are dried to the shrinkage limit (Guo, 2009), the time required for tailings drying is primarily associated with the rates of first-stage drying.

In subsequent sections, this paper will describe how the potential evaporation for northern Alberta was determined. Also described is development of drying rates using literature provided tailings inputs as run in a geotechnical model. Finally, the actual meteorological data is compared to the modeled evaporative rates to determine timeframes to reach geotechnical targets.

Drying times were estimated from the hourly potential evaporation rates for northern Alberta and from the variable evaporative efficiencies for MFT. The example tailings are assumed to have an initial void ratio of 2.5 and a target void ratio of 1.0 (Guo, 2009; Jeeravipoolvarn et al., 2009). The tailings were assumed to be placed on a drying bed as a 10-cm lift (Wells and Riley, 2007).

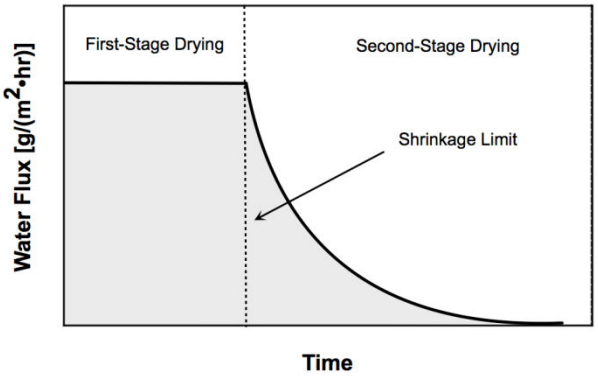

Figure 1. Evaporative water loss rate is constant during first-stage drying. However, once the shrinkage limit is reached, second-stage drying begins. Second-stage drying is characterized by a slowing water loss rate. (Cargill, 1985)

POTENTIAL EVAPORATION

The hourly potential evaporation rates were estimated from the 2002 weather data for Lac La Biche, Alberta (54.8°N, 121.0°W) (NCDC, 2002) using the ASCE hourly reference evapotranspiration equation (ASCE, 2005). Missing hourly weather data was filled by assuming persistence from the previous hour. The net radiation component of the ASCE approach was modified to consider the effects of cloud cover using the algorithms found in the EPA's PCRAMMET software (EPA, 1999). Also, the default albedo value and air-phase resistance factors in the ASCE approach were changed from values for cropland to values more representative of mud flats (Arya, 2001). The potential evaporation calculations assumed a flat tailings surface and assumed that the drying bed was not inclined toward the sun. The estimated hourly potential evaporation rates for June 15 through June 24 and for October 15 through October 24 are plotted in Figure 2. Figure 2 indicates that a greater potential exists for water evaporation during June than during October.

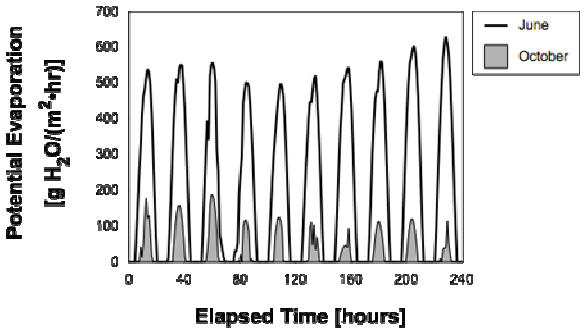

Figure 2. The estimated potential evaporation rates for the 10 days following June 15 are greater than those for the 10 days following October 15.

EVAPORATIVE EFFICIENCY

The evaporative efficiency of the tailings as a function of the potential evaporation rate was estimated using a seepage model for unsaturated flow conditions. The relationship between actual evaporation rate and the potential evaporation rate was determined when the voids were initially water saturated. The actual evaporative flux was estimated using the VADOSE/W software package (GEO-SLOPE, 2010), which uses a finite-element approach to solve transient unsaturated flow problems for which the thermal and climatic boundary conditions are defined.

Material Properties

Representative material properties for the MFT were obtained from published literature. Assumed index properties such as particle size distribution (D_{60} =0.003 mm and D_{10}=0.00005 mm) and Atterberg limits (liquid limit of 59 percent) were for MFT found in Syncrude's Mildred Lake Settling Basin (Guo, 2009). The assumed relationship between hydraulic conductivity and void ratio was as follows (Bromwell, 1983):

$$k = 8.94 \times 10^{-11} e^{4.25} \quad (1)$$

in which k is the hydraulic conductivity [m/s] and e is the void ratio.

Additional assumed parameters were the material thermal conductivity [3.0 J/(sec•m•°C)] and the mass specific heat capacity [710 J/(kg•°C)]. These are typical values for the shale and sandstone range and for soil minerals, respectively (GEO-SLOPE, 2010).

The volumetric water-content function for the material was estimated from the saturated volumetric water content (i.e. porosity) and the index properties D_{60}, D_{10}, and liquid limit using the modified Kovacs method (Aubertin et al, 2003). A porosity of 0.6 was used in estimating the volumetric water-content function and was obtained from the assumed void ratio of 1.5.

The volumetric water-content function was used to estimate a hydraulic conductivity function using the van Genuchten method (van Genuchten, 1980). This method requires as inputs the volumetric water-content function, saturated hydraulic conductivity, and residual volumetric water content. The saturated hydraulic conductivity was obtained from equation (1) using a void ratio of 1.5. The resulting saturated hydraulic conductivity was $5.0087 \cdot 10^{-10}$ m/s. The residual volumetric water content was assumed to be 10% of the saturated volumetric water content. Additionally, an assumed value of $1.0 \cdot 10^{-5}$ 1/kPa was used for the coefficient of volume compressibility. The material was assumed to be isotropic in terms of hydraulic conductivity.

With seepage parameters established for the MFT, the thermal parameters were estimated. The thermal conductivity function was estimated from the volumetric water-content function and the material thermal conductivity as described above using the Johansen method (Johansen, 1975). The volumetric specific heat function was then estimated using the volumetric water-content function and the mass specific heat capacity described above using the de Vries method (GEO-SLOPE, 2010).

Approach

First, a steady-state seepage calculation was executed to provide the initial thermal and porewater pressure distributions. The upper thermal boundary condition was set at 20 °C and the lower hydraulic boundary condition was fixed at a total head of 10 cm, which established hydrostatic porewater pressures throughout the material lift with the phreatic surface located at the tailings surface. No drainage was allowed from the bottom boundary.

Second, a transient seepage calculation was executed for a period of three days using potential evaporation values ranging from 83 to 833 g/m^2•hr (2 to 20 mm/day). The potential evaporation was placed as the upper boundary condition at the tailings surface, while the upper thermal and lower hydraulic boundary conditions from the steady-state analysis were removed. Again, no drainage was allowed from the bottom boundary. A flux section to record actual evaporation during transient cycling was placed along the upper boundary. The actual evaporation (AE) at 2 hours of elapsed time was then compared to the potential evaporation (PE) applied as the upper boundary condition.

Estimated Values

The estimated evaporative efficiency (AE/PE) for the example MFT varied with potential evaporation (PE). As illustrated in Figure 3, at potential evaporation rates below about 300 g/m^2•hr, the tailings are able to release water at rates approaching the potential evaporation rate and the evaporative efficiency is about 1.0. Above 300 g/m^2•hr, the tailings are unable to release water at the potential evaporation rate. The evaporative efficiency decreases with increasing potential evaporation.

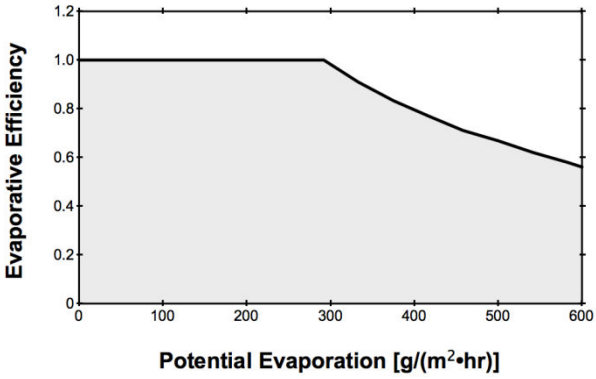

Figure 3. The evaporative efficiency for the first-stage drying of the example MFT varies with the potential evaporation rate.

ACTUAL EVAPORATION RATES

The estimated impact of the evaporation efficiency correlation (Figure 3) on the actual evaporative water-loss rates is illustrated in Figure 4, where

the actual evaporative water-loss rate is equal to the potential evaporation rates multiplied by the appropriate evaporative efficiency. Figure 5 compares the hourly actual water-loss rates to the hourly potential evaporation rates for the 10 days following June 15. The actual drying rates are slower than the potential evaporation rate, especially at higher potential evaporation rates. Thus, at high potential evaporation rates, the properties of the tailings limit the rate of evaporative water loss and affect the time required for drying.

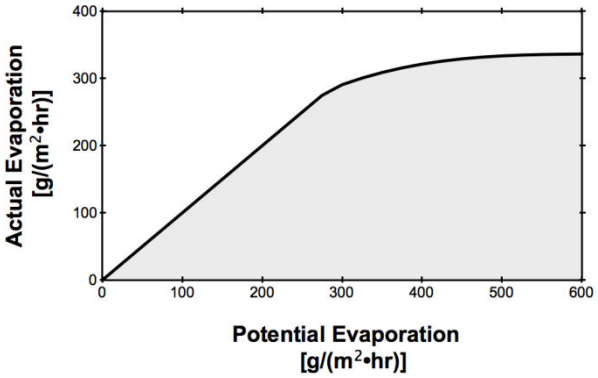

Figure 4. Estimated actual evaporation as a function of the potential evaporation assuming the evaporation efficiency correlation provided in Figure 3.

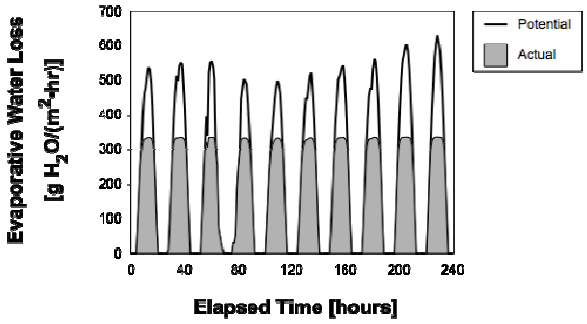

Figure 5. Estimated hourly potential and actual evaporative water-loss rates for the 10 days following June 15. The properties of the tailings limit the rate of evaporative water loss. The plotted actual water-loss rates are based on the evaporative efficiency correlation provided in Figure 3.

DRYING TIMES

To give an example, a 10-cm thick lift of theoretical MFT needs to lose about 42,857 grams of water per square meter of surface area when dried from an initial void ratio of 2.5 to a target void ratio of 1.0. The time required to evaporate this amount of water depends on when the lift is placed on the drying bed. Figure 6 compares the time requirements for drying assuming that placement occurs at noon on the 15th day of the month. Estimated drying times range from 11 days for a June 15 placement to 131 days for an October 15 placement. The plotted drying times for cold months (i.e., the late fall, winter and early spring months) are shown for completeness; however, these should be regarded as crude estimates because this approach does not consider the latent heat for the freezing and thawing of water. In the summer months tailings dry in less than 2 weeks, while in spring and fall drying requires up to 3 weeks.

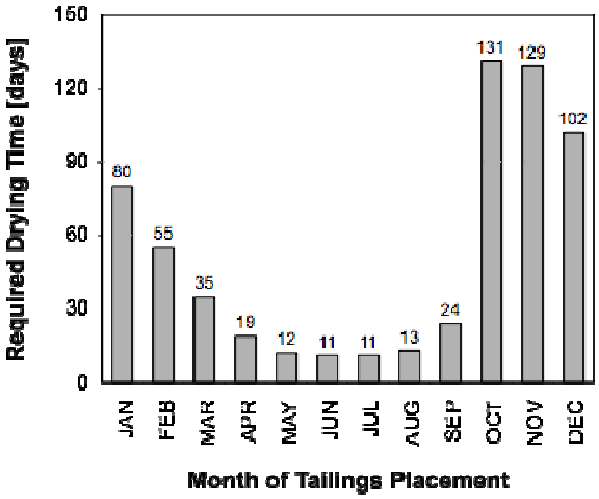

Figure 6. Estimated time requirements for drying oil sands tailings from a void ratio of 2.5 to a void ration of 1.0. The plotted values are based on the assumed evaporative efficiency correlation provided in Figure 3.

The evaporative efficiency approach above can provide reasonable estimates of the time required for first-stage drying. Wells and Riley (2007) observed that a 10-cm thick lift of MFT showed an increase in the solids content (by weight) from 35 to 80 percent in about 18 days in July 2003. Assuming a specific gravity of 2.7 for the solids,

the increase in percent solids means that about 72,150 grams of water needed to be evaporated per square meter of tailings surface area. The evaporative efficiency approach estimated that 18 days would be required to evaporate this mass of water from a square meter of MFT if the tailings were placed on the drying bed in early July. If the tailings were placed on the bed in the middle of July, 19 days would be required.

SUMMARY

The presented approach provides an initial estimate of the time required for the first-stage drying of fine tailings. Estimated drying times are based on the hourly potential evaporation rates provided by the ambient weather conditions, the evaporative efficiency of the oil sands tailings, and the mass of water that must be evaporated from the tailings to meet the target undrained shear strength of 5 kPa. The atmospheric drying potential is relatively uniform between May and August and, during this period, the modeled results show that tailings characteristics limit actual evaporation rates. Meteorological conditions appear to limit evaporation in months outside this seasonal range.

This study demonstrated that the time required for the first-stage drying of fine tailings is not defined soley by potential evaporation. During the summer, actual evaporation rates are limited by the evaporative efficiency of the fine tailings. Drying times based only on potential evaporation will underestimate time requirements.

Accurate estimates of drying times require knowing the evaporative efficiency of the tailings. Evaporative efficiencies can be estimated by hydraulic modeling (as was done in this study) based on the physical properties of the fine tailings. Evaporative efficiencies should be confirmed experimentally either by field or laboratory studies. An advantage of laboratory studies (e.g., wind tunnel studies) is that the potential evaporation can be more easily monitored.

Once the evaporative efficiency correlation for a fine tailings is established, the impact of operational changes on drying times can be assessed. For example, the effects of lift thickness and initial water content on drying times can be evaluated. By quantifying drying times as a function of weather conditions and of the physical properties of the tailings, the approach described in this paper can assist in optimizing the design and operation of a drying bed.

REFERENCES

Arya, S. P. 2001. *Introduction to Micrometeorology Second Edition*, Academic Press, San Diego, CA.

ASCE. 2005. *The ASCE Standardized Reference Evapotranspiration Equation*. American Society of Civil Engineers, Reston, VA.

Aubertin, M., M. Mbonimpa, B. Bussiere, and R. P. Chapuis. 2003. A physically based model to predict the water retention curve from basic geotechnical properties. *Canadian Geotechnical Journal* 40(6): 1104-1122.

Bromwell. 1983. Geotechnical investigation of Mildred Lake oil sand tailings sludge disposal. Bromwell Engineering, Inc., Lakeland, Florida.

Cargill, K. W. 1985. *Mathematical Model of the Consolidation/Dessication Processes in Dredged Material, Final Report*. Technical Report D-85-4. US Army Engineer Waterways Experimental Station, Vicksburg, MS.

EPA. 1999. *PCRAMMET User's Guide*. U.S. Environmental Protection Agency, Office of Air Quality Planning and Standards, Research Triangle Park, NC. EPA-454-B-96-001.

GEO-SLOPE. 2010. *Vadose Zone Modeling with VADOSE/W 2007. An Engineering Methodology. Fourth Edition*. Geo-Slope International, Ltd., Calgary, Alberta.

Guo, C. 2009. *Rapid densification of the oil sands mature fine tailings (MFT) by microbial activity*. Ph.D. dissertation, University of Alberta, Edmonton, Alberta.

Jeeravipoolvarn S., Scott J. D. and Chalaturnk R. J. 2009. Geotechnical characteristics of in-line thickened oil sands tailings. In: Sego, D., M. Alostaz, and N. Beier (eds), *Tailings and Mine Waste '09: Proceedings of the Thirteenth International Conference on Tailings and Mine Waste*, Banff, Alberta, Canada, pp. 813-828.

Johansen, O. 1975. *Thermal conductivity of soils*. Ph.D. thesis. Trondheim, Norway (CRREL Draft Translation 637, 1977) ADA 044002.

Simms, P., A. Dunmola, and B. Fisseha. 2009. Generic predictions of drying time in surface deposited thickened tailings in a “wet” climate. In: Sego, D., M. Alostaz, and N. Beier (eds), *Tailings and Mine Waste ’09: Proceedings of the Thirteenth International Conference on Tailings and Mine Waste*, Banff, Alberta, Canada, pp. 749-757.

van Genuchten, M. T. 1980. A closed-form equation for predicting the hydraulic conductivity of unsaturated soils. *Soil Science Society of America Journal* 44: 892-898.

Wells, P. S. and D. A. Riley. 2007. MFT drying–case study in the use of rheological modification and dewatering of fine tailings through thin lift deposition in the oil sands of Alberta. In: Fourie, A. B. and R. J. Jewell (eds), *Paste 2007: Proceedings of the 10th International Seminar on Paste and Thickened Tailings*, pp. 271-284.

EXPERIMENTAL RESEARCH ON MUD FARMING OF FINE OIL SANDS TAILINGS

Yutian Yao, Frits van Tol, Leon van Paassen, Bert Everts, Arno Mulder
Geo-Engineering Section of Department of Geotechnology, Delft University of Technology, Delft, the Netherlands

ABSTRACT

Oil sand tailings are produced when bitumen is extracted from surface mined oil sands. The fine part of these tailings has very poor consolidation and dewatering properties. This paper deals with the feasibility of mud farming to accelerate the water release of fine oil sands tailings. Based on the experience with sub-areal drying of dredged sludge from the Rotterdam harbor basins, Delft University of Technology has explored the feasibility of mud farming to dewater fine oil sand tailings. The characteristics of both dredged sludge and fine oil sand tailings were compared and several experiments were carried out on thickened tailings (TT) from Muskeg River Mine, Alberta, Canada. A series of experiments was performed in which containers of different height were filled with TT and exposed to different climatological conditions, both in climate rooms and in the open air.

INTRODUCTION

Mud farming is a geotechnical engineering technique which is mainly used to dewater fine grained slurries. Mud farming uses sub-areal drying as dewatering technique. The slurry is deposited in a disposal site in thin layers, in order to maximize the benefits of the evaporation. After a certain drying period further filling or removal and re-use takes place. With the joint effect of evaporation and self weight consolidation, both the moisture content and compressibility of the mud reduce, while the density and shear strength increase. With proper management of surface water, an overconsolidated soil profile can be obtained due to the high suction stresses.

In the Netherlands, fine material originating from the rivers Rhine and Meuse, settles in the Rotterdam harbour basins. For nautical reasons this material was and still is being dredged. In the seventies and eighties the disposal strategy for this dredged sludge was sub-areal drying (or mud farming). The results gained have demonstrated the effectiveness of mud-farming in dewatering and consolidation of dredged sediments. The related engineering experience will be presented in the following sections. In a later stage the pollution of the sediments prevented the use of ripened sludge on land and at present the dredged sediments are stored in large, man-made disposal ponds.

Oil sands tailings, the waste production of tailings from the oil extraction plant, are a mixture of sand, silt, clay, water and approximately 1% to 2% remaining bitumen. The present strategy is to pump these tailings into large ponds where the mixture segregates forming a layer with high sand content at the bottom and a thick layer of unconsolidated fines on top, the so-called mature fine tailings (MFT). Thickening of fine tailings in thickeners has been implemented by Shell Albian Sands and other technologies such as inline flocculation of fluid fine tailings, and centrifugation of flocculated fluid fine tailings are in advanced stages of development. There is a strong interest to develop economical means to dispose fine oil sands tailings effectively. Mud-farming is one of the options.

Delft University of Technology conducted a study to evaluate whether fine oil sands tailings can be disposed and dried based on the Dutch experience with dredged sludge. In this paper mud farming of Rotterdam harbor dredged sludge is reviewed, followed by the experimental studies on fine oil sand tailings. In order to conclude about the feasibility of using mud-farming to dewater fine oil sand tailings in the area of the oil sands mines in Canada the governing parameters and climatological conditions are compared with the Dutch ones.

CASE STUDY OF MUD FARMING

Background

The Rotterdam Port Authorities and the Dutch Ministry of Transport and Waterways have more than 50 years of experience of dredging and depositing the sediments from the Rotterdam Harbour. The following strategy was followed:

- from 1960 – 1980
  the sludge was deposited in confined disposal sites on land;
- from 1970 – 1980
  a part of the sludge was converted to usable clay (to maintain parks and greens of the city and as cover on dike embankments);
- from 1985 – present
  the polluted part of the sludge (yearly 10 million m3) is stored in a man-made disposal site of 150 Mm3 near shore;
  the remaining part of the sludge is dumped into the sea.

The mud is deposited at relative low density (bulk density less then 1200 kg/m3) and consolidates under its own weight, which is extremely time consuming (Projectnota, Slufter, 1984).

Layout Of Disposal Sites On Shore

A typical layout of a disposal site for dredged sludge is shown in Figure 1. The disposal site is subdivided into a number of smaller units with a surface area between 200,000 and 500,000 m2. The size of each unit is kept within certain (upper and lower) limits according to the quantity of material to be stored, about 60,000 m3 weekly. This resulted in layers of about 1 to 1,5 m to be stored subsequently in the units. Such an entire disposal site covered about 2 up to 4 km2. After sufficient drying of a deposed layer a new one was deposited. In general not more then 5 layers were deposited on top of each other. Among the units, discharge canals with settling basins were created. The excess water is discharged through the canal into a basin; after the settlement of the fine particles, the water is discharged to open water.

Dewatering

After the filling and the drainage of free water the dredged sludge must go through a ripening process, in order to become suitable for use (planting, cultivating, road building, etc.). The ripening process consists of removing the water on top of the settled sludge. Once the stagnant water has been removed, evaporation causes an unsaturated zone in the sludge with very high suction pressures leading to volume reduction. On top of the vertical subsidence, the volume reduction also leads to horizontal tensile stresses, resulting in crack formation. Cracking improves the permeability of the top layer and enables air to reach into the sediment resulting in increasing the evaporation and boosting the dewatering process.

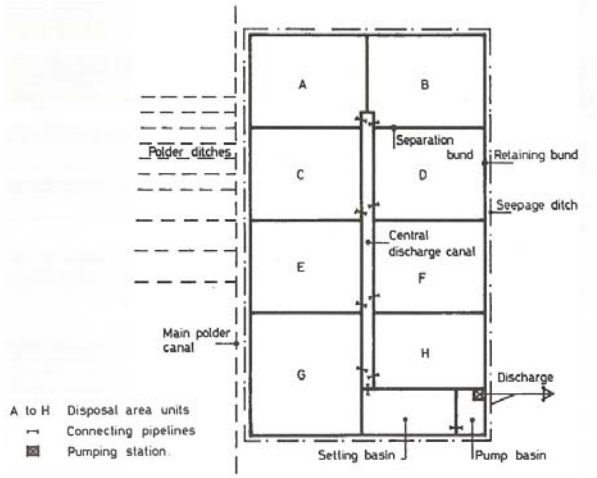

Figure 1. Typical layout of a disposal site for dredged sludge (D'Angremond et al, 1978).

Furrowing

The evaporation can be further encouraged by furrowing, which is able to remove the released water as much as possible. Technically this can be done by two types of devices shown in Figure 2: the Amphirol (for the first stages of furrowing) and the disc wheel (for later stages). As long as no cracking occurs, rainwater is collected in the furrows and runs off the surface of the mud. The effective ripening time per year is thus considerably shortened. For an unfurrowed disposal site in The Netherlands it is estimated that ripening takes place only during 3 months per year. By furrowing, the period in which ripening occurs can be extended up to even 10 months per year.

With proper management, consolidated and trafficable land can be obtained by mud farming within a limited time frame. The experience gained in Rotterdam during drying dredged sludge is worthy of being transferred to other projects.

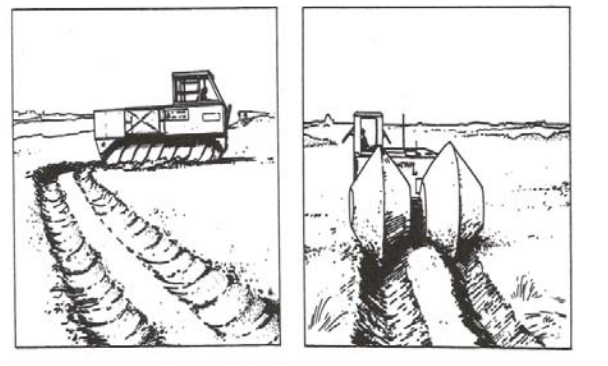

Figure 2. Sketches of two types of device: Amphirol (left) and Disc wheel (right).

Conditions For Successful Mud-Farming

From the Rotterdam experience the following conditions are considered crucial for successful mud-farming:

1. The material to be treated must exhibit suction behavior, with very high suction pressures in unsaturated conditions. This behavior is predominantly determined by the composition of the material, in particular the clay and organic matter content (Rijniercse, 1983). To assess the feasibility of the mud-farming technique for the TT from Albian Sands a comparison of material composition with the Dutch harbor sludge will therefore be made in this paper.

2. Sedimentation is required. The fines must settle in order to have a clear separation between water and sludge. This is essential for the start of the drying process. It will be delayed in case the fines remain in suspension. With a number of sedimentation tests this behavior has been determined.

3. Furthermore a significant precipitation deficit is required during a considerable period. Therefore the climatic conditions at Fort McMurray are compared with the Dutch situation.

LABORATORY TESTS

From March to August, 2010 an experimental program was undertaken by TU Delft to evaluate the feasibility of mud farming of fine oil sand tailings. The methods and results are presented in this section.

Materials

The fine tailings used in this research originate from Muskeg River Mine, Fort McMurray, Canada. At Albian Sands the tailings are separated with hydro cyclones at site. The overflow of cyclones is thickened and forms a tailing called TT (Thickened Tailings). The property index of the materials used is presented in Table 2 where the properties between dredging sludge and fine oil sands tailings are compared.

TT sludge was supplied in four oil drums (159 L). The drums were rolled for several minutes, before samples were taken. Each sample of TT was mixed with a blender before use in the experiment. Two sampling procedures were distinguished, according to the deposit age. Type A is rather fresh, newly sampled without exposure to air since shipping from Canada. Type B has been exposed to air and deposited in capped containers for at least two months. The initial water content and density at the start of the experiments for both two types were almost the same.

Methods

In this research, the TT samples were placed in different conditions to learn the behavior during mud faming process. To carry out these tests, 11 glass containers in dimension of 30cm by 30cm of cross section area were manufactured. The containers were filled with different heights of TT. Then the containers were placed in climate rooms with different temperatures and in the open air, sheltered from rains. During the tests, water released by the tailings was removed as soon as possible for both the outdoor and climate room samples. When the surface of soil dried out, a cannel, 2 cm deep and 3 cm wide was made horizontally across the center part over the surface. There were also 3 containers in climate rooms without water removal as control tests. The height, the water content and the shear strength of the tailings were monitored during the tests. Table 1 provides specifications of the tests.

Results

Control tests

After filling the containers, the mud level immediately began to settle. At the beginning the fine particles settled fast and after only one day a

clear mud-water interface was observed. As the sedimentation process went on, the mud level continue to drop, but also the water surface dropped due to the evaporation in climate rooms. The settlement rate of mud level declined after some time however the settlement rate of water surface remained almost the same. The heights of mud level and water level varied with time are shown in Figure 3.

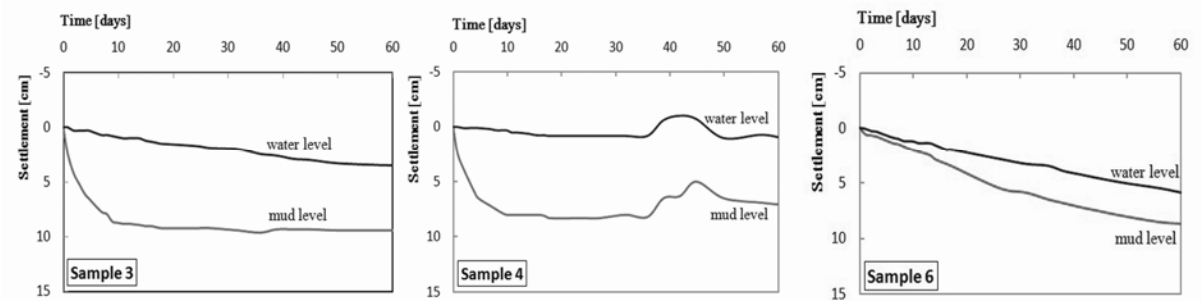

Figure 3. Settlements of mud level and water level with time for control tests.

From the graphs it is evident that sedimentation behavior of each sample is a bit different. For sludge type A (sample 3 and 4) the initial settlement rate is rather high (3 cm/day) and decreases to virtually zero within 10 days, while for sludge type B the initial settlement rate is rather low (0.2 cm/day) and decreases gradually over the observation period of 60 days. After 60 days all samples show similar total settlement between 8 and 10 cm. Temperature did not seem to have a large effect on amount and rate of settlement. For sample 4, (type A at 20^{o}C) there was an obvious rebound in both water and mud level curves at the time of 35 days, a similar phenomenon took place in sample 3 (type A at 10^{o}C) but not so pronounced. For sample 6 (type B, 20^{o}C), there was not any rebound of curves at all and the curve seemed much linearly. The rebound of the curves of sample 3 and 4 are probably caused by the gas bubbles produced as the results of decomposition of organic materials in the tailings. As the gas accumulates the mud expands and the mud and water level raises. It seems that the samples which are placed in higher temperature and with shorter deposit age show more gas production than the other ones.

Climate room tests

The climate room samples were dewatered by removing the freshwater as soon as possible and dried under the effects of evaporation under static but different conditions. Figure 4 presents the changes of sample heights with time in climate room tests. The mud surface settlement curves in Figure 4 are very similar to the ones illustrated in Figure 3. Due to the gas production, consolidation processes of tailings were to some extent retarded. In addition, compared with curves in Figure 3, the climate room tests with water removal have slightly larger settlements after a period of 60 days, between 9 and 12cm. Removing water accelerates the ripening process particularly in the top part of the sludge. The water content of the mud just beneath (10mm) the surface part of samples was determined and shown in Figure 5. From the graphs, it is found that the water content of sample 7 (type A,20□) which has passed the liquid limit decreases much faster than sample 8 (type A, 10□). This is probably because of the difference in evaporation rate as a result of different temperature. Sample 8 and sample 11, both in temperature of 10° have different surface water content after 60 days of consolidation probably because sample 11 is 10cm higher than the other one which needs longer time for drying.

Outdoor tests

The outdoor tests started late March and ended in early August. The local temperature and humidity profile of the tests period is presented in Figure 6 (http://www.weerzoetermeer.nl). The changes in sample heights with time during the tests are given in Figure 7. The outdoor mud-farming experiments (sample 1 and 5) show similar settlement rates as the climate room experiments. The difference in settlement behavior between type A (sample 1) and type B (sample 5) is rather small in the

outdoor tests compared to the climate room tests. Both outdoor and climate room tests show about 12 cm of settlement after 60 days. A ditch is made after 20 days and after 35 to 40 days the first cracks appear. Sample 2, which has a height of 40 cm shows similar relative settlement rate. The results of water content and shear strength measurements just beneath the surface are shown in Figure 8.

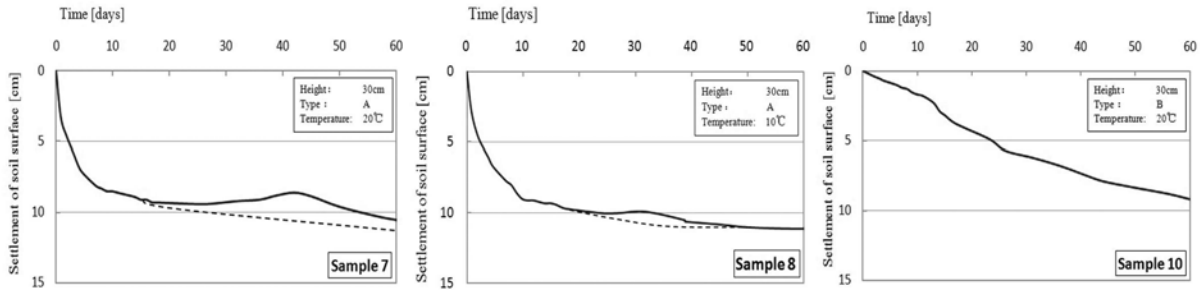

Figure 4. The settlements of mud surface during climate room tests.

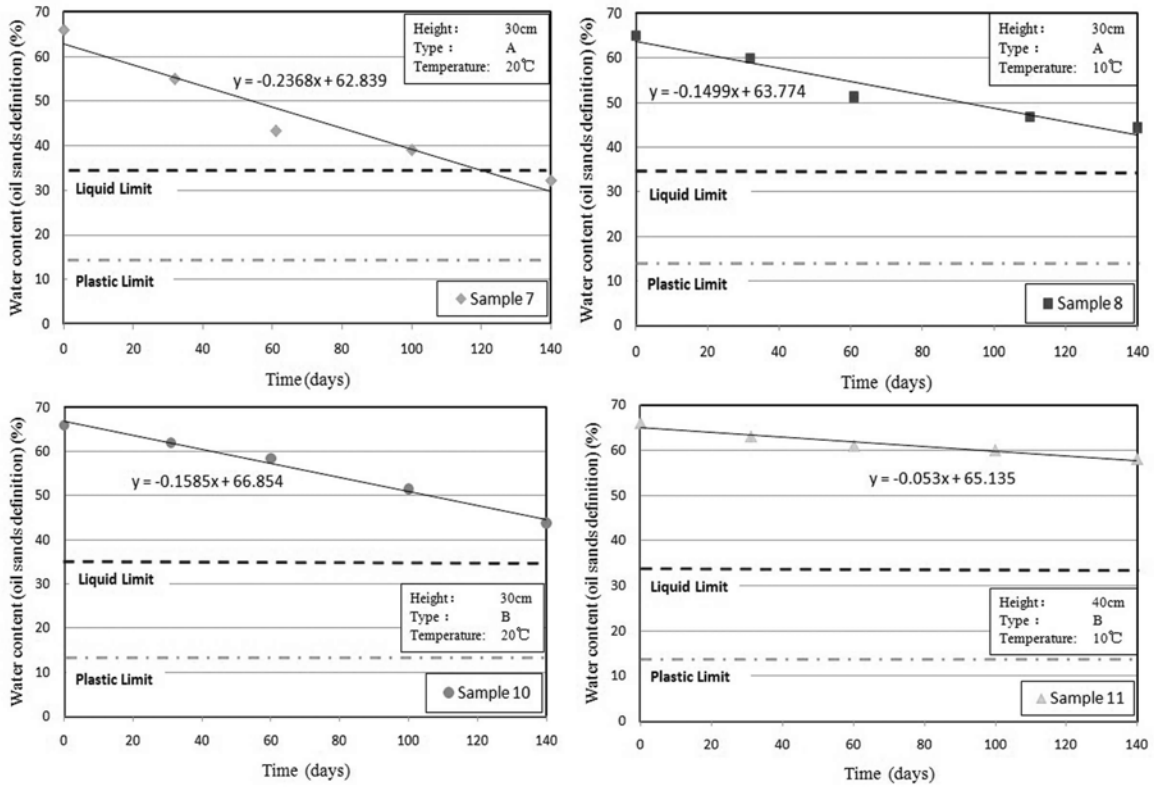

Figure 5. Water content on the surface part of the mud (Liquid limit and plastic limit are in oil sands definition).

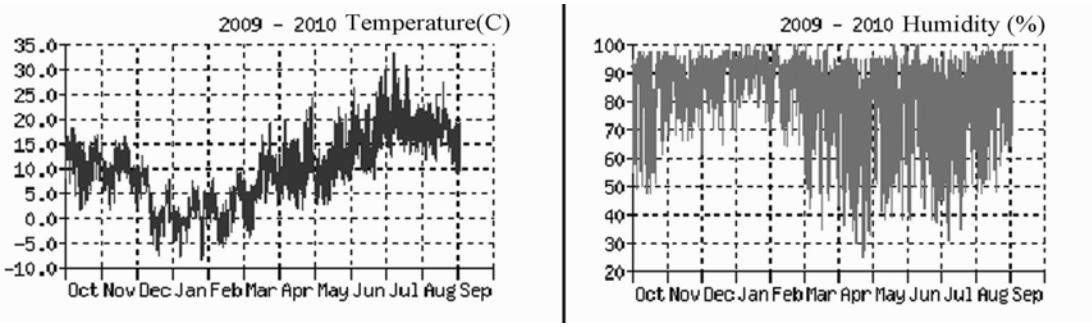

Figure 6. Air temperature and humidity profiles for outdoor tests.

T.A. Newson and M.Fahey, (2003) illustrated the state of fine tailings during the mud farming process in Figure 9. Compared with the results of the outdoor containers tests in Figure 8 it can be seen that point A in Figure 9 corresponds in the tests with a water content of 65%, which is far above the liquid limit. As the material dries, the water content decreases and the liquid limit is reached at 35%. The volume of the samples continues to decrease and the water content of samples 1 and 5 passes the plastic limit after 100 – 120 days, point B in Figure 9. With ongoing drying the soil becomes un-saturated and will eventually reach the shrinkage limit. The shrinkage limit of the TT has not been assessed.

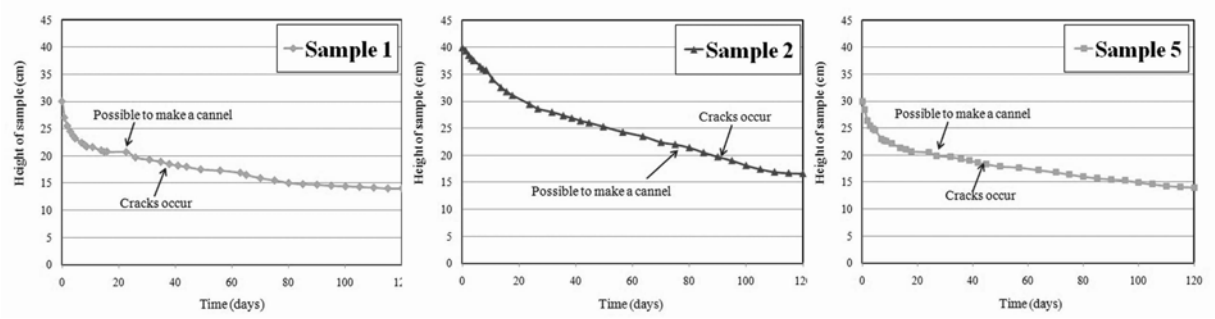

Figure 7. Sample heights in time of outdoor tests.

The strength of the top material in the outdoor test increased in all the samples in particular during the last stage. The reached strength values in sample 1 and 5 respectively 115 and 90 kPa correspond with the strength of remolded clay near the plastic limit, according to Atkinson and Bransby (1978) and Peck et al. (1996). Figure 10 shows a top view of the outdoor samples at the end of the test period.

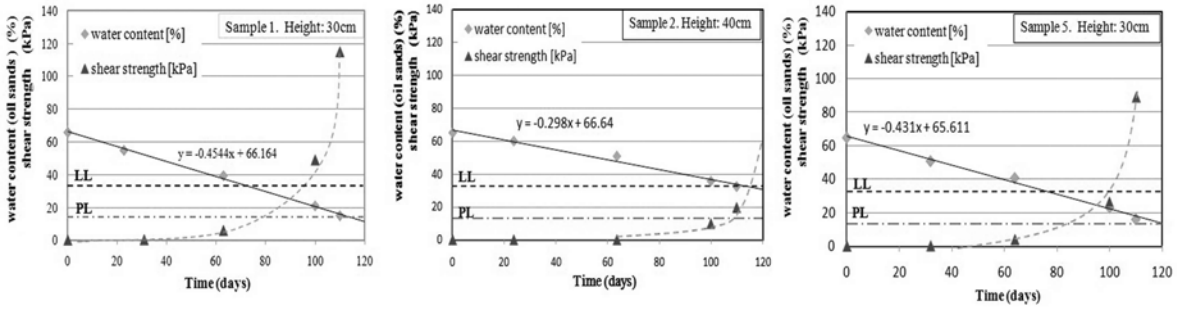

Figure 8. Water content and shear strength of outdoor samples in time.(LL and PL are in oil sands definition).

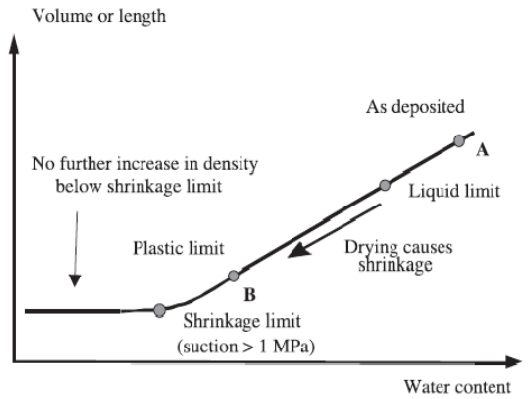

Figure 9. State change of tailings during mud farming (T.A. Newson and M.Fahey, 2003).

ANALYSIS AND DISCUSSIONS

Concerning the criteria for successful mud farming stated above in 2.5 the following analyses are made to evaluate the feasibility of mud farming of fine oil sands tailings. Firstly, the composition and index properties of fine oil sands tailings are compared with dredging sludge on which mud farming is very effective. Table 2 presents the properties of dredging sludge, MFT and TT taken from literatures and those obtained in laboratory tests at Delft University. As stated above, the required suction behavior is mainly determined by the clay and organic matter content. The TT has a lower clay content and the type organic matter is quite different. Therefore it would be very useful to carry out a few tests to assess the water retention characteristics (Qiu and Sego, 2001). In order to compare the amount of water to be extracted from the dredging sludge and the TT the total range, from the water content at deposition Wdep until the water content at plastic limit (PL) must be considered. This total range for dredging sludge and TT is respectively 40% - 45% and 50% - 55%. Thus the conditions for TT are somewhat unfavorable as more water must be extracted.

Figure 10. Final states of the tests: Sample 1(left) sample 2(middle) and sample 5 (right)

Regarding the second condition for mud farming, the sedimentation behaviors of the two materials should be compared. From the Project nota Slufter, (1984), it can be seen that a column of dredging sludge with initial bulk density of 11.5kN/m3 settles in about 80 minutes, when the consolidation starts. This rather fast sedimentation is attributed to the fact that the sludge has been dredged in salt or brackish water condition and it is known that salt acts as flocculant. Illustrated in figure 4, the sedimentation and consolidation processes of TT are difficult to distinguish. Moreover, the rate of sedimentation is much lower than that of the dredging sludge. Nevertheless the TT separates in a few days in water and mud, which makes it possible to remove the stagnant water.

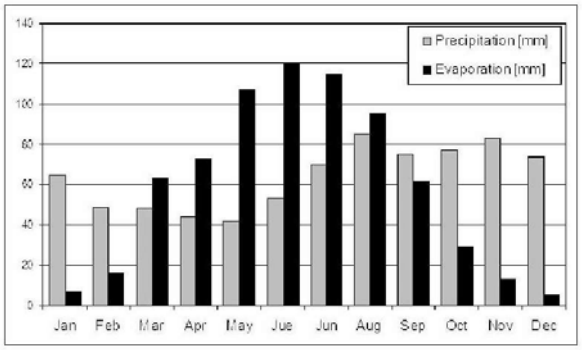

Figure 11. Average monthly precipitation vs. evaporation in the Netherlands.

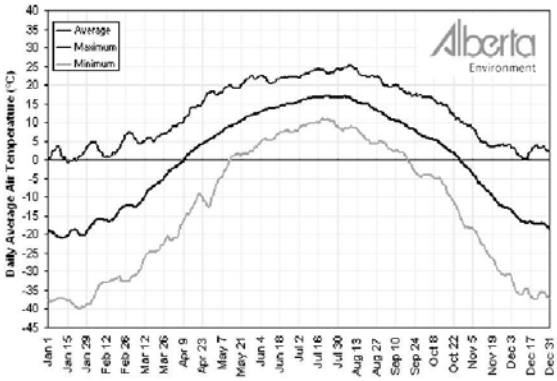

Figure 12. Daily average air temperature at Fort McMurray.

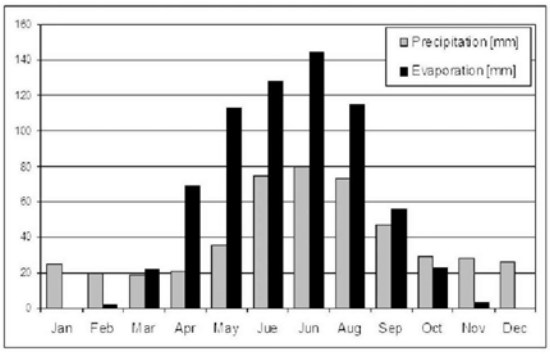

Figure 13. Average monthly precipitation vs. evaporation at Fort McMurray.

The last point is the climatic conditions which govern the mud farming process. Two climatological factors determine the feasibility of mud farming. Evaporation is the drive for the drying process and thus for mud farming. Therefore a large precipitation deficit is essential. On the other hand at very low temperatures freezing of the top layer occurs and evaporation stops. So these conditions are compared between the Netherlands and Fort McMurray. In Figure 6, the annual temperature profiles of average daily temperature and humidity in the Netherlands in 2010 is showing a mild climate with no long lasting cold periods. A precipitation deficit is available from March to August with a monthly average of 40mm. (Figure 11). The climate in Fort McMurray, Alberta, Canada is quite different from the conditions in the Netherlands. The daily average temperature at Fort McMurray is shown in Figure 12 and the precipitation/evaporation is provided in Figure 13. Looking carefully into these graphs, it can be concluded that the temperature, precipitation and evaporation in the Fort McMurray area from half April up to end of September are proper for mud farming. The total precipitation deficit in that period could be as high as 200 - 250 mm and exceeds the average deficit in the Netherlands. Outside the mentioned period in Fort McMurray the temperatures are below zero. This means that in those months the ripening process will stop. Considering the fact that the three criteria for successful mud-farming are met, it seems that this technique can be applied to ripen fine oil sand tailings in the Fort McMurray area in the summer period, potentially in combination with other techniques such as freezing and thawing during the winter months.

CONCLUSIONS & RECOMMENTATIONS

This paper presented practical experience with successful mud farming of dredging sludge. Based on a comparison of the properties of dredging sludge and fine oil sand tailings (TT) and the local climate conditions mud farming appears to be a feasible technique to dewater fine oil sand tailings in thin layers. Laboratory experiments on thickened tailings from Albian Sands confirm that with mud farming an acceptable water content and strength can be obtained.

For the further research of mud farming on oil sands tailings, the following measures are recommended. (1) carry out field test , (2) assess water retention curve of fine oil sand tailings (MFT and TT), (3) simulate drying process (field and containers tests) with a numerical model, (4) determine optimal flocculants for fast sedimentation and (5) define a deposition strategy for whole seasonal cycle (accounting for the freezing during winter) and (6) select a specific type of vegetation to optimize the evaporation.

REFERENCES

D'Angremond, K., J. Brakel, A.J. Hoekstra, W.C. Kleinbloesem, L. Nederlof and J. de Nekker. 1978, Assessment of certain European Dredging practices and dredged material containment and reclamation methods", Technical Report D-78-58, U.S. Army Engineer

Rijniersce, K. 1983, A simulation model for physical soil ripening, Ministry of Transport and Waterways, Rijksdienst IJsselmeerpolders, Flevobericht nr 203.

Project-report Slufter, Physical processes, consolidation, trafficability and water management, 1984, Rotterdam public Works and Ministry of Transport and Waterways, (in Dutch)

Wichman, B. G. H. M. 1999, Consolidation behavior of gassy mud: theory and experimental validation, Doctor's thesis, Delft University of technology, Delft, the Netherlands, 157 p.

Qiu, Y. and D. C. Sego, 2001, Laboratory properties of mine tailings: Canadian Geotechnical Journal, v.38, p. 183-190.

Van Kessel, T. and W. G. M. van Kesteren, 2002, Gas production and transport in artificial sludge depot: Waste Management, v. 22, p.19-28.

Elprama, R and A.F. van Tol, 2003, Twenty years of dredging sludge deposit in man-made basin, Proceedings of XIII ECSMGE, Vanicek et al. Prague, v.1, p. 61- 66.

Pollock, G.W., E.C. McRoberts, G. Livingstone, G.T.McKenna and J.G. Matthews, 2000. Consolidation behaviour and modelling of oil sands composite tailings in the Syncrude CT prototype, Tailing and Mine Waste '00, Balkema, Rotterdam.

Newson, T. A. and M. Fahey, 2003, Measurement of evaporation from saline storages: Engineering Geology, v. 70, p. 217-233.

Sobkowicz, J. C. and N. R. Morgenstern, 2009, A geotechnical perspective on oil sands tailings, Proceedings of Tailings& Mine Waste conference, 2009.

Van Tol, F, H.J. Everts and Y. Yao, 2010, Report on Feasibility of Dutch dewatering techniques in oil sands tailings. Delft University of Technology, Delft, the Netherlands.

Table 1. Overview of small-scale mud farming tests.

Sample ID		Sample height (cm)	Air Temperature (℃)	Average air Moisture content (%)	Type of sample (A/B)
Outdoor tests	1	30	Max.: 5 to 33℃ Min.: -3 to 12℃	40%-95%	A
	2	40			A
	5	30			B
Climate room tests	7	30	20	65±5	A
	8	30	10	70±5	A
	10	30	20	65±5	B
	11	40	10	70±5	B
Control tests	3	30	10	70±5	A
	4	30	20	65±5	A
	6	30	20	65±5	B

Table 2. Properties of dredging sludge and fine oil sands tailings.

Items	Dredging sludge	Oil sand tailings		
		MFT	TT	TT (this study)
Grain size and composition				
Clay content (< 2 μm) [%]	22 – 32	30 - 50	5-20	12 - 15
Sand content (> 63 μm) [%]	20- 30 (dredged) 3 – 5 (deposited and segregated)	5 (>44 μm)	20-30(>44 μm)	25-30 (> 63 μm) 30-35 (>44 μm)
Fines content (< 63 μm) [%] (< 44 μm) [%]	94.8 – 96.7	95	75 - 90	70 -75 65-70
Organic matter [%]	8			
Bitumen (of total mass)[%] (of fines mass)[%]		1 - 2 5 -10	1- 2 5 - 6	1.5-2.0
Bulk density kN/m^3	12 (dredged) 11.5–11.6(deposited)			12.1
Density of solids kN/m^3	24.5			23.8
Porosity n	0.85 – 0.9			0.84
Void ratio e = n/(1-n)	5.5 - 9			4.3
Water content (oil sands definition)*	0.70 – 0.80		0.5 – 0.6	0.65 – 0.67
Solid content SC= 1-W	0.30 – 0.2		0.4 – 0.5	0.33 – 0.35
SFR_{44} **		0 – 0.1	1 – 1.5	0.54
Liquid limit WL	115 -137 %		40 – 70%	47 – 53%
Plastic limit	33 – 71 %	27%	16-27%	15 – 15.5%
Plasticity index	62 – 83 %	25%	20-30%	32 – 38%

* In oil sands industry definition which is defined as the ratio of water mass and total mass, W=w/T.
** SFR_{44}= Sand Fine Ratio, The ratio of sand content (>44μm) and fines content (<44μm).

LABORATORY AND FIELD EXPERIENCE WITH RIM DITCH DEWATERING OF MFT

Randy Mikula[1], Alebachew Demoz[1] and Rick Lahaie[2]
[1]CanmetENERGY, Devon, Alberta
[2]Syncrude Canada Limited, Edmonton, Alberta

ABSTRACT

Among the new technologies being evaluated for the treatment of fluid fine tailings, rim ditch dewatering is showing some promise. Recent laboratory scale investigations culminated in a 50,000 m^3 test of the technology at Syncrude's Mildred Lake settling basin. Using a high molecular weight, medium charge density polymer to modify the clay behaviour in the MFT (mature fine tailings), approximately 80,000m^3 of MFT was deposited, while withdrawing approximately 30,000m^3 of water suitable for recycle to the extraction process. The laboratory work leading up to the field test program will be discussed, along with the preliminary results of the field test.

INTRODUCTION

Background

Syncrude Canada is aggressively pursuing a variety of tailings management alternatives that will result in dewatered MFT tailings. This paper describes the results of a test program carried out in the summer of 2009 designed to evaluate rim ditching, or accelerated dewatering, a technology in use in the Florida phosphate industry. In essence, this technology relies on the removal of water from the deposit surface, either at a low spot in the deposit, or via the construction of a rim ditch to collect and remove both rain runoff and deposit dewatering volumes. Preliminary testing of this concept was undertaken at CanmetENERGY in early 2008. The large-scale (14 m^3) evaluations, in which deposits using lime and gypsum additives were compared to a control deposit of MFT, yielded positive results. At the same time, a variety of lime and gypsum additives were evaluated in small-scale tests along with some polymer candidates. It was believed that if the flow behaviour of the oil sand MFT could be modified to develop the same order of strength as the swelling clays found in Florida, then the Florida phosphate technology could be directly applied to oil sand tailings.

The rim ditching method, when adapted for oil sand tailings, relies on accelerated dewatering due to polymer treatment of MFT and the continuous removal of the water released from the deposited material. Based on the success of a 5-m^3 lab pilot scale test at CanmetENERGY using only polymer treatment of the MFT, a field pilot test was conducted by Suncrude Canada Ltd. in the summer of 2009 using a 10m deep, 51,000-m^3 pit to contain the deposited MFT.

RESULTS AND DISCUSSION

The polymer treatment was conducted in a continuous mode with two in line injections to MFT pumped out of a pond using a dredge. The variability in the solids content of the feed MFT required some control and monitoring of the treatment process in order to maintain proper dosing and mixing conditions. The feed MFT solids content was measured hourly by gravimetric analysis, and showed a Gaussian-type distribution with most of the feed in the range of 30 to 35 wt%, and a mean of 32.6 wt%.

The MFT feed was treated with polymer flocculant (A3338) manufactured by SNF at dosages of 750 to 1000 grams per tonne of solids. The effect of the treatment on dewaterability was monitored in the field using capillary suction time (CST) measurements, along with rheology or flow behaviour measurements.

A key to success in the polymer applications for MFT dewatering is the mixing environment. In order to assess the success of the mixing in terms of maximizing water release, it is necessary to have some measure to gauge the dewaterability of the polymer-treated MFT. The capillary suction time (CST) test and shear flow measurements using a field rheometer were used to monitor and even adjust the polymer treatment in real time on an hourly basis. In CST measurements, the MFT is poured into a small open tube resting on a filter paper placed on a flat plastic plate fitted with concentric electrodes. The water is extracted by

capillary suction and its rate of extraction provides a measure of the dewaterability. The time taken by the water front to reach the concentric electrodes is an inverse measure of the dewaterability. Untreated MFT has CST values in excess of 3000 s and, when the polymer was properly mixed, this index was observed to be significantly less than 1000 s.

The pilot layout

Figure 1 shows a schematic of the pilot layout with the polymer injection points and mixing system. Figure 2 shows a photograph of the site just before it was filled. The pit volume was approximately 50,000m^3, and was it filled initially only from the end discharge point, with the filling added from the mid discharge point after the pit was approximately 60% filled. The MFT delivery to the pilot was very consistent at about 33%. Figure 3 shows the distribution of MFT variability throughout the test period.

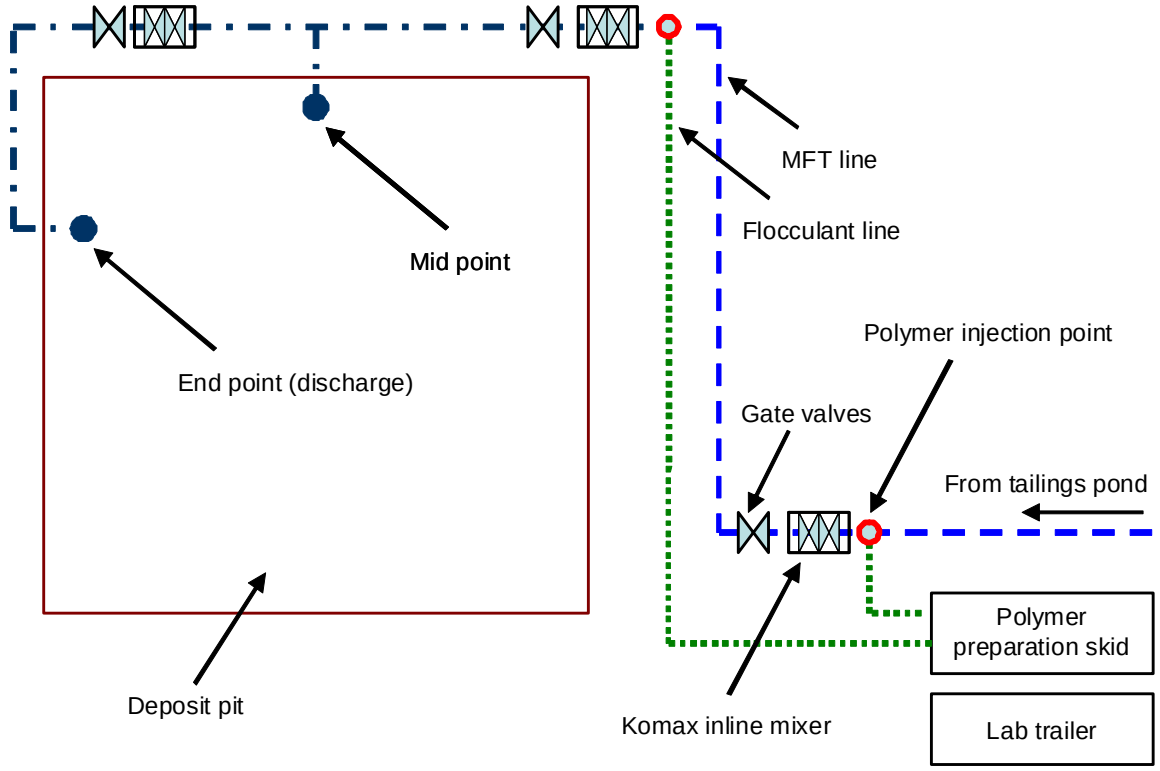

Figure 1. Schematic of the rim ditch deposit showing the dual deposition points and the polymer injection and mixing configuration.

The deposit fill rate and water release

In spite of the consistency of the MFT feed, some adjustment of the polymer dosage was required in order to maintain a high level of dewaterability in the initial deposit. The dewaterability was monitored using a modified capillary suction test. The criteria used for acceptable dewaterability was a capillary suction time (CST) of less than 1000s. Figure 4 shows that in general, this criteria was met for this deposit. During deposition, the dewatering rate was so significant that in the 35 days required to fill the 50,000m^3 test pit, over 80,000m^3 of treated MFT was deposited. This was possible because the initial dewatering released over 30,000m^3 of water.

Figure 5 shows the material balance for this test program at its completion in August of 2009. The initial treated MFT solids of about 30% was very quickly improved to 43% on average. Clearly, at the bottom of the deposit, denser material would be expected.

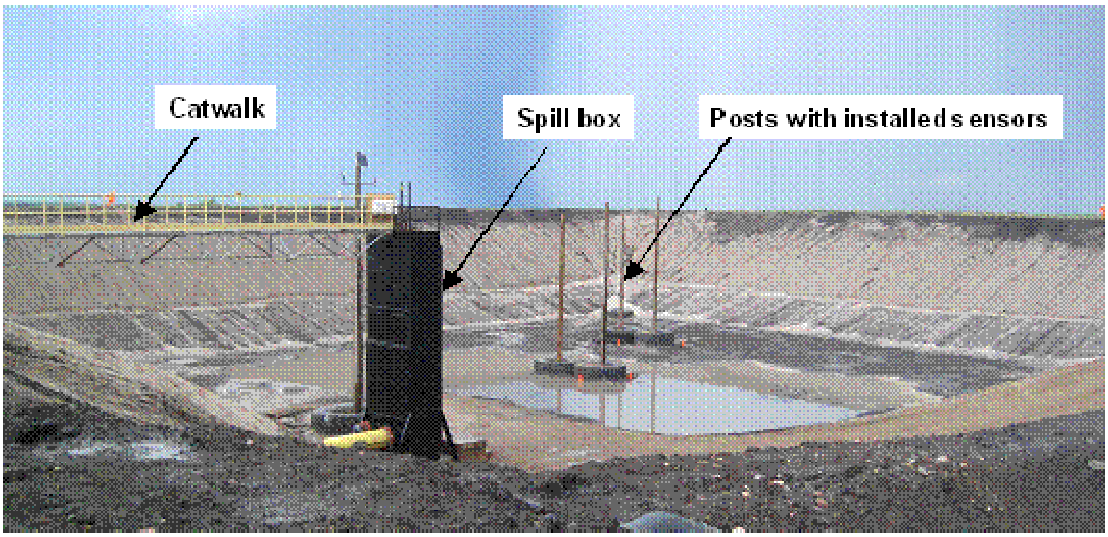

Figure 2. Photograph of the test site showing the spill box to collect release water and the geotechnical program monitoring equipment.

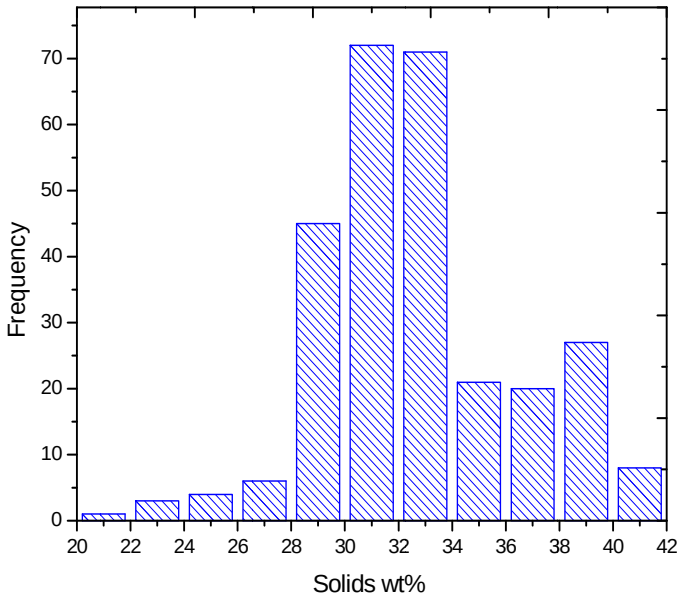

Figure 3. Distribution of MFT solids content for the duration of the test.

Initial release water quantity and quality

The initial release water was monitored for solids content and residual polymer in the field. The capillary suction test can be used as a reliable monitor for polymer concentrations in the 10ppm range, as shown in Figure 6. Although water was not pumped from the deposit unless the solids content was less than 1%, it was not possible to apply any criteria for the release of any potential residual polymer. However, batch extraction testing showed that there was no impact on extraction performance for a medium grade ore using the early release water from the rim ditch pilot. These results are shown in Figure 7.

Initial deposit performance

Tables 1 and 2 show the solids and clay content of the MFT to the pit and from selected sampling sites approximately 30 days after the pit was filled.

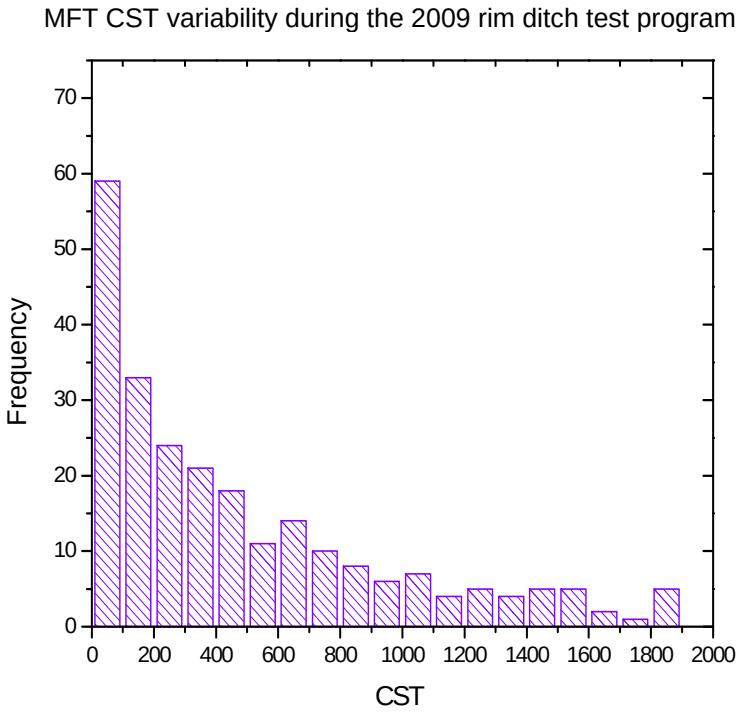

Figure 4. Distribution of CST values for the duration of the test program.

The data in Table 1 suggest that the clay content is lower for higher solids content MFT samples. This data illustrates that in spite of a higher than average clay content (50% clay on solids is often considered to be average), the dewatering rate is significant. The top samples in the two locations illustrated here show some significant differences in solids content, probably due to the water coming up from lower in the deposit and diluting the upper low lying areas. No evidence of segregation of the MFT is evident from the consistency in the clay content as a function of depth. Figure 8 shows vane shear measurements taken along the length of a dock constructed atop the deposit and extending approximately to the middle of the deposit. At only the 2m depth, yield points between 3 and 7 kPa are already observed.

Core samples collected from several sites in the pit were evaluated for solids and clay contents. These results are shown in Table 2. The clay content of the solids was found to be independent of depth, showing that the flocculation was stable and that no segregation of the solids occurred. The average solids contents of sites 3 and 5 were 46.5 wt% and 45.5 wt% (average of top and bottom layers), respectively.

These values are in close agreement with the average solids contents of the deposit calculated from the mass balance data in Figure 5. The total volume of water pumped out of the pit on September 26 was 37187m^3, giving a solids content of 46.7 wt%.

Table 1. Solids and clay content of selected composite MFT feed samples from the 2009 rim ditch test program.

Date (2009)	Solids (wt%)	Clay by XRD (wt%)
July 31	29.9	64.8
July 21	28.9	63.0
August 16	36.2	50.2

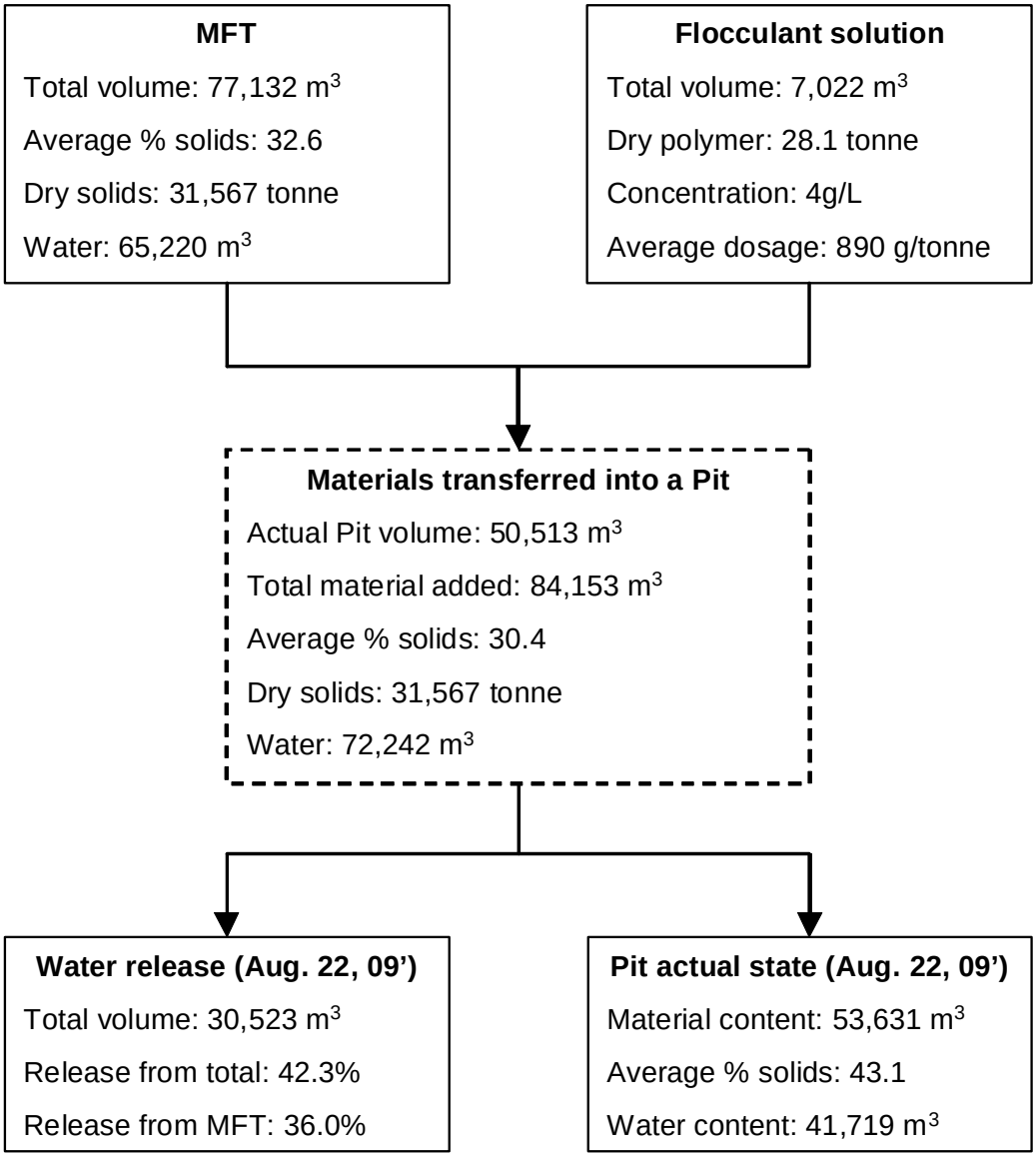

Figure 5. Material mass balance for the rim ditch pilot test from July 15 to August 22, 2009

Table 2. Solids and clay contents of selected sample points in the 2009 rim ditch pit 30 days after filling.

Sample Depth (m)	Solids (wt%)	Clay (wt%)
Site 3 (26/09/09)		
0.0–0.25	36.43	60.33
8.25–8.75	47.46	59.22
8.75–9.05	56.52	61.99
Site 5 (25/09/09)		
0.0–0.25	26.62	64.14
8.75–9.25	48.78	63.56
9.25–9.40	64.31	66.37

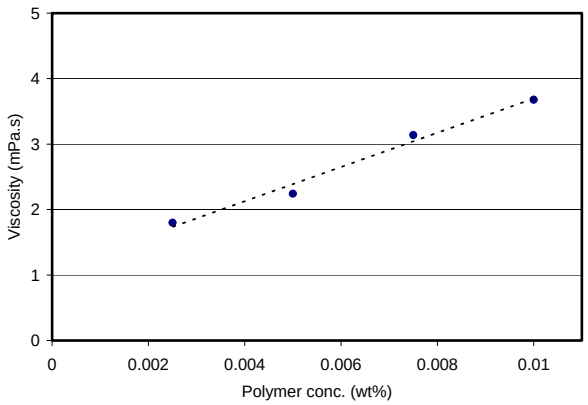

Figure 6. The relationship between CST and residual polymer in the release water.

CONCLUSIONS

The CST or capillary suction test was found to be a useful field test for the direct measurement of the proper mixing and therefore the optimum dewaterability of the rim ditch MFT. Favourable dewatering for the rim ditch deposit (as determined from the CST) could be achieved with 750 to 1000g polymer per tonne of solids.

More than 80000 m^3 of material was deposited in the test pit (74100 m^3 of MFT mixed with 6700 m^3 of polymer solution) over 35 days of the pilot operation. Approximately 37300 m^3 of the water, which corresponds to 550% of the volume of polymer solution water used to treat the MFT, had been recovered after about 3 months from the start of the deposition.

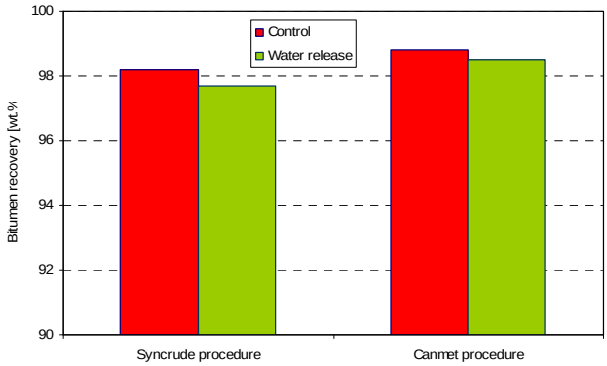

Figure 7. Batch extraction test results showing no impact on extraction recovery or froth quality using the release water from the rim ditch pilot test program. The froth quality for the control sample was reduced relative to the ore extracted with rim ditch release water.

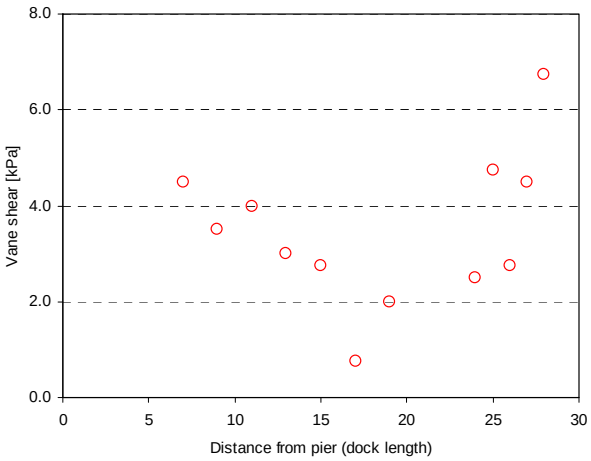

Figure 8. Vane shear testing conducted approximately 30 days after the pit was filled.

The water release was initially very rapid although the recovery rate began to slow down about 15 days after the end of deposition. The polymer treated tailings deposited at about 30% solids dewatered to approximately 43% solids in the time it took to fill the test pit and to 48% solids in less than 90 days with all of the released water being suitable for recycle to the extraction process. Initial (after 60 days) hand held vane shear testing

of the deposit showed values (at the 2m depth) of 3 to 7kPa, indicating a dewatering trajectory that may fulfil the requirements of the new ERCB tailings management directive. Further and more thorough assessments of the dewatering and strength development will determine the ultimate utility of this tailings management approach, but the initial results are very favourable.

ACKNOWLEDGEMENTS

The authors would like to thank Syncrude Canada Limited for permission to publish this paper. The authors would also like to thank Truong Dang-vu, Michelle Barber and Paulina Wong for technical support, and PERD for providing some financial support to Natural Resources Canada.

EXPERIMENTAL RESEARCH ON ACCELERATED CONSOLIDATION USING FILTER JACKETS IN OIL SANDS TAILINGS

Yutian Yao, Leon van Paassen, Frits van Tol, Bert Everts and Arno Mulder
Section Geo-engineering, Department of Geotechnology, Delft University of Technology, The Netherlands

ABSTRACT

Prefabricated Vertical Drains (PVD) can be applied to accelerate the consolidation of oil sands tailings. Due to the fine soil particles and/or the residual organic matter in the tailings, the geotextile filter jackets risk clogging or blinding, which can lead to the significant reduction in the discharge capacity of the PVD. The objective of this study is to evaluate the filtration behavior of filter jackets when applied in thickened oil sands tailings. Filtration column tests were conducted in the laboratory on three types of filter jackets. The experimental results were interpreted using FSCONBAG, a computer program designed to simulate the consolidation behaviour of dredging sludge. Directly after starting the tests, the flow rate through the filters decreased significantly over a test period of 2-3 weeks. It appeared that the filter jackets kept on functioning well during the test, while the filtration behaviour of the thickened tailings controlled the thickened tailings/geotextile system could be well described with the FSCONBAG finite strain consolidation model.

INTRODUCTION

Prefabricated Vertical Drains (PVD), also known as Wick drains or band drains, are widely used to accelerate consolidation of soft clays nowadays. When installed in soft soils, PVD can create a short path for the trapped pore water to escape and thus speed up the rate of consolidation. PVD are comprised of a drainage core wrapped in a geotextile filter jacket which has two basic functions: first to retain soil particles; and second, to allow water to pass from the soil into the PVD core. As noted by McGown (1976), Bell and Hicks (1980), D.T.Bergado et.al (1996), an effective geotextile filter jacket in the soil may function as follows: A small amount of fine particles moves into or through the filter jacket leaving the coarser particles to bridge and arch outside of it. The zone of fine particles immediately behind the soil bridge network is called a “filter cake”. Once the soil filter is established, no further particle movement will occur and the soil-geotextile jacket system is in equilibrium; hence, the geotextile filter jacket retains the soil particles and prevents its migration into the PVD core.

The establishment of a stable and effective soil filter by the geotextile filter jacket depends on the following:

1. The physical and mechanical properties of the geotextile filter jacket e.g. pore size, porosity and compressibility of geotextiles etc.
2. The characteristics of the soil, e.g. particle size distribution, porosity, permeability, and cohesiveness.
3. External stresses and strains imposed on the soil-PVD system.
4. The prevailing hydraulic conditions, e.g. laminar or turbulent flow, unidirectional or reversible flow, and dynamic or pulsating flow.

For well–graded sandy and silty soils, a good selection of the geotextile filter jacket is essential for the successful application of PVD. For fine tailings, the potential migration of fine particles during the drainage and consolidation might present a higher risk of clogging of the filter jackets compared with coarser grained soils. Thus the application of PVD in fine oil sands tailings needs to be studied.

Bell and Hicks (1980) present three different clogging mechanisms for geotextile filter jackets, distinguished as follows:

1. Clogging of the core, by passage through the jackets of too much fine particles;
2. Clogging of the filter jacket by particles trapped within the fabric structure;
3. Blinding of the jackets by formation of a filter cake due to filtration of the sludge.

In addition to above mechanisms, the proper functioning of the PVD in fine oil sands tailings can also be hampered by:

4. Decreased permeability of consolidated sludge around the drain.

5. Clogging of the filter jacket by the residual bitumen in the oil sands tailings.

Oil sands tailings, the waste production of oil sands from the extraction plant, are a mixture of sand, silt, clay, water and approximately 1% to 2% un-recovered bitumen. Oil sands tailings are pumped into tailing ponds where sand is used to build containment structures and beaches and the clay-sized mineral particles flow with water into a settling basin for settling and water clarification. Thickening of fine tailings in high rate thickeners has been implemented at the Shell Albian Sands operations and other technologies such as paste thickened tailings, inline flocculation of fluid fine tailings, and centrifugation of flocculated fluid fine tailings are in advanced stages of development. There is a strong interest and incentive to accelerate the rate of consolidation of fine oil sands tailings deposits and the application of PVD is one of the options. Liu & McKenna (1998) conducted a pre-feasibility study including laboratory testing and numerical modeling to obtain parameters for the potential application of PVD in Composite Tailings (CT, oil sands tailings with a relative high sand content). Wells & Caldwell (2009) presented a field test of the application of PVD in Fort McMurray in a high fines content tailings deposit produced through Suncor operations. At the Shell Albian Sands oil sands operations tailings are classified by hydro-cyclones in which the coarse fraction is separated from the tailings. The cyclone overflow, which contains the fines and water, is further processed in high rate tailings thickeners to recover warm water that can be immediately reused in bitumen processing while producing Thickened Tailings (TT) slurry. Compared with CT, TT has a much higher fines content (up to 70% of particles finer than 44 μm) and water content far above the LL which may cause the clogging of the geotextile filter jackets by migrating particles.

In order to study the performance of geotextile filter jacket of PVD in oil sands tailings, especially the TT, laboratory filtration tests were performed to observe the clogging behavior of filter jackets. The results of the laboratory test were analyzed using FSCONBAG, a computer program designed to simulate the consolidation behavior of dredging sludge based on finite strain consolidation theory.

MATERIALS AND METHODS

Slurry

The soil used in the test is TT taken from Albian Sands Muskeg River Mine at Fort McMurray, Canada. Table 1 provides a summary of engineering properties of material used. The water content is defined as the ratio of mass of water and the total mass. Fines are defines as particles smaller than 44 μm. Figure 1 shows the comparison between TT used in the test and other oil sands tailings plotted in the Ternary Plot (Scott & Cymerman, 1984). The TT sample used in the test fits well within the area of classical classification of TT (Shahid Azam & J. Don Scott, 2005).

Table 1. Properties of thickened tailings used in the laboratory experiments.

Index	Value
Water content* (ASTM D2216)	65.0%
Bulk density of sludge	1.20g/cc
Particle Density (Ultra pycnometer)	2.29g/cc
Void ratio	4.3
Liquid limit (ASTM D4318)	52%
Plastic limit (ASTM D4318)	15%
Plasticity index (ASTM D4318)	37%
SFR(44μm)** (BS1377)	0.54
Fines content (BS1377)	65%
D30	6.3μm
D50	11μm

* Water content is defined as the ratio of water mass and total mass, W=w/T.

** SFR= Sand Fine Ratio, The ratio of sand content (>44μm) and fines content (<44μm).

Geotextile

The filtration tests were conducted with three non-woven geotextiles (DuPont). The filter jacket samples represent the widely used geotextiles that are applied as standard filter jacket of PVD in the consolidation of soft soils. Table 2 shows the properties of geotextile filter jackets used in the tests. These filter jackets are readily distinguished

by the differences in their unit weight and permeability, i.e. white colored polyester geotextile (LDFD) is light weight and more permeable while the grey colored ones (D165&5417HS) are heavy weight and less permeable. All the three geotextiles were used without any modifications.

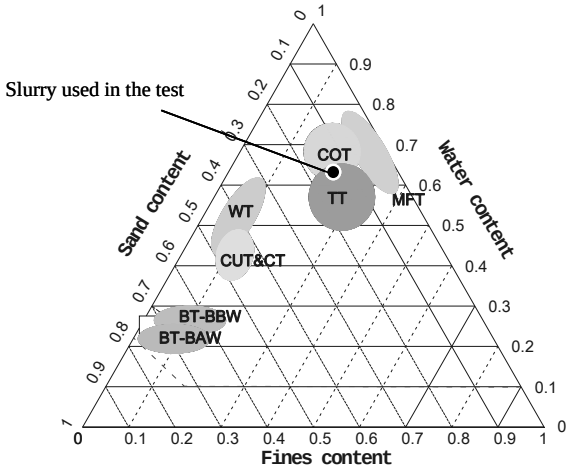

Figure 1. Comparison of TT used and classified tailings products plotted in Ternary Plot (Scott & Cymerman, 1984).

Test aparatus

The apparatus used for testing was fabricated at the Department of Geotechnology, Delft University of Technology, the Netherlands (Yao, et al, 2010). The design (Figure 2) was based on the set-up for the Gradient Ratio Test (GRT-ASTM1992) as described by Palmeira et al. (1996). Three perspex glass cylindrical moulds, 100 mm diameter each, were mounted on top of each other and tightly screwed, forming the filtration column. The three major parts of the column are the pressure chamber, filtration chamber and collection chamber with heights of 300 mm, 200 mm and 100 mm respectively. A constant hydraulic pressure was applied in the pressure chamber using compressed air, which is maintained at the required value using a pressure controller. Air at the controlled pressure is then admitted to the bladder in the air/water bladder cell thus supplying water to the pressure chamber at constant pressure without direct contact between air and water. The filtration chamber is the part where the thickened tailings remain throughout the test. Tailings sludge in the filtration chamber is dewatered through a geotextile filter supported by a wire mesh placed between the filtration chamber and collection chamber. Pressure transducers are installed in the wall of filtration chamber to monitor the pore pressure in the sludge during the test. The measurement of outflow is achieved by weighing the accumulative discharged water, collected in a cup below the outlet. In order to prevent evaporation, the cup was sealed with plastic paper with a hole letting the filtrate drop in. The weight of discharged water and the pore pressures in the tailings are monitored and recorded automatically by a Data Acquisition System.

Table 2. Properties of geotextiles used in the experiments.

Items	TYPAR D165	TYPAR 5417HS	LDFD
Material	Polypropylene	polypropylene	polyester
Unit weight (g/m^2)	165	140	95
Effective area (cm^2)	60	60	60
Thickness 20kPa (mm)	0.39	0.40	0.30
Elongation at break (%) MD	50	50	39
Tensile strength (kN/m)	12.9	11.7	6
Opening size O_{95} (μm)	<75	75	75
Opening size O_{95wet} (μm)	---	75	<65
Permeability (mm/s)	11	12	39
Permittivity (1/s)	0.3	0.3	---

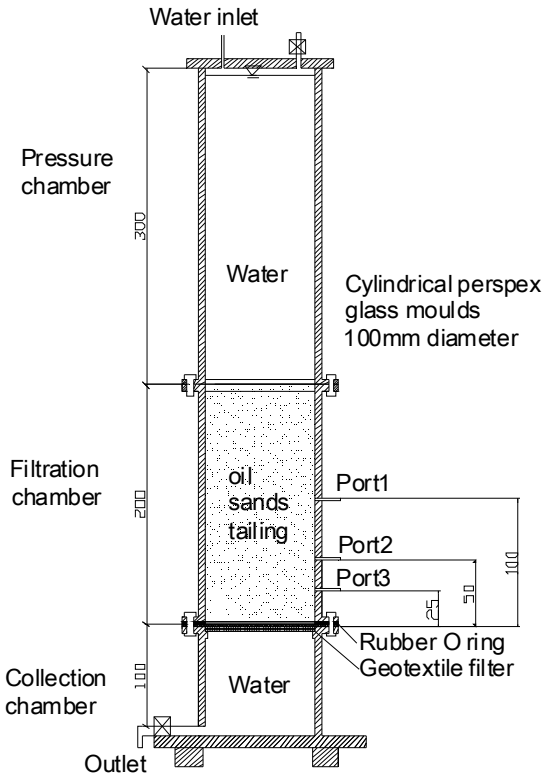

Figure 2. Schematic diagram of filtration column.

Measurements

A detailed description of the sample preparation and apparatus installation is provided by Yao et al. (2010). During the tests, the height of sludge, the pore pressures at two horizons and the amount of discharged water are monitored. After completion of the tests, the water content of the sludge samples and the increased weight of geotextiles are determined.

Applied pressure

The magnitude of imposed hydraulic pressure was set to simulate the pressure/potential at the depth where PVD would be installed in the field. Initially the fine tailings are considered a 'heavy' fluid (Wells & Caldwell, 2009). The driving force which promotes water flow from the tailings into the vertical drain is equal to difference between the total head (hydraulic potential) within the tailings column and the total head within the core of an individual drain. When the PVD are installed, for tailings with bulk density (ρ_t) of 12 kN/m^3, the expected fluid pressure hence potential in the tailings (P_t) at a depth (h_t) is $P_t=\gamma_t h_t=\rho_t g h_t$. Inside the drain the potential $P_d=\gamma_w h_w=\rho_w g h_w$. In case that the density of water (ρ_w) is less than the unit weight of the tailings, there is a net pressure difference between the outside and the inside of the vertical drain and hence flow of tailings water from the tailings into the wick drain. The dewatering process continues after the soft tailings approach their liquid limits and begin to generate effective stresses. Once the fluid-like tailings begin to experience grain-to-grain contact the hydraulic conductivity of the tailings begins to reduce the flow of tailings water into the wick drain. This is the phenomenon referred to as consolidation.

Initially, the pore pressure at the bottom of the filter is equal to the applied pressure in the pressure chamber on top of the water column and self weight of the slurry in the chamber. Once the valve at the bottom is opened, the water in the collection chamber is directly connected to open air. Thus the pore pressure at the bottom side of the geotextile filter jacket is constantly zero. In the test the pressures imposed on the sludge samples with geotextile of LDFD and 5417HS were constant 20 kPa and 10 kPa respectively. For geotextile of D165, however, the pressure was set initially to 10 kPa and doubled when the flow rate became stable. The pressures imposed on the filter jackets were approximately representing the pressure difference of PVD at the depth between 5 m and 10 m in the pond. Tests were stopped when the flow was negligible or some abnormal phenomenon occurred .The duration of the tests varied from 20 to 40 days.

Analysis using FSCONBAG

The results of the laboratory test were analyzed using FSCONBAG, a computer program designed to simulate the consolidation behavior of dredging sludge based on finite strain consolidation theory (Greeuw & Best, 1999).

According to this model, the consolidation behavior of dredging sludge is described by two relationships with void ratio (e) as shown in Figure 3.

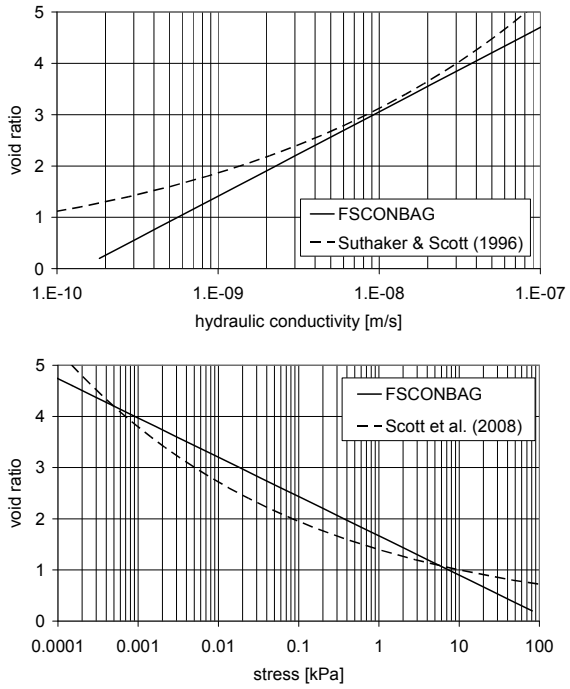

Figure 3. Relationships between void ratio and hydraulic conductivity (left) and and effective stress (right), as used in FSCONBAG.

The hydraulic conductivity (K) is defined by:

$$K = K_0 \exp\left(n_1 + n_2 e\right)$$

In which K_0 = 1 m/s, n_1 = -22.7 and n_2 = 1.4 and the effective stress, (σ') is defined by:

$$\sigma' = \sigma'_0 \exp\left(m_1 + m_2 e\right)$$

In which σ'_0 = 1 kPa, m_1 = 5 and m_2 = -3. The constants were defined by fitting the calculated results to the measurements of the downward flow in test 3. The relationships show reasonable correspondence with literature values on similar tailings as described by Suthaker & Scott (1996) and Scott et al. (2008) (Sobkowicz and Morgenstern, 2009).

RESULTS AND DISCUSSION

Observations during the tests

Figure 4 and 5 show the results of the three filtration tests.

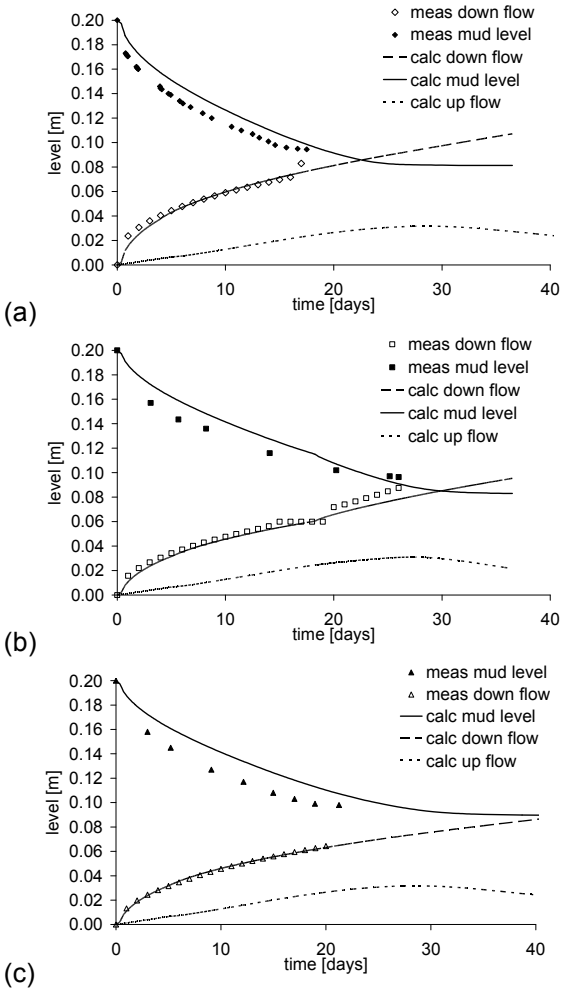

Figure 4. Consolidation and settlement behavior of the sludge with each filter sample: (a) LDFD at 20 kPa), (b) D165 at 10 and 20 kPa (c) 5417HS at 10 kPa.

The measured mud level and cumulative down flow in figure 4 show similar trends for all tests in spite of the differences in the permeability of the geotextiles as well as the different pressures applied. In the first several seconds there was an immediate large flow coming out from the outlet, followed by a sharp decrease of flow, and finally gradually decreasing trend. After 10 to 15 days the discharged flow rate became almost constant in each test. The filtrate water contained some fines at the beginning but remained completely clean after a while, which demonstrated that the jacket functioned correctly, not allowing too much of fines to get into the core of the drains.

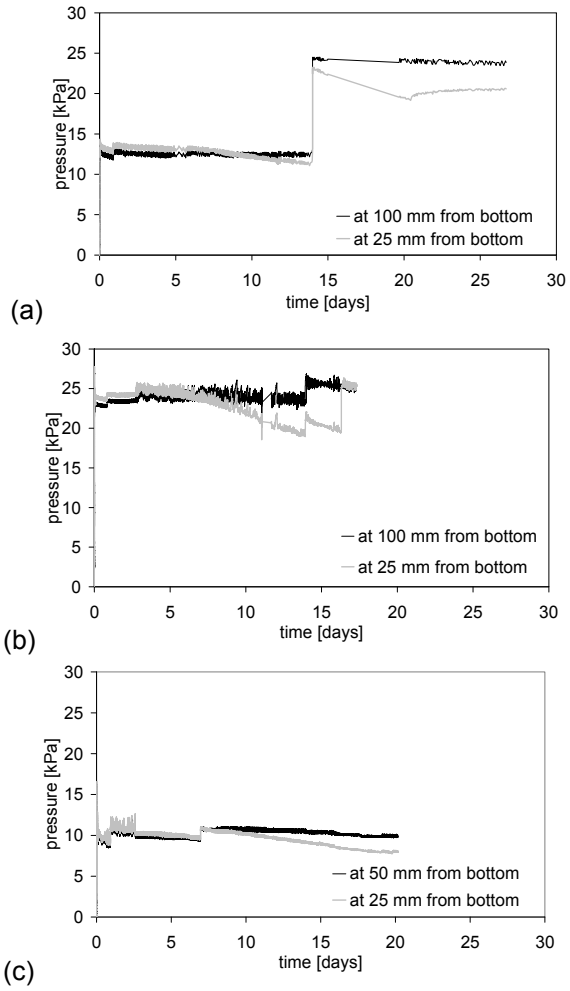

Figure 5. Measured pore pressures of the sludge with each filter sample: (a) LDFD at 20 kPa), (b) D165 at 10 and 20 kPa (c) 5417HS at 10 kPa.

The measured settlements of the mud level, were significantly larger than the cumulative down flow, indicating that part of the consolidation water drained upwards, which was not measured but shown by the calculations. Still a difference existed between the calculated settlements - which is the sum of the cumulative up and down flow – and the measured settlement, which is attributed to the settling of solid particles in the sedimentation stage of the filtration tests. According to the calculations, when the end of the consolidation period is reached, the downward flow rate reaches a constant value (about 1 mm/day to 1.5 mm/day), induced by the hydraulic gradient over the consolidated soil/geotextile system.

The pore pressure was measured at different levels in the sample (Figure 5). Initially the lower sensor recorded a slightly higher pore pressure due to the difference in hydrostatic pressure. In a later stage the effect of bottom drainage and consolidation was reflected in the decreasing pressure at the lowest transducer. The tests lasted for 17 to 26 days. Towards the end of tests (a) and (b), the flow rate increased as well as the pore pressures. This was probably caused by shrinkage and cracks which occurred at the sample along the wall of cylinder (Figure 6), creating a shortcut for drainage. On the other hand, at the outer surface some gas bubbles were observed. These gas bubbles might have disturbed the pressure measuring by the transducer because of poor contact with the sample.

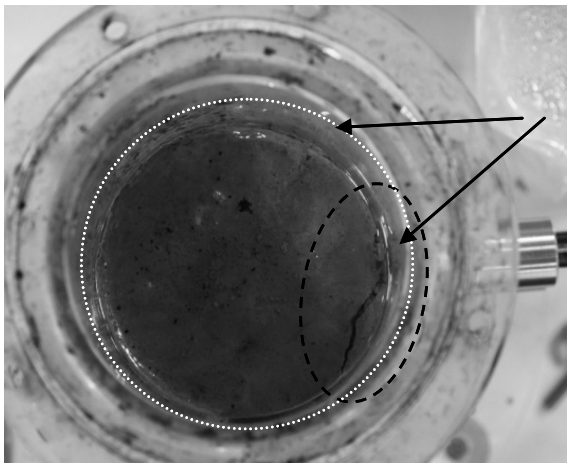

Figure 6. Shrinkage and cracks occurred at the end of the test at the surface of soil sample.

For long-term performance of a filter jacket as illustrated in figure 4 (a) and (c), the higher imposed pressure (20kPa, relative to 10kPa) result in a slightly higher flow rate. Also we noticed that the flow rate in (b) increased when the pressure was doubled, but continued to decrease gradually afterwards. Finally, according to Figure 5 (c), the pore pressures remain constant after 18 days of consolidation.

The calculated pressures over the height of the samples (Figure 7) show a rapid decrease in maximum excess pore pressure during the first 3.7 days of consolidation. This consolidation results in an increase in effective stress and decrease in pore pressure mostly below the bottom two centimeters of the sludge sample. The zone of reduced pore pressures (or increased effective stress slowly moves up until

after about 40 days the sample is fully consolidated. At the final stage the hydraulic gradient increases significantly due to the reducing permeability as a function of the decreasing void ratio with depth.

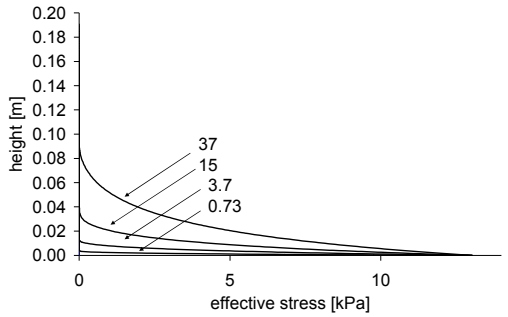

(a)

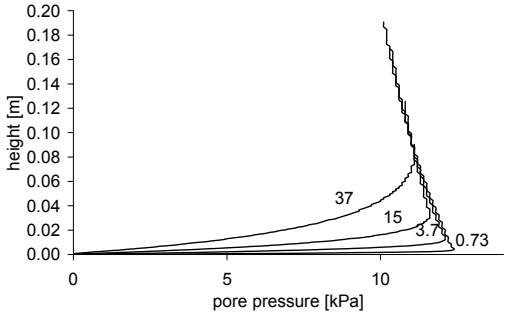

(b)

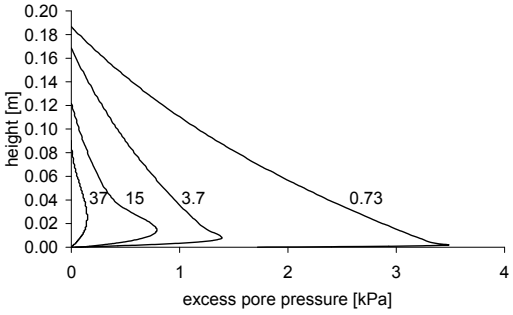

(c)

Figure 7. Calculated effective stress (a), pore pressure (b) and excess pore pressure (c) over the height of the mud at an hydraulic head of 10 kPa on top of the sample.

Analysis of soil sample

Figure 8 shows the void ratio along the height of the soil sample after the test derived from the measured water contents and from the calculations in FSCONBAG. The measured void ratio shows good correlation with the calculated value for all three tests. At the top of the consolidated sample, the void ratio is close to its original value, while close to the bottom the void ratio is reduced to a value of 1 (which corresponds with a water content of about 30%). The measured void ratios close to the bottom are higher than the calculated values, which might be due to the bridging of particles close to the filter or loss of some fine particles in or through the filter. A higher pressure on top of the sample leads only to a slightly lower void ratio at the bottom of the sample.

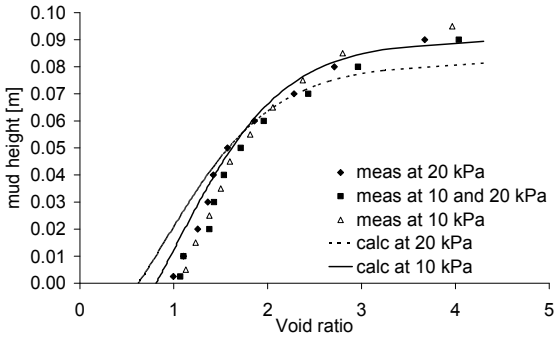

Figure 8. Void ratio along the height of soil sample after the test.

Analysis of geotextile filters

Figure 9 shows the filters before and after the use. It is clear that fine soil particles and bitumen had accumulated on and in the filters. The LDFD filter, shows dirt up to the edges of the filter, which is due to the rubber O-ring used in the first test. This ring was not thick enough to prevent seepage between filter jacket and sidewall. For the other tests a double O-ring was used and seepage was successfully avoided (Figure 10b).

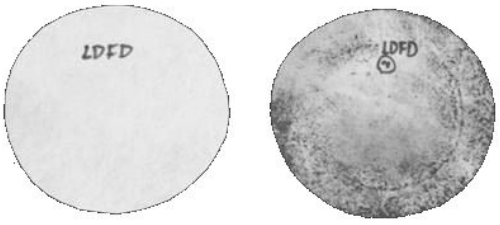

(a)

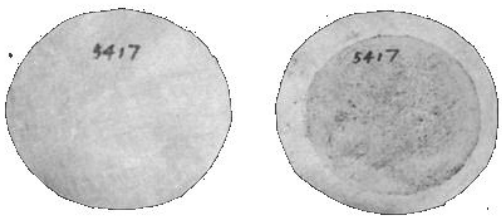

(b)

Figure 9. Geotextile filter jacket before (left) and after the test (right): (a) LDFD, (b) 5417HS.

Although the filters were covered with some fine soil or bitumen they were not seriously clogged.

Table 3 compares the dry weight of all the filter jackets before and after the test. The increase in weight of the filters during the test demonstrates that a certain amount of soil particles were trapped among the geotextile fibers. Additionally, it is interesting to find that for all the filters, the relative increments are almost identical, which may prove that in this test the difference of the three geotextiles does not affect the clogging behavior.

Table 3. Weight comparison of the filters before and after the test.

Geotextile filters	LDFD	5417HS	D165
Dry weight before (g)	1.49	1.92	2.33
Dry weight after (g)	1.77	2.28	2.76
Net increase (%)	18.8	18.8	18.5

The authors used the same test apparatus to measure the hydraulic conductivity of the filter after the completion of the test and removal of the sludge using a constant head method. It was found impossible to determine the flow rate with sufficient accuracy because the filter was still too permeable. Therefore it is considered that the permeability of the jacket is not the limiting factor in the soil/geotextile system.

The performances of filter jackets with respect to the possible clogging mechanisms in the test as mentioned before are evaluated as follows:

1. The geotextile filter jackets were able to retain the tailings particles. Only a few fine particles migrated through the filter jackets during the beginning of the test. Clogging of the cores of PVDs is very unlikely to happen in reality.
2. The increased weight of the filter jackets after the tests demonstrated that some particles were trapped among the fibers of the geotextile jackets, however, this phenomenon was not significant to seriously reduce the permeability.
3. Blinding of the filter jackets by formation of a clear filter cake that stuck to the surface of the filter jackets was not observed when the samples were dismantled from test apparatus.
4. The solid content around the filter jackets increased during consolidation and the permeability of the soil decreased along with the void ratio. After the completion of the tests the permeability was reduced by a factor of about 1000. The measured results were reasonably corresponding with the calculations in FSCONBAG, while the soil properties used in the simulations corresponded with literature values on similar tailing material. Using the finite strain consolidation model of FSCONBAG, other configurations with higher slurry levels, other types of oil sands tailings and different drainage conditions can be simulated. However, the model still requires to be improved in order to consider multidirectional flow and settlement (the currently used version only considers 1D consolidation) and enable the use of non-linear relationships between void ratio and the logarithmic of hydraulic conductivity and effective stress
5. The residual bitumen did not accumulate on the filter jackets after the test. This was concluded after visual inspection of jackets.

Finally, the fact that the used filter jackets were still very permeable after the tests confirms that they are not clogged by oil sands TT in the filtration tests.

CONCLUSIONS

The filtration behavior of thickened oil sands tailings has been studied using different geotextiles filter jackets and applied hydraulic pressure gradients. The following major conclusions may be derived.

1. Permeability of the sludge/geotextile system decreases with increasing solid content of soil sample irrespective of the type of geotextile used and pressure applied on the system.
2. The bitumen as well as the fines in the sludge does not cause serious blinding or clogging of filter jackets. During the test period as long as 40 days of application, the filter jackets functioned properly.
3. The layer of consolidated fine tailings adjacent to the jackets decreases the permeability of the system dramatically, but does not affect functioning of the filter jacket. In other words, it is the consolidation behavior controlling the permeability characteristics of TT; the filter jackets do not control the long-term filtration performance of the system.

4. The soil sample under higher pressure gains higher solid content compared with others with the same filter jacket. There is no direct relation found in the test between the pressure difference and clogging behavior of filters.
5. In this study it is found that gas production may occur, but the produced gas will escape soon and not hamper the consolidation process in a considerable way.
6. This study which evaluates the performance of geotextiles with oil sands fine tailings has practical significance in the design of PVD for tailing pond applications.

ACKNOWLEDGMENT

The authors want to acknowledge Shell (Game changer) for their support, Albian Sand for supplying the test material, Dr. Greeuw for his support in the use of FSCONBAG and Cofra for the deliverance of the filter jackets.

REFERENCES

ASTM (2000) Annual book of standards. Philadelphia: American Society for Testing and Materials.

Azam, S. and Scott, J. D. 2005. Revisiting the ternary diagram for tailings characterization and management. Waste Geotechnics, December:43-46.

Aziz, A.A., Mohammed, T.A. and Omar, H. 2008. Filtration performance of a silt/geotextile system within a triaxial permeameter. Proceedings of the 4th Asian Regional Conference on Geosynthetics, 2008:415-419.

Greeuw, G. and Best H. 1999. Manual FSCONGAS version 2.1, report nr. CO-378630/49, Delft Geotechnics (Deltares)

Liu, B.Y. and McKenna, G.1998. Application of Wickdrains in consolidated tailings (personal communication).

McGown, A. 1976. The properties and uses of permeable fabric membranes. Proceedings of the Workshop on Materials and Methods for Low Cost Road, Rail and Reclamation Works, Lee, Ingles and Yeaman, Eds. published by the University of New South Wales, Leura, Australia, September ,1976: 663-710.

Palmeira, E.M., Fannin, R.J. and Vaid, Y.P. 1996, A study of the behaviour of soil-geotextile systems in filtration tests, Canadian Geotechnical Journal, 33: 899-912

Pollock, G.W., Mc Roberts, E.C., Livingstone, G., Mc Kenna, G.T. and Matthews, J.G. 2000. Consolidation behaviour and modelling of oil sands composite tailings in the Syncrude CT prototype, Tailing and Mine Waste ’00. Rotterdam: Balkema.

Rao, G.V., Gupta K.K. and Pradhan, M.P.S. 1991. Long-term filtration behavior of soil-geotextile system. Geotechnical Testing Journal, Vol.15, No.3: 238-247.

Sobkowicz, J.C. and Morgenstern, N.R. 2009. A Geotechnical perspective on oil sand tailings. Tailings & Mine Waste ’09. University of Alberta, held in Banff, Alberta, November 2009.

Scott, J.D. and Cymerman, G.J. 1984. Prediction of viable tailings disposal methods. ASCE Proceedings of a symposiuim on sedimentation and consolidation models: 522-544. San Francisco, California, USA.

Scott, J.D., Jeeravipoolvarn, S. and Chalaturnyk, R.J. 2008. Tests for Wide Range of Compressibility and Hydraulic Conductivity of Flocculated Tails. Proceedings of the 61st Canadian Geotechnical Conference, Edmonton, Alberta: 738-745.

Suthaker, N.N. and Scott, J.D. 1996. Measurement of Hydraulic Conductivity in Oil Sand Tailings Slurries. Canadian Geotechnical Journal, N33: 642-653.

Wells, P.S. and Caldwell, J. Vertical “wick” drains and accelerated dewatering of fine tailings in oil sands. Tailings & Mine Waste ’09. University of Alberta, held in Banff, Alberta, November 2009.

Yao,Y., A.F.van Tol, H.J.,Everts and A. Mulder. 2010. Proceedings of 14th International Conference on Tailings and Mine Waste. Vail, Colorado, USA.

SEGREGATION AND DIFFERENTIAL SETTLING IN FLOCCULATED TAILINGS

Raymond S. Farinato, Amir Mahmoudkhani, Tom Fenderson, and Philip Watson
Atlanta R&D Centre, Kemira, Atlanta, Georgia, USA

ABSTRACT

In order to comply with federal regulations, dewatered oil sands tailings slurries must become trafficable, defined as having yield strength above 10 kPa after 5 years. Achieving this level of yield strength requires not just a sufficient concentration of solids, but also adequate interparticle forces that result in sufficiently strong networks. Complicating matter is the broad particle size distribution characteristic of oil sands tailings, ranging from microns to millimeters, typically divided at the 44 μm mark into 'fine' and 'coarse' particle categories. In addition to interparticle interactions and solids volume fraction, the particle size distribution will impact material properties of settled beds and their subsequent dewatering rates after thickening. Mineralogy, on the other hand, defines the nature of surface properties and morphology of the particles, and hence dewatering of this heterogeneous system.

Tailings also naturally stratify during settling according to Stokes' Law, with coarse particles concentrated at the bottom of a sedimented bed and fines at the top. This segregation and stratification can also impact mechanical and dewatering properties. Adding an efficacious flocculant or coagulant will alter the settling properties of the treated tailings, thereby having the potential to alter stratification, mechanical and dewatering properties of the settled bed.

Model blends of coarse and fine oil sands tailings were prepared in fixed proportions, and the effects of these size distributions on stratification after gravity settling, with and without the addition of polymeric flocculants and inorganic additives, were determined. Floc and settled bed morphologies were observed microscopically, while mechanical properties were determined rheologically. These properties were determined as a function of the initial particle size distribution, treatment type and height in the settled bed.

INTRODUCTION

Background

Ever since commercial production of oil from the Athabasca oil sands began in 1967, one of the challenges has been tailings disposal. Production of 1 barrel of bitumen typically results in 1.8 metric tons of waste solids in the form of a low-solids tailings slurry (Cabrera, et al., 2009). Tailings slurries are discharged into ponds where the solids slowly settle and dewater. However, ERCB Directive 74 (2009) has required a re-evaluation of the procedures currently in use. In order to achieve the stated target properties, tailings must rapidly dewater and the recovered solids composition must have sufficient shear strength such that it is strong enough to support traffic within 5 years. This will require improvements in settling rates and extent of dewatering in much of the current practices.

Solid-liquid separation of finely divided suspensions often requires chemical treatment to enhance settling rates and to tailor the morphology of the settled bed to result in adequate dewatering rates and extents. This is especially true under circumstances where the settling and dewatering is driven mainly by gravity, as is the common practice in oil sand tailings management. Chemical treatment can include the addition of simple salts, pH modifiers, coagulants, flocculants, or combinations thereof. Such treatments are designed to form aggregates by destabilizing suspended fine solids through either a process of coagulation, flocculation, or both. As always, water chemistry is an important factor in the action of these chemicals by virtue of its affect on speciation of the additives as well as the solid surfaces.

Aggregate formation not only affects settling rate and completeness of separation, but it also governs the structure of the settled bed, which in turn affects dewatering and compressibility of the network of particles. These features impact the ultimate material properties of the dewatered solids and the rate at which those final properties are attained. Thus to obtain appropriate mechanical

properties of the final paste, the structure of the network of aggregated particles must be properly engineered.

Aggregated (coagulated or flocculated) tailings suspensions comprise a very wide range of sizes (sub-micron to over a millimeter) and morphologies, leading to complex settling and dewatering processes, especially since much of the action occurs in either a hindered settling regime or within a compressible network. Such behavior might reasonably result in stratified properties within the settled bed, which will impact dewatering behavior.

Our main purpose in the study reported here was to gain some insight into features of settled beds of oil sand tailings prepared using different chemical treatments. A blend of solids derived from fractionated oil sand tailings was used as the substrate in order to ensure a high level (40 wt-%) of fine particles (< 44 microns). The particles were a mixture of minerals, including silicates, swellable and non-swellable clays, and toluene-insoluble organic material (presumably asphaltenes). The mixture contained virtually no toluene-soluble organics.

Suspensions of this mixture were treated with a variety of coagulants and flocculants, and allowed to settle in cylinders at room temperature. Samples from various depths in the settled beds were excised and analyzed. Sampling from different depths in the settled bed allowed characterization of any stratification. In addition to using analysis methods commonly employed in the oil sands industry (e.g. solids content and dynamic rheometry), we utilized techniques from other disciplines wherein beds of aggregated solids are also studied. These methods included capillary suction time (CST) to evaluate drainage properties, and steady-state floc size distributions as a function of mixing intensity to evaluate aggregate strength.

EXPERIMENTAL

Tailings & Treatments

Oil sand tailings from a variety of sources in Athabasca region of Alberta, Canada were extracted with hot toluene in a Soxhlet apparatus over a period of four hours. The extracted solids were dried and sieved into two fractions (< 44 microns and > 44 microns). These were mixed in a weight ratio of 60% coarse to 40% fines in a master batch. This ratio was selected to mimic tailings from a very low-grade oil sand ore. 10 wt-% slurries of these solids were made in tap water prior to treatment and settling.

Chemical treatments included:

1) gypsum (MP Biomedicals; ACS reagent grade)
2) polymer A (Kemira; flocculant grade poly(acrylamide(70)-co-acrylate(30))
3) polymer N (DOW; flocculant grade polyethylene oxide)
4) mixture of #2 and mixed inorganic coagulants

The flocculant grade water-soluble polymers were of comparable weight average molecular weights, approximately 5 million Daltons.

Settling Apparatus & Sampling

Settling tests were performed in either 100-mL or 1-L graduated cylinders. Treatment chemicals were mixed into the tailings slurry using a perforated disk mounted on a steel rod. Three transits of the disk (up and down) through the slurry were sufficient for mixing. Plastic 1-L graduated cylinders with tapped holes at several heights were used to sample at different bed depths. The tapped holes (3/16”, 28 TPI) were plugged during the settling and bed formation stages. These plugs were removed in order to extract samples (typically 20 mL) of the settled bed for analyses. The samples thus extracted were divided for analyses (oven solids [2 hrs @ 120 °C], CST, PSD, rheometry). A photograph of a 1-L cylinder with sampling ports is shown below.

Capillary Suction Time (CST)

The Capillary Suction Time (CST) test has been used since the 1970’s as a practical, yet empirical method for characterizing dewatering and the state of colloidal materials in watsewater treatment facilities (Scholz, 2005). The main use for the CST is to determine filterability of the flocculated solids after the addition of coagulant and/or flocculant aids.

The dewatering properties of materials excised from settled beds of treated tailings were measured using a capillary suction time method as described in Standard Method APHA 2710 G (APHA, 1999). CST measurements were carried out using a CST instrument from Venture

Innovations Inc. (California, USA). The CST is the time interval it takes an aqueous solution to traverse between two radial positions in a filter paper (Whatman No. 1, 11 cm) under the influence of capillary suction. A low CST value implies good sludge dewatering; i.e. the water from the paste releases quickly with little impediment. Each measurement was conducted at least in triplicate and the average presented here. The time for distilled water blanks (10.8 ± 0.7 sec) was subtracted from sample times to improve comparisons and to account for variation in characteristics of the filter paper used.

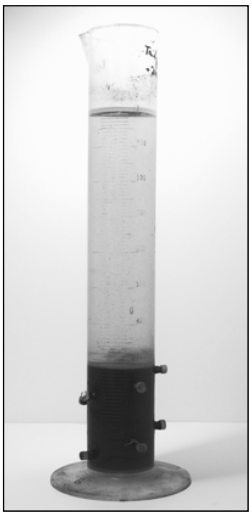

Figure 1. 1-L settling cylinder with sampling ports

Particle Size Determination

Particle size distributions (PSD) were determined with a Malvern Mastersizer S, which measures the angular dependence of scattered light (mainly in the forward direction). Paste samples were dispersed in the impeller driven flow loop of the Mastersizer. The flow loop contained Milli-Q water without additional chemical dispersants. Particle size distributions were computed as equivalent-sphere size distributions based on Mie scattering and Fraunhofer diffraction formalisms applied to the scattering data. The optical constants (λ = 432.8 nm) used for these computations were a complex refractive index of 1.5295, 0.000i for the solids and a real refractive index of 1.3300 for the continuous phase. Measurements were taken during each test at 30, 60, 120, 240, and 360 seconds after addition of the solids to the diluent under continuous agitation at a single impeller speed. This procedure allowed us to assess whether a steady-state size distribution had been achieved. Typically we used the size distributions after 120 sec of mixing for comparisons, since steady state was achieved by this time. By using this procedure at different impeller speeds and comparing steady-state distributions at these various impeller speeds we were able to assess the strength of aggregates.

Material from the 1-L sampling cylinders was gathered by one of two methods. A small portion of the solids from each bed depth was added directly into the Mastersizer dilution cell. The second method was to take dewatered solids from CST measurements, re-suspend them in water with mild shaking, and then measure their PSD.

Material from 100-mL cylinder tests was sampled as an ensemble. A portion of the flocculated bed was wet-sieved through a 106-micron screen and the PSD of the -106 micron fraction was measured. This procedure was used in order to focus on changes in the finer fraction of solids derived from each treatment.

Dynamic Rheometry

Rheological investigations were conducted at 22°C on an Anton-Paar MCR 300 rheometer equipped with 50-mm parallel plates set to a gap of 1 mm. Aliquots of flocculated tailings that had been removed from different heights of the 1-L graduated cylinder were added to the rheometer via 2-mL disposable Pasteur pipettes. Measurements began with an amplitude sweep in which the oscillatory strain was logarithmically increased from 0.001 to 100% while the oscillatory frequency was held constant at 10 s^{-1}. The linear viscoelastic region was determined from this data by noting the range of amplitudes where the storage modulus G' had a flat slope.

Next, frequency sweeps were performed on fresh samples by holding the amplitude to a constant value within the linear viscoelastic region and then logarithmically decreasing the frequency from 100 to 0.1 s^{-1}. We used a strain of 0.01% for the lower-solids flocs taken from the cylinder at heights at the 250 and 150 mL marks, and a strain of 0.1% for the flocs withdrawn at the 25 mL mark.

RESULTS

Treatment doses were chosen based on experience with tailings of this nature and some preliminary screening data. These doses were:

1) Gypsum: 200 g/dry T
2) Polymer A: 80 g/dry T
3) Polymer N: 80 g/dry T
4) Dual: mixed inorganic coagulant @ 1000 g/dry T and polymer A @ 100 g/dry T

After mixing the tailings and chemicals the settled bed typically formed from the top down; i.e. the column of settling slurry formed a discernable interface with the clarified volume above it and this interface dropped with time, finally forming a compact bed. The initial settling rates for the various treatments ranked as follows, in increasing order: untreated < gypsum < dual < polymer N < polymer A.

Stratification of Solids Content & CST Values

The figures 2 and 3 below are assays of the solids and CST values vs bed depth for settled beds of tailings treated with either gypsum, polymer A, polymer N, or a dual treatment consisting of a mixed inorganic coagulant and polymer A. The 'lower cut' sample was taken at a position ¼ of the bed height from the bottom, the 'middle cut' sample was from ½ of the bed height from the bottom, and the 'top cut' was from ¾ of the bed height from the bottom. Settling was allowed to proceed overnight to ensure equilibration. Final bed heights ranged from around the 230-mL to 280-mL marks. Standard deviations for the CST measurements averaged about 3%.

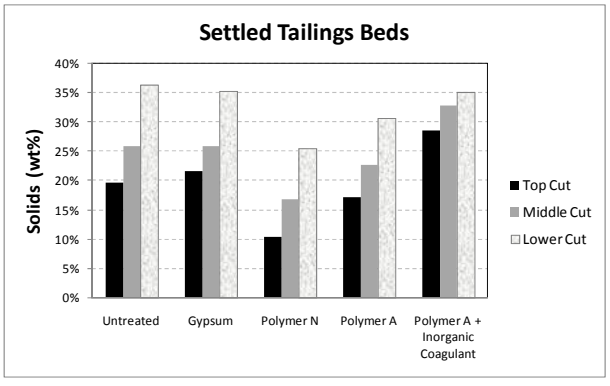

Figure 2. Settled bed solids content vs. bed depth

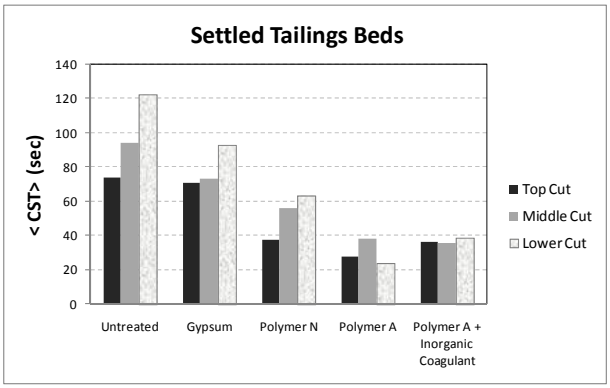

Figure 3. Settled bed CST vs. bed depth

Clearly these data depict stratification in most of the settled beds. An increase in solids with depth is expected from the gravitational forces operating on these compressible networks (figure 2). Note that the polymer flocculant treatments resulted in generally more expanded beds with better dewatering rates (lower CST values) than did treatment with just gypsum. Even though the anionic flocculant (polymer A) produced higher solids beds compared to the nonionic flocculant (polymer N), it still had measurably better dewatering rates (figure 3).

The settled beds produced from tailings treatments with either polymer A alone, or polymer A in combination with mixed inorganic coagulants had much less stratification of dewatering rates than the other treatments. In fact, the dual treatment resulted in a dewatering rate independent of depth in the settled bed. Except for the tailings treated with polymer A, dewatering was slower (larger CST value) at greater depths in the settled bed.

Particle Size Distributions

Steady-state particle size distributions under fixed mixing conditions have been used to assess the floc strength and breakage pattern of flocculated solids, mainly in wastewater treatment applications (Jarvis, et al, 2005). We applied this method to flocculated oil sand tailings in the impeller-type mixer that is a component of the Malvern Mastersizer S.

Samples of settled tailings treated in 100-mL cylinders were recovered and gently wet-screened to collect the < 106 micron fraction, which was then diluted directly in the Malvern mixer. This pre-fractionation was done in order to have better definition of the size distributions in the sub-200-micron range. The bed volume in the

100-mL cylinders was typically about 20 mL, so no attempt was made to determine stratification in these small bed volumes; the bed was sampled at about the half-height mark. Note that the amounts of material added to the Malvern mixer result in very high dilution ratios (i.e. a few tenths of a gram of solids in 100 mL of water). Steady-state particle size distributions were determined at several impeller speeds; however, only results for three speeds that span the entire range are shown in the plots below for visual clarity.

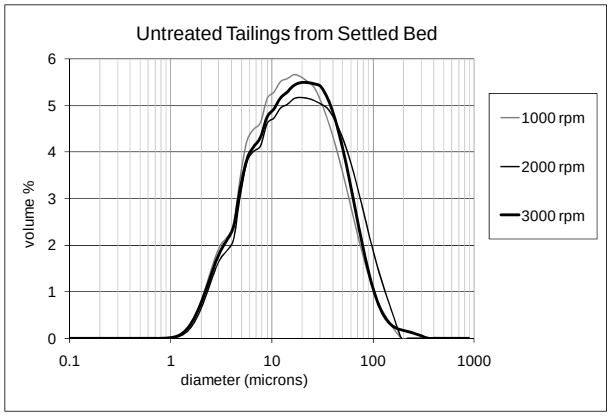

Figure 4. Effect of impeller speed on untreated tailings from settled bed

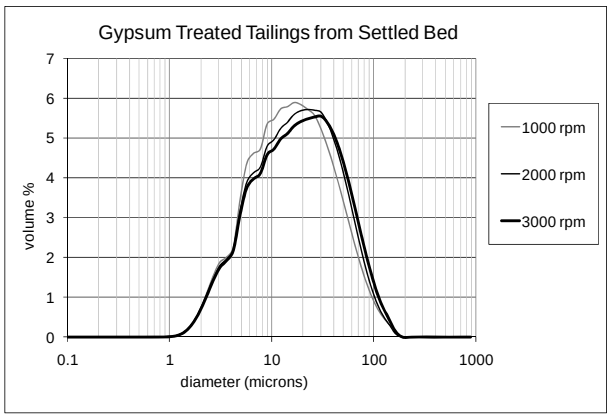

Figure 5. Effect of impeller speed on gypsum treated tailings from settled bed

Floc fragmentation was most clearly evident in the tailings treated with either polymer N, polymer A alone, or the mixed inorganic coagulant and polymer A (dual treatment).

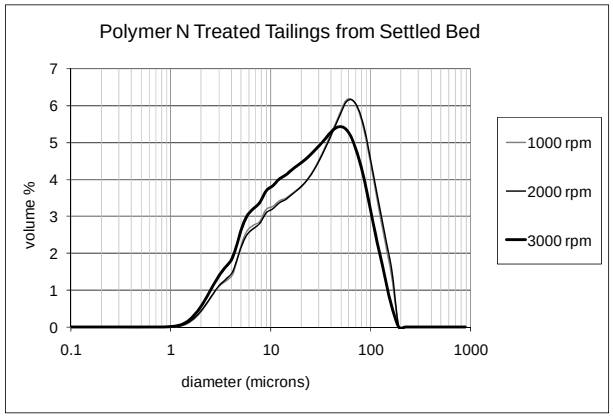

Figure 6. Effect of impeller speed on Polymer N treated tailings from settled bed

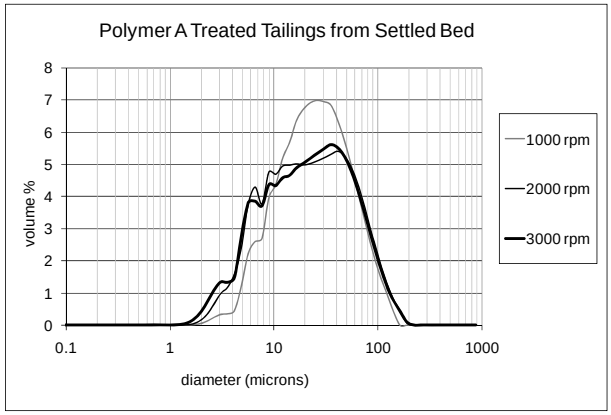

Figure 7. Effect of impeller speed on Polymer A treated tailings from settled bed

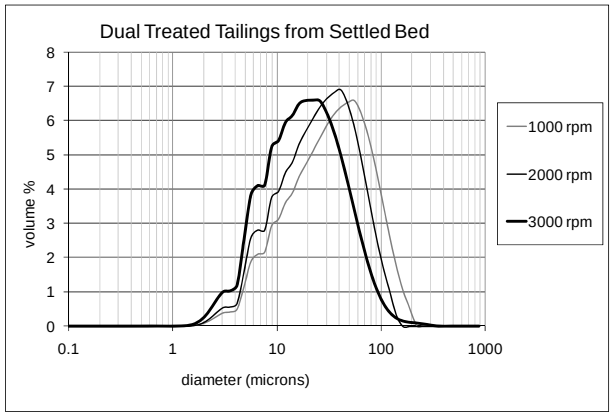

Figure 8. Effect of impeller speed on dual treated tailings from settled bed

The untreated and gypsum-treated tailings exhibited no evidence of agglomerate fragmentation under the impeller speeds employed.

We also investigated stratification effects in the settled beds from 1-L cylinder tests. Treated tailings samples extracted from different bed depths were all sized under steady-state conditions at 2000 rpm impeller speed. Those results are shown in the figures below. Recall that the 'bottom' sample was taken at a position ¼ of the bed height from the bottom, the 'middle' sample was from ½ of the bed height from the bottom, and the 'top' sample was from ¾ of the bed height from the bottom.

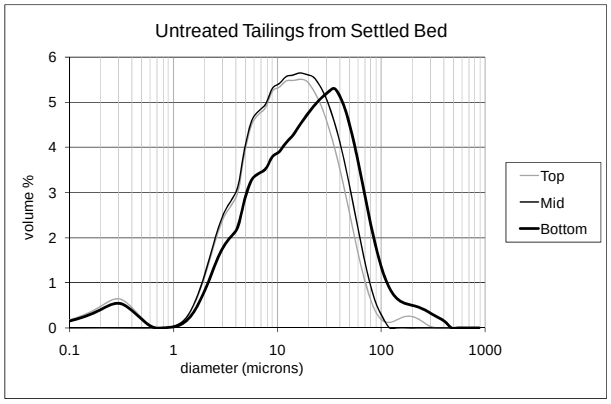

Figure 9. PSDs for untreated tailings from different depths in the settled bed

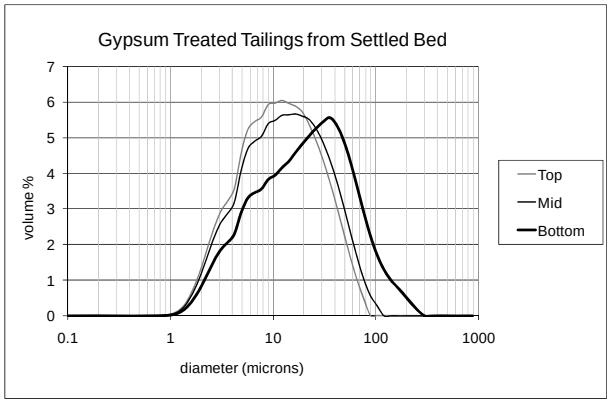

Figure 10. PSDs for gypsum treated tailings from different depths in the settled bed

There was clearly stratification with respect to particle size distributions for the untreated tailings, as well as those treated with gypsum or polymer N. Interestingly, treatment with polymer A appeared to mitigate stratification.

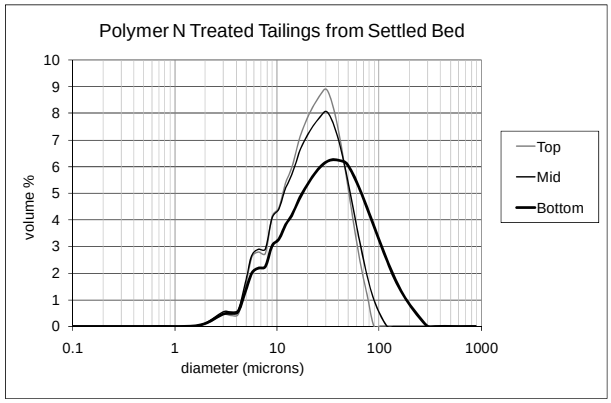

Figure 11. PSDs for polymer N treated tailings from different depths in the settled bed

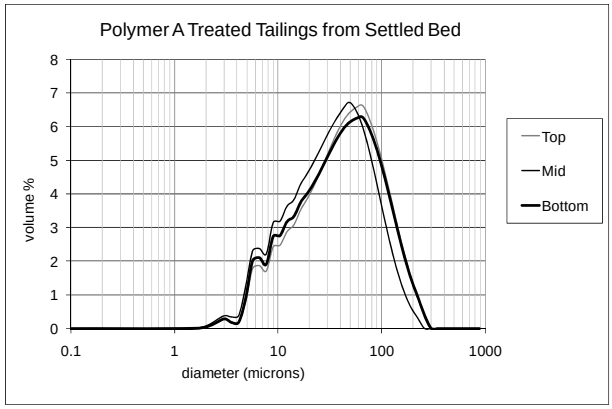

Figure 12. PSDs for polymer A treated tailings from different depths in the settled bed

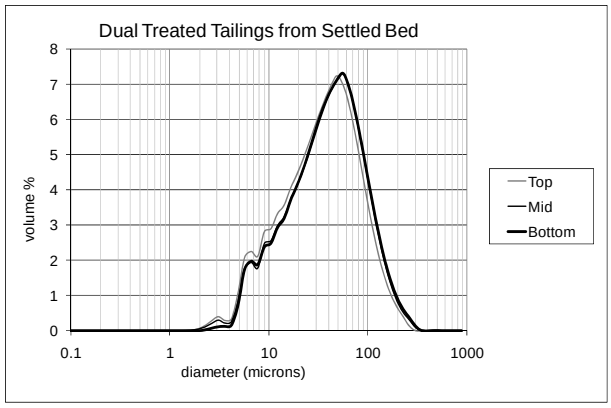

Figure 13. PSDs for dual treated tailings from different depths in the settled bed

Recall that polymer A also mitigated stratification as determined from the CST dewatering results. Thus, while polymer A and polymer N both flocculate suspended fines, they produce different structures in the bed network.

Dynamic Rheometry

Some insight on the microstructure of networks of flocculated particles may be acquired from their rheological behavior, especially from oscillatory rheometry (McFarlane, et al, 2005). The dynamic rheometry data shown in the figures below are in the form of damping factors, tan(δ), which equal the ratio of the loss modulus to the storage modulus (G"/G').

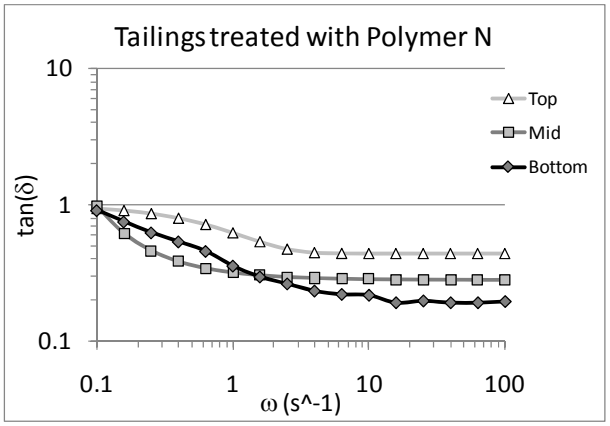

Figure 14. Oscillatory rheometry of settled tailings treated with polymer N at several depths in the bed.

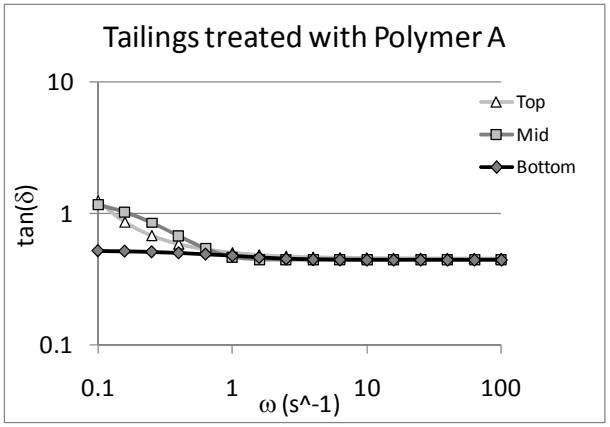

Figure 15. Oscillatory rheometry of settled tailings treated with polymer A at several depths in the bed.

Except at very low frequencies, the flocculated beds have damping factors between 0.1 and 1, indicating the presence of weak network structures. For tailings treated with polymer N the values of tan(δ) decrease deeper into the settled bed. Recall that the wt-% solids increased with depth in the bed for the same system (see figure 2). So the network became more elastic with depth. Conversely, the samples obtained from different column heights within the tailings bed treated with polymer A showed little difference in tan(δ) as a function of depth in the bed, despite the increase in wt-% solids with depth in the bed. The oscillatory rheometry data are consistent with the conclusions drawn from CST and solids measurements. Stratification is evident in the settled tailings treated with polymer N; however, the tailings treated with polymer A exhibited more uniformity with depth in the settled bed.

DISCUSSION

A consistent story emerges from the data presented above. Even though the analytical methods used do not yield very precise structural details about the networks that constitute the settled beds, we found that the methods are sensitive enough to identify important differences amongst tailings treated with different coagulants and flocculants. Indeed there were the expected density and dewatering gradients in the settled beds simply due to gravitational forces; however, it was not expected that some treatments could greatly mitigate the stratification of dewaterability.

Untreated tailings did settle slowly with time to form a compact bed with stratified material properties and the poorest dewaterability. Aggregates did not form, as evidenced by the PSDs that did not change with mixing intensity.

Tailings treated with gypsum settled into a stratified bed that had a similar density profile as the untreated tailings; however, the dewaterability was slightly improved. This might be expected from the application of a coagulant that compressed the electrical double layers in the electrostatically stabilized fine particle fraction, thereby creating very small aggregates from the fines. This picture is supported by the PSD data as a function of mixing intensity.

Treatment of the tailings with the two polymers produced substantially different settled beds compared to those made from the gypsum-treated

or untreated tailings. Either polymer tended to result in a less dense settled bed; more so with polymer N than with polymer A. Dewatering was also significantly improved in both cases; although more so with polymer A. The tailings flocculated with either polymer tended also to be more shear sensitive. All of these behaviors are consistent with aggregate formation due to polymer bridging of some of the fine solids. An example of flocculated tailings from treatment with polymer A is shown in the photomicrograph below.

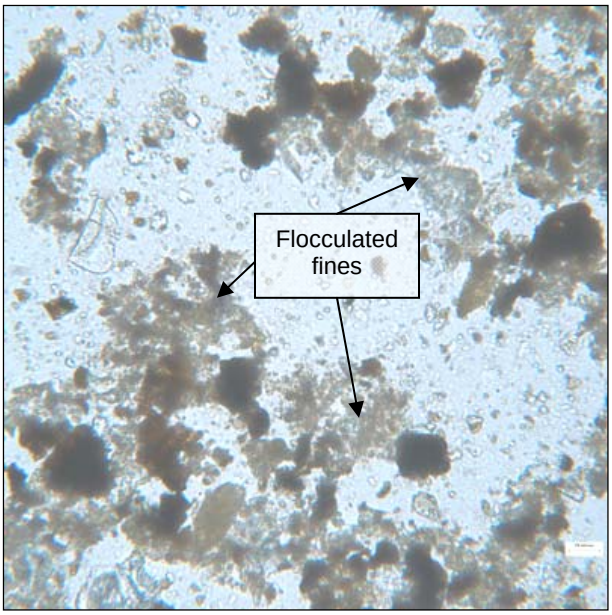

Figure 16. Optical photomicrograph of tailings fine particles flocculated with polymer A. Scale bar (lower right) is 20 microns.

The fact that polymer N formed less dense settled beds than did polymer A suggests that those aggregates may be somewhat stronger. However, the configuration of the network formed from tailings treated with polymer A dewaters measurably better than that made with polymer N. If the tailings network formed with polymer N were simply less dense, then one would expect it to dewater more rapidly. Since this was not the case we have to assume the two networks are not simply related by an affine transformation (i.e. a simple scaling with no change in microstructure).

The dual chemical (inorganic coagulant + polymer A) treatment created a settled bed that retained high solids content, good dewaterability and a mitigation of stratification. The aggregates were susceptible to shear breakage; however, it is uncertain whether this is detrimental or beneficial in a large-scale setting.

The conclusions discussed above may be put in the form of a simple cartoon (see Figure 17) that captures the essentials of our hypotheses regarding the networks formed from chemically treated tailings.

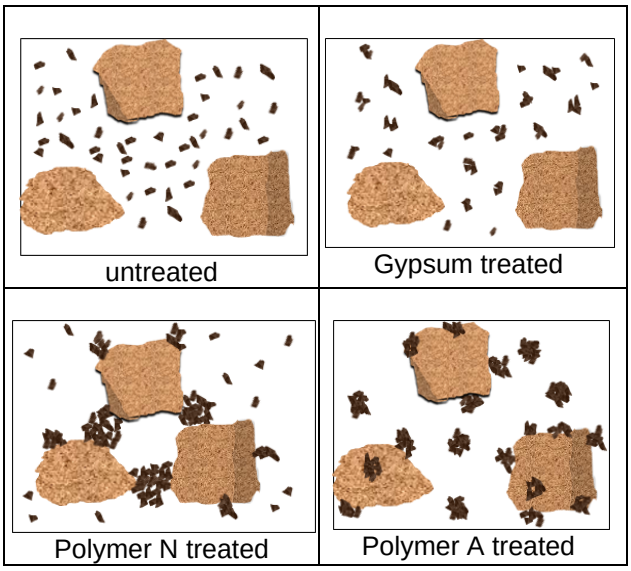

Figure 17. Schematic representation of our hypothesis.

SUMMARY

We have shown that several simple measures of chemically treated oil sand tailings, some of which have not traditionally been used in oil sands research, can yield insight into the networks formed in settled beds. Stratification of solids content and dewaterability in these settled networks was quantified. This allowed us to determine treatments where this stratification was mitigated. Optimum treatments where the settled bed has high solids, good dewaterability and minimal stratification can and were identified using this system of metrics.

REFERENCES

S. C. M. Cabrera, J. Bryan, B. Komishke and A. Kantzas. 2009. Study of the settling characteristics of tailings using nuclear magnetic resonance technique. International Journal of Mining, Reclamation and Environment, 23:33 - 50.

Energy Resources Conservation Board Directive 074, Tailings Performance Criteria and Requirements for Oil Sands Mining Schemes (Released: February 3, 2009); http://www.ercb.ca/docs/documents/directives/directive074.pdf

M. Scholz, 2005. Review of recent trends in Capillary Suction Time (CST) dewaterability testing research. Ind. Eng. Chem. Res. 44, 8157.

Standard Methods for the Examination of Water and Wastewater. 20th Edition, 1999. American Public Health Association, American Water Work Association, Water Environment Federation, Washington, D.C.

P. Jarvis, B. Jefferson, J. Gregory and S. A. Parsons. 2005. A review of floc strength and breakage. Water Research, 39:3121-3137.

A. J. McFarlane, J. Addai-Mensah and K. Bremmell. 2005. Rheology of flocculated kaolinite dispersions. Korea-Australia Rheology Journal, 17:181-190.

Al-PAM ASSISTED FILTRATION OF MATURE FINE TAILINGS PRODUCED FROM OIL SANDS DEVELOPMENT

Aurangzeb Alamgir, Jacob Masliyah and Zhenghe Xu
University of Alberta, Edmonton, Alberta, Canada

ABSTRACT

Filtration is considered as a dewatering option after flocculating MFT, as it produces stackable solids for backfill (land reclamation) and the highest quality and quantity of water (filtrate) for recycle. In this study, performance as filtration aids of an in-house synthesized, organic-inorganic hybrid flocculant, Al-PAM is compared with a commercial Magnafloc 1011 for treating oil sands mature fine tailings (MFT). Through this study, an optimal process configuration for MFT dewatering is established in terms of MFT dilution, flocculent dosage and recycle of MFT release water as dilution water.

The results showed that the commercial Magnafloc was ineffective as filtration aid for treating MFT. The raw MFT was found irresponsive to Al-PAM flocculant addition. An MFT dilution from 30 wt% solid to 10 wt% solid was identified to be optimal for Al-PAM to be an effective filtration aid, in the context of both flocculant dosage and materials handling. A novel two-step process: Al-PAM flocculation and thickening of diluted MFT using thickener overflow, followed by filtration of thickener underflow to produce a stackable filter cake and virtually solids-free filtrate for recycle was found to be the most appealing. The presence of residual Al-APM in the clarified water was proven to be beneficial when used as MFT dilution water with scaled Al-PAM addition. This study clearly shows that Al-PAM assisted filtration is a viable solution to reduce the volume and liability of MFT while increasing the rate of process-affected water recycle.

INTRODUCTION

Oil sands industry has attracted a worldwide attention due to its massive scale and potential to secure global fuel supply. From Canada's prospective there is no question whether this fuel source should be fully developed or not. However Canada being a responsible nation needs to respond more objectively to international calls regarding the environmental concerns. No doubt the industry is doing everything possible to remove the tag of DIRTY OIL from our enviable energy source. However, despite of all technical advances, especially in oil sands tailings management, it seems that the issue has yet to be fully addressed. More dedicated and joint efforts are required to help industry flourish in a world-wide acceptable manner.

Hot water extraction process is considered water intensive and produces a huge amount of tailings, more than 3 meter cubes for every barrel of bitumen produced. In most of current commercial plants, tailings produced are pumped to large settling ponds referred to as tailings ponds. In tailings ponds, the coarse solids settle quickly as sand beach while the fine particles settle slowly. Many years of settling of fine solids result in the formation of a stable suspension containing about 30 wt% solid, known as Mature Fine Tailings, MFT. Continuous accumulation of MFT is causing a great economic and environmental concern due to its poor consolidation and water release characteristics.

Accumulation of MFT adversely affects ecosystems and poses a risk to wild life in the surrounding area. To resolve oil sands tailings issues, the recently released ERCB directive 074 (ERCB, 2009) sets the following appropriate tailings management objectives for oil sands mines:

- Minimize and eventually eliminate long term storage of fluid tailings in the form of reclamation landscape;
- Create a solid landscape at the earliest opportunity to facilitate progressive reclamation;
- Reduce containment of fluid fine tailings in an external tailings disposal area during operation;
- Maximize intermediate process water recycle to increase energy efficiency and reduce fresh water intake;
- Minimize resource sterilization associated with tailings ponds; and
- Ensure that the liability for tailings is managed through reclamation of tailings ponds.

For better management of oil sands tailings in commercial oil sands operations, the settling characteristics of the fine solids must be improved by an economic and environmentally friendly

approach. Several patents and reports describing techniques to increase the efficiency of the consolidation process are available in open literature. The approaches proposed include:

- Changing pH of the slurry (Baillie and Malmberg, 1969; Schutte, 1974; and Speight and Moschopedis,1977);
- Using flocculating agents (Moschopedis et al, 1977; and Kessick, 1982);
- Agglomeration of fines (Maloney, 1976; Majid and Sparks, 1993)
- Bacterial enhanced-consolidation (Raymond et al, 1970)
- Freeze thaw dewatering (Elliott, 1975)
- Use of intense sound waves (Fear and Camp, 1972)
- Electrophoretically assisted gravitational settling (Flintoff and Plitt, 1976)

These techniques can be applied individually or in combination to shift the segregation boundaries. The segregation characteristics have also been manipulated with chemical amendments.

Through intensive research and development initiatives a number of sound consolidation techniques have been evolved. Composite tailings process and paste technology are already in practice and have their own pros and cons. The objective of this research is to investigate the potential of an in-house synthesized, organic-inorganic hybrid polymer, Al-PAM as flocculating agent of MFT. Sedimentation and filtration tests were conducted to assess settling and densification performance of MFT. This endeavour is intended to optimize dewatering characteristics of MFT.

The ultimate aim of this research is to prove a novel process concept of MFT management and to identify the optimal conditions for production of self-supportive deposits from MFT, in terms of

i) Type and dosage of polymer
ii) Degree of MFT dilution
iii) Process configuration

Optimization of these conditions ultimately results in a maximum recovery of water that is suitable for reuse in oil sands extraction process.

MATERIALS AND METHODS

Following samples of MFT and polymers were used in the course of current study.

Mature Fine Tailings, MFT

The focus of study was to explore the performance of different polymers on densification and filtration of MFT under different experimental conditions. MFT samples from Syncrude Canada were used in this study. The original MFT was analyzed to contain 66 wt% water, 31 wt% solid and 3 wt% of bitumen.

The particle size distribution of the solids in MFT was determined using a Malvern Mastersizer 2000 particle size analyzer. The results show that 96% particles were less than 44 µm (fines) and d_{50} was 6.5 µm.

For each set of tests, a subset of the samples was obtained by vigorously mixing the MFT using an electrically powered mixer for 30 minutes prior to taking a representative sample of the original MFT into 3-L glass bottles.

Flocculants

In current study commercial Magnafloc1011 and Al-PAM were used as flocculants. Magnafloc1011 was purchased from Ciba Specialty Chemicals. It has an average molecular weight of about 17.5 million Daltons and ionic charge density of around 27%. Al-PAM was synthesized in-house and its molecular weight was characterized by viscosity measurement. In the preliminary work, Al-PAM of different molecular weight and aluminum content was used and the Al-PAM with the best performance was identified. The intrinsic viscosity of the selected Al-PAM was 750cm/g. This Al-PAM was used throughout the study.

MFT Dilution

Addition of polymers to raw MFT (31% solid) did not show any improvement on settling and filtration. The dilution of MFT to 15 wt% solids with flocculant addition did not demonstrate visible improvement in both settling and filtration either. Dewatering at measurable rates was observed only when MFT

was diluted to 10 wt% solids or lesser. Since water chemistry plays an important role in controlling the settling behaviour of particles in a suspension, the water extracted from same MFT by pressure filtration was used for dilution of MFT. Tests were performed on raw MFT and MFT diluted to 15 wt%, 10 wt% and 5 wt% solids.

EXPERIMENTAL PROCEDURES

Polymer Addition

Stock solutions of 1000 ppm Al-PAM and Magnafloc1011 were prepared. Magnafloc stock solution, referred to as Magnafloc, was placed on a vibrating plate and Al-PAM solution was kept in a mechanical shaker, both for 24 hours to ensure complete dissolution. The prepared stock solutions were used only for one day. To prepare MFT suspension, 90 g of MFT slurry was taken and homogenized in a 250 mL beaker. To make a total suspension of 100 g, 10 mL of polymer solution was added to 90 g of MFT sample in the following manner:

- Polymer stock solution was added at 0.1 mL/s addition rate to the prepared MFT suspension under agitation at 350 rpm;
- The agitation stopped as soon as polymer addition was over;
- The resultant suspension was poured into a 100-mL graduated cylinder (settling) or 500-mL filter press.

For settling experiments, the cylinder was inverted three times and then placed on a bench. Filtration was started as soon as the flocculated suspension was transferred to the filter press.

Settling Test

Quick formation of big and dense flocs with high mechanical strength represents a better performance of polymer as flocculant. In case of settling the effectiveness of a polymer as flocculant is often measured by:

i) The initial settling rate (ISR), i.e. the slop of settling curve (h/H vs. time) at time 0;
ii) The solid content in the sediment;
iii) The turbidity of the supernatant.

While settling, a clear liquid slurry interface, known as mud line, is seen to descend. The height of the mud line (h) is recorded as a function of settling time. A settling curve is constructed by plotting h/H vs. time, where H represents the initial height of the slurry. The initial settling rate was calculated from the slop of initial settling curve. After the first five minutes of settling, 20 mL of supernatant was removed from the top of the graduated cylinder with the help of a syringe. The turbidity of this supernatant was measured with a HF-Micro laboratory turbidity meter. Turbidity of the supernatant was expressed in Nephelometric Turbidity Unit (NTU).

Settling was continued for one hour after which the entire supernatant was carefully removed. The sediment was weighed and then dried in an oven at 105 ^{o}C for 24 hours. The dried sediment was weighed again and its water content was calculated. These parameters are used to determine the optimum flocculant dosage for MFT thickening.

Filtration Test

Filtration apparatus used in this study is a small laboratory scale unit with 500-mL capacity and 45.8-cm^2 filtration area. All tests were performed under constant pressure of 15 kPa. The filter press is interfaced with a computer loaded with custom-programmed filtration software. For each filtration test, the weight of the filtrate from an electronic balance is continuously recorded by the computer. Filtration results are shown as a plot of filtrate weight vs. filtration time. For all samples, initially filtration rate is relatively high and almost linear but with passage of time it levels off. If filtration is allowed to continue for a sufficient period of time, a filter cake could be produced. In this case, the cake formed is dried in an oven at 105°C to a constant weight for cake moisture analysis. The performance of polymers as filtration aid is evaluated in terms of initial filtration rate (i.e., the slop of the initial linear portion of the filtration plot), filtration time and/or moisture content of filter cake.

Filtration of Sediment

When neither settling nor the filtration, as a single dewatering process, could produce a desirable outcome, an idea of coupling these two processes was proposed. The idea was to thicken the diluted MFT by settling after flocculation, followed by filtration of the sediment. Al-PAM was added to MFT suspension only prior to settling. For most of the suspensions investigated in this study, one hour settling appeared to be sufficient to produce sediment of desired solid content. Settling performance of the samples was measured in terms

of ISR, turbidity of the supernatant and solid content of the sediment. Thickened slurry (sediment) was filtered under regular filtration conditions. Dewatering efficiency by filtration was measured in terms of filtration rate, filtration time and filter cake moisture content.

Water Recycle

Two streams of water are recovered during the experiment i.e. supernatant and filtrate. Either of these two streams could be used for dilution of MFT. Here decision is made to use supernatant for dilution. Filtrate is almost solid free water and could be used in bitumen extraction process.

RESULTS

With proper dilution, both settling and filtration rates of slurries seemed to increase with increasing polymer dosage up to a certain value after which, a further increase in polymer dosage decreases settling and filtration rates.

Settling

Initial Settling Rate (ISR)

As shown in Figures 1 and 2, both commercial Magnafloc and in-house synthesized Al-PAM showed little improvement in ISR of raw MFT. MFT dilution to 15 wt% solid showed little effect.

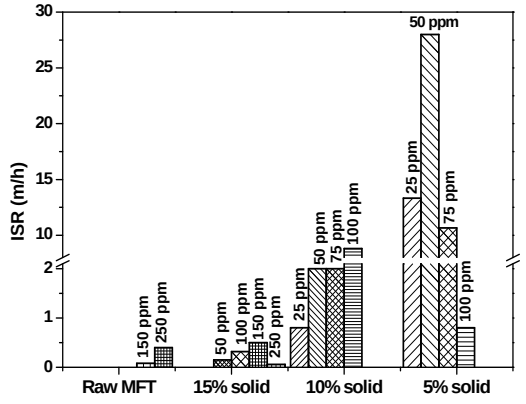

Figure 1. Initial settling rate of MFT with Magnafloc as flocculant.

However, after dilution to 10 wt% and 5 wt% solid, polymer addition showed a pronounced improvement on solids settling of diluted MFT. For MFT dilution to 10 wt% solid, for example, the fastest ISR was 8.8 m/h and 6.25 m/h for Magnafloc at 100 ppm and Al-PAM at 75 ppm, respectively. In the case of dilution to 5 wt% solid, the fastest ISR was 28 m/h and 18.2 m/h for Magnafloc and Al-PAM, respectively, both at 50 ppm. It is evident that at optimal dosages, Magnafloc is more effective than Al-PAM in flocculating MFT after proper dilution, determined by ISR.

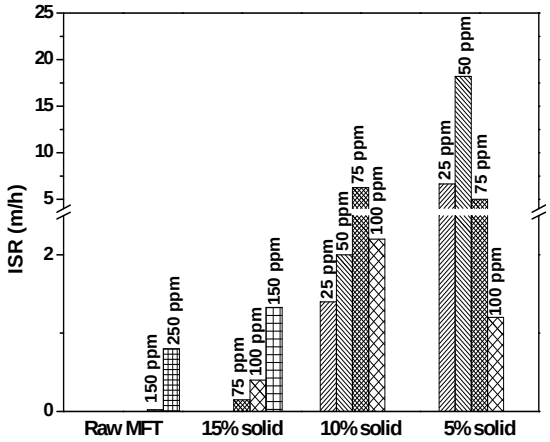

Figure 2. Initial settling rate of MFT with Al-PAM as flocculant.

Turbidity of Supernatant

Turbidity of supernatant was measured after flocculant addition and settling of five minutes. As shown in Figures 3 and 4, the supernatant of raw MFT and diluted MFT to 15 wt% solid remains highly turbid at all polymer dosages.

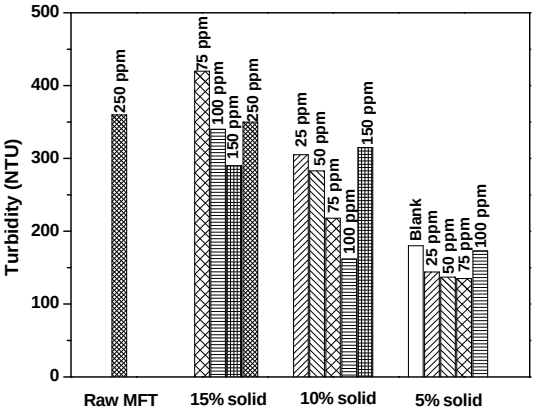

Figure 3. Turbidity of supernatant produced after settling of MFT with Magnafloc as flocculant.

After proper MFT dilution, turbidity of the decanted supernatant decreased with increasing polymer dosage up to optimum value. A further increase in

dosage resulted in an increase in supernatant turbidity. For MFT diluted to 10 wt% solid, the lowest turbidity values were 162 NTU and 156 NTU for Magnafloc at 100ppm and Al-PAM at 75ppm, respectively. In the case of MFT dilution to 5 wt% solid, the lowest turbidity values were 135 NTU and 127 NTU for Magnafloc at 75ppm and for Al-PAM at 50ppm, respectively. Clearly, high dilution is beneficial for producing higher quality supernatant and Al-PAM is more effective that Magnafloc in flocculating ultrafine particles, measured by lower turbidity of supernatants.

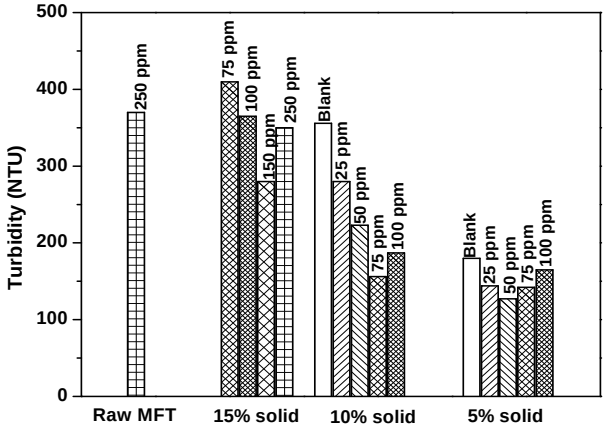

Figure 4. Turbidity of supernatant produced by settling of MFT with Al-PAM used as flocculant.

Solid Content of Sediment

Solid content analysis of the sediment was made after one hour of settling. Shorter settling time was found insufficient for most of the samples to produce desirable sediment. The result in Figures 5 and 6 show that flocculation of diluted MFT does not improve densification of the sediments. After MFT dilution to 10 wt% solids, for example, the maximum solids content was determined to be 30 wt% and 29 wt% with 75 ppm Magnafloc and Al-PAM addition, respectively.

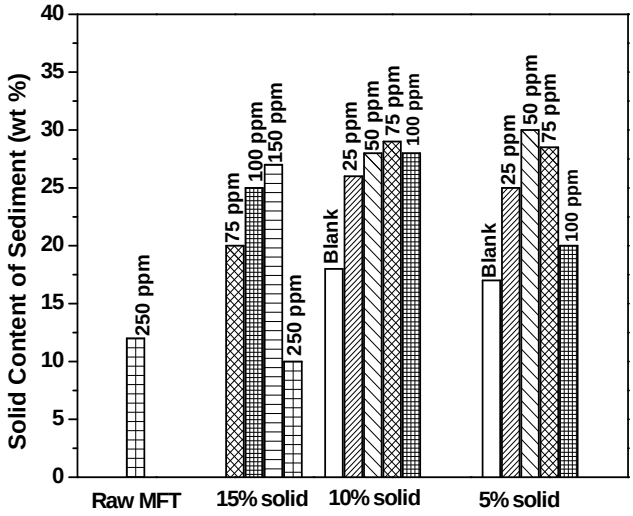

Figure 5. Solid content of sediment after settling of MFT with Magnafloc as flocculant.

FILTRATION

Although commercial Magnafloc performed slightly better than Al-PAM in settling, it could not enhance dewatering of MFT by filtration as shown in Figure 7. In contrast, Al-PAM was found to be effective in enhancing filtration of diluted MFT as discussed next.

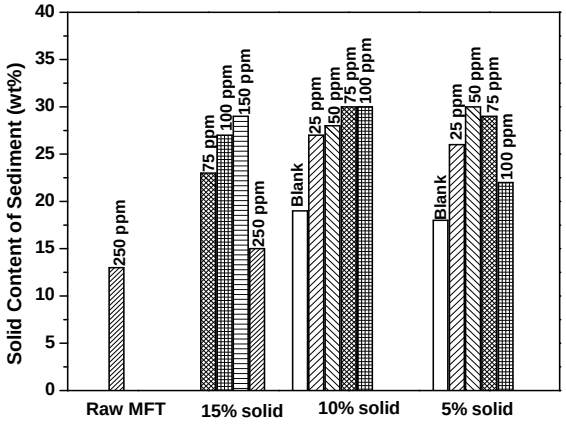

Figure 6. Solid content of sediment after settling of MFT with Al-PAM as flocculant.

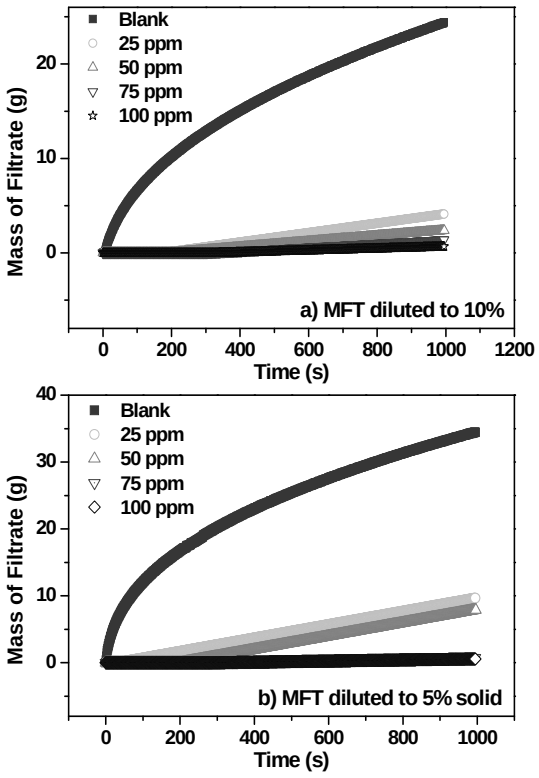

Figure 7. Filtration rate of MFT diluted to 10% and 5% solids using Magnafloc as filtration aid.

Filtration Rate

Typical filtration curves obtained with Al-PAM addition are shown in Figure 8. For a given suspension, filtration rate decreases with time. Ultimately the filtration curve becomes horizontal, indicating the completion of filtration. Even with optimum polymer dosages, filtration rate of raw MFT and diluted MFT to 15 wt% solid was very slow. With further dilution, Al-PAM addition significantly improved filtration rate of diluted MFT. With a dilution to 10 wt% solid, filtration for 1000 seconds yielded 25 grams of filtrate without polymer addition. Addition of 25 ppm, 50 ppm and 75 ppm of Al-PAM increased the filtration rate progressively, yielding 52 grams, 56 grams and 63 grams filtrates, respectively. A further increase in Al-PAM dosage to 100 ppm caused a slight decrease in filtration rate. In the case of dilution to 5 wt% solid, filtration for 1000 seconds yielded 35 grams of filtrate without polymer addition. The addition of 25 ppm, 50 ppm, 75 ppm and 100 ppm yielded 69 grams, 79 grams, 63 grams and 55 grams of filtrate, respectively. Filtration results suggest that the optimum dosage of Al-PAM for MFT diluted to 5 wt% and 10 wt% solid is 50 ppm and 75 ppm, respectively.

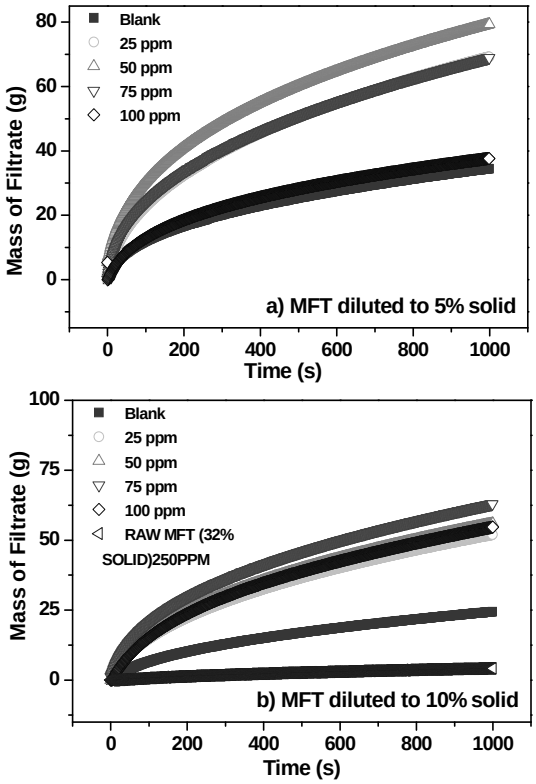

Figure 8. Filtration rate of MFT diluted to 10 and 5 wt% solids using Al-PAM as filtration aid.

Filtration Time

In the context of this research, filtration time refers to the time for which filtration needs to continue to produce a cake with a desirable moisture content. It was identified that a filter cake of 23 wt% moisture content produced from MFT is stackable and the filtration time to reach this moisture content is defined as filtration time. Strictly speaking, the moisture content cannot be controlled to the same value for different experiments. In this study, it varies from 22 wt% to 23 wt%.

The effect of MFT dilution on filtration time at optimal Al-PAM dosage is shown in Figure 9. At MFT dilution to 10 wt% solids, the shortest filtration time of 25 minutes is achieved at 75 ppm Al-PAM addition. With MFT dilution to 5 wt% solids, the shortest filtration time of 19 minutes is achieved at 50 ppm Al-PAM addition. Although the dilution of MFT to 5 wt% solids produced a filter cake of 23 wt% solids at a slightly shorter filtration time at

lower Al-PAM dosage, MFT dilution to 10 wt% solids remains to provide a better overall filtration performance as it could treat a larger volume of raw MFT (5 vs. 4 units of raw MFT) at a lower Al-PAM dosage (225 ppm vs. 300 ppm Al-PAM per unit volume of raw MFT).

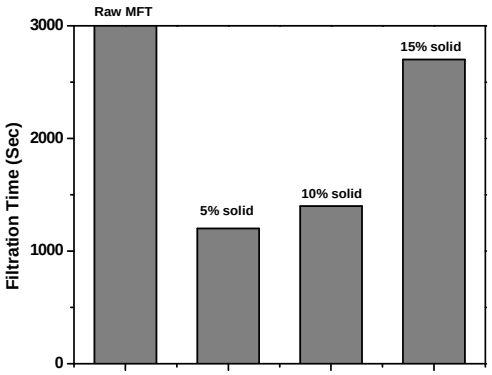

Figure 9. Comparison of filtration time of MFT at different dilutions with their respective optimal Al-PAM dosages to produce a cake of 23 wt% moisture content.

Filtration of Sediments

Although flocculation-assisted filtration of diluted MFT seems promising, filtration of a large volume of diluted MFT to a desirable cake moisture content of 23 wt% requires a relatively long filtration time. There is a need to reduce the filtration time to the level that is practically acceptable. The idea here is to filter a much smaller volume of sediments after flocculation and thickening of diluted MFT. With this approach, the dilution can be accomplished by the clarified water in the original MFT after flocculation and thickening without using fresh water. The filtrate would represent a net water recovery from MFT. As shown in Figure 10, applying this concept to an MFT diluted to 10 wt% solids reduced filtration time from 25 minutes to 8 minutes to produce cake of 23 wt% moisture, representing a significant reduction. In the case of MFT dilution to 5 wt% solids, the filtration time was reduced from 19 minutes to 7 minutes.

As shown in Figure 11, the filtrate produced by filtration is much clear than clarified water by settling. The sediments after flocculation and thickening, on the other hand, remain fluid, while the filter cake of 23 wt% moisture appears stackable, as shown in the inset of Figure 10. The findings from this study prove that flocculation-assisted sediment filtration is a viable solution to treating MFT.

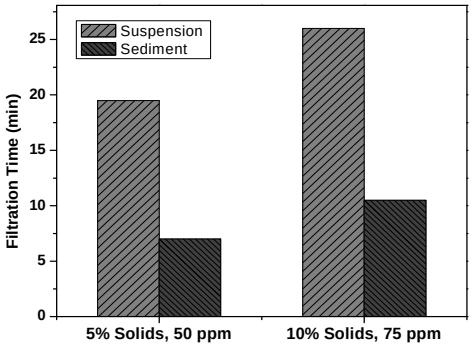

Figure 10. Comparison of filtration time for diluted MFT and corresponding thickened sediments after flocculation at optimal Al-PAM dosage to produce cake with 23 wt% moisture.

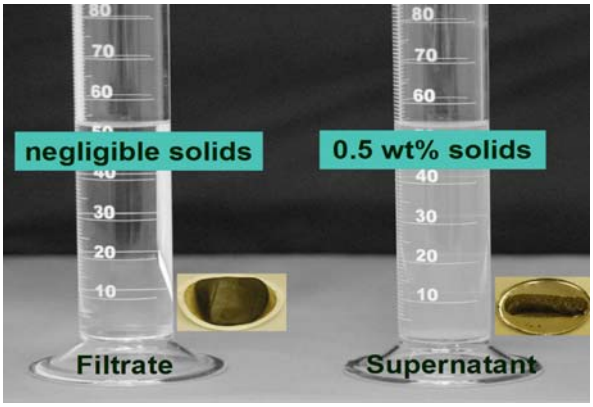

Figure 11. Comparison of release water clarity by thickener and filtration and fluidity of sediments and filter cake (inset).

WATER RECYCLING

In filtration of sediments after flocculation and thickening, two streams of water, i.e., clarified supernatant and filtrate are produced. Recycle of residual Al-PAM if present in the clarified water would reduce Al-PAM dosage. This hypothesis was tested by using the clarified water as dilution water for MFT. MFT dilution, on the other hand, may appear strange when the aim of dewatering is to consolidate MFT and recover water from it. However, if the clarified water could be used as

dilution water, the process itself would generate net gain of water from filtration. This concept is tested here. The results in Figure 12 show a slight decrease in filtration time by diluting MFT with the clarified water (supernatant of settling) for the first two cycles, confirming the presence of residual Al-PAM in the clarified water and its beneficial effect on flocculation of diluted MFT. However, a slight increase in filtration time was observed after the 3rd and 6th recycle of the clarified water for MFT dilution to 10 wt% and 5 wt%, respectively. The observed increase in filtration time could indicate a continue accumulation of residual Al-PAM in the clarified water, which may exceed the optimal dosage. It is also possible that the ultrafine particles accumulate in the clarified water. The presence of ultrafine particles is known to adversely affect filtration performance.

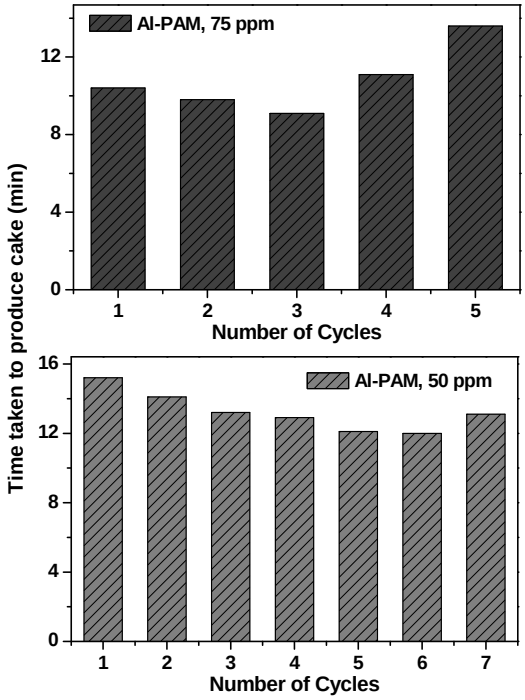

Figure 12. Effect of water recycling on filtration time.

CONCLUDING REMARKS

Enhancement of MFT dewatering requires destabilization of gel-like MFT structure and particle aggregation by improving attractive interactions among particles. In present study, stable MFT structure was destroyed by MFT dilution while polymers were used to flocculate the particles. An ideal flocculant should have the capability to flocculate fine particles effectively, producing large and porous flocs of high water permeability. It appears that Al-PAM is capable of accomplishing this objective due to its cationic nature of imbedded aluminum hydroxide colloids. The effective flocculation of ultrafine particles was confirmed by lower turbidity of supernatant after settling of diluted MFT with Al-PAM addition than with Magnafloc addition. MFT diluted to 10 wt% solid was determined to achieve optimal results. When MFT diluted to 10 wt% solid was filtered with 75 ppm Al-PAM addition, a filtration cake of 23 wt% moisture content was produced after 25 minutes of filtration. To shorten the filtration time, a novel two stage dewatering process was introduced: flocculation and thickening of diluted MFT followed by filtration of sediments.

Filtration time could be shortened considerably from 25 minutes to 10 minutes by this process to produce a filter cake of 23 wt% moisture. Integrated with water management, the clarified water can be used to dilute raw MFT and clear filtrate generated for recycle, reducing fresh water intake for bitumen extraction. In Figure 12, the process diagram of this novel MFT management scheme is compared with conventional thickening or filtration processes.

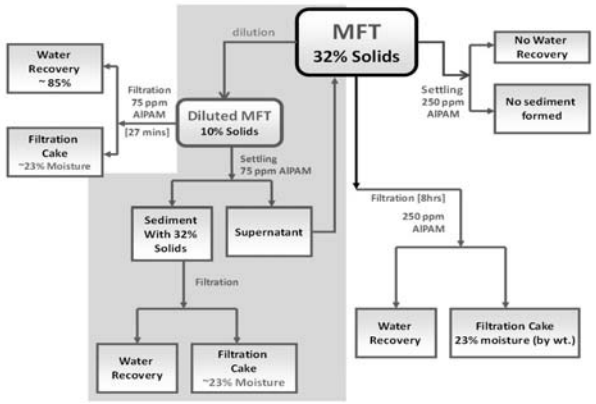

Figure 13. Schematic flow sheet of the overall optimum process configuration.

ACKNOWLEDGEMENT

The study was funded by Natural Sciences and Engineering Research Council of Canada (NSERC) under Industrial Research Chair Program in Oil Sands Engineering. The assistance of Al-PAM synthesis by Dr. Lana Algha and valuable discussions with Ms Tara (Xiaoyan) Wang are also greatly appreciated.

REFERENCES

Camp, F. W., 1976, The Tar Sands of Alberta, Canada, 3rd Ed., Cameron Engineers Inc., Colorado, U.S.A.

Chase, R. P., 1979, Settling Behavior of Natural Aquatic Particulates, University of Chicago, Illinois, USA.

Cymerman, G., Kwong, T., Lord, T., Hamza, H., Xu, Y., 1999, Thickening and disposal of fine tails from oil sands processing, The 3rd UBC-McGill International Symposium on Fundamentals of Mineral Processing, Metallurgical Society, Montreal, Canada, pp. 605-619

Ezeagwul, K. E., 2008, Studies on Flocculation of Kaolin Suspension and Mature Fine Tailings, M.Sc thesis, University of Alberta, Edmonton, Canada

Fine Tailings Fundamental Consortium (FTFC), 1995, Advances in Oil Sands Tailings Research, Alberta Department of Energy, Edmonton, Alberta, Canada.

Kaminsky, H., 2008, Characterization of an Athabasca Oil Sands Ore Process Stream, PhD. Thesis, University of Alberta, Edmonton, Canada.

Kasongo, T., Zhou, Z., Xu, Z., Masliyah, J. H., 2000, Effect of clays and calcium ions on bitumen extraction from Athabasca oil sands using flotation, Can. J. Chem. Eng., 78, 674 - 681.

Li, H., Jun Long., Zhenghe Xu., Masliyah, J. H., 2008, Novel polymer aids for low-grade oil sand ore processing. Can. J. Chem. Eng., 86, 168-176.

MacKinnon, M. D., Mathews, J. G., Shaw, W. H., Cuddy, R. G., 2001. Water quality issues associated with composite tailings (CT) technology for managing oil sands tailings, Inter. J. Mining, Reclamation & Environment, 15, 235 - 256.

Masliyah**,** J. H., Zhiang, Z., Xu, Z., Czarnecki, J., Hamza, H., 2004. Understanding water-based bitumen extraction from Athabasca oil sands, Can J. Chem. Eng., 82, 628-654.

Wang, X., 2009, Polymer Aids for Settling and Filtration of Oil Sands Tailings, M.Sc thesis, University of Alberta, Edmonton, Canada

Yang, W.Y**.,** Qian, J.W., and Shen, Z.Q., 2004. A novel flocculant of $AI(OH)_3$-polyacrylamide ionic hybrid, J. Colloid Interface Sci., 273, 400-405.

OPTIMIZING MFT DEWATERING BY CONTROLLING POLYMER MIXING

Alebachew Demoz, Vicente Munoz, and Randy Mikula
Natural Resources Canada, Canmet Energy Research, 1 Oil Patch Drive, Devon, Alberta, T9G 1A8

ABSTRACT

In order to minimize water chemistry changes during MFT (mature fine tailings) treatment and to enhance the performance of various tailings management schemes, polymer usage has become popular. Typically, high molecular weight, medium charge density polyacrylamides are used to modify the clay behaviour and enhance dewatering. Polymers, unlike inorganic rheology modifying additives, have a relatively narrow operational or mixing window in order to achieve optimal results. There are several fundamental or direct approaches to evaluating the mixing efficiency in order to create a tailings mix that will dewater rapidly. This paper will discuss the mixing parameters that are important in maximizing dewatering performance, including the development of several simple index tests that have been proven useful in field testing programs.

INTRODUCTION

High-molecular-weight polymer flocculants are being used for accelerated dewatering of mature fine tailings (MFT). Two anionic polymers were used to flocculate MFT containing 98 wt% fines. Different types of impellers were used as mixing tools for the flocculation process. The flocculation outcome was evaluated based on the amount and rate of water release and the capillary suction time (CST). There was a clear peak in the rate of water release and a minimum in the CST as a function of mixing time, clearly showing that there is an optimal mixing energy that corresponds to the most rapid dewatering of flocculated MFT.

Steady-state and dynamic rheological studies show that flocculant enhances the elastic property of MFT. Under optimal mixing conditions the primary flocs form aggregates with large pores and channels that result in higher rates of water release. Stereo microscopic imagery confirmed the above and also showed that over-shearing reduces the aggregate size.

High molecular weight polymers accelerate the dewatering of mineral suspensions by serving as binding agents of the solids and enhancing floc strength (Gregory, 1989). For a variety of MFT dewatering approaches, the initial first step is the efficient addition of the process additive. It has been shown that MFT will not dewater and develop strength without some chemical or physical intervention. As the mechanical energy goes down, the polymer (or other additive) concentration has to go up. As will be shown later, the dewatering rate of MFT due to addition of a given polymer depends upon the hydrodynamic conditions under which it is added to the MFT. Therefore, physical mixing variables such as agitation intensity, duration, and equipment used are of considerable importance in maximizing the effectiveness of a flocculant. If used outside its optimal operating envelope, a potentially excellent flocculant could appear mediocre.

In this study, we want to show that the dewatering rate of polymer-treated MFT is actually related to the energy input of mixing. This dependency is demonstrated by correlating the energy input directly to the first-order phenomenon and desired outcome: the quantity and rate of water release. In order to examine the effect of mixing energy on the floc size and, in turn, the dewaterability, microscopic images of untreated MFT, readily dewatering flocculated MFT, and over-sheared flocculated polymer-treated MFT are included here. The rheology of a dispersion reflects the strength of its microstructure and structural changes were also probed using steady-state and dynamic rheological measurements.

EXPERIMENTAL

Mixing trials were conducted using different impeller types, mixing speeds, and mixing durations in the polymer treatment of MFTs. The mixing parameters of torque and speed were continuously recorded using an InstruNet™ model 100 data acquisition system by Omega Engineering.

The MFT and polymer mixture were agitated using an overhead Heidolph RZR 2051 stirrer rated at analogue outputs from the unit were digitized to monitor both the rotation speed and motor torque during mixing tests. The signals were filtered to remove high-frequency readings (above 40 Hz) and were sampled at 0.65 s per point.

Four different but commonly used mixing impellers were used in this study, namely, vane impeller, hydrofoil, Rushton turbine (RT), and pitched-blade impeller (PBT). All of the tests, except for the one using the hydrofoil Lightnin A310 impeller, were conducted under what are considered wide-gap mixing conditions. The mixing vessel had four baffles 10 mm wide and spaced 90º apart. The diameter and capacity of the vessel were 120 mm and 2 L. Either 900 g or 1 kg of MFT was used for each set of mixing tests.

Two medium charge density anionic polyacrylamide, commercial flocculants were used in these tests. A3335, average molecular weight of 17 x 10^6 g/mol, and A3338, average molecular weight of 18 x 10^6 g/mol, both supplied by SNF (GA, USA). The polymer dosage is reported based on the solids content of the MFT and is usually given in grams of polymer per tonne of solids in the MFT.

The CST measurements were conducted using a Triton Electronics meter, type 319 multi-CST. All CST measurements were conducted in triplicate and the mean values were used in the analyses. Alternatively, the dewatering rates was measured by the released water volumes from settling columns; the mud lines of the polymer-treated MFT samples were recorded in 1-L graduated cylinders after 24 h of settling.

Rheological measurements were carried out at 25.0ºC using an ARG2 or ARES-G2 rheometer (TA Instruments, New Castle, DE, USA) equipped with Peltier plate temperature control. Cone-plate geometry (40-mm cone diameter, 1º cone angle, 1-mm gap) were used to perform the measurements. The samples were protected against drying by putting low-viscosity mineral oil around the exposed circumference of the sample.

Low-magnification images of the untreated MFT and flocculated MFT were obtained using a Carl Zeiss DiscoveryV20 stereo microscope equipped with a Carl Zeiss AxioCam high-resolution camera. The stereo microscope and the camera were controlled with AxioVision software. Due to the large volume of the aggregated samples and the insufficient depth of field, extended-focus rendering was used to create a sharp image over the entire field of view.

RESULTS AND DISCUSSION

Particle size characterization of the MFT solids showed that 60.3 wt% and 99.2 wt% of the solids were smaller than 2 µm and 44 µm, respectively. Flocculation and dewatering is generally less challenging with MFT samples containing coarse sand particles. The small solids and clay particles have to be incorporated into flocs and into larger aggregates in order for the fines to form a structure that will release water from the MFT. The flocculation outcome can be evaluated directly by measuring the water release from settling columns or CST measurements in macro-level tests. These direct evaluation methods were chosen as the first step in demonstrating the energy of mixing as a controlling property in achieving a more readily dewatering polymer-treated MFT.

The rheology of MFT is unlike that of most other solid dispersions due in large part to the clays. As anisotropic particles with net negative platelet charges and net positive edge charges, the clay particles are responsible for the formation of a network structure in the MFT. This structure is strong enough to appear as elastic flow at applied shear stresses below the yield shear stress. At prolonged shear or a higher shear rate, the network structure breaks down and the MFT shows viscous flow. This confers a thixotropic property which, in MFT, takes hours to rebuild. MFT deforms under modest stress, and totally fractures under shear stress greater than the yield stress. Once the structure is broken down, the strength keeps on decreasing, resulting in a higher shear rate for a given stress. Beyond the yield stress, the MFT flow can best be described by the Bingham model.

The apparent viscosities of the polymer flocculant solutions at concentrations used to treat MFT are up to three orders of magnitude higher than that of water. The flow curves of the flocculant solutions show yield stress and a power-law relationship. High-molecular-weight polymer solutions are invariably viscoelastic and the Herschel-Bulkley equation of state (equation 1), or one of its simplified forms describes their flow properties:

$$\sigma = \sigma_o + k\gamma^n \quad (1)$$

where σ, is shear stress (Pa), σ_o is yield shear stress, k is the consistency index, n, is the power law index, and γ is the shear rate (1/s).

The high-molecular-weight flocculants bring smaller particles together and bridge small flocs to form large aggregates. This change in structure is evident in steady-shear flow measurements of polymer-treated and untreated MFT as shown in Figure 1. The addition of polymer solution leads to a considerable increase in viscosity because of the association of fine particles. At low shear stress, the flocculated MFT shows resistance to flow (plastic response) and has a corresponding high viscosity. Generally, MFT shows non-Newtonian flow when the solids content is 15 wt% and higher. Shear thinning occurs when the network that gives rise to the increased strength gets disrupted by shear.

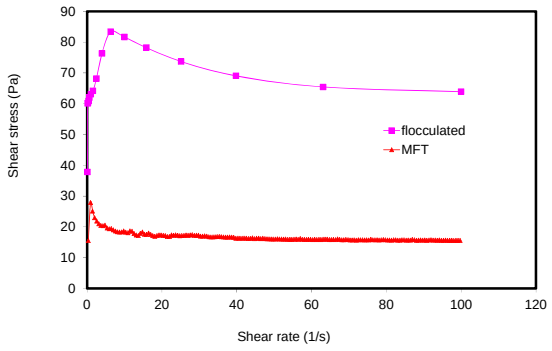

Figure 1: Difference in the steady-shear flows of 43-wt% solids MFT and after it was flocculated with A3338 at 1000 g/tonne solids.

Controlling the entire agitation process is essential since it affects the MFT flocculation outcome. The power dissipated by the agitation (mixing energy) may be one of the basic underlying parameters that determine the dewaterability of MFT treated with a given polymer. This aspect was examined by monitoring the motor torque of the overhead stirrer at selected constant impeller speeds and evaluating the polymer-MFT mixing outcome based on the amount of water released and/or the CST of the flocculated MFT (Sholz, 2006). These results, which demonstrate a direct link between the energy input and polymer treatment for different types of impellers and impeller speeds using the two anionic commercial polymer flocculants, are presented below.

The polymer-MFT mixing tests were conducted for a fixed set of geometries and a constant mass of MFT so as to limit differences in the flocculation outcomes to the effects of mixing energy in general and the time of mixing and rotation speed of impellers in particular (Paul et al., 2004), Chappel et al., 2002)). Figure 2 shows the outcomes for five batches of MFT mixed using the RT impeller at a constant speed of 600 rpm and varying mixing times using A3335 polymer solution. The peak in the amount of water released after 24 h and the point of lowest CST are of interest as a basis for determining the optimal mixing time or energy input that produces a readily dewatering flocculated MFT (Sholz, 2006).

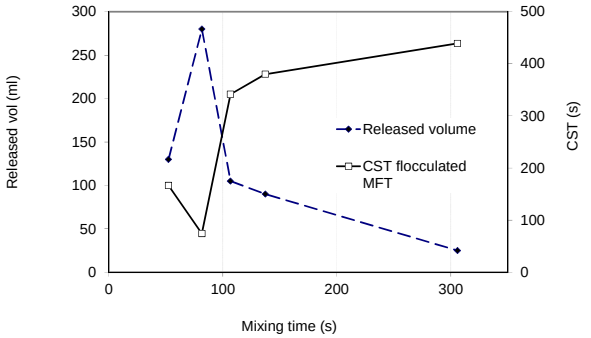

Figure 2. Dewaterability of 1 kg of 21-wt% TS MFT treated with 0.2-wt% A3335 polymer solution. The polymer dosage was 1000 g/tonne and mixing was conducted using an Rushton Turbine (RT) impeller at 600 rpm.

The sharp changes in the water release and CST show that the transition from an under-mixed to an over-sheared flocculation condition can occur within a rather narrow range of mixing times (or energy inputs).

The impeller Reynolds numbers, Re, for the experimental work reported here were 1000 < Re < 9000. This is intermediate between turbulent flow (Re > 20,000) and laminar flow (Re < 10) (Paul et al., 2004), Chappel et al., 2002)). A specific power input per unit volume or mass can be calculated from these types of results for use in scaled-up industrial mixing applications. It is also reasonable to assess the mixing in this study in

terms of the energy input since it can serve as a common basis for comparing differing mixing conditions. The integral of the dynamic torque versus time-of-mixing plot at constant impeller speed can give the energy of mixing, as follows:

$$\varepsilon = 2\pi N \int_0^t (M - M_o)\, dt \qquad (2)$$

where ε is the mixing energy (J), t is the mixing time (s), M is the torque during flocculation, and M_o is the no-load torque (N·m).

The untreated MFT was initially stirred to disperse the solids, warm up the mixer motor, and precondition the sample. The preconditioning step provides the baseline torque for comparison with the torque during polymer flocculation. The torques obtained in the MFT preconditioning step, as well as the no-load (empty vessel) torques were linearly correlated with the impeller rotation speed. However, in contradistinction to the expectation that increased torque would be required to maintain the same rotation speed after flocculation (a process that produces a higher-viscosity mixture), the torque for the treated MFT at steady state was smaller than the torque for untreated MFT. In short, the motor torque at steady state for a given rotation speed had the order: no load < flocculated MFT < untreated MFT.

For mixing to be effective, it is a minimum requirement that the impeller should disperse the flocculant and create a homogenous treated MFT. At lower speeds, larger impellers are required to achieve a given degree of flocculation within a reasonable time. Figure 3 shows that the optimal mixing period is shortened with increasing rotation speed . It shows the flocculation response for another combination of impeller type (PBT), Re (higher rotation speed), and increased solids content of MFT. Consistent with the other systems, the flocculation response was found to peak and then fall sharply beyond 4 min of mixing. The same dependence of mixing time and dewaterability was also obtained using the airfoil A310 impeller.

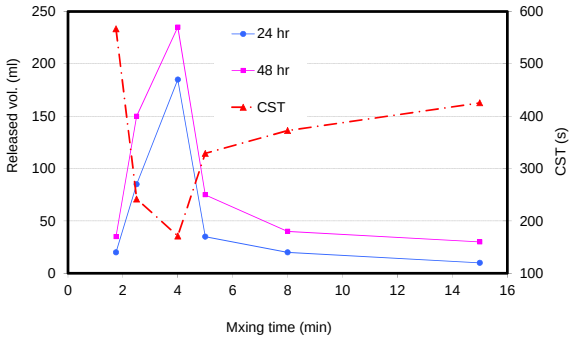

Figure 3. Dewaterability after treatment of 900 g of 34-wt% TS MFT with 0.1-wt% A3338 solution using a PBT impeller at 850 rpm. The polymer dosage was 1000 g/tonne.

Different combinations of impellers, flocculants, and MFT solids loadings were considered and in each case it was empirically shown that there is an optimal energy of mixing to produce readily dewatering flocculated MFT. Whether the mixing energy influences the floc structure, floc size, or both was examined using microscopy and rheological measurements. The flocculation produced large aggregates that are distinctly visible in Figure 4, micrograph B. Further mixing appears to have disrupted the weak bridging interaction between flocs, reducing the size of the aggregates. However, the over-sheared condition did not revert the flocculated solids to the dispersed original state of the untreated MFT (Figure 4, micrograph A versus micrograph C). The images with flocculant indicate a basic structure of flocs around a certain size distribution which join to form the aggregates. These primary flocs appear intact even after mixing beyond the optimal condition. A more detailed image size analysis would be required to ascertain this. The images show that over-shearing, beyond the optimal condition, reduced the porosity of the channels and therefore lead to reduced dewatering.

The flocculation and aggregation lead to a network structure having viscous and elastic behaviors that can be examined by dynamic oscillatory rheological measurements.

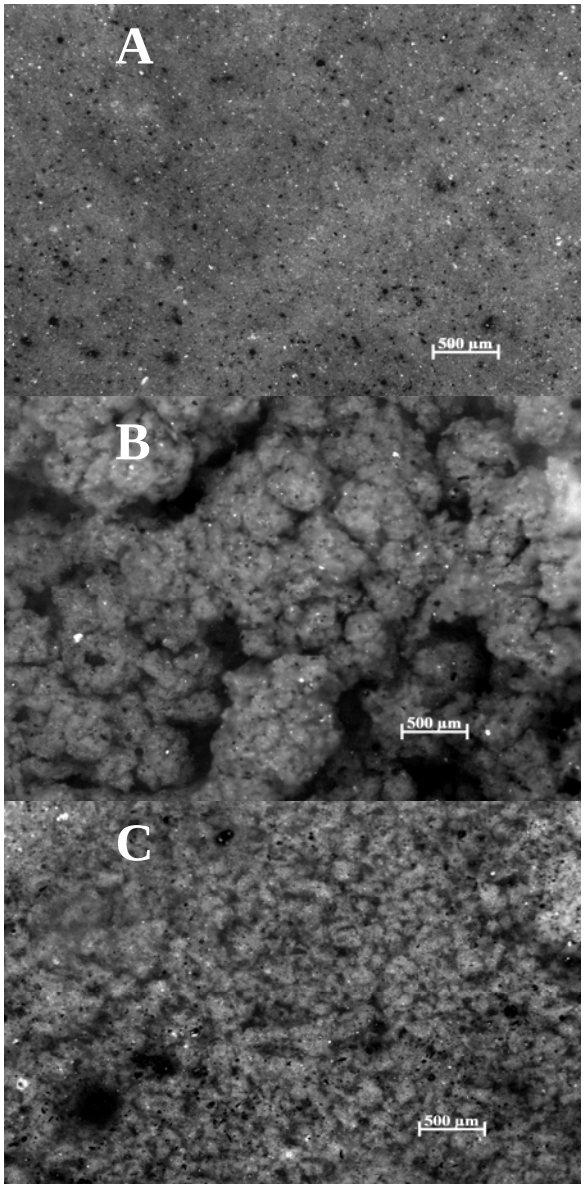

Figure 4. Stereo micrographs obtained at the same magnification comparing the effect of mixing energy on the same MFT: A) untreated MFT; B) 1000 g/tonne A3338, flocculated and optimally mixed; and C) same flocculated MFT as in B, but over-sheared. The darkest zones are water-filled channels.

A strain amplitude sweep from 0.01 to 25% on MFT (whose steady-state shear flow is given in Figure 1) show that the viscoelastic property is in the linear range for strain below 1%. In a frequency sweep (Figure 5), the dominance of the storage modulus over the loss modulus is observed for the optimally mixed, flocculated MFT and even for over-sheared flocculated MFT. The high storage modulus of the over-sheared flocculated MFT, in agreement with the microscopic images, indicates that the over-shearing did not destroy the primary flocs. This suggests that the over-shearing affected only the weaker, easier-to-fracture bridging networks of the aggregates. The dominant storage moduli in the kilopascal range are characteristic of gel like substances consisting of three-dimensional networks of physical bonds (Ferry, 1980, and Macosko. 1994)). Where the elastic modulus dominates, the dispersion structure can be considered as a network of closely packed hard spheres.

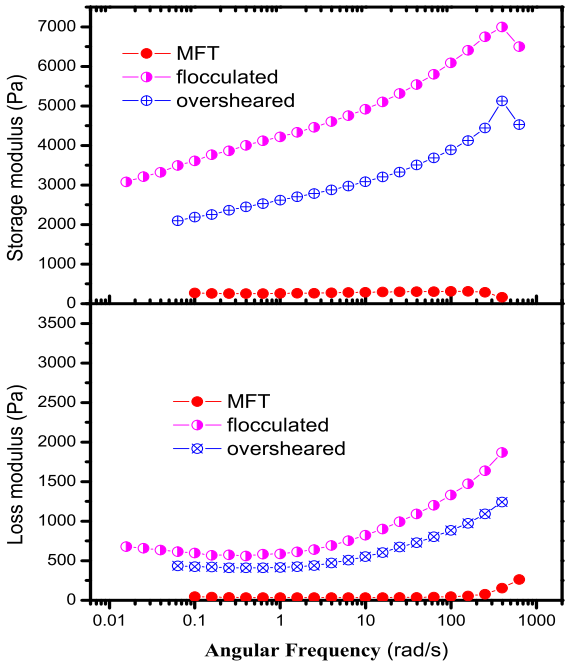

Figure 5. Dynamic moduli of 43-wt% solids MFT at 0.1% strain amplitude.

SUMMARY

The focus of polymer-assisted accelerated dewatering is usually directed towards selecting the best polymer available for the application. However, control of the flocculation process is of no less importance than the specific polymer selected. The benefits of operating at the optimal physical conditions are attractive, particularly when

compared to the challenges of developing new flocculants.

The amount of released water and/or the CST were used to evaluate the flocculation process. The CST was found to be inversely proportional to the rate of water release, and could therefore be used confidently as a quick indicator of the dewaterability of treated MFT with normal solids loading. Vane, Rushton Turbine (RT), Pitched Blade Turbine (PBT), and airfoil impellers, which are used in a wide range of applications, were used for mixing. Different permutations of impeller speed, MFT solids content, and polymer type (straight vs branched) were tested. In every case, there was a clear peak in the amount of water released or a minimum in the CST corresponding to an optimal mixing energy and resulting in a well-flocculated and readily dewatering MFT. Since this optimal energy input was observed for different types of impellers whose mixing regimes vary considerably, it is reasonable to expect that mixing energy would play a similar role when in-line mixers are utilized, which is generally how flocculation treatment is conducted on an industrial scale.

The results of both the rheology and microscopy confirm that the flocculant creates a floc population distributed around a primary floc size. The flocculant also causes bridging of the primary flocs to form larger aggregates. The aggregates provide large void spaces through which released water can escape. Over-shearing breaks up the large aggregates and reduces the pore sizes, thus reducing the rate of water release. Microscopic imagery directly confirms the flocculation, aggregate formation, and aggregate breakup in the over-sheared state.

ACKNOWLEDGMENT

Funding for this research was provided by the Canadian Program for Energy Research and Development (PERD).

REFERENCES

Chapple, D., Kresta, S.M., Wall, A., Afacan, A., (2002). “The effect of impeller and tank geometry on power number for pitched blade turbine” *Trans IChemE,* 80, 364-372.

Ferry, J.D., (1980) “Viscoelastic Properties of Polymers,” 3rd edn.,Wiley, New York, 1980

Gregory, J., (1989) “Fundamentals of Flocculation”, CRC Critical Reviews in Environmental Control, 19, 185-230.

Macosko, C.W., (1994) “Rheology: Principles, Measurements, and Applications, VCH Publisher, New York, 1994.

Paul, E. L., Atiemo-Obeng, V.A., Kresta, S.M. (Eds), (2004). “Handbook of Industrial Mixing” Wiley-Interscience, *Hoboken, NJ, USA*

Scholz, M., (2006). “Revised capillary suction time (CST) test to reduce consumable costs and improve dewaterability interpretation.” *J. Chem. Technol. Biotechnol,* 81, 336-344.

FLOCCULATION KINETICS OF KAOLINITE: ROLE OF AQUEOUS PHASE SPECIES

Peter House[1], Chen Wang[2] and Nav Dhadli[1]
[1] Shell Canada Ltd., 3655 36 ST NW, Calgary, Alberta, Calgary Research Center
[2] University of Alberta, Edmonton, Alberta, Canada

ABSTRACT

Numerous population balance studies have investigated the flocculation kinetics of pure kaolinite clays with anionic polyacrylamide (A-PAM). However, few studies address, quantitatively, the role of aqueous phase species on both aggregate growth and breakage rates. In this work, a fully replicated 2^k factorial study is conducted on the effect of pH, electrolytes and chelating agents on the flocculation kinetics of A-PAM and kaolinite. For tests conducted at pH 7, aggregate growth rates are found to be much faster in the presence of electrolytes; however, the corresponding rate of aggregate breakage is also much faster. This effect is likely caused by a shift in the adsorption mechanism of A-PAM to kaolinite in the presence of electrolytes from hydrogen bonding (at pH 7) to a very non-specific Van der Waals type attraction. This mechanism is further supported by a significantly subdued effect of pH when electrolytes are present in solution. Flocculation kinetics of kaolinite in oil sands process waters are found to share this relative insensitivity to changes in pH – likely a result of their saline nature.

INTRODUCTION

Use of polymeric flocculants at oil sands mining operations has expanded greatly in the past decade. Consumers of flocculants include: high rate thickener operations at Shell Albian Sands; tailings reduction operations (TRO) at Suncor; and numerous studies of pilot scale centrifuges, accelerated de-watering and paste thickeners across several operators. To ensure efficient use of flocculants there is a need to understand how process design and operational parameters influence the kinetics of aggregation. Particularly, how clay chemistry, aqueous phase chemistry and a flow field interact to produce growth and breakage of clay aggregates produced upon addition of anionic polyacrylamide.

Aggregate production is described, mathematically, using population balance models (PBMs). Kinetic expressions for aggregate growth and breakage are usually given as a function of the flow field. For example, aggregate growth related processes are usually described with a population balance of the form (Kim and Kramer (2007)):

$$\left.\frac{dN_k}{dt}\right|_{Growth} = \frac{1}{2}\sum_{i=1,i+j=k}^{k-1}\alpha\beta_{ij}N_iN_j - \sum_{i=1}^{\infty}\alpha\beta_{ik}N_iN_k \qquad [1]$$

where, N_i is the number density of aggregates containing *i* particles, α is the efficiency with which collisions between particles or aggregates results in aggregation, and β_{ij} is the collision frequency of aggregates of size *i* and *j*. Collision frequency, for simple shear flows, is given by Smoluchowski (1916) kinetics:

$$\beta_{ij} = \frac{4}{3}\dot{\gamma}(ai + aj)^3 \qquad [2]$$

where, $\dot{\gamma}$ is the local shear rate in the flow field and a_i is the radius of an aggregate containing *i* number of particles. The efficiency of collisions, however, is dictated by the interactions between particulate and aqueous phase chemistry. This term provides a link between what is occurring on the micro-scale (i.e. adsorption of polymer) and the particle level (i.e. aggregation). Expanding on the link between micro-scale behavior and particle level observations has been the topic of several works.

La Mer and Smelie (1956) investigated the effect of flocculant coverage on collision efficiencies of the form given in Equation 1. In this work, collision efficiency was discussed in the context of Figure 1 – a collision between two particles with or without adsorbed flocculant. Their proposed expression for collision efficiency was provided as a sum of the possible interactions,

$$\alpha = \alpha_1\theta_1\theta_2 + \alpha_{12}\theta_1(1-\theta_2) + \alpha_{21}\theta_2(1-\theta_1) + \alpha_2(1-\theta_1)(1-\theta_2) \qquad [3]$$

Where, θ_i is surface coverage of flocculant relative to maximum possible surface coverage for particles of type i (range is [0, 1]); α_1 is the collision efficiency associated with polymer coated patches for particles of type 1 and 2, α_{12} is the collision efficiency associated with a polymer coated patch on a particle of type 1 and an uncoated patch on a particle of type 2; α_{21} is the collision efficiency associated with a polymer coated patch on a particle of type 2 with an uncoated patch on a particle of type 1 and α_2 is the collision efficiency between two uncoated particles.

Empirically, collision efficiencies associated with type 1 and type 2 interactions are generally very low in electrostatically stabilized systems, due to steric repulsion (for type 1 collisions) and electrostatic stabilization (for type 2 collisions). A complementary observation is, for collisions to be efficient, a fraction of one particle containing polymer must collide with a fraction of another particle that does not. Furthermore, if aggregation is to occur the nature of the surface that does not already contain polymer must be such that it is energetically favorable for polymer adsorption to occur.

Since the work of La Mer and Smelie (1956) there have been several attempts to express collision efficiencies as a function of the net interaction energy between particles using modified DLVO theory (see, for example, Ahmad et al. (2008)). However, when bridging flocculation is the primary mechanism through which aggregation is achieved, the net interaction energy between particles changes as aggregates interact with the flow field. For example, changes in polymeric conformation that occur during aggregate breakage can render polymers incapable of bridging repulsive length scales due to electrostatic forces. Conformational changes could include chain scission of the polymer (Van de Ven (1981)) or an extension of the polymer from a looped structure to a linear chain that adsorbs in a flat conformation precluding particulate bridging (Taylor et al. (2002)). A number of papers have introduced PBMs that treat the effects of aggregate breakage on polymeric structure empirically (Pelton (1981); Heath et al. (1999); Heath et al. (2006)). These models address these effects by allowing for a gradual reduction in the rate constant for aggregate growth or an increase in the rate constant for aggregate breakage.

Pelton (1981) considered the effect of breakage by defining a fraction of the particle surface available for bonding (similar to La Mer and Smelie (1956)). Each aggregate breakage event was assumed to de-activate a fraction of the particle surface available for particulate bonding. Effectively, this led to a gradual decay in the collision efficiency between particles/aggregates. Pelton did not speculate on mechanisms at the micro-scale, but it is likely that the model captured (indirectly) the concept of steric repulsion shown in Figure 1a.

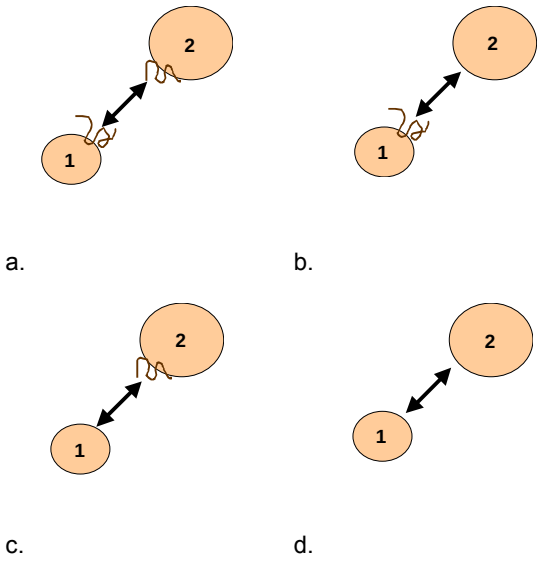

Figure 1. Categorization of particle-particle interactions leading to flocculation or coagulation: a) interaction of type 1; b) interaction of type 12; c) interaction of type 21; d) interaction of type 2.

More recent studies have attempted to link what is known about adsorption mechanisms of polyacrylamides to the observed floc strength of kaolinite-A-PAM aggregates. Taylor et al. (2002) experimentally determined anionic polyacrylamide adsorption capacities and kinetics of kaolinite at pH 4.5 and pH 8.5. Consistent with previous works (Nazbar et al. (1984); Pefferkorn et al. (1985)), they found that adsorption capacities at pH 4.5 are significantly higher than at pH 8.5. In this work, the reduced adsorption capacity at pH 8.5 was attributed to the loss of hydrogen bonding sites. This occurs due to hydrolysis of hydroxide functional groups at the kaolinite edge which are known to hydrogen bond with carbonyl functional groups of polyacrylamides. Taylor et al. (2002) concluded that aggregate strength would be significantly lower at pH 8.5 versus pH 4.5 due to a reduction in the net interaction energy between bridged particulates (fewer hydrogen bonds).

Flocculation kinetics were not measured, but it is likely that under the conditions investigated by Taylor et al. collision efficiencies would also be significantly lower at pH 8.5 due to a reduction in the active surface area for flocculant adsorption.

Although the effect of changes in pH is certainly of practical interest, there are other influencing factors which are known to significantly alter the mechanism of polyacrylamide attachment to kaolinite, such as electrolytes (Lee et al. (1991)). In the absence of cations in solution, almost all adsorption of anionic polyacrylamide to kaolinite occurs via hydrogen bonding with hydroxyls found on the kaolinite edge surface (Nazbar et al. (1984); Pefferkorn et al. (1985)). These groups display acid-base behavior, which explains the sensitivity to pH (Avena (2006). However, most commercial process waters are highly saline. According to Lee et al. (1991), presence of cations in the aqueous phase should expand the available surface for flocculant adsorption, especially on the basal face of kaolinite where non-specific Van der Waals attachment was found to occur.

In this work, the sensitivity of flocculation kinetics of a Georgia kaolinite with A-PAM to calcium ion concentration (Ca^{2+}), pH, and a chelating agent for calcium is studied. An attempt is made to link the observed flocculation growth and breakage rates to what is known about adsorption mechanisms under the conditions of testing.

Theory and Background: Population Balance Model

To facilitate quantitative interpretation of results it is useful to evaluate kinetic data in terms of the regression coefficients of a population balance model. Observations in the preliminary phase of experimentation indicated population balances describing flocculation of kaolinite with A-PAM would have to capture three rate-based phenomena: aggregate growth, aggregate breakage and de-activation of the clay surface caused by aggregate breakage. None of the existing literature models captured all of these phenomena in a satisfactory manner for the conditions employed in the present work. Therefore, some slight modifications to existing literature PBMs were made.

First, the general population balance framework of Kim and Kramer (2007) was used for model development.

$$\frac{dN_k}{dt} = \frac{1}{2}\sum_{i=1,i+j=k}^{k-1}\alpha\beta_{ij}N_iN_j - \sum_{i=1}^{\infty}\alpha\beta_{ik}N_iN_k - S_kN_k^b + \sum_{l=k+1}^{\infty}\Theta_{lk}S_lN_l^b \quad [4]$$

In Equation 4, S_k is a breakage kernel and Θ_{lk} determines the number of daughter aggregates of size k produced by breakage of an aggregate of size l (Θ_{lk} is commonly referred to as the breakup distribution function). The first two summation terms in Equation 4 arise from aggregate growth events, while the remaining two terms represent aggregate breakage events. The first summation term describes the growth rate of aggregates of size k, due to the aggregation of two smaller granules. The second summation term describes the rate of disappearance of aggregates of size k resulting from aggregation with other granules in the suspending medium. The product of the collision efficiency and collision frequency, found in the growth related terms of Equation 4, can be modeled using Equation 5. In Equation 5, the details of the flow field and collision efficiency are lumped into a single kinetic constant, k_G, for aggregate growth. The rationale behind not decoupling conditions of the flow field from collision efficiency is the flow field was not varied in any of the tests in the present work. Therefore, changes in the growth constant can be interpreted as changes in flocculation efficiency without detailed knowledge of the flow field.

$$\alpha\beta_{ij} = k_G\left(a_i + a_j\right)^3 \quad [5]$$

However, modification of Equation 5 was necessary to capture the observed decay in the growth rate of aggregates after the onset of aggregate breakage. Consequently, a dimensionless term for the effective surface area available for flocculation was included, similar to Heath et al. (1999), making the PBM used here:

$$\frac{dN_k}{dt} = k_G\theta_{eff}\left\{\sum_{i=1,i+j=k}^{k-1}\frac{1}{2}\left(a_i + a_j\right)^3N_iN_j - \sum_{i=1}^{\infty}\left(a_i + a_j\right)^3N_iN_k\right\} - S_kN_k^b + \sum_{l=k+1}^{\infty}\Theta_{lk}S_lN_l^b \quad [6]$$

where, θ_{eff}, is defined as the ratio of the effective surface area at time *t* to the initial effective surface area for flocculation. Therefore, at time *t=0*, $\theta_{eff} = 1$ and decays proportional to the rate of

aggregate breakage, which is the source of effective surface de-activation. The rate of de-activation was assumed to follow first order kinetics, with linear proportionality to the rate of aggregate breakage.

$$\frac{d\theta_{eff}}{dt} = -k_D\left\{\sum_k^{\infty} S_k N_k^b\right\}\theta_{eff} \qquad [7]$$

where the exponent *b* was taken to be 1, consistent with Heath et al. (1999, 2006). The breakage kernel was taken from Kramer and Kim (2007), but modified to account for the observation that a critical floc diameter, $d_{agg,c}$, was asymptotically approached (Kramer and Clark (1999)) during testing (see Equation 8).

$$S_k = k_1\dot{\gamma}^{k_2}\left(d_{agg,k}^{k_3} - d_{agg,c}^{k_3}\Big|_{\dot{\gamma}}\right) \qquad [8]$$

In Equation 8, k_3 was taken to be unity as per Heath et al.(1999, 2006); $d_{agg,c}$ was assumed constant as shear rates were not varied; and, because experiments were performed under conditions of constant flow field, k_1 and k_2 can be lumped into one parameter, as shown below in Equation 9:

$$\begin{aligned} S_k &= k_B\left(d_{agg,k} - d_{agg,c}\right) & d_{agg,k} &> d_{agg,c} \\ S_k &= 0 & d_{agg,k} &< d_{agg,c} \end{aligned} \qquad [9]$$

where, k_B is an aggregate breakage constant; and, $d_{agg,k}$ is diameter of an aggregate containing *k* particles. The aggregate diameters were calculated from Kim and Kramer (2007),

$$d_{agg,k} = d_{p0}(k)^{1/D_f} \qquad [10]$$

where, d_{p0}, is taken to be the mean diameter of particles prior to flocculation; and, D_f is the fractal dimension of the aggregate (assumed to be 2.3).

The final requirement for computation of breakage kinetics is an expression for the breakage distribution function, Θ_{lk}. In this work, the breakage distribution function was assumed to follow binary breakup criteria, as per Heath et al. (2006).

$$\Theta_{lk} = 2\delta(l-2k) + \delta(l-(2k-1)) + \delta(l-(2k+1)) \qquad [11]$$

where, δ, is the Dirac function. The above expression, is essentially a mathematical representation of three scenarios that can result in the formation of an aggregate of size *k*. This can be easily illustrated by taking k=2 and referring to Figure 2. According to the binary distribution condition aggregates formed during breakage are of equal size or the closest approximation to this.

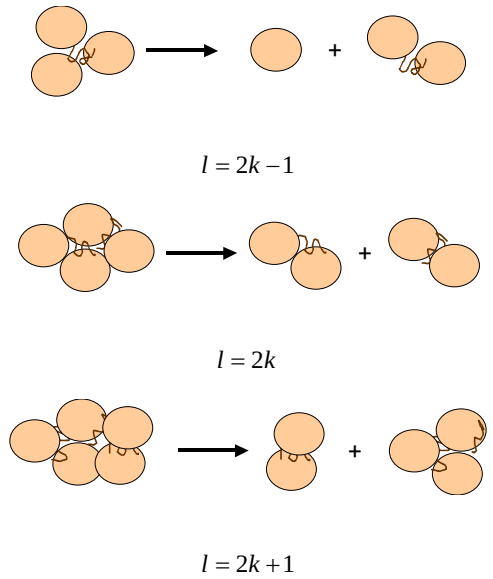

Figure 2. Pictorial representation of breakage distribution function used in this work.

For example, when an aggregate consisting of three particles breaks, daughter aggregates, of size two and one, form. Similarly, when an aggregate of four particles breaks, two daughter aggregates, of size two, form. Therefore, the Dirac function equals one for the cases *l = 2k-1, 2k* and *2k+1*.

MATERIALS AND METHODS

Flocculant Preparation

Anionic polyacrylamide powder (AF-246) having a charge density of ~30 % was obtained from Hychem Ltd.. AF-246 powder was dissolved in deionized water to a concentration of 0.5 wt.% 24 hours in advance of all test work. Immediately prior to use, the solution of A-PAM was diluted to 0.1 wt.% to ensure rapid mixing between the polymer and kaolinite suspension. The flocculant dose used in each test was 800 g/ton of kaolinite.

Kaolinite Suspension

The kaolinite used in this work was a kGa-1b Georgia Kaolinite obtained from Purdue University (see Pruett and Webb (1993) for details). For all tests, 0.4 liters of 5 wt.% kaolinite suspension was prepared by mixing kaolinite with de-ionized water at pH 7 in a 0.5 L pyrex beaker provided by Lasentec for use with the FBRM probe. Aqueous phase chemistry was then adjusted to the set-points provided in Table 1.

When pH adjustments were necessary, a solution of 10 wt.% sodium hydroxide from Fischer Scientific was added drop-wise until pH 9 was measured using a pH probe from Mettler Toledo. Calcium Chloride di-hydrate ($CaCl_2.2H_2O$) from EMD (CX0130-2) and reagent grade EDTA from J.T. Baker (8991-01) were used to adjust Calcium and EDTA levels to the desired concentrations.

Table 1. Set-points for test variables

Test #	pH	Calcium Concentration, mol/L	EDTA Concentration, mol/L
1	7	0.0025	0.0025
2	7	0.0025	0
3	7	0	0.0025
4	7	0	0
5	9	0.0025	0.0025
6	9	0.0025	0
7	9	0	0.0025
8	9	0	0

FBRM Setup

A Lasentec model D600S/T from Mettler Toledo, with a laser speed of 2 m/s, was used for in-situ particle size measurement during flocculation studies. The probe was positioned 2 mm above a 4-blade impeller (rotating at 400 RPM), provided as a standard item with the D600S/T for laboratory studies. Signals collected were averaged over 5 seconds intervals.

In-situ Measurement of Flocculation Kinetics

Prior to flocculant addition, the 0.5 L pyrex beaker containing the kaolinite suspension was prepared as per the set-points given in Table 1. The FBRM-impeller setup was then immersed in the beaker and the mean-squared chord length was monitored for a minimum of 20 minutes or until it stabilized. Prior to flocculant addition, data was logged to establish a baseline particle size. One minute after data logging began, 800 g AF-246/ton of kaolinite was added as a 0.1 wt.% solution in a single dose delivered with a rapid pour from a 50 mL graduated cylinder.

Duplicate measurements of each set-point in Table 1 were conducted to ensure reproducibility of FBRM measurements. The average of the replicate measurements was used in the regression of data.

RESULTS AND DISCUSSION

Data collected for the experimental conditions in Table 1 was averaged over 2 replicate runs for each condition and plotted in Figures 3 and 4. The PBM fit of Equations 6, 7 and 9 is also shown in this figure – values for regression coefficients are provided in Table 2. At pH 7, Calcium accelerated the rate of aggregate growth and the corresponding rate of aggregate breakage (see Figure 3). Regression of the PBM indicated a four-fold increase in the growth constant, which is reflective a four-fold increase in the collision efficiency at time zero. This suggests that there was a large increase in the surface area of the kaolinite particles available for A-PAM adsorption when Calcium is present at 0.0025M. However, aggregates that formed, upon addition of Calcium, were weaker and broke to a final aggregate size that was much smaller. This is consistent with the findings of Lee et al. (1991) that when salts are not present in high concentration, almost all adsorption of A-PAM occurs on the kaolinite edge surface where hydrogen bonding with hydroxyl groups is possible. Under these conditions (i.e. an absence of cations), for aggregation to happen, edge to edge collisions between particles are necessary. Whereas, when higher concentrations of cations were present, Lee et al. (1991) found that a very non-specific Van der Waals induced adsorption of A-PAM occurred on both edge and planar surfaces of kaolinite particles. Behavior of this kind would render far more of the kaolinite surface available for A-PAM adsorption, therefore increasing collision efficiencies. However, the net attraction between A-PAM and kaolinite particles would be far less than if an abundance of edge surface hydrogen bonding sites were the dominant location for flocculant adsorption (as would be expected at pH 7). Consequently, aggregates should be expected to be weaker at pH 7 when high concentrations of cations are present, as is observed in Figure 3a.

As the pH of the aqueous phase was increased, from pH 7 to pH 9 (see Figure 3b), the rate of flocculant growth decreased and the final aggregate size observed was much smaller. This behavior was anticipated as hydrolysis of a significant quantity of hydroxyl groups occurs with a pH increase of this magnitude (Taylor et al. (2002); (Nazbar et al. (1984); Pfefferkorn et al. (1985)). These groups are responsible for hydrogen bonding with the carbonyl functional groups on the polyacrylamide chains. Fewer hydrogen bonding sites should reduce the effective area for flocculant adsorption, thereby lower collision efficiencies and the strength of aggregates, as noted by Taylor et al. (2002). When Calcium was added at pH 9, however, the observed behavior was quantitatively very similar to that at pH 7. This suggests that hydrogen bonding, under the experimental conditions of this study, is not of primary importance to flocculation behavior when high concentrations of divalent ions are present.

Attempts were made to reverse the effects of Calcium addition through the addition of EDTA, which is known to chelate Calcium ions. When EDTA was added at 0.0025M (see Figure 4a) at pH 7, there was a near quantitative match for the observed flocculation kinetics with and without Calcium at a 1:1 mole ratio. Although, flocculation kinetics were very different than those performed in de-ionized water at pH 7. Specifically, aggregates grew faster and were much weaker, qualitatively similar to previous observations resulting from Calcium addition. It is likely that the sodium introduced when EDTA was added increased the available surface area for flocculant adsorption in much the same manner as Calcium. The extent to which growth rates were increased was not as dramatic as in Test #2. This is likely the consequence of the reduced valency of the sodium ion which should result in lower net interaction energies between A-PAM and the clay surface according to DLVO theory (Ahmad et al. (2008)).

In Figure 4b, when EDTA was added at pH 9, the effect of Calcium was also largely inhibited. In both tests conducted with EDTA at pH 9, the kinetics were similar to tests conducted at pH 7. However, aggregates were weaker, as would be expected due to the reduction in net interaction energy that occurs due to acid-base behavior of kaolinite particles that is displayed in this pH range.

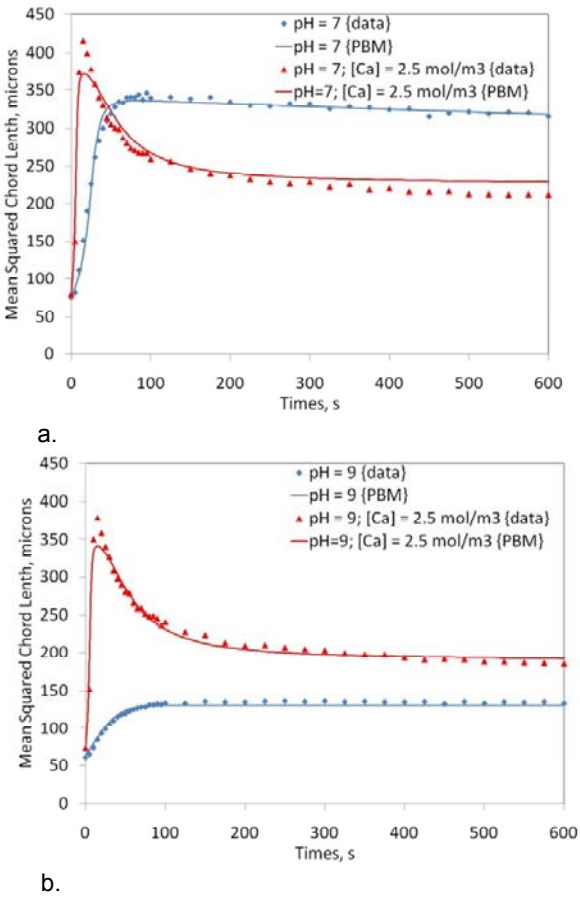

Figure 3. FBRM Data and PBM fit for aqueous phase chemistry corresponding to: a) pH = 7; pH = 7, [Ca^{2+}] = 2.5 mol/m^3; b) pH = 9; pH = 9, [Ca^{2+}] = 2.5 mol/m^3

Table 2. Model regression coefficients for test runs in Table 1

Test #	K_G	K_B	K_D	D_c, microns
1	0.034	2.01	4.97E-9	301
2	0.1448	291	3.2E-8	286
3	0.117	31.1	2.86E-7	271
4	0.112	193	3.01E-7	288
5	0.021	0.203	1.68E-9	79.6
6	0.134	175	2.5E-8	252
7	0.093	372	5.43E-6	297
8	0.112	169	3.14E-7	266

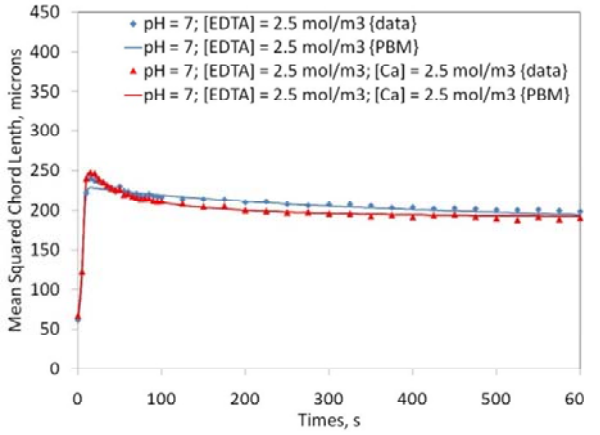

a.

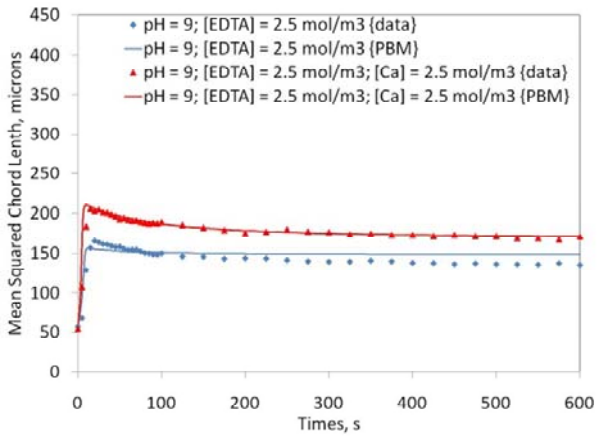

b.

Figure 4. FBRM Data and PBM fit for aqueous phase chemistry corresponding to: a) pH = 7; pH = 7, [EDTA] = 2.5 mol/m^3; b) pH = 9; pH = 9, [EDTA] = 2.5 mol/m^3

Kinetics of Kaolinite Flocculation in Reclaim Water

To complement the more systematic work conducted using de-ionized water, tests were conducted at pH 7 and pH 9 with water sampled from the external tailings facility at Muskeg River Mine (MRM). This water is known to contain high concentrations of both monovalent and divalent cations. Results of the testing and regression of FBRM data are provided in Table 3 and Figure 5.

Table 3. Model regression coefficients for test conducted with MRM reclaim water

pH	KG	KB	KD	Dc, microns
7	0.116	187	2.45E-7	251
9	0.134	223	1.26E-7	271

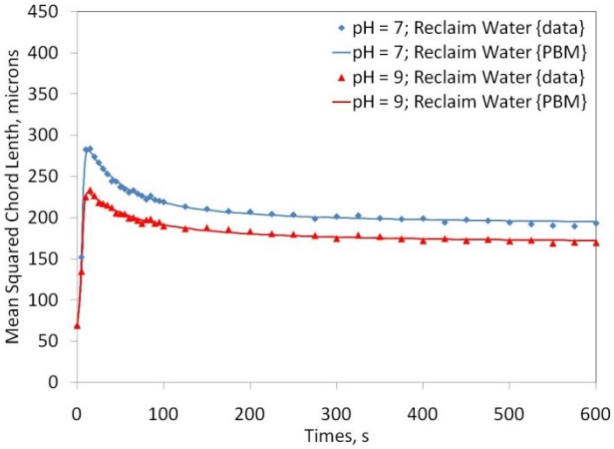

Figure 5. FBRM Data and PBM fit for aqueous phase chemistry corresponding to: a) Reclaim water adjusted to pH 7; b) Reclaim water adjusted to pH 9.

Sensitivity to pH in these tests was similar to the saline waters tested previously, but very different from kinetic data obtained from flocculation in de-ionized water. This suggests that flocculant adsorption due to non-specific Van der Waals type adsorption, and not hydrogen bonding, is of primary importance to flocculation kinetics in saline commercial process waters for mineralogy similar to that studied here.

CONCLUSION

A 2^k factorial study of pH, electrolyte (Calicum ions) and chelating agent (EDTA) concentration was performed. In the absence of electrolytes, flocculation kinetics of kaolinite with A-PAM were found to be extremely sensitive to pH – consistent with the understood adsorption mechanism. Aggregates formed more slowly and were weaker at higher pH. However, when high concentrations of divalent cations were present the sensitivity of kinetics to pH was greatly subdued. Interestingly, at pH 7 aggregates form much more quickly, but were weaker when Calcium was added. This appears to be in harmony with a shift in the A-PAM adsorption mechanism from hydrogen bonding at the kaolinite edge surface to a less specific Van der Waals type of attraction reported by Lee et al. (1991). Qualitatively, similar behavior was observed when EDTA was added to the aqueous phase of kaolinite suspensions. It is thought that the presence of sodium ions resulted in a similar shift in the A-PAM adsorption mechanism.

However, collision efficiencies were lower than when Calcium was added (by itself), which is expected from the lower valency of the Sodium ion.

Commercial process water from MRM was found to be qualitatively similar to saline water, in the sense that sensitivity of flocculation kinetics to pH was not nearly as prominent as is observed in de-ionized water. This suggests that a non-specific Van der Waals type of adsorption is responsible for most adsorption of A-PAM in saline commercial process waters for mineralogy similar to that studied here.

NOMENCLATURE

α	Collision Efficiency
β_{ij}	Collision Frequency between aggregates of size i and size j (m^3/s)
$\dot{\gamma}$	Shear rate of flow field (s^{-1})
θ	Fraction of particulate surface area available for flocculant adsorption
a_i	Radius of aggregate containing a total of i particles (m)
$d_{agg,c}$	Critical aggregate diameter, below which, no breakage occurs (m)
$d_{agg,k}$	Diameter of aggregate containing a total of k particles (m)
D_f	Fractal dimension of aggregates
d_{p0}	Diameter (mean squared chord length) of kaolinite particles (m)
k_B	Breakage constant ($m^{-1}.s^{-1}$)
k_G	Growth constant (s^{-1})
N_i	Number density of aggregates containing a total of i particles ($Number/m^3$)
S_k	Breakage Kernel for aggregates containing a total of k particles (s^{-1})

ACKNOWLEDGEMENTS

The authors would like to thank Shell Canada Ltd. for access to laboratory facilities and members of the AMIRA 266F project for their technical assistance and insightful discussions.

REFERENCES

Kim, J. and Kramer, T. Adjustable Discretized Population Balance Equations: Numerical Simulation and Parameter Estimation for Fractal Aggregation and Break-up, Colloids and Surfaces A: Physicochemical and Engineering Aspects 292, pp. 173-188, 2007.

Smoluchowski M. Drei Vortage uber diffusion brownsche bewegung and koagulation vol kolloidteilchen. Physick zeitschrift 17, pp. 557-, 1916.

La Mer, V.K. and Smelie, Flocculation, subsidence and filtration of phosphate slimes. I. General, Journal of Colloid Science 11, pp. 608-616, 1956.

Ahmad, A.L., Chong, M.F. and Bhatia, S. Population Balance Model (PBM) for flocculation process: Simulation and experimental studies of palm oil mill effluent (POME) pretreatment, Chemical Engineering Journal 140, pp. 86-100, 2008.

Van de Ven, T.G.M. Effects of Polymer Bridging on Selective Shear Flocculation, Journal of Colloid and Interface Science 81, pp. 290-291, 1981.

Taylor, M. L., Morris, G.E., Self, P.G. and Smart, R.St.C., Kinetics of Adsorption of High Molecular Weight Anionic Polyacrylamide onto Kaolinite: The Flocculation Process. Journal of Colloid and Interface Science 250, pp. 28-36, 2002.

Pelton, R.H. A model for flocculation in turbulent flow, Colloids and Surfaces 2, pp. 277-285, 1981.

Heath, A.R., Fawell, P.D., Bahri, P.A. and Swift, J.D. Population balance modeling of flocculation processes. CHEMICA. Perth; September, 1999.

Heath, A.R., Bahri, P.A., Fawell, P.D. and Farrow, J.B., Polymer Flocculation of Calcite: Population Balance Model, AIChE Journal 52, pp. 1641-1653, 2006.

Nazbar, L., Pefferkorn, E. and Varoqui, R. Polyacrylamide-Sodium Kaolinite Interactions: Flocculation Behavior of Polymer Clay Suspensions, Journal of Colloid and Interface Science 102, pp. 380-388, 1984.

Pefferkorn, E., Nabzar, L., Carroy, A. Adsorption of Polyacrylamide to Na Kaolinite: Correlation between Clay Structure and Surface Properties, Journal of Colloid and Interface Science 106, pp. 94-103, 1985.

Lee, L.T., Rahbari, R., Lecourtier, J. and Chauveteau, G. Adsorption of Polyacrylamides on

the Different Faces of Kaolinites, Journal of Colloid and Interface Science 147, pp. 351-357, 1991.

Avena, Marcelo J. Acid-Base Behavior of Clay Surfaces in Aqueous Media, Encyclopedia of Surface and Colloid Science 1, pp. 17-46, 2006.

Pruett, R.J. and Webb, H.L. Sampling and Analysis of KGa-1B Well-Crystallized Kaolin Source Clay, Clay and Clay Minerals 41, pp.514-519, 1993.

UNDERSTANDING AL-PAM ASSISTED OIL SANDS TAILINGS TREATMENT

Lina Guo, Yadollah Maham, Jacob Masliyah and Zhenghe Xu
University of Alberta, Edmonton, Alberta, Canada

ABSTRACT

Built on the demonstrated success of Al-PAM, an in-house synthesized, organic-inorganic hybrid polymer, for flocculation and filtration of fresh oil sands extraction tailings, this research aims at understanding working mechanisms of Al-PAM as filtration aid for oil sands fresh tailings management. The effect of Al-PAM properties (MW and Al content) and tailings characteristics (fines content and bitumen content) on flocculant-assisted tailings filtration was studied to optimize the design of Al-PAM for tailored application to oil sands tailings treatment. The objective is to produce stackable filter cake suitable for land reclamation and high quality filtrate for recycling.

Al-PAM of higher molecular weight was found to be more effective as settling and filtration aid for fresh oil sands tailings treatment. High Al content in Al-PAM was determined to be beneficial for settling and filtration. Removal of bitumen from fresh laboratory extraction tailings did not improve settling and filtration performance of Al-PAM. Effective flocculation of ultra-fines particles in fresh tailings was identified to be a key contributor to excellent performance of Al-PAM in filtration of fresh oil sands extraction tailings. Filtration of flocculated sediments using high molecular weight and high Al content in Al-PAM is proven to be an appealing solution to oil sands tailings treatment.

INTRODUCTION

Oil sand tailings are aqueous suspensions of coarse sand, fine solids, and clays with some fugitive bitumen attached to them. They are the reject stream of pH between 8 and 9 after bitumen extraction from the oil sand ores. As any other natural resource processing industries, the reject stream is fed to large tailing ponds for storage and water recycle. After discharge to the tailings ponds, the coarse sands settle quickly, while much of the fine solids and residual bitumen remain suspended, leading to the formation of mature fine tailings (MFT) which contains typically 30wt% solids after 2-3 years of setting. Further consolidation of MFT without any treatment would take hundreds of years (Coulson et al., 1991; Eckert et al., 1996).

Reducing fresh water intake and eliminating tailings ponds have been a major challenge facing the oil sands industry. Our approach as illustrated in Figure 1 is to produce stackable tailings for direct disposal to the mined pit as tailings are produced. With this approach a maximum amount of warm process water can be recycled without need to create tailings ponds. Recycling warm water not only reduces fresh water intake, but also reduces energy requirement to heat the otherwise cold process water for hot water extraction process. In our earlier study, a novel organic-inorganic hybrid polymer, Al-PAM was shown to enhance settling (Li et al., 2008) and filtration (Wang et al., 2010) of oil sands extraction tailings.

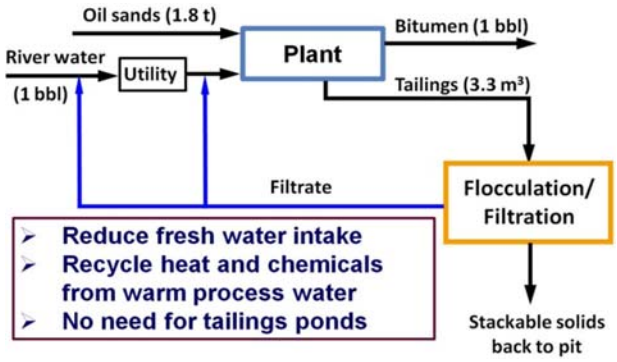

Figure 1. Concept and benefits of flocculation followed by filtration of oil sands tailings.

Filtration has been proposed as an alternative for oil sands tailings management (Xu et al., 2008; Wang et al., 2010). Filtration as an oil sands extraction tailings solution is attractive as it not only produces stackable solids for immediate land reclamation, but also allows recycle of a maximum amount of warm process water. In this study, we investigate the effect of Al-PAM characteristics, such as molecular weight and aluminum content in Al-PAM on flocculation and filtration of laboratory fresh oil sands tailings. Aiming at commercialization of flocculant-assisted filtration for treating large volume of oil sands tailings, a new process configuration

was investigated by filtering the sediments after clarification with flocculant addition.

MATERIALS AND METHODS

Flocculant

In this study, three organic-inorganic hybrid polymers, known as Al-PAMs of different molecular weights and aluminum contents were synthesized, following similar procedures described by Yang et al. (2004), Li et al. (2008) and Wang et al. (2010). In Al-PAM synthesis, the molecular weight was controlled by varying initiator concentrations while aluminum content was controlled by aluminum to acrylamide monomer mass ratio. The aluminum hydroxide colloids were prepared using aluminum chloride and ammonium carbonate, $(NH_4)_2CO_3$. The synthesized Al-PAM was characterized by viscosity measurement and aluminum analysis to determine molecular weight and aluminum content in Al-PAM. The intrinsic viscosity and aluminum content of various Al-PAMs are given in Table 1. For the convenience of discussion, the polymers are coded by numbers 4, 6 and 8 to present low, medium and high molecular weight while letter R and H are used to indicate low and high aluminum content, respectively. The code Al-PAM6R, for example, indicates an Al-PAM of medium molecular weight (2.5 million Da) and low aluminum content (0.1 wt%).

For comparison, a commercially available, partially hydrolyzed polyacrylamide of high molecular weight around 17.5 million Daltons and a medium charge density around 27 % (Straszewska et al., 1980) was also used as flocculant. This commercial flocculant purchased from Ciba Specialty Chemicals is known as Magnafloc 1011 (MF1011), formally as Percol 727.

Table 1. Physical properties of polymer flocculants used in this study

Polymer	[η]* (mg/L)	MW (10^6 Da)	Al Content§ (wt%)	Zeta Potential† (mV)
MF1011	13968	17.5	N/A	anionic
Al-PAM4R	437	1.5	0.10	+0.18
Al-PAM6R	675	2.0	0.09	+0.20
Al-PAM6H	650	2.0	0.24	+0.16
Al-PAM8R	835	2.5	0.11	+0.17

Note: *intrinsic viscosity was measured using Al-PAM solutions of pH 5.6-6.2 at 25 ± 0.05°C; §the Al content of polymers on dry power basis was determined using AA (AA880, Varian) and confirmed with IC (DX-600, Dionex); †zeta potential was measured at pH 5.6-6.2 with an average standard deviation of 0.005 mV.

Laboratory Oil Sands Extraction Tailings

To apply flocculation-assisted filtration to fresh oil sands extraction tailings, oil sands extraction tailings are produced by laboratory extraction units using an oil sands ore from Syncrude Canada Ltd. (Fort McMurray, Canada). The oil sands ore used in this study is a medium grade ore containing 9.6 wt% bitumen and 82 wt% solids among which 25.5 wt% solids are finer than 44 μm, known as fines.

To obtain oil sands extraction tailings for flocculation and filtration tests, flotation tests were conducted using a Denver flotation cell, following the procedures described by Kasongo et al. (2000) and Wang et al. (2010). Flotation was conducted at 80°C and pH 8.4. The agitation speed was kept at 1500 rpm and air flow rate at 120 mL/min. The bitumen recovery after 60 min flotation was 91.7%.

Settling Tests

The settling tests were performed by following the procedures described by Wang et al. (2010). For each settling test, 100 g of tailings slurry were placed in a 250-ml beaker and mixed at 500 rpm for 2 minutes. A desired level of flocculant was then added to the slurry under mixing at 300 rpm. After mixing, the slurry was transferred into a 100-ml graduated cylinder and mud-line position was recorded as a function of settling time. The results were plotted in the form of settling curve (mud-line position vs time) from which initial settling rate (ISR) was derived by taking the slope of initial settling

curve. After settling for 10 minutes, the turbidity of the supernatant was measured using Turbidimeter (HF Scientific DRT-15CE Portable Turbidimeters, Fisher Scientific). It should be noted that flocculant dosages in this paper are expressed on the basis of slurry weight of tailings. Flocculant stock solutions were prepared in deionized water to 500 ppm concentration one day prior to their use. Unless otherwise stated, the pH of settling tests was fixed at 8.4.

Filtration Tests

The filtration tests were carried out using a laboratory filtration unit (LPLT300, Fann Instrument Company). As described by Wang et al. (2010), a specially hardened filter paper of 2-5 μm pore size (N87000, Fann Instrument Company) was used as filter media. The slurry was mixed in a similar manner as in the settling test, but performed in the filtration cell. After mixing, the tailings slurry was immediately filtered under 15 kPa pressure. The weight of filtrate was monitored continuously by an electric balance interfaced with a computer.

RESULTS AND DISCUSSION

Flocculation

Effect of Molecular Weight

The ability of Al-PAMs and MF1011 to flocculate actual oil sands tailings was investigated using laboratory-generated oil sands extraction tailings. The results of settling tests using the laboratory extraction tailings of 10-11 wt% solids are shown in Figure 2. It is evident that increasing Al-PAM concentration up to 30 ppm increases ISR of laboratory extraction tailings for all the Al-PAMs, indicating that Al-PAM is capable of flocculating fine solids in oil sands extraction tailings. At Al-PAM concentrations above 30 ppm, ISR appears to level off, regardless of molecular weight of Al-PAM. However, there is a general trend of increasing ISR with increasing molecular weight of Al-PAM. For a given charge density, increasing molecular weight of Al-PAM is anticipated to enhance bridging of particles due to increased length of bridging, leading to enhanced settling of fine solids.

In contrast, MF1011 at lower polymer concentrations of less than 25 ppm showed a better performance than Al-PAM in particle flocculation, exhibiting a higher ISR. This better performance of MF1011 is attributed to larger molecular weight and higher charge density, allowing more flexible polymer chains for more effective bridging. At polymer concentrations higher than 10 ppm, increasing MF1011 concentration showed little improvement in flocculation as seen by leveling off of ISR. Above polymer concentrations of 30 ppm, Al-PAM of medium to high molecular weights outperformed MF1011.

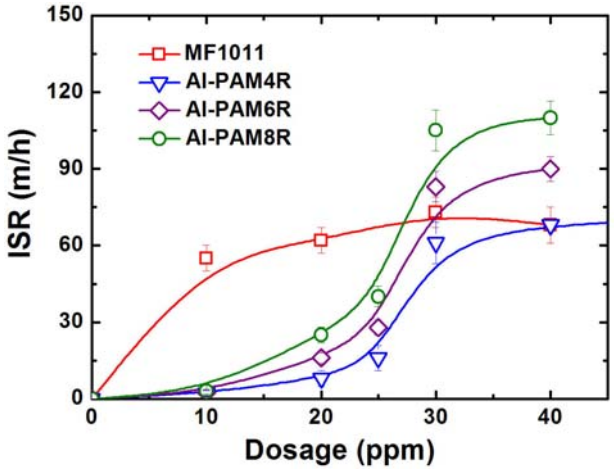

Figure 2. Initial settling rate (ISR) of laboratory oil sands extraction tailings after flocculation by a series of polymers at different dosages.

Although ISR is traditionally used to assess the performance of polymer flocculant, the turbidity of supernatant provides an equally important measure of flocculation, emphasizing the impact of flocculant addition on ultrafine particles. The measured turbidity of supernatant after settling of flocculated laboratory oil sands extraction tailings for 10 min is shown in Figure 3.

It is interesting to note a continuous decrease in supernatant turbidity with increasing Al-PAM concentration. In comparison, Al-PAMs of higher molecular weights performed slightly better, in particular at lower Al-PAM concentrations. At 30 ppm Al-PAM dosage, all Al-PAM showed essentially the same performance, reducing the turbidity of supernatant below 30 NTU. Compared to the inset of Figure 3, the supernatant is essentially solids free. The significant improvement in supernatant turbidity emphasizes importance of cationic characteristics of Al-PAM, which neutralizes charges of fine solid particles and acts as a coagulant. In contrast, the turbidity of supernatant of laboratory oil sands extraction tailing after MF1011

addition remained high at 1350 NTU over the entire MF1011 dosage. This observation suggests that negatively charged MF1011 is not effective in coagulating ultrafine particles, leaving them to remain suspended, as seen in the inset of Figure 3. The suspended ultrafine particles are anticipated to have a significant negative impact on filtration, which will be addressed in the next section.

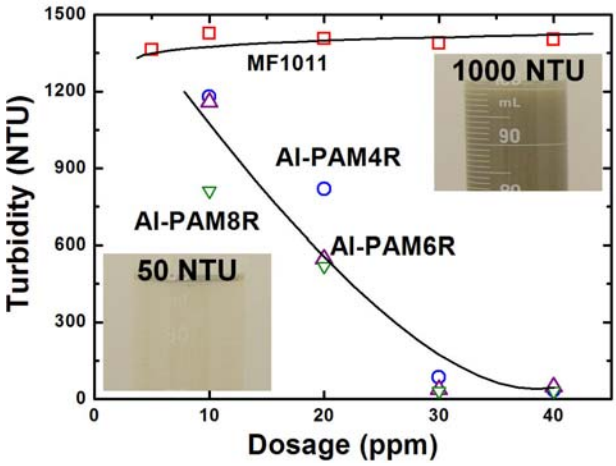

Figure 3. Turbidity of supernatant after settling for 10 min of laboratory oil sands extraction tailings flocculated by a series of polymers at different dosages.

Effect of Aluminum Content

Figure 4 shows that for a given molecular weight, increasing aluminum content in Al-PAM enhances significantly particle flocculation and hence settling. Higher aluminum content in Al-PAM also reduces turbidity of supernatant as shown in Figure 5, clearly demonstrating beneficial effect of increasing aluminum content in Al-PAM on fine particle flocculation.

To understand the observed effect of increasing aluminum content in Al-PAM on increasing particle settling and reducing turbidity of supernatant, the zeta potential of fine solid particles is measured as a function of Al-PAM concentration at a fixed suspension pH of 8.4. Although the zeta potential of Al-PAM at these two aluminum contents is essentially the same as shown in Table 1, the zeta potential results in Figure 6 show a much reduced negative zeta potential values with the addition of higher aluminum content Al-PAM than lower aluminum content Al-PAM at moderate Al-PAM dosages (20 to 30 ppm), suggesting a stronger attachment and higher adsorption density of higher aluminum content Al-PAM than lower aluminum content Al-PAM.

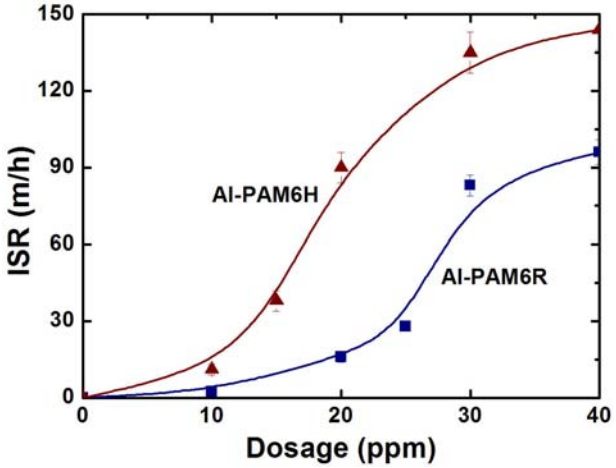

Figure 4. Effect of aluminum content in Al-PAM on initial settling rate of flocculated laboratory oil sands extraction tailings.

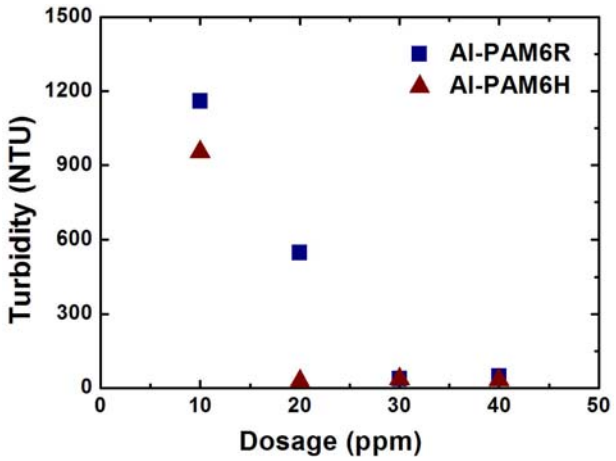

Figure 5. Effect of aluminum content in Al-PAM on supernatant turbidity of flocculated laboratory oil sands extraction tailings.

For a given molecular weight, Al-PAM of higher aluminum content is anticipated to have more aluminum hydroxide binding sites for attaching to fine particle solids, leading to an increased binding strength and adsorption density. Clearly charge neutralization of particles plays a critical role in enhancing particle flocculation, as it reduces repulsive forces between particles and hence allows closer proximity for more effective bridging flocculation by Al-PAM branches (loops and tails).

Filtration

Effect of Molecular Weight

Although MF1011 was able to increase settling rate of laboratory oil sands tailings, the addition of MF1011 before filtration reduced slightly filtration rate, as shown in Figure 7 (MF1011). In contrast, Al-PAM addition greatly enhanced filtration rate as also shown in Figure 7.

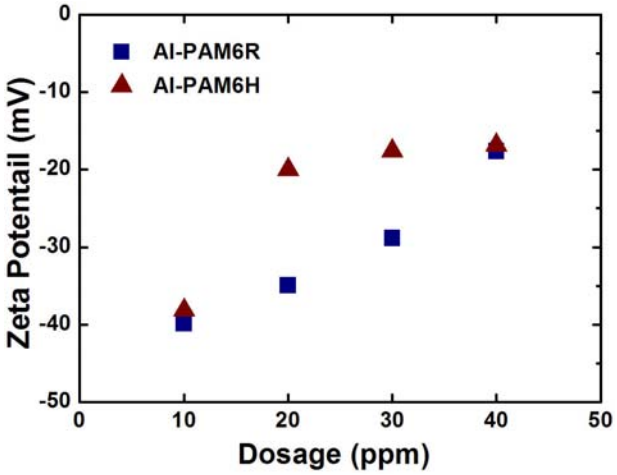

Figure 6. Effect of aluminum content in Al-PAM on zeta potential of laboratory oil sands oil sands extraction tailings.

The results in Figure 7 show that at a given aluminum content, increasing molecular weight of Al-PAM decreased its concentration required to reach optimal filtration rate. Taking the slope of the initial filtration curve as the filtration rate, a quantitative comparison of filtration rate at optimal Al-PAM dosage in Figure 8a revealed that not only optimal Al-PAM dosage decreased with increasing Al-PAM molecular weight, the initial filtration rate also increased with increasing molecular weight of Al-PAM. The increase in filtration rate translates to a reduced filter press for treating a given volume of tailings. Furthermore, increasing molecular weight of Al-PAM also decreased slightly the moisture content of filter cake as shown in Figure 8b. Clearly high molecular weight of Al-PAM is beneficial for filtration of oil sands tailings. It should be noted however that Al-PAM of the highest molecular weight (Al-PAM8R) is prone to overdose as shown in Figure 7 (Al-PAM8R).

The observed enhancement of filtration rate corresponds well with observed enhanced settling rate of oil sands tailings with Al-PAM addition as shown in Figures 2 and 3: Al-PAM of highest ISR and lowest turbidity of supernatant produced the highest filtration rate at lowest optimal dosage. Effective flocculation, in particular of fines to form loosely packed flocs helps to create passages for filtrate to flow through. The reason why MF1011 did not improve the filtration, although it enhanced settling of solids, is likely related to high turbidity of supernatant, a sign of ineffective flocculation of fines. The presence of these fines in supernatant is likely to plug the pore channels needed for water to flow through during filtration. A flocculant of both coagulation and flocculation characteristics appears to be effective filtration aids for oil sands tailings filtration.

Effect of Aluminum Content

To investigate the effect of aluminum content in Al-PAM on its filtration performance, filtration tests were conducted using higher aluminum content Al-PAM (Al-PAM6H). Comparing the results in Figure 9 for Al-PAM6H with the results of Al-PAM6R in Figure 7, it is evident that high aluminum content of Al-PAM reduces optimal dosage: 20 ppm for Al-PAM6H vs 30 ppm for Al-PAM6R. This is consistent with optimal Al-PAM dosage of flocculation shown in Figure 5. At optimal dosage, however, the filtration rate is similar, indicating a similar structure of flocs and hence filter cake.

Effect of Fines in Supernatant

To confirm detrimental role of suspended fines in supernatant in oil sands extraction tailings, filtration tests with supernatant refilling were performed. In this set of tests, oil sands extraction tailings were obtained using a laboratory hydrotransport extraction system (Wallwark, 2004). In each test, 80 mL of supernatant from flocculated laboratory oil sands extraction tailings were filtrated through the filter cake formed by filtering Al-PAM8R flocculated laboratory oil sands extraction tailings.

The results obtained using laboratory oil sands extraction tailings at lower bitumen recovery (62.2%) are shown in Figure 10. For comparison, the filtration curve of laboratory oil sands tailing flocculated by Al-PAM8R is also included in this figure. It is interesting to note that the filtration rate of process water through the filter cake is slower than direct filtration of laboratory extraction tailings flocculated with 30 ppm Al-PAM8R. The lower filtration rate of filtering process water is attributed to the full development filter cake. The filtration through the filter cake of supernatant after settling of

Al-PAM8R flocculated laboratory extraction tailings for 5 min is slower than filtration of process water, indicating the presence of a limited amount of fine solids in the supernatant as indicated by visible turbidity of supernatant as shown in the insert of Figure 3.

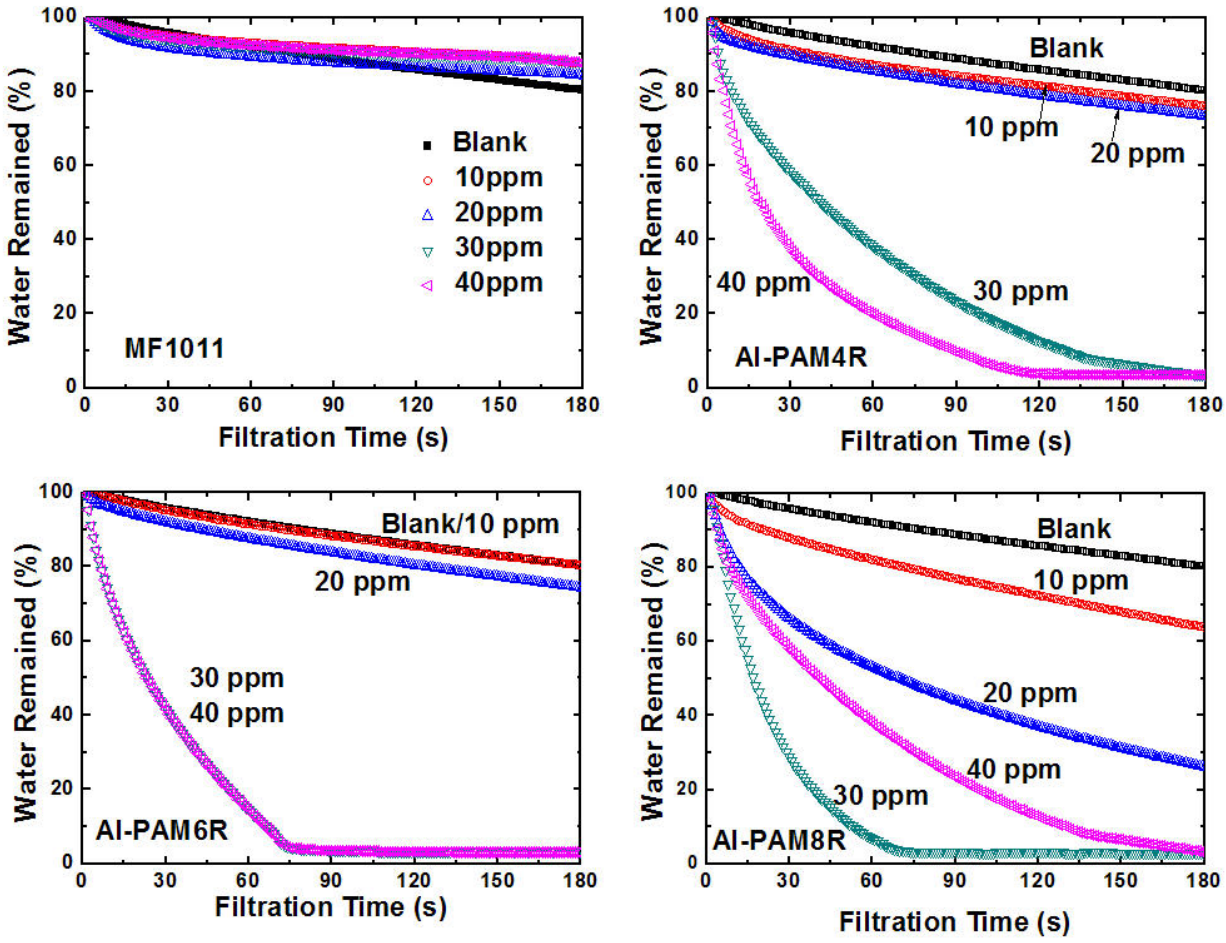

Figure 7. Effect of polymer addition on filtration of laboratory oil sands extraction tailings.

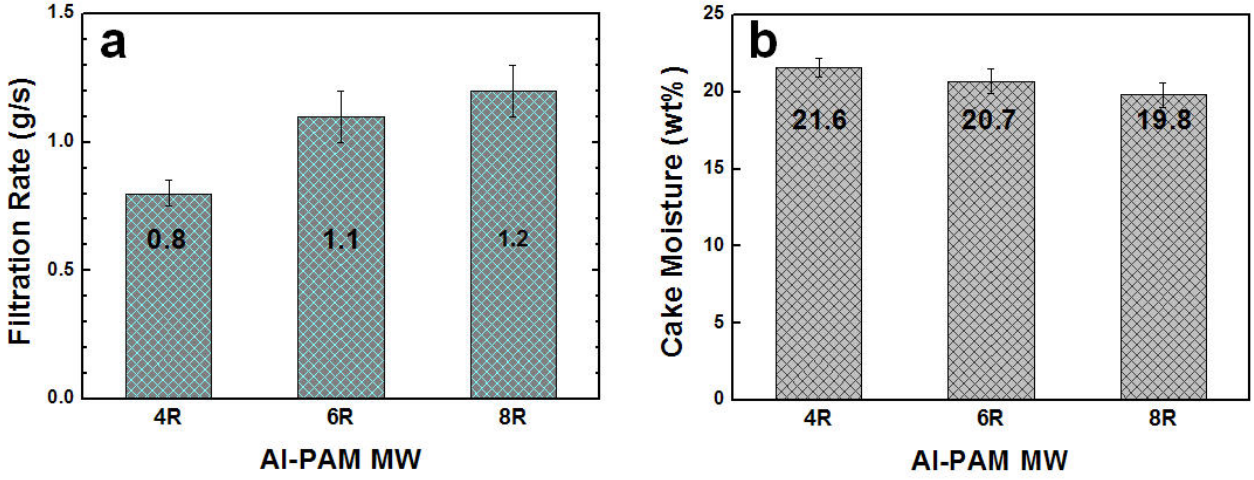

Figure 8. Effect of molecular weight of Al-PAMs at optimal dosages on filtration rate of laboratory oil sands extraction tailings and moisture content of filter cake.

In contrast, the filtration of supernatant produced by MF1011 proceeded at much slower rate, indicating the blockage of channels in the filter cake by fine particles suspended in the supernatant as shown in the inset of Figure 3.

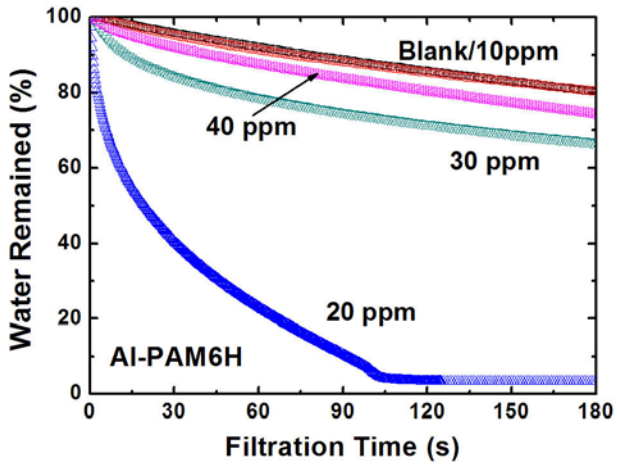

Figure 9. Effect of high aluminum content Al-PAM addition on filtration of laboratory oil sands extraction tailings.

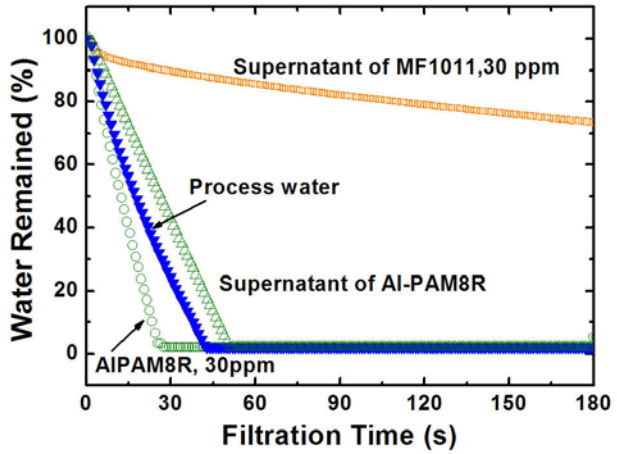

Figure 10. Effect of suspended fine solids in supernatant on filtration of laboratory oil sands extraction tailings.

The results of supernatant filtration confirm that the suspended solids in supernatant of MF1011 flocculated laboratory oil sands tailings are responsible for poor filtration performance of laboratory oil sands tailings. This finding provides a direction in searching for filtration aids: a good filtration aid should be not only capable of producing large and loosely packed flocs of desired mechanical strength, but also able to effectively flocculate fines.

Novel Filtration Process

Although filtration of oil sands extraction tailings after flocculation with optimal dosage of high molecular weight Al-PAM (Al-PAM8R) appears promising, the filtration time of 40 s remains relatively high, in particular considering filtration of large volume of oil sands extraction tailings. It is therefore more attractive if one could reduce filtration time. In this regard, filtration of sediments of flocculated oil sands extraction tailings is considered. The concept of filtering the sediments of flocculated oil sands extraction tailings is shown in Figure 11.

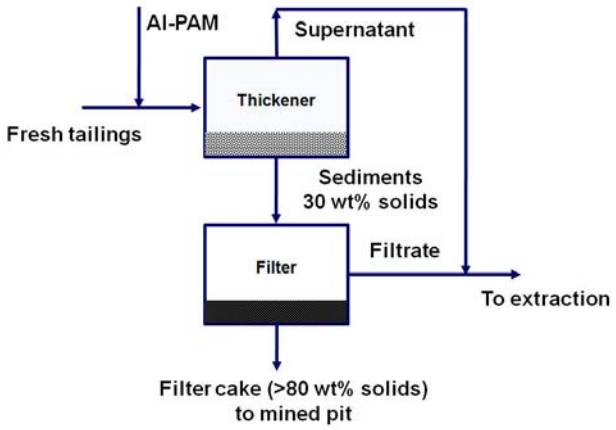

Figure 11. Concept of a novel two-step filtration process for treating large volume of oil sands extraction tailings: filtration of sediments after flocculation and thickening.

In this case, only small volume of sediments after thickener of flocculated oil sands extraction tailings needs to be run through the filer press. To prove the concept, filtration tests were conducted using oil sands extraction tailings obtained with laboratory hydrotransport extraction system. In this set of tests, supernatant was removed after settling for 5 min of flocculated oil sand extraction tailings and only sediments were filtered. The results in Figure 12 shows a significant decrease in filtration time from 20 s to 8 s by filtering sediments only after flocculation of oil sands extraction tailings using Al-PAM8R. More important, filtration of MF1011 flocculated sediments became feasible although it takes a bit longer to complete and the filter cake contains a slightly higher moisture content as

compared with the case of filtering sediments produced by Al-PAM8R.

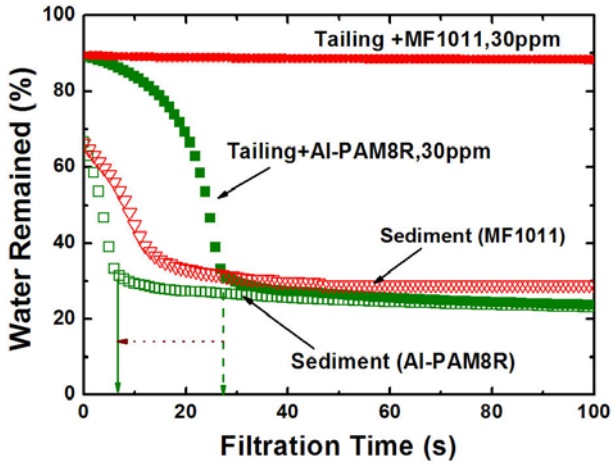

Figure 12. Filtration of sediments in comparison with direct filtration of flocculated laboratory oil sands extraction tailings.

It should be noted that this study focused mainly on the effect of Al-PAM design on flocculation and filtration. Less effort was made to characterize mechanical properties of formed aggregates, which determine the integrity and handling of sediments.

For the purposes of applying Al-PAM to treating warm oil sands extraction tailings and recycle of warm process water, further effort is needed to investigate the effectiveness of Al-PAM at oil sand extraction tailings temperatures as tailings are produced. For the purpose of water recycling, it is critical to determine the effect of residual chemicals (flocculants) in filtrate on processing of oil sands ores.

CONCLUSIONS

From this study, the following conclusions are derived.

1) Organic-inorganic hybrid Al-PAM is confirmed to be effective in flocculating oil sands extraction tailings for enhanced filtration.
2) Higher molecular weight and/or higher aluminum content of Al-PAM are found to be more effective for both thickening and filtration of oil sands extraction tailings.
3) Effective flocculation of ultrafine particles is the key for flocculant to be an effective filtration aids for oil sands extraction tailings.
4) Filtration of sediments after flocculation-assisted thickening reduces filtration time significantly, making filtration more practical.
5) Innovation in design of flocculants will provide a practical solution to management of oil sands tailings.

ACKNOWLEDGEMENT

The study was funded by Natural Sciences and Engineering Research Council of Canada (NSERC) under Industrial Research Chair Program in Oil Sands Engineering. We would like to thank Dr. Xianhua Feng and Dr. Lana Alagha for providing assistance on synthesis of Al-PAMs. Valuable discussions with Ms Tara (Xiaoyan) Wang and Ms Margo Chan are also greatly appreciated.

REFERENCES

Coulson, J.M., Richardson, J.F., Harker, J.H., Backhurst, I.R., 1991, Chapter 7: Liquid Filtration in Particle Technology & Separation Processes, Coulson & Richardson's Chemical Engineering Vol. 2, 5th edition, Butterworth-Heinemann, Oxford.

Eckert, W. F. Masliyah, J. H., Gray M. G., Fedorak, P. M., 1996, Prediction of sedimentation and consolidation of fine tails, AIChE J., 42, 960-972.

Kasongo, T., Zhou, Z., Xu, Z., Masliyah, J. H., 2000, Effect of clays and calcium ions on bitumen extraction from Athabasca oil sands using flotation, Can. J. Chem. Eng., 78, 674 - 681.

Li, H., Jun Long., Zhenghe Xu., Masliyah, J. H., 2008, Novel polymer aids for low-grade oil sand ore processing. Can. J. Chem. Eng., 86, 168-176.

Straszewska, D., Kovar, J., Bohdanecky, M., 1980, A note on the viscosity of dilute-solutions of polymer mixtures, Colloid Polymer Sci., 258, 600-604.

Wallwork, V., Xu, Z., Masliyah, J., 2004, Processability of Athabasca oil sand using a laboratory hydrotransport extraction system (LHES), *Can. J. Chem. Eng.*, 82: 687-695.

Wang, X., Feng, X., Xu, Z., Masliyah, J., 2010, Polymer aids for settling and filtration of oil sands tailings, Can. J. Chem. Eng. 88, 403-410.

Xu, Y.M., Dabros, T., Kan, J. M., 2008, Filterability of oil sands tailings, Process Safety and Environmental Protection, 86(B4), 268-276.

Yang, W.Y**.,** Qian, J.W., and Shen, Z.Q., 2004, A novel flocculant of $Al(OH)_3$-polyacrylamide ionic hybrid, J. Colloid Interface Sci., 273, 400-405.

Session 3

New Concepts

OIL SANDS TAILINGS TREATMENT VIA SURFACE MODIFICATION OF SOLIDS WITH POLYMERS

D. Soane, W. Ware, R. Mahoney, and K. Kincaid
Soane Energy LLC, Cambridge, MA, USA

ABSTRACT

A new water treatment technology has been developed that is capable of rapidly separating clays and other fine particulates from oil sands tailings streams. The process immediately liberates water for reuse in the bitumen extraction process and generates non-segregating solids that are suitable for dewatering and deposition. The process can reduce the need for long term storage of tailings in ponds and accelerate land reclamation.

This platform technology, termed the ATA (for Anchor-Tether-Activator) process, comprises three basic components: an Anchor particle, a Tether polymer and an Activator polymer. The oil sand extraction tailings stream is first split into a fines stream and coarse stream via a hydrocyclone. The hydrocyclone fines overflow is dosed with an Activator polymer, altering surface properties and causing the suspended clay fines to aggregate. The coarse sand in the hydrocyclone underflow serves as the Anchor particle and is coated with a monolayer of Tether polymer. The Tether-bearing Anchor particles exhibit a strong affinity to the Activated clay fines in the tailings. When the two treated streams are recombined, the Tether-bearing Anchor particles self-assemble with the aggregated clay fines in the Activated tailings, forming robust complexes that quickly settle.

Two output streams emerge from the ATA process: a clarified water stream that can be reused in the oil sands extraction process, and dewatered solids that possess sufficient mechanical integrity for reclamation. Benefits of the ATA process include: rapid dewatering of tailings, reduction in tailings ponds, reduced energy consumption due to the recycle water retaining a substantial amount of sensible heat, and a reclaimable, non-segregating solids stream. Recent developments include shear testing of ATA solids to simulate fluid transport conditions. Results are presented to demonstrate that ATA solids are capable of pipeline transport.

INTRODUCTION: FINE FLUID TAILINGS FROM OIL SANDS OPERATIONS

Mining operations often produce waste streams that contain fine particulates dispersed in aqueous phases. These fine particles can include clays, fine sands, silt, and organic matter. In order to remove these fine particles from the process stream to enable water recycling, either energy-intensive dewatering processes or long term settling must be employed.

The naturally occurring oil sand deposits in Northern Alberta, Canada are geologic formations composed of heavy petroleum hydrocarbons commingled with solid inorganic material. Large volumes of heated water are used commercially to extract the hydrocarbons from the inorganic solid matrix. This extraction process, along with mechanical stresses on the ore minerals, causes fine particles to become dispersed in the aqueous phase. After recovery of the petroleum values, the remaining waste stream, or tailings, is an alkaline solution containing fine suspended clays and other minerals, along with some residual hydrocarbons. In current practice, these tailings are stored in artificial ponds where the suspended solids are allowed to settle over a period of many years. During this settling period, residual heat energy is dissipated to the environment.

Management of tailings from bitumen extraction operations remains a challenge for oil sands producers. Existing tailings ponds cover an area of over 130 million square meters and contain about 720 million cubic meters of fine fluid tailings.[1] This is a condition that is not sustainable over the long term. The Energy Resources Conservation Board (ERCB) of Alberta recently issued Directive 074, titled “Tailings Performance Criteria and Requirements for Oil Sands Mining Schemes”, mandating that oil sands operators reduce fine tailings storage 30% by 2012 and 50% by 2013. Long term objectives of the ERCB Directive are:

- Eliminate tailings and wastewater storage on site
- Create a trafficable landscape for reclamation at the earliest opportunity
- Maximize the use of recycled process water to increase energy efficiency and reduce freshwater consumption
- Reduce the total footprint of the tailings ponds

CURRENT PRACTICES AND LIMITATIONS

In the formation of traditional tailings ponds, whole tailings (WT) are pumped directly from the extraction plant into manmade containment ponds. Coarse particles (>44 µm) settle quickly to form a beach near the WT outfall, while the fine particles (<44 µm) remain suspended in the aqueous phase. Over time, the fine particles partially settle within the aqueous phase to form mature fine tailings (MFT), a semi-solid sludge layer with approximately 30% solids by weight.

Oil sands operators have been developing alternatives to traditional tailings treatments for many years. The goal of these alternatives is to reduce the growth of tailings ponds and to recycle the water that they contain. Two alternative technologies are currently in use for capturing fines and recycling process water: Composite Tailings (CT) and Thickened Tailings (TT).

Composite Tailings

For this process, whole tailings at the extraction plant are initially processed with a hydrocyclone to produce an underflow stream of coarse particles and overflow stream of fine tailings. The fines stream is pumped into tailings ponds to consolidate into MFT. The underflow is combined with MFT dredged from the tailings ponds at a sand-to-fine ratio (SFR) between 3:1 and 4:1, and is then treated with gypsum as a coagulant. The resultant mixture is pumped to a disposal area for settling. The CT process allows operators to remediate their current inventories of MFT.

It was initially believed that CT deposits would quickly become trafficable solids that could be used for reclaiming the landscape. However, it has been determined that the dewatering rate of CT prevents the mixture from forming a geotechnically stable solid.[2] A number of factors make the CT process a delicate one, for example CT requires precise dosing of the components, which can be adversely affected by inconsistencies in the MFT composition or the coarse particle stream composition. CT is also shear-sensitive, allowing the coarse (sand) fraction to segregate from the CT mixture unless careful material handling is employed. Due to these limitations, the CT process alone may not allow operators to satisfy the ERCB requirements. As another drawback, the CT process requires the use of gypsum as a coagulant, which results in the presence of residual calcium ions in the recycle water stream. Since bitumen extraction is sensitive to the presence of divalent cations, water recycled from CT would require further treatment to safeguard the extraction process.

Thickened Tailings

The thickened tailings (TT) process treats whole tailings (WT) as this stream exits the extraction plant. The WT are separated by a hydrocyclone into a fine fraction (overflow) and a coarse fraction (underflow). The overflow is then mixed with flocculants and allowed to settle in large vessels. In the settling vessels, clarified water rises to the top while the flocculated fines settle to form a sludge at the bottom. One advantage of the TT process is the rapid clarification of water for recycling with limited heat loss. However, the TT process also produces a sludge that is not a geotechnically stable solid. This sludge, not suitable for land reclamation, must be either treated further or stored in containment areas. When thickened fine tailings are treated with course particles and coagulant as a further treatment, they yield a mixture called non-segregating tailings (NST). NST have some of the same limitations as CT, such as shear sensitivity.

THE ATA PROCESS

The Anchor-Tether-Activator (ATA) process employs surface-active polymers to cause the fines in the tailings to complex with heavier sand particles, so that the fines can be separated from the aqueous environment and compacted into a stable solid. The solids produced by the ATA process dewater efficiently, are non-segregating, have high mechanical stability, and are consistent with ERCB goals for tailings management. The ATA process also has the benefit of treating fresh WT, eliminating the need for long-term storage of

fines in tailings ponds. In addition, the rapid settling of the solids allows water to be recycled quickly with minimal heat loss.

The key to the ATA technology is the interaction between the Anchor-Tether complex and the Activated fines. The ATA process, shown in Figure 1 below, comprises three components: 1) an Activator polymer that is added to the fine tailings stream; 2) a Tether polymer that has a high affinity for the Activator; and 3) an Anchor particle that is coated with the Tether polymer. First, the Activator is added to the fine tailings causing the fines to aggregate together (Fig.1, Step A). Simultaneously, the Tether polymer is added to the coarse particles, coating the particles with a monolayer and changing their surface behavior (Fig. 1, Step B). When the two streams are combined (Fig. 1, Step C), the Activated fines spontaneously bind to the Tether-Anchor complex creating solid clusters. These clusters can be separated from the water via sedimentation or filtration. If any of the three ATA components (Anchor, Tether, or Activator) is left out, the solids do not settle out to form a stable, non-segregating complex with good drainage properties.

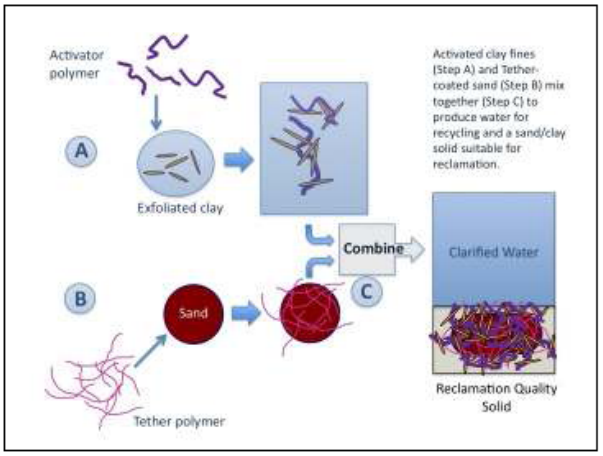

Figure 1. Schematic of the ATA mechanism

The ATA process is compatible with existing oil sands operations. For example, using existing technologies, whole tails can be separated into overflow and underflow using a hydrocyclone. Activator can then be mixed into to the hydrocyclone overflow. The underflow can be used to provide a readily available stream of Anchor particles to be treated with Tether. Unlike other technologies, the ATA process produces both warm recycle water containing less than 0.1% suspended solids and a dewatered solid that suitable for land reclamation. Table 1 below offers a comparison between the ATA, CT, TT, and NST processes.

Table 1. Comparison of Soane Energy ATA process with the CT, TT, and NST processes

Tailings Process Characteristics	ATA	CT	TT	NST
PROCESS:				
Capable of treating whole tails	Yes	No	Yes	Yes
Capable of treating MFT	Yes	Yes	No	No
WATER PRODUCED:				
Heat recovery possible	Yes	No	Yes	Yes
Water recycle time	Immediate	15+years	Immediate	Immediate
Safe for extraction (low Ca)	Yes	No	Yes	No
SOLIDS PRODUCED:				
Reclaimable	Yes	Partially	No	Partially
Self containing	Yes	No	No	No
Trafficable	Yes	Yes	No	Yes

ATA PERFORMANCE – SHEAR STABILITY

Stability to shear conditions is necessary to enable fluid transport of the ATA slurry from the point of formation to the point of dewatering or the dedicated disposal area. We have tested shear stability for the ATA process as follows.

Shear Rate vs. Settling Rate

To simulate pipeline transport, ATA solids were exposed to a wide range of shear conditions in a specially designed shear cell. The shear cell is calibrated to deliver a known shear rate based on the fluid properties of water. As a point of reference, the low end of this range (400 s^{-1}) is just enough mixing to keep all of the agglomerated solids suspended and the upper end of the range (1000 s^{-1}) is highly turbulent flow. This range is consistent with shear rates (10 - 1000 s^{-1}) reported[3] for pipe flow. After mixing ATA solids at a constant shear rate for one minute, the solids were allowed to settle and a settling rate was determined by observing the solid-liquid interface. Unsheared ATA showed a settling rate that approached 200 m/hr. The settling rate steadily decreased as the shear rate of the test was increased, with ATA settling at 12 m/hr after 1000 s^{-1} of shear (Figure 2). This decrease in settling rates indicates that the size of the ATA aggregates was decreasing but the solids are still

capable of separating by gravity. The reduced aggregate size does not indicate that the fines/sand complex in ATA is destroyed; later tests show that the coarse and fine aggregated particles remain cohesive under these conditions.

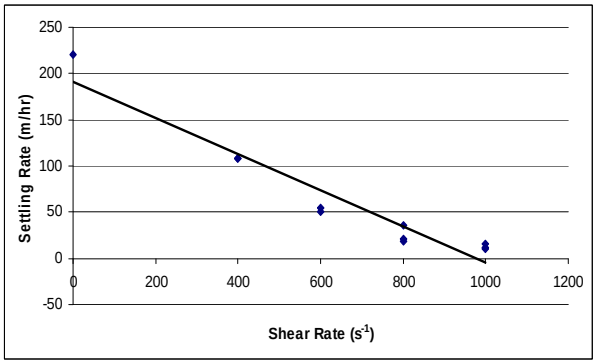

Figure 2. Settling rate of ATA solids vs. shear rate

Shear Rate vs. Segregation Index

While the size of ATA complexes was reduced by exposure to shear, this does not reflect a lower extent of fines capture in the sheared ATA. The integrity of the coarse-to-fines attachment can be measured by a Segregation Index (SI) under different shear conditions. Segregation Index is a measurement of a concentration gradient within a solids sample, calculated by determining the difference in moisture content of equal layers of the solid as follows.

*Segregation Index = (((average moisture) - (layer moisture)) / (average moisture)) * 100*

Segregation Index is also used to quantify the percent fines capture (FC), where FC is defined as 100-SI. A fines capture of less than 95% (SI above 5) is considered segregating. Conversely, when the SI is below 5, the solid in question is considered nonsegregating.[4]

Under ideal conditions, all layers of the solid have equal moisture content and equal fines content, indicating no stratification of coarse sandy material at the bottom of the deposit and no layer of fines at the top. To measure SI experimentally, ATA solids were sheared under different conditions then allowed to settle and the moisture content of four layers of the solids bed was measured. As shown in Figure 3, ATA was non-segregating when exposed to high rates of shear (up to 1000 s^{-1}) for one minute. However, when ATA samples were exposed to shear for 10 minutes, segregation was observed. These results suggest that ATA complexes are not broken apart upon short-term exposure to shear, and that limited pipeline transport of ATA slurry is possible.

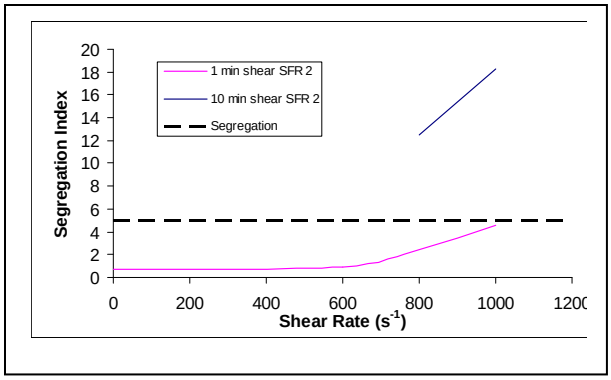

Figure 3. Segregation Index of ATA solids vs. shear rate

Shear Rate vs. Resistance to Filtration

Filterability is essential to some proposed dewatering mechanisms for ATA solids. The resistance to filtration (*r*) is a measure of the ability of a filtrate to pass through a filter medium such as a bed of solids. To determine the *r* value, the filtration rate is measured experimentally and the inverse of the filtration rate is plotted against the volume of filtrate. The linear portion of this plot can be described by the equation:[5]

$$\frac{t}{V} = \frac{\mu r \omega}{2PA^2} V + \frac{\mu r L_m}{PA}$$

Where *t* is filtration time (s); *V* is the filtrate volume (m^3); μ is the viscosity of the filtrate (Pa s); ω is the mass of the solids cake per unit filtrate volume (kg/m^3); *r* is the specific resistance of the filter cake (m/kg); *P* is the pressure on the top of the filter cake (Pa); *A* is the filter area (m^2); and L_m is the theoretical thickness of the filter medium. In this type of plot, the slope, *b*, and intercept, *a*, are:

$$a = \frac{\mu r L_m}{PA} \qquad b = \frac{\mu r \omega}{2PA^2}$$

At a constant pressure, resistance to filtration (*r*) can be calculated as:

$$r = \frac{2PA^2}{\mu\omega} b$$

Experiments were conducted to measure the resistance to filtration after shearing the ATA solids at different shear rates as described above. The shear-induced reduction in ATA aggregate size does influence the filtration of ATA solids. The smaller structures cause the ATA solids to have smaller pore openings and a higher resistance to filtration (Figure 4). However, even after exposure to high shear rates ATA has a relatively low *r* value, less than 5.0E+07 m/kg. For comparison, a Thickened Tailings (TT) mixture was prepared and the *r* value was determined to be 3.0E+10 m/kg, significantly higher than ATA. This finding is consistent with reported literature values of 2.4E+09 to 3.2E+12 m/kg for TT.[5]

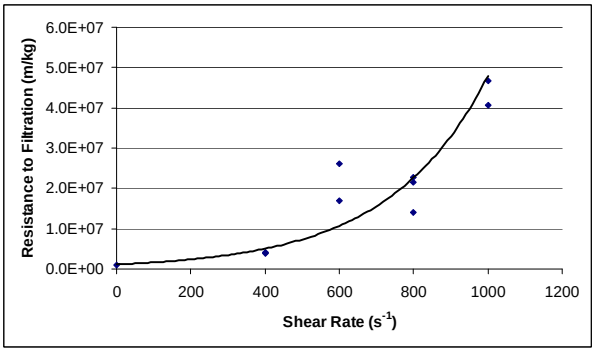

Figure 4. Resistance to filtration as a function of shear rate

The results of shear exposure testing show that sheared ATA solids have a reduced size of aggregates, yet the fines remain captured. The amount of shear stability is consistent with the demands of pipeline transport over limited distances. Also, filtration of ATA solids is shown to be a viable dewatering mechanism.

ENVIRONMENTAL IMPACT

By collecting the fine fluid tails within a nonsegregating sand matrix, the ATA process yields a mechanically stable solid that is suitable for land reclamation. In order to meet ERCB Directive 074 requirements, ATA solids must meet or exceed the metrics summarized here:

- Deposit must have a minimum undrained shear strength of 5 kPa after 1 year
- Deposit must be ready for reclamation within 5 years after deposition
- Deposit must form a trafficable surface with undrained shear strength of 10 kPa

The ATA process causes the rapid release of process water, allowing the water to be reclaimed with minimal heat loss. The warm water can then be recycled directly into the extraction process or sent through a heat exchanger. The goal is to reclaim 70% of the ATA process water at a thermal loss of 5°C. This benchmark has both economic and environmental advantages. By capturing the energy in the recycled water, the ATA process can reduce the need to burn natural gas as a source of heat. This can reduce the operating cost of bitumen extraction and reduce greenhouse gas emissions.

Operators with existing tailings ponds are able to satisfy 75 - 80% of their freshwater demand by recycling water from their ponds. The balance is obtained from the local surface waters. However, new operators have not accumulated the clarified water reserves, and therefore must draw the majority of their water from the local water supply. It is estimated that the oil sands industry uses 100 million gallons of water per day. As the industry grows, that number is projected to rise to 264 million gallons per day, potentially straining the local watershed.[6] A new operator with a fully implemented ATA tailings management system would be able to significantly reduce their freshwater demand and improve the long term sustainability of the industry.

REFERENCES

ERCB website, www.ercb.ca

M.D. MacKinnon, J.G. Matthews, W.H. Shaw, and R.G. Cuddy (2001) Water quality issues associated with implementation of composite tailings (CT) technology for managing oil sands tailings, International Journal of Surface Mining, Reclamation, and Environment, Vol. 15, No. 4, pp. 235-256.

H.A. Barnes (2000) Handbook of Elementary Rheology, Table 1, University of Wales.

Y.T. Mihiretu (2009) Fundamentals of Segregation, PhD thesis, University of Alberta.

Y. Xu, T. Dabros, J. Kan (2008) Filterability of oil sands tailings, Journal of Process Safety and Environmental Protection, Vol. 86 pp. 268-276.

Griffiths M, Woynillowicz D (2003) Oil and Troubled Waters: Reducing the impact of the oil and gas industry on Alberta's water resources, Pembina Institute, April 2003.

RECOVERY OF HYDROCARBONS FROM MATURE FINE TAILINGS OF OIL SANDS EXTRACTION

T. Thomas[1], A. Afacan[1], J. Masliyah[1], Z. Xu[1], Y. Wang[2] and J. Liu[2]
[1]University of Alberta, Edmonton, Alberta, Canada
[2]China University of Mining Technology, Xuzhou, China

ABSTRACT

Bitumen recovery by hot water-based extraction process produces waste streams known as tailings that are currently discharged to tailing ponds. When discharged, the coarse solid particles in the tailings stream settle out quickly, while the fine solids accumulate over years of settling to a solid content of 30-35 wt%. This fluid fine sludge, known as mature fine tailings (MFT), traps 1-3 wt% hydrocarbons within its stable slurry structure. The remediation of these mature fine tailings is one of major challenges facing the oil sands industry. This study was intended to investigate potential recovery of residual hydrocarbons in the MFT by froth flotation. Using a laboratory Denver flotation cell operated in a batch mode, the effect of MFT dilution ratio, flotation hydrodynamics and aeration ratio on hydrocarbon recovery kinetics was studied. Flotation was found to be capable of recovering more than 80% of the hydrocarbons contained in the MFT. The hydrocarbon rich froth produced by a continuous column flotation cell was treated by naphtha-based froth cleaning which was found to produce hydrocarbon product similar to diluted bitumen obtained in bitumen extraction process, suitable for upgrading.

INTRODUCTION

Bitumen in oil sands is a non-conventional form of crude oil. Oil Sands are unconsolidated deposits of sands impregnated with a high molar mass and viscous form of petroleum known as bitumen. The largest oil sands deposit found in Alberta entails a recoverable crude oil of 175 billion barrels, second only to Saudi Arabia's reserves of conventional oil (Alberta Energy Utilities Board, 2006). These oil sands are a mixture of sand (mineral solids constituting about 80-85 wt%), water (3 to 7 wt %), mineral rich clays (about 15-30 wt% of mineral solids less than 44 μm in diameter) and heavy viscous bitumen which is substantially heavier than conventional crude oil hydrocarbons (about 7-16 wt%) Masliyah and gray, 2007). The current extraction method based on the Hot Water Extraction Process, (HWEP) (Clark, 1994) produces a clean bitumen product as the feed to the up-grader. Bitumen recovery by the HWEP is typically more than 90%. The HWEP produces waste streams known as tailings which are difficult to handle. The tailings containing sand particles, dispersed fines and water along with residual bitumen are hydraulically transported and deposited in the tailings ponds. The coarse particles in the tailings when discharged segregate to form a sloping beach that becomes dykes for the tailings ponds (FTFC, 1995). The remaining fines settle slowly and accumulate over a few years to form a stable sludge containing about 30-35 wt% solids and 1-3 wt% hydrocarbons (Cymerman, et al., 1999). This sludge is referred to as mature fine tailings (MFT). About 0.25 m^3 of mature fine tailings is generated from production of one barrel of synthetic bitumen (Nelson, 2006). The residual hydrocarbons in MFT could be a good source of hydrocarbons that are otherwise toxic in nature due to the presence of traces amount of naphthenic acids in the residual hydrocarbons. If a technology is available to economically recover these hydrocarbons, it could reduce the ever visible environmental footprint of the oil sands extraction processes.

The main objective of this study is to investigate potential recovery of the hydrocarbons from MFT using a laboratory Denver flotation cell operated in a batch mode. The effect of MFT dilution, mixing and aeration on hydrocarbon recovery kinetics is studied. The hydrocarbon recovered was cleaned using current naphthenic froth cleaning process currently practiced in the oil sands industry (Masliyah and Gray, 2007).

MATERIALS AND METHODS

Materials

Syncrude mature fine tailings (MFT) provided by the Oil Sands Tailings Research Facility (OSTRF) was used in this study. The composition of the MFT determined using Dean Stark (Soxhlet extraction)

method is given in Table 1. The errors shown in the table represent the standard deviation obtained from five representative samples. It can be seen that the MFT is a suspension consisting of water, fine solids and hydrocarbons. The average particle size of fine solids is determined to be d_{50}= 17.7 µm. The raw MFT is extremely viscous and difficult to process without dilution.

Table 1. Composition (wt%) of MFT used in this study

Hydrocarbons	Solids	Fines*	Water
3±0.3	35±0.1	97±0.5	62±0.1

*number represent percent solids finer than 44 µm.

Experimental Procedures

Denver flotation cell

A schematic diagram of the Denver flotation cell is shown in Figure 1. The cell manufactured by the Denver Company is modified to include a custom-made water jacket around a one-litre flotation cell made of 316 Stainless Steel. The water jacket is connected to a Neslab water bath from which water at a given temperature was circulated, thereby ensuring a constant temperature within the cell. Aeration for froth flotation of the hydrocarbons is achieved by passing air through the impeller shaft. The air flow rate is measured using a pre-calibrated Matheson flow meter (No 7641 C/W602). The agitator (impeller) is driven by ½ HP Baldor Industrial Motor manufactured by the Baldor Electric Company. The agitation speed of the batch flotation tests is determined using a tachometer. The pH of slurry is measured using a portable pH meter from OAKTON Eutech Instruments, pH 110.

In each test, the diluted MFT was preheated to 35 ºC before being fed into the Denver flotation cell, and maintained at 35 ºC through flotation tests. The slurry in the Denver flotation cell was agitated at 1500 rpm for 5 minutes without air addition. The floatation was carried out for about 20 minutes with continuous air addition at a given flow rate of 150 mL/min, unless otherwise stated. The froth was collected into pre-weighed thimbles over different time intervals of 3, 5, 10 and 20 minutes.

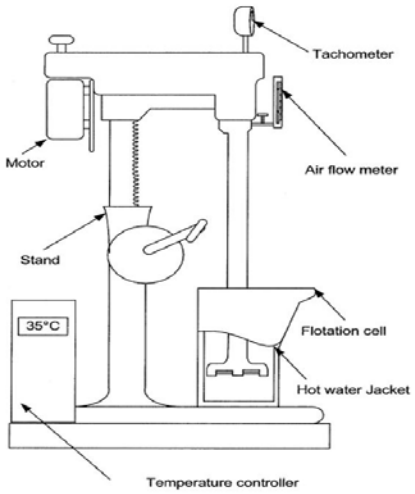

Figure 1. Schematics of a laboratory Denver flotation cell

The composition of froth was analyzed using Dean Stark apparatus, which allowed determination of hydrocarbon recovery and amount of unwanted mineral solids in the recovered bitumen froth. The flotation performance is evaluated by cumulative hydrocarbon recovery and froth quality by solids to hydrocarbon ratio as defined below. Cumulative recovery, *R(t)* is defined as the percentage of bitumen in the feed that is recovered over a given flotation period, i.e.,

$$R(t) = \frac{Hydrocarbon\ \ in\ Froth}{Hydrocarbon\ in\ Feed} \text{x} 100 \qquad (1)$$

Assuming that the batch flotation process in the Denver flotation cell follows a first order process, the recovery rate, *R(t)* can be calculated by:

$$R(t) = R_m(1 - e^{-k\,t}) \qquad (2)$$

where R_m is the maximum possible recovery at infinite flotation time, *k* is the flotation rate constant and *t* is the cumulative flotation time.

Flotation column

In view of treating larger batches of tailings and with an onus towards continuous operations, the dynamics derived from the batch flotation operations were used in developing a methodology for continuous operations. For this purpose, a flotation column shown in Figure 2 was used for

continuous flotation tests. The column is made of Pyrex glass with an inner diameter of 100 mm. The column contained three peristaltic pumps (Masterflex I/P) to control the flow rate of feed, tailings and recirculation streams. A 20-L baffled feed mixing tank with an overhead mixer is used to prepare feed slurry.

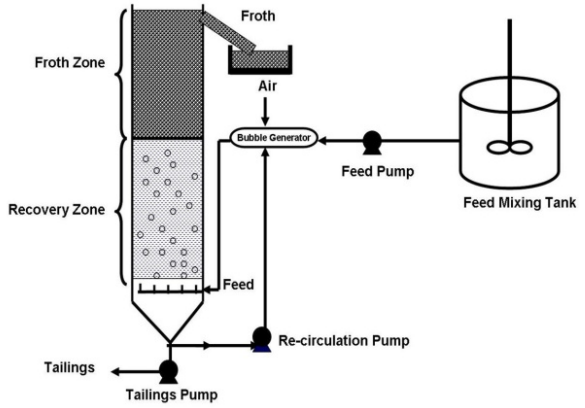

Figure 2. Schematics of a continuous flotation column

For each test, the slurry was prepared in the mixing tank. The MFT samples were diluted with process water at a 1:2 mass ratio. The slurry temperature was kept constant at 35 ºC. This was accomplished by heating the process water to the required temperature prior to mixing with MFT sample in the feed mixing tank. The column was first filled with process water at 35 ºC. The recirculation pump was started to establish the continuous flow condition. The feed slurry was then introduced into the flotation column. Once froth zone was established and the initial froth was produced, the tailings pump started. The feed, tailings and froth samples were taken after an initial operation of 30 minutes at each condition to ensure the steady state operation of the flotation. The collected samples were analysed for their hydrocarbon, solids and water content using Dean Stark apparatus. Recovery of hydrocarbons, *R* is calculated by:

$$R = \frac{F\,P\,x_{FP}}{F\,x_F} \qquad (4)$$

where *P* and *F* are the mass flow rate of froth product and feed streams, and x_{FP} and x_F are the mass fraction of hydrocarbons in froth and feed streams, respectively.

RESULTS AND DISCUSSION

Effect of Dilution Ratio, N

The effect of MFT dilution ratio, using Aurora recycle water (process water) on the recovery of hydrocarbons from the MFT was first studied. The MFT samples were diluted with process water to a mass ratio of 1:N (where N = 0, 1 and 2). In this set of tests, the agitation speed and air flow rate were set at 1500 rpm and 150 mL/min, respectively. The feed slurry temperature was kept at 35ºC. The froth samples were collected into different pre-weighed thimbles over time intervals of 3, 5, 10 and 20 minutes. The hydrocarbon recovery in each time intervals was calculated using Equation (1). Figure 3 shows the recovery of hydrocarbons as a function of flotation time at different dilution ratios.

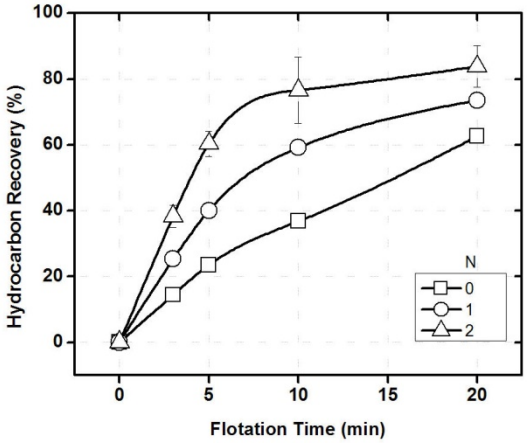

Figure 3. Effect of dilution ratio, N on hydrocarbon recovery from diluted MFT

Increasing the dilution ratio with process water is shown to increase hydrocarbon recovery. At a dilution ratio of 2, for example, the hydrocarbon recovery could reach as high as 80%. Dilution is necessary because MFT is extremely viscous, hindering the contact of hydrocarbons with air bubbles and hence their flotation.

Figure 4 compares hydrocarbon recovery and solids to hydrocarbon ratio (SHR) at different dilution ratios. Increasing the dilution ratio is shown to decrease the amount of solids recovered in the froth product, i.e., drastically improve the quality of hydrocarbon froth. Increase in dilution ratio decreases the solids content in the feed slurry and hence solid carry over into the froth, even though the water recovery is also increased with dilution

ratio as shown in Table 2. It is clear that increasing dilution ratio of MFT is highly beneficial for improving both MFT recovery and froth quality.

The flotation parameters, such as the ultimate recovery, R_m and flotation rate constant, k (min^{-1}) obtained by fitting the flotation experiment data given in Figure 3 to Equation (2) using non-linear regression wizard of the Origin 7.5 software, are shown in Table 2. It can be seen that the ultimate recovery, R_m is higher (85%) for flotation of MFT with no dilution as compared with two times dilution (N=2). However the corresponding flotation rate constant, k is four times smaller. It indicates that a much shorter flotation times is needed to achieve a desired hydrocarbon recovery at higher dilution. Further increase in dilution ratio of feed is not attempted in this study, as higher dilution would lead to handling of excessive large volumes by flotation cells in practice, which would reduce the residence time for treating the same volume of raw MFT. The dilution ratio was kept at 1:2 for the remaining tests.

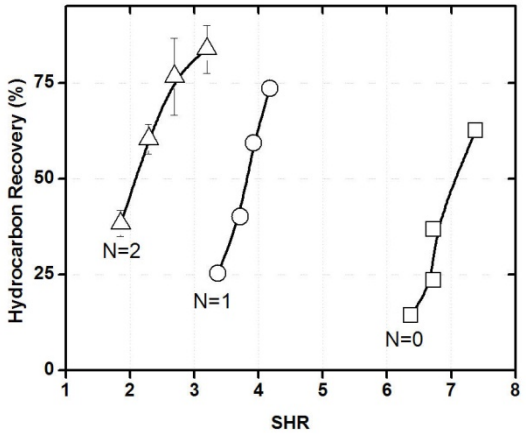

Figure 4. Effect of dilution ratio, N on hydrocarbon recovery and froth quality measured by solids to hydrocarbon ratio (SHR)

Table 1. Hydrocarbon recovery parameters of MFT flotation at different dilution ratio

Dilution ratio N	Cumulative recovery (%)	R_m (%)	k (s^{-1})	SHR	Water/Hydrocarbon ratio
0	62	97.4	0.05	7.4	12.1
1	74	78.4	0.14	4.2	23.2
2	84	85.5	0.22	3.2	26.4

Effect of Dilution Medium

To determine the source of water for MFT dilution prior to its flotation and its effect on hydrocarbon recovery, different types of water were used. The MFT were diluted with process water, de-ionized water and tap water. To eliminate the effect if any caused by the variation in pH of the three different sources of water, the pH of the other two sources of water was adjusted to the same pH value of 8.2 as the Aurora recycle water prior to dilution. The froth flotation was conducted under identical conditions of 1500 rpm agitation and 150 mL/min aeration rate at 35 °C. Table 3 shows a comparison of hydrocarbon recovery obtained with different dilution water. A negligible variation in hydrocarbon recovery was observed among the three sources of water, demonstrating that hydrocarbon recovery is independent of source of dilution water. Dilution is therefore thought to mainly reduce the viscosity of the slurry and entrainment of fine solids to hydrocarbon froth.

Table 3. Effect of dilution medium on hydrocarbon recovery from diluted MFT

Dilution medium	Cumulative Recovery (%)
Process water	83.8
De-ionized water	89.9
Tap water	89.6

Effect of Aeration Rate

The effect of aeration rate on hydrocarbon recovery from diluted MFT was also studied. In this set of tests, the MFT was diluted with process water at 1:2 mass ratio, the pH was maintained at 8.2, the solution temperature at 35 °C, flotation time at 20 minutes and agitation speed at 1500 rpm. Air flow rate varied from 25, 150, 525 to 730 mL/min. Figure 5 shows hydrocarbon recovery as a function of flotation time at various air flow rates. It can be seen that hydrocarbon recovery

increases with increasing air flow rates. Increasing the air flow rate is anticipated to produce more bubbles and hence larger bubble surface area flux, increasing attachment of hydrocarbons with bubbles and resulting in higher hydrocarbon recovery rate as shown in Table 4. However the overall hydrocarbon recovery (R_m) for all air flow rates is essentially similar, although there is a slight trend of increasing hydrocarbon recovery with increasing aeration rate.

Table 4. Effect of air flow rate on recovery parameters of hydrocarbons by flotation

Air flow rate (mL/min)	Recovery (%)	R_m (%)	k (s^{-1})
25	78	83.5	0.18
150	83	85.5	0.22
525	86	85.8	0.26
730	89	88.5	0.43

Figure 6 shows the hydrocarbon recovery and froth quality profile at different aeration rate. Increasing aeration rate shows a continuous increase in froth quality, i.e., less solids were recovered in the froth at a given hydrocarbon recovery. It appears that increasing aeration rate caused a significant increase in collisions of mineralized (hydrocarbon-covered) bubbles, leading to an increased coalescence and hence increased hydrocarbon load per unit floated bubble surface area and reduced recovery of water per unit recovery of hydrocarbons. Both contribute to an improved hydrocarbon froth quality. Hence high air flow rates are highly desirable for a higher hydrocarbon recovery and froth quality.

Figure 7 shows that flotation rate constant increased only marginally with increasing aeration rate up to 550 mL/min. However a significant increase in flotation rate with further increase in aeration rate was observed. Although it is anticipated that flotation rate constant increases with increasing aeration rate due to increase in the number of bubbles or bubble surface area with increasing aeration rate, the reason for the sharp increase in flotation rate constant with increasing aeration rate above 550 mL/min remains to be established.

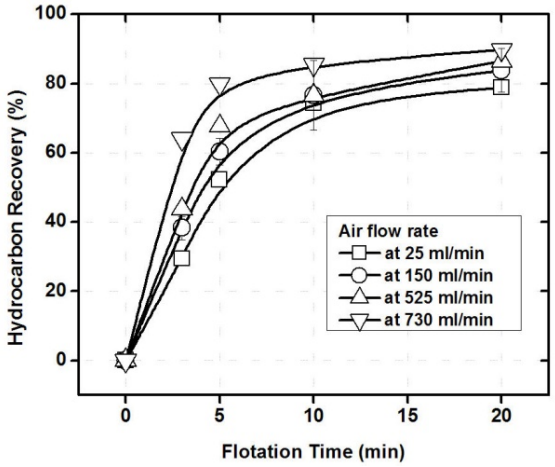

Figure 5. Effect of air flow rate on hydrocarbon recovery from diluted MFT

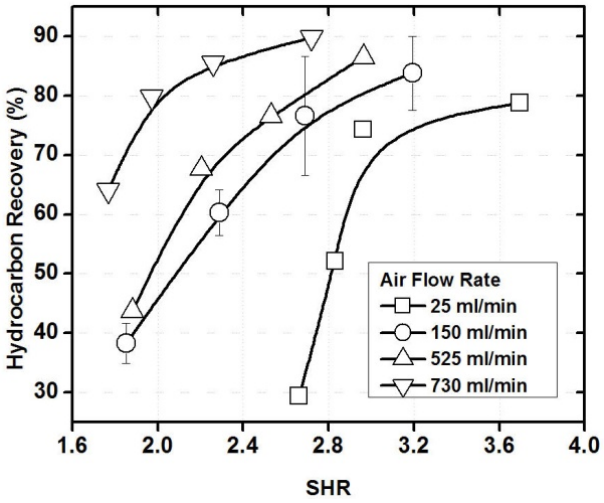

Figure 6. Effect of air flow rate on hydrocarbon recovery and froth quality measured by solids to hydrocarbon ratio (SHR)

Effect of Agitation Speed

Effect of agitation speeds on hydrocarbon recovery from MFT was studied. In this set of tests, the slurry temperature and air flow rate were kept constant at 35 °C and 150 mL/min, respectively. Three different agitation speeds of 900, 1500 and 2100 rpm were used. Figure 8 shows hydrocarbon recovery as a function of time.

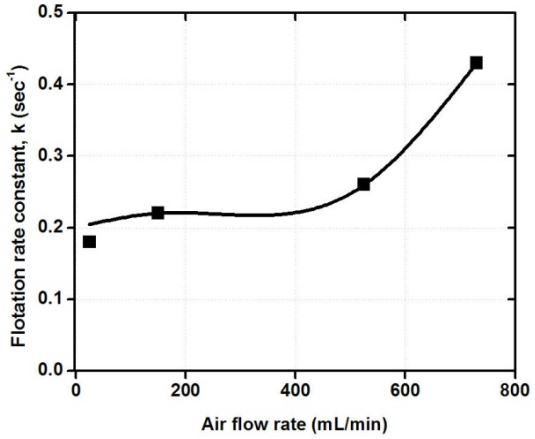

Figure 7. Effect of air flow rate on flotation rate constant of hydrocarbon recovery from MFT

It can be noted that the hydrocarbon recovery increases with increasing agitation speed. Increasing agitation speed increases the shear of the slurry, possibly leading to an increased liberation of hydrocarbons from the solids. Increasing agitation speed also increases breakup of air bubbles, producing smaller air bubbles of higher total surface area for contacting hydrocarbons and hence, leading to a faster flotation rate and increasing overall bitumen recovery. Furthermore, higher agitation speed increases the collision between air bubbles and liberated hydrocarbons, contributing to an increase in hydrocarbon recovery. Overall, increasing agitation speed increases ultimate hydrocarbon recovery and flotation rate constant as shown in Table 5.

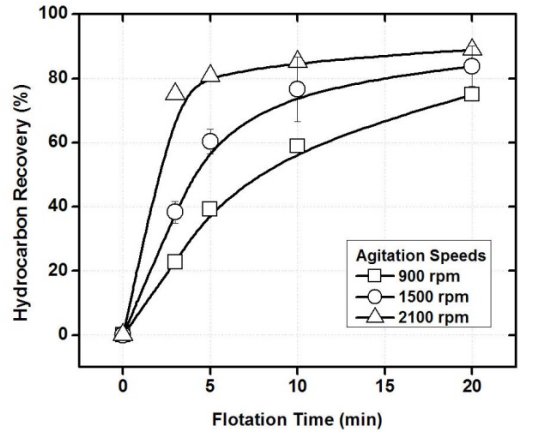

Figure 8. Effect of agitation speed on hydrocarbon recovery from diluted MFT

It is interesting to note an exponential increase in flotation rate constant with increasing agitation speed as shown in Figure 9. This finding further supports that increasing agitation speed reduces size of bubbles and increases collision between air bubbles and liberated hydrocarbons, collectively increasing flotation rate.

Table 5. Effect of agitation speed on recovery parameters of hydrocarbons by flotation

Agitation speed (rpm)	Recovery (%)	R_m (%)	k (s^{-1})
900	75	82.6	0.12
1500	84	85.5	0.22
2100	89	86.4	0.64

The results in Figure 10 show a negligible effect of agitation speed on froth quality as all the data points collapse essentially on a single hydrocarbon recovery and froth quality curve. Overall, high agitation speed is beneficial for recovery of hydrocarbons from MFT by a mechanical flotation cell.

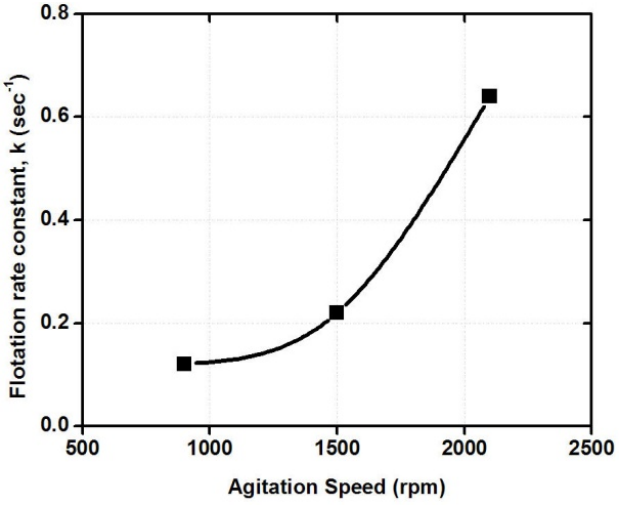

Figure 9. Effect of agitation speed on flotation rate constant of hydrocarbon recovery from MFT

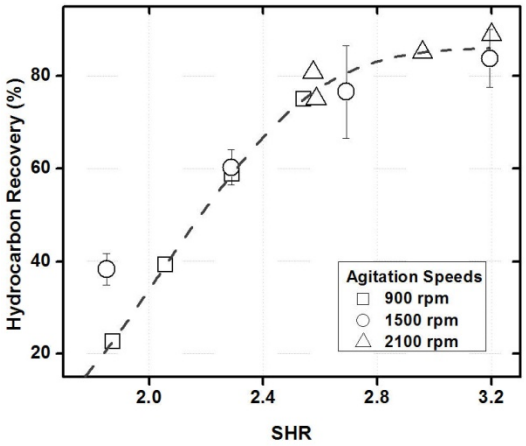

Figure 10. Effect of agitation speed on hydrocarbon recovery and froth quality measured by solids to hydrocarbon ratio (SHR)

Hydrocarbon Recovery by a Continuous Flotation Column

After establishing the potential of flotation technology for recovery of hydrocarbons from MFT in a batch Denver flotation cell, recovery of hydrocarbons was also studied using a continuous flotation column. The slurry or feed for the flotation column was prepared in the feed mixing tank by diluting the MFT with Aurora recycle process water to a 1:2 mass ratio. The prepared slurry was found to have a hydrocarbon concentration of 1 wt% and a solid concentration of about 12 wt%. The flotation was carried out at 35 ^{o}C. The slurry was fed into the column and the froth was collected after 30 minutes of flotation to ensure the steady state. The froth collected was analyzed for its hydrocarbon and solids content using the Dean Stark method. The results in Figure 11 show that after 30 minutes, the hydrocarbon recovery is constant at about 80%, indicating a steady state. The solids content in both froth and tailings remained at about 12 wt%, indicating entrainment of solids to the froth. Flotation column is seen to be suitable for recovering hydrocarbons from the diluted MFT.

Hydrocarbon Froth Cleaning

Since hydrocarbon recovered in froth containing about 15-20 wt% hydrocarbon and 12-14 wt% solids remains poor quality, froth cleaning is essential prior to the upgrading operations as practiced in bitumen extraction process.

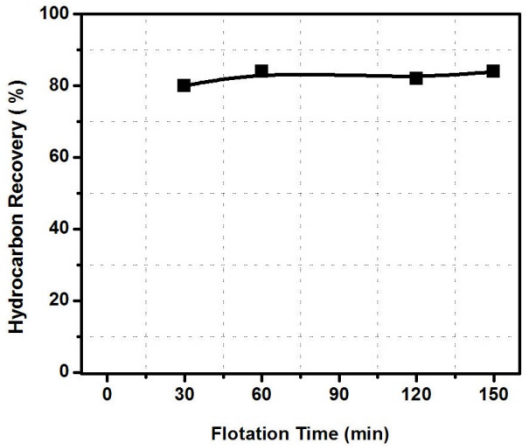

Figure 11. Hydrocarbon recovery from diluted MFT by a laboratory continuous flotation column

There are two commercial bitumen froth treatment processes used in oil sands industry: the naphthenic froth treatment (NFT) process used by Syncrude Canada Ltd., Suncor Energy Inc. and Canadian Natural Resources Ltd., and the paraffinic froth treatment (PFT) process practiced by Albian Sands Energy. The NFT process uses naphtha as the diluent at a naphtha-to-bitumen mass ratio of 0.6–0.75, while the PFT process uses paraffinic solvent of C_5-C_6 mixtures as the diluents at an alkane-to-bitumen mass ratio of 2.1-2.5. In this study, naphtha was used to assist separation of remaining water and solids in the froth by gravity method. The naphtha was added to the hydrocarbon froth at a naphtha-to-hydrocarbon ratio of about 0.65. The diluted hydrocarbon froth was then centrifuged at a relatively low centrifugal speed of 3500 rpm for 30 minutes. The centrifuged froth was allowed to stand still. Three distinct layers were formed. The hydrocarbon layer on the top was removed carefully and dried under vacuum to evaporate the diluent. The water content in the hydrocarbon layer is then determined using a Karl Fischer titrator. The water content in the clean hydrocarbon is shown in Table 6. Two different runs of column flotation using two MFT samples from Syncrude were analysed. It can be seen that despite a large amount of water in the hydrocarbon froth, the addition of naphtha has been successful in rejecting water from the froth from about 73.7% to 0.2% with a negligible amount of solids at a hydrocarbon recovering of more than 98% of the hydrocarbons in the froth. It is important to note that the hydrocarbons recovered from MFT contain significantly higher asphaltene content than bitumen, but can be cleaned to the quality for upgrading.

Table 2. Composition of feed, hydrocarbon froth and cleaned hydrocarbon froth

No	MFT (wt%)			Hydrocarbon froth (wt%)			Naphtha/ Hydrocarbon (wt:wt)	Water in cleaned froth (wt%)
	Hydrocarbon	Solids	Water	Hydrocarbon	Solids	Water		
1	2.12	30	67.88	14.17	12.07	73.76	0.65	0.28
2	2.78	29.41	67.81	16.55	11.33	72.12	0.65	0.23

SUMMARY

In this study, potential recovery of hydrocarbons from mature fine tailings (MFT) of Syncrude Canada was investigated using a laboratory scale Denver flotation cell. With proper dilution, independent of type of dilution medium, flotation was found capable of recovering about 80% of hydrocarbons in MFT. The flotation conditions such as dilution ratio, mixing speed and air flow rate showed significant effect on hydrocarbon recovery and froth quality. Cleaning of the froth with naphtha produced a hydrocarbon product containing less than 0.3 wt% water and negligible amount of solids, i.e., a hydrocarbon product suitable for upgrading. Despite a hydrocarbon content of less than 2 wt% in MFT, recovery of valuable hydrocarbon source in MFT using conventional flotation methods makes it a lucrative proposition, simply due to the massive scope and scale of the tailings produced from oil sands mining operations.

ACKNOWLEDGEMENTS

The study was funded by Natural Sciences and Engineering Research Council of Canada (NSERC) under Industrial Research Chair Program in Oil Sands Engineering. We also would like to thank OSTRF for providing us with MFT samples.

REFERENCES

Alberta Energy and Utilities Board. *Alberta's Energy Reserves and Supply Outlook 2006–2015*, 2006.

Masliyah, J.H., Gray, R.M., *Extraction and Upgrading Oil Sands Bitumen (Intensive Short Course Notes),* 2007.

Clark, K., Hot Water Separation of Alberta Bituminous Sand. *The Canadian Institute of Mining and Metallurgy,* 201-214, 1994.

Fine Tailings Fundamental Consortium (FTFC), Advances in Oil Sands Tailings Research, Alberta Department of Energy, Edmonton, Alberta, 1995.

Cymerman, G., Kwong, T., Lord, T., Hamza, H., Xu, Y., Thickening and Disposal of fine Tails from Oil Sand Processing, in *Proceedings, 3rd UBC-McGill International Symposium on Fundamentals of Mineral Processing (CIM),* Met Soc, Montreal, 1999, pp. 605-619.

Nelson, R., Strategic Needs for Energy Related Water Use Technologies, Alberta's Environment Conference, Edmonton, February 2006.

OIL SANDS MINE PLANNING AND WASTE MANAGEMENT USING GOAL PROGRAMMING

Eugene Ben-Awuah and Hooman Askari-Nasab
Mining Optimization Laboratory (MOL)
University of Alberta, Edmonton, Alberta, Canada

ABSTRACT

Strategic mine planning and waste management is an important aspect of surface mining operations. Recent environmental and regulatory requirements makes waste management an integral part of mine planning in the oil sands industry. In oil sands mining, due to the limitation of lease area, the pit phase advancement is carried out simultaneously with the construction of tailings dykes in the mined out areas of the pit. These dykes are constructed to hold tailings that are produced during the processing of the oil sands. Most of the materials used in constructing these dykes come from the oil sands mining operation (overburden and interburden) making it necessary to have a plan for supplying the dyke material. The research problem here is determining the order of extraction of ore, dyke material and waste to be removed from a predefined ultimate pit limit over the mine life that maximizes the net present value of the operation – a strategic schedule. The strategic schedule to be developed is subject to a variety of economic, technical and physical constraints.

We have developed, implemented, and tested a proposed mixed integer goal programming theoretical framework for oil sands open pit production scheduling with multiple material types. The formulation uses binary integer variables to control mining precedence and continuous variables to control mining of ore and dyke material. There are also goal deviational variables that must be set up by the planner. The optimization model was implemented in TOMLAB/CPLEX environment.

The developed model proved to be able to generate a uniform schedule for ore and dyke material. It also provides the planner the flexibility of choosing goal deviational variables leading to improved NPV.

INTRODUCTION

Mining is the process of extracting a beneficial natural resource from the earth (Newman et al., 2010). The extraction process can be an underground or open pit mining operation and this research will be restricted to the latter. An important aspect of mining engineering is mine planning. Whittle (1989) defined open pit mine planning as the process of finding a feasible block extraction schedule that generates the highest net present value (NPV) subject to some operational and technical constraints. Depending on the size of the deposit, the mine plan can be divided into short-term, medium-term and long-term with planning durations ranging from 1 month to 30 years.

Long-term production schedules are the main backbone that drives the activities of the mine throughout its life. The main focus of this research will be on long-term production scheduling optimization process. The process attempts to maximize the net present value of the overall profit to be generated from the mining operation within some operational and technical constraints such as mining and ore processing capacities, grade blending and block extraction sequencing.

Oil sands mining comprise the mining of overburden material and the McMurray formation. The overburden material is barren and the McMurray formation contains bitumen which is the desirable mineral. About 80% of the oil sands ore after processing finds its way to the tailings dam, making the tailings facility and waste management important aspects of this operation. Due to lack of lease area, these tailings facilities are sited mostly in-pit and embankments or dykes are constructed to contain the tailings. Most of the materials used in constructing these dykes come from the mining operation which makes it necessary to have a plan for supplying the dyke material.

Depending on the dykes' designs, they have different configurations at different locations within the dyke and hence require different material types. Some of the dyke construction methods

shown in Figure 1 are: 1) upstream, 2) downstream, and 3) centerline construction methods. More literature that provides details on dyke construction methods for tailings facilities are provided by Vick (1983) and Sego (2010). These dykes are constructed simultaneously as the mine phase advances and the dyke footprints are released. Figure 2 shows a mining phase advancement schedule at Syncrude Canada Ltd. and this schedule is used to decide the in-pit dyke construction schedule (Syncrude, 2009). This emphasizes the need for a simultaneous development of a life of mine ore and dyke material schedule that can support the mining operation and this will be the main focus of this research.

Currently, scheduling of dyke material is done after mining has started and this may result in inconsistent production of dyke material at different periods during the mine life. It is also a regulatory requirement that life of mine schedules for tailings management strategies are documented and reported annually resulting in the need for a more systematic approach towards oil sands waste management (McFadyen, 2008).

The oil sands mine long-term production planning problem will be modeled numerically as an optimization problem using a mixed integer goal programming model. The optimization problem will be coded using MATLAB (Mathworks Inc., 2009) and solved with TOMLAB/CPLEX which is a large scale mixed integer programming solver. This solver uses a branch and cut algorithm (Holmström, 2009).

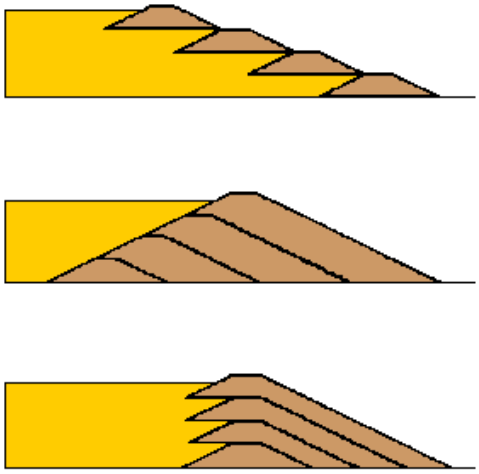

Figure 1. a) Upstream, b)downstream, and c) centerline construction methods (after Vick, 1983)

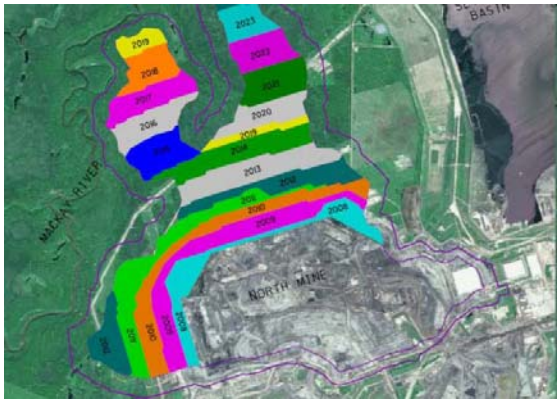

Figure 2. Syncrude Canada Ltd: North mine development sequence (after Syncrude, 2009)

SUMMARY OF LITERATURE REVIEW

Exact optimization methods have proved to be robust in solving the LTPP problem. They have the capability of considering multiple material types and multiple elements during optimization. This flexibility of mathematical programming models leads to the generation of production schedules with higher NPV than heuristic methods. Goal programming (GP) is an exact optimization technique that has been used for production scheduling in the industry. The advantage of this technique is that it allows for flexible formulation and the specification of priorities among goals or targets. This formulation also allows some form of interaction between the decision maker and the optimization process (Zeleny, 1980; Hannan, 1985). Depending on its use, some alterations are made to the formulation structure. Goal programming was applied to the mine scheduling problem using multiple criteria decision making formulation by Zhang et al. (1993). Multiple goals were considered based on their priorities. The model was tested for a surface coal mine production scheduling and implemented using a branch-and-bound method in 'C' programming language environment. This model was developed for a single ore type process. Chanda and Dagdelen (1995) used goal programming and an interactive graphics system for optimal blending in mine production. Their model sets up the blending problem with multiple goals and attempts to minimize the deviation from the goals using a Fortran 77 computer program based on simplex method of linear programming. The model was tested for a coal mine deposit, but due to some interactions involved in solving the problem,

optimal solution cannot be always guaranteed. A mineral dressing criteria was defined by Esfandiri et al. (2004) and used in the optimization of an iron ore mine. A 0-1 non-linear goal programming model was defined based on multiple criteria decision making and the deviations for economics, mining and mineral dressing functions were minimized. This formulation was solved using LINGO software. The model was found to have limitations and constraints that are numerous for practical application.

Other mine and production related problems have been solved using goal programming with some modifications. Oraee and Asi (2004) used a fuzzy goal programming model for optimizing haulage system in an open pit mine. Due to the variations in operating conditions caused by technical, operational, and environmental factors for a mechanical shovel, their model use fuzzy numbers to represent parameters for these operating conditions in optimization. They argue that, their model generates a more realistic results than those based on random numbers derived from probability distributions. A 0-1 goal programming model was developed by Chen (1994) for scheduling multiple maintenance projects for a mineral processing equipment at a copper mine. Using 0-1 decision variables and multiple scheduling periods, the model scheduled for four projects, 40 jobs and nine types of resources. In comparison to a heuristic method that was already used by the mine, the goal programming model reduced the project duration, total project cost and overall workload. Many industrial production planning and project selection decision making problems have been solved making use of the advantages of goal programming formulations (Jääskeläinen, 1969; Mukherjee and Bera, 1995; Leung et al., 2003; Lee et al., 2010).

Other exact optimization techniques that have been used for mine production scheduling are mixed integer programming (MIP) and linear programming (LP). Initial works that was carried out by Johnson (1969), Gershon (1983) and Dagdelen (1985) developed linear programming (LP) and mixed integer programming (MIP) formulations that uses integer variables for optimizing mine schedules. Their formulations could not ensure feasible solutions for all cases and could not overcome the issue of solving large integer programming problems. An integer programming formulation that was developed by Dagdelen and Johnson (1986) uses Lagrangian relaxation and subgradient optimization algorithm to solve the LTPP problem. This formulation could not be implemented on large scale problems and could not handle dynamic cut off grades. Subsequent integer programming models developed by Akaike and Dagdelen (1999) and Caccetta and Hill (2003) use 4D-network relaxation, subgradient optimization algorithm, and branch and cut algorithm respectively to solve the LTPP optimization problem but these models also could not be implemented on large scale problems or handle dynamic cutoff grades.

MIP formulations that was developed by Ramazan and Dimitrakopoulos (2004) attempt to reduce the number of binary variables and solution times by setting certain variables as binary and others as continuous. This resulted in partial mining of blocks that have the same ore value affecting the NPV generated. Ramazan et al. (2005) and Ramazan (2007) developed an MIP model that uses an aggregation method to reduce the number of integer variables in scheduling. This formulation was solved based on fundamental tree algorithm and was used in scheduling a case with 38,457 blocks within the final pit limit. The problem was broken down into four push-backs based on the nested pit approach using WHITTLE (Gemcom Software International, 2008) and formulated as separate MIP models. This would not guarantee a global optimum solution of the problem. Boland et al. (2009) presented an LP approach to generate mine production schedules with block processing selectivity. They however did not present enough information on the generated schedules to enable an assessment of the practicality of the solutions from mining operation point of view.

Recent research work by Askari-Nasab and Awuah-Offei (2009) on the application of exact optimization methods to the LTPP problem has lead to the development of mixed integer linear programming (MILP) models that use block clustering techniques to solve the problem of having large number of decision variables. With a combination of their MILP models and a block clustering algorithm, Askari-Nasab and Awuah-Offei (2009) applied their models to a large scale problem. The formulations use a combination of continuous and binary integer variables. The continuous variables control the portion of a block to be extracted in each period and binary integer variables control the order of block extraction or precedence of mining-cuts through a dependency directed graph using depth-first-search algorithm. The concept of mining-cuts using clustering

techniques is reinforced as an option for solving MILP problems for large scale deposits. The formulation was successfully implemented on an iron ore mine intermediate scheduling case study over twelve periods in TOMLAB/CPLEX (Holmström, 2009) environment. This model does not consider multiple material types.

Due to the advantages that are presented by GP and MILP, some efforts have been made to combine these two techniques and used together for solving industrial problems. This hybrid termed as mixed integer goal programming (MIGP) has been used for scheduling and budgeting problems in nursing, business administration and manufacturing industries (Selen and Hott, 1986; Ferland et al., 2001; Liang and Lawrence, 2007; Nja and Udofia, 2010). MIGP formulation is the proposed model in this paper for application to the oil sands mine LTPP problem.

After carefully reviewing the literature on GP, MILP, and MIGP formulations, and oil sands mining and waste management, a formulation has been developed to attempt solving the problem of LTPP for oil sands mining operations. The model has been used to generate a long-term production schedule for ore, dyke material and waste.

PROBLEM DEFINITION

Mine management is always faced with the problem of achieving multiple goals with the available limited resources. In oil sands mining, due to the limitation of lease area, the pit phase advancement is carried out simultaneously with the construction of tailings dykes in the mined out areas of the pit, one section at a time. These dykes are constructed to hold tailings that are produced during the processing of the oil sands. Dykes with different configurations are required during the construction. Most of the materials used in constructing these dykes come from the oil sands mining operation (overburden and interburden). It is assumed that the material sent to the processing plant (ore) must have a specified amount of bitumen and percentage fines as well as the material sent for dyke construction (dyke material). Any other material that does not meet the requirements of ore or dyke material is sent to the waste dump.

The main problem here is determining the order of extraction of ore, dyke material and waste to be removed from a predefined ultimate pit limit over the mine life that maximizes the net present value of the operation – a strategic schedule. Figure 3 shows a schematic representation of the problem definition. Figure 3 illustrates the scheduling of an oil sands ultimate pit block model containing *N* blocks. Each block *n*, is made up of ore o_n, dyke material d_n, and waste w_n. The material in each block is to be scheduled over *T* periods depending on the goals and constraints associated with the mining operation. For period t_1, the ore material scheduled is o_n^1, the dyke material scheduled is d_n^1, and the waste material scheduled is w_n^1.

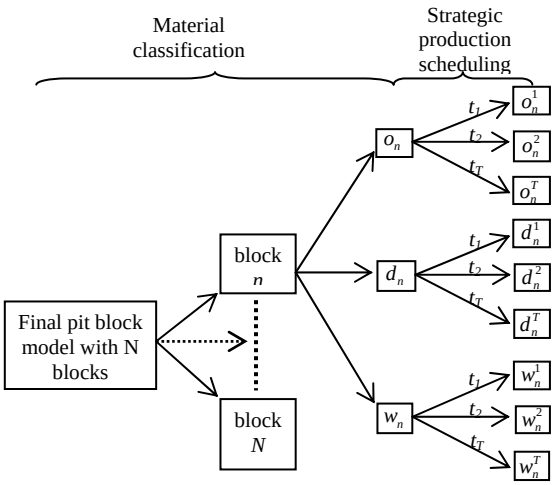

Figure 3. Schematic representation of problem definition

The strategic schedule to be developed is subject to a variety of economic, technical and physical constraints. The constraints control the mining extraction sequence, ore and dyke material blending requirements and mining, processing and dyke material goals. The mining, processing, and dyke material goals specifies the quantities of material allowed for the mining operation, processing plant and dyke construction respectively.

The strategic schedule is the main driver for the profitability of the oil sands mining operation. The schedule controls the NPV of the operation and enables a robust waste management planning strategy. Improper waste management planning can lead to environmental issues causing immediate mine closure by regulatory agencies and major financial liabilities.

OREBODY BLOCK MODELING, ULTIMATE PIT LIMIT, AND SOME ASSUMPTIONS

In long-term mine planning, one of the significant steps in the planning process is orebody block modeling. This is made up of the geologic and economic block models which serve as the backbone that drives the activities of the mine throughout its life. It is used for assessing the cash flow of the entire mining operation and then further exploited in subsequent mine planning processes such as optimization, pit design, production scheduling, waste management, equipment selection and plant design. Block models are three-dimensional arrays of rectangular blocks used to model orebodies. Each attribute in a block model represents one characteristic of the volume of material. These attributes include but are not limited to rock types, grades, density and dollar value. These attributes are stored in individual models, which have the same number of rows, columns and levels (Hustrulid and Kuchta, 2006). To determine the size of the block model needed to define the orebody, attributes like the shape and size of the orebody, the mining method, the mining bench height, and mining equipment selection need to be taken into consideration.

The source data for the geologic block model is the information from the drill holes logged from the exploration of the orebody. It is also required that the modeler understands the basic geology of the formation of the orebody and its country or host rock. Cost and revenue information such as mining cost, processing cost and mineral selling price are used in generating the economic block model (Askari-Nasab, 2009).

In geologic modeling, reliable estimation or simulation techniques are provided by Geostatistics to generate block attributes at locations where no data is available. A common estimation technique described as the “workhorse” in Geostatistics is Kriging (Deutsch, 2002). Inverse distance weighting (IDW) is another spatial interpolation algorithm that has been used over the years (ArcGIS, 2010) for geologic modeling. IDW is used for building the geologic model of the large scale data used for this research.

It is assumed that the blocks within the block model are made of smaller regions known as parcels. A parcel is part of a block for which the rock-type, tonnage and element content are known. A block can be made up of zero or more parcels and the total tonnage of the parcels may sum up to the block tonnage or it may be less. The difference, which is waste of unknown rock-type, is known as undefined waste. Neither the location nor the shape of a parcel within a block is defined but the spatial location of each block is defined by the coordinates of its center. Based on the ore tonnage and the grade in each block, the quantity of contained mineral are calculated (Gemcom Software International, 2008; Askari-Nasab and Awuah-Offei, 2009).

It is assumed that the orebody will be extracted using open pit mining techniques and a classical ultimate pit limit design will be generated based on the graph algorithm (Lerchs and Grossmann, 1965; Hustrulid and Kuchta, 2006). This pit outline contains reserves that maximize the profit. As demonstrated by Askari-Nasab and Awuah-Offei (2009), the ultimate pit limit generated directly when an optimal long-term scheduling algorithm is used will become a subset of the conventional ultimate pit limit that is generated using the Lerchs and Grossman’s algorithm (Lerchs and Grossmann, 1965). With this basis, the process of finding the optimal long-term strategic schedule will be divided into two steps: 1) determine the ultimate pit limits, and 2) generate a production schedule within the ultimate pit limit.

Clustering

One of the main problems associated with finding the optimal long-term production schedule is that, the size of the problem grows exponentially as the number of blocks increases (Askari-Nasab and Awuah-Offei, 2009) resulting in insufficient computer memory during optimization. This is caused by an increase in the number of decision variables and constraints resulting mainly from the block mining precedence. An efficient way of dealing with this problem is by applying a clustering technique. Clustering is a technique used for aggregating blocks in a block model. In the clustering algorithm to be used in this research, blocks within the same level or mining bench are grouped into clusters based on the attributes: location, rock-type, and grade distribution. These clusters of blocks are referred to as mining-cuts and they have similar attribute definitions to that of the blocks such as coordinates representing the spatial location of the mining-cut.

This block aggregation approach will summarize ore data as well as maintain an important

separation of lithology. The total quantity of contained elements in the blocks will be modeled for the mining-cuts to ensure the accuracy of the estimated values. This approach also ensures the planning of a practical equipment movement strategy based on the contained elements and tonnages in the mining-cuts. The clustering algorithm to be used for this research is a fuzzy logic clustering algorithm (Kaufman and Rousseeuw, 1990; Askari-Nasab and Awuah-Offei, 2009).

It is important to note that, clustering of blocks in a block model to mining-cuts reduces the degree of freedom of variables or resolution of the problem when finding the mining sequence that maximizes the NPV of the operation. This may lead to reduced NPV values as compared to a high resolution block level optimization (Askari-Nasab and Awuah-Offei, 2009).

APPLICATION OF MIXED INTEGER GOAL PROGRAMMING (MIGP) MODEL

Notation

The notations used in the formulation of the oil sands strategic production scheduling problem has been classified as sets, indices, subscripts, parameters and decision variables.

Sets

N= {1,…..,N} set of all blocks in the model.

$D_n(J)$ for each block, *n*, there is a set $D_n(J) \subset N$ which includes all the blocks that must be extracted prior to mining block *n* to ensure that block *n* is exposed for mining with safe slopes, where J is the total number of blocks in the set $D_n(J)$

$C_n(L)$ for each block, *n*, there is a set $C_n(L) \subset D_n(J)$ defining the immediate predecessor blocks that must be extracted prior to extraction of block *n*, where L is the total number of blocks in the set $C_n(L)$.

Indices and subscripts

A parameter, *f*, can take three indices and a subscript in the format $f_{n,l}^{e,t}$. Where:

$t \in \{1,.....,T\}$ index for scheduling periods.

$n \in \{1,.....,N\}$ index for blocks.

$e \in \{1,.....,E\}$ index for element of interest in each block.

$l = \{m,\ p,\ d\}$ subscripts for mining, processing or dyke construction respectively.

Parameters

d_n^t the discounted profit obtained by extracting block *n* in period t.

v_n^t the discounted revenue obtained by selling the final product within block *n* in period *t* minus the discounted processing cost of all the ore material in block *n*.

p_n^t the extra discounted cost of mining all the material in block *n* as dyke material for construction.

q_n^t the discounted cost of mining all the material in block *n* as waste.

g_n^e the average grade of element *e* in ore portion of block *n.*

$\underline{g}^{t,e}$ the lower bound on the required average head grade of element *e* in period *t.*

$\overline{g}^{t,e}$ the upper bound on the required average head grade of element *e* in period *t*.

f_n^e the average percent of fines in ore portion of block *n*.

$\underline{f}^{t,e}$ the lower bound on the required average fines percent of ore in period *t.*

$\overline{f}^{t,e}$ the upper bound on the required average fines percent of ore in period *t*.

f_n^d the average percent of fines in dyke material portion of block *n*.

$\underline{f}^{t,d}$ the lower bound on the required average fines percent of dyke material in period *t.*

$\overline{f}^{t,d}$ the upper bound on the required average fines percent of dyke material in period *t*.

o_n the ore tonnage in block *n*.

w_n the waste tonnage in block *n.*

d_n the dyke material tonnage in block *n*.

T_m^t the mining goal in period *t* (tonnes).

$d_1^{-,t}$ the negative deviation from the mining goal in period *t* (tonnes).

T_p^t the processing goal in period *t* (tonnes).

$d_2^{-,t}$ the negative deviation from the processing goal in period *t* (tonnes).

T_d^t the dyke material goal in period *t* (tonnes).

$d_3^{-,t}$ the negative deviation from the dyke material goal in period *t* (tonnes).

$d_3^{+,t}$ the positive deviation from the dyke material goal in period *t* (tonnes).

$r^{e,t}$ the proportion of element *e* recovered in time period t (processing recovery).

$p^{e,t}$ the price of element *e* in present value terms per unit of product.

$s^{e,t}$ the selling cost of element *e* in present value terms per unit of product.

$c^{e,t}$ the cost in present value terms per tonne of ore for processing.

k^t the cost in present value terms per tonne of dyke material for dyke construction.

m^t the cost in present value terms of mining a tonne of waste in period *t*.

Decision variables

$x_n^t \in [0,1]$ a continuous variable representing the portion of block *n* to be extracted as ore and processed in period *t*.

$z_n^t \in [0,1]$ a continuous variable representing the portion of block *n* to be extracted as dyke material and used for dyke construction in period *t*.

$y_n^t \in [0,1]$ a continuous variable representing the portion of block *n* to be mined in period *t*, which includes both ore, dyke material and waste.

$b_n^t \in [0,1]$ a binary integer variable controlling the precedence of extraction of blocks. b_n^t is equal to one if the extraction of block *n* has started in period t, otherwise it is zero.

Modeling of economic block value

The objective function of the MIGP model for strategic LTPP is to maximize the net present value of the mining operation. The concept of economic block value is based on ore parcels which could be mined selectively. The profit from mining a block is a function of the value of the block and the cost incurred in mining, processing and dyke construction. The discounted profit from block *n* is equal to the discounted revenue obtained by selling the final product contained in block *n* minus the discounted cost involved in mining block *n* minus the extra discounted cost of mining dyke material (Askari-Nasab and Awuah-Offei, 2009). This has been simplified into Eqs. (1) to (4).

$$d_n^t = v_n^t - q_n^t - p_n^t \quad (1)$$

Where:

$$v_n^t = \sum_{e=1}^{E} o_n \times g_n^e \times r^{e,t} \times \left(p^{e,t} - s^{e,t} \right) - \sum_{e=1}^{E} o_n \times c^{e,t} \quad (2)$$

$$q_n^t = \left(o_n + d_n + w_n \right) \times m^t \quad (3)$$

$$p_n^t = d_n \times k^t \quad (4)$$

The mixed integer goal programming model

Using multiple criteria decision making analysis, the objective function of the MIGP model for strategic LTPP as applied in oil sands mining, can be formulated as maximizing the NPV. This is shown by Eq. (5). The complete MIGP model comprising of the objective function, goal function and constraints can be formulated as:

$$Max \sum_{t=1}^{T} \sum_{n=1}^{N} \left(v_n^t \times x_n^t - p_n^t \times z_n^t - q_n^t \times y_n^t \right) \quad (5)$$

Goal functions:

$$\sum_{n=1}^{N} \left(\left(o_n + w_n + d_n \right) \times y_n^t \right) + d_1^{-,t} = T_m^t \quad (6)$$

$$\sum_{n=1}^{N} \left(o_n \times x_n^t \right) + d_2^{-,t} = T_p^t \quad (7)$$

$$\sum_{n=1}^{N} \left(d_n \times z_n^t \right) + d_3^{-,t} - d_3^{+,t} = T_d^t \quad (8)$$

Constraints:

$$\underline{g}^{t,e} \le \sum_{n=1}^{N} g_n^e \times o_n \times x_n^t \Big/ \sum_{n=1}^{N} o_n \times x_n^t \le \overline{g}^{t,e} \quad (9)$$

$$\underline{f}^{t,e} \le \sum_{n=1}^{N} f_n^e \times o_n \times x_n^t \Big/ \sum_{n=1}^{N} o_n \times x_n^t \le \overline{f}^{t,e} \quad (10)$$

$$\underline{f}^{t,d} \le \sum_{n=1}^{N} f_n^d \times d_n \times z_n^t \Big/ \sum_{n=1}^{N} d_n \times z_n^t \le \overline{f}^{t,d} \quad (11)$$

$$x_n^t + z_n^t \le y_n^t \quad (12)$$

$$b_n^t - \sum_{i=1}^{t} y_s^i \le 0 \quad (13)$$

$$\sum_{i=1}^{t} y_n^i - b_n^t \le 0 \quad (14)$$

$$b_n^t - b_n^{t+1} \le 0 \quad (15)$$

$$d_1^{-,t},\ d_2^{-,t},\ d_3^{-,t},\ d_3^{+,t} \ge 0 \quad (16)$$

$$\forall t \in \{1,...,T\} \quad e \in \{1,...,E\} \quad d \in \{1,...,D\}$$

$$n \in \{1,...,N\} \quad s \in C(L)$$

Eqs. (6), (7), and (8) are the goal functions which define the mining, processing and dyke material goals that are required to be achieved. Eqs. (9), (10), and (11) specify the limiting requirements for ore bitumen grade, ore fines and dyke material fines. Eq. (12) ensures that the total material mined in each period does not exceed the sum of the ore and dyke material mined. Eqs. (13), (14) and (15) check the set of immediate predecessor blocks that must be mined prior to mining block *n*. Eq. (16) ensures that the negative and positive deviations from the targeted mining, processing and dyke material goals are always positive.

APPLICATION OF THE MIGP MODEL FOR STRATEGIC PRODUCTION SCHEDULING

The problem being looked at here is finding the sequence of extracting ore, dyke material and waste blocks from a predefined ultimate pit over the mine life so that the NPV of the operation is maximized. The production schedule is subject to some physical, technical and economic constraints such as mining extraction sequence and mining and processing capacities.

The formulation presented here for open pit strategic production scheduling has the objective of maximizing the NPV of the mining operation whilst achieving the multiple goals of ore and dyke material requirements. The block sizes used for production scheduling must be similar to the selective mining units; otherwise, the generated schedule may not be feasible in practice. The proposed MIGP model uses binary integer decision variables, b_n^t to control precedence of block or mining-cut extraction and continuous variables, y_n^t, x_n^t, and z_n^t are used to model extraction, processing and dyke material requirements respectively at block or mining-cut level. Continuous deviational variables, $d_1^{-,t}$, $d_2^{-,t}$, $d_3^{-,t}$, and $d_3^{+,t}$ have been defined to support the goal functions that control extraction, processing and dyke material. These deviational variables provide a continuous range of units (tonnes) that the optimizer chooses from to satisfy the defined goals.

Precedence of block/mining-cut extraction

The mining precedence constraints are the main reason for the increase in the number of constraints and the complexity of the scheduling problem. Previous mining precedence constraint set-ups enforces that, before a block is mined all blocks on top of it must be mined first. For the example shown in Figure 4, before block 1 is mined, the 24 blocks above it must be mined first. This results in 24 mining precedence constraint

equations in each period for block 1. This increases the size of the problem quickly making the optimization intractable (Askari-Nasab and Awuah-Offei, 2009).

The mining precedence constraint in the MIGP formulation has been modeled using the directed graph theory (Askari-Nasab and Awuah-Offei, 2009). Eqs. (13) to (15) in the model control the relationship of block extraction precedence by the binary integer variable, b_n^t. Specifically, Eq. (13) ensures that only the set of immediate predecessor blocks on top of a block need to be extracted prior to extracting the block. This is represented by the set $C_n(L)$ in the formulation. Eq. (14) ensures that if extraction of block *n* is started in period *t,* then block *n* has not been extracted before. Eq. (15) ensures that b_n^t is equal to one if extraction of block *n* has started by or in period *t*, otherwise it is zero. This means once the extraction of a block starts in period *t*, this block is available for extraction during the subsequent periods. Figure 4 shows the set that has to be mined for extracting block 1: $C_1(L) = \{2, 3, 4\}$.

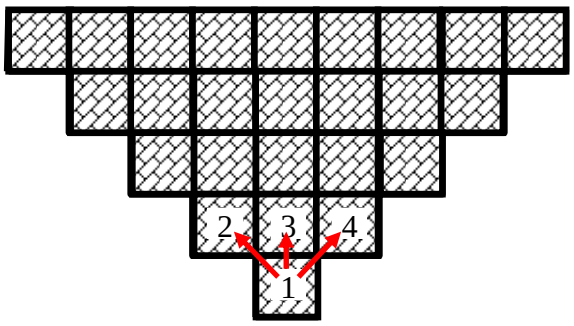

Figure 4. Block extraction precedence in the MIGP formulation

This results in 3 mining precedence constraint equations in each period for block 1 as compared to 24 in previous formulations. This decreases the size of the mine production scheduling optimization problem considerably.

Solving the optimization problem

The use of the MIGP formulation for an orebody model usually results in a large scale optimization problem. One of the recent optimization solvers capable in handling such problems is the ILOG CPLEX (ILOG Inc., 2007). This optimizer was developed based on branch and cut algorithm and makes the solving of MIGP models possible for large scale problems. Branch and cut is an algorithm which combines different optimization techniques for solving integer programming problems. This algorithm is a hybrid of branch-and-bound and cutting plane methods (Horst and Hoang, 1996; Wolsey, 1998).

This research uses TOMLAB/CPLEX (Holmström, 2009) as the MIGP model solver. The CPLEX solver engine (ILOG Inc., 2007) has been successfully integrated with MATLAB (Mathworks Inc., 2009) working environment by TOMLAB/CPLEX. An optimization termination criterion that the user set in CPLEX is the gap tolerance (EPGAP). The gap tolerance sets an absolute tolerance on the gap between the best integer objective and the objective of the best node remaining. It instructs CPLEX to stop as soon as it has found a feasible integer solution proved to be within the set EPGAP.

RESULTS AND DISCUSSIONS

We have developed, implemented, and tested the proposed MIGP model presented in this research in TOMLAB/CPLEX environment (Holmström, 2009). The performance of the proposed model is analyzed based on net present value, mining production goals and smoothness of the generated schedules. The model was tested on a Dell Precision T3500 computer at 2.4GHz, with 3GB of RAM. A relative tolerance of 5% on the gap between the best integer objective and the feasible integer solution was set for a large scale data.

Table 1 shows numerical results from the MIGP model for an oil sands ultimate pit data set containing 61490 blocks. The blocks were clustered to 302 cuts and scheduled over 20 periods. The ultimate pit contains five 15m benches from elevation 325m to 265m. The ultimate pit was obtained using WHITTLE (Gemcom Software International, 2008). Each block represents a volume of 50m x 50m x 15m of rock and each mining cut contains about 200 blocks. The model contains 4866.2 million tonnes of material with 2792.5 million tonnes of ore. The ore bitumen grade ranges from 7 to 16.5% with an average grade of 11.6%. The ore fines grade ranges from 0 to 59.9% with an average grade of 9.0%. It also contains 1697.8 million tonnes of dyke material. The dyke material fines grade ranges from 0 to 49.3% with

an average grade of 4.9%. Bitumen and fines grades need to be controlled within an acceptable range for processing plant feed and dyke construction.

Table 1. Results from the MIGP model for large scale data

MIGP NPV ($M)	MIGP NPV (no dyke cost) ($M)	Root Node Gap (%)
11201.2	11770.0	5.09

It is desired to keep an average processing plant head grade with bitumen content between 7 and 16% and fines content less than 30%. The dyke material is required to have bitumen content less than 7% and fines content less than 50%. Our goal is to generate a uniform schedule based on the availability of material, the plant processing and dyke construction requirements. Further to this, we intend to keep a steady stripping ratio of about 0.7 when the mining of ore starts. This would ensure that the mining equipment capacity will be uniform throughout the mine life.

An important feature of this MIGP formulation, that makes it a robust and flexible platform for mine planning, is that apart from the NPV maximization, the planner has control over the setting of goals and their deviational variables and upper and lower limits of grades. The planner can also decide on tradeoffs between NPV maximization and goal achievement.

The results show that during the first two years, due to the formation of the oil sands deposit, dyke material was the most abundant as a result of the presence of the overburden material which must be stripped. Once the overburden material is mined, ore becomes available from period 3 until the end of the mine life. The dyke material was ramped down after period 2 due to the dwindling reserves of interburden dyke material. The mining capacity was uniform throughout the mine life. Figures 5, 9, and 10 show the schedules for ore, dyke material, and waste mined over the 20 scheduling periods. The total amount of material mined was 4757.5 million tonnes. This is made up of 2428.8 million tonnes of ore, 1064.0 million tonnes of dyke material and the rest being waste.

It is our target to blend the run-of-mine ore to meet the quality and quantity specification of the processing plant and dyke construction. As more detailed planning is done in the short and medium term, the blending problem becomes more prominent. The plant head grade and the dyke material grade that was set were successfully achieved in all the periods. The ore material bitumen grade was between 11 and 12.5% with fines grade between 7% and 13%. The dyke material fines grade was also between 0 and 12%. These can be seen in Figures 6, 7, and 8.

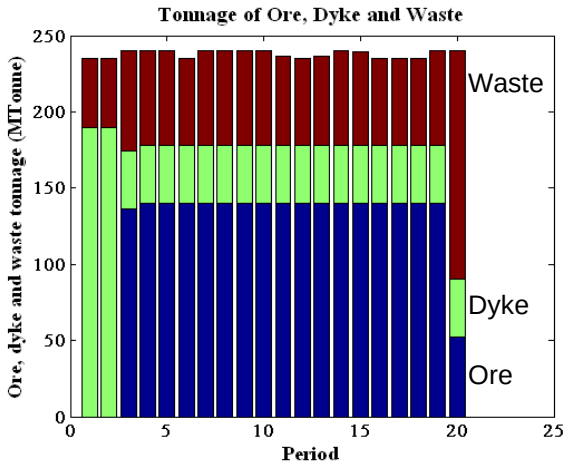

Figure 5. Tonnage of ore, dyke material and waste per period

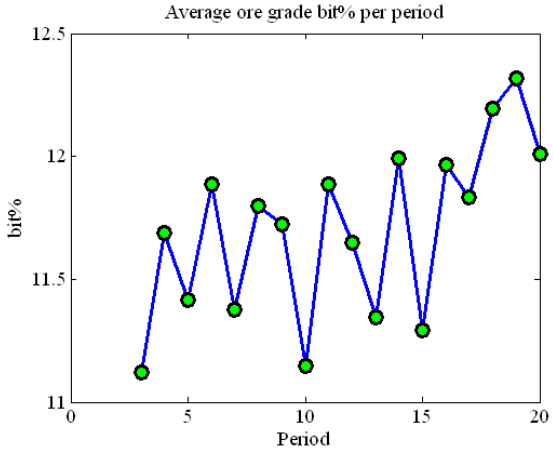

Figure 6. Average bitumen grade of ore per period

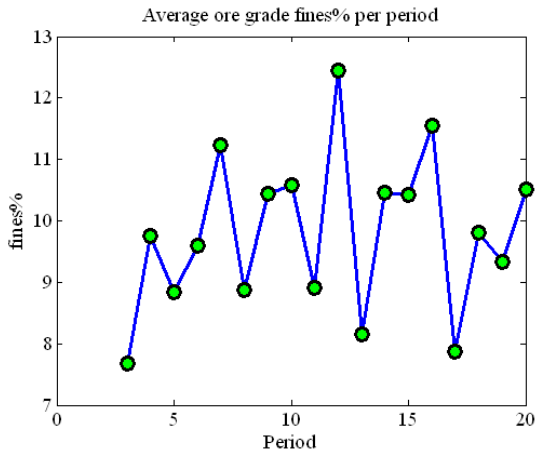

Figure 7. Average fines grade of ore per period.

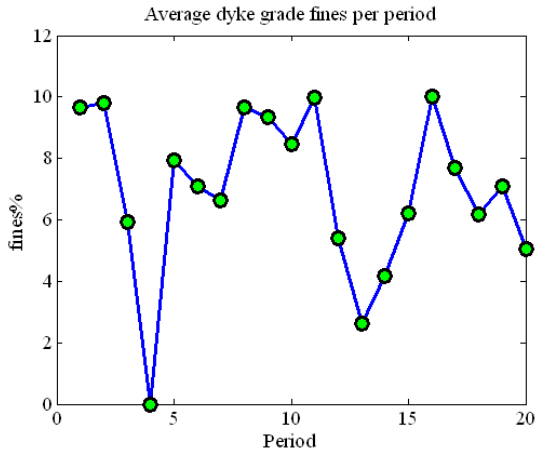

Figure 8. Average fines grade of dyke material per period

CONCLUSIONS AND FUTURE RESEARCH WORK

This paper discussed the current application of mixed integer programming and goal programming to the open pit long-term production scheduling problem and some of the limitations. Further to this, we looked at the use of mixed integer goal programming formulations in solving industrial problems due to the advantages derived from this hybrid formulation. In this paper, we have developed, implemented and tested a MIGP optimization formulation for open pit production scheduling of multiple material types. The oil sands mining case was used. This requires that a production schedule is generated for ore, dyke material and waste. These schedules ensure that whilst ore is fed to the plant, there is scheduled material available for dyke construction. This enables adequate space for the in-pit storage of tailings from the plant.

The formulation uses binary integer variables to control mining precedence and continuous variables to control mining of ore and dyke material. There are also goal deviational variables that must be set up by the planner. The optimization model was implemented in TOMLAB/CPLEX environment.

The developed model proved to be able to generate a uniform schedule for ore and dyke material. It also provides the planner the flexibility of choosing goal deviational variables to achieve a uniform schedule and improved NPV. Similarly, tradeoffs between achieving a goal and maximizing NPV can be made.

Further research will focus on developing a horizontal direction block extraction sequence constraint that will enforce a more systematic way of mining. This becomes more significant in the short term due to the equipment maneuverability requirements in oil sands mining.

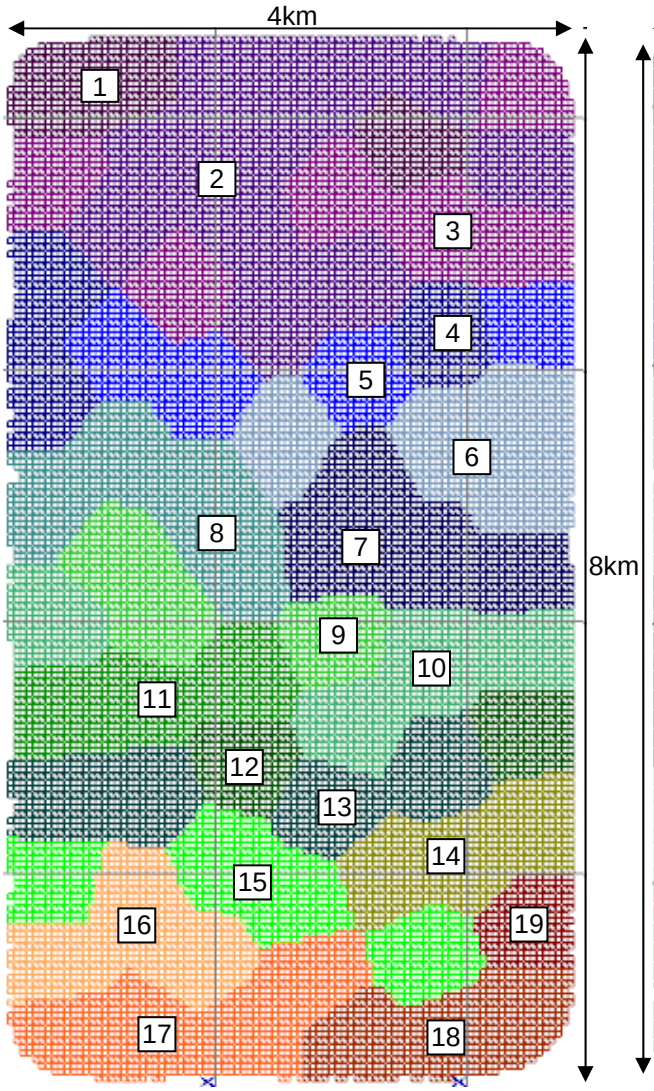

Figure 9. Plan view showing periods cuts were mined – level 310m

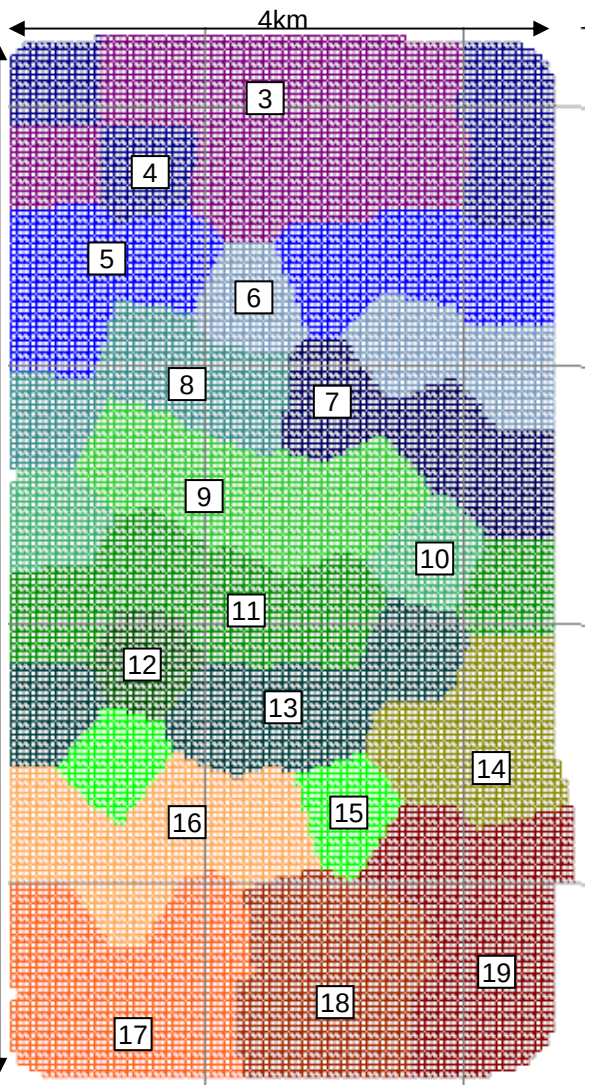

Figure 10. Plan view showing periods cuts were mined – level 295m

REFERENCES

Akaike, A. and Dagdelen, K. (1999). *A strategic production scheduling method for an open pit mine*. Paper presented at 28th International Symposium on the Application of Computers and Operations Research in the Mineral Industry, pp. 729-738.

ArcGIS (2010). How inverse distance weighted interpolation works. *ArcGIS Resource Center,* Retrieved July 19, 2010 from: http://help.arcgis.com/en/arcgisdesktop/10.0/help/index.html#//00310000002m000000.htm

Askari-Nasab, H. (2009). *Surface mine design and optimization.* University of Alberta, Edmonton. Pages C7-15.

Askari-Nasab, H. and Awuah-Offei, K. (2009). Mixed integer linear programming formulations for open pit production scheduling. University of Alberta, Mining Optimization Laboratory Report One, Edmonton, 1-31.

Askari-Nasab, H. and Awuah-Offei, K. (2009). Open pit optimization using discounted economic block value. *Transactions of the Institution of Mining and Metallurgy, Section A, Mining Industry*, *118*,(1), 1-12.

Boland, N., Dumitrescu, I., Froyland, G., and Gleixner, A. M. (2009). LP-based disaggregation approaches to solving the open pit mining production scheduling problem with block processing selectivity. *Computers and Operations Research*, *36*,(4), 1064-89.

Caccetta, L. and Hill, S. P. (2003). An application of branch and cut to open pit mine scheduling. *Journal of Global Optimization*, *27*, 349-365.

Chanda, E. K. C. and Dagdelen, K. (1995). Optimal blending of mine production using goal programming and interactive graphics systems. *International Journal of Mining, Reclamation and Environment*, *9*,(4), 203-208.

Chen, V. Y. X. (1994). A 0-1 goal programming model for scheduling multiple maintenance projects at a copper mine. *European Journal of Operational Research*, *76*, 176-191.

Dagdelen, K. (1985). Optimum multi-period open pit mine production scheduling by Lagrangian parameterization. PhD Thesis, University of Colorado, Golden, Colorado, Pages 325.

Dagdelen, K. and Johnson, T. B. (1986). *Optimum open pit mine production scheduling by Lagrangian parameterization*. Paper presented at 19th International Symposium on the Application of Computers and Operations Research in the Mineral Industry, Society of Mining Engineers (AIME), pp. 127-142.

Deutsch, C. V. (2002). *Geostatistical reservoir modeling.* Oxford University Press, New York. Pages 376.

Esfandiri, B., Aryanezhad, M. B., and Abrishamifar, S. A. (2004). Open pit optimization including mineral dressing criteria using 0-1 non-linear goal programming. *Mining Technology, Transactions of the Institutions of Mining and Metallurgy*, *113*, A3-A13.

Ferland, J. A., Berrada, I., Nabli, I., Ahiod, B., Michelon, P., Gascon, V., and Gagne, E. (2001). Generalized assignment type goal programming problem: application to nurse scheduling. *Journal of Heuristics*,(7), 391-413.

Gemcom Software International (2008). Whittle strategic mine planning software. Ver. 4.2, Vancouver.

Gershon, M. E. (1983). Optimal mine production scheduling: evaluation of large scale mathematical programming approaches. *International Journal of Mining Engineering*, *1*, 315-329.

Hannan, E. L. (1985). An assessment of some criticisms of goal programming. *Computers and Operations Research*, *12*,(6), 525-541.

Holmström, K. (2009). TOMLAB /CPLEX (Version 11.2). Tomlab Optimization, Pullman, WA, USA.

Horst, R. and Hoang, T. (1996). *Global optimization: deterministic approaches.* Springer, Berlin; New York. 3rd ed, Pages 727.

Hustrulid, W. A. and Kuchta, M. (2006). *Open pit mine planning and design.* Taylor and Francis/Balkema, Second ed, Pages 735.

ILOG Inc. (2007). ILOG CPLEX 11.0 User's manual September. Ver. 11.0.

Jääskeläinen, V. (1969). A goal programming model of aggregate production planning. *The Swedish Journal of Economics*, *71*,(1), 14-29.

Johnson, T. B. (1969). *Optimum open-pit mine production scheduling*. Paper presented at 8th International Symposium on Computers and Operations Research, Salt Lake City, Utah, USA. pp. 539-562.

Kaufman, L. and Rousseeuw (1990). *Finding groups in data: an introduction to cluster analysis.* Wiley, New York. Pages 342.

Lee, J., Kang, S., Rosenberger, J., and Kim, S. B. (2010). A hybrid approach of goal programming for weapons systems selection. *Computers and Industrial Engineering*, *58*, 521-527.

Lerchs, H. and Grossmann, I. F. (1965). Optimum design of open-pit mines. *The Canadian Mining and Metallurgical Transaction*, *68*, 17-24.

Leung, S. C. H., Wu, Y., and Lai, K. K. (2003). Multi-site aggregate production planning with multiple objectives: a goal programming approach. *Production Planning and Control*, *14*,(5), 425-436.

Liang, F. and Lawrence, S. (2007). A goal programming approach to the team formation problem. Leeds School of Business, University of Colorado, 8.

Mathworks Inc. (2009). MATLAB Software. Ver. 7.9 (R2009b).

McFadyen, D. (2008). Directive 074. Energy Resources Conservation Board, Calgary, 14.

Mukherjee, K. and Bera, A. (1995). Application of goal programming in project selection decision - A case study from the Indian coal mining industry. *European Journal of Operational Research*, *82*, 18-25.

Newman, A. M., Rubio, E., Caro, R., Weintraub, A., and Eurek, K. (2010). A review of operations research in mine planning. *Institute for Operations Research and the Management Sciences*, *40*,(3), 222-245.

Nja, M. E. and Udofia, G. A. (2010). Formulation of the mixed-integer goal programming model for flour producing companies. *Asian Journal of Mathematics and Statistics*, *3*,(3), 201-210.

Oraee, K. and Asi, B. (2004). *Fuzzy model for truck allocation in surface mines*. Paper presented at 13th International Symposium on Mine Planning and Equipment Selection, Routledge Taylor and Francis Group, Wroclaw, Poland. pp. 585-593.

Ramazan, S. (2007). *Large-scale production scheduling with the fundamental tree algorithm - model, case study and comparisons*. Paper presented at Orebody Modelling and Strategic Mine Planning, The Australian Institute of Mining and Metallurgy, Perth, Western Australia. pp. 121-127.

Ramazan, S., Dagdelen, K., and Johnson, T. B. (2005). Fundamental tree algorithm in optimising production scheduling for open pit mine design. *Institute of Materials, Minerals and Mining and Australasian Institute of Mining and Metallurgy*, *114*,(A), 45-54.

Ramazan, S. and Dimitrakopoulos, R. (2004). *Recent applications of operations research and efficient MIP formulations in open pit mining*. Paper presented at SME Annual Meeting, Society for Mining, Metallurgy, and Exploration, Cincinnati, Ohio. pp. 73-78.

Sego, D. C. (2010). Mine waste management. Course notes, University of Alberta, Geotechnical Center, Edmonton, 83.

Selen, W. J. and Hott, D. D. (1986). A mixed-integer goal-programming formulation of the standard flow-shop scheduling problem. *Journal of the Operational Research Socitey*, *37*,(12), 1121-1128.

Syncrude (2009). Annual tailings plan submission: Syncrude Mildred Lake. Syncrude Canada Ltd, Fort McMurray, 45.

Vick, S. G. (1983). *Planning, design, and analysis of tailings dams.* John Wiley and Sons, New York. Pages 369.

Whittle, J. (1989). The facts and fallacies of open pit design. Whittle Programming Pty Ltd.

Wolsey, L. A. (1998). *Integer programming.* J. Wiley, New York. Pages 264.

Zeleny, M. (1980). Mathematical programming with multiple objectives. *Computers and Operations Research*, *7*,(1-2), iii.

Zhang, Y. D., Cheng, Y. P., and Su, J. (1993). Application of goal programming in open pit planning. *International Journal of Mining, Reclamation and Environment*, *7*,(1), 41-45.

Session 4

Water/Chemistry

NAPHTHA INTERACTION WITH BITUMEN AND CLAYS: A PRELIMINARY STUDY

Michael Afara, Vicente Munoz, and Randy Mikula
Natural Resources Canada, CanmetENERGY Research, 1 Oil Patch Drive, Devon, Alberta, T9G 1A8

ABSTRACT

Naphtha association with bitumen and clays in froth treatment tailings is not well understood, in spite of the importance of minimizing losses of both naphtha and bitumen from this process stream. The use of head space analysis combined with microscopic observations can help in the understanding of these associations, and to determine the relative importance of clay mineralogy and/or bitumen content. This paper discusses preliminary results from a project where the roles which bitumen and clays play in naphtha release from tailings are investigated.

INTRODUCTION

There are generally three tailings streams associated with surface mined oil sands operations. These are the sand or coarse tailings, the fluid fine tailings, and the froth treatment tailings. The froth treatment tailings result from the processes that are required to remove mineral and water from the bitumen froth in order for it to be processed in the upgrader and refinery. The froth treatment process inevitably involves solvent in order to reduce the bitumen viscosity to the point where removal of the solids and water is accomplished with settlers or centrifuges. Up until recently, the solvent of choice has been a naphtha component from the upgrading or refinery operations. Shell-Albian has moved to a paraffinic solvent which, at the expense of some precipitated asphaltenes, allows for the production of diluted bitumen that can meet a pipeline specification. In either case, a froth treatment tailings stream is created that has mineral, water and hydrocarbon with a solvent contamination. Because of the relatively small volume of bitumen produced relative to the other streams, this is the smallest of the tailings streams. The froth treatment tailings is passed to a diluent stripper before being discharged to the tailings ponds, but the diluent removal in this step is never perfect.

The ERCB has established guidelines for the release of solvent to tailings ponds from the froth treatment tailings at a level of 4 barrels of solvent for every 1000 barrels of bitumen production. The fraction of this solvent that might ultimately evaporate and contribute to VOC (volatile organic carbon) loading to the environment is not well understood. This understanding is complicated by the fact that naphtha is a component of the bitumen in the ore. Although the C5 and C6 (pentane and hexane) solvents that dominate the paraffinic solvents are not a significant part of the ore hydrocarbon components, the test methods would have applicability for those tailings as well. This paper focuses on the naphtha solvent process.

Naphtha available from the froth treatment process is not all immediately available to the atmosphere via evaporation since most of the froth treatment tailings are not near the surface of the tailings ponds. A thorough understanding of the actual environmental availability would have to include partitioning between the froth treatment tailings, the water column, and ultimately the atmosphere. This preliminary study is only a cursory look at the broad interactions between the solvent, bitumen, and mineral components in the froth treatment tailings.

METHODS

Gas Chromatography Mass Spectrometer (GC/MS)

The combination of static headspace together with gas chromatography/mass spectrometry (HS-GC/MS) is a powerful technique for analyzing volatile organic compounds in a closed system. HS-GC/MS was carried out using an Agilent network gas chromatography equipped with mass selective detector and connected to a headspace sampler. Samples (5 g) are spiked with naphtha by method of injection, and equilibrated at room temperature for a 24-hour period prior to analysis. Gases evolved into the vial's headspace during equilibration are swept into the GC by He gas. The gases are separated based on their retention times on the column, and then analyzed by MS, which utilizes methods that monitors specific ions using

Selected Ion Recording. The total hydrocarbon peak areas were recorded for individual sample analyzed and then compared to control (naphtha-spiked deionized water).

Micro Flame Ionization Detector

The micro flame ionization detector (FID) detects organic compounds by measuring an electrical current generated by electrons from burning carbon particles in the sample. Evolved gas- micro flame ionization detector (EG-FID) is a novel technique for analyzing gases evolved from a volatile material, and unlike GC/MS cannot identify the volatile material. This technique has an FID coupled to a gas jar, with a valve for turning on and off gas flow. EG-FID analysis was carried out using Photovac's handheld micro FID instrument with a detection range of 0.1-50,000 ppm VOCs. In this technique, the sample in a 15-mL vial is spiked with solvent and then placed in a 1-L gas jar which is connected to the instrument. The samples are allowed to equilibrate for 2-hours before turning on the gas flow. Once the valve is turned on, the evolved gases are moved into the FID and the readings are recorded from the instrument.

Naphtha Partitioning in Water

Naphtha is extremely insoluble in water, and quickly evaporates when mixed with water. The rate at which naphtha evaporates in water was monitored in terms of *ppm* of naphtha added and expressed as % naphtha released. Deionized water (2.5g) in a headspace vial was spiked with 3000 *ppm* naphtha and immediately capped to avoid loss of VOCs. The sample was left to equilibrate for 24 hrs, and then analyzed by headspace GC/MS, a specific GC/MS technique which analyzes volatile compounds released to the 'headspace" of a closed vial. This was used as a control to test naphtha interaction in various other systems.

Bitumen and Clay Interaction with Naphtha

Naphtha, a well known diluent used in multiphase system separation, ends up in the tailings pond where it evaporates into the atmosphere. In the tailings pond, naphtha may interact with the bitumen and/or clay component, and this may effect its rate of evaporation in such system. We studied this interaction using pure bitumen and clay (kaolinite) systems in order to understand the overall effects of naphtha on MFT. Bitumen-naphtha interaction was studied by making varying amounts of 3000 *ppm*-naphtha-spiked bitumen (0.5, 1, 1.5 or 2%) mixed with DI-water in a headspace vial, and then analyzing for VOC release by headspace GCMS and comparing it to control (DI-water, no bitumen). Similarly, clay-naphtha interaction was studied by spiking varying amounts of kaolinite (1, 2, 5 and 10%) in a headspace vial with 3000 *ppm* naphtha and monitoring VOC release by chromatography and comparing it to control (DI-water, no clay). To rule out non-specific interaction between kaolinite and naphtha, we examined the effect of sand on VOC release by spiking varying amounts of sand slurry with naphtha and monitoring its release by GC/MS. All experiments were compared to control and the results were expressed as percentage of total hydrocarbon peaks of naphtha released to the headspace vial compared to control.

Distribution of Naphtha, Toluene and Hexane

The distribution of naphtha, toluene and hexane in MFT and its components was studied by spiking the components with the solvent, and monitoring its release by EG-FID. In this experiment, 5g of MFT was spiked with either *3000ppm* of naphtha, or *1500ppm* of toluene or hexane and the amount of solvent released was monitored. In order to determine the distribution of solvents in bitumen, 1.2% bitumen was spiked with the same amount of solvents. Solvents were also added to 42% dean-starked solids and kaolinite to study its distribution of solvents. Lastly, a mixture of 1.2% bitumen and 42% solids was spiked with the solvents, and the amount of solvents released was measured.

Naphtha Release from MFT

Based on the model studies of naphtha release from bitumen-clay mixtures, we designed an experiment to study its release from MFT. This MFT contains 3.5% bitumen and 42% solids. In this experiment, the MFT in a headspace vial was spiked with 3000 *ppm* naphtha, and the rate of VOC release was monitored by headspace GC/MS after a 24-hr equilibration. In order to determine the effects of solids present in the MFT, we tested the effect of increasing solids content on naphtha release from MFT. The original MFT contained 42% solids and this was increased to 52 and 65% solids by addition of dean-stark MFT solids to the original MFT. Similarly, we tested for the effects of increasing bitumen on the original MFT by adding toluene-solubilized bitumen to the MFT, thus

increasing the bitumen content to 7 and 14% from the original 3.5%. In all, samples were spiked with 3000 *ppm* of naphtha and the rate of VOC release was analyzed by GCMS. All experiments were compared to VOC release from DI-water and expressed as percentage of control.

RESULTS AND DISCUSSION

By using the amount of solvent found in the headspace vial under controlled conditions as a baseline, the effect of clays, mineral, and bitumen can be evaluated. Standard clays were evaluated along with solids extracted from MFT and bitumen extracted from an ore sample. Figure 1 shows the naphtha released (as a fraction of the control) with increasing bitumen content. Naphtha interaction with bitumen is clearly reducing the naphtha evaporating into the head space vial under controlled conditions. Figure 2 shows the same experiment with kaolinite clay and in this case, although there is a clear reduction, it is not nearly as significant as with the bitumen.

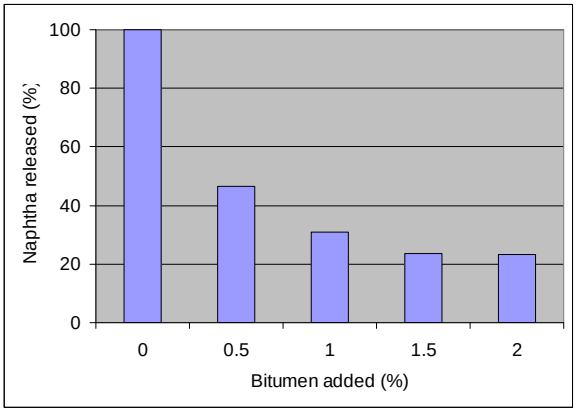

Figure 1. Naphtha evaporated with bitumen addition.

This is not surprising given the fact that naphtha is naturally associated with the bitumen. It is significant that there is such a significant reduction in evaporation given the hydrophilic nature of the standard kaolinite. Even the froth extraction process minerals are generally hydrophobic as shown in the Figure 3 micrograph of froth treatment process diluted bitumen. The top micrograph shows clays in the diluted bitumen. The clays (red color) are trapped in water globules stabilized by structured bitumen (green color). This micrograph was acquired using simultaneous acquisition in the fluorescence and reflectance modes. The bottom image is the same field of view showing only the fluorescence channel. The structures in the bitumen can be seen clearly and the water globules and clays do not fluoresce so they are shown as black components in the image. In this image it is very clear that only a small fraction of the mineral is associated with the dil-bit, with the vast majority of the minerals in the water phase.

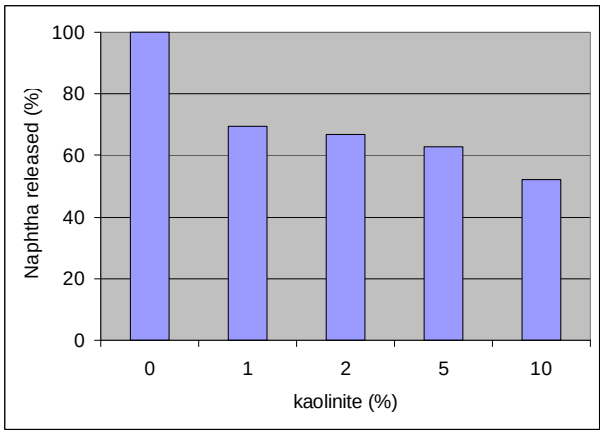

Figure 2. Naphtha evaporated with kaolinite addition.

Further investigations on the reduction of solvent evaporation due to interaction with minerals and bitumen are summarized in Figure 4. This shows naphtha, toluene, and hexane interactions with a variety of samples in order to establish the relative importance of the mineral component compared to the bitumen component. In this case, the solids extracted from the MFT are as effective as the MFT in limiting solvent evaporation. Kaolinite is not as effective as any of the other combinations, confirming the results in Figure 2. The effect of bitumen is seen to be the greatest for the hexane solvent compared to the naphtha or the toluene (a common naphtha solvent surrogate). In spite of the repeated tests (the range in the data is shown in the Figure 4 error bars) this is a phenomena that needs to be confirmed with further larger scale studies.

An explanation for the apparent synergistic effect of the MFT dean stark solids and bitumen in reducing the solvent evaporation (Figure 4) might be due to the fact that dean stark extracted solids are generally much more hydrophobic than the solids before dean stark extraction. In effect, therefore, the addition of solids from the dean stark process is also increasing the available hydrocarbon to bridge an interaction of solvent with bitumen.

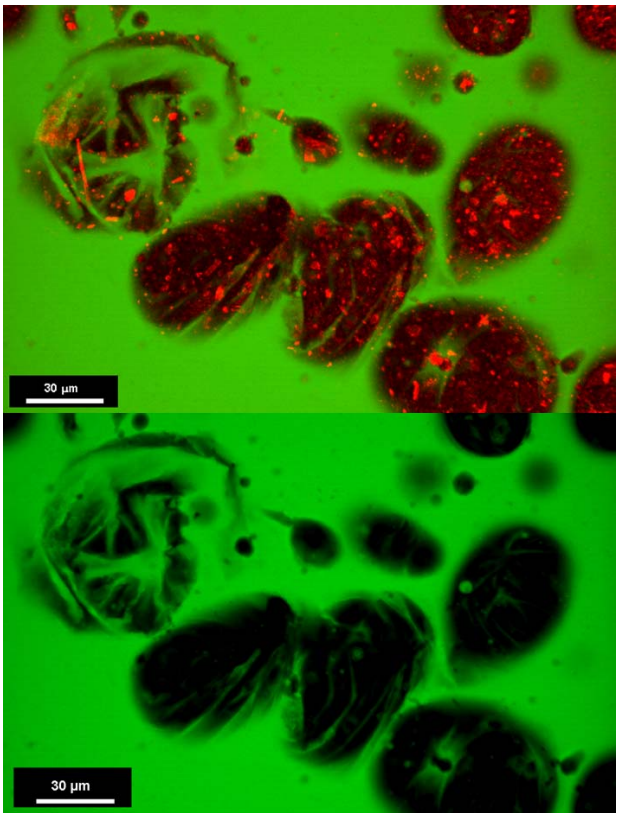

Figure 3. Minerals in diluted bitumen.

The experiments summarized in Figure 5 attempt to answer the question about hydrocarbon contamination on dean stark prepared solids by adding dean stark solids to increase the apparent solids content in an MFT sample. Increasing the solids content from 42% (control) to 65% made no difference in the solvent evaporation into the head space.

Addition of bitumen to the same sample significantly decreased evaporation, even to the point of an MFT sample that was not spiked with naphtha. Not surprisingly, the data shows that there is a strong interaction of naphtha with bitumen that reduces its availability to the atmosphere. What is surprising is the apparent strong interaction of bitumen with hexane and clearly further work is required. Paradoxically, these very preliminary results suggest that bitumen lost to froth treatment tailings may in fact help to mitigate evaporation of lost solvent to the atmosphere. In addition, the small scale of the head space experiments implies that on a commercial scale with the tailings under many meters of water, the release to the atmosphere may be further mitigated.

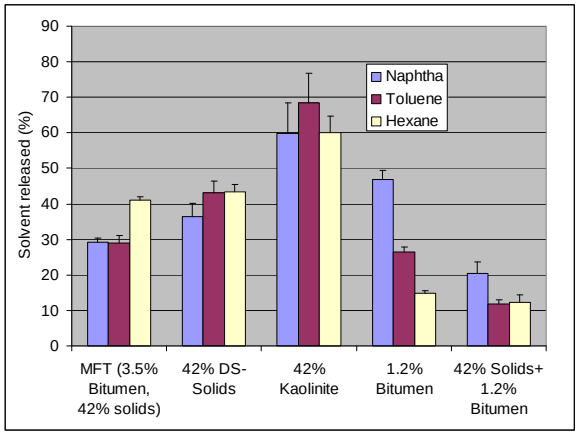

Figure 4. Naphtha, toluene, and hexane with a variety of components.

SUMMARY

A test protocol has been developed that allows for empirical evaluation of solvent interactions with the mineral and hydrocarbon components in an oil sands process stream. By mixing naphtha with tailings solids and with bitumen it has been possible to establish the relative importance of those components in mitigating solvent evaporation.

The results from this preliminary study show that relatively small amounts of bitumen help to reduce the solvent evaporation rate significantly. Mineral solids play an important role, but still much less significant than for bitumen. Hexane solvents also showed a significant decrease in evaporation with bitumen, even though, unlike naphtha, they are not a significant portion of the native bitumen. Further work is required to quantify these initial observations.

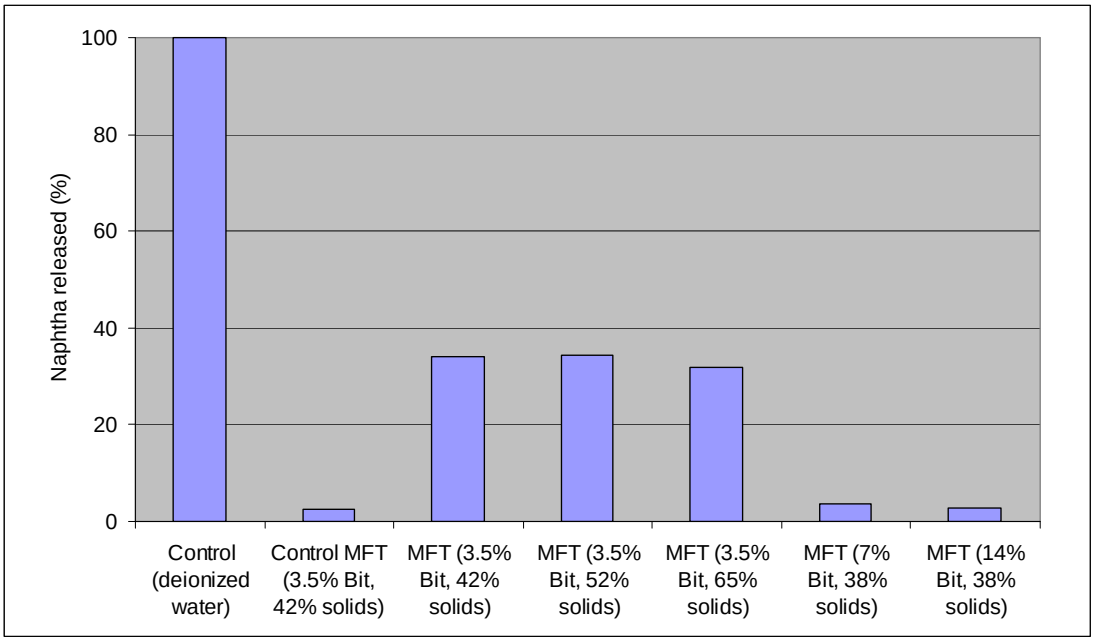

Figure 5. Naphtha released for a combination of dean stark solids and bitumen.

NAPHTHA EVAPORATION FROM OIL SANDS TAILINGS PONDS

Kim Kasperski, Vicente Munoz, and Randy Mikula
Natural Resources Canada, CanmetENERGY Research, 1 Oil Patch Drive, Devon, Alberta, T9G 1A8

ABSTRACT

Naphtha release from tailings ponds is often modeled based on data from a 1996 publication by Kasperski and Munoz titled "Vapour Pressure Properties and Hydrocarbon Distribution in the Plant 4 Tailings Stream". In the last several years this paper has been used to provide evidence for the idea that 40% of the naphtha going to the tailings ponds is available to the environment. The data in the Kasperski and Munoz paper in fact does not support the conclusion that only 40% of the naphtha is evaporating from the tailings ponds. The areas of confusion will be outlined with the hope that in the future other evidence will be used to model solvent evaporation from tailings ponds.

INTRODUCTION

CanmetENERGY often uses the concept of recoverable versus unrecoverable bitumen in analyses of bitumen in tailings ponds or other sources. This terminology is based on microscopy based assessments of the hydrocarbon morphology in various process streams. Hydrocarbon that is not associated with mineral matter is easy to see under the microscope as spherical entities. Hydrocarbon components which have a strong affinity for mineral components are designated as not recoverable. Clearly under the right process conditions, it would be possible to recover all of the hydrocarbon, but the use of recoverable and unrecoverable in terms of the microscopic morphology helps to determine limits to bitumen (or other hydrocarbon) recovery under relatively non-aggressive flotation conditions. Figures 1 and 2 show bitumen in tailings where the Figure 1 recoverable bitumen is clearly spherical and not associated with the mineral components. The bitumen in Figure 2 however, is clearly strongly associated with the mineral phase and recovery of this would involve a chemical intervention to break the bitumen mineral interaction or alternatively the recovery of a very poor bitumen product. This concept of recoverable and non-recoverable hydrocarbon is very useful in the optimization of a recovery process since it might be unproductive to try to improve recovery in a situation where the easy to recover hydrocarbon is available and further improvements in total recovery could only be at the expense of a product quality.

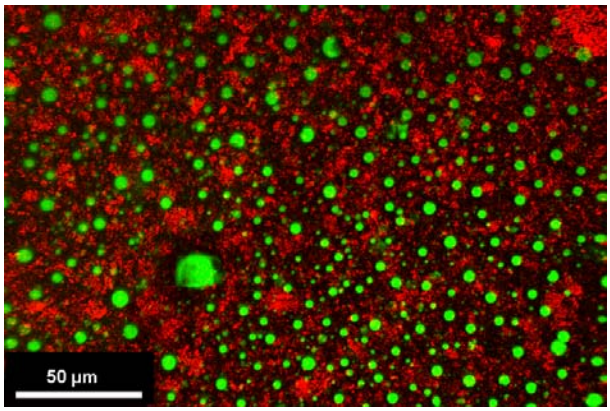

Figure 1. Recoverable bitumen in a tailings sample. The bitumen is in green and the mineral components are red. The dark areas are water. Note the largely spherical nature of the bitumen.

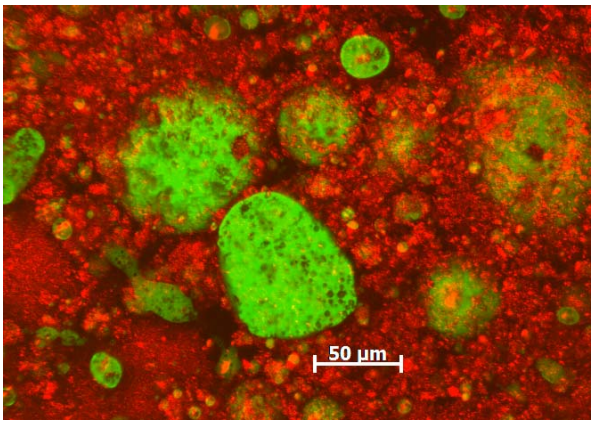

Figure 2. Unrecoverable bitumen in a tailings sample. The bitumen is in green and the mineral is red. Note the predominance of bitumen closely associated with mineral.

In the 1996 report "Vapour Pressure Properties and Hydrocarbon Distribution in the Plant 4 Tailings Stream". Divisional Report WRC 96-35,

Kasperski and Munoz use the recoverable and unrecoverable hydrocarbon concept to help understand the diluent distribution in the samples studied.

Ultimately this might help to assess the performance of technologies to reduce solvent loading on the Plant 16 diluent scrubber in the Suncor oil sands operation.

In spite of the fact that the purpose of this report is to determine factors that may govern solvent recovery for feed to a solvent recovery unit, references to this report have been used to support conclusions about solvent evaporation potential from a tailings pond. Clearly the solvent distributions and behaviour of diluent recovery unit tailings would not be related to diluent recovery unit feed the latter of which is the topic of the aforementioned paper. This note is meant to illustrate in a clear manner why the data in this report should not be used to support solvent release estimates from the tailings ponds.

RESULTS AND DISCUSSION

Figure 3 is repeated from the Kasperski and Munoz paper and in the Suncor nomenclature of the time, it shows that Plant 4 tailings are the feed to the Plant 16 diluent stripper. The microscopic evaluation of the feed to the diluent stripper uses the concept of recoverable and unrecoverable hydrocarbon, and this concept is clearly defined. In the course of this definition, the authors state *"The non-recoverable oil has been defined as the oil found strongly associated with solids".*

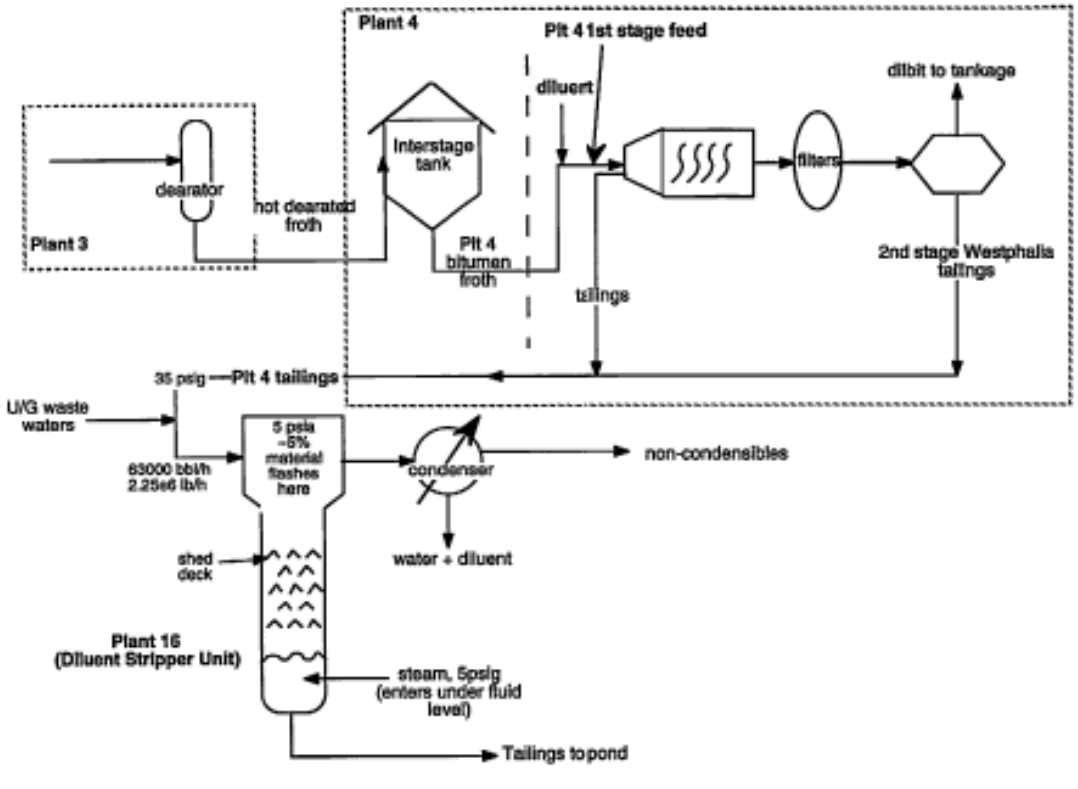

Figure 3. Figure 1 reproduced from the Kasperski and Munoz report 96-35.

Later, the authors went on to estimate, based on the microscopy that *"between 40 and 50% of the hydrocarbon was associated with solids",* Thermogravimetric analysis of the Plant 4 tailings was done in order to better understand the distribution of diluent and bitumen. In this analysis,

the Plant 4 tailings were centrifuged in order to separate the solids from the aqueous phase. The aqueous phase would contain dissolved solvent as well as the recoverable hydrocarbon as defined by the microscopic morphology. Thermogravimetric analysis of the samples in this case involves heating the samples and monitoring the weight loss. At the same time, an infrared detector is used to monitor the composition of the evolved gases. In this way, weight losses due to hydrocarbon components can be distinguished from water loss or carbon dioxide from mineral decomposition. This data is shown in Figure 4 which is a reproduction of figure 6 in the original report.

Table 6 - Weight losses observed during thermogravimetry of Plant 4 samples. All values are the means±S.D. of three runs.

TG Region	Weight Loss (wt%)			
	Hydrocarbon Fraction of Plant 4 Feed	Aqueous Fraction of Plant 4 Tails	Solid Fraction of Plant 4 Tails (from centrifugation)	Solid Fraction of Plant 4 Tails (from filtration)
Drying	61.3 ± 4.0[b]	98.5 ± 0.8	42.2 ± 0.9	55.4 ± 0.7
Water	1.9 ± 0.7	97.4 ± 0.7	34.9 ± 3.4	46.1 ± 3.0
Hydrocarbon[a]	59.4 ± 4.7	0.9 ± 1.5	7.3 ± 4.3	9.3 ± 3.7
Pyrolysis	33.1 ± 4.1	0.8 ± 0.2	11.6 ± 0.1	10.6 ± 0.1
Oxidation	3.5 ± 0.9	0	2.5 ± 0.2	3.1 ± 0.1
Ash (wt remaining)	2.0 ± 2.4	0.7 ± 0.8	43.8 ± 1.0	30.9 ± 0.6
Oxidation/pyrolysis	0.11 ± 0.02	0	0.21 ± 0.02	0.29 ± 0.01

[a] Value obtained by difference.
[b] This value is comparable to that obtained from the vacuum distillation analysis (Table 2).

Figure 4. Table 6 reproduced from the Kasperski and Munoz report.

The distribution of diluent between the water and solid phases can be calculated if the total amounts of each are available. This calculation is done by the authors in Appendix C (reproduced as Figure 5) and it can be seen that the proportion of diluent calculated in this way is 40%, generally in agreement with the qualitative microscopy assessment.

Unfortunately, many estimates of the availability of solvents to the environment from tailings ponds (VOC's or volatile organic compounds) have interpreted the previous discussion of the data in the Kasperski and Munoz report to mean that only about 40% of the naphtha solvent going into the tailings pond would be available to the environment as a VOC loading. The association of diluent with solids in no way means that it would not eventually move from the water column to the air. The assessment of recoverable versus unrecoverable hydrocarbon by microscopy methods simply is an estimate of the ease with which these hydrocarbons could be recovered. In spite of the terminology, it does not imply that these hydrocarbons could not be recovered under any circumstances. Similarly, in terms of the Kasperski and Munoz report, it does not mean that the diluent would never be available to the environment via evaporation.

In spite of the fact that the report is dealing with feed to a diluent stripper, the authors clearly address the idea of diluent evaporation when they state on page 22 of their report "*This data shows that all the diluent could be vaporized even at a lower temperature, as long as enough time was allowed.*"

In order to determine the distribution of diluent, the assumptions made are that all diluent is evaporated during the drying step and that none of the observed hydrocarbon is from bitumen. The first assumption is based on observations made during TG-EGA analysis of pure diluent. The second assumption is based on studies which have shown that for mixtures of bitumen with solvents or water, the amount of components in the vapour phase that came from the original bitumen was negligible (2). The diluent distribution is then calculated as follows:

Mass tailings sample centrifuged = 900.1 g
Mass aqueous phase after centrifugation = 776.7 g
Mass solids after centrifugation = 123.4 g

Per cent diluent in aqueous phase (hydrocarbon from TG drying step) = 0.9 wt%
Per cent diluent in solids (hydrocarbon from TG drying step) = 7.3 wt%

Mass diluent in aqueous phase = 776.7 x 0.009 g
= 6.99 g
Mass diluent in solids = 123.4 x 0.073 g
= 9.01 g
Fraction of total diluent that is in aqueous phase = 6.99/(6.99+9.01)
= 44 wt%
Fraction of total diluent that is in solids = 9.01/(5.99+9.01)
= 56 wt%

Total diluent content in tailings = (6.99+9.01)/900.1
= 1.8 wt% (vs 0.6 wt% from Dean-Stark and diluent analysis)

Figure 5. Excerpt from Appendix C showing the distribution of diluent between the mineral and aqueous phases in the plant 4 tailings.

SUMMARY

Currently the ERCB (Energy Resources Conservation Board) allows 4 volumes of solvent to be lost to tailings for every 1000 volumes of bitumen produced. It is not justifiable to use the Kasperski and Munoz report CWRC 98-35 to support a contention that only 40% of this total would be available to the environment and contribute to VOC's. Notwithstanding the fact that the report is investigating the properties of feed to a diluent stripper, and not feed to a tailings pond, the authors state clearly that given enough time, all of the diluent could evaporate. Furthermore, a review of environmental impact assessments will reveal that at various times, this report has been used to support reductions in paraffinic solvent evaporation to the environment. This is not to say that other mechanisms might be at work to limit solvent evaporation to some fraction of the 4 barrels solvent per 1000 barrels of bitumen production, along with other evidence, but the Kasperski and Munoz report would not be among them.

REFERENCE

Kasperski, K.L., and Munoz, V.A., Vapour Pressure Properties and Hydrocarbon Distribution in a Plant 4 Tailings Stream, Fuel Processing Laboratory, Western Research Centre, October 1996, Divisional Report WRC 96-35.

OIL SANDS PROCESS-AFFECTED WATER CONTAMINATION TRANSPORT THROUGH PEAT SOILS: LABORATORY AND GREENHOUSE STUDY

F. Rezanezhad[1], J.S. Price[1], L. Rochefort[2], R. Pouliot[2], R. Andersen[2,3], C. Daly[4]
[1]Department of Geography, University of Waterloo, Canada
[2]Department of Phytology, University of Laval, Canada
[3]Macaulay Land Use Research Institute, Aberdeen, UK
[4]Suncor Energy Inc., Fort McMurray, Canada

ABSTRACT

In the Athabasca oil sands region, peatlands cover up to half of the local landscape, and peat materials are commonly used in reclamation. Despite the importance of contamination and toxicity caused by Oil Sands Process-affected Water (OSPW), little is known about its transport in peat soils. To address this lack of knowledge, the transport and attenuation processes of OSPW through peat soils and its effects on peatland vegetation were assessed with laboratory and greenhouse experiments. A potentially significant barrier to reclamation is the presence of salts, heavy metals and organic acids in the groundwater from OSPW, which have a toxic effect on plants. Toxicity of OSPW is related to the elevated concentration of naphthenic acids (NAs) and sodium (Na). However, its transport through peat is significantly delayed by sorption and by diffusion into immobile water contained in the peat matrix. Laboratory experiments showed approximately 94% of the 43.5 mg l^{-1} of OSPW was sorped by 1 kg of peat. For Na ~84% sorption occurred with 382 mg l^{-1} kg^{-1} of peat. The adsorption of NAs and Na on peat fitted Freundlich linear isotherms with adsorption coefficients of 6.05 and 3.64 l/kg, respectively. The complex dual-porosity structure of peat (both open and dead-end pores) and the high cation exchange capacity of the peat are the important factors in attenuating contaminant transport. In this study, to examine the plant responses and identify species most tolerant to the expected levels of contamination, field conditions were recreated (~ 40 mg l^{-1} NAs and 385 mg l^{-1} Na) in a randomized design in the greenhouse with two treatments: 1) mosses (*Sphagnum warnstorfii* and *Tomentypnum nitens*) and 2) vascular plants (*Carex aquatilis* and *Calamagrostis stricta*). After two growing seasons of receiving contaminated water, the vascular plants continued to reproduce without showing stress from oil sand process water contamination but mosses showed a slight decline in health towards the end of the second growing season. The goal of this research was to observe how OSPW contaminated water is transported through peat as well as to observe how fen vegetation reacts to a realistic contamination scenario.

INTRODUCTION

Oil sands mining in the Athabasca oil sands region disturbs large tracts of land as the vegetation-soil layer must be removed in order to access the oil sands beneath. Peatlands are a dominant feature of this landscape and are, therefore, greatly affected oil sands mining. Oil companies are obliged by law to return post-mined land to improved or equivalent capacity, and restore a part of their lease back to peatlands. Processing oil sands in this region produces large volumes of wet tailings material including sand, silts and clays in suspension, soluble organic chemicals, ammonia, heavy metals, salts and oil sand process-affected water (OSPW). Many of the current pressing problems of environmental concern in this region involve transport of OSPW contaminated with sodium (Na) and naphthenic acids (NAs) (Alberta Environmental Protection, 1996), since they may be at concentrations toxic to aquatic plants and animals (Trites and Bayley, 2005; Apostol *et al*., 2004). Therefore, one of the greatest barriers to peatland creation will be the elevated amount of toxins (naphthenic acid, metals and salinity) present in the post-mined landscapes. Na and NAs are readily transported through porous geological media with little attenuation beyond mechanical dispersion (Gervais and Barker, 2005). However, their movement into peatlands has received very little attention. Given the broad spatial coverage of peatlands (Vitt and Chee, 1989), use of peat in artificial soil cover during reclamation (Shurniak and Barbour, 2002) and the recent thrust to reclaim post-mined landscape to fen peatlands (Price *et al*., 2010), determining the transport and fate of OSPW in peat soils is essential.

Groundwater flow in peat directly influences how effectively solutes are removed or dispersed by chemical (Hill and Siegel, 1991), physical (Price and Woo, 1988; Ours *et al*., 1997), and microbiological processes (Todorova *et al*., 2005). Transport of contaminants through the peat may experience ion exchange, ion exclusion, chemical and biological transformations, volatilization, dissolution and precipitation, biodegradation and dispersion (Tindall and Kunkel, 1999), but advection (into open and connected or active pores) and matrix diffusion (into closed pores) are typically assumed to be the dominant mechanisms controlling non-reactive solute transport in peat (Reeve *et al.,* 2001). Solute passing through open and connected pores is abstracted through diffusion into closed pores (Loxham and Burghardt, 1983; Price and Woo, 1988; Viraraghavan and Ayyaswami, 1989; Hoag and Price 1997). Very little information is available in the literature on the transport properties of OSPW in peat soils. Janfada *et al*., (2006) found NAs to be strongly adsorbed by organic matter, and are subject to degradation by microbial action (Herman *et al*., 1994).). Hadwin *et al*., (2005) found that exposure to slightly higher than naturally occurring levels of naphthenic acids shifted the microbial community structure to one that is capable of metabolizing NAs. Thus, there may be some capacity for wetlands to remove NAs from process-affected water (Toor *et al*., 2007).

Both increasing salinity and NAs inhibit water uptake and might reduce plant growth (Munns and Termaat, 1986; Kamaluddin and Zwiazek, 2002). There is a concern that the combined effects of NAs and salinity may intensify plant water stress in reclamation areas (Apostol *et al*., 2004). Therefore, the combined effects of salinity and NAs could result in potentiation, where the effect of two substances is not additive, but greater than expected (Walker *et al*., 2006). Much research has been carried out on the response of boreal forest species (Renault, 1998; Renault, 1999; Renault, 2000; Renault, 2001; Apostol *et al*., 2004) as well as marsh species (Brendell-Young *et al*., 2000; Crowe *et al*., 2001; Crowe *et al*., 2002; Cooper, 2004) species to OSPW. However, little research has been carried out on peatland species (Trites and Bayley, 2005) and no research has been carried out on peatland mosses.

In this study, laboratory and greenhouse experiments were run to assess the transport and attenuation processes of NAs and Na through peat and to investigate how oil sands process-affected waters will affect peatland vegetation, specifically fen vegetation. The main objectives are to: (1) derive a clear understanding of the transport, sorption mechanisms and the interaction of the NAs and Na with the peat matrix; (2) understand how the structure and properties of peat affects OSPW transport and retardation; and (3) investigate how typical fen vegetation will react to a realistic contamination scenario in a controlled macrocosm environment.

METHODOLOGY

Laboratory Experiments

The peat used in this study was obtained from fens of the Athabasca oil sands region; these being the dominant local peatland type (Vitt and Chee, 1989), and shipped to University of Waterloo for laboratory experiments and University of Laval for greenhouse experiments. The soil was moderately decomposed rich-fen sedge-peat (pH=7.4). The peat was highly disturbed by digging operations and repacked. The OSPW was obtained from the Suncor Energy oil sands operation with initial concentration of 525 mg l^{-1} for Na and 53 mg l^{-1} for NAs.

Batch tests (Freeze and Cherry, 1979; Pignatello, 2000) were used to determine the equilibrium times for adsorption of Na and NAs in the peat. A known mass of peat (~120 g) was placed into nine 200 ml glass vials (sealed with a cap) with 120 ml of diluted OSPW (70% OSPW) with initial concentration of 382 mg l^{-1} for Na and 43.5 mg l^{-1} for NAs. The samples were agitated on a constant mixer for 24h. The solute was extracted from the paste by suction lysimeter after 1h, 3h, 6h, 18h, 24h, 48h, 3 days, 7 days and 14 days. The same procedures were used for seven different concentrations as 100%, 70%, 55%, 30%, 15%, 5% and 1% of OSPW). After the batch experiments were completed, the peats were dried at 80˚C for a period of a week and the measured concentrations were adjusted on the basis of its oven-dry weight.

All water samples were analyzed for total NAs using Fourier Transform Infrared spectroscopy (FT-IR) developed by Jivraj *et al*., 1995; and for total Na using Perkin Elmer model 3100 atomic absorption spectroscopy.

Greenhouse Experiments

To understand the movement of NAs and Na through a peat matrix under moss and vascular plant covers and observe how these fen plants growing in peat will react to OSPW input, a randomized design was used with two treatments: 1) mosses (*Bryum pseudotriquetrum* and *Pohlia nutans*) and 2) vascular plants (*Carex aquatilis* and *Calamagrostis stricta*) in a greenhouse at University of Laval. The moss cover has no underground root system but its cover can impact the moisture and temperature of the underlying peat matrix. However, the cover of *Carex aquatilis* and *Calamagrostis stricta* have an extensive belowground root system which could affect the way NAs and Na flows through the peat matrix. The interaction of the plants with the contaminated substrate will therefore be different under a moss vs. vascular cover. These treatments were replicated two times, for a total of 4 containers (120 × 80 × 76 cm) (Figure 1). The peat containers were saturated slowly with rain water (collected in a cistern) rising from input manifolds at the base of the containers in several input steps and then it was held at saturation for 24h. The saturated containers were completely drained for 24h and then OSPW (with initial Na and NAs of ~385 mg l^{-1} and ~40 mg l^{-1}, respectively) was introduced at the base of the containers until a water table of -15 cm was achieved. The OSPW was pulled upward by evapotranspiration and the water table was held at -15 cm by filling the inflow device every two days. The water level was monitored every 15 minutes in the containers using pressure transducers.

The greenhouse experiments were continued for a two growing seasons (started from April 2009 to June 2010 with a 3 months stop with setting the containers outside to simulate winter) to see how contaminated water migrates sufficiently into the root zone and affects the vegetation. The precipitation was simulated as the field condition in Fort McMurray (~70 mm/month) for the first 5 months of first growing months (April to August) and then drier (~10 mm/month) for the last 3 months of first growing season and all second growing season. Humidity and temperatures also was simulated and controlled as the field condition. The photoperiod for the duration of the experiment was 16 hours. The daytime humidity was 50% and the night time humidity 60%. The temperature was 19 ^{o}C during the day and 10 ^{o}C at night.

Eight vegetation assessments were carried out in two growing seasons. The first was at the end of March (before contaminants are added), the second was in June, the third was at the mid-August and the last was at the end of October for the first growing season. In the second growing season vegetation assessments were carried out every five weeks from February to June 2010. During these assessments, the percentage cover of the plants, a plant health index as well as the shoot length and number of leaves for the vascular plants was measured. For the moss species the percentage cover and plant health index were noted. The plant health index was a scale from 1 to 7 with 1 being 100% healthy and 7 being 100% dead.

Along with monitoring of plant's health, the concentration and flux of these solutes were assessed simultaneously to determine the critical NAs and Na concentrations, duration and timing of exposure; and to track the transport and attenuation processes through peat by plant uptake. For this, one container for each treatment (one with vascular plants and one with mosses) was instrumented with 4 suction lysimeters to extract solute from four depths (-5, -10, -15, -25 cm) (Figure 1). A two week sampling period was selected and a 70 ml sample was taken from each depth and stored for Na and NAs analysis. The water samples taken by suction lysimeters were transported to the Department of Geography and Environmental Managements at the University of Waterloo for Na and NAs analysis.

Figure 1. Mosses and vascular plants ccontainers with installed instruments.

RESULTS AND DISCUSSIONS

Laboratory Experiments

The batch tests showed rapid and significant adsorption of Na and NAs to the peat. After adding OSPW, stable concentrations of Na and NAs were achieved within 1h with no discernable trend and no significant difference occurring thereafter for the two-week duration of the experiment. The amount of Na and NAs adsorbed depends on mass of peat suspended per volume of solution and solution concentration. The adsorption rates computed from batch tests results showed that 308 mg of Na in a 382 mg l^{-1} Na OSPW solution were sorped in 1kg of peat (80%). By comparison, NAs sorption on peat was 41 of 43.5 mg l^{-1} kg^{-1} peat in OSPW (94%). The amount of Na and NAs adsorbed also depends on the concentration of the solution (Table 1).

Table 1. Na and NAs adsorption for the 7 batch test containers with different initial input concentrations. MDL is the method detection limit.

	% of OSPW	100%	70%	55%	30%	15%	5%	1%
Sodium (Na)	input (mg)	99	71.1	54.2	30.7	15.4	4.3	1.8
	adsorbed (mg)	82.8	57.9	45.4	24.8	11.4	3.0	1.1
	adsorption rate	83.4%	81.4%	83.7%	80.0%	74.0%	69.7%	61.1%
Naphthenic Acids (NAs)	input (mg)	10.9	8.4	6.7	3.2	1.6	0.6	0.2
	adsorbed (mg)	10.2	8.0	6.3	2.9	<MDL	<MDL	<MDL
	adsorption rate	93.5%	95.2%	94.0%	90.0%	---	---	---

Lower initial concentrations resulted in decreased adsorption by a proportion equivalent to the slope of the so-called Freundlich isotherm (Figure 2). The Freundlich isotherm is an equilibrium isotherm that represents the mass of contaminant adsorbed per unit dry mass of soil or organic matter versus the concentration of the contaminant and the equation is expressed as (Freeze and Cherry, 1979):

$$S=K_{ads}C^{b}, \qquad (2)$$

where S is the amount of a solute adsorbed onto the solid phase (mg kg^{-1}), C is the concentration of the solute in the liquid phase (mg l^{-1}), K_{ads} is the Freundlich adsorption coefficient representing the extent of sorption (l kg^{-1}), and b is the Freundlich exponent constant representing the degree of non-linearity of sorption. If the constant b has a value of 1, the Freundlich isotherm is identical to the linear isotherm. The slope of the log-log Na and NAs adsorption (K_{ads}) and the constant b obtained by Freundlich fitting are presented in Figure 2. The Freundlich adsorption isotherms for Na and NAs showed an excellent fit to the measured adsorption data (R^2 = 0.99). The b values in the Freundlich isotherms were approximately equal to 1, implying that the isotherms were likely to be linear. These linear isotherms show the influence of concentration on the extent of adsorption on peat by the linear partitioning of solutes between liquid and solid phases. As the K_{ads} in the Freundich equation is related primarily to the capacity of the adsorbent for the adsorbate and b is a function of the strength of adsorption, higher K_{ads} for NAs than Na, 6.05 and 3.64 l kg^{-1} values, respectively in Figure 2, shows a stronger sorption of organic compound NAs to peat than Na, resulting in higher percentage of NAs adsorption.

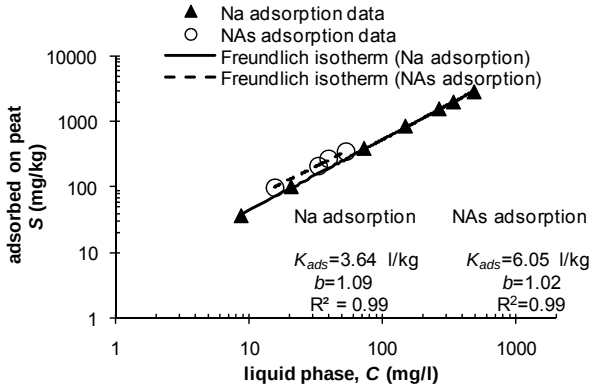

Figure 2. Na and NAs adsorption on peat presented by the slope of the Na and NAs in solid phase (*S*) versus liquid phase (*C*) (Freundlich isotherm).

In Rezanezhad *et al*., (in review), the physical and hydraulic properties of the same peat samples were studied and with the dual-porosity model fitted to the observed data, three hypotheses were assumed for the dual pore size distributions in peat that affect solute transport. These guiding hypotheses differentiate pore size distributions *as*: (*I*) open and connected macropores where most solute transport probably occurs; (*II*) closed or partially closed cell remains with more or less intact walls and (*III*) hyaline cells and dead-end or isolated pore spaces where solute transport is attenuated and retarded by diffusion into these spaces.

Greenhouse Experiments

The depth from peat surface to the water level, measured using pressure transducers installed

inside the containers, varied over the duration of the experiment with evapotranspiration and precipitation rate. The water level depths for the mosses were higher than for the vascular plants, which had higher evapotranspiration in a similar condition of humidity, precipitation and temperature. The average amount of contaminant introduced to the moss and vascular plant containers was approximately 3 and 15 liters per week in the first five months of first growing season, respectively, and then increased to approximately 9 and 25 liters per week for all other months, respectively. The total OSPW used in the moss and vascular plant containers was ~415 and ~1120 liters, respectively.

The results of the contaminant transport in moss and vascular plant containers showed that OSPW introduced at the base of the containers (with initial Na and NAs concentration of 385 mg l^{-1} and 40 mg l^{-1}, respectively) was pulled upwards by evapotranspiration over the growing periods. Higher evapotranspiration from the vascular plants in comparison to the mosses increased the upward migration of water and contaminant compared to the mosses. At the base the resulting Na and NAs concentration increased after 14 months of experiments. NAs did not migrate into the rooting zone or was lower than the method detection limit of the system in the first growing season, but Na did migrate.

Table 2 shows the results of liquid phase (*C*) and solid phase (*S*) Na and NAs concentrations distributed at different depths for both moss and vascular plant containers at the last day of experiment. The liquid phase Na and NAs mass profiles were obtained based on liquid phase Na and NAs concentrations and the volume of solution available at each depth. The liquid-phase concentration profile is dependent on the adsorption of Na and NAs in each layer. Based on total amount of introduced OSPW (~415 and ~1120 liters for moss and vascular plant containers respectively), initial water content of the peat, liquid phase Na and NAs concentrations at each depth and the Freundlich adsorption isotherm coefficients obtained for Na and NAs (Figure 2), the mass of adsorbed Na and NAs on the peat was determined in the solid phase. The partition of solute mass between liquid and solid (adsorbed) phase with depth is shown in Figure 3 and 4 for Na and NAs respectively. The results showed that the amount of adsorbed Na and NAs onto the peat is approximately an order of magnitude larger than Na and NAs in liquid phase (Figure 3 and 4).

Table 2. Liquid phase (*C*) and solid phase (*S*) Na and NAs concentrations distributed at different depths for moss and vascular plant containers at the last day of experiment. The plant uptakes were calculated by percentage of subtracted total solid phase mass (adsorbed mass on peat) and liquid phase from total input mass to the total input mass.

depth	mosses container				vascular plants container			
	Na		NAs		Na		NAs	
	C(mg)	*S*(mg)	*C*(mg)	*S*(mg)	*C*(mg)	*S*(mg)	*C*(mg)	*S*(mg)
-5 cm	1191	28825 (17.5%)	50	1372 (7.7%)	23548	115248 (24.9%)	210	3827 (5.3%)
-10 cm	1395	32160 (19.5%)	112	1895 (10.7%)	25692	110626 (23.9%)	653	6891 (9.6%)
-15 cm	2543	33797 (20.5%)	223	6056 (34.2%)	16732	63426 (13.7%)	623	24942 (34.9%)
-25 cm	6608	55688 (33.8%)	437	7012 (39.6%)	17734	84965 (18.4%)	1244	31410 (44.0%)
total	11737	150470	822	16335	83706	374265	2730	67070
total input (mg)	164526		17694		461034		71271	
plants uptake (mg)	2318 (1.4%)		537 (3.0%)		3062 (0.6%)		1470 (2.0%)	

In the moss container, the increase in concentration in the liquid phase was sequentially delayed at higher elevations in the profile (Figure 3a and 4a). At -25 cm below the peat surface 33.8% and 39.6% of total introduced mass of Na (164,526 mg) and NAs (17,694 mg), respectively, was adsorbed after 14 months. At -15 cm, -10 cm and -5 cm, the adsorption rate was 20.5%, 19.5% and 17.5% for Na and 34.2%, 10.7% and 7.7% for NAs, respectively (Table 2). At these levels, the adsorbed concentrations are lower than at the -25 cm level because: a) the greater distance means it takes solute longer to get there and b) the fluid arriving there has had the solute stripped from it by sorption in the lower layers. But, this was different for Na in the vascular plant container where after ~180 days the liquid concentration at the -5 cm and -10 cm level matched that of the layer below it, as Na accumulated there by higher evapotranspiration at the surface of this container. After 14 months, the final Na concentration of the -5 cm and -10 cm layer in the vascular plant container exceeded that of the -15 and -25 cm layer (Table 2 and Figure 3b). The plants uptake was calculated by percentage of subtracted total solid phase mass (adsorbed mass on peat) and liquid phase mass from total input mass to the total input mass. Uptake of Na and NAs were found as 1.4% and 3.0% for mosses and 0.6% and 2.0% for vascular plants, respectively.

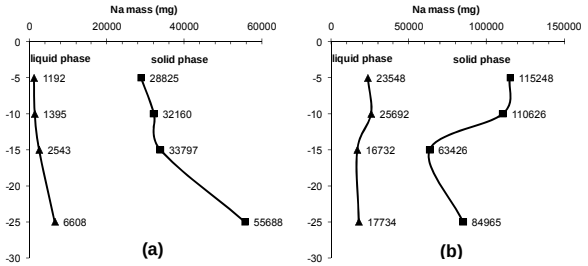

Figure 3. Na mass profiles with depth for liquid phase and solid phase (adsorbed on peat) for mosses (a) and vascular plants (b) at the last day of experiment.

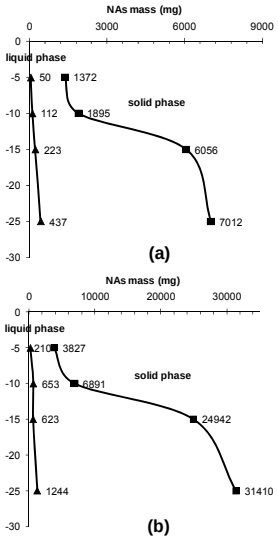

Figure 4. NAs mass profiles with depth for liquid phase and solid phase (adsorbed on peat) for mosses (a) and vascular plants (b) at the last day of experiment.

After two growing seasons of receiving OSPW, the vascular plants did not show signs of poor health but mosses showed a slight decline in health towards the end of the second growing season due to effects of OSPW (Figure 5). Both vascular plants, particularly *Carex aquatilis*, continued to reproduce during both growth season of the experiment. These results indicate that peat has an exceptional ability to absorb the contaminants in the OSPW water. This means that the vascular plants have at least two growing seasons to establish before they must cope with stress caused by salinity and other toxins in OSPW, and probably longer where the peat layer is thicker.

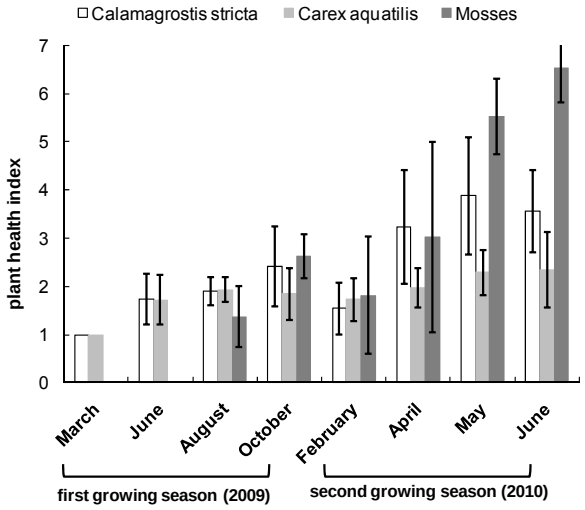

Figure 5. Vascular plants and mosses health index tested over two growing seasons. For the plant health index, a value of 1 indicates 100% healthy, and a value of 7 indicates 100% dead.

CONCLUSIONS

This study examined the movement of oil sands process-affected water through peat substrate and the survival, growth and regeneration/germination of different fen plant species grown in peat treated with process-affected water. The physical and hydraulic properties of peat soils and sorption coefficient explain the mechanisms of sorption and physical-chemical factors affecting the concentration of potentially toxic compounds in the rooting zone. Our experiments suggested that the complex dual-porosity structure of peat is an important factor on attenuation process in groundwater transport and the presence of this structure has a strong effect on solute transport.

Batch tests showed no significant difference between Na and NAs absorption after 1h versus 2 weeks, thus naphthenic acids and sodium were concluded to undergo rapid sorption to the peat soil (~94% of NAs and ~80% of Na when one litter of OSPW solution containing 43.5 and 382 mg l^{-1} of NAs and Na, respectively, was added to one kilogram of peat). The adsorbed Na and NAs also depended on the concentration of the solution where the lower initial concentrations resulted in lower adsorption by a proportion equivalent to the slope of the linear Freundlich isotherm.

After two growing seasons of receiving contaminated water the vascular plants were in good health and continued to reproduce. This was facilitated by the peat, which absorbed most of the contaminants allowing the vascular plants to grow without apparent stress from oil sand process water contamination. In fact, all vascular plants continued to grow between the two growing seasons although the simulated precipitation decreased in the last months of first growing season and the second season, which increased the amount of OSPW water entering the system.

Finally, the information gathered from these laboratory and greenhouse experiments will be taking a clear step towards addressing the future outcomes of oil sand affected landscapes. With this information, reclaimed landscape designs will be able to position peatlands in landscapes according to the amount of contamination they will tolerate.

ACKNOWLEDGMENTS

This study was part of Suncor fen creation research program and funding for this project was provided by Suncor Energy Inc. We thank Shirley Chatten (University of Waterloo, Department of Earth and Environmental Sciences) and Alex MacLean (Wilfrid Laurier University, Department of Geography and Environmental studies) for the water sample analysis.

REFERENCES

Alberta Environmental Protection. 1996. Fort McMurray-Athabasca subregional integrated resource plan. Edmonton, AB.

Apostol, K.G., Zwiazek, J.J., MacKinnon, M.D. 2004. Naphthenic acids affect plant water conductance but do not alter shoot Na^+ and Cl^- concentrations in jack pine (Pinus banksiana) seedlings. Plant and Soil, **263**, 183-190.

Brendell-Young, L.I., Bennett, K.E., Crowe, A., Kennedy, C.J., Kermode, A.R., Moore, M.M., Plant, A.L., Wood, A. 2000. Ecological characteristics of wetlands receiving an industrial effluent. Ecological Applications, **10**: 310-322.

Cooper, N.J. 2004. Vegetation community development of reclaimed oil sands wetlands. M.Sc Thesis. University of Alberta, Edmonton, Canada.

Crowe, A.U., Han, B., Kermode, A.R., Brendell-Young, L.I., Plant, A.L. 2001. Effects of oil sands effluent on cattail and clover: photosynthesis and the level of stress proteins. Environmental pollution, **113**: 311-322.

Crowe, A.U., Plant, A.L., Kermode, A.R. 2002. Effects of an industrial effluent on plant colonization and on the germination and post-germinative growth of seeds of terrestrial and aquatic plant species. Environmental pollution, **117**: 179-189.

Freeze, R.A., Cherry, J.A. 1979. Groundwater. Prentice-Hall, Englewood Cliffs, NJ. 604 pp.

Hadwin, A.M., Del Rio, L.F., Pinto, L.J., Painter, M., Routledge, R., Moore, M.M. 2005. Microbial communities in wetlands of the Athabasca oil sands: genetic and metabolic characterization. FEMS microbial Ecology, **55**: 68-78.

Herman, D.C., Fedorak, P.M., MacKinnon, M., Costerton, J.W. 1994. Biodegradation of naphthenic acids by microbial populations indigenous to oil sands tailings. Canadian Journal of Microbiology, **40**: 467–477.

Hill, B.M., Siegel, D.I. 1991. *Groundwater flow and the metal content* of peat. Journal of Hydrology, **123**: 211-224.

Hoag, R.S., Price, J.S. 1997. The effects of matrix diffusion on solute transport and retardation in undisturbed peat in laboratory columns. Journal of Contaminant Hydrology, **28**: 193- 205.

Gervais, F., Barker, J. 2005. Fate and transport of naphthenic acids in groundwater. *Bringing Groundwater Quality to the Watershed* Scale (Proc. GQ 2004, 4th Internat. Groundwater Quality Conference), IAHS Publ., **297**: 305-310.

Janfada, A., Headley, J.V., Peru, K.M., Barbour, S.L. 2006. A Laboratory Evaluation of the Sorption of Oil Sands Naphthenic Acids on Organic Rich Soils. Journal of Environmental Science and Health Part A, **41**: 985-997.

Jivraj, M.N., MacKinnon, M., Fung, B. 1995. Naphthenic acids extraction and quantitative analyses with FT-IR spectroscopy. Syncrude Analytical Methods Manual, fourth ed. Syncrude

Canada Ltd. Research Department. Edmonton, AB.

Kamaluddin, M., Zwiazek, J.J. 2002 Naphthenic acids inhibit root water transport, gas exchange and leaf growth in aspen (*Populus tremuloides*) seedlings. Tree Physiology, **22**: 1265–1270.

Loxham, M., Burghardt, M. 1983. Peat as a barrier to the spread of micro-contaminants to the groundwater. In: C.H. Fusehman and S.A. Spigarelli (Editors), Proc. Int. Syrup. on Peat Utilization, Bemidji State University, Bemidji, MN. Bermidji State University, Bermidji, pp. 337-349.

Munns, R., Termaat, A. 1986. Whole-plant response to salinity. Australian Journal of Plant Physiology, **13**: 143–190.

Ours, D.P., Siegel, D.I., Glaser, P.H. 1997. Chemical dilation and the dual porosity of humified bog peat. Journal of Hydrology, **196**: 348-360.
Pignatello, J.J. 2000. The measurement and interpretation of sorption and desorption rates for organic compounds in soil media. Advanced in Agronomy, **69**: 1- 73.

Price, J.S., McLaren, R.G., Rudolph, D.L. 2010. Landscape restoration after oil sands mining: conceptual design and hydrological modelling for fen reconstruction. International Journal of Mining, Reclamation and Environment, **24**(2): 109-123.

Price, J.S., Woo, M.K. 1988. Wetlands as waste repositories? Solute transport in peat. Proc. Nat. Student Conference on Northern Studies, 18-19 November 1986, Assoc. of Canadian Universities for Northern Studies, Ottawa, Ont., pp. 392-395.

Reeve, A.S., Siegel, D.I., Glaser, P.H. 2001. Simulating dispersive mixing in large peatlands. Journal of Hydrology, **242**: 103-114.

Renault S., Lait, C., Zwiazek, J.J., MacKinnon, M.D. 1998. Effect of high salinity tailings waters produced from gypsum treatment of oil sand tailings on plants of the boreal forest. Environmental Pollution, **102**: 177-184.

Renault, S., Paton, E., Nilsson, G., Zwiazek, J.J., MacKinnon, M.D. 1999. Responses of boreal plants to high salinity oil sands tailings water. Journal of Environmental Quality, **28**: 1957-1962.

Renault, S., Zwiazek, J.J., Fung, M., Tuttle, S. 2000. Germination growth and gas exchange of selected boreal forest seedlings in soil contantaining oil sands tailings. Environmental Pollution, **107**: 357-365.
Renault, S., Crosser, C., Franklin,J.A., Zwiazek, J.J. 2001. Effects of NaCl and Na_2SO_4 on red-osier dogwood (*Cornus stolonifera* Michx) seedlings. Plant and Soil, **233**: 261-268.

Rezanezhad, F., Price, J.S. 2010. Movement and Absorption Mechanisms of Oil Sands Process-affected Water in Dual-porosity Peat Soils: A Laboratory Experiment. Journal of Contaminant Hydrology, in review.

Shurniak, R.E., Barbour, S.L. 2002. Modeling of water movement within reclamation covers on oilsands mining overburden piles. American Society of Mining and Reclamation, 3134 Montavesta Rd. Lexington KY 40502.

Tindal, J.A., Kunkel, J.R. 1999. Unsaturated Zone Hydrology for Scientists and Engineers. Prentice Hall, New Jersey, 624 p.

Todorova, S.G., Siegeland, D.I., Costello, A.M. 2005. Microbial Fe(III) reduction in a minerotrophic wetland – geochemical controls and involvement in organic matter decomposition. Applied Geochemistry, **20** (6): 1120-1130.

Toor, N., Liber, K., MacKinnon, M., Fedorak, P. 2007. The role and effectiveness of wetlands for mitigation of oil sands process affected waters CEMA Progress Report November 1, 2007.

Trites, M., Bayley, S.E. 2005. Effects of Salinity on Vegetation and Organic Matter Accumulation in Natural and Oil Sands Wetlands. Final Report CEMA Reclamation Working Group Grant 2005-0018.

Vitt, D.H., Chee, W.L. 1989. The vegetation, surface water chemistry and peat chemistry of moderate-rich fens in central Alberta, Canada. Wetlands, **9**: 227-261.

Viraraghavan, T., Ayyaswami, A. 1989. Batch studies on septic tank effluent treatment using peat. *Can. J. Civ. Eng*., **16**(2): 157-161.

Walker, C.H., Hopkin, S.P., Sibly, R.M., Peakall, D.B. 2006. Principles of Ecotoxicology, third edition. Taylor and Francis Group, New York.

A REVIEW OF THE NATURE OF NAPHTHENIC ACID OCCURRENCE, TOXICITY, AND FATE IN REFINERY AND OIL SANDS EXTRACTION WASTEWATERS

C. Eickhoff, P. Heaton, R. Vermeersch, J. Laroulandie, J. Keating, P. Howes, B. Chubb
Maxxam Analytics, Canada

INTRODUCTION

Concerns regarding the fast growing oil sands industry and the risk of contamination associated to the naphthenic acids have risen into environmental and regulatory groups. Naphthenic acids which occur naturally in crude oils and bitumen have been identified and characterised as primary toxicants in wastewaters associated with oil refineries and oil sands extraction activities. Respecting the zero policy discharge, the petroleum industry has accumulated large volumes of oils sands process water into tailings ponds and wetland. The toxicity and persistence of naphthenic acids is important to consider in terms of potential effects to aquatic organisms such as fish, invertebrates and aquatic plants. Environmental managers may encounter issues with toxicity arising from naphthenic acids or other related wastewater components related. This article summarizes the current available literature regarding the toxicity and fate of naphthenic acids in the environment. Strategies for identifying toxicity caused by naphthenic acids or other components in wastewaters will also be presented.

CHEMISTRY OF NAPHTHENIC ACIDS

Naphthenic acids (NAs) are an unspecific mixture of many different hydrocarbon compounds having a variety of molecular weights, number of cycloalkane rings, and alkyl side chains. Naphthenic acids are natural constituents of oil sands ore and are readily dissolved in the alkaline extraction water. NAs are classified as a complex mixture of alkyl-substituted acyclic and cycloaliphatic carboxylic acids with the general formula $C_nH_{2n+z}O_2$ (Figure 1), where n represents the carbon number and z represents a homologous group series number related to the number of five or six carbon rings within the structure.

In general, the physical and chemical characteristics of naphthenic acids can be described as the overall mixture as summarised in Table 1. However, a recent investigation (Clemente et al., 2003) demonstrated that the concentration and composition of components in NAs are different when extracted from oil sands tailings ponds, oil sands ore, or commercial sources. Commercial preparations usually have few acids with carbon numbers above 20, whereas it is common to find acids with carbon numbers >20 in NA from OSPW (Oil Sands Process-affected Water) and crude oil. Therefore, the different molecular structures and sidechains found within naphthenic acids create individual compounds with various physical, chemical, and toxicological properties. For example, the polarity of naphthenic acids increases with molecular weight while the volatility decreases with higher molecular weight.

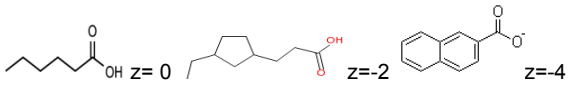

Figure 1. Example of chemical structures of naphthenic acids

Due to the carboxylic acid moiety attached to a hydrophobic group, NAs act as surfactants. The number of hydrophilic groups, which increase the water solubility of NAs, depends on the makeup of the complex mixture.

Naphthenic acids are weak acids having pKa values of approximately 5. The water solubility of NAs is directly related to the pH of the solution. The greatest proportion of total acids in solution at pH >5 exist in the ionic form which is more soluble. Acid solutions favor the protonated form which is less soluble in water. Solubility has been estimated using EPIWIN (USEPA, 2000-2009) for complex mixtures which may contain hundreds or thousands of structures. The estimated solubility of NAs ranged from 0.0003 to 2.1 mg/L depending on the molecular weight and pH (American Petroleum Institute Petroleum HPV Testing Group, 2003).

Identifying the composition of NA mixtures is still a challenge and requires further analytical development. Recent advances in analytical

techniques have identified additional compounds within mixtures of NAs including O_4 structures, and some NAs contain compounds with more than one carboxylic acid moiety (Frank et al., 2010).

UV and IR analyses have shown the presence of pyrroles, thiopenes, and phenols in NA purified from a California crude oil. TLC of California crude demonstrated that the NAs fraction contains 3 mol% phenol, 5 mol% nitrogen, 2% of which are indoles, and 8.5 mol% sulfur (Seifert and Teeter, 1969). Hsu et al. (2000) demonstrate that 40% of the NAs did not contain the carboxylic acid functional group while in a California crude oil acids aromatics groups make up for 3.1%. It seems that some NA mixtures do not fit the general formula $C_nH_{2n+z}O_2$.

Further work need to be carry to better understand the differences in the composition of NAs and the influences on aquatic toxicity. To date, the fate of these compounds and the role they play in NAs toxicity is not known.

Table 1. Chemical and Physical Properties of NAs (Whitby, 2010)

Parameter/property	General Description
Colour	Freshly distilled NAs are colourless, but storage of refined NAs leads to development of colours from dark red to bright or pale yellow, dark amber, yellowish brown and black
Odour	Freshly distilled NAs are odorless but storage heads to development of odour from the presence of phenol and sulfur impurities
State	Viscous liquid
Viscosity at 40 °C	40 – 100 mPa s. (depending on grade of oil)
Solubility	Completely soluble in vegetable and mineral oils and all organic solvents at room temp. Soluble in water at alkaline or neutral pH <50 mg/L
Molecular weight	Generally between 140 and 450 amu
Boiling Point	250 – 350 °C
Dissociation constant, pKa	5 - 6
Refractive index	≈ 1.5
Log Kow (octanol water partition coefficient)	≈ 4 at pH 1, ≈ 2.4 at pH 7, ≈ 2 at pH 10
Density	0.97 – 0.99 g/cm^3
Specific gravity at 20°C	0.95 – 0.98
% of phenolic compounds by weight	0.05 – 15
% of unsaponifiables by weight	1 - 20

Note: Values vary greatly with NA source and composition between freshly distilled and stored or aged compounds.

NAPHTHENIC ACIDS IN THE ENVIRONMENT AND THE EXTRACTION PROCESS

Naphthenic acids are natural constituents of oil sands ore. They can represent up to 50% by weight of the total acidic proportion in crude oil (Headley et al., 2004). In the aquatic environment, NAs occur in low concentration in the environment. NAs concentrations measured in Northern Alberta rivers near Fort McMurray are generally below 1 mg/L. In the same area, the concentration of NAs in natural groundwater ranged between <4 mg/L in near-surface and >55 mg/L in basal and limestone aquifers (CEATAG, 1998). The introduction of NAs into the aquatic environment may occur directly by contact with crude oil, a spill, or effluent released into the surface and ground water system. On the other hand, rivers have over time naturally carved valleys through oil sands deposits (Figure 2). Therefore, due to water-solubility of the NAs at neutral condition, NAs (as naphenates) are mobilised into the environment.

In order to extract the bitumen contained in oil sands material, oil sands mining use a large amount of alkaline hot water. During this process, naphthenic acids and other acidic compounds, readily dissolved in the caustic extraction water, are solubilised and removed from the crude oil (Brient, 1995). The extraction process produces large volumes of wastewater, fine tails, and non-recovered bitumen which, under the zero discharge policy, have to be stored in large settling ponds. Concentration in tailings waters was measured as high as 110 mg/L (CEATAG, 1998).

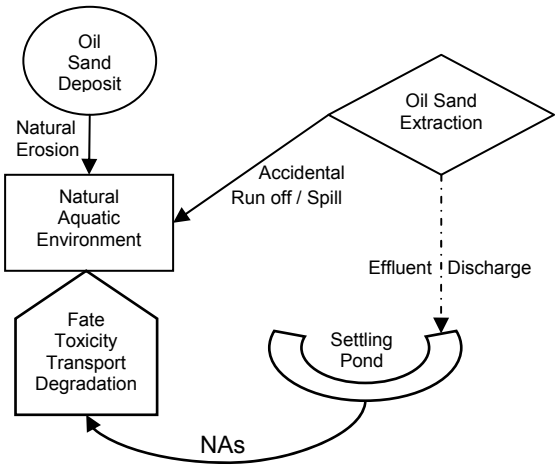

Figure 2. NAs introduction into the environment

The accumulation of effluent containing high concentrations of NAs in settling ponds in Canada is a great concern for the oil sands extraction industry. At operation shutdown, reclamation of the settling ponds into viable terrestrial and aquatic systems, with NAs concentration below toxic levels, will have to be conducted by the industry. Therefore, research regarding the toxicology, fate, transport and degradation of residual levels of NAs has been conducted to address this concern, as well as development of efficient analytical methods to determine concentrations in water, soil, sediment, and exposed species such as fish or plants.

AQUATIC TOXICITY OF NAPHTHENIC ACIDS

NAs are recognised as one of the most toxic compounds in oil sands water extraction and refinery tailings effluents (Clemente and Fedorak, 2005). Toxicity regarding these organic compounds is related to their mixture content, its complexity and physico-chemical properties in the medium analysed. Oil sands deposits, formed by biodegradation of mature petroleum, are composed of hundreds of different compounds, and each deposit has a composition to some extent different from another. Therefore, concentration, contents and complexity of NAs, solubilised during the bitumen extraction from a particular deposit, may be dissimilar from another source.

NAs surfactants qualities and moderate water-solubility at neutral or alkaline pH exposes aquatic organisms to the toxic effects of dissolved NAs (as naphthenates). In this paper, recent acute, chronic and bioaccumulation testing with NAs compounds, both naturally occurring and commercially prepared, are presented as well as the influence of environmental parameters, molecular weight, and aging process on NAs toxicity. The following toxicity data presents a summary of aquatic toxicity studies from oil sands tailings effluents or commercial preparations from many different sources tested in the lab or field, and therefore, it is not possible to distinguish which of the specific NAs contribute the most to the toxicity.

Acute Toxicity

Usually, pollutant's toxicity is preliminarily measured by conducting bioassays for acute toxicity. In the present review, all studies reported have not been conducted using bioassays tested according to standard guidelines (i.e. OECD, EC, ASTM, USEPA) to characterise the toxicity of NAs. However, the American Petroleum Institute Petroleum HPV Testing Group intends to conduct OECD 203 Fish Acute Toxicity Tests, 202 Daphnia sp. Acute Immobilisation Tests and 201 Alga Growth Inhibition Tests.

Available older acute toxicity data shows that naphthenic acids are moderately to highly toxic to fish (ranging from 2.5 to 75 mg/L (Table 2), zooplankton and luminescent bacteria (Table 3).

The augmentation of oil sands mining sites and therefore the number of settling ponds increases the occurrence of measuring NAs and other hydrocarbon compounds in the aquatic environment. Even a low level concentration of NAs can result in stress and toxic effects for fish and other aquatic organisms.

NAs are described as complex mixtures of low to high molecular weight (MW) compounds, thus recent studies looked into the role of different NAs

fraction on toxicity. Holowenko et al. (2002) confirmed that the composition of NAs affects the toxicity. NAs toxicity is not directly correlated to the concentration of NAs but to the contents and the complexity of the mixture (CEATAG, 1998). However, toxicity decreases with NAs concentration.

Frank et al. (2008a) designed a study to fractionate an NA extract mixture by MW to assess each fraction's toxicity. Fractions were separated by Kugelrohr distillation, in which fractions collected at higher boiling points contained NAs of greater carbon content as well as a greater degree of cyclicity. Microtox® assays showed that the lowest molecular weight NAs had higher toxicity (EC50: 41.9 ± 2.8 mg/L) than the highest MW NAs collected (EC50: 64.9 ± 7.4 mg/L). Although these results seem to support field observations of microbial degradation of low MW NAs decreasing OSPW toxicity (Holowenko, 2002), it was unclear why larger NAs, presumably with greater hydrophobicity, would be less toxic.

Further studies by Frank et al. (2008b) analysed the isolated NA fractions by proton NMR. The analysis revealed that an increase in molecular weight of NAs correlated with an increase in carboxylic acid content. Acute toxicity bioassays were conducted where *Daphnia magna* were exposed to mono- and dicarboxyl NA-like surrogates. Among surrogates with a single carboxylic acid group, increasing molecular weight resulted in an increase in toxicity (LC50s: 10 ± 1.3 mM and 0.59 ± 0.20 mM for the respective lowest and highest MW NA-like surrogates).

Table 2. Fish acute testing reported before 2000

Fish name	Species name	Endpoint	Results	Reference
Zebra fish	*Brachydanio rerio*	96h TLm	16.3 mg/L	Cairns et al. 1965
Zebra fish embryo	*Brachydanio rerio*	48h TLm	3.5 mg/L	Cairns et al. 1965
Three spine stickleback	*Gasterosteus aculeatus*	96h LC50	2.5 - 5 mg/L	Dorn 1992
Chum salmon	*Oncorhynchus keta*	10d LC50	25 mg NA/L	Dokholyan & Magomedov 1983
Kutum	*Rutilus frisii kutum*	10d LC50	50 mg NA/L	Dokholyan & Magomedov 1983
Young Roach	*Rutilus rutilus caspicus*	10d LC50	50 mg NA/L	Dokholyan & Magomedov 1983
Sturgeon	*Acipenser gueldenstaedti*	10d LC50	50 mg NA/L	Dokholyan & Magomedov 1983
Adult Roach	*Rutilus rutilus caspicus*	10d LC50	75 mg NA/L	Dokholyan & Magomedov 1983
Caspian round goby	*Neogobius melanostomus*	10d LC50	75 mg NA/L	Dokholyan & Magomedov 1983
Rainbow trout	*Oncorhynchus mykiss*	96h LC50	7% v/v OSPW	MacKinnon & Boerger 1986

Table 3. Other acute aquatic testing reported

Organism	Species name	Endpoint	Results	Reference
Bacteria (Microtox®)	*Vibrio fischeri*	5 or 15 min IC50	5 mg NA/L	Clemente et al. 2004
Bacteria (Microtox®)	*Vibrio fischeri*	15 min IC50	20 - 30% v/v OSPW	MacKinnon & Boerger 1986
Bacteria (Microtox®)	*Vibrio fischeri*	15 min IC20	10% v/v OSPW	MacKinnon & Boerger 1986
Algae (Diatom)	*Navicula seminulum*	96h LC50	26.0 – 80.5 mg/L	Academy of Natural Sciences 1960
Zooplankton	*Nephargoides maeoticus*	MAC	0.15 mg NA/L	Dokholyan & Magomedov 1984
Zooplankton	*Daphnia magna*	48h LC50	2% v/v OSPW	MacKinnon & Boerger 1986

Sublethal and Chronic Toxicity

However, with the addition of a second carboxylic acid group to the same NA-like surrogates, the toxicity was significantly reduced (LC50s: 10 ± 1.3mM and 27 ± 2.2mM for the respective monocarboxyl and dicarboxyl NA-like surrogates of similar MW). As the addition of carboxylic acid groups decreases the hydrophobicity of the NAs, and higher MW NAs were found to have higher carboxylic acid content, this may offer an explanation as to which lower molecular weight NAs in OSPW have been found to be more toxic. Recently, several studies were conducted to evaluate NAs sublethal and/or chronic toxicity. Those studies measured long-term effects related to changes such as metabolism, growth, reproduction success or survival. Several early life stage or chronic toxicity studies were conducted with fish and amphibians to understand and document the long-term effects of OSPW and sediment.

Peters et al. 2007 conducted early life stage bioassays with yellow perch and Japanese medaka to either MLSB water or Na-NA standards. The purified Na-NA standards were found to be more toxic to fish than native OSPW. Perch were consistently more sensitive than medaka in the frequency of deformity and larval length endpoints. Yellow perch showed no fertilization success (100% conc.), optic-cephalic abnormalities and spinal deformities. A concentration response was observed in the frequency of deformed perch embryos in both treatments. Japanese medaka embryos showed developmental problems with early heart formation. Many of the deformities observed for medaka were associated with the circulatory system and osmoregulation. Other signs of arrested development were associated with yolk sac assimilation and edema.

A similar early life stage study using early life stages fathead minnow and white sucker exposed to OSPW shows larval malformations effects including edemas, hemorrhages, and skeletal, craniofacial and eye defects (Colavecchia et al., 2007). Oil sands were two fold more toxic to fathead minnows (TPAH LC50 = 47-330 µg/g) than to white sucker (TPAH LC50 = 95-860 µg/g) larvae.

OSPW have the potential to disrupt the normal endocrine functioning in exposed fish through alterations to both reproductive and glucocorticoid hormone biosynthesis. Sex hormones (testosterone and estradiol) levels in the plasma were significantly reduced in both males and female goldfish. Reduction of sex hormone levels in females seemed to be greater than in males (Lister et al. 2008). Reductions in sex hormone levels could have impacts on fish fecundity.

White sucker were exposed to oil sands sediments during early life stages showed significant premature hatching, reduced growth, and malformations. Most common larval deformities included edemas (pericardial, yolk sac, and subepidermal) hemorrhages, and spinal defects (Colavecchia et al. 2006).

Since the oil sands industry will have to reclaim all settling ponds to a natural aquatic ecosystem, amphibians will also be exposed to NAs. Pollet (2000) exposed Boreal toad (*Bufo boreas*) and wood frog (*Rana sylvatica*) tadpoles to OSPW representative of a range of effluents expected to occur on oil sands lease sites at mine closure. Endpoints evaluated included survival, growth, development and frequency of deformities. The *B. boreas* tadpoles displayed significantly reduced growth and prolonged developmental time compared to controls, and *R. sylvatica* showed decreased survival and reduced rates of growth when exposed to process waters. One strain of *R. sylvatica* was highly sensitive and displayed no growth and poor survival in all exposures, suggesting different tolerances among amphibian populations. Based on this study it was concluded that wetlands formed from oil sands effluent will not support viable amphibian populations.

Bioaccumulation Potential

Chronic fish studies demonstrate that exposure to OSPW or settling pond sediment significantly influences larval survival, fertilization, development and biochemical responses in fish and amphibians. In addition, OSPW has the potential to taint fish flesh giving the flesh off-odor or off-flavour. A study by Koning and Hrudey (1992) showed that fish exposed to OSPW for 24h were tainted after judgment by a sensory panel, evidence of accumulation of OSPW components in the flesh of the fish.

In fact, tissue concentration can be the result of water or feed exposure. Hellou et al. (1989) investigated the metabolism of two small commercially produced naphthenic hydrocarbons (n-butylcyclohexane and t-butylcyclohexane) in rainbow trout. This study showed that trout will

conjugate naphthenic acids to glucuronide metabolites which can be determined in the bile of exposed fish. This study reveals that naphthenic acids can be absrobed, metabolised, and excreted by fish. Therefore, fish are unlikely to biomagnify small NAs as they can be metabolised and excreted. However, larger and more complex NAs were not studied. Development of further analytical techniques could help to evaluate NAa exposure by measuring metabolites in fish bile. as described by Hellou et al. (1989). This research would also help to address the potential for bioaccumulation of larger molecular weight NAs in fish.

Although studies cited in this paper demonstrate that NAs have various lethal and sublethal effects on fish and other aquatic organisms, until recently there has been no analytical method developed to specifically measure NAs accumulation in fish tissue.

Development of a new quantitative analytical method helped to examine the bioaccumulation of potential NAs in fish. Young et al. (2007) conducted 96h static renewal tests with rainbow trout fry exposed to three different treatments: 1) fed with pellets containing 1.5 mg NA/g food, 2) water exposure containing 3 mg NA/L and 3) OSPW exposure containing 15 mg NA/L. Samples of fish were homogenised and extracted and the mixture of free fatty acids and naphthenic acids were isolated from the extract using strong anion exchange chromatography. After this clean up, the extract was analysed by GC/MS. Each type of treatment revealed concentrations of NAs in fish tissue except fish not exposed to NAs. The minimum detectable concentration was approximately 1 mg NA/kg of fish tissue.

More recently, a newly developed analytical method using GC/MS-SIM to measure NAs in fish has been developed with a lower detection limit of 0.1 mg/kg of fish flesh (Young et al., 2008). The analytical method was used to measure uptake and depuration of commercial NAs in laboratory experiments. Rainbow trout were exposed to 3 mg NA/L for 9 days. The mean concentration of NAs in fish exposed from days 2 to 9 (when fish were at equilibrium) was 5.6 ± 1.9 mg/kg. A BCF of approximately 2 was estimated at pH 8.2. Within 1d after the fish were transferred to freshwater, about 95% of the NAs were depurated. The concentration of NAs dropped to 0.3 ± 0.3 mg/kg. The analytical method was also used to determine if NAs were present in four species of wild fish. Northern pike (*Esox lucius*), lake whitefish (*Coregonus clupeaformis*), white sucker, (*Catostomus commersoni*), and walleye (*Sander vitreus*) were collected in waters near oils ands. Flesh samples from 23 wild fish were analysed and 18 had no detectable NAs. Four fish contained NAs at concentrations from 0.2 to 2.8 mg/kg. These studies suggest that NA have a relatively low bioaccumulation potential in fish.

Mode of Toxicity

The presence of hydrophobic alkyl groups and a hydrophilic carboxylic moiety suggests that the sodium salts of NAs are surfactants. Observed acute toxicities for NA-like surrogates to aquatic organisms rose with increasing MW (hydrophobicity) and decreased with greater carboxylic acid content. Because of the lack of functional groups that would be expected to target a specific receptor, the solubility of NAs in OSPW as ionic salts, and the surfactant properties of NAs, the probable mode of acute toxic action for NAs is narcosis (Frank et al., 2008a & 2010). Narcosis is a nonspecific mode of toxic action in which a hydrophobic compound permeates the lipid bilayer of a cell disrupting membrane function including surface tension, fluidity and thickness and ultimately produces cell death.

Factors influencing NAs toxicity

On site, settling ponds are exposed to environmental conditions which can modify pH, salinity, temperature and degradation of the NAs. These changes can either affect the compound's properties, and therefore its bioavailability and toxicity, or affect the organism's metabolism, and thus the uptake of the compound.

At pH 8.2 (e.g.: Athabasca River), only 0.63% of NAs (pKa 6) exist in their protonated form. Thus, over 99% of the acids exist as soluble naphthenates (Young et al., 2008). Therefore, acidification of the tailings ponds, which increases the NAs adsorption onto the sediment, decreases their bioavailability in the water, and reduces OSPW toxicity measured by Microtox® (MacKinnon and Boerger, 1986).

Since sodium and sulfate levels are elevated in OSPW due to ions leaching during the water extraction process of the bitumen, Nero et al. (2006) investigated the effects of salinity as a modifying factor for the toxicity of NAs using young yellow perch. Different mixtures of NAs (commercial (CNAs) vs. extracted from OSWP

(ENAs)) were examined to determine if differences in NA composition affected gill and liver endpoints. Exposure to NAs resulted in 100% mortality to perch in ≤96 h at the highest test concentrations (CNAs 3.6 mg/L, ENAs 6.8 mg/L). Addition of $NaSO_4$ reduced toxicity at lower concentrations of NAs. Acute toxicity of CNAs (80% mortality) was higher than ENAs (0% mortality) at lower concentrations (1.8 mg CNA/L, 1.7 mg ENA/L). The study confirms that young yellow perch were highly sensitive to NAs exposure. Yellow perch exposed to NAs (commercial or extracted) and salt showed a high level of gill proliferative alterations in the form of epithelial chloride and mucous cell proliferations. Changes had significant impacts on gill surface area, which may have consequences for gas exchange and NAs uptake. Liver damage was observed associated with degenerative and inflammatory alterations. Salt may have had some effect on response to NAs depending on the chemical composition of the NAs.

DEGRADATION

Several laboratory and field studies have been conducted on the biodegradation of surrogate naphthenic acids (those that fit the formula $C_nH_{2n+z}O_2$), commercially available naphthenic acids, and naphthenic acids in waste waters. NAs are often investigated as a group or mixture, as analytical methods did not typically allow for individual compounds to be identified due to the group's complex nature.

Due to the moderate water solubility (up to 50 mg/L), NAs should partition to the water column and be available to micro-organisms for degradation. However, as a group, NAs have been identified as persistent biomarkers and weakly degradable (McMartin et al., 2004).

Biodegradation

Generally, biodegradation of NAs is an aerobic process; however, anaerobic biodegradation has been identified in deep subsurface reservoirs (Aitken et al., 2004; Boll et al., 2002; Jones et al. 2008; Larter, 2003; Widdel and Rabus, 2001). Research has shown that NAs can be metabolised by microbes in a manner similar to hydrocarbons. Microbes indigenous to oil sands tailings are capable of degrading complex mixtures of commercial sodium salts of naphthenic acids, as well as mixtures of organic acids extracted from oil sands tailings (Herman et al., 1993, 1994). Several different micro-organisms, including *Acinetobacter anitratum, Alcaligenes faecalis*, and *Pseudomonas putida*, have been shown to metabolise model NAs by aerobic β oxidation pathways, which involve the formation of a new carboxylic acid with two carbons fewer than its predecessor (Whitby, 2010). Of the studies reviewed, degradation of NAs was observed primarily via microbial degradation (in water and sediment). Microbial populations respond to NA substrates through increased CO_2 production (mineralisation), O_2 consumption, and enhancement of metabolism with the addition of nutrients. In one study, commercial preparations of NAs were shown to be degraded in aerobic cultures from OSPW. NA concentrations dropped from approximately 100 to <10 mg/L, accompanied by a release of about 60% carbon from the NAs as CO_2 in as little as 10 days of incubation. The toxicity of the culture supernatant also reduced as measured by the Microtox® test (Clemente and Fedorak 2004). Similarly, Herman et al. (1994) determined that microbial degradation of a commercial NA converted approximately 50% of the carbon into CO_2. The toxicity of the commercial mixture to *Vibrio fischeri* (Microtox®) was attenuated following degradation. The same study showed that approximately 20% of the organic carbon present in an oil sand tailings (OST) extracted mixture was biodegraded, resulting in a significant reduction in toxicity as measured by the Microtox® assay.

Analysis by GC/MS provided information on the effects of biodegradation on NA mixtures, including changes to their composition and the determination that lower molecular weight (MW) acids (n = 5-13) were degraded more readily than the higher MW acids. Although biodegradation rates of surrogate NAs were relatively rapid in the laboratory, NAs in tailings ponds are more complex and are expected to degrade more slowly in the environment (Clemente and Fedorak 2004).

Field studies monitoring the detoxification of oil sands tailings by natural processes have indicated that the acute toxicity of oil sands tailings is reduced within 1 year, while removal of chronic toxicity requires 2-3 years (Boerger et al. 1992; MacKinnon and Boerger, 1986, 1991).

Little information is available on the effects of NAs on biofilm structure and actual transformation of complex NA mixtures. Lake biofilms are complex community structures of diverse microbial species that obtain nutrient and energy supplies from passing water and play a major role in the carbon

cycling in natural waters (Wetzel 1993). Headley et al. (2010), examined the dissipation (combined sorption and biodegradation) of NAs by lake biofilms using rotating annular bioreactors. Dissipation rates were dependent on the NA mixture composition and a combination of factors indentified including molecular structure, molecular mass and inhibition by some components containing S and/ or N acids).

Environmental conditions were also examined (Lai et al. 1996) as factors that affect the biodegradation rate of NAs. The effects of temperature, dissolved oxygen concentration and phosphate addition on the rate of CO_2 released from two NA surrogates were monitored. Tailings pond water micro-organisms were used to examine the degradation of representative mono- and dicyclic NA surrogates. The results of this study found that the monocyclic NA was degraded more quickly (10-15% in 4 weeks) than the dicyclic NA surrogate (2-4% in 8 weeks), supporting the observation that NA biodegradation is inversely proportional to the degree of cyclicity (Morales et al. 1993). Addition of phosphate resulted in a twofold increase of NA degradation in the first 4 weeks with an augmentation in O_2 consumption. However, degradation declined to rates equivalent to those without phosphate addition. The observed plateau was not related to phosphate limitation. Decreases in dissolved oxygen concentrations or temperature reduced the rate of biodegradation.

Lab studies showed that natural OSPW-derived NA may not degrade in laboratory experiments under the same conditions as commercially available NA. Therefore caution must be taken when comparing biodegradation studies with commercial NA to native NA mixtures (Headley et al. 2010).

Photolysis

Studies using photolysis have also been conducted to determine the efficacy of a variety of UV/vis radiation sources for reducing the concentration of NAs as well as the aryl hydrocarbon (Ah) receptor binding as a measure of potential toxicity. Photolysis at UV_{254} was the most effective radiation source for affecting mixture composition although the concentration of the compounds studied was not significantly reduced in river water. Interferences such as humic acids and other organic substances potentially absorb light thereby reducing the effect of light on the NAs. In general, natural and artificial sunlight are not efficient at reducing the range of NA compounds or mixtures in a relatively clear natural water source. It is anticipated that photolysis by natural means in coloured tailings ponds will be negligible and will neither affect the concentration nor the toxicity of NAs. However, incorporation of photolytic treatment at UV_{254} may reduce the concentration of some NA and may reduce overall aquatic toxicity based on the Ah receptor assay (McMartin et al., 2004).

Phytoremediation

Two naphthenic acids mixtures (extracted from tailings pond water and commercial) were compared to examine the removal of NA by aquatic macrophytes cattail, *Typha latifolia*; common reed, *Phragmites australis*; and hard stem bulrush, *Scirpus acutus* (Armstrong et al. 2008). It was observed that the oil sands extracted mixture was less phytotoxic to the wetland plants than the commercial mixture. But that the commercial mixture was sequestered by plants to a larger degree than the oil sands extracted mixture. Certain NAs were sequestered more than others. Two ring NAs with a carbon number ranging from 12 to 15 displayed the greatest loss of abundance, whereas some NAs, carbon number 16 to 18 increased in abundance of non-cyclic straight chained or branched NAs. Changes in different forms of NAs was masked when looking at total NA concentrations. Dissipation of NA in the medium may have been due to adsorption or metabolism by root associated micro-organisms but the exact mechanism of loss is unknown. Cattail was the most sensitive plant species that showed altered water uptake after 10 days of exposure. The common reed was the most tolerant species tested particularly to low NA concentrations (30 mg NA/L). The common reed had the highest dissipation of NAs of the planted treatments exposed to (60 mg NA/L). Commercial NAs have a lower mass range of components (157 – 297 m/z) compared to the oil sands NAs (195 – 325 m/z) from the Athabasca Basin. The lower molecular weight NAs appeared to be more phytotoxic than the higher MW NAs. It may be inferred that lower MW NAs are able to dissipate from hydroponic medium in the presence of plants either through adsorption or absorption into plant roots. The results of the study indicate that plants alone may not mitigate NAs from OSPW tailing ponds. In addition caution should be taken when comparing the toxicity and environmental fate of commercial NA mixtures with NAs present in OSPW.

Aging process

The maturation or aging process occurring in a tailings pond can affect NAs properties and toxicity. Field studies have demonstrated that the acute toxicity of OSPW decreases when effluent has been allowed to degrade in tailings ponds for 1 to 24 months (MacKinnon and Boerger, 1986 and Lai et al., 1986).

More recently, Hersikorn et al. (2010), performed in situ tests on wood frog tadpoles in wet landscape wetlands containing oil sands tailings of various ages. Tadpoles in wetlands exposed to young OSPM (Oil Sands Process-affected Materials) showed the lowest survival, but when exposed to old OSPM, tadpole survival was similar to young and old reference wetlands. Therefore, toxicity from OSPM diminishes over time, and aged OSPM may support amphibian populations. It was unclear which components of OSPM were causing the toxic effects (NAs, PAH, etc.). Another study, comparing the effect of OSPW and mature tailings, suggested that fathead minnows could survive and grow in matured fine tailings (MFT) oil sands processed water (Siwik et al., 2000). Most importantly, MFT may have a synergistic effect on growth during short periods of early growth, suggesting that fish may not show significant adverse effects in mature fine tailings OSPW. In addition, NAs and other toxic agents may be less toxic or may have degraded over time in these aged waters.

A study suggested that the oldest water from experimental reclamation ponds contains more oxidised NAs species than parent NAs on average, suggesting that NAs are slowly degraded by hydroxylation. It is also possible that oxidised NA species are more persistent than parent NAs and their relative concentrations increase as the concentration of parent NAs declines. NAs with lower carbon numbers may partition faster into the atmosphere, thus some loss of lower MW NAs may not be through biodegradation but through partitioning (Han et al. 2009).

Lo et al. (2006) determined fractions with higher proportions of multi-ring structures exhibited lower toxicity. It was proposed that multi-ring structures are more highly branched and therefore more resistant to microbial degradation. Conversely, Clemente and Fedorak (2005) and Toor et al. (2008) found NAs with lower molecular weights and fewer rings may be more susceptible to biodegradation. This causes a reduction in the acute toxicity of tailings water, yet some chronic toxicity remains and is thought to be due to remaining NAs with high molecular weight and more ring structures.

CONCLUSION

Recent research has confirmed that NAs is highly toxic to aquatic organisms. Extracted from the bitumen or commercially produced, these compounds have shown harmful acute, sublethal, and chronic biological effects. Sublethal and chronic fish studies demonstrate that exposure to OSPW or settling pond sediment significantly influences larval growth, survival, fertilisation, development (circulatory, deformity, etc) and hormone production in fish and amphibians. The application of some of state-of-the-art methods has demonstrated the potential of bioaccumulation of NAs, and its excretion mode by fish. Several studies suggested that NAs fractions with different MW have dissimilar toxicity. Bioassays with the NA-like surrogates indicated that toxicity was likely a function of hydrophobicity, with the probable mode of toxicity being narcosis. Biodegradation can change the composition of the NA mixture and in general, lower MW acids and those with the lowest number of rings degrade more readily than the higher MW acids. This causes a reduction in the acute toxicity of tailings water, yet some chronic toxicity remains and is thought to be due to remaining NAs with high molecular weight and more ring structures. Further studies to fully characterize the toxicity associated to each NAs fraction and to examine toxicity to other species such as invertebrates and fish are continuing as researchers investigate the environmental fate and effects of NAs and OSPW.

REFERENCES

Aitken, C. M., Jones, D. M., and Larter, S. R. 2004. Anaerobic hydrocarbon biodegradation in deep subsurface oil reservoirs. Nature, 431: 291-294.

American Petroleum Institute Petroleum HPV Testing Group 2003. Test Plan for Reclaimed Substances: Streams containing Naphthenic acids, phenolics disulfides acids or caustics. Consortium Registration # 1100997: 22 p.

Armstrong, S. A., Headley, J. V., Peru, K. M. and Germida, J. J. 2008. Phytotoxicity of oil sands

naphthenic acids and dissipation from systems planted with emergent aquatic macrophytes. Journal of Environmental Science and Health, Part A, 43: 1, 36-42.

Boerger, H., MacKinnon, M., van Meer, T., and Verbeek, A. 1992. Wet landscape option for reclamation of fine tails. Environmental Issues and Waste Management in Energy and Minerals Production – Proceedings of Second International Conference on Environmental Issues and Management of Waste in Energy and Minerals Production, Calgary, Alta., pp. 1249-1261.

Boll, M., Fuchs, G., and Heider, J. 2002. Anaerobic oxidation of aromatic compounds and hydrocarbons. Current Opinion in Chemical Biology, 6: 604–611.

Brient, J.A., Wessner, P.J., Doyle, M.N. Naphthenic acids. In Kirk-Othmer Encyclopaedia of Chemical Technology, 4th Ed.; Kroschwitz, J.I., Ed.; John Wiley and Sons: New York, NY, 1995; 1017–1029.

Clemente, J. S., Fedorak, P. M. 2005. A review of the occurrence, analyses, toxicity, and biodegradation of naphthenic acids. Chemosphere, 60: 585–600.

Clemente, J.S., MacKinnon, M.D. and Fedorak, P.M. 2004. Aerobic biodegradation of two commercial naphthenic acids preparations. Environmental Science & Technology, 38: 4, 1009-1016.

Clemente, J.S.; Prasad, N.G.N.; MacKinnon, M.D.; Fedorak, P.M., 2003. A statistical comparison of naphthenic acids characterized by gas chromatography–mass spectrometry. Chemosphere 50: 1265-1274.

Colavecchia, M.V., Hodson, P.V. and Parrott, J.L. 2006. CYP1A induction and Blue Sac disease in early life stages of white suckers (*Catostomus commersoni*) Exposed to Oil Sands. Journal of Toxicology and Environmental Health, Part A, 69: 10, 967-994.

Colavecchia, M.V., Hodson, P.V. and Parrott, J.L. 2007. The Relationships among CYP1A induction, toxicity, and eye pathology in early life stages of fish exposed to oil sands. Journal of Toxicology and Environmental Health, Part A, 70: 18, 1542-1555.

Conrad Environmental Aquatics Technical Advisory Group (CEATAG) 1998. Naphthenic Acids Background Information Discussion Report; Alberta Department of Energy: Edmonton, AB, Canada,.

Dokholyan, B.K. and Magomedov, A.K. 1983. Effect of sodium naphthenate on survival and some physiological-biochemical parameters of some fishes. Journal of Ichthyology, 23: 6, 125-132.

Frank, R.A., Kavanagh, R., Burnison, B.K., Arsenault, G., Headley, J.V., Peru, K.M., Van Der Kraak, G., Solomon, K.R. 2008a. Toxicity assessment of collected fractions from an extracted naphthenic acid mixture. Chemosphere, 72: 1309-1314.

Frank, R.A., Fischer, K., Kavanagh, R., Burnison, B.K., Arsenault, G., Headley, J.V., Peru, K.M., Van Der Kraak, G. and Solomon, K.R. 2008b. Effect of carboxylic acid content on the acute toxicity of oil sands naphthenic acids. Environmental Science & Technology, 43: 2, 266-271.

Frank, R. A., Sanderson, H., Kavanagh, R., Burnison, B.K., Headley, J.V. and Solomon, K.R. 2010. Use of a (Quantitative) Structure-Activity Relationship [(Q)Sar] Model to Predict the Toxicity of Naphthenic Acids. Journal of Toxicology and Environmental Health, Part A, 73: 4, 319-329.

Han, X., MacKinnon, M.D., Martin, J.V. 2009. Estimating the *in situ* biodegradation of naphthenic acids in oil sands process waters by HPLC/HRMS. Chemosphere, 76: 63-70.

Headley, J.V. and McMartin, D.W. 2004. A review of the occurrence and fate of naphthenic acids in aquatic environments. Journal of Environmental Science and Health, Part A, 39: 8, 1989-2010.

Headley, J.V., Peru, K.M., Adenugba, A.A., Du, J. and Mcmartin, D.W. 2010. Dissipation of naphthenic acids mixtures by lake biofilms. Journal of Environmental Science and Health, Part A, 45: 9, 1027-1036.

Hellou, J., Banoub, J.H. and Ryan, A. 1989. Fate of naphthenic hydrocarbons in the bile of rainbow trout (*Salmo gairdneri*). Environmental Toxicology and Chemistry, 8: 871-876.

Herman, D.C., Fedorak, P.M., and Costerton, J.W. 1993. Biodegradation of cycloalkane carboxylic acids in oil sand tailings. Canadian Journal of Microbiology, 39: 576–580.

Herman, D.C., Fedorak, P.M., MacKinnon, M.D. and Costerton, J.W. 1994. Biodegradation of naphthenic acids by microbial populations indigenous to oil sands tailings. Canadian Journal Microbiology, 40: 467-477.

Hersikorn, B.D., Ciborowski, J.J.C. and Smits, J.E.G. 2010. The effects of oil sands wetlands on wood frogs (*Rana sylvatica*). Toxicological & Environmental Chemistry, 92: 8, 1513-1527.

Holowenko, F.M., MacKinnon, M.D. and Fedorak, P.M. 2001. Naphthenic acids and surrogate naphthenic acids in methanogenic microcosms. Water Research, 35: 11, 2595–2606.

Holowenko, F.M., MacKinnon, M.D., Fedorak, P.M., 2002. Characterization of naphthenic acids in oil sands wastewaters by gas chromatography–mass spectrometry. Water Research 36, 2843–2855.

Hsu, C.S., Dechert, G.J., Robbins, W.K., Fukuda, E.K. 2000. Naphthenic Acids in Crude Oils Characterized by Mass Spectrometry. Energy Fuels, 14: 217-223.

Jones, D.M., Head, I.M., Gray, N.D., Adams, J.J., Rowan, A.K., Aitken, C.M., Bennett, B., Huang, H., Brown, A., Bowler, B.F.J., Oldenburg, T., Erdmann, M., et al., 2008. Crude-oil biodegradation via methanogenesis in petroleum subsurface reservoirs. Nature, 451: 176-180.

Koning, C.W. and Hrudey, S.E. 1992. Sensory and Chemical Characterization of Fish Tainted by Exposure to Oil Sand Wastewaters. Water Science Technology, 25: 2, 27–34.

Lai, J.W.S., Pinto, L.J., Kiehlmann, E., Bendell-Young, L.I. and Moore, M. M. 1996. Factors that affect the degradation of naphthenic acids in oil sands wastewater by indigenous microbial communities. Environmental Toxicology and Chemistry, 15: 9, 1482-1491.

Larter, S.R. 2003. The controls on the composition of biodegraded oils in the deep subsurface. Part 1: Biodegradation rates in petroleum reservoirs. Organic Geochemistry, 34: 601–613.

Lister, A., Nero, V., Farwell, A., Dixon, D.G., Van Der Kraak, G. 2008. Reproductive and stress hormone levels in goldfish (*Carassius auratus*) exposed to oil sands process-affected water. Aquatic Toxicology, 87: 170-177.

Lo, C.C., Brownlee, B.G., Bunce, N.J. 2006. Mass spectrometric and toxicological assays of Athabasca oil sands naphthenic acids. Water Research, 40: 655-664.

MacKinnon, M., and Boerger, H. 1986. Description of two treatments for detoxifying oil sands tailings pond water. Water Pollution Research Journal of Canada, 21: 496-512.

MacKinnon, M.D., and Boerger, H. 1991. Assessment of a wet landscape option for disposal of fine tails sludge from oil sands processing. Proceedings of the Petroleum Society of CIM and AOSTRA 1991 Technical Conference, Banff, Alta., April 21-24, 1991. Alberta Oil Sands Technology and Research Authority (AOSTRA), Edmonton, Alta. AOSTRA-CIM Pap., No. 9 1-124.

McMartin, D.W., Headley, J.V., Friesen, D.A., Peru, K.M. and Gillies, J.A. 2004. Photolysis of naphthenic acids in natural surface water. Journal of Environmental Science and Health, Part A, 39: 6, 1361-1383.

Merlin, M., Guigard, S.E., Fedorak, P.M. 2007. Detecting naphthenic acids in waters by gas chromatography–mass spectrometry. Journal of Chromatography A, 1140: 225–229.

Morales, A., Hrudey, S.E. and Fedorak, P.M. 1993. Mass spectrometric characterization of naphthenic acids in oil sands wastewaters. Analysis of biodegradation and environmental significance. Edmonton AB: Alberta Department of Energy, Oil Sands Research Division.

Nero, V., Farwell, A. Lee, L.E.J, Van Meer, T., MacKinnon, M.D., Dixon, D.G. 2006. The effects of salinity on naphthenic acid toxicity to yellow perch: Gill and liver histopathology. Ecotoxicology and Environmental Safety, 65: 252-264.

Peters, L. A., MacKinnon, M., Van Meer, T., van den Heuveld, M. R., Dixon, D. G. 2007. Effects of oil sands process-affected waters and naphthenic acids on yellow perch (*Perca*

flavescens) and Japanese medaka (*Orizias latipes*) embryonic development. Chemosphere, 67: 2177-2183.

Pollet, I. and Bendell-Young, L.I. 2000. Amphibians as indicators of wetland quality in wetlands formed from oil sands effluent. Environmental Toxicology and Chemistry, 19: 10, 2589–2597.

Seifert, W.K., Teeter, R.M. 2969. Preparative thin-layer chromatography and high-resolution mass spectrometry of crude oil carboxylic acids. Analytical Chemistry, 41: 786-795.

Siwik, P.L., Vanmeer, T., MacKinnon, M.D. and Paszkowski, C.A. 2000. Growth of fathead minnows in oilsand-processed wastewater in laboratory and field. Environmental Toxicology and Chemistry, 19: 7, 1837-1845.

Toor, N., X., Han, E., Franz, M., MacKinnon, J., Martin, and K. Liber. 2008. Biodegradation of complex naphthenic acid mixtures and a probable link between congener profiles and aquatic toxicity. 35th Annual Aquatic Toxicity Workshop, 5–8 October 2008, Saskatoon, SK, Canada.

EPIWIN (software) U.S. Environmental Protection Agency for EPI Suite™. 2000 – 2009

Wetzel, R.G. 1993. Microcommunities and microgradients: linking nutrient regeneration, microbial mutualism, and high sustained aquatic primary production. Netherlands Journal of Aquatic Ecology, 27: 3–9.

Whitby, C. 2010. Microbial naphthenic acid degradation. Advances in Applied Microbiology, 70: 93-125.

Widdel, F., and Rabus, R. 2001. Anaerobic biodegradation of saturated and aromatic hydrocarbons. Current Opinion in Biotechnology, 12: 259–276.

Young, R.F., Orr, E.A., Goss, G.G., Fedorak, P.M. 2007. Detection of naphthenic acids in fish exposed to commercial naphthenic acids and oil sands process-affected water. Chemosphere, 68: 518-527.

Young, R.F., Wismer, W.V., Fedorak, P.M. 2008. Estimating naphthenic acids concentrations in laboratory-exposed fish and in fish from the wild. Chemosphere, 73: 498-505.

ARE "NAPHTHENIC ACIDS" FROM OIL SANDS TAILINGS WATERS REALLY NAPHTHENIC ACIDS?

Phillip M. Fedorak[1], David M. Grewer[1,2], Rozlyn F. Young[1], Randy M. Whittal[2]
[1]Department of Biological Sciences, University of Alberta, Edmonton, Alberta, Canada
[2]Department of Chemistry, University of Alberta, Edmonton, Alberta, Canada

ABSTRACT

About 30 years ago, researchers reported that the acute toxicity of oil sands tailings waters was associated with the acid-extractable organics from these waters. Because the Fourier transform infrared (FTIR) spectra of these extracts were similar to the spectra of commercially available naphthenic acids, these extracted compounds have been referred to as "naphthenic acids". It is widely agreed that naphthenic acids have the general formula $C_nH_{2n+Z}O_2$. Using state-of-the-art ultrahigh resolution electrospray ionization Fourier transform ion cyclotron resonance mass spectrometry (ESI-FT-ICR MS), we analyzed the acid-extractable organics from seven oil sands tailings waters for ions corresponding to $C_nH_{2n+Z}O_2$, with combinations of n = 8 to 30, and Z = 0 to -12. The mass spectra of these extracts showed between 1300 and 1900 ions, with >99% of the ions having m/z between 145 and 600. Remarkably, only 4.5% to 6.9% of these ions corresponded to naphthenic acids ($C_nH_{2n+Z}O_2$). When the ion abundances in the mass spectra were considered, only 10.7% to 35.6% of the total abundance could be assigned to the naphthenic acids. Thus, >60% of the compounds in the extracts of oil sands tailings waters were not naphthenic acids. Based on these findings, the term "naphthenic acids", which has been used to describe the toxic, acid-extractable compounds in tailings waters, should be replaced by a more general term such as "oil sands tailings water acid-extractable organics". Naphthenic acids are components of the "oil sands tailings water acid-extractable organics", but this term would not be as misleading as "naphthenic acids".

INTRODUCTION

Background

IUPAC recognizes the term "naphthenic acids" and provides the following definition: "acids, chiefly monocarboxylic, derived from naphthenes" (McNaught and Wilkinson, 1997). From the same reference, the definition of naphthenes is "cycloalkanes especially cyclopentane, cyclohexane and their alkyl derivatives." According to McNaught and Wilkinson (1997) both terms seem to be obsolete, except in the petroleum and petrochemical industries.

Naphthenic acids are described by the general formula $C_nH_{2n+Z}O_2$, where n is the number of carbon atoms in the molecule and Z is a negative, even integer that specifies hydrogen deficiency in the case of cyclic naphthenic acids (Brient et al., 1995). In this communication, we refer to these as "classical" naphthenic acids, and examples of some of these are given in Figure 1.

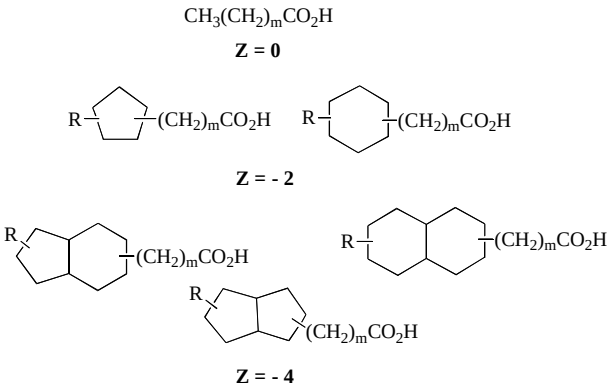

Figure 1. Examples of some classical naphthenic acids structures. R is alkyl, and m is the number of CH_2 units.

Barrow et al. (2009) analyzed naphthenic acids from the oil sands area, and found acids with formula $C_nH_{2n+Z}O_x$, where x = 2 to 5. Similarly, Han et al. (2009) detected mono- and di-oxide naphthenic acids (i.e. $C_nH_{2n+Z}O_3$ and $C_nH_{2n+Z}O_4$) in extracts from Syncrude oil sands process-affected waters (OSPW). Lee (1940) introduced the term "oxy-naphthenic acids" to describe compounds that form after mild oxidation of these acids. We have chosen to use this term to include acids with x = 3, 4, or 5.

OSPW are toxic to a range of organisms (Clemente and Fedorak, 2005), thus these waters

are not intentionally released to receiving waters, but they are retained on-site in accordance with existing policies and practices. MacKinnon and Boerger (1986) reported on two treatments to detoxify oil sands tailings pond water. They wrote "toxicity appears to be due primarily to polar organic carboxylic acids (naphthenic acids)". This seems to be the first time that the term "naphthenic acids" was used to describe the toxic extractable compounds in tailings pond waters. In the early stages of investigating the toxicity of OSPW, it was reasonable to consider the oil sands acid-extractable organics to be naphthenic acids, because there were few analytical methods available to characterize the organic acids.

The Fourier transform infrared (FTIR) spectroscopy method described by Jivraj et al. (1995) has become the oil sands industry standard method for quantifying naphthenic acids in water. Samples are acidified and extracted with dichloromethane (DCM). Then, after concentrating the organic extract, the intensities of the absorbances of the monomeric and dimeric forms of the carboxylic groups (at 1743 and 1706 cm^{-1}, respectively) are measured.

Over the past decade, many reports have focused on the analyses of OSPW by various methods, most of which utilize some form of mass spectrometry to characterize the naphthenic acids (for a review, see Headley et al., 2009). The availability and application of these new techniques have provided a better understanding of the composition of the acid-extractable components in OSPW.

Ultrahigh resolution electrospray ionization Fourier transform ion cyclotron resonance mass spectrometry (ESI-FT-ICR MS), is a powerful method that has been used to study naphthenic acids composition from various sources (Barrow et al., 2010; Scott et al., 2009; Smith et al., 2008). This method has indicated that there is a wide variety of acids in the extracts of OSPW, many of which do not fit the formula of the classical naphthenic acids ($C_nH_{2n+Z}O_2$). The objective of the current study was to use ESI-FT-ICR MS to determine how prevalent the classical naphthenic acids and the oxy-naphthenic acids are in acid extracts of OSPW from various sources.

MATERIALS AND METHODS

Sources and extraction of samples

Seven water samples were used in this study. These included OSPW from Syncrude [Mildred Lake Settling Basin (MLSB); West-in Pit (WIP); and two experimental reclamation ponds: Pond 9 and Demo Pond], from Suncor [Pond 2/3 and Pond 9], and from the Albian Pond.

Water samples were adjusted to pH~10.5 with 2 M NaOH to ensure dissolution of carboxylic acids in the aqueous phase. Subsequent centrifugation of each sample at 10,400 *g* for 20 min removed any particulate matter. The supernatant liquid was then recovered and acidified with concentrated HCl to pH~1.5 in preparation for organic extraction.

FTIR and elemental analyses

The industry standard FTIR spectroscopy method was used to estimate the naphthenic acids concentration in each sample. A 50-mL portion of sample was diluted to 250 mL with water and the pH adjusted to ~1.5 before being extracted three times with 10-mL portions of dichloromethane (DCM), concentrated and analyzed (Scott et al., 2008).

Analyses for C, H, N, S, and O content of the DCM extracts were done using the Carlo Erba EA 1108 elemental analyzer in the Analytical and Instrumentation Laboratory at the University of Alberta (Department of Chemistry).

ESI-FT-ICR MS

In order to determine the content of classical and oxy-naphthenic acids within each OSPW extract, analyses were carried out using ultrahigh resolution ESI-FT-ICR MS. A small amount (<10 mg) of each OSPW sample extract was dissolved in DCM (~1 mg/mL) then diluted 500 to 1000 times in 3:1 methanol:toluene giving a final concentration of about 1 to 2 µg/mL. The samples were analyzed by direct infusion negative ion electrospray on a Bruker 9.4 T Apex-Qe FTICR mass spectrometer (Bruker Daltonics, Billerica, MA) at a flow rate of 2 µL/min. Data were collected over the m/z range of 145 to 2000 with an ion-accumulation time in the external hexapole collision-cell of 10 s prior to injection to the ICR cell using side-kick trapping. Time-domain data sets (4M data points) were summed (16 acquisitions) to enhance signal-to-noise. The spectra were initially

calibrated externally using a mixture of n-C17 and n-C26 saturated carboxylic acids. This calibration was verified at m/z 561 with protoporphyrin IX. After acquisition of each data set, internal calibration was completed using the series of ions containing $C_nH_{2n+Z}O_2$. Mass accuracy across the full mass range was much less than 1 ppm (RMS), with 95% of ions falling within ± 0.02 mDa or 0.1 ppm and up to 99% within ± 0.2 ppm.

Data analyses from the above protocol were then performed using the acquired mass spectra. The data were converted to '.txt' files in the form of mass and abundance lists. Exact masses of acids (m/z = ±0.001) fitting the formula $C_nH_{2n+Z}O_x$, were calculated for all combinations of n = 8 to 30, Z = 0 to -12, and x = 2 to 5 while considering the occurrence of ^{12}C and one occurrence of ^{13}C for each combination of n, Z, and x.

The calculated masses were then tabulated and each individual mass subjected to the 'grep' command line text search utility written for Unix. The 'grep' command searches files for lines matching a given regular expression and prints them in an output file for review. An example of this protocol is as such: |grep '[exact mass]' *.txt|. Exact masses of this form were rounded to two decimal places to avoid losing any mass ions due to rounding errors. The resulting list of raw data was reviewed to find those masses accurate to m/z = ±0.001 and, where occurring, each exact mass and its relative abundance were recorded.

RESULTS AND DISCUSSION

Naphthenic Acids Concentrations and Elemental Analyses

The concentrations of naphthenic acids in the oil sands tailing waters, as determined by FTIR, are given in Table 1. The concentrations ranged between 35 and 63 mg/L in the ponds that receive or recently received fresh tailings (MLSB, WIP, Pond 2/3, Pond 5, and Albian tailings pond). The lowest concentrations of naphthenic acids in oil sands waters were observed in the experimental reclamation ponds at Syncrude, called Demo Pond (also known as Demonstration Pond, SCL 12, and Big Pit) and Pond 9 (also known as SCL 9 and TPW).

The latter two ponds were constructed in 1993 (Siwik et al., 2000; Han et al., 2009). Demo Pond contained nearly equal volumes of mature fine tails and fresh cap water which had not been used in the extraction process. Pond 9 was filled with tailings pond water, without any mature fine tails. During natural ageing of tailings water, the naphthenic acids concentrations, determined by FTIR, decrease (Schramm et al., 2000; Han et al., 2009) and this is reflected by their lower concentrations observed in Table 1.

Table 1 also summarizes the results from the elemental analyses of acid-extractable organics from the tailings waters. Each OSPW extract contained S (ranging from 1.06% in Pond 9 extract to 4.30% in the Albian extract). Some of the S in the extracts may be due to sulfate ($R–O–SO_3^-$) and sulfonate ($R–SO_3^-$) surfactants that have been reported to be in the aqueous phase of NaOH-extracts of oil sands ore (Schramm and Smith, 1987). All but one sample (Albian) contained N, with a maximum N content of 0.69% (Table 1).

Given the complexity of the oil sands tailings, it is not surprising that N- or S-containing organics can be detected in these extracts. However, the elemental analyses indicate that considering these OSPW extracts to be only classical or oxy-naphthenic acids (represented by the general formula $C_nH_{2n+Z}O_x$), which has been the case in many studies (e.g. Bataineh et al., 2006; Han et al., 2009; Headley et. al., 2010; Offier et al., 2009; Rogers et al., 2002), is an oversimplification and is incorrect.

ESI-FT-ICR MS Analyses: Numbers of Ions

Mass spectra were obtained from the ESI-FT-ICR MS analyses for compounds in the m/z range of 145 to 2000. The mass spectra of these extracts showed between 1300 and 1900 ions (Table 2), with >99% of the ions having m/z between 145 and 600. The numbers of ions corresponding to classical naphthenic acids ($C_nH_{2n+Z}O_2$) ranged from 75 to 102 (Table 2). No ions were found for values of n ≥ 30. Remarkably, these numbers accounted for only 4.5% to 6.9% of the ions with m/z 145 to 600.

The numbers of ions that corresponded to oxy-naphthenic acids ($C_nH_{2n+Z}O_x$), x = 3 to 5, were also determined for each OSPW extract (Table 2). The counts ranged from 143 to 201 and the oxy-naphthenic acids were more numerous than the classical naphthenic acids. Nonetheless. the sum of the numbers of ions corresponding to classical and oxy-naphthenic acids found in the OSPW extracts accounted for only 14 to 17% of

the total number of ions detected by ESI-FT-ICR MS (Table 2). Clearly, based simply on the numbers of ions found in the analyses of the OSPW extracts, the majority of the ions detected are not classical or oxy-naphthenic acids.

Table 1. Naphthenic acids concentrations in OSPW and elemental composition (% by weight) of acid extracts of oil sands tailings waters.

Sample	Naphthenic acids by FTIR (mg/L)	C	H	O	N	S
Syncrude MLSB	44	70.10	8.68	15.98	0.68	3.80
Syncrude WIP	60	69.82	8.70	16.40	0.51	3.38
Syncrude Pond 9	20	59.71	6.82	20.22	0.24	1.06
Syncrude Demo Pond	14	–[a]	–	–	–	–
Suncor Pond 2/3	63	71.12	9.13	16.34	0.69	3.85
Suncor Pond 5	38	67.34	8.45	17.68	0.38	2.91
Albian Pond	35	69.28	8.34	16.24	0.00	4.30

[a] Not analyzed because of insufficient sample.

Table 2. Summary of ion counts from ESI-FT-ICR MS analyses of acid extracts of oil sands tailings waters.

Sample	Total number of ions	Classical naphthenic acids ($C_nH_{2n+Z}O_2$). Number of ions	% Total number of ions	Oxy-naphthenic acids. Number of ions	% of Total number of ions [a]
Syncrude MLSB	1849	102	5.5	161	14
Syncrude WIP	1312	83	6.3	121	16
Syncrude Pond 9	1680	75	4.5	158	14
Syncrude Demo Pond	1691	95	5.6	185	17
Suncor Pond 2/3	1416	98	6.9	133	16
Suncor Pond 5	1873	95	5.1	201	16
Albian Pond	1497	89	5.9	143	15

[a] Based on sum of classical and oxy-naphthenic acids ions.

Table 3. Abundances of ions from ESI-FT-ICR MS analyses of acid extracts of oil sands tailings waters

Sample	Total Abundance of ions ($x10^6$) (arbitrary units)	Classical naphthenic acids ($C_nH_{2n+Z}O_2$). (%) of Total Abundance	Oxy-naphthenic acids. (%) of Total Abundance	Sum[a] of (%) of Total Abundance
Syncrude MLSB	2032	28.6	11.7	40.3
Syncrude WIP	951	24.4	11.7	36.1
Syncrude Pond 9	1782	10.7	27.1	37.8
Syncrude Demo Pond	1743	17.0	30.4	47.4
Suncor Pond 2/3	1165	35.6	10.3	45.9
Suncor Pond 5	2033	19.8	22.9	42.7
Albian Pond	1295	19.5	16.7	36.2

[a] Based on sum of classical and oxy-naphthenic acids ions.

ESI-FT-ICR MS Analyses: Abundance of Ions

The data in Table 2 show that only a relatively small proportion (≤18%) of the detected ions in the extracts from OSPW corresponded to classical ($C_nH_{2n+Z}O_2$) or oxy-naphthenic acids ($C_nH_{2n+Z}O_x$, x = 3 to 5). However, the ions that fit these formulae might be very abundant and therefore account for the majority of the ion abundances detected. Thus, we compared the sums of measured abundances for the classical and oxy-naphthenic acids to the total abundance in each spectrum (Table 3).

Considering the Syncrude MLSB extract, the total abundance of ions (arbitrary units) was 2032 x 10^6 (Table 3). The abundance of all of the ions corresponding to classical naphthenic acids accounted for 28.6% of the total abundance. In total, the abundance of ions with x = 3, 4 and 5 (the oxy-naphthenic acids) in the MLSB sample (Table 3) accounted for 11.7% of the total abundance.

Both the classical and oxy-naphthenic acids were found in all of the extracts (Table 3). The classical naphthenic acids were more abundant in the Syncrude MLSB, Syncrude WIP and the Suncor Pond 2/3 samples. The abundance of the oxy-naphthenic acids was much more prevalent in the two experimental reclamation ponds, Syncrude Pond 9 and Demo Pond. Han et al. (2008) demonstrated that aerobic microbial activity led to the formation of hydroxylated naphthenic acids, converting $C_nH_{2n+Z}O_2$ acids to $C_nH_{2n+Z}O_3$ acids. The higher abundance of the oxy-naphthenic acids in the two experimental reclamation ponds suggests that microbial activity may have oxidized the classical naphthenic acids over the years when no fresh tailings were added to these ponds.

As was the case with the numbers of ions in the mass spectra, the abundances of the ions corresponding to classical and oxy-naphthenic acids were only a fraction of the total ion abundances. Just 36.1 to 47.4% of the total ion abundances correspond to classical and oxy-naphthenic acids (Table 3). Thus, >50% of the ions could not be assigned to any of the molecular species that were considered in this study.

These Findings And Oil Sands Environmental Issues

"Naphthenic acids" are considered to be a major environmental problem associated with the oil sands industry and these acids are frequently mentioned in articles dealing with environmental health in the oil sands area (e.g. Kean, 2009; Tenenbaum, 2009). The complexity of naphthenic acids has been demonstrated in many studies (Bataineh et al., 2006; Dzidic et al., 1988; Fan, 1991; Han et al., 2008; Martin et al., 2008) and the analytical challenges are well recognized.

Because of the commonly used term "naphthenic acids", we started with the assumption that the classical naphthenic acids ($C_nH_{2n+Z}O_2$) would be major constituents of these OSPW extracts. However, based on simple peak counts from the ESI-FT-ICR MS analyses, the classical naphthenic acids were only a minor portion of the compounds in these extracts. Extending the peak counts to include oxy-naphthenic acids (x = 3 to 5) accounted for fewer than 20% of the peaks in the OSPW extracts (Table 2). When the abundances of the various peaks were considered (Table 3), the classical and oxy-naphthenic acids made up <50% of the peak abundances in the OSPW samples.

In addressing the toxicity of naphthenic acids to various organisms, some researchers have used naphthenic acids from OSPW (Madill et al., 2001; Rogers et al., 2002; Apostol et al., 2004; Nero et al., 2006; Gentes et al., 2007; Peters et al., 2007) in their studies. As is evident from our ESI-FT-ICR MS analyses, there are many compounds other than naphthenic acids and oxy-naphthenic acids in these preparations, and this fact confounds the conclusions that the classical naphthenic acids are the components responsible for toxicity. Similarly, previous biodegradation studies that have focused only on the classical naphthenic acids (e.g. Scott et al., 2005; Del Rio et al., 2006; Han et al., 2009; Headley et al., 2010) have unknowingly overlooked more than one-half of the compounds present in OSPW.

Part of the problem is semantics. Using the term "naphthenic acids" to describe a group of carboxylic acids (i.e. $C_nH_{2n+Z}O_2$) in the OSPW implies that these acids are the major components in OSPW and gives the false sense that we have a good understanding of the makeup of mixtures of acids in such waters. From the data presented in this paper, it is clear that the compositions of mixtures called "naphthenic acids" are not as simple as anticipated and the make-ups of these complex mixtures are far from being adequately understood. Therefore, it appears to be time to replace the term "naphthenic acids", which has been used for about 30 years to describe these

toxic extractable compounds, with a new term such as “oil sands tailings water acid-extractable organics (OSTWAEO)”. Classical and oxy-naphthenic acids are components of OSTWAEO, but the term OSTWAEO would not be as misleading as the currently used term “naphthenic acids”.

“Naphthenic acids” constitute an important parameter for monitoring and regulating potential OSPW releases in the oil sands area. However, our current inability to characterize the majority of the compounds in OSTWAEO creates a serious regulatory problem. In addition, the results from this study indicate that a better characterization of the components that make up OSTWAEO is required to help understand the key components that exert toxicity on various organisms. Similarly, improved characterization of these acids will aid in the application of chemical or microbial treatments for the detoxification of these waters.

ACKNOWLEDGEMENTS

Funding for the FT-ICR MS instrument was provided by the Canadian Foundation for Innovation and the Alberta Science and Research Investments Program. Research funding was provided by the Canadian Water Network and NSERC. We thank Syncrude, Suncor and Albian for the OSPW samples. We acknowledge the assistance of J. Klassen, W. Moffat, and D. Zinz.

REFERENCES

Apostol, K.G., Zwiazek, J.J., MacKinnon, M.D. 2004. Naphthenic acids affect plant water conductance but do not alter shoot Na^+ and Cl^- concentrations in jack pine (*Pinus banksiana*) seedlings. Plant and Soil **263**:183-190.

Barrow, M.P., Headley, J.V., Peru, K.M., Derrick, P.J. 2009. Data visualization for the characterization of naphthenic acids within petroleum samples. Energy & Fuels **23**: 2592–2599.

Barrow, M.P., Witt, M., Headley, J.V., Peru, K.M. 2010. Athabasca oil sands process water: Characterization by atmospheric pressure photoionization and electrospray ionization Fourier transform ion cyclotron resonance mass spectrometry. Analytical Chemistry **82**: 3727-3735.

Bataineh, M., Scott, A.C., Fedorak, P.M., Martin, J.W. 2006. Capillary HPLC/QTOF-MS for characterizing complex naphthenic acids mixtures and their microbial transformations. Analytical Chemistry **78**: 8354-8361.

Brient, J.A., Wessner, P.J., Doyle, M.N. 1995. Naphthenic acids. In: Kroschwitz J.I., editor. Encyclopedia of chemical technology, 4th ed. John Wiley & Sons, New York; pp. 1017-1029.

Clemente, J.S., Fedorak, P.M. 2005. A review of the occurrence, analyses, toxicity, and biodegradation of naphthenic acids. Chemosphere **60**: 585-600.

Del Rio, L.F., Hadwin, A.K.M., Pinto, L.J., MacKinnon, M.D., Moore, M.M. 2006. Degradation of naphthenic acids by sediment micro-organisms. Journal of Applied Microbiology **101**: 1049–1061.

Dzidic, I., Somerville, A.C., Raia, J.C., Hart, H.V. 1988. Determination of naphthenic acids in California crudes and refinery wastewaters by fluoride-ion chemical ionization mass-spectrometry. Analytical Chemistry **60**: 1318-1323.

Fan, T.-P. 1991. Characterization of naphthenic acids in petroleum by fast atom bombardment mass spectrometry. Energy & Fuels **5**: 371-375

Gentes, M.-L., Waldner, C., Papp, Z., Smits, J.E.G. 2007. Effects of exposure to naphthenic acids in tree swallows (*Tachycineta bicolor*) on the Athabasca oil sands, Alberta, Canada. Journal of Toxicology and Environmental Health, Part A **70**: 1182-1190.

Han, X., Scott, A.C., Fedorak, P.M., Bataineh, M., Martin, J.W. 2008. Influence of molecular structure on the biodegradability of naphthenic acids. Environmental Science & Technology **42**: 1290-1295.

Han, X., MacKinnon, M.D., Martin, J.W. 2009. Estimating the in situ biodegradation of naphthenic acids in oil sands process waters by HPLC/HRMS. Chemosphere **76**: 63–70.

Headley, J.V., Peru, K.M., Barrow, M.P. 2009. Mass spectrometric characterization of naphthenic acids in environmental samples: a review. Mass Spectrometry Reviews **28**: 121-134.

Headley, J.V., Peru, K.M., Adenugba, A.A., Du, J.-L., McMartin, D.W. 2010. Dissipation of naphthenic

acids mixtures by lake biofilms. Journal of Environmental Science and Health, Part A **45**: 1027-1036.

Jivraj, M.N., MacKinnon, M., Fung, B. 1995. Naphthenic Acids Extraction and Quantitative Analyses With FT-IR Spectroscopy. In: Syncrude Analytical Methods Manual. 4th ed. Syncrude Canada Ltd. Research Department, Edmonton, Canada.

Kean, S. 2009. Eco-alchemy in Alberta. Science **326**:1052-1055.

Lee, D.D. 1940. Thermosetting resin reaction product of furfural with an oxy-naphthenic acid. U.S. Patent number 2,207,624.

MacKinnon, M.D., Boerger, H. 1986. Description of two treatment methods for detoxifying oil sands tailings pond water. Water Pollution Research Journal of Canada **21**: 496-512.

Madill, R.E.A., Orzechowski, M.T., Chen, G., Brownlee, B.G., Bunce, N.J. 2001. Preliminary risk assessment of the wet landscape option for reclamation of oil sands mine tailings: Bioassays with mature fine tailings pore water. Environmental Toxicology **16**:197-208.

Martin, J.W., Han, X., Peru, K.M., Headley, J.V. 2008. Comparison of high- and low-resolution electrospray ionization mass spectrometry for the analysis of naphthenic acid mixtures in oil sands process water. Rapid Communications in Mass Spectrometry **22**: 1919-1924.

McNaught, A.D., Wilkinson, A. 1997. IUPAC Compendium of Chemical Terminology, (2nd edn). Wiley-Blackwell: Chichester, Oxford. (Available at http://old.iupac.org/publications/compendium/)

Nero, V., Farwell, A., Lee, L.E.J., Van Meer, T., MacKinnon, M.D., Dixon, D.G. 2006. The effects of salinity on naphthenic acid toxicity to yellow perch: Gill and liver histopathology. Ecotoxicology and Environmental Safety **65**: 252-264.

Oiffer, A.A.L., Barker, J.F., Gervais, F.M., Mayer, K.U., Ptacek, C.J., Rudolph, D.L. 2009. A detailed field-based evaluation of naphthenic acid mobility in groundwater. Journal of Contaminant Hydrology **108**: 89–106.

Peters, L.E., MacKinnon, M., Van Meer, T., van den Heuvel, M.R., Dixon, D.G. 2007. Effects of oil sands process-affected waters and naphthenic acids on yellow perch (*Perca flavescens*) and Japanese medaka (*Orizias latipes*) embryonic development. Chemosphere **67**: 2177–2183.

Rogers, V.V., Wickstrom, M., Liber, K., MacKinnon, M.D. 2002. Acute and subchronic mammalian toxicity of naphthenic acids from oil sands tailings. Toxicological Science **66**: 347-355.

Schramm, L.L., Smith, R.G. 1987. Two classes of hot anionic surfactants and their significance in water processing of oil sands. Canadian Journal of Chemical Engineering **65**: 799-811.

Schramm, L.L., Stasiuk, E.N., MacKinnon, M. 2000. Surfactants in Athabasca oil sands slurry conditioning, flotation recovery, and tailings processes. In: Schramm, L.L., editor. Surfactants, fundamentals and applications in the petroleum industry. Cambridge University Press, Cambridge, UK; pp. 365-430.

Scott, A.C., MacKinnon, M.D., Fedorak, P.M. 2005. Naphthenic acids in Athabasca oil sands tailings waters are less biodegradable that commercial naphthenic acids. Environmental Science & Technology **39**: 8388-8394.

Scott, A.C., Young, R.F., Fedorak, P.M. 2008. Comparison of GC-MS and FTIR methods for quantifying naphthenic acids in aqueous samples. Chemosphere **73**: 1258-1264.

Scott, A.C., Whittal, R.M., Fedorak, P.M. 2009. Coal is a potential source of naphthenic acids in groundwater. Science of the Total Environment **407**: 2451-2459.

Siwik, P.L., van Meer, T., MacKinnon, M.D., Paszkowski, C.A. 2000. Growth of fathead minnow in oilsands-processed wastewater in laboratory and field. Environmental Toxicology and Chemistry **19**: 1837–1845.

Smith, D.F., Schaub, T.M., Kim, S., Rodgers, R.P., Rahimi, P., Teclemariam, A., Marshall, A.G. 2008. Characterization of acidic species in Athabasca bitumen and bitumen heavy vacuum gas oil by negative-ion ESI FT-ICR MS with and without acid-ion exchange resin prefractionation. Energy & Fuels **22**: 2372–2378.

Tenenbaum, D.J. 2009. Oil sands development A health risk worth taking? Environmental Health Perspectives **117**: A150-A156.

PARALLEL FACTOR ANALYSIS (PARAFAC) OF NAPHTHENIC ACIDS IN PROCESS AFFECTED WATER

A.M. Ewanchuk, M. Alostaz, A.C. Ulrich, D. Sego
Dept. of Civil and Environmental Engineering, University of Alberta, Edmonton, AB, Canada T6G 2W2

ABSTRACT

Naphthenic acids are known contaminants that are released during the extraction process in the oil sands industry and are contained in process affected water. These compounds cause corrosion issues within the refining units and demonstrate toxic effects to various organisms. Fluorescence technology has been used to produce unique excitation-emission matrices (EEMs) for oil sands produced naphthenic acids as a characterization technique. Due to the varying nature of the naphthenic acid mixture the fluorescence signals obtained are overlapping and complex. In the case of overlapping signals a decompositional method can be used, such as parallel factor analysis (PARAFAC). This multivariable statistical procedure was used to decompose EEM data and differentiate the underlying components of the naphthenic acid mixture. This statistical technique aids in fluorescence characterization and understanding of naphthenic acids in process affected water.

INTRODUCTION

Naphthenic Acids in the Oil Sands

The Athabasca oil sands deposits in northern Alberta, Canada, represent one of the largest oil deposits in the world with reserves of 173 billion barrels proven to be recoverable (Alberta Government 2009). These oil sands contain large amounts of naphthenic acids released during the extraction process and carried throughout the mining plant in the process water (Janfada et al. 2006).

Large volumes of water are required for the extraction process, approximately three barrels of fresh water for every barrel of oil produced (Allen 2008). Water that is not able to be recycled within the system is transferred to tailings pond impoundments. This process affected water contains sands and clays which settle within the ponds (Allen 2008, Headley & McMartin 2004). The naphthenic acids are then concentrated and contained within the impoundments. Naphthenic acids are an issue in the oil sands industry as they have been shown to be toxic to various organisms and cause corrosion issues within the refinery units in the extraction process (Allen 2008; Clemente & Fedorak 2005; Headley & McMartin 2004; Slavcheva 1999; Babaian-Kibala 1994).

Naphthenic acids are monobasic carboxylic acids and are composed primarily of alkyl-substituted cycloaliphatic carboxylic acids (Brient et al. 1995). Traditionally naphthenic acids are considered to be of the form $C_nH_{2n+Z}O_2$, where n is the number of carbons and Z is a zero or negative, even integer that specifies the homologous series (Clemente & Fedorak 2004). The Z value ranges from 0 to -12 and indicates the hydrogen deficiency resulting from the ring formation. Ring structures typically contain five or six carbons with each multiple of -2 signifying another ring (Brient et al. 1995). Figure 1 shows some typical structures of naphthenic acids, with R representing the alkyl functional group.

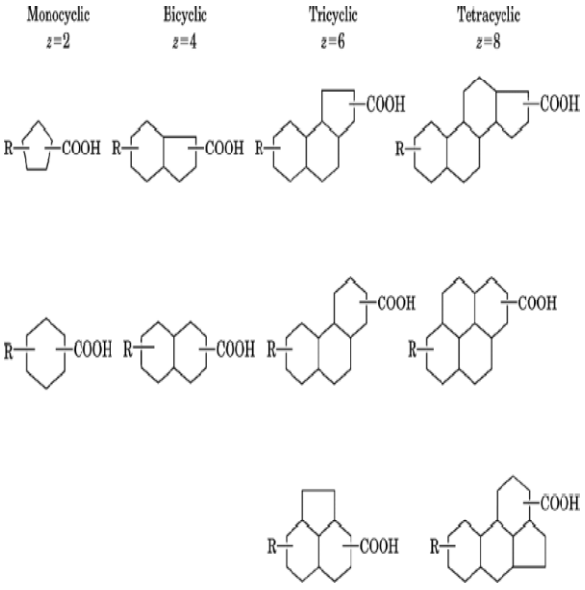

Figure 1. Naphthenic Acid Structures (Brient et al. 1995)

Naphthenic acids found in the tailings ponds have been found to contain various levels of impurities, and do not fall within the general formula $C_nH_{2n+Z}O_2$. The presence of pyrolles, thiophenes, and phenols has been detected in the naphthenic acid portion of a Californian crude oil using UV and IR analysis (Seifert et al. 1969). Similarly thin layer chromatography has identified the presence of phenol, nitrogen and sulphur within the naphthenic acid fraction of a Californian crude oil (Seifert & Teether 1969). In addition mass spectrometry methods were able to determine compositions containing oxygen, ozone, tetraoxygen (O_4), O_2S, O_3S and O_4S within a heavy crude from South America (Headley et al. 2009).

Concentrations of naphthenic acids within the tailings ponds have been found in the range of 40-120 mg/L, (Holowenko et al. 2001). The current method used by oil sands operators to quantify naphthenic acids is through the use of Fourier Transform Infrared (FTIR) spectroscopy (Jivraji et al. 1995). This method requires time consuming sample preparation, is unable to isolate individual species and can overestimate naphthenic acid concentration by almost double (data not shown). Quantification is based on comparing the petroleum based naphthenic acids to commercially produced naphthenic acids. Recently fluorescence technology has been used to generate unique signatures that aid in characterization and understanding of naphthenic acids in process affected water.

In this paper fluorescence technology is applied to the process affected water from three oil sands operations and the underlying components of naphthenic acids are determined using a statistical technique, PARAFAC. Similar techniques are subsequently applied to commercially produced naphthenic acids.

Background

Fluorescence spectrometry as an analytical technique has many benefits. The fluorescence signals obtained are unique to each particular compound, and thus can be used in identification for analytical purposes (Lackowitz 2006). Samples require little or no preparation, and are not affected or destroyed during measurement (Alostaz et al. 2008a). In addition fluorescence methods are readily reproducible, simple and cost effective (Brown et al. 2009). Fluorescence spectrometry has been used as an analytical technique in several different applications. Petroleum products such as gasoline, diesel, and heavy crude oil that contain polycyclic aromatic hydrocarbons (PAHs) have been shown to produce unique EEMs that can be used to track and determine contamination (Alostaz et al. 2008a). Synchronous fluorescence spectrometry has been used for detecting natural organic matter, as well as PAHs and petroleum contaminants (Kavanagh et al. 2009).

Petroleum derived naphthenic acids will display characteristic fluorescence signals when exposed to ultraviolet wavelengths between 260-350 nm. By exposing the samples to multiple excitation wavelengths a three dimensional plot known as an excitation-emission matrix (EEM) can be constructed (Rho & Stewart 1978). Previous studies have identified a prominent peak occurring at an excitation wavelength of 290 nm and an emission wavelength of approximately 346 nm for process affected waters (Brown et al. 2009; Mohammed et al. 2008).

Due to the complex nature of the naphthenic acid mixture the fluorescence signals produced are overlapping and complex. In the case of overlapping signals a decompositional method can be used, such as parallel factor analysis (PARAFAC). The use of PARAFAC in fluorescence analysis has been demonstrated in previous studies with petroleum products and crude oil where overlapping signals have been obtained (Alostaz et al. 2008a,b).

PARAFAC is a multivariable statistical procedure that can be used to decompose EEM data and differentiate the components of the mixture (Alostaz et al. 2008b). Fluorescence EEMs are arranged into a three way array with the dimensions dependant on the number of samples analysed at different concentrations, and the number of excitation and emission wavelengths. Using an alternating least squares approach, the method determines a function that approximates the data (Bro 1997). The PARAFAC model decomposes the fluorescence array into three loading matrices, estimated relative concentration, excitation and emission loading matrices. The optimal number of components is determined by looking at the residuals between the data and the function; the deviation of the data and the model, known as the core consistency and the number of distinct component peaks visible.

MATERIALS AND METHODS

Sources and preparation of samples

For this study process affected water samples were obtained from three different oil sand operations. Process affected water from Company A was obtained from a recycle line located in the extraction plant. Samples for Company B and C were obtained directly from the oil sands tailings pond. Samples were refrigerated at 4^{o}C and stored in plastic containers. Prior to analysis, samples were filtered using vacuum filtration and 0.45 µm nylon filters to remove suspended particles in the samples that cause light scatter during measurement. Commercial naphthenic acids were obtained from Sigma Aldrich.

Fluorescence and Absorbance Measurements

A Varian Cary Eclipse spectrometer was used for fluorescence measurements using the 90^{o} degrees detection setup. Samples were analyzed in clear quartz cuvettes measuring 1.24x1.24x4.5 cm. Excitation-Emission Matrices were generated using Varian Cary Eclipse software at a scan rate of 600 nm/min. Emission wavelengths were collected from 240 to 600 nm with 1 nm increments at excitation wavelengths ranging from 250 to 450 nm with 10 nm increments. The bandwidth (slit width) was 10 nm and 5 nm for excitation and emission, respectively. Both excitation and emission filters were set to automatic.

Fourier Transform Infrared Spectroscopy

Naphthenic acid concentration was determined using Fourier transform infrared (FTIR) spectroscopy. Filtered PA water samples of 500mL were raised to a pH of 11.5 with the addition of NaOH. Dichloromethane is then added to the PA water in increments of 25mL three times and is subsequently removed. The samples are then acidified to a pH of 2 using HCl. Dichloromethane is then added in 25mL increments three times in order to quantitatively extract the naphthenic acids. The dichloromethane with the extracted naphthenic acids is then allowed to dry overnight. Fresh dichloromethane is then added prior to analysis. This is a modified extraction method similar to the industry standard used (Jivraji et al. 1995). The FTIR equipment then measures the absorbance of the monomeric and dimeric forms of the carbonyl groups at their respective wavelengths of 1743 and 1706 cm^{-1}. The results are then quantified by calibration curves derived from the commercially available Sigma Aldrich naphthenic acids.

PARAFAC

PARAFAC requires a series of EEMs of the analyte in question in different concentrations. The process affected water samples from the three companies were diluted with deionized water in increments of 10%, starting from undiluted samples (100%) down to 10% for a total of 10 samples. The Sigma Aldrich naphthenic acids were diluted with methanol and were prepared in concentrations of 10, 20, 50, 100 and 200 ppm. The required arrays were prepared using MATLAB R2009b and the additional PARAFAC toolbox version 5.2 add on.

RESULTS

Petroleum Derived Naphthenic Acids

Naphthenic acid concentration was determined using Fourier transform infrared (FTIR) spectroscopy. The resulting concentrations were 68 ppm for Company A, 44 ppm for Company B and 32 ppm for Company C. EEMs were obtained for each of the three companies at undiluted and diluted levels. The undiluted EEM for Company A is shown in Figure 2. Diluted samples produced similar EEMs, with the intensity decreasing with each diluted level (data not shown). Companies B and C also produced similar results. In all cases the prominent peak was determined to be at an excitation wavelength of 290 nm and an emission wavelength of approximately 346 nm. For the undiluted samples the peak intensities obtained were found to be 511 au for Company A, 637 au for Company B and 373 au for Company C. Intensities were found to linearly decrease with each subsequent dilution for all three companies (data not shown). These values have not been corrected for absorbance.

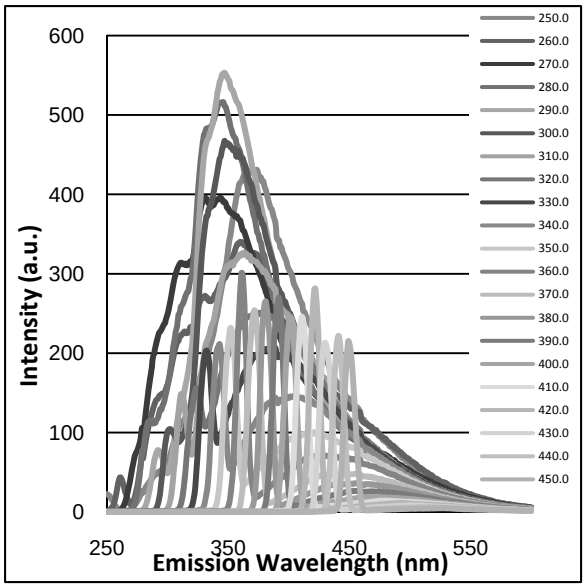

Figure 2. Excitation-Emission Matrix for process-affected water from Company A, 68ppm

PARAFAC analysis was performed to establish the optimal number of components that could be determined from the naphthenic acids in the samples. Based on the residuals between the function and the data, and the core consistency, the optimal number of components was determined to be five. Figure 3a illustrates an example of the distribution of residuals from the PARAFAC analysis. The residuals are described by noise instead of systematic variation in the data. Figure 3b shows an example of the core consistency for a PARAFAC model. The core consistency represents the deviation between the data and the model, with the core elements shown as both open and closed circles. The open circles are ideally non zero whereas the closed circles are ideally zero, and will follow the dashed line.

PARAFAC models for each company determined that the estimated concentration of each of the determined components decreased with each dilution. Figure 4 depicts the estimated concentrations for each component determined for Company A. Similar results were determined for companies B and C (results not shown).

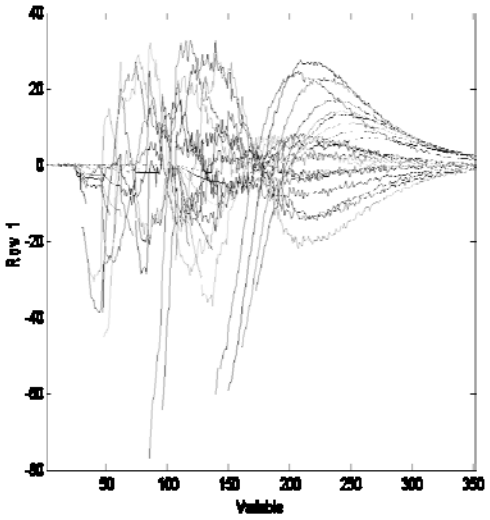

a)

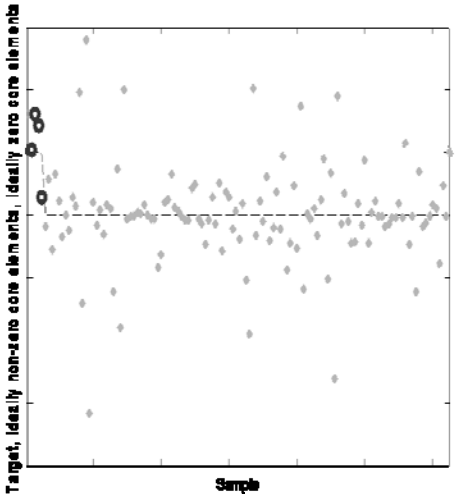

b)

Figure 3. Example of residual and core consistency results from PARAFAC model

Figures 5 through 7 depict the five components determined for the emission loading for each of the three companies.

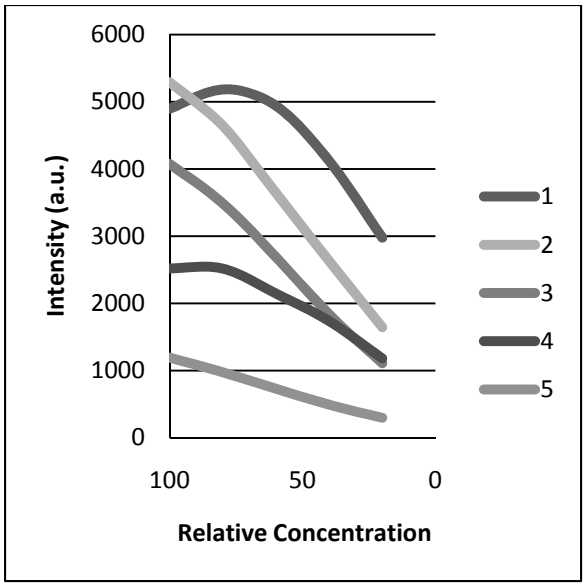

Figure 4. Estimated relative concentration of each component

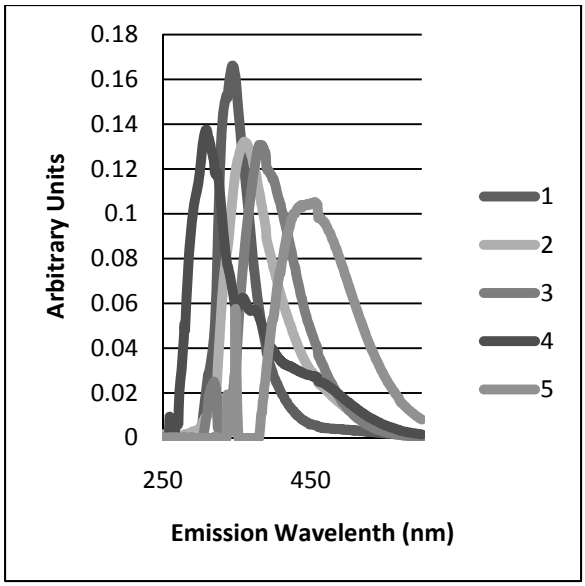

Figure 5. Emission Loadings of Company A

Commercially Produced Naphthenic Acids

A similar dilution series of commercially available naphthenic acids was prepared for PARAFAC analysis. The resulting EEM for a solution of 100 ppm is shown in Figure 8. Unlike the petroleum derived naphthenic acids, the prominent peak intensity was found to be at an excitation wavelength of 270 nm and an emission wavelength of 313 nm. Intensities for the subsequent dilutions were found to decrease linearly (data not shown).

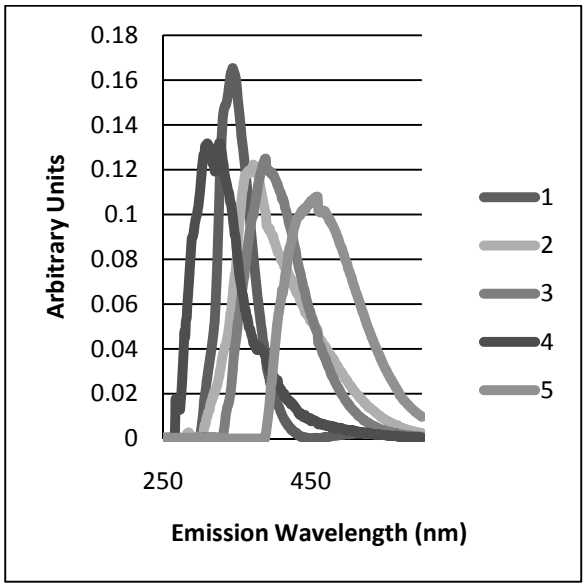

Figure 6. Emission Loadings of Company B

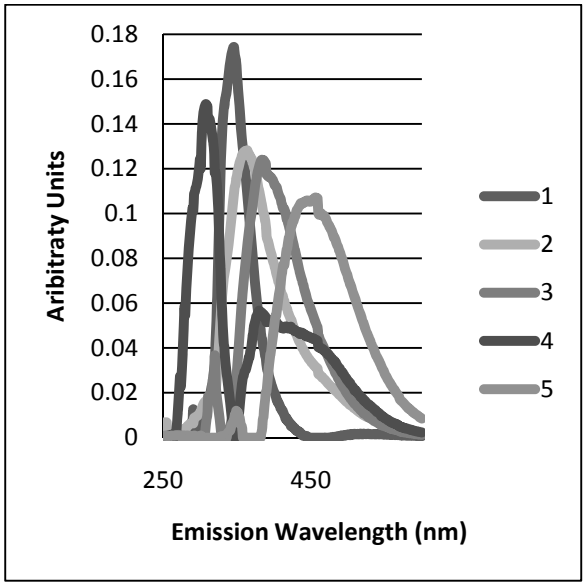

Figure 7. Emission loadings of Company C

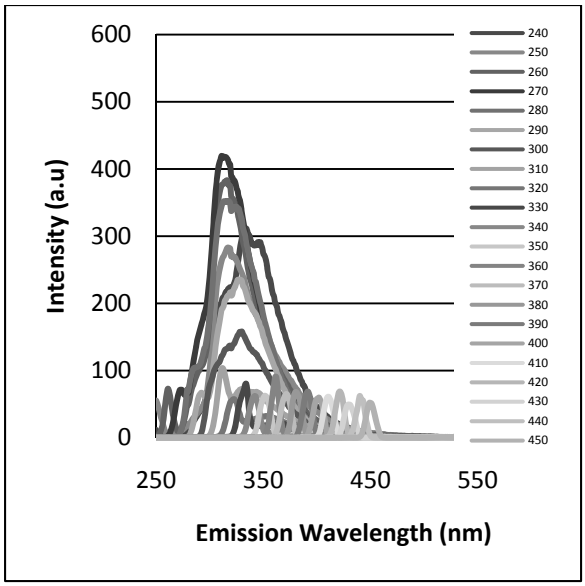

Figure 8. Sigma Aldrich naphthenic acids in methanol at a concentration of 100 ppm.

Similar to the petroleum derived naphthenic acids, a five component model was developed for the Sigma Aldrich naphthenic acids. The resulting emission loading is shown in Figure 9.

DISCUSSION

The fluorescence EEMs generated for each dilution series showed that intensity decreased with each increasing dilution. Similar results were found in previous work done by Brown et al. (2009). For this study intensities were not corrected for absorbance. By correcting for absorbance inner filtering effects are taken into account, due to the right angle fluorometry (Tucker et al. 1992). Previous work has shown that the linear correlation in a dilution series does not depend on correction for absorbance. PARAFAC analysis of process affected water from each of the three oil sands operations determined that five distinct components could be determined from the overall EEM signature. The relative concentration of each component decreased correspondingly with each increasing dilution for all dilution series. The relative concentrations of each component between companies differed, and were reflective of the concentrations determined by FTIR.

Despite the varying concentrations from each of the three companies, from both the FTIR and fluorescence analysis, the underlying emission loading components were alike. The five components determined were found to be in relatively the same emission wavelengths locations with similar corresponding intensity peaks.

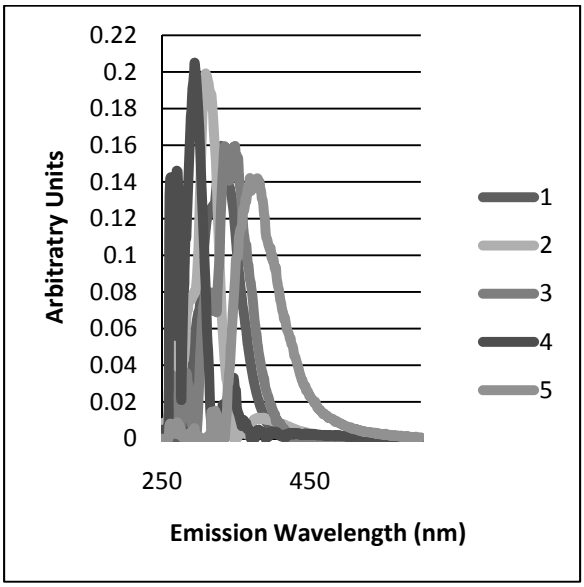

Figure 9. Components of Commercially Produced Sigma Aldrich Naphthenic Acids

The EEMs from the commercially produced naphthenic acids from Sigma Aldrich showed a similar decreasing intensity trend with the increasing dilutions. However the prominent peak was found to be at a lower excitation wavelength, and in general the emissions collected were shifted to lower wavelengths, as compared to the petroleum derived naphthenic acids. The relative concentrations of each component were found to decrease with the dilution series similar to the petroleum naphthenic acids, however the underlying components were found to be shifted. The peak excitation wavelengths were shifted to lower wavelengths for each component and the corresponding intensities were unlike those determined previously. This raises an issue as the Sigma Aldrich naphthenic acids are what the FTIR concentrations are calibrated against. The petroleum derived naphthenic acids show they are made up of different components, but yet are still compared to the commercial naphthenic acids for quantification. The Sigma Aldrich naphthenic acids were diluted using methanol as a solvent, whereas the petroleum derived naphthenic acids

were diluted with deionized water. The commercially produced acids are not miscible with water, and thus methanol was required as a solvent.

Future Work

The underlying principle components that have been determined for each of the three companies can now be further analyzed and correlated to naphthenic acid structures or molecular weight, using other methods of characterization. High performance liquid chromatography (HPLC) can be used in conjunction with mass spectrometry methods, such as high resolution mass spectrometry (HRMS) and is an enhanced technique over FTIR analysis (Bataineh et al. 2006; Han et al. 2009). HPLC/HRMS has been shown to be more selective as FTIR will respond to any carboxylic acid present, not just naphthenic acids (Han et al. 2009). The principle components identified can subsequently be utilized in a second statistical technique, soft independent method of class analogy (SIMCA). SIMCA allows for data from an unknown sample to be compared to the determined principle components and subsequently assess the similarities between the two datasets. This allows for the detection of compounds other than naphthenic acids in the unknown mixture which could cause interference during fluorescence.

CONCLUSION

The use of Parallel Factor Analysis (PARAFAC) has the ability to determine underlying components from an excitation-emission matrix (EEM) of overlapping and complex signals. PARAFAC analysis was performed on process affected water from three different oil sands operations and commercially produced naphthenic acids. Five primary components were determined for each of the three oil sands companies. Despite varying concentrations of each water sample, the primary components determined were found to occur at approximately the same excitation wavelength and have similar intensities. The underlying components of the commercially produced naphthenic acids were found to occur at lower excitation wavelengths, and differing intensities. These commercially produced naphthenic acids are what are used for current quantification techniques, yet they do not fully represent the true petroleum derived naphthenic acids.

ACKNOWLEDGEMENTS

The authors would like to acknowledge the support from the Natural Sciences and Engineering Research Council of Canada (NSERC) and the Oil Sands Tailings Research Facility (OSTRF).

REFERENCES

Alberta Government. 2009. Alberta's Oil Sands. [online] Available from http://www.oilsands.alberta.ca/ [accessed August 27, 2010]

Allen, E.W. 2008. Water treatment in Canada's oil sands industry I: Target pollutants and treatment objectives. Journal of Environmental Engineering and Science, 7: 123-128.

Alostaz, M. 2008. Improved ultraviolet induced fluorescence (UVIF)-standard cone penetration testing (CPT) system to detect petroleum hydrocarbon contaminants. PhD thesis, University of Alberta.

Alostaz, M., Biggar, K., Donahue, R., and Hall, G. 2008a. Petroleum contamination characterization and quantification using fluorescence emission excitation matrices (EEMs) and parallel factor analysis (PARAFAC). Journal of Environmental Engineering and Science. 7: 183–197.

Alostaz, M., Biggar, K., Donahue, R., and Hall, G. 2008b. Soil type effects on petroleum contamination characterization using ultraviolet induced fluorescence excitation-emission matrices (EEMs) and parallel factor analysis (PARAFAC). Journal of Environmental Engineering and Science 7: 661–675.

Babaian-Kibala, E. 1994. Phosphate ester inhibitors solve naphthenic acid corrosion problems. Oil and Gas Journal, 92: 31-35.

Bataineh, M., Scott, A.C., Fedorak, P.M., and Martin, J.W. 2006. Capillary HPLC/QTOF-MS for Characterizing Complex Naphthenic Acid Mixtures and Their Microbial Transformation. Analytical Chemistry, 78: 8354-8361.

Brient, J.A.; Wessner, P.J.; Doyler, M.N. Naphthenic acids. In Kirk-Othmer Encyclopedia of Chemical Technology, 4th ed.; Kroschwitz, J.I.,

Ed.; John Wiley and Sons: New York, 1995; 1017-1029.

Bro, R. 1997. PARAFAC Tutorials and Applications. Chemometrics and Intelligent Laboratory Systems. 38(2):149-171.

Brown, L. D., M. Alostaz, A. C. Ulrich. 2009. Characterization of Oil Sands Naphthenic Acids in Oil Sands Process-Affected Waters Using Fluorescence Technology. In 62nd Canadian Geotechnical Conference, Halifax, Nova Scotia, 1-7.

Clemente, J.S. and Fedorak, P.M. 2004. Evaluation of the analyses of tert-butyldimethysilyl derivatives of naphthenic acids by gas chromatography – electron impact mass spectrometry. Journal of Chromatography, 1047(2004): 117-128.

Clemente, J.S. and Fedorak, P.M. 2005. A review of the occurrence, analyses, toxicity, and biodegradation of naphthenic acids. Chemosphere, 60(2005): 585-600.

Han, X., MacKinnon, M. D., Martin, J.W. 2009. Estimating the in situ biodegradation of naphthenic acids in oil sands process waters by HPLC/HRMS. Chemosphere, 76(2009): 63-70.

Headley, J.V. and McMartin, D.W. 2004. A Review of the Occurrence and Fate of Naphthenic Acids in Aquatic Environments. Journal of Environmental Science and Health, A39(8): 1989-2010.

Headley, J.V., Peru, K.M., and Barrow, M.P. 2009. Mass Spectrometric Characterization of Naphthenic Acids in Environmental Samples: A Review. Mass Spectrometry Reviews. 28: 121-134.

Holowenko F, MacKinnon M and Fedorak P. 2001. Naphthenic acids and surrogate naphthenic acids in methanogenic microcosms. Water Resources, 35: 2596–2606.

Janfada, A. et al. 2006. A Laboratory Evaluation of the Sorption of Oil Sands Naphthenic Acids on Organic Rich Soils. Journal of Environmental Science and Health, A41: 985-997.

Jivraj, M., M. Mackinnon, B. Fung (1995). Naphthenic Acid Extraction and Quantitative Analysis With FT- IR Spectroscopy. In Syncrude Analytical Manuals, 4th Edition, Research Department, Syncrude Canada Ltd., Edmonton, AB

Kavanagh, R.J., Burnison, B.K., Frank, R.A., Soloman, K.R., Van deer Kraak, G. 2009. Detecting oil sands process-affected waters in the Alberta oil sands region using synchronous fluorescence spectroscopy. Chemosphere 76: 120–126.

Lakowicz, J.R. 2006. Principles of Fluorescence Spectroscopy, 3rd Ed. Springer Science+Business Media, LLC, New York, NY.

Mohammed, M.H., Wilson, L.D., Headley, J.V., and Peru, K.M. 2008. Screening of oil sands naphthenic acids by UV-Vis absorption and fluorescence emission spectrophotometry. Journal of Environmental Science and Health Part A 43: 1700–1705.

Rho, J.H., and Stewart, J.L. 1978. Automated Three-Dimensional Plotter for Fluorescence Measurements. Analytical Chemistry, 50(4): 620-625.

Seifert, W., and Teeter, R. 1969. Preparative Thin-Layer Chromatography and High Resolution Mass Spectrometry of Crude Oil Carboxylic Acids. Analytical Chemistry, 41(6): 786-795.

Seifert, W., Teeter, R., Howells, W.G., and Cantow, M. 1969. Analysis of Crude Oil Carboxylic Acids after Conversion to Their Corresponding Hydrocarbons. Analytical Chemistry, 41(12): 1639-1647.

Slavcheva, E., Shone, R., Turnbull, A., 1999. Review of naphthenic acid corrosion in oil refining. British Corrosion Journal 34: 125–131.

Tucker, S.A., Amszi, V.L., Acree, W.E. 1992. Primary and Secondary Inner Filtering: Effect of K2Cr2O7 on fluorescence emission intensities of quinine sulphate. Journal of Chemical Education, 69(1): A8-A12.

PORTABLE NAPHTHENIC ACID SENSOR FOR OIL SANDS APPLICATIONS

M.T. Taschuk[1], Q. Wang[1], S. Drake[1], A. Ewanchuk[2], M. Gupta[1],
M. Alostaz[2], A. Ulrich[2], D. Sego[2], Y.Y. Tsui[1]
[1]Dept. of Electrical and Computer Engineering, University of Alberta, Edmonton, AB, Canada T6G 2V4
[2]Dept. of Civil and Environmental Engineering, University of Alberta, Edmonton, AB, Canada T6G 2W2

ABSTRACT

Napthenic Acids (NA) are a byproduct of oil sands operations which may be toxic. Current methods for NA detection and concentration measurements in process-affected water (PAW) require site samples to be sent to an analytical chemistry facility, a costly and time-consuming step. To eliminate this bottleneck, we have developed a field-portable fluorescence sensor capable of detecting NA in water at concentrations below 10 mg L^{-1} in seconds.

Our prototype sensor is also capable of detecting NA at the tens of ppm level in PAW without any sample preparation. Our device uses ultraviolet light-emitting diodes and a compact charge-coupled device spectrometer to excite and measure NA fluorescence signatures. Our system is capable of measuring the full excitation-emission spectrum of NA in PAW, with excitation wavelengths between 265 nanometers (nm) and 340 nm and emission wavelengths between 200 nm and 800 nm. In this paper we report on our instrument design, develop an optical theory to characterize the performance, characterize NA sensitivity, and report avenues for further improvements and miniaturization of our device.

INTRODUCTION

Background

Monitoring the presence, migration and biodegradation of naphthenic acids (NA) in oil sands process-affected waters (PAW) is an essential component of assessing and mitigating their environmental and operational impacts. NA are toxic to aquatic life (Clemente and Fedorak, 2005; Allen, 2008) and are a major source of corrosion in the oil industry (Slavcheva *et al.,* 1999).

Previous studies have demonstrated that petroleum NA show characteristic fluorescence when excited by ultraviolet (UV) light in the range of 260 nm to 350 nm (Kavanagh et al., 2009; Brown et al., 2009). One approach to acquiring such signatures is an excitation-emission matrix (EEM), which requires recording fluorescence spectra from multiple excitation wavelengths. EEM measurements can, in principle, determine which of the NA family is present in a given sample. Such analysis is useful for assessing the toxicity of PAW, which depends on the molecular weight of the NA contaminants (Frank *et al.*, 2009).

Portable instruments for fluorescence characterization of hydrocarbons in various matrices have been studied for many years (Alarie *et al.*, 1993; Baird and Nogar, 1995; Hart and JiJi, 2002; Obeidat *et al.*, 2008). As low-cost, high power optical sources and improved battery technologies have become available, portable instruments have decreased in size and weight. However, instrument performance has remained roughly constant, producing limits of detection (LOD) in the parts-per-million (ppm) and parts-per-billion (ppb) range.

Early work by Alarie *et al.* had a similar objective to the work described here (Alarie *et al.*, 1993). They designed a portable instrument for on-site contaminant detection, including hydrocarbons in groundwater and hazardous waste sites. The instrument was a ruggedized version of a lab instrument, occupying a suitcase sized (48 cm by 40 cm by 21 cm) optical system. A similar volume of batteries was required to run the system, and the total weight was 22.5 kg. The system was highly sensitive, achieving low ppm to high ppb LOD. A similar system was reported by Baird *et al.* a few years later (Baird and Nogar, 1995). Although the system was smaller (16 cm by 16 cm by 20 cm), its chemical detection performance was not clearly described.

As ultraviolet light-emitting diodes (LED) became commercially available, portable instruments

began to use this low-cost source (Hart and JiJi, 2002; Obeidat *et al.*, 2008). The first use of LEDs for obtaining excitation-emission matrices (EEM) was by Hart et al. (Hart and JiJi, 2002), using seven LEDs at wavelengths between 370 nm and 636 nm. A 1/4 m imaging spectrometer (Oriel MS260i) was used with a cooled charge-coupled device (CCD) detector. The system obtained LOD in the ppb to part-per-trillion (ppt) level for fluorescent dyes. Although the system developed by Hart *et al.* is not portable due to the spectrometer, it is a clear demonstration of the capabilities of LEDs as an excitation source.

A fully portable system using LEDs and an Ocean Optics spectrometer was reported by Obeidat *et al.* (Obeidat *et al.*, 2008). This EEM-capable system is small and light weight (1.5 kg, 24 cm by 15 cm by 5 cm). The wavelengths used were between 405 nm and 640 nm. System performance was characterized using fluorescent dyes and several plant extracts; nanomolar LOD were achieved for the dyes and the plant extracts could be distinguished using the EEM.

In this paper we present a portable fluorescence instrument for characterization of NA in PAW from the oil sands industry. Our prototype is a step towards miniature sensors for detecting hydrocarbons, and will be used to characterize fluorescence signatures and demonstrate the utility of LEDs for compact oilsands instrumentation. Although our long-range goal is a miniature device, the current instrument has utility as a screening instrument for field use. We test prototype performance with diesel and NA in water, demonstrate NA detection below 10 ppm, and demonstrate that our system can detect NA in PAW with no sample preparation.

INSTRUMENT DESIGN & CHARACTERIZATION

Instrument Specifications

Our completed prototype is shown in Fig. 1. The sensor uses LEDs at different UV wavelengths for fluorescence excitation. The UV emission is focused on the sample by an off-axis parabolic mirror. The same mirror collimates the sample's fluorescent emission for analysis with a compact CCD spectrometer (Ocean Optics). This version has been encased in ABS plastic pipe to provide a robust container for use in the field. Table 1 gives detailed specifications.

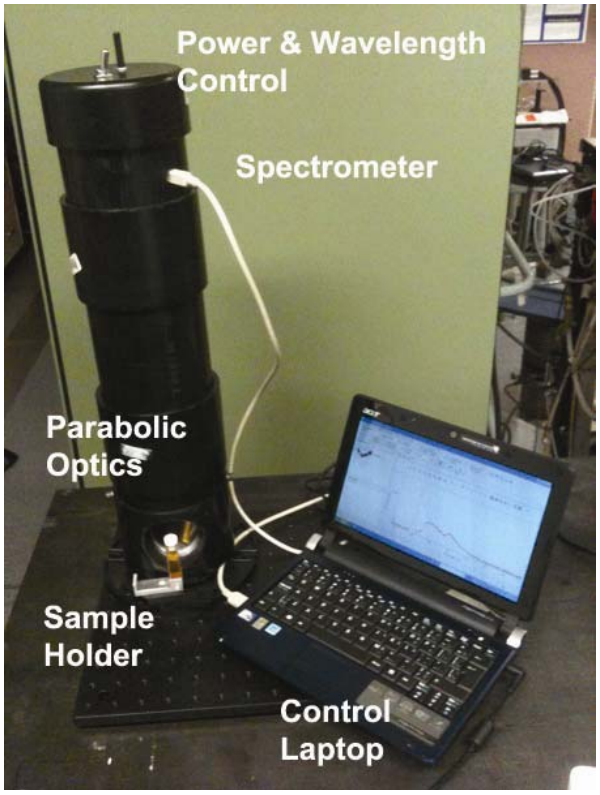

Figure 1: Picture of completed prototype encased in ABS pipe. From top to bottom, control switches to select excitation wavelength, compact CCD spectrometer (inside ABS pipe), parabolic optics for focusing UV LEDs, sample holder and laptop to control spectrometer. Not shown: LED array, control circuitry and emission relay optics.

Optical Theory

To better understand the expected behaviour of the instrument, we have derived the special case of a distributed fluorescent emitter in an absorbing analyte for our instrumental characteristics and geometry, which differs from conventional bench top instruments. This analysis allows comparison of prototype performance with the theoretical limits, and gives insight into how to improve the instrument. Consider the case of an infinitesimal slice of PAW inside the cuvette at a distance *x* from the cuvette's front face, excited by a LED. The fluorescent emission observed by the instrument can be written as:

$$d\phi = e^{-\alpha_{emit} x}\Theta(x)dx \qquad [1]$$

where α_{emit} is the absorption coefficient of the analyte at the emission wavelength, and $\Theta(x)$ is the fluorescent brightness in units of μJ Sr^{-1} cm^{-3}. The expected fluorescence strength is given by the quantum efficiency of the analyte, η, and the energy absorbed, E_{abs}.

Table 1: Instrument specifications.

Specification	Value
Physical	
Diameter	12 cm
Height	53 cm
Weight (no base plate)	4 kg
Weight (with base plate)	8.5 kg
Excitation	
Repetition Rate	1 kHz
Pulse Width	10 μs
265 nm	11 mW
280 nm	18 mW
295 nm	19 mW
310 nm	25 mW
320 nm	14 mW
340 nm	16 mW
Emission	
f/#	4
Spectral Resolution	380 pm

Applying the Beer-Lambert law, and differentiating for the expected absorption of the infinitesimal slice, $\Theta(x)$ can be written as

$$\Theta(x) = \frac{\eta}{4\pi} E_{abs}(x) = \frac{\eta}{4\pi} E_{target} \alpha_{excite} e^{-\alpha_{excite} x} \qquad [2]$$

where E_{target} is the incident energy on the sample, α_{excite} is the analyte's absorption coefficient at the excitation wavelength, and the factor of 4π corrects for the isotropic fluorescent emission. The total expected emission can be found by integrating Eqn. 1 and is

$$\Phi(E_{target}, \alpha_{excite}, \alpha_{emit}) = \int_0^{L_c} \frac{\eta}{4\pi} E_{target} \alpha_{excite} e^{-\alpha_{excite} x} e^{-\alpha_{emit} x} dx \qquad [3]$$

$$\Phi(E_{target}, \alpha_{excite}, \alpha_{emit}) = \frac{\eta}{4\pi} E_{target} \frac{\alpha_{excite}}{\alpha_{excite} + \alpha_{emit}} \left[1 - e^{-L_c(\alpha_{excite} + \alpha_{emit})}\right] \qquad [4]$$

where L_c is the length of our cuvette. We estimate the depth of field of our parabolic mirror at ≈ 2 cm, so the cuvette length presents the limiting factor. Following the treatment described previously (Taschuk *et al.*, 2008), it is possible to write the expected signal produced by our prototype, *S*, as

$$S = LTR_{detector} \Phi(E_{target}, \alpha_{excite}, \alpha_{emit}) \qquad [5]$$

where *L* is the detector luminosity, with units of Sr cm^2, *T* represents the detector losses (unitless), and *R* is the detector gain with units of Counts μJ^{-1}. In the limit of strong absorption, $\alpha >> L_c$, the fluorescence signal will be saturated and will not depend on concentration. In the limit of weak absorption, $\alpha << L_c$, the fluorescence signal will be negligible. For the case of $\alpha \sim L_c$, we expect a quasilinear behaviour.

We tested the expected behaviour using diesel in chloroform, which allowed us to test a wide concentration range. A representative diesel signal is shown in Fig. 2a, which shows the fluorescence signature for a 4 parts per thousand concentration. The peak at 265 nm is reflected light from the excitation LED. Diesel signals were numerically integrated from 300 nm to 460 nm; the results for different concentrations are given in Fig. 2b. The line in Fig. 2b is a best fit to Eqn. 5; an absorption coefficient of ≈ 4200 cm^{-1} is obtained.

Overall, the expected behaviour is observed: a quasilinear region at low concentrations followed by a saturated signal at higher concentrations. However, at very high concentrations, the model fails to capture the observed behaviour. One possible explanation for this discrepancy is the rapidly changing Fresnel losses as one moves from a solution dominated by diesel to one dominated by chloroform. Another effect that has not been captured is solvent fluorescence quenching, which may affect the results here (Patra and Mishra, 2002).

Further work will be required to incorporate these effects. Such work will also allow a direct evaluation of some of the instrumental factors. Although t is possible to estimate luminosity, some prototype components are not fully specified by the manufacturer, rendering a reliable estimate of detector responsivity very difficult. However, this will require precise knowledge of the analyte solutions used to characterize the instrument.

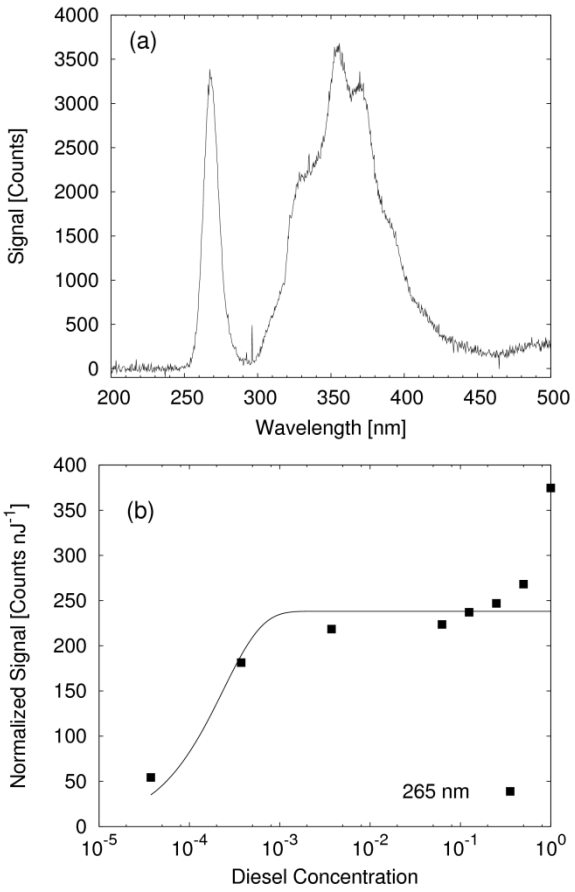

Figure 2: (a) Representative diesel spectrum at a concentration of 4 10^{-3} in chloroform. Diesel signatures were integrated numerically and are shown in (b) for different concentrations. The line in (b) is a best fit of Eqn. 5 to the data, excluding the bulk diesel data point. An absorption coefficient of ~ 4200 cm^{-1} is obtained.

Signal Analysis

Figure 3 gives a representative background corrected spectrum collected by our. Good fits to the LED signatures and primary PAW fluorescence peak are achievable with a skew normal distribution (O'Hagan and Leonard, 1976):

$$P(x) = 2\exp\left(-\frac{(x-x_0)^2}{2\sigma^2}\right)\left[1+\mathrm{erf}\left(\frac{a(x-x_0)}{\sqrt{2}}\right)\right] \quad [6]$$

where α is a measure of distribution asymmetry. This is an empirical fit only. Best fits to the LED peak, the PAW fluorescence peak, and a green defect associated with the UV LED are also shown in Fig. 3. The fit may be used to remove the LED signature, or to numerically integrate the fluorescent intensity observed by the prototype. The green defect will be easily removed with a short-pass filter in a future prototype.

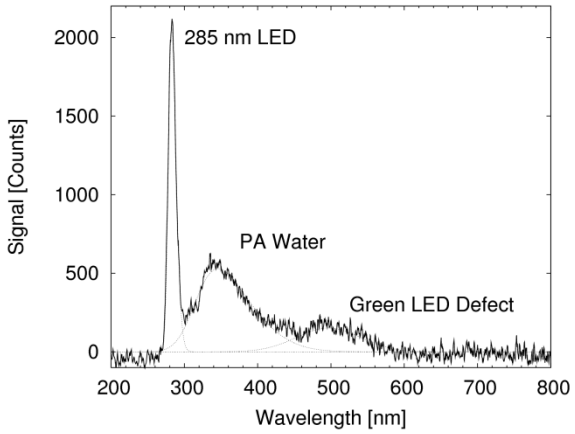

Figure 3: Characteristic spectrum from our prototype. Three components have been identified and fit. From left to right, the scattered light from the LED, the NA peak, and a green artifact from the UV LEDs.

Dark current in Ocean Optics spectrometers can add significant background to the spectra acquired with our prototype. For each integration time used here, a background spectrum was taken with no light incident on the detector. This background was subtracted from all spectra prior to analysis.

INSTRUMENTAL PERFORMANCE

Comparison with Benchtop Instrument

Our prototype output was compared with that from a benchtop fluorescence spectrometer for PAW samples at different excitation wavelengths. Since the linewidth of the excitation light in the bench top instrument is much narrower than that of the prototype, it was necessary to remove the scattered light from the LEDs, using the procedure described above.

The normalized spectra from both instruments are shown in Fig. 4.

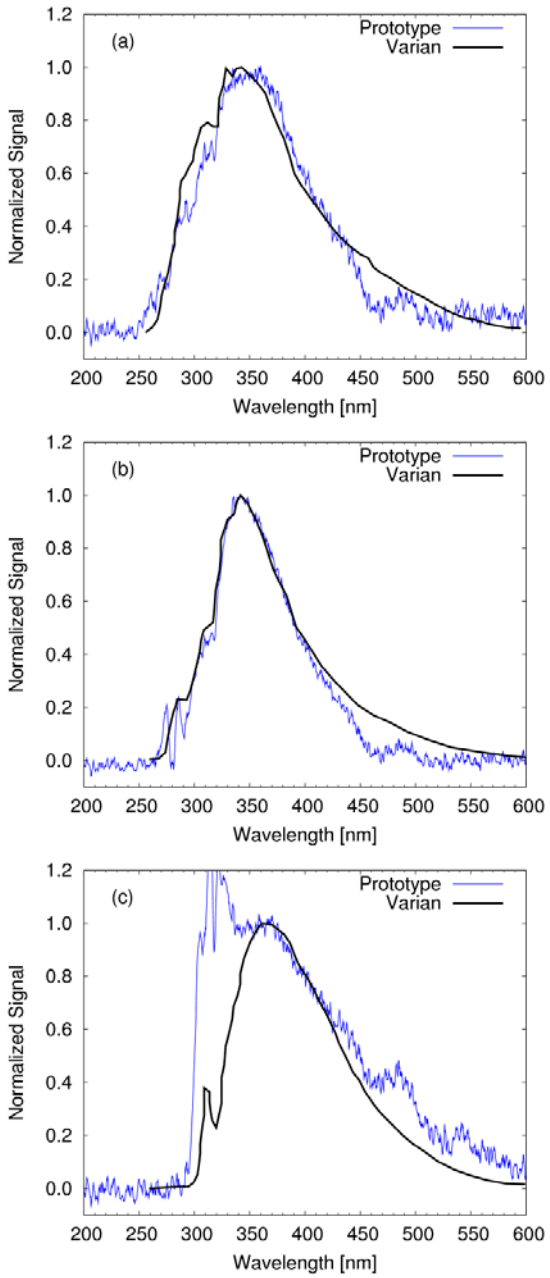

Figure 4: Comparison of normalized spectra obtained with prototype and bench-top standard at excitation wavelengths of (a) 270 nm, (b) 280 nm and (c) 310 nm. With reflected light from the UV LEDs has been removed, the agreement between the prototype and standard instrument is excellent. In some cases removal of the LED signature is not yet optimized, and will require further work.

Qualitatively, the agreement between the two instruments is excellent. In cases where the LED signature fully overlaps with the emission spectrum, the LED removal will require further work. However, in the context of a screening instrument, the current performance is considered acceptable.

NA limit of detection in filtered PAW

To determine if our prototype could detect NA at industrially relevant levels, samples from three industrial sites were measured. Prior to fluorescence measurements, samples were filtered for particles larger than 450 nm. Concentration of NA in the filtered PAW was determined using Fourier-transform infrared spectroscopy (FTIR), which required additional sample preparation using a process similar to that outlined by Jivraj *et al.* (1995).

FTIR sample preparation starts with 500 mL of filtered PAW; sample pH is raised to 11.5 by adding NaOH. Subsequently, 25 mL of dichloromethane (DCM) is added to the sample. The sample is shaken, and the DCM is drained. This entire process is repeated three times. The sample's pH is then lowered to 2 by adding HCl; and rinsed three times with 25 mL of DCM. The DCM is allowed to evaporate overnight, and NA residue is collected on the beaker. The residue is collected by adding 30 mL DCM to the beaker, and then measured in the FTIR. To determine concentration the 1706 cm^{-1} and 1743 cm^{-1} peak heights are measured and combined. The FTIR is calibrated using commercially available NA (Sigma Aldrich), rather than petroleum-derived NA.

To produce samples at different concentrations filtered PAW samples were diluted with deionized. The fluorescence from each sample was measured at each excitation wavelength. The quartz cuvettes used to hold the samples were triple rinsed with deionized water between measurements. Integration time was 5 seconds, and 5 averages were used for a total measurement time of 25 seconds. Background removal was as described above.

For each spectrum, the NA fluorescence peak was fit with a skew Gaussian distribution. The peak was numerically integrated to calculate total signal strength. Noise was estimated from the standard deviation of pixel-to-pixel variation in an adjacent region of the spectrum with no features. The signal-to-noise ratio (SNR) is defined as

$$SNR = \frac{\int S(\lambda) d\lambda}{\sigma \sqrt{N_{channels}}} \quad [7]$$

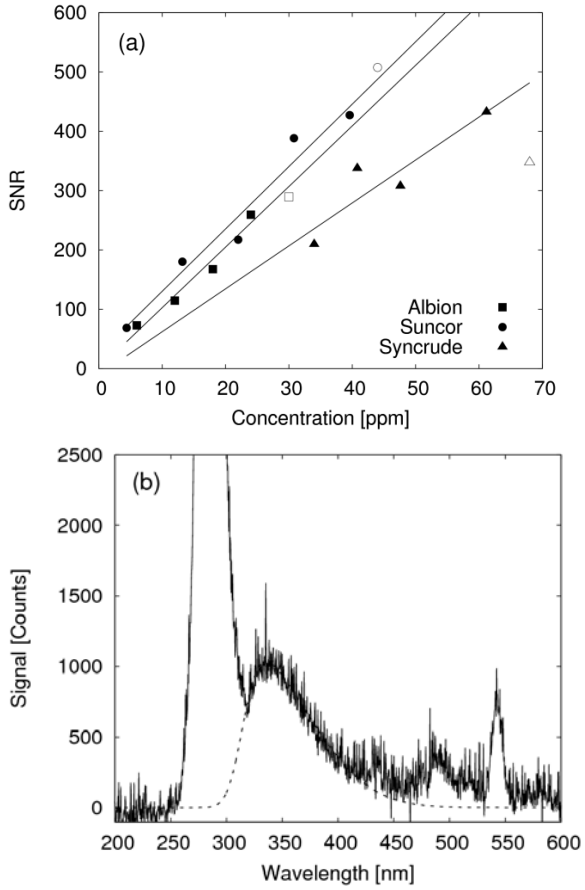

Figure 5: (a) Signal-to-noise ratio as a function of NA concentration, and best linear fits to the data set. (b) Sample spectrum for 13 ppm NA in filtered PAW. The PAW peak at 340 nm is still clearly visible, even without removal of the LED signature. Excitation wavelength was 285 nm, integration time was 5 seconds, and 5 spectra were averaged. The open symbols are unfiltered samples and were excluded from the fits.

where S is as defined in Eqn. 5, σ is single channel noise, and $N_{channels}$ is the peak width. Noise is scaled to the peak width using the conventional $N^{1/2}$ from Poisson noise. The SNR for the three different sites and an excitation wavelength of 285 nm is given in Fig. 5a. Differences are observed between different sample sources, but are linear within them. SNR is remains excellent at the 10 ppm level.

NA signatures in unfiltered PAW

The performance of our prototype on unfiltered samples was also tested, and the results are shown in Fig. 6. These samples were cloudy, indicating significant scatter in the visible wavelengths. However, despite increased scattering, the NA signature can be clearly observed in the unfiltered samples for all three industrial sites. This is a promising result, as it indicates that the prototype can measure samples obtained from the field with little or no preparation.

DISCUSSION

We have developed a field portable LED-based fluorescence spectrometer that can measure NA at industrially relevant levels. Although this initial result is promising, we feel that there are significant improvements that can be made to enhance its performance, and greatly reduce its size. The following is a discussion of alternative techniques for NA detection and opportunities for improving performance of our prototype. In general, the tradeoff is between ease-of-use and/or measurement time and performance.

For example, laser-induced fluorescence (LIF) routinely achieves LOD in the ppb range, but requires high power lasers. There is a broad literature on LIF for hydrocarbon detection in water (Kenny *et al.*, 1987; Taylor *et al.*, 1993; Filippova *et al.*, 1993; Lewitzka *et al.*, 1999). The performance is excellent, but high-powered lasers are not well-suited for field use, and are certainly not portable. Several standard chemical techniques have been applied to detection of NA in water, including gas chromatography mass spectroscopy (GC-MS) and Fourier-transform infrared spectroscopy (FTIR) (Scott *et al.*, 2008), capillary high-performance liquid-chromatography quadrupole time-of-flight mass-spectroscopy (HPLC/QTOF-MS) (Bataineh *et al.* 2006) and synchronous flourescence spectroscopy (SFS) (Kavanagh *et al.*, 2009). Scott *et al.* (2008) have compared GC-MS and FTIR for quantifying NA concentrations, and found that GC-MS is about 100 times more sensitive with a LOD of 10 ppb. Moreover, Scott *et al.* (2008) report that FTIR consistently reports a higher concentration that GC-MS, although the ratio varies with sample source.

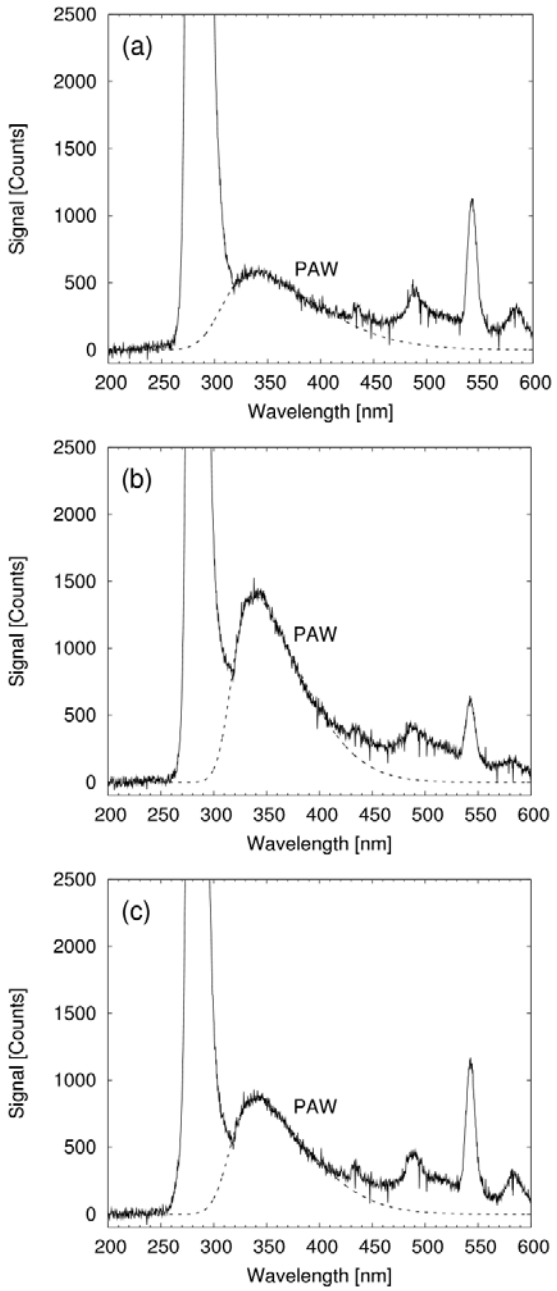

Figure 6: Fluorescence signature of NA in unfiltered PAW from (a) Albian, (b) Suncor and (c) Syncrude. The NA peak is clearly visible in all samples, even without removing the LED signature. This indicates that the prototype can be successfully applied in the field with little or no sample preparation. The features above 500 nm are leaked room light.

This result is troubling for the calibration of our instrument, and other work that depends on FTIR. It was already clear from the LOD work presented above that discrepancies exist between the concentration reported by the FTIR and the fluorescence intensity reported by our instrument, as seen in Fig. 5. When considered in combination with the observations of Scott *et al.* (2008), it is clear that obtaining additional calibration standards should be a priority. Despite these issues, the factor reported by Scott *et al.* suggests that the performance of our prototype is better than that reported here. It is possible that the performance reported here will improve, pending additional investigations.

Bataineh *et al.* (2006) have developed an HPLC/QTOF-MS technique for characterizing NA and studying biological remediation. They report excellent absolute detection limits in the pg range. The technique is also capable of NA speciation by carbon number and Z-series, and should lead to a better understanding of NA toxicity and the efficacy of the different NA remediation techniques. However, significant sample preparation is required to achieve the performance reported by Bataineh *et al.*, and is not well suited to field use.

From the perspective of a field instrument, more promising is the comparison of our instrument with the lab based work by Kavanagh *et al.* (Kavanagh *et al.*, 2009). While the LOD from Kavanagh's work is not clear, they report signals down to a few mg L^{-1}. The performance of our prototype is in the same range, and we expect improvements are possible.

While the other techniques can achieve significantly better performance than our prototype, none of them are well-suited for field use, and all of them require sample preparation. Here we have demonstrated a prototype instrument that detects NA in water at the ppm level, with little or no sample preparation. Moreover, several opportunities exist for improving the performance of our instrument in future versions.

Inspection of Eqn. 4 and Eqn. 5 suggests two avenues for improving performance: increased power on target (E_{target}) and increased luminosity (L). It is clear from our model and the results presented in Fig. 2 that the only method for increasing signal levels it to increase E_{target}; the other parameters, η and α are physical constants of the analyte. Optical power can be improved by increasing the number of LEDs in the system, or by waiting for increased power in a LED package - doubling time for LED power is approximately 2.3 years (Steele, 2007). The other route to

improved performance is to increase the luminosity of our system through increased f-number or aperture size. Both should be possible with improved optical design.

CONCLUSION

Monitoring the presence and migration of NA in PAW is desirable for environmental and economic reasons; reducing the potential for toxic releases and improving the lifetime of oil sands industrial plants, respectively. We have developed a field portable LED-based fluorescence spectrometer that can measure NA below the 10 ppm level. Our prototype uses LED wavelengths between 265 nm and 340 nm as an excitation source, and a compact CCD Ocean Optics spectrometer as a detector. Although other techniques can achieve better limits of detection, our instrument is field-portable, and capable of measuring NA in PAW without sample preparation. In addition to this initial promising result, through development of an optical theory for our device we have identified several feasible routes to improving performance of our instrument in future versions.

ACKNOWLEDGEMENTS

The authors gratefully acknowledge Professor Michael Brett of the University of Alberta and the NRC National Institute for Nanotechnology for valuable discussions. In addition, we gratefully acknowledge funding from the Natural Sciences and Engineering Research Council of Canada (NSERC), the Oil Sands Tailings Research Facility (OSTRF), the Canadian Institute for Photonics Innovations (CIPI), the Canada School of Energy and Environment (CSEE), Alberta Innovates Technology Futures (AITF) and the Integrated Nanosystems Research Facility at the University of Alberta.

REFERENCES

Alarie, J., T. Vo-Dinh, G. Miller, M. Ericson, D. Eastwood, R. Lidberg, M. Dominguez (1993). Development of a battery-operated portable synchronous luminescence spectrofluorometer. Rev. Sci. Instrum., **64**:2541– 2546.

Allen, E. W. (2008). Process water treatment in Canada's oil sands industry: I. Target pollutants and treatment objectives. J Environ Eng Sci, **7**:123–138.

Baird, W., N. Nogar (1995). Compact, self-contained optical spectrometer. Applied Spectroscopy, **49**:1699– 1704.

Bataineh, M., A.C. Scott, P.M. Fedorak, J.W. Martin (2006). Capillary HPLC/QTOF-MS for Characterizing Complex Naphthenic Acid Mixtures and Their Microbial Transformation. Analytical Chemistry **78**: 8354 - 8361

Brown, L. D., M. Alostaz, A. C. Ulrich (2009). Characterization of Oil Sands Naphthenic Acids in Oil Sands Process-Affected Waters Using Fluorescence Technology. In 62nd Canadian Geotechnical Conference, Halifax, Nova Scotia, 1-7.

Clemente, J., P. Fedorak (2005). A review of the occurrence, analyses, toxicity, and biodegradation of naphthenic acids. Chemosphere, **60**:585–600.

Filippova, E., V. Chubarov, V. Fadeev (1993). New possibilities of laser fluorescence spectroscopy for diagnostics of petroleum-hydrocarbons in natural-water. Can J Appl Spectrosc, **38**:139–144.

Frank, R. A., K. Fischer, R. Kavanagh, B. K. Burnison, G. Arsenault, J. V. Headley, K. M. Peru, G. V. D. Kraak, K. R. Solomon (2009). Effect of Carboxylic Acid Content on the Acute Toxicity of Oil Sands Naphthenic Acids. Environ. Sci. Technol., **43**:266–271.

Hart, S., R. JiJi (2002). Light emitting diode excitation emission matrix fluorescence spectroscopy. Analyst, **127**:1693–1699.

Jivraj, M., M. Mackinnon, B. Fung (1995). Naphthenic Acid Extraction and Quantitative Analysis With FT- IR Spectroscopy. In Syncrude Analytical Manuals, 4th Edition, Research Department, Syncrude Canada Ltd., Edmonton, AB.

Kavanagh, R. J., B. K. Burnison, R. A. Frank, K. R. Solomon, G. V. D. Kraak (2009). Detecting oil sands process-affected waters in the Alberta oil sands region using synchronous fluorescence spectroscopy. Chemosphere, **76**:120–126.

Kenny, J., G. Jarvis, W. Chudyk, K. Pohlig (1987). Remote laser-induced fluorescence monitoring of ground- water contaminants: prototype field instrument. Instrumentation Science & Technology, **16**:423–445.

Lewitzka, F., U. Buenting, P. Karlitschek, M. Niederkrueger, G. Marowsky (1999). Quantitative analysis of aromatic molecules in water by laser-induced fluorescence spectroscopy and multivariate calibration techniques. Proceedings of SPIE, **3821**:331.

Obeidat, S., B. Bai, G. D. Rayson, D. M. Anderson, A. D. Puscheck, S. Y. Landau, T. Glasser (2008). A multi-source portable light emitting diode spectrofluorometer. Applied Spectroscopy, **62**:327–332.

O'Hagan, A., T. Leonard (1976). Bayes estimation subject to uncertainty about parameter constraints. Biometrika, **63**:201–203.

Patra, D., A. Mishra (2002). Total fluorescence quantum yield and red shift of total fluorescence maximum as parameters to investigate polycyclic aromatic compounds present in diesel fuel. Spectroscopy Letters, **35**:125–136.

Scott, A. C., R. F. Young, P. M. Fedorak (2008). Comparison of GC-MS and FTIR methods for quantifying naphthenic acids in water samples. Chemosphere, **73**:1258–1264.

Slavcheva, E., B. Shone, A. Turnbull (1999). Review of naphthenic acid corrosion in oil refining. Brit Corros J, **34**:125–131.

Steele, R. V. (2007). The story of a new light source. Nat Photonics, **1**:25–26.

Taschuk, M.T., Y. Godwal, Y.Y. Tsui, R. Fedosejevs, M. Tripathi, B. Kearton (2008). Absolute characterization of laser-induced breakdown spectroscopy detection systems. Spectrochim Acta B, **63**:525–535.

Taylor, T., G. Jarvis, H. Xu, A. Bevilacqua, J. Kenny (1993). Laser-based fluorescence EEM instrument for in-situ groundwater monitoring. Instrumentation Science & Technology, **21**:141-162.

INTENSIVE HEAT METHOD FOR USING NON-SEGREGATE FINE TAILING FOR GENERATING HOT PROCESS WATER AND STABLE SOLIDS THAT CAN SUPPORT TRAFFIC

Maoz “Moose” Betzer-Zilevitch, Ex-Tar Technologies Inc., Alberta, Canada

ABSTRACT

This paper presents a revolutionary method of solving the non-segregate fine tailing water problem through the use of intensive heat processes, while recovering the water and heat and using it in an oilsands open-mine extraction mining facility. The new process includes the internal combustion of low quality fuel, such as sulphur rich petcoke, as the heat source for generating the hot water used for the bitumen extraction. This eliminates the use of natural gas for generating hot water.

The method presented minimizes the need for settling fine tailings basins and enables a sustainable tailing practice of “reclaiming as you go”. The sulphur content of the low grade carbonic fuel contributes to the soil stabilization. The revolutionary method can use the water softening process sludge waste, such as WLS (Warm Lime Softener), widely used for OTSG water treatment in EOR facilities (like SAGD or CSS). The reaction generates calcium sulphite or calcium sulphate, possibly an-hydrate, which increases the soil stability of a land-fill in order to support traffic. The process includes a DCSG (Direct Contact Steam Generator) reactor that can transfer the liquid MFT to solid particles and gas (steam). When using petcoke as the fuel, for each one ton/hour of combusted petcoke, about 100ton/hour of 90C heated process water is generated. 6-12 tons/hour of MFT can be converted into hot process water and dry solids.

Due to the direct contact internal heat exchange, this method has a high thermal efficiency which minimizes the amount of emitted CO_2 for generating the hot process water used for bitumen extraction.

INTRODUCTION

Background

Tailing pond water is a by-product of the oil, water and sand separation process. The tailing pond problem is continually escalating with oilsands mining development. The mature tailing water contains suspended fine sediments, clay, heavy metals, hydrocarbons like bitumen, diluent, PAHs (Polycyclic Aromatic Hydrocarbons) and Naphthenic Acids, sulphate, and sodium salinity. In recent years, due to the introduction of solvents as part of the extract froth treatment, the tailings include a larger percentage of asphaltin and solvent remains. To achieve good bitumen separation and recovery, heat and extensive mixing energy is introduced to the water and ore mixture. This increases the entropy in the tailing slurry. To reverse this process and separate the tailings to their components (solids and water), more energy- in the form of mechanical (acceleration/pressure) or thermal (heat) energy- is required. The search to achieve reverse processing to separate the solids and the water without a significant energy investment is similar to the search for the “Perpetuum Mobile”. The most available energy source is the sun, which, combined with low air humidity, can evaporate the water out from fine tailings, thus separating the solids in a stable form that can support traffic. The problem in the Wood Buffalo area is the lack of sun energy, combined with high air humidity and low temperatures during most of the year. This makes the removal of the water from the MFT (Mature Fine Tailing) very challenging. With global warming, the precipitation in this northern area can even increase, which will accelerate this problem. The proposed solution presented in this paper is to replace the sun energy as the driving energy source for drying the MFT (Mature Fine Tailings) with intensive heat generated from combustion energy where the heat and the water derived from the MFT is not wasted as it is used in the bitumen extraction process. The solids can be disposed of efficiently, in a way that they can support traffic.

The following self explanatory block diagram describes this overall concept.

The tailings are fed into the DCSG (Direct Contact steam generator):

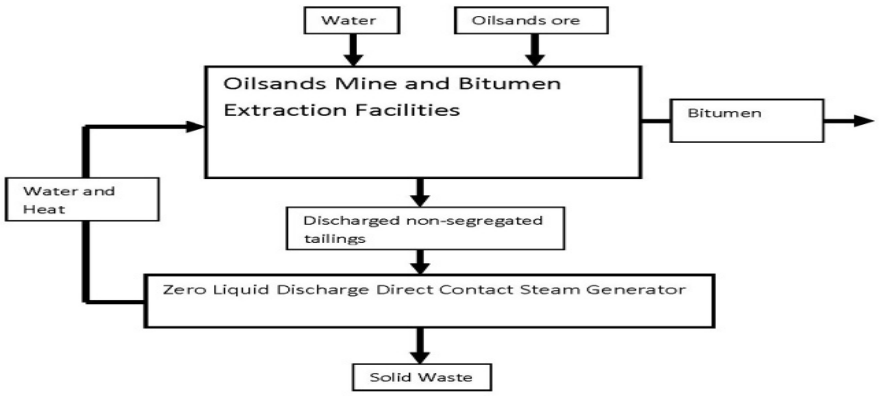

Figure 1. ZLD Oilsands mine block diagram.

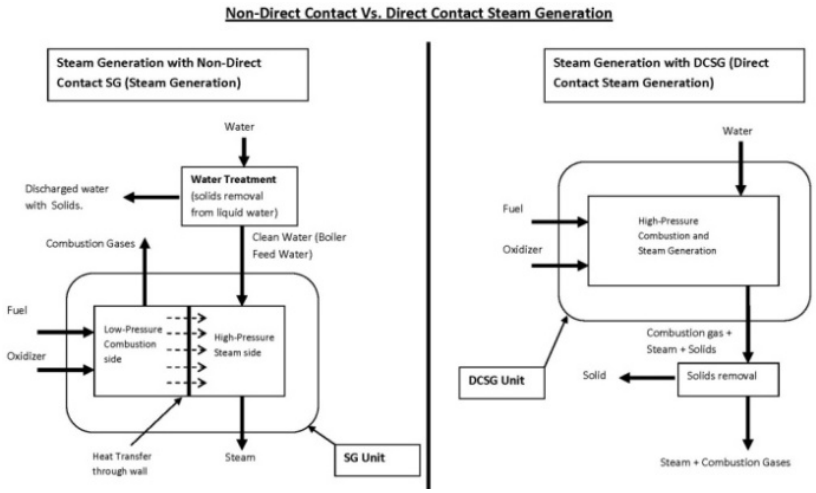

Figure 2. Direct contact VS. Non-direct contact steam generation

The DCSG is a key element in the proposed technology. The principal is simple and effective.

The following figure describes the basic principle of a Direct versus a Non-direct steam generator:

In “Direct Contact Steam Generation” (DCSG), the heat is transferred between the liquid water and the combustion gas through the direct mixing of the two flows (the tailings and the combustion gases). In the DCSG, the combustion pressure is similar to the produced steam pressure and the combustion gases are mixed with the steam. The DCSG can also be referred to as a direct contact evaporator or direct contact dryer. In a Non-Direct Steam Generator (like a steam boiler with a steam drum and a mud drum) or a “Once Through Steam Generator” (OTSG), the heat transfer and combustion gases are not mixed and the heat transfer is done through a wall (typically a metal wall), where the pressure of the generated steam is higher than the pressure of the combustion. This allows for the use of atmospheric combustion pressure and high pressure steam. The product is pure steam (or a steam and water mixture, as in the case of the OTSG) without combustion gases. Because the non-direct heat transfer, the water quality should be controlled to control mineral build-ups or should include a means to remove build-ups and scaling should be used.

It is possible to use a partial combustion gasifier as the DCSG, while generating syngas, as presented in Figure 3.

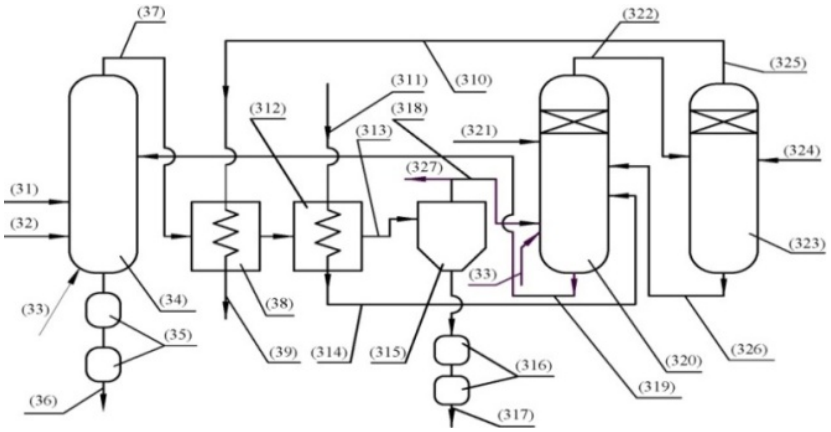

Figure 3. Partial combustion gasifier DCSG.

Valuable products, like hydrogen, can be recovered from the syngas. In the following figure, a fluidised bed gasifier 34 is used to generate syngas. Additional fine tailings 319 can be injected to recover a portion of the partial combustion heat and can be converted to steam, making the gasifier a DCSG. The produced syngas 313, after solids are removed from it, can be used for hydrogen production in a hydrogen plant.

The following section will briefly describe 3 examples for possible DCSG solutions that can be used for treating the MFT:

1. *DCSG with up-flow fluid bed combustion:*
   This option is briefly described below. Additional tailings 52 are injected at the upper section of the pressurized fluid bed boiler 51 or gasifier. A portion of the heat is used to generate HP (high pressure) steam through the heat exchanger 56 inside the boiler while the rest is used to generate steam through direct contact with the injected tailings.

2. *Vertical Up-flow DCSG (direct contact steam generator) with tailings injection and liquid bottom collecting bath:*

Combusted, heated gas 5 is generated in AREA 1 with the use of a pressurized combustor, possibly as a component of a pressurized boiler. The combustion gases are introduced into vertical up-flow steam generator 1. The vertical vessel includes several sections as follows:

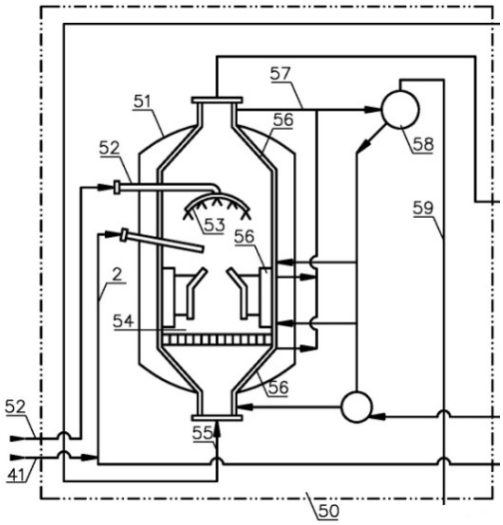

Figure 4. Pressurized Fluid Bed boiler and DCSG with tailings injection.

3.

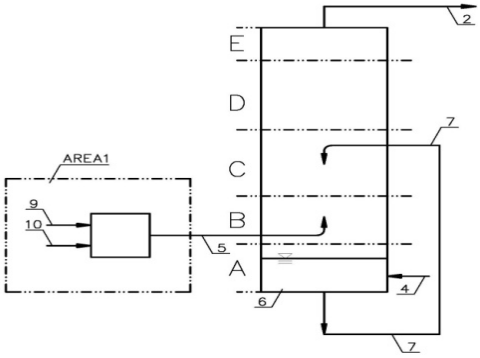

Figure 5. Vertical up-flow direct contact steam generator.

Section A- located at the bottom of the vessel including liquid bath water 6. At section A, the water can be maintained at the saturated temperature or lower. The water section will collect and mobilize any solid particles not carried on by the up-flow combustion gas and steam mixture and any liquid water droplets that were not converted to steam. Tailings flow 7 is continually recycled and injected into the up-flow gas stream in Section C.

Section B (located above the liquid water bath) - hot combustion gases 5 are injected into this section. Another option is to integrate combustion into the vessel of the steam generation facility 1, wherein combustion will occur in Section B, internally generating the pressurized combustion gases in section B. The hot combustion gases flow upwards in section B, creating the up-flow effect.

Section C is located above section B and it includes the mixture of the tailings from the bottom of the vertical vessel, possibly with additional tailings. It is used to generate an up-flow of gas and solid particles carried by the momentum of the liquid water changing into gas. The amount of injected tailings is such that most of the water will be converted into steam and that dry solid particles will be carried on by the up-flow gas stream and will be removed from the steam generator reactor in a gas and solid form. The discharged up-flow from section C into section D is a non-saturated, “dry” mixture of steam and combustion gas where the steam is super-heated at the partial pressure it is subjected to.

Section D is located above section C and it is a homogenizer and steam generation section. In section D, the direct contact heat transfer between the up-flow combustion gas and the carried-on liquid droplets is completed. Liquid tailings are converted into a homogeneous mixture of steam and dry solid particles that were carried on with the liquid water from section A. Section E is located at the top of the vertical vessel. The homogeneous mixture of the up-flow steam, gas and dry solid particle mixture 2 is discharged from this section. The product leaving section E is a flow of high - pressure dry steam and combustion gas with solid particles.

Fuel 1, oxidizer 2, and low quality water, like tailings, 3 are supplied to a high pressure combustor 6 at section A, which is located at the top of the vertical vessel. The fuel 1 may be coal slurry, petcoke slurry, or hydrocarbons (such as untreated heavy low quality crude oil, VR (vacuum residuals), asphaltene, or any available carbon or hydrocarbon fuel). The oxidizer gas 2 can be enriched air or oxygen. The combustion is stoichiometric, and the amount of heat energy generated is greater than in partial combustion, resulting in extremely high temperatures, especially if oxygen is used as the oxidizer. The temperature is controlled by the water injected into the combustor 3. The water can be supplied with the fuel in a slurry form. The combustion section can include a radial heat exchanger 9 that is located near the vessel wall. The heat exchanger heats a saturated, solid free steam and gas flow 10 to generate a dry, super heated steam and gas flow or generate high pressure pure steam. The combustion gas with the generated solids, possibly in liquid form (like melted slag), flows downward to the direct contact steam generation in section B. In this section, tailings 7 are injected and dispersed into the down flowing gas flow. The tailings are converted into gas, which leaves the solids in a dry particle form mixed with the gas. The gas and solids flow to the discharge section, located low in the vessel. In this section, the gas flow is deflected, this forces a change in direction to improve the mixture and to prevent accumulation of large solid particles, possibly in a sticky form, and possible liquid droplets from discharging with the gas flow out from the system where it can settle in the down-flow pipe and equipment. At the bottom of the vessel, there is the fluid bed section D where cold gas 4 circulates and flows upwards to suspend the solids bed. Solids are discharged from the bottom of the vessel 5 to maintain the bottom fluid bed solids level. The up-flow velocity above flow 4 in section D and below discharge flow 8 in section C, is in the range of 0.2m/sec to 3m/sec to support the upward carry-on solids with a particle size of up to 1.2 mm.

4. Internally Fired Rotating DCSG:

The internally fired rotating DCSG is formed from a pressurized sloped vessel 71 which includes an internal combustion head at its high point. Fuel 75 and oxidizing gas 76 are injected through the combustion head 78 and combusted inside the pressurized sloped vessel. The vessel includes internal rotating enclosure 715 that further includes chains 72 connected to the rotating enclosure in the sloped vessel 71. Tailings 77 are injected into and around the combustion reaction area 73 to control the combustion temperature and to protect the combustion area structure section 74 while generating steam. Additional low quality water 77 is injected below the combustion head to prevent

an excessive reduction in the combustion temperatures as the temperature to support combustion is significantly higher than the temperature for steam generation. The combustion area is insulated 713 to protect against the high temperatures. The heat transfer is enhanced by the use of chains 72 that are connected to the rotating enclosure 715. The chains also remove solid build-up deposits, to keep the rotating vessel clean. The rotating vessel can include a partial separation 714 to enhance the heat exchange between the different phases. The steam and combustion gas 717 are discharged from the vessel discharge section 71 through pipe 716 which is located at the upper section of the low end of the sloped vessel. The internal rotating enclosure 715 is supported on rotating wheels 710. The solids are discharged through a screw 720 that collects the discharged solids falling by gravity from the low end of the rotating enclosure. The solids are then collected by the rotating screw where they are discharged through valve 721 to maintain the pressure. The solids are in a dry particle form or in a stable slurry form- a stackable non-flowable form. The discharge screw is located perpendicular to the rotating enclosure to collect the solids or the concentrated slurry. Because the solids or the slurry are not flowable, a perpendicular single or double screw can be used, where the rotating screw energy is used for mixing and mobilizing the solid particles. The apparatus includes a stationary pressure vessel 71 with an internal rotating enclosure 715 to simplify the feed and discharge connections. However, it should be obvious to use a rotation seal for the connections and use a pressure controlled rotating vessel with swivels for the connections, at least at low and medium pressures of up to 15bar.

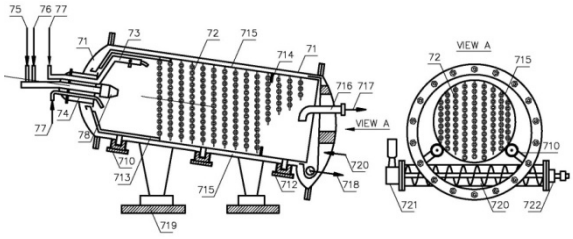

Figure 6. Internally Fired Rotating DCSG.

ELIMINATING THE TAILING POND

The DCSG can be integrated with an open mine oilsands extraction facility as described in Figure 7 below, where the hot process water for the ore preparation is generated by recovering the heat and condensing the steam 52 generated from the fine tailings 61 and the combustion gases, without the use of a tailing pond. This concept will require major changes to the mining logistics as it replaces the hydro-transport with major screening and trucking efforts as a means of transporting the course tailings 51, mainly sand, and the dry MFT 53, mainly clay, generated by the DCSG, back to the pit.

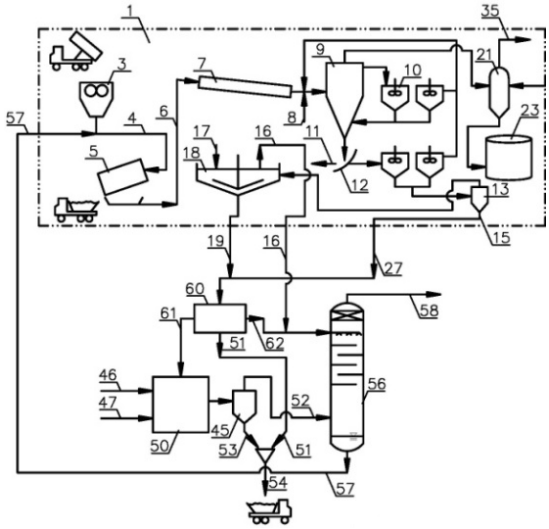

Figure 7. Oil sands mine without the use of tailing pond.

SIMULATIONS

1. The following flow table is a simulation of the inventive process that was done using VMG Sim simulation program.

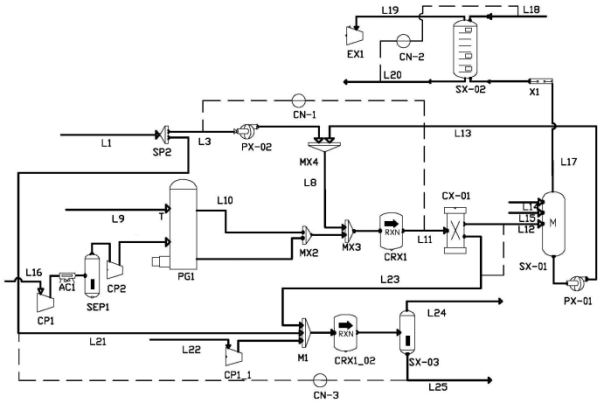

Figure 8. Process simulation diagram.

The following example, described in Figure 8 and Tables 1 and 2, is a simulation of the process. Coal feed with a high sulfur content in a slurry form, together with compressed air, was fed into a Plasma gasifier PG1. The system pressure is 10 bar. The coal flow burned in the process is 1.08 mt/hour. The amount of sulfur in the coal was increased in the simulation to 13.8%, which is more than four times the amount of sulfur in low grade coal, in order to check the sensitivity of the process. Some air by-passes the gasifier and is mixed with the syngas to generate additional heat and for full combustion. Flow L8, composed of tailing pond water and make-up water, is supplied with the lime stone to SX-01 and mixed with the combusted syngas to generate a stream of gases and solids. The L8 flow includes the pond water (MFT), together with the recycled water, that includes the solids that by-pass the solid separator and the lime stone solids. The L8 flow is 11.3 mt/hour at a temperature of 105C and has a 24% solids content by weight. The discharge from CRx1, called flow L11, is the discharge from the DCSG before removing the solids. Pond water with 23% solids is supplied to the process at a rate of 6.2 mt/hour and at a temperature of 25C. Water L15 and lime stone is supplied to SX-01. Water flow L15, is different from the process water used after heating, for mixture with the oilsand ore. It can include fine tailings as long they will stay in a liquid form, even after adding the lime stone and the by-pass solids. Another option is to eliminate the whole stage of SX-01 and replace it directly with the “Water Recovery Tower” SX-02, where the solid remains are scrubbed by the oilsands plant hot process water (stream L20) and the lime stone is supplied with the petcoke fuel or with the “Pond water” (MFT water that will replace the L8 flow in the present simulation). One option is to supply dry solids from separator CX-01 to mixer M1 where they are mixed with additional MFT (therefore removing additional MFT from the tailing pond) and with low pressure air to oxidize the generated $CaSO_3$ to gypsum and to increase the water content in the solids to reduce potential dust while still having a stable, solid material that can be used as back-fill and to support traffic. The saturated steam and combustion gas mixture from multi feed separator SX-01, named L17, is at a temperature of 166C, has a mass flow of 20.4 mt/hour and includes 50% steam, and the rest is the combustion NCG. Flow L17 is directed to the water recovery tower SX-02 where it is washed with cold water L18 which is the water supplied from the oilsand mine plant and used, after heating, for the extraction process for mixing with the oilsands ore. The cold water L18 flow is at a temperature of 20C and has a mass flow of 89.3 mt/hour. The cold non condensable gases expand on turbo-expander EX1 with an efficiency of 48% and generate 240hp. Another option is to use lower process pressures. In this case, there will be no need to recover the pressurized gas energy as the energy invested in compressing the oxidizer will be minimized as well. The produced hot water L20 temperature is 90C with a mass flow of 99.7 mt/hour. The additional water in the heated process water is due to the steam condensation from flow L17, which includes 50% steam. The produced hot water L20 is directed to the oilsand plant, where it is mixed with the oilsands ore for extracting the tar. The CO_2 product ratio (defined as the amount of product hot water at 90C) generated per 1 kg of generated CO_2 is 40 [kg H2O/kgCO2], (without considering the air compression electrical consumption).

Table 1.

/L11 (Material Stream)				
Prop Pkg: Gasification 2010				
Connections				
Material Inlets				
	Connection		Up Stream Unit Op	
In	CRx1		---	
Material Outlets				
	Connection		Down Stream Unit Op	
Out	CX-01		---	
External Signal Connections				
	Connection		Value	
T [C]	/CN_Reactor_Outlet_T.In		250.0	
Equilibrium Results				
PropName	Bulk	Vapour	Liquid0	
Phase Fract	1.00	0.95	0.05	
T [C]	250.0	250.0	250.0	
P [kPa]	1061.93	1061.93	1061.93	
MoleFlow [kgmole/h]	922.33	875.64	46.70	
MassFlow [kg/h]	23178.30	20048.52	3129.78	
Fraction [Fraction]				
WATER	0.6059	0.6292	0.1681	
CARBON DIOXIDE	0.0640	0.0674	0.0006	
CARBON MONOXIDE	1.09E-04	1.15E-04	5.75E-07	
OXYGEN	0.0031	0.0033	0.0000	
HYDROGEN	5.06E-05	5.33E-05	5.29E-07	
ARGON	0.0036	0.0038	0.0000	
NITROGEN	0.2798	0.2946	0.0011	
gALUMINUM OXIDE	7.13E-04	1.34E-41	1.41E-02	
gCALCIUM OXIDE	3.42E-07	6.45E-45	6.76E-06	
gDIIRON TRIOXIDE	2.03E-04	3.82E-42	4.01E-03	
gDISODIUM OXIDE	7.99E-05	1.51E-42	1.58E-03	
gSILICON DIOXIDE	0.0340	0.0000	0.6706	
AMMONIA	1.02E-10	1.08E-10	2.16E-12	
CARBONYL SULFIDE	5.04E-12	5.04E-12	5.04E-12	
HYDROGEN SULFIDE	6.54E-11	6.54E-11	6.54E-11	
METHANE	0.00E+00	0.00E+00	0.00E+00	
SULFUR DIOXIDE	9.79E-04	1.03E-03	4.42E-05	
SULFUR	8.45E-11	8.45E-11	8.45E-11	
DeGypsum*	7.42E-05	1.40E-42	1.47E-03	
CalciumSulfite*	0.0069	0.0000	0.1354	
gMAGNESIUM	1.51E-04	2.84E-42	2.98E-03	
NITRIC OXIDE	4.42E-04	4.65E-04	3.05E-07	
SULFUR TRIOXIDE	1.28E-05	1.34E-05	1.10E-06	
NITROGEN DIOXIDE	5.33E-07	5.61E-07	8.73E-09	

Table 2.

/L20 (Material Stream)				
Prop Pkg: APRNGL				
Connections				
Material Inlets				
	Connection		Up Stream Unit Op	
In	Water_Recovery_Tower		---	
Material Outlets				
	Connection		Down Stream Unit Op	
Out	---		---	
External Signal Connections				
	Connection		Value	
T [C]	/CN_Hot_Water_T.In		90.0	
Equilibrium Results				
PropName	Bulk	Vapour	Liquid0	
Phase Fract	1.00	0.00	1.00	
T [C]	90.0	90.0	90.0	
P [kPa]	1050.00	1050.00	1050.00	
MoleFlow [kgmole/h]	5528.22	0.00	5528.22	
MassFlow [kg/h]	99682.60	0.00	99682.60	
Fraction [Fraction]				
WATER	0.9995	0.0690	0.9995	
CARBON DIOXIDE	3.18E-04	1.75E-01	3.18E-04	
CARBON MONOXIDE	2.99E-09	2.85E-04	2.99E-09	
OXYGEN	9.61E-07	8.17E-03	9.61E-07	
HYDROGEN	4.03E-09	1.32E-04	4.03E-09	
ARGON	1.05E-06	9.37E-03	1.05E-06	
NITROGEN	6.44E-05	7.33E-01	6.44E-05	
AMMONIA	1.30E-11	1.30E-11	1.30E-11	
CARBONYL SULFIDE	1.33E-14	1.33E-14	1.33E-14	
HYDROGEN SULFIDE	9.84E-13	9.84E-13	9.84E-13	
METHANE	0.00E+00	0.00E+00	0.00E+00	
SULFUR DIOXIDE	1.57E-04	4.21E-03	1.57E-04	
SULFUR	3.21E-12	3.21E-12	3.21E-12	
NITRIC OXIDE	4.07E-08	1.16E-03	4.07E-08	
SULFUR TRIOXIDE	1.95E-06	2.04E-05	1.95E-06	

2. The following results show a simulation of a hot water generation method for oilsand mining extraction facilities, with Fine Tailing water recycling, as described in Figure 9, for two different system pressures.

The cold process water 8 includes recycled process water together with fresh make-up water that is supplied from local sources (like the Athabasca River in the Wood Buffalo area). Another bi-product from the open mine oilsands plant is Fine Tailing (FT) 5 which, after a time, is transferred to a stable Mature Fine Tailings (MFT). Hot pressurized combustion gas or a mixture of fuel and oxidizer 1 is fed to enclosure 3. The hot combustion gases are mixed in enclosure 3 with a flow of FT 5 from Block A1. Most of the liquid water in the FT is converted to steam. The remaining solids 4 are removed from the steam and combustion gas mixture 21. Another option is to inject the carbon or hydrocarbon fuel and oxidizer gas into the steam generation reactor 3 and then combust them. Energy is released in the form of heat to generate hot combustion gas. The FT 5 can be injected with the fuel into the combustion to control the combustion temperature. The mixture of pressurized steam and combustion gas is mixed with the cold process water from Block 1A in a direct contact heat exchanger 7. A non-direct commercially available heat exchanger can be used as well. The cold process water 8 is heated to generate hot process water 9 that is supplied

back to operate the Open Mine Oilsand plant 1A. The steam generated from the FT, and possibly from the combustion, is condensed and recovered with the hot process water supplied back to Block A1. The pressurized Non Condensable Gases (NCG) from the combustion process are released at 2 or are further used or treated (not shown).

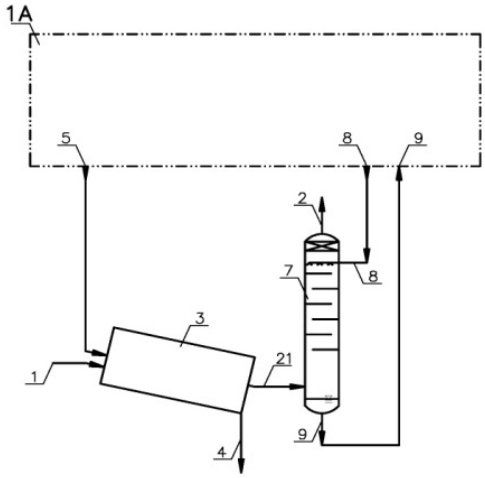

Figure 9. DCSG from tailing stream combined with extraction process water heating.

The simulation balance was done for 1 ton/hour of petcoke. The simulation shows the amount of generated hot process water as a function of the process water temperature. The results shows that for the particular process feeds and assumptions, generating high temperature water at 90C will require a higher combustion pressure system. If the temperature of the process water can be slightly reduced (to the range of 80C-85C), the system pressure can be reduced to 103kpa, without significant impact on the overall process performance. The biggest advantage for reducing the system pressure will be a reduction in the TIC cost and the operation costs. The cost and complexity of a Pressurized Fluid Bed Boiler will be significantly lower for pressures as low as 103kpa in comparison to a typical combustion pressure of 1000kpa, as is generally used for generating electricity.

LABRATORY TEST RESULTS

(Remark: The laboratory test program is currently underway. The test results will include toxicity tests of the water generated from MFT by the DCSG at different operation conditions).

1. Tailing sample analysis using GC/MS:

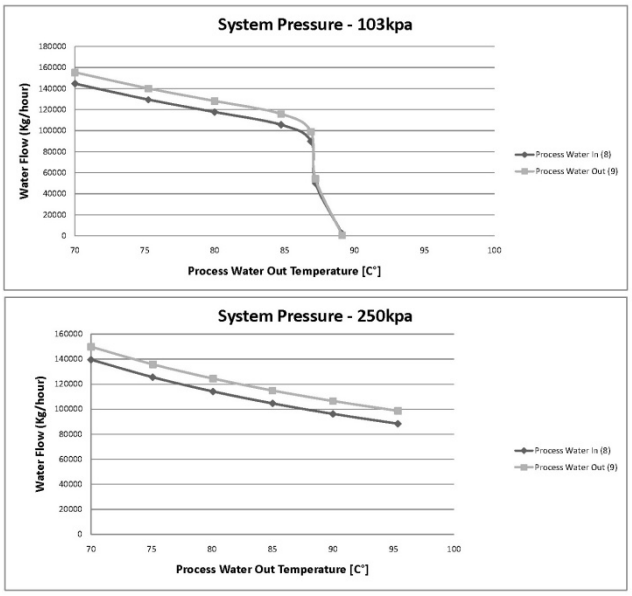

Figure 10. Simulation balance for the impact of the system pressure on the hot process water generation.

The analysis was done on a MFT sample received from OSTRF.

The following graph (Figure 11) is an illustration of the analysis results for MFT volatile compounds, up to boiling point of 150C.

The following graph (Figure 12) is an illustration of the analysis results for MFT volatile compounds, up to boiling point of 300C.

2. Heavy metals and toxicity analysis:

The toxicity was analysed using Microtox method. The heavy metals were tested using ICP. Table 5 summarizes the analysis results.

Fig.1: GC/MS chromatogram of volatile organic compounds

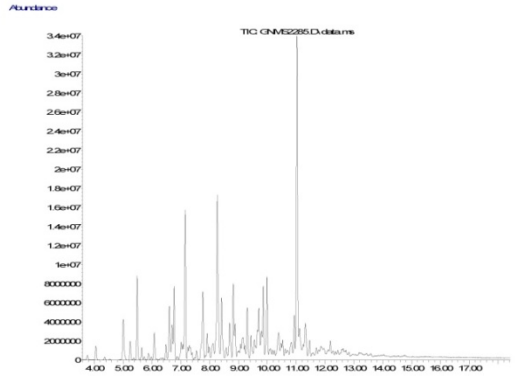

Figure 11.

Fig.2: GC/MS chromatogram of semi volatile organic compounds

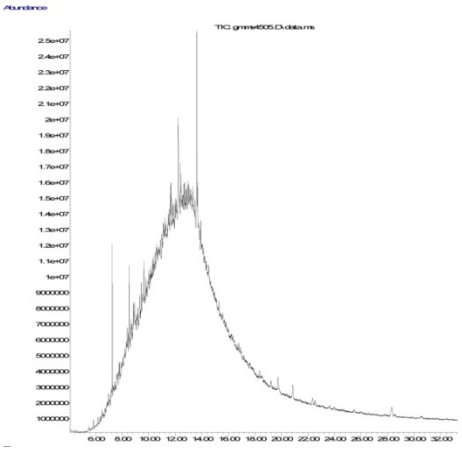

Figure 12.

The laboratory results are summarized in the following tables:

Table 3

No	R_t (min)	Chemical name	Structure
1	3.76	2-Methylbutane	
2	4.05	Pentane	
3	5.0	2-Methylpentane	
4	5.24	3-Methylpentane	
5	5.48	Hexane	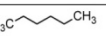
6	5.65	4-Methyl-2-pentene	
7	6.08	Methylcyclopentane	
8	6.48	Methylcyclopentene	
9	6.6	2-Methylhexane	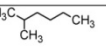
10	6.7	Cyclohexane	
11	6.76	3-Methylhexane	
12	7.15	Heptane	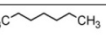
13	7.76	Methylcyclohexane	

Table 4

No	R_t (min)	Chemical name	Structure
14	8.25	2-Methylheptane	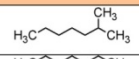
15	8.4	3-Methylheptane	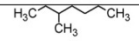
16	8.7	Isomer of Dimethylcyclohexane	
17	8.82	3-Ethylhexane	
18	8.88	Isomer of Dimethylcyclohexane	
19	9.3	2-Methyloctane	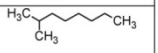
20	9.7	Trimethylcyclohexane	
21	9.86	Methyloctane	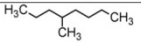

3.

Table 5

15/07/2010 : **Date**

REMARKS		RESULT		UNITS	TEST	#
[1]		<5.0		mg/kg (dry solids)	ICP-ב - (As) ארסן	280304
[1]		<2.0		mg/kg (dry solids)	ICP-ב - (Cd) קדמיום	280314
[1]		<1.0		mg/kg (dry solids)	ICP-ב - (Hg) כספית	280326
[1]		17.2		mg/kg (dry solids)	ICP-ב - (Pb) עופרת	280344
		25.9		%	solids	380012
[1]		89		(Light reduction),%	Microtox toxicity	380208
[1]		10		%	EC 50 ריכוז אפקטיבי	380995
		30489		mg/kg (dry solids)	TPH (FTIR, Blue Book) Met	388683

1. Poly Aromatic Hydrocarbons (PAH) analysis:

Table 6

Poly Aromatic Hydrocarbons PAH's

30ml/50.2g	Delution Ratio	8270	(EPA) Method
20/07/10	Date	mg/kg	Units

Tested Chemical	Result
Naphtalene	LOQ
Acenaphthylene	LOQ
Acenaphtene	**0.37**
Fluorene	LOQ
Phenanthrene	**1.55**
Anthracene	LOQ
Fluorantene	LOQ
Pyrene	**0.89**
Benzo(a)Anthracene	LOQ
Chrysene	**1.67**
Benzo(b)fluoranthene	LOQ
Benzo(k)fluoranthene	LOQ
Benzo(a)Pyrene	LOQ
Indeno(1,2,3-cd)pyrene	LOQ
Dibenzo(a,h)anthracene	LOQ
Benzo(ghi)perylene	LOQ

LOQ - Reporting levels are equal or smaller than 0.15mg/kg

CONCLUSIONS

The presented solution is ultimately focused on the Fine Tailings as the main driver, with additional potential benefits of the ability to use low grade fuel, like petcoke, as the heat source and the potential improvement of the heat balance due to the direct nature of its heat transfer that may allow a reduction of the discharged combustion gas temperature.

The present solution does not interfere with, or change, the oil sands extraction process, a proven

large scale process. It also does not change the mining side, or the hydro-transport as a transference means. The major change from the proposed technology will be on the utility side and the way the process water is heated. It can work with any type of tailings, including tailings that have a larger percentage of asphaltins due to improved froth solvent de-asphalting treatment processes.
The presented solution is robust and its working principles are driven directly from the basic physics, achieving the "Reclaiming as You Go" goal.

ACKNOWLEDGMENTS

Virtual Materials group for their generosity in allowing me use their VMG Sim. simulation program and especially for Marco Satyro and Glen Hay for their professional help and support.

Dr. Dave Sego from U of A for providing tailing samples for laboratory tests.

REFERENCES

Figure #1, ZLD Oilsands mine block diagram. Canadian Patent application CA 2,694,847, filed February 26, 2010, titled: "System and method for zero liquid discharge".

Figure #2, Direct contact VS. Non-direct contact steam generation. Canadian Patent application CA 2,684,817, filed November 12, 2009, titled: "Steam generation process and system for enhanced oil recovery".

Figure #3, Partial combustion gasifier DCSG. US Patent US 7,694,736 issued April 13, 2010, titled: "Integrated system and method for steam-assisted gravity drainage (SAGD)-heavy oil production to produce super-heated steam without liquid waste discharge".

Figures #4, Pressurized Fluid Bed boiler and DCSG with tailings injection. US Patent application US 12/635,597, filed December 10, 2009, titled: "Steam generation process for enhanced oil recovery".

Figure #5, Vertical up-flow direct contact steam generator. Canadian Patent application CA 2,676,720, filed August 28, 2009, titled: "Vertical zero liquid discharge direct contact up-flow steam generator system and method".

Figure #6, Internally Fired Rotating DCSG. Canadian Patent application CA 2,694,847, filed February 26, 2010, titled: "System and method for zero liquid discharge".

Figures #7, Oilsands mine without the use of tailing pond. Canadian Patent application CA 2,665,747, filed May 12, 2009, titled: "Usage of oil facilities waste sludge and fine tailings water for generation of hot water and steam for bitumen production".

Figures #8, Process simulation diagram. US Patent application US 12/636,729, filed December 12, 2009, titled: "System and method for minimizing the negative environmental impact of the oilsands industry".

Figures #9, DCSG from tailing stream combined with extraction process water heating. US Patent application US 12/636,729, filed December 12, 2009, titled: "System and method for minimizing the negative environmental impact of the oilsands industry".

Figures #10, Simulation balance for the impact of the system pressure on the hot process water generation. US Patent application US 12/636,729, filed December 12, 2009, titled: "System and method for minimizing the negative environmental impact of the oilsands industry".

Session 5

Soft Tailings Stabilization/Reclamation

CONCEPTUAL DESIGN OF A REMOTE SYSTEM FOR CHARACTERIZING OILSANDS TAILINGS DEPOSITS

M.G. Lipsett, Benoit Rivard
University of Alberta, Edmonton, Alberta, Canada

ABSTRACT

Oilsands tailings have variability in post-depositional shear strength that can make reclamation challenging. Collecting information on the characteristics of a deposit is often difficult, especially when tailings have very little bearing strength. A general concept is described for remote sensing of surficial characteristics of tailings deposits, and recent progress on the technology platform and sensor suite is described. A prototype robot system has been developed, and experiments have been conducted for estimating soil parameters. A robotic tooling package has been designed to take samples and to make geotechnical measurements. Issues of navigation have been considered for the range of conditions expected on actual deposits, and alternatives to wheeled vehicles are discussed. Two types of hyperspectral imaging cameras have been field tested on coarse tailings deposits and beside a wet soft tailings impoundment. Some mineralogical features are readily visible in the spectra, but additional work is required before soil properties can be estimated using hyperspectral cameras.

INTRODUCTION

Background

Oilsands tailings comprise coarse silica sand and fine silts and clays in water with residual bitumen. Coarse tailings are beached, trapping some fines in the pores with water. Structures are built with sand, including dykes, which are designed to maintain negative pore pressure for stability and low leakage. Fine solids are generally dispersed during the water-based bitumen separation process, and the fines do not readily form densifying sediments. Natural densification can occur, possibly through microbial action and local changes in water chemistry that affect clay lamellar structures, with subsequent loading to promote densification. The composite or consolidated tailings (CT) process combines gypsum as a coagulant with sand loading to accelerate densification. Thickened tailings processes (TT) use flocculants to form agglomerates that will sediment quickly and in appropriate conditions form dewatered (dense) deposits that have enough shear strength to cover with reclamation material. New processes are using beaching of flocculated tailings in low lifts to dessicate quickly, or centrifugation of flocculated tailings, to produce dense tailings with sufficient bearing strength to support a load.

The shear strength of a tailings deposit depends on the loading requirements. Only a few pascals of shear strength are necessary to form a shallow slope (on the order of 1% gradient); however, more than 50 kPa is usually necessary to support mobile equipment. Vibratory motions of machinery moving on an undrained soft tailings deposit may promote liquefaction. (This also occurs on coarse tailings deposits immediately after beaching, and in areas that are saturated).

While CT has been in commercial use for a number of years, it has been observed that the post-depositional characteristics of CT deposits can have considerable variability in sand to fines ratio and shear strength. It is likely that new tailings processes will also experience some variability in deposit characteristics. Where a shear strength specification must be met, variability in a deposit will be problematic for subsequent earthmoving activities to lay down multiple lifts of engineered tailings and reclamation material.

Some method for monitoring the characteristics of soft tailings deposits will therefore be important to control the post-depositional shear strength.

Ideally, properties of a deposit would be done from a distance. Remote sensing using airborne cameras or satellite imagery can reveal some soil surface characteristics, allowing for fast mapping. It may also be possible to use remote sensing techniques to reveal properties of soft tailings soil through noncontact measurements. In that case, a remote sensing system may be sufficient to show whether there is high variability in the deposit characteristics. Depending on the dimensions of the containment pond, measurements could be made from an array of towers on the perimeter of

the pond, provided that the towers are high enough to allow an appropriate field of view. An alternative approach would be to make periodic fly-overs with aircraft, which may be piloted or drones.

In many soils, moisture content can be estimated using spectral features in the short-wave-infrared (SWIR) range of the light spectrum that are characteristic of water, as water absorption increases significantly beyond 1 µm. Reflectance spectrometry has been used for estimating bitumen content in oil sands ore [Lyder et al 2010, Rivard et al. 2010], and for estimating the particle size density of solids estimation based on reflectance features [Rivard et al. 2009]. To date, there has been no parametric study of reflectance spectra features related to key characteristics of soft tailings: moisture content, particle size distribution, mineralogy, and undrained shear strength.

A potential obstacle is the requirement for illumination. Natural sunlight may be limited by weather, time of day, and seasonal conditions of observations and affect the detection of features of interest. A high frequency of observations may help to overcome these limitations by providing a valuable subset of quality observations.

Most soil characteristics are best determined using direct measurements. Table 1 lists some methods proposed for soil characterization and strength [Viscerra & McBratney 1998].

Non-contact sensors mounted on a vehicle are likely to be more practical to implement on a mobile platform. As well, for a vehicle to navigate successfully, it must be able to detect and avoid obstacles (including impassable areas). Near infra-red (NIR) sensors may be capable of measuring a variety of characteristics related to soil shear strength at a short distance for local navigation. A cone penetrometer or dynamic penetrometer (which determines California bearing number) can be automated to estimate the shear strength at the surface and at depth. A geographic information system can be used to archive soil measurements at a set of locations determined using a global positioning system receiver.

A number of approaches have been employed (or proposed) for monitoring soft soil deposits. These systems rely on manual sampling or measurements done using a craft that can navigate over water and soft mud. Navigation is problematic because the pore pressure and strength of the sand and fines is highly variable and prone to liquefaction in some situations. Equipment is prone to getting stuck, and sinkholes may present a risk to workers (and equipment).

Table 1: Potential Soil Characterization Methods

Soil Property	Sensor Type	Practicality
Water Content	Near Infra-red (NIR)	Good
	Mid-Infrared	TBD
	Ground Penetrating Radar	Good
	Microwave Reflectance	Good
	Electrical Resistance/Impedance	Limited
	Capacitance	Limited
Clay Content	NIR	Good
	Mid-Infrared	Good
Organic Matter	NIR	Good
	660nm Single Wavelength Sensor	Good
Strength	Penetrometer	Limited

Floating wheeled vehicles, such as an Argo™, rely on some soil shear strength for wheels to drive the machine, and low friction when riding on mud with too little bearing strength for the tires to support the mass of the vehicle. In soft tailings such a machine can become bogged down. A novel screw propulsion system was employed on the Amphiroll (also called a marsh screw or an Archimedean screw tractor), originally developed in the Netherlands and the former Soviet Union. This craft had limited success because it required two drives and had mechanical reliability problems operating in soft mud [Anon].

Amphibious vehicles are a good alternative, particularly those that are air-driven: hovercrafts and airboats. Driving against mud in a range of weather can present operability challenges and may require a range of control strategies. The most successful platform would likely be a hovercraft, although it is somewhat more

expensive than other vehicles and requires more maintenance to ensure reliable operation. Small commercial hovercrafts are available, and are designed to operate in muddy conditions.

There is, however, a real advantage to driving against the soil: the potential to use traction measurements to estimate soil parameters without having to make ongoing measurements with dedicated tooling.

Three general options were considered for collecting this information from locations on a soft tailings deposit:

a) permanent sensors installed by full-time personnel working from an amphibious vehicle, with wiring strung back to a base station or a wireless telemetry system;
b) manual sampling and testing by full-time personnel working from an amphibious craft;
c) telerobotic vehicle using an amphibious craft as a platform, with automatic tooling for sampling and testing.

A remote sensing solution was not assessed because the proof-of-concept of relating remote sensing measurements directly to geotechnical properties has not yet been established. If this capability can be developed, then it may become a preferred option; for this reason, an assessment of remote sensing for tailings characterization has been undertaken.

A high-level net-present-value analysis of capital and operating costs (including operator labour, maintenance, consumables, and lab analysis) shows that each of the three options is roughly equivalent in cost over twenty years with a 5% discount rate. Other factors then become important, such as worker safety and timely data collection. An automatic sampler with instrumentation is likely to be more accurate than a manual method. There is no particular reason why people have to collect samples from the deposit to determine the soil characteristics, except that the elements of a remote system have not been integrated and commercialized. A vehicle capable of navigating on soft tailings could be converted to telerobotic or even fully autonomous control, and tooling can be developed to make measurements of soil properties and to take samples, while reducing risk to workers. Thus an argument for pursuing a robotic method can be made based on safety and performance.

A concept has developed for a robotic system to navigate to a defined location on a tailings structure, collect penetrometer data and samples at the surface and at depth, and return the samples for analysis. The potential to use remote sensing information has also been considered from a navigation standpoint to determine safe passage, and to provide a first-order characterization of the surface and support the selection of sampling sites.

SYSTEM CONCEPT

The ground-based soil characterization system concept comprises a tooling package to acquire samples and to take geotechnical measurements, a robotic vehicle to go to a location for measurements, and a ground station to allow a human operator to plan the task, monitor progress, and take control of the system when necessary.

Tooling Package

A basic design was developed for a tooling package for measuring shear strength and taking samples; this design was intended for testing on a laboratory-scale field robot, a modified Parallax QuadRover. Key specifications were:

- Mass not exceeding Quadrover's 46 kg (100 lbs) load capacity;
- Minimal disturbance of a sample during collection and transport;
- Ability to collect and store multiple samples; and
- Ability to measure and collect samples at a depth of 0.5 metre, with potential to extend to greater depths
- Remotely operable.

A number of design concepts were assessed before opting for the design shown in Figure 1.

This design meets all of the specifications, and comprises the following subsystems:

- A set of sample capsules designed for very soft soil or stiffer soil (shown in Figure 2);
- A mechanism to connect a sample capsule to an actuator;
- A shear strength measurement device using a commercial strain-gauge-based load cell;
- A hydraulic actuation system to lower the tool into the soil and withdraw it; and

- A sample storage magazine, which indexes to allow the tool to affix an empty container, collect a

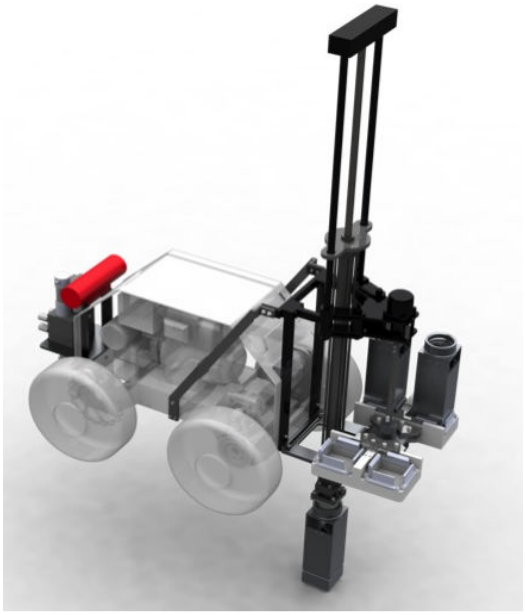

Figure 1. Tailings sampler concept design showing tooling package on a small wheeled rover.

A design has also been developed for an extensible mechanism with multiple lengths of tool and integrated power and communication. While the tool package is designed to mount to QuadRover, it can be mounted on a range of vehicles, which would allow the prototype to be tested in field conditions mounted on an appropriate craft.

Robotic Vehicle Platform

For development purposes, a wheeled vehicle is used for preliminary laboratory studies such as navigation. Issues of traction control are considered, to prevent the vehicle from becoming stuck. This is an important feature even for teleoperated vehicles, to allow the machine to maintain traction.

For a wheeled vehicle, soil-wheel interactions can be measured to estimate soil properties [Wong 1993]. The Quadrover was modified to estimate

- cohesion stress,
- internal friction angle, and
- shear displacement angle under the wheel by measuring speed, torque, wheel angular velocity, and sinkage.

Figure 2. Sample holders for soft & firm tailings

Operator Ground Station

The human operator interacts with the robotic system through a ground station, which is simply a graphical computer interface that allows the human to tell the robot a set of commands to perform, and to see what the robot is doing. The user interface also allows status information about the machine to be displayed, like a vehicle dashboard.

Figure 3 shows a screenshot of the graphical display of the ground station program, which was developed using Cocoa and Composer software packages. The current version of the navigation software has the following capability:

- receives and parses data sent from the on-board sensors
- displays a map, with an editable picture and coor-dinate system
- receives input from the user to create and update waypoints, by clicking on the map or inserting GPS coordinates
- flags to tell the robot where to sample or use any other equipment
- animates a horizon and display video from a con-nected webcam
- generates trajectories and error-handling functions to direct the robot from waypoint to waypoint
- has features to control turning radius at waypoints
- sends NMEA strings to the control board for ki-nematic control of the robot.

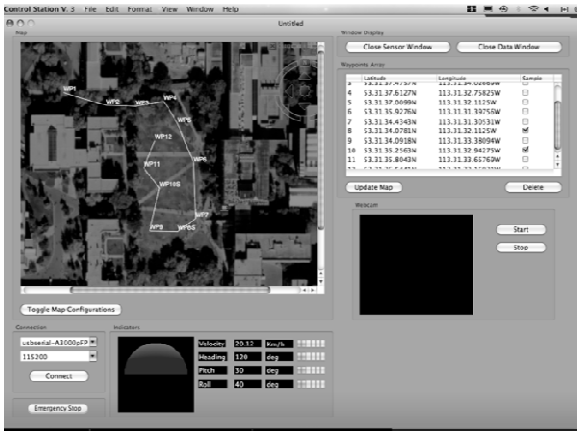

Figure 3. Screenshot of the operator interface for controlling the mobile robot system

Wireless links to a ground control station enable robot monitoring and control from a distance. The robot uses a hierarchical control system, with microcontrollers executing low-level sensing and actuation, and an on-board 2.13 GHz Intel-based microcomputer (MacMini) handling most path planning and sensor processing. The sensing, actuation, and control system are illustrated in Figure 4.

The only image-based sensors currently on the robot simple webcams to acquire images for display on the remote operator ground station.

A high-level fault-modes-and-effects-analysis has been done to consider how the operation of a robotic system must integrate safely with normal tailings operations.

EXPERIMENTS

Laboratory-Scale Prototype Robotic Vehicle

The robot vehicle and ground station were tested outdoors on hard ground. The vehicle was able to track within ~1 m of a set of waypoints using GPS.

Laboratory experiments were done to estimate traction in dry sand. The slip ratio of each wheel S is the key state indicator for the vehicle; the slip ratio is related to the difference between intended wheel velocity (tire circumference velocity) and actual wheel velocity (travelling velocity), and is defined by the following equation:

$$S = \begin{cases} \dfrac{(r\dot{\theta}_w - v_w)}{r\dot{\theta}_w} & (r\dot{\theta}_w > v_w : accelerating, S\ positive) \\ \dfrac{(r\dot{\theta}_w - v_w)}{v_w} & (r\dot{\theta}_w < v_w : braking, S\ negative) \end{cases} \quad (1)$$

where r is the radius of the wheel, θ_w is rotation angle of the wheel ($\dot{\theta}_w = \omega$), $r\dot{\theta}_w$ is tire circumferential speed, and v_w is linear speed of the wheel. These two values are relatively simple to measure accurately in real-time onboard the vehicle. The soil shear stress τ and normal stress σ imparted in the material below the wheel is related; the torque T on a wheel is the sum of the shear stress acting on the area of the wheel that is contacting the soil:

$$T = r^2 b \int_{\theta_r}^{\theta_f} \tau(\theta) d\theta, \quad (2)$$

where

$$\tau(\theta) = \left[c + \sigma(\theta) tan\phi\right]\left[1 - e^{-r/\{k\left[\theta_f - \theta - (1-s)(sin\,\theta_f - sin\,\theta\right]\}}\right] \quad (3)$$

c is the cohesion of the soil, k is the shear displacement under the wheel, and ϕ is the internal friction angle of the soil [Yoshida]. The angle from vertical to the front contact with soil is θ_f and the angle to back contact is θ_r. These angles were estimated from sinkage depth measurements.

The vehicle was operated in dry level sand 15 cm deep, over a five metre run at a set speed. Measured variables were: angular velocity of front and rear wheels (which was controlled), linear velocity of the vehicle, normal force on each wheel, static sinkage depth, dynamic sinkage depth, and torque. This data was used in this set of equations to find least-squares estimates of the soil parameters to be c= 0.72, ϕ= 40°, and k.=0.03. Parameters c and ϕ agreed fairly closely with published results, but k was a factor of ten low. The torque and sinkage measurements were somewhat noisy, which contributed to errors.

A prototype sample capsule was tested in low strength 2Pa soft tailings. Despite the tailings having high water percentage, the prototype sealed watertight. The adaptor was then tested on 6 kPa soil, prepared using Devon silt, and the hooks effectively captured soil.

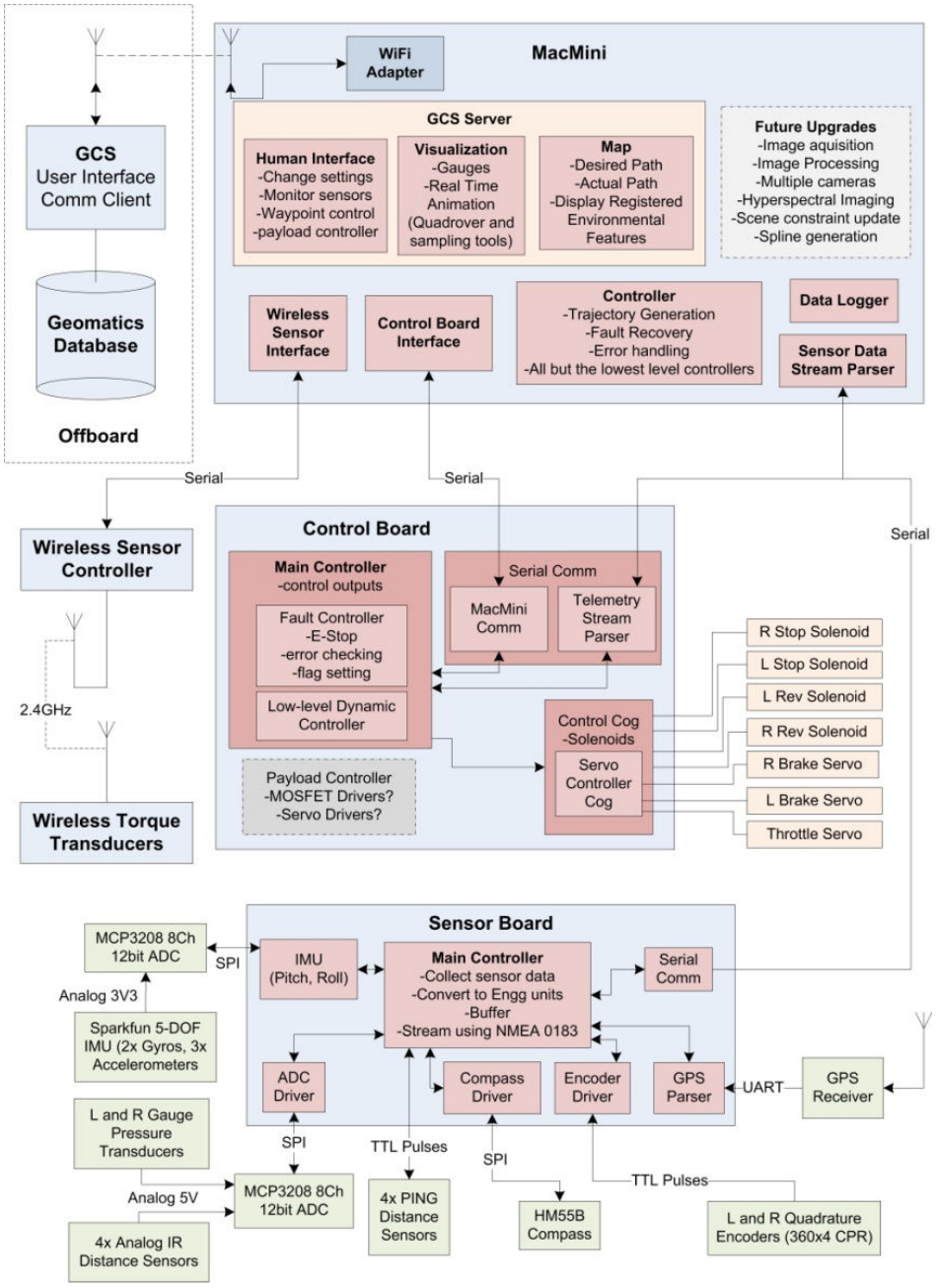

Figure 4. Control system block diagram

Remote Sensing Tests at an Operating Oilsands Plant

A Telops hyperspectral imaging camera was evaluated in field conditions at Albian Sands. The camera was tripod mounted and images were taken sensing passively emitted surface radiance from a coarse tailings beach and an ore face. The hypercam acquired images of 320 x 256 pixels with a spectrum for each pixel in the 7.7 – 11.5 µm range. Image analysis indicates that emission spectra recorded features predominantly attributed to clay and quartz sand mineral constituents of the coarse tailings deposit. From these data detailed maps of surface material classes can be generated encompassing as many as ten different surface classes with subtle differing mineralogical characteristics resulting from the depositional processes. Such maps could be readily used to

support hazard avoidance navigation of a rover of the tailings and for selection of sample locations.

Figure 5 displays image spectra for surfaces dominated by fines and sand and these spectra respectively capture key spectral features of clay (near 1000 cm^{-1}) and quartz particles (1100 and 1200 cm^{-1}). A visible-light photograph of the coarse tailings area is shown in Figure 6. Using a measure of the strength of the clay and quartz sand features, a simple map was generated to showcase the spatial variation in the amount of fine solids at the surface of a coarse tailings beach, shown in Figure 7. This map defines two dominant types of surfaces based on the relative abundance of fines.

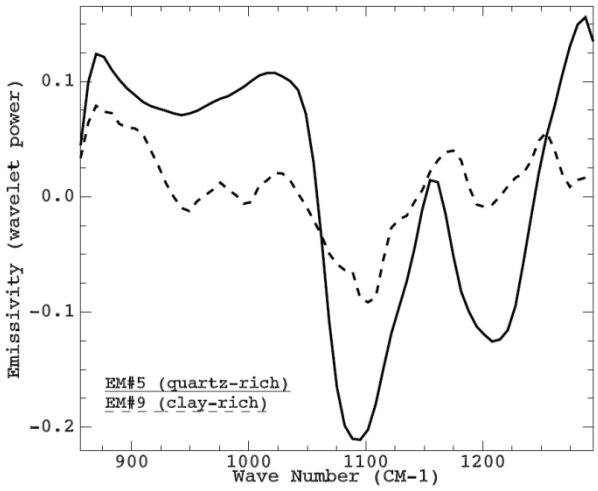

Figure 5. Image spectra of tailings, with dashed line representing fines-rich surface and solid line representing sand-rich surface.

FUTURE WORK

Additional remote sensing work will be done to relate spectral features to soft tailings surface characteristics (grain size and moisture content), using instruments such as a portable active FTIR spectrometer for reflectance measurement in the 2-22μm range, and a long-wave hyperspectral camera to image tailings towards developing in situ tailings characteristics. Thermography of tailings over diurnal periods may provide a good indicator of the moisture content of tailings as temperatures fluctuate.

Resolving issues of on-board sensing and perception for navigation and control are also part of future work. A number of enhancements will be made to the robotic vehicle for traction parameter estimation. Wireless strain gauges will be installed on the wheels to measure wheel shaft torque. Electrohydraulic servovalves will allow for proportional vehicle speed control. A more accurate method of measuring tire sinkage will be implemented. The vehicle will then be tested outdoors for longer runs and higher speeds, which will allow for more accurate soil strength parameter estimates at the surface, and traction control.

Figure 6: Visible image of a coarse tailings deposit, with gold square and circular black calibration panels shown in the centre of the image, and released water and pit wall shown in the background.

A prototype will be built of the tooling package that can mount on the laboratory-scale mobile robot. This package will be tested on soils of known properties to calibrate the instrumentation and to test the automatic samplers. The design already includes features for reliability in field conditions.

Alternative platforms will be considered, such as autonomous hovercraft control schemes. There may be options to use field prototype low-ground pressure wheeled robotic vehicles, such as a space rover platform developed by Norcat.

Another alternative now being considered instead of a land vehicle is a robotic aircraft UAV to carry the sensor package. This is only appropriate if unique spectral features can be correlated to soil characteristics. Others are integrating combined visible/near-infrared (VNIR) cameras for remote helicopters.

Figure 7. Black & white Hypercam processed image showing the classification of sand-rich regions in brighter tones and fines-rich regions in darker tones.

The ground station has been developed for either land or air vehicle operation; but additional functionality remains to be added to control the sensor package and sampler. Once these subsystems have been developed and tested, then system integration and field trials can be conducted on a small deposit, and then actual deposits.

ACKNOWLEDGMENTS

This work was supported by several sources: the University of Alberta School for Energy and the Environment, the Faculty of Engineering, the Faculty of Science, and the Natural Sciences and Engineering Research Council of Canada.

Robot vehicle prototype development was done under the direction of Mike Lipsett by Stephen Dwyer, with Nicolas Olmedo developing the ground station interface for robot teleoperation and autonomous navigation on hard ground. Traction measurements were done by Jamie Yuen, Stephen Dwyer, and Nicolas Olmedo. The sampling tool basic design was developed by Meaghan Janssen, Nikolai Kummer, Keith Martin, and Brendan Ferguson. Hyperspectral images were acquired, analyzed, and interpreted by Benoit Rivard and Jilu Feng, with support from Louis Brault at Telops. The cooperation and on-site support from staff at Albian Sands is greatly appreciated, particularly from Jonathan Matthews, Brad Balaski, Ivor Winland, and Rod Clarke.

REFERENCES

Anonymous.
http://www.amphibiousvehicle.net/amphi/D/dafrolling/dafrolling.html
Accessed Sept 25, 2010.

Lipsett. M.G. & Dwyer, S.C. A Robotic System to Characterize Soft Tailings Deposits. Proc Mine Waste 2009, Banff Nov. 2009.

Lyder, D., Feng, J., Rivard, B., Gallie, A., and Cloutis, E. 2010. Remote bitumen content estimation of Athabasca oil sand from hyperspectral infrared reflectance spectra. Fuel 89: 760-767.

Rivard, B., Feng, J., Gallie, A., and Cloutis, E. 2009. Characterization of oil sand bitumen content and grain size properties using infrared reflectance spectroscopy. 11th Geoide annual conference, Vancouver, BC, May 27-29 2009.

Rivard, B., Lyder, D., Feng, J., Gallie, A., Cloutis, E., Dougan, P., Gonzalez, S., Cox, D., Lipsett, M. 2010. Bitumen content estimation of Athabasca oil sand from broad band infrared reflectance spectra. Can. J. Chem. Eng. 88(5): 830-838.

Viscarra, RA; McBratney, AB, 1998. “Laboratory evaluation of a proximal sensing technique for simultaneous measurement of soil clay and water content.” Geoderma 85, pp. 19-39.

Yoshida. K. Terramechanics-based analysis and traction control of a lunar/planetary rover. Field and Service Robotics, 24:225–234, 2006.

CAPPING SOFT TAILINGS FROM A FLOATING PLATFORM

Michael Costello[1], Eric Hedblom[1] and Walther Van Kesteren[2]
[1]Barr Engineering Company, Minneapolis, MN, USA,
[2]Deltares, Delft, The Netherlands

ABSTRACT

Traditional tailings basins are built by perimeter discharge, working from the high ground and allowing fines to accumulate in the middle. These Fluid Fine Tailings (FFT) are difficult to cap and consolidate from the side because they are displaced by denser sand. A combination of coarse and fine tailings with gypsum called Composite Tailings and Consolidated Tailings (CT), have more sand than FFT and are generally stronger. They are often present as a heterogeneous mixture of particle sizes in large tailings basins. FFT and often CT are untrafficable when final reclamation begins. There is a different way to cap these materials. Using the water pool as a floating platform for access, capping sand can be placed by raining and rainbowing onto the submerged tailings from a discharge barge.

Raining is a process of sprinkling thin uniform lifts of sand through the water column on top of tailings. Rainbowing is similar, but the thin uniform lift is applied by shooting a continuous sand slurry from a water cannon. Both technologies operate over scales ranging from very small demonstration projects to rates on the order of 2,000 to 5,000 cubic meters per hour. Even a higher production is possible, depending of the available equipment and restrictions, such as thickness of the sand layer.

These techniques have been used successfully for full scale remediation of aquatic habitats on sediment with shear strengths as low as 150 Pa, water contents up to 500%, and high oil content. In flumes, capping has been successful on sediments as weak as 15 Pa.

This paper presents the foundation for the success of this method, equipment available to implement this technology, a summary of relevant case histories under conditions similar to oil sand tailings, available byproduct materials that are well suited for capping, limitations and restrictions of the technology, and concepts for creating reclamation landforms using these techniques.

BACKGROUND

Water-based capping from a floating platform places initially thin and uniform lifts of granular material on top of soft compressible sediments. It takes advantage of the unique accessibility and mobility afforded by floating platforms, potentially high production rates via slurry delivery, and the reduced unit weight of submerged sand to achieve gentle uniform loading.

Gentle placement and uniformity of initial loading avoids lateral displacement of weak underlying tailings which is commonly seen from typical beaching operations. Capping of soft sediments is proven technology for at least 30 years (Ling 1998). It has been conducted at water depths ranging from 0-62 m (Verduin 2002). It is often used to isolate contaminated sediments from the benthic community in the top 15 cm of sediment, and from the water column using 20-100 cm of sand. Some sub aqueous caps have been built up to 9 m thick for habitat diversity in littoral zones (Thompson 2003). Contaminated sediment cap areas range from very small to 4.6 sq km.

Near Amsterdam in the Netherlands, islands in the IJmeer have been constructed on extremely soft soils covering a total area of 218 ha, using 25,000,000 m^3 of sand. These islands together form a brand new extension of the city of Amsterdam, called IJburg, which will house 45,000 inhabitants.

THE FOUNDATION OF CAPPING

Capping causes the effects shown in Figure 1 and allows bridging of surface loads over deeper soft sediment.

Caps can be supported on weak tailings if loaded gently and uniformly with initially thin lifts. Table 1 lists a dozen project with soft sediment.

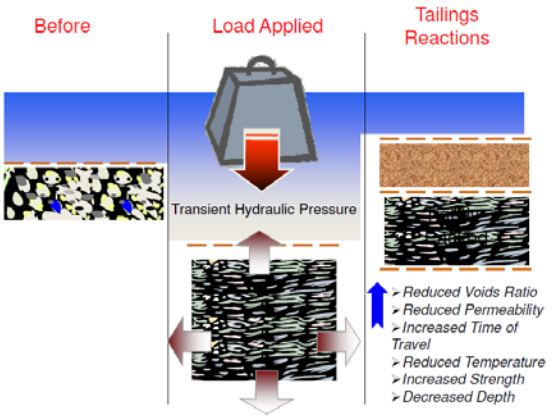

Figure 1. Effects of placing caps on tailings.

Table 1. Examples of capping projects on soft sediments.

Site	Water Content W/S wt %	Surface Shear Strength kPa	References
Hiroshima Bay, Japan	90 +	0.5	Ling 1998
Matsushima Bay, Japan	225-370	0.1	Ling 1998
Lake Biwa, Japan	135	1	Ling 1998
Stryker Bay, USA	36-284	0.3-0.8	Hedblom 2002
Annacostia River, USA		0.5-1.0	Reible 2004
Soda Lake, USA	161-455	0.2-0.5	Thompson 2003
KPC Ward Cove, USA	Avg. 415	0.14- 4.8	Verduin 2002
LA Harbor Dredge Disposal	Avg. 161	0.4-0.6	Verduin 2002
LA Harbor Cap	Avg. 111	0.2-1.0	Verduin 2002
Iburg Project, Netherlands	>119	0.7-1.0	Verduin 2006
Mocks Pond	>500	Low	Thompson 2003
Hudson River, USA	230-250	Avg. 1.0	Verduine 2005

Bearing capacity analysis is used to determine the initial lift height for subaqueous sand layer placement. Typically, it assumes no undrained strength gain with depth (Ling 1998), which is commonly true for thick deposits of FFT and a conservative assumption for CT. For sediment with undrained cohesive strengths (C_u) of 1 to 2 kPa, an initial allowable mineral sand thickness is between 20 and 50 cm (Ling 1998). Subsequent lifts can be thicker due to strength gains from initial consolidation.

With a sufficient tapering transition slope or abutting against a beach or other stable structure, slope failure at the edges of a cap can be controlled or eliminated. The required taper slope is determined by analysis of log-spiral or circular failure mechanisms, and squeezing failure over the whole depth of the soft sediment. The taper slope itself is controlled by the discharge rate and velocity across the water. If necessary due to spatial constraints, geotextiles and geofabric tubes can be used for more sudden transitions. Typical transition zone lengths are 5 times cap thickness (Palermo 1998), and is a function of the layer thickness of the soft sediment.

It is important to initially apply the sand slowly and uniformly to avoid foundation problems and loss of sand. Also, allow sufficient time between lifts to dissipate built up pore pressure. This is often on the order of a day or three, so is not a time constraint when placing a large cap.

Laboratory column tests, consolidation tests on soft tailings, and finite strain analysis predict how caps will perform. In Figure 2, the rate of release of gas and porewater are shown for two capping sands over tarry sediment in a column test. The reduced discharge rate can be used to calculate the post-capping permeability of the capped sediment. The total volume release is coupled to the settling curve in time and is determined by effective stress (compressibility), permeability and creep data.

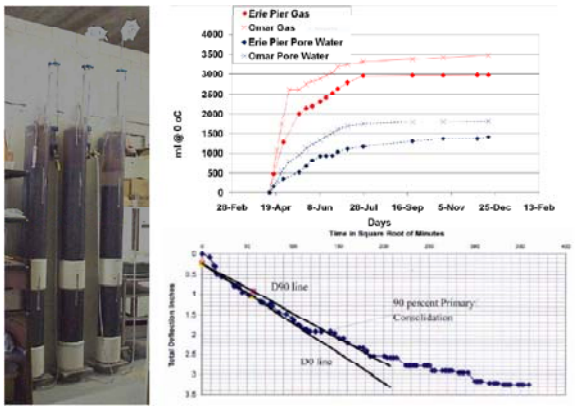

Figure 2. Capped column tests.

Figure 3. Seepage Induced Consolidation (SIC) test apparatus.

Effective stress, permeability and creep data can be measured for very soft sediments with the SIC apparatus shown in Figure 3. With FFT or CT, the SIC test is also capable of determining conditions for gas and bitumen to begin flowing within the tailings.

Figure 4 shows some of the DELCON model results for capped conditions, including the effect of consolidation on the permeability of the underlying tailings and the magnitude and rate of expected consolidation. DELCON can also report strength gain, the fate of discharged fluids, and gas production from gassy tailings.

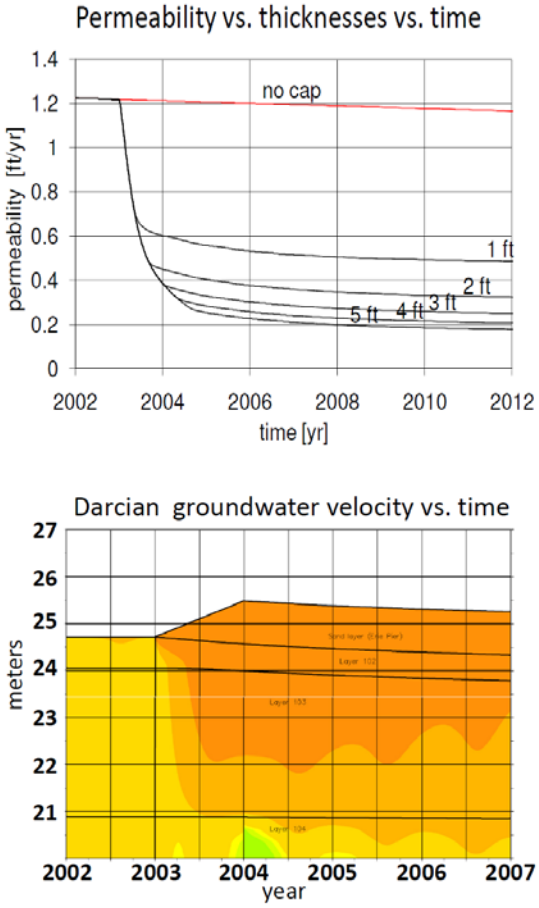

Figure 4. DELCON consolidation model results on consolidation of caps illustrating the types of analyses appropriate to capping evaluation and design.

EQUIPMENT

Quite a variety of methods have been developed for placement of sand from a floating platform. They can generally be grouped into three categories: (1) Surface diffusers (either mechanically or hydraulically fed), (2) Sub-surface diffusers, which together are described as "raining" technology, and (3) rainbowing, which features the added benefit of projecting the sand 100-300 m beyond the platform. Examples of each are shown in Figures 5, 6 and 7.

Figure 5. Surface diffusion of hydraulically delivered sand, raining sand through the water column to gently place it on soft tailings.

Softer tailings require tighter controls on the uniformity and thickness of the initial lifts. Positioning is important because it controls the uniformity of the layer thickness. If a cap layer is to be uniformly thick, the solids must be discharged at a consistent rate, and the discharge location must constantly and consistently move over the area to be capped. Since the floating platform is essentially frictionless on the water, positional controls are necessary to assure this type of movement.

Typically, positions are controlled by cables, spuds or propulsion. Three or four cables can be anchored and used to pull the discharge across the capping area. Spuds are vertical poles deployed at several positions on the barge. With this setup, the barge maneuvers into a position and sets its spuds into the sediment. The spuds then allow it to pivot, producing a radial discharge pattern. Finally, the barge can operate with thrusters to maneuver against wind and the drag of the slurry line to control its position. Venturi jet thrusters can be used in shallow water without scouring recently

placed capping sand, and is probably the best approach for position control when capping in large oil sand tailings basins. Where possible, temporarily raising the pool elevation can help provide deeper draft.

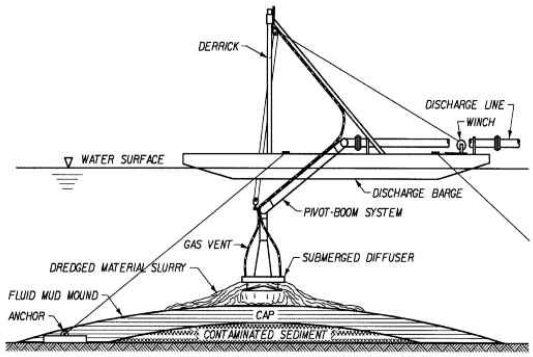

Figure 6. Sub-surface sand diffuser to spread sand at the bottom of the water column. (Palermo 1998)

Figure 7. Rainbowing sand from a slurry cannon. (Thompson 2003)

In-mine pits are often smaller and have high wall that may provide anchoring opportunities.

Global Positioning Systems (GPS) have enabled well controlled lifts, and in combination with slurry discharge data provide detailed records of how and where a cap was placed. Sonar soundings can be used as well unless consolidation in a scale important to the thickness is expected.

PRODUCTION RATES AND COSTS

Production rates vary considerably depending on the scale of the project, the maximum feasible initial lift height, the rate at which subsequent lifts can be increased in height, availability of sand, pumping capacity, positioning controls, discharge equipment capacity and environmental restrictions. In the realm of capping contaminated sediments in a natural setting, production rates of 50-100 m^3 per hour are typical to place 20-100 cm of sand. In these cases, resuspension of contaminated sediment is a big constraint, and the scale is usually less than a dozen hectares, so equipment is relatively small. Sand is usually purchased and hauled to the site where it is slurried for delivery typically as a 15 cm to 1 m thick cap. Figure 5 shows a 10 inch line placing about 60 m^3 per hour. A recent study of these types of capping projects over areas ranging from 0.4 to 20 hectares cost $32 to $97 (CAD) per cubic meter (Palermo et al 2009).

At this time in the Netherlands, the 2nd Maasvlakte (a large harbor extension in the port of Rotterdam) is under construction using rainbowing techniques to make upland harbor area from the bed of the North Sea. 325 million cubic meters of sand are being distributed over an area of about 2,000 ha. This project cost € 2,900,000,000 ($CAD 11.83 /$m^3$). These costs include dredging sand from 10-15 km off shore, hauling the sand in a ship, and rainbowing the sand onto the seabed and building it into upland areas suitable for port activities. The average thickness of capping fill was 16 m.

Figure 8 illustrates the setup of a large scale rainbowing water cannon like that used on the Rotterdam project. Below that is a surface diffuser capable of a similar scale of operation. Note that the surface diffuser operates as about six side-by-side channelized diffusers.

CASE HISTORIES

Deltares Flume Test

In an effort to examine how sand can be placed on soft sediment, Deltares conducted flume tests on very low strength sediment. In a flume containing essentially muddy water with shear strength of 15 Pa, capping sand was applied using a sub-aqueous diffuser, gently sprinkling two layers onto the very soft sediment. While controlled conditions in a flume are more stable than in a tailings basin, the experiment sheds light on the process of capping soft tailings with sand. The capping process is visible in Figure 9 showing two layers of capping.

The first lift shows some sand loss into the very soft sediment. It shows localized pore water discharge channels, which were created before placing any sand. These channels appear in the first phase of consolidation, where permeability determines the settling rate and effective stresses are negligible. If loading becomes uneven, these discharges can become piping, with pore water discharged to the water pool while sand falls into the soft tailings along the edges of the upward discharge. The process is called fingering. This is why uniform loading is important. As sediment strength increases, the risk of this type of failure diminishes rapidly.

In order to retain the aquatic depths at the site while adding capping material, a temporary surcharge was added to push the cap into the soft sediments. This created upland conditions for a period of three years while consolidation proceeded. The excess sand was later removed and reused elsewhere on the site, leaving a wetland cap and restored littoral zone.

The 4.5 hectare area to be capped was isolated with sheet piling, which provided rigid controls in combination with the shoreline for a cable operated positioning system. See Figure 11. An initial lift of 15 cm was placed using the surface diffuser shown in Figure 5 on these sediments with initial shear strength of about 0.6 kPa (Table 1).

To prevent migration of dissolved polycyclic aromatic hydrocarbons, a geotextile mat containing activated carbon and sand (to assure negative buoyancy) was deployed and a variety of settlement instrumentation was set on top of the carbon mat as shown in Figure 12. Raining by surface diffusion was used to bring the bed up to the water line and articulated dump trucks and dozers built the upland surcharge from there. Crushed washed limestone was delivered by ship for the sand supply. Its high angularity helped prevent mixing at the sediment interface (Figure 12), and created a stable trafficable working surface for installing instruments (15 cm layer) and for 40 ton trucks (1-1.5 m).

AVAILABLE BYPRODUCT MATERIALS

Dutch landbuilding guidance for landmaking in the Rotterdam harbor is for relatively coarse sand (D50 = 250 um, with a maximum of 5% less than 63 um to control turbidity). The approximate permeability of this material is 1 x 10 -4 to 1 x 10 -5 m/s. The high permeability is so this foundation material can function as a drain for consolidation pore water and, for placement above the water line, to drain infiltrating rain water quickly for rapid development of trafficability.

Figure 8. Large scale production surface diffuser (complements of Van Oord) with rainbowing above and raining by surface diffuser below.

Analog oil sands byproduct materials include the coarsest portion of coarse tailings and coke produced in the upgraders. Based on the author's experience, typical washed coarse oil sand tailings

have a D50 of about 100 um. This finer sand is more difficult to drain, but could be upgraded via hydrocyclones.

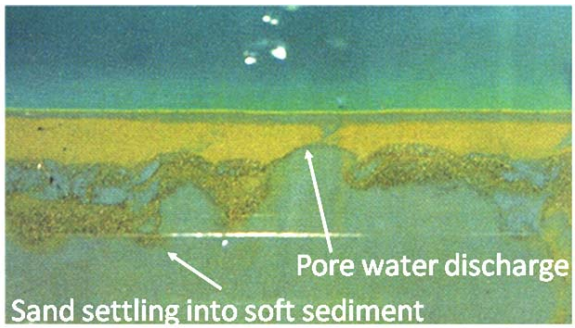

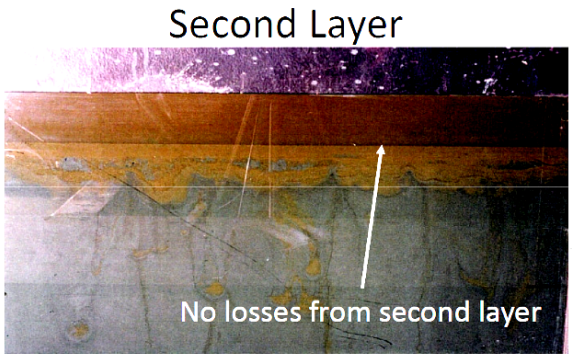

Figure 9. Capping sand applied to 15 Pa sediment in a laboratory flume with a sub-aqueous diffuser. Photo of first layer is shown above photo of the second layer.

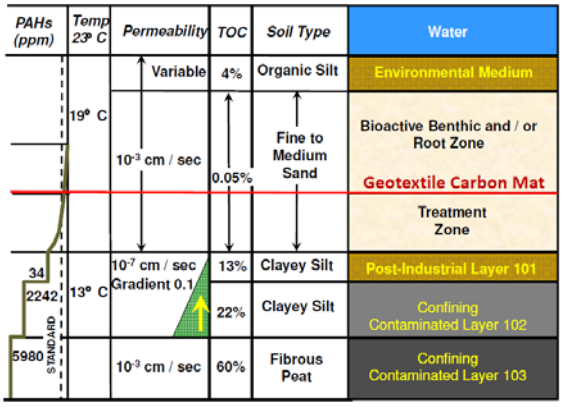

Figure 10. Features of an environmental cap at Stryker Bay. Permeability values are after consolidation.

Figure 11. Surcharge cap installation at Stryker Bay.

Tailings sand applies weight to the consolidating tailings even when under water. For FFT, tailings sand should be delivered in a thin initial lift. With FFT with lower solids and shear strength, there may be initial mixing with FFT via fingering, then would be more stable for the next lift. Capping more competent CT or NST, initial lifts can be thicker and mixing with tailings is unlikely.

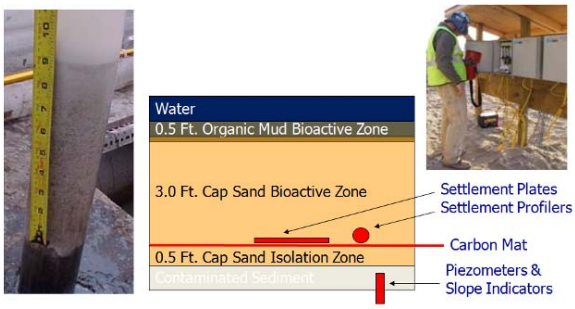

Figure 12. Core showing boundary between capping sand and underlying soft sediment, and a description of the settlement instrumentation to monitor the effect of the surcharge. Instrumentation data was collected on shore.

Coke is typically already sufficiently coarse, and has a lower bulk density than coarse tailings. Crushed coke can be angular while other coke is well rounded. Angularity increases its friction angle allowing it to bridge over soft sediments and support traffic more easily than the more rounded coke or tailings sand. Its lower bulk density allows it to be placed underwater without applying a significant load on the underlying sediment. Coke is buoyant on FFT and CT. A surcharge load can

be applied when the coke is dewatered or when it is placed above the water line. Its light weight also allows it to be thrown farther when rainbowing.

To be most economical, this high specification material is most important in the drainage layer. Lower cost materials could be used above the drains.

LIMITATIONS AND RESTRICTIONS

In contrast to beaching, it is important to place capping material in appropriately thin uniform lifts. If capping is applied shore to shore, there is no restrictions on the edges. If the cap does not extend shore to shore, then a transition slope must be used to taper the edge. These slopes are set by stability analysis. If the cap needs a steeper slope, geotextiles or geofabric tubes should be considered to transition the differential loading.
It is also important that the sand does not cement after deposition from bacterial or chemical changes when consolidated pore water with dissolved ions (salt, CO2, gypsum) is percolating through the sand cap. Cementing sand will result in large monolith sheets that are not stable on the soft sediment.

RECLAMATION CONCEPTS

Aquatic Habitats

Sand placement via a floating platform can be a useful tool for reclamation of tailings basins into stable aquatic habitat. They are effective when:

- Accelerating the consolidation of the underlying tailings,
- Providing a “treatment zone” for organic contaminants to biodegrade before reaching the benthic zone or water column,
- Isolating a developing bioactive benthic zone from direct contact with solid or adsorbed contaminants, and
- Degassing sediments via consolidation.

Sub-aqueous sand placement is a viable method for development of sub-aqueous habitat such as expanding littoral zones, establishing a specific sediment medium for habitat development, or diversifying shallow habitat and shoreline edges.

When converting the FFT portion of a tailings basin into a wetland complex, capping from a water-based platform can be an important method to make the soft area trafficable for aquatic habitat. For example, using combinations of raining followed by rainbowing, geotechnically stable foundations can be constructed for subsequent development of fens or bogs. Such technology can integrate with adjacent uplands reclamation, water level controls, and flushing of saline and possibly toxic pore water.

Upland

One approach to creating uplands over CT, NST or possibly even over FFT, as illustrated in Figure 13, is to initially raise the pool elevation as high as possible within the constraints of required freeboard and dyke safety, then rain high permeability sand (coke or coarse tailings) from a surface diffuser through the water column. The initial lift height is determined based on specific strength of the underlying tailings.

Improve the sand's ability to convey consolidation water by deploying wicks into the tailings (Wells, 2009) and drain tile in the capping sand (as necessary) from a floating platform. Then rainbow more high permeability mineral sand. Draw down the water table by pumping from the drainage layer to uniformly surcharge the underlying tailings.

Consolidate the tailings and gain access for land-based equipment. Continue to place more uniform lifts until the desired trafficable conditions and expected consolidation are achieved. As strength of consolidated tailings increases, more efficient methods of construction can be used, such as Syncrude’s hummock and swale approach to diversify the landform and create a natural and productive upland landscape. At this point, if not before, the dewatering pumps can be removed.

CONCLUSIONS

Prior experience in sediment remediation and coastal constructing demonstrate that capping soft tailings from a floating platform is technically and economically viable. There are a wide range of tools and several potentially economic materials with which to construct caps from a water platform. These techniques offer alternatives to capping FFT or CT that may be used to overcome limitations of traditional beaching when reclaiming

tailings basins into trafficable aquatic or upland habitat.

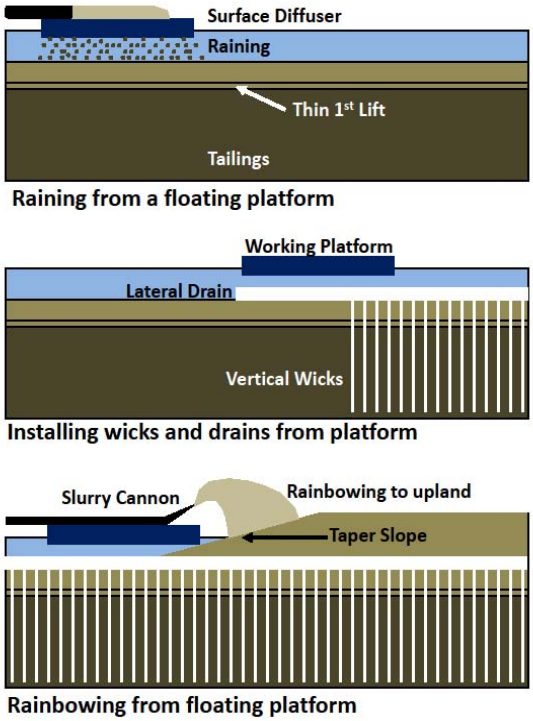

Figure 13. Schematic illustration of capping soft tailings via raining, wicking and drainage, and rainbowing.

REFERENCES

Hedblom, E. 2002. "Appendix GH, Geology-Hydrogeology," in: Costello, M. Data Gap Report, St. Louis River/Interlake/Duluth Tar Site, Duluth, Minnesota.

Ling, H., Leshchinsky, D. 1996. Appendix C: Case Studies on Geotechnical Aspects of In-Situ Sand Capping," in: Palermo, M., Guidance for In-Situ Subaqueous Capping of Contaminated Sediments, EPA 905-B96-004, Great Lakes National Program Office, Chicago, IL.

Palermo, M., Maynord, S., Miller, J., and Reible, D. 1998. Guidance for In-Situ Subaqueous Capping of Contaminated Sediments, EPA 905-B96-004, Great Lakes National Program Office, Chicago, IL.

Palermo, M., Mohan, R., Costello, M., 2009. "Setting In-lieu Fee Structure for Sediment Remediation on the Elizabeth River," Consultant Memorandum to the Elizabeth River Project and Living River Restoration Trust.

Reible, D., 2004. "Lessons being Learned from the Anacostia Active Capping Demonstration", Sediment Management Work Group Conference.

Thompson, T., Hartman, G. Houck, C, Lally, J. Paulson, R., 2003. "Methods for Capping Soft Unconsolidated Sediments," Proceedings: In Situ Contaminated Sediment Capping Workshop, Cincinnati, OH.

Thompson, T., Houck, C., Paulson, R., Fitzpatrick, A., 2003. "Environmental Costs and Benefits of Capping in a Wildlife Habitat: The Soda Lake Wyoming Case Study," Proceedings: In Situ Contaminated Sediment Capping Workshop, Cincinnati, OH May.

Wells, P.S., 2009."Vertical 'Wick' Drains and Accelerated Dewatering of Fine Tailings in Oil Sands," Proceedings of Tailings and Mine Waste Conference, Banff Alberta.

Van Kesteren, W. 2002. "Appendix GT3, DELCON Assessment of Gas and PAH Fluxes and PAH Flux management Plan," in: Costello, M. Data Gap Report, St. Louis River/Interlake/Duluth Tar Site, Duluth, Minnesota

Van Kesteren, W., Huls, H. 2002. "Appendix BT, Bench Test Report," in: Costello, M. Data Gap Report, St. Louis River/Interlake/Duluth Tar Site, Duluth, Minnesota.

Verduin, J., 2003. "Successfully Capping Soft Sediments," Proceedings: In Situ Contaminated Sediment Capping Workshop, Cincinnati, OH.

Verduin, J. Lynch, B., 2005. "Capping Very-Low-Strength Hexacholorbenzene-Impacted Sediments: A Case Study," in: Olfenbuttel, R. and White, P. (Eds.), Remediation of Contaminated Sediments: Finding Achievable Risk Reduction Solutions. Proceedings of the Third International Conference on Remediation of Contaminated Sediments (New Orleans, Louisiana. ISBN 1-57477-150-7, published by Battelle Press, Columbus, OH,

Verduin, J. 2002. "Appendix GT4, Cap Foundation and Slope Stability Analysis," in: Costello, M. Data Gap Report, St. Louis River/Interlake/Duluth Tar Site, Duluth, Minnesota.

CONSOLIDATION PROJECTIONS FOR THICKENED TAILINGS

Bill Shaw[1], Al Hyndman[2] and John Sobkowicz[3]
[1]WHS Engineering
[2]Magnus Limited, North Saanich, British Columbia
[3]Thurber Engineering, Calgary, Alberta

SUMMARY

Clay-dominated fluid tailings produced in oil sands mining operations represent a challenge for the industry. About 800 million cubic metres of this material reside as a fluid slurry with 30% - 40% solids (by total mass) in above-grade containment ponds. While the majority of fines can be contained within the sand matrix making up most of the solid tailings or sequestered under water caps in in-pit lakes, at least some portion of the fines will need to be managed through creation of trafficable, fines dominated (cohesive) deposits produced from thickened extraction fines (TT) or reprocessing fine fluid tailings from the tailings settling ponds (MFT). Methods are currently being tested and implemented at a commercial scale to dewater this slurry so that the resulting fine-particle material can be incorporated into closure landscapes.

The consolidation behavior of cohesive deposits is very sensitive to the compressibility and the hydraulic conductivity of the consolidating mass. The time required to attain densities and strengths suitable for reclamation may vary by years or decades for materials that appear to have similar composition.

This paper describes modeling results for thickened tailings which are based on the observed performance of available test deposits, using a finite strain model. Three field-scale tests at the Syncrude Aurora North Mine and one test at the Shell Muskeg River Mine were selected for their relevance in projecting consolidation behavior for multiple-layered TT deposits. There is a large range in predicted consolidation rates and strengths for a particular deposit, depending on which compressibility and permeability properties are selected, from which field test. Some of these meet the strength criteria in ERCB Directive 074, (5 kPa within one year of deposition and 10 kPa of surface strength within 5 years of deposition completion); others do not.

The model results for a 10-year generic TT deposit indicate that surface capping and initial reclamation would be attainable within five years of TT deposit completion, for all cases. In summary: For TT behaving in a manner typical of the better-performing field deposits, (faster consolidation and better strength gain), the Directive 074 criteria of 10 kPa will be met within 2 years of filling the DDA. The upper metre of the deposit will require a minimal cap load to achieve this condition. A closure landscape could be constructed within five years of the end of deposition.

For TT behaving in a manner typical of the poorer-performing field deposits, “floating” caps or other soft ground techniques will have to be employed for the initial access and capping efforts. A closure landscape could be constructed within 5 to 10 years of the end of deposition, although this time frame might be shortened by the use of enhanced vertical drainage, once the cap is in place.

Initial surface reclamation can commence shortly after capping. Final contouring of the surface drainage features for mine closure would be completed when remaining surface subsidence from full consolidation is in the range of 2 metres or less.

Understanding the deposition parameters leading to better or poorer-performing field deposits requires further research, with the objective of more consistently obtaining better performance. Results now available from additional deposits, created by Shell at the Muskeg River Mine (MRM) site, need to be incorporated into the model results reported herein.

Modeling projections are needed for other fines dominated deposits created from processing MFT including:

- Centrifuge cake.
- Thin-lift layering of polymer-treated MFT.
- Accelerated dewatering (a.k.a., “rim ditching”).

With the exception of the 2009, 10-metre thick accelerated dewatering deposit at the Syncrude Mildred Lake test site, there are no deep deposits

with a multi-year history of monitoring to provide data for meaningful model projections. As commercial-scale demonstrations of these methods are now being implemented, it is important to acquire field data over a longer time period so that future planning and projections of consolidation performance can be based upon valid modeling. Collaboration among oil sands operators should result in accelerating the expansion of knowledge in this important area.

INTRODUCTION

Fluid fine tailings produced from surface mining of oil sands operations have been the subject of much attention and in some cases considerable misinformation in the media and on the internet. The causes, consequences and management methods under development have been described in Hyndman & Sobkowicz 2010 and in Sobkowicz & Morgenstern 2009.

In summary, fluid fine tailings result from the segregation of fines from the coarse sand tailings as the sand settles on tailings beaches. The water that runs off the beach contains fine solids, both of which go into a containment pond. The fines settle slowly from the water, reaching a solids content of about 30% (by total mass) within two years. This material is referred to as “Mature Fine Tailings” (or MFT). Ten to twenty years after deposition, MFT may reach a solids content of 35% to 40%.

There are three general methods of incorporating fines into the mine closure landscape:

The fines can be incorporated into the sand tailings matrix.

The fines can be sequestered under a water cap in an in-pit lake.

The fines can be processed to create a fines-dominated (cohesive) solid deposit.

The following table lists the methods in use or under active development for each of the three categories.

Table 1. Fines Sequestration Methods

Fines in sand	Fines-dominated (Cohesive)	Water-capped Fluid Fines
Conventional beaching	MFT centrifugation	Storage under water in an in-pit lake
CT (mixture of sand and MFT)	MFT thin layer dewatering	
NST (mixture of sand and TT)	MFT accelerated dewatering (“rim ditching”)	
	TT deposition	

Each of these methods is described in Hyndman & Sobkowicz (2010).

The rate at which each of these types of deposit is ready for reclamation varies:

- For the case where fines are stored within the sand, deposits consolidate relatively quickly and achieve strength with surface loading. Reclamation can be started shortly after deposition.
- For water-capped MFT, geotechnical strength is not a factor. Reclamation occurs as the resulting pond bio-remediates to an environmentally acceptable condition.
- For cohesive deposits, a near fully consolidated state can take years or decades.

It is the consolidation behaviour of these latter deposits, and of thickened tailings in particular, that is the subject of this paper.

The consolidation rate of deep, multiple-layered, clay-dominated deposits is very sensitive to the compressibility and the hydraulic conductivity of the material, (the latter declines as consolidation takes place). A deposit with one or two thin lifts may undergo an initial dewatering (upon deposition), and then if left alone, may further dewater through environmental effects such as evaporation or freeze-thaw. This type of deposit can develop strength relatively quickly. However,

when multiple layers are deposited at a continuous and relatively quick rate, (i.e., quicker than the rate of consolidation), dewatering and significant strength gain can take many years.

CONSOLIDATION PROJECTIONS

Test Data Sources

Data from four relevant deposits were used to develop consolidation projections:

1. Cell B
2. Column 8
3. Column 19

} Syncrude Aurora North Mine 2001-3 thickener trials.

4. Shell TTF Cell 1 at the Muskeg River Mine (2007 trial).

The test conditions for each of the above deposits are outlined below:

Deposition Conditions	SCL Aurora Cell B	SCL Aurora Column 19	SCL Aurora Column 8	Shell TTF Cell 1
Thickener	10 metre high rate (CONRAD)	1.5 metre Eimco Pilot (4.5 metre height)	10 metre high rate (CONRAD)	10 metre Paste
Polymer & addition rate, grams per tonne	CIBA 1235 93	CIBA 1235 86-100	CIBA 1235 92	Hychem AF246 210 (+ 100g Ca^{2+}/m^3 H_2O)
Average solids at deposition, Mass%	42.8	55.6	46.6	60.2
Fines/(Fines+water) at deposition, Mass%	29.7	37.9	32.5	47.1
Sand/Fines Ratio	0.77	0.95	0.81	0.70
Pump type	Centrifugal	Peristaltic	Centrifugal	Positive Displacement
Size of Deposit	1 m depth 15 m width by 250 m length	4.35 m depth 1.5 m diameter	5 m depth 3 m diameter	4.75 m depth 35 m width and 65 m length
Filling Period	307 hours TT intermittent discharge August 27 to September 27, 2003. Approximately 6856 m^3 of TT was placed in Cell B at an initial slurry average density of 1.36 t/m^3. The calculated volume in October, 2003 was 3777 m^3 and the average deposit density was 60% solids. See Cell B deposition timeline - Attachment 1A.	22 hours TT was deposited on Sept 23, 24 and 25, 2003 - a total of 22 hours to fill.	3 hours TT was deposited continuously from 2 pm to 5 pm, Aug 14 2002.	319 hours TT intermittent discharge over 4 months from Sept 5, 2007 to Dec 4, 2007. See Cell 1 deposition timeline -Attachment 1B.

Note: Factors not included in the above table, such as clay content, variation in composition and environmental effects may affect consolidation and strength attainment.

The measured compressibility and back-calculated hydraulic conductivity for all four deposits are shown in Attachment 2. It is clear from these plots that:

- Cell B and Column 19 show more favourable TT behaviour, with a lower compressibility and a higher hydraulic conductivity (indicating a higher consolidation rate).
- Column 8 and the Shell thickener show higher compressibility and lower hydraulic conductivity (indicating a slower consolidation rate).

The observed differences in compressibility and hydraulic conductivity for these deposits do not appear to be large (on the plotted curves), but as will be evident in the next section, small differences in these properties can lead to substantial differences in rate of consolidation.

The peak and residual undrained shear strength data for the field pilots are shown in Attachment 3. It should be noted that there were difficulties in calculating the vertical effective stress due to lack of measured pore pressures for some deposits (in which case, pore pressures were estimated). It is clear from the peak strength plot that:

- Only Column 8 and the Shell thickener show undrained strengths that are consistent with the calculated vertical stress profile and with critical state soil mechanics principles, indicating a c_u/p' ratio of about 0.35.
- The other deposits apparently have much higher c_u/p' ratios, most obvious on the peak undrained shear strength plot, but also to some extent existing on the residual shear strength plot.
- Residual strength data is only available for the Cell B deposit. This material exhibited a large strength loss at high shear strain, i.e., a high strength "sensitivity".

The reasons for the differences in the strength behavior noted above are not obvious. One issue is the lack of good pore pressure data. Another is the impact of environmental effects on the deposits, which has not been well documented.

Modeled Consolidation Results (Generic TT Case)

The data from these four deposits were then used to model the consolidation trajectories of TT in a realistic example deposit:

- 10-years of deposition at a rate of 1.2 tonnes of solids per m^2 per year.
- Thickened tailings with sand/fines ratio of 0.8.
- Solids content of 50% as deposited {≈ 36% F/(F+W)}
- Maximum deposit depth at completion: 20 metre.
- Sand cap – 6 metres total (2 metres per year over 3 years).

Consolidation and strength over time were projected using a finite strain model, using material parameters as shown in each of the four sets of curves shown in Attachment 2. Note that it is very important to use a *self-consistent* set of permeability and compressibility curves, both derived from the same deposit, for a particular analysis. Selection of "average" or "best estimate" unrelated curves from the two plots will lead to very misleading projections.

The finite strain analyses predict the variation in solids content and effective stress in the deposit with time. Projected strength profiles are calculated by applying what is judged to be an appropriate c_u/p' ratio to the calculated vertical effective stress. The projected solids content and strength profiles are shown on the following charts. For ease of comparison, 5 kPa and 10 kPa peak undrained shear strength lines have been highlighted for reference.

TT Deposit Properties - Column 19 Parameters

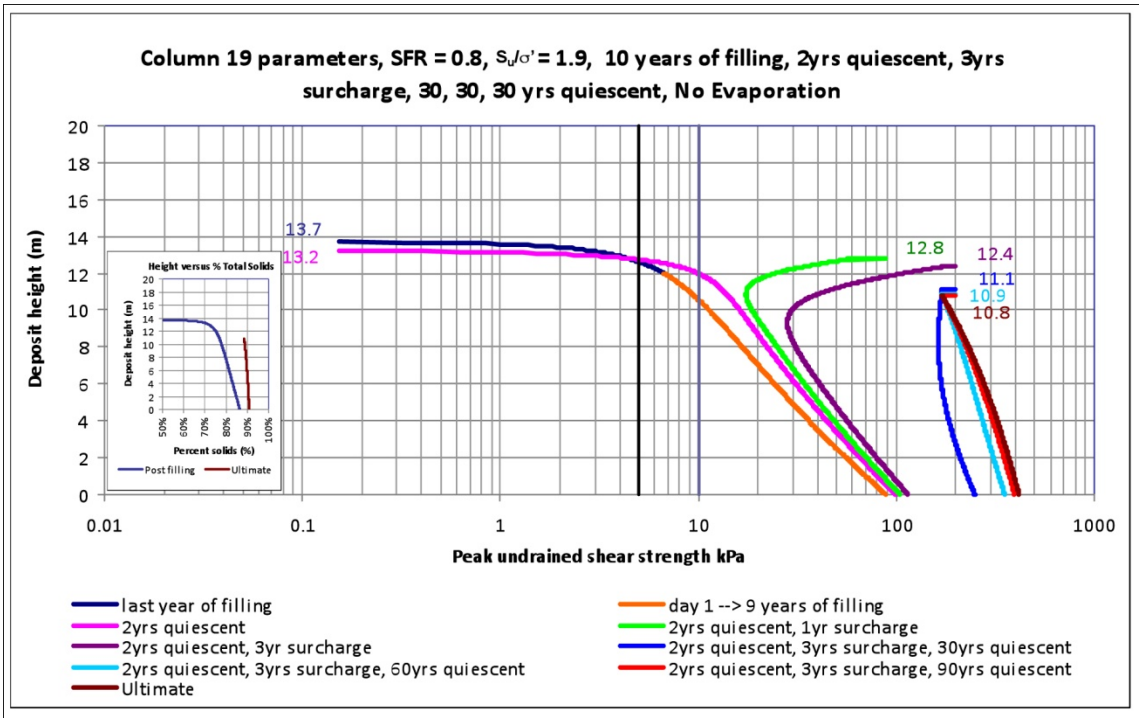

TT Deposit Properties - Cell B Parameters

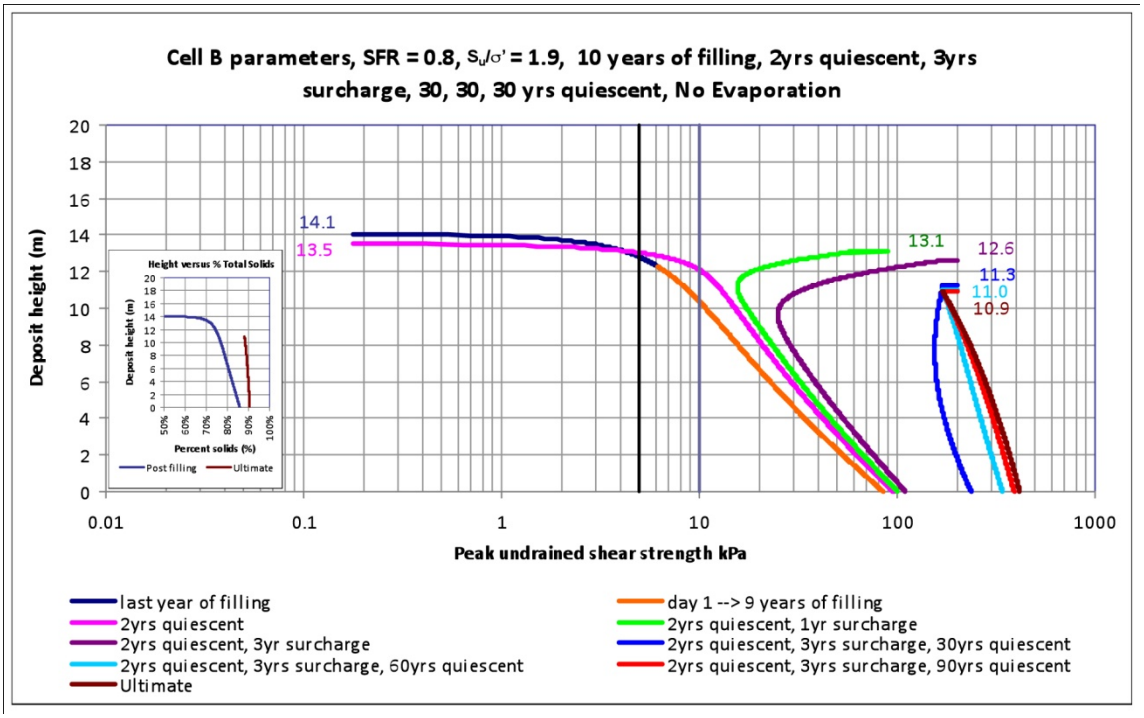

TT Deposit Properties - Shell Cell 1 Parameters

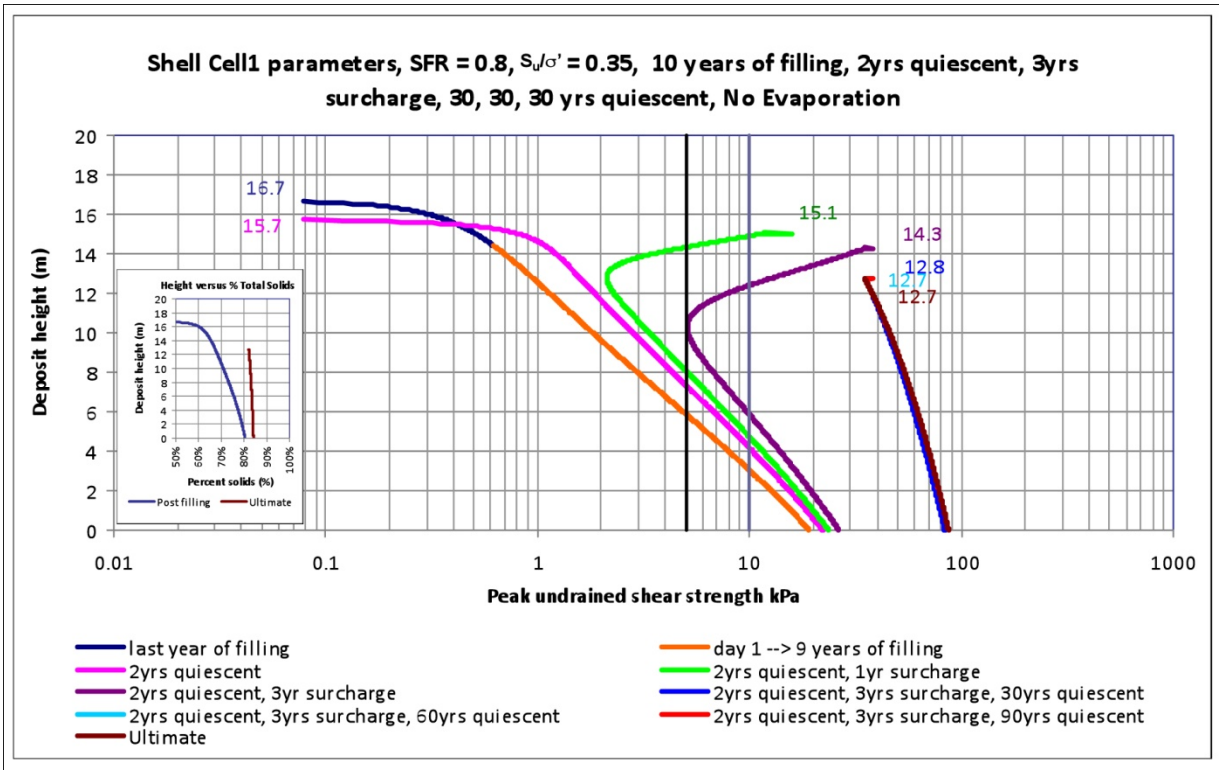

TT Deposit Properties – Column 8 Parameters

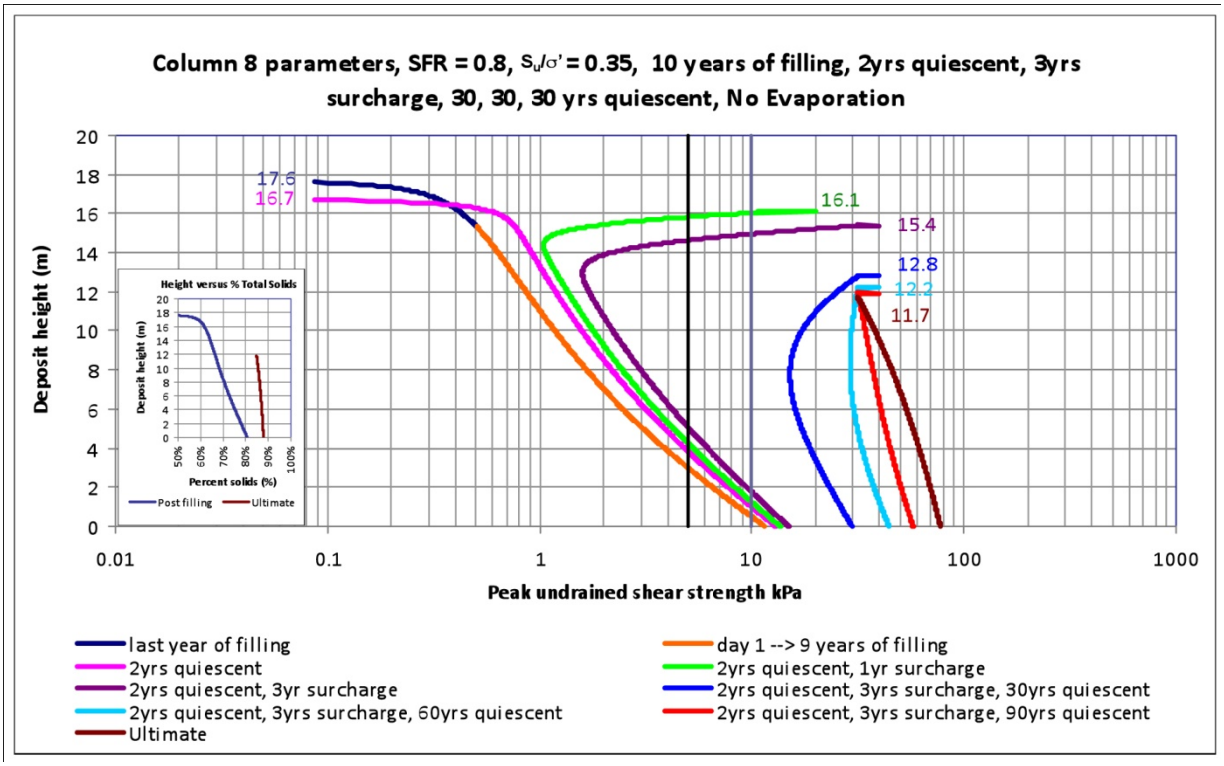

The analyses based on the Cell B and Column 19 data predict somewhat faster rates of consolidation than the analyses based on the Column 8 and Shell Cell 1 data, as is evident in the deposit heights at the completion of TT deposition, shown in the following chart. The projected strength profiles are also shown in this chart. Note, however, that the strength predictions based on Cell B / Column 19 data used a higher c_u/p' ratio – a value of 1.9, compared to a value of 0.35 for the Column 8 / Shell Cell 1 predictions. These values were selected to show the possible range of behaviour in the deposit. If the c_u/p' ratio for the Cell B / Column 19 predictions is reduced to 0.35, the projected strength profiles are more in line with the Shell Cell 1 curve.

The strength predictions for the four cases *after sand* capping are compared in the following three charts. The results indicate that *final land form* construction and *surface drainage* contouring, to build a closure landscape, could begin almost immediately following sand capping, based on the Column 19 and Cell B data (using the higher cu/p' ratio). However, if

the deposit behavior follows the Shell Cell 1 or Syncrude Column 8 trajectory and the lower c_u/p' ratio, land form construction and surface contouring would need to be deferred for 5 to 10 years following placement of the sand cap to reach a position of acceptable residual subsidence (less than about 2 metres). It may be possible to shorten this time by accelerating dewatering and strength attainment, using additional methods such as working the deposit surface with special mobile equipment to enhance atmospheric drying.`

TT Deposit Strength after the Filling Period

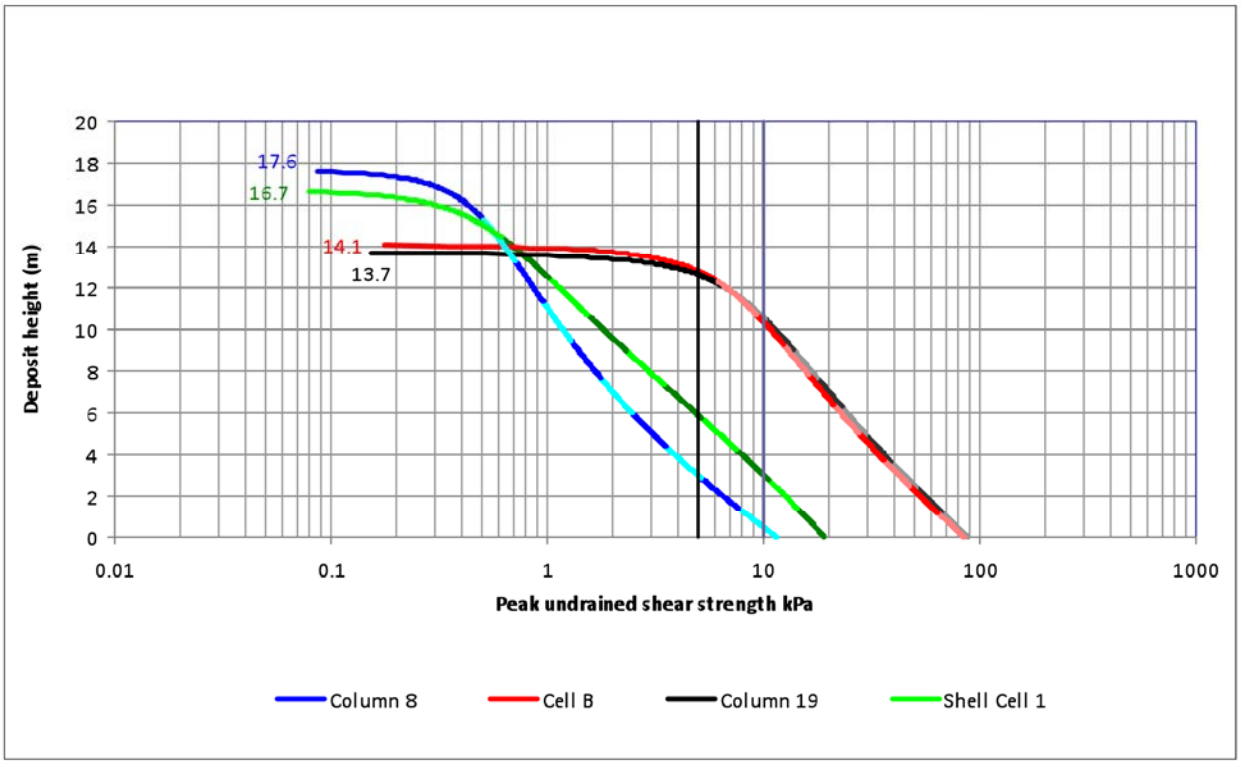

TT Deposit Right after Sand Capping

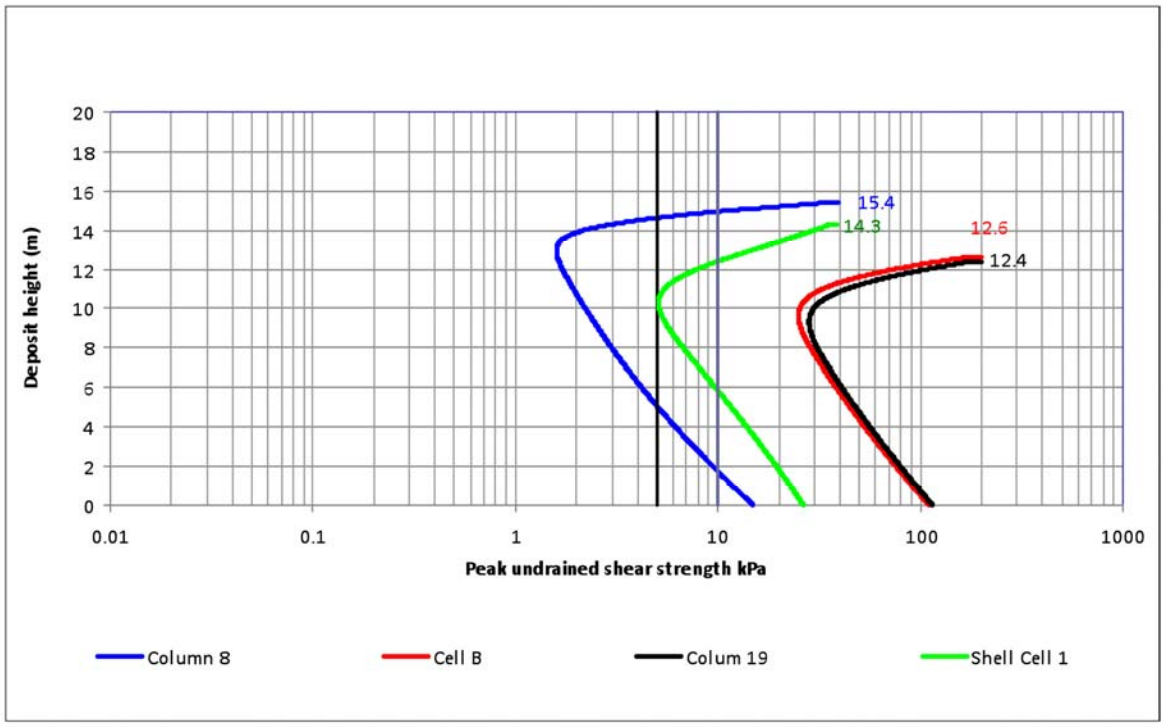

TT Deposit Properties 5 Years after Capping

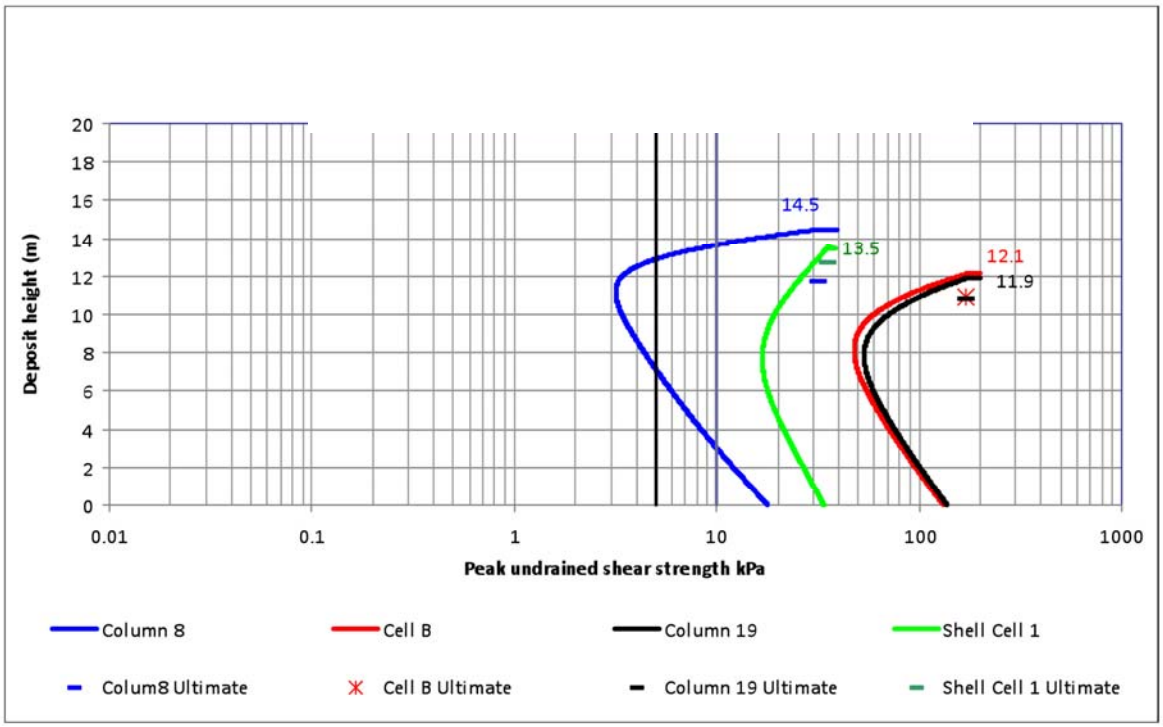

TT Deposit Properties 10 Years after Sand Capping

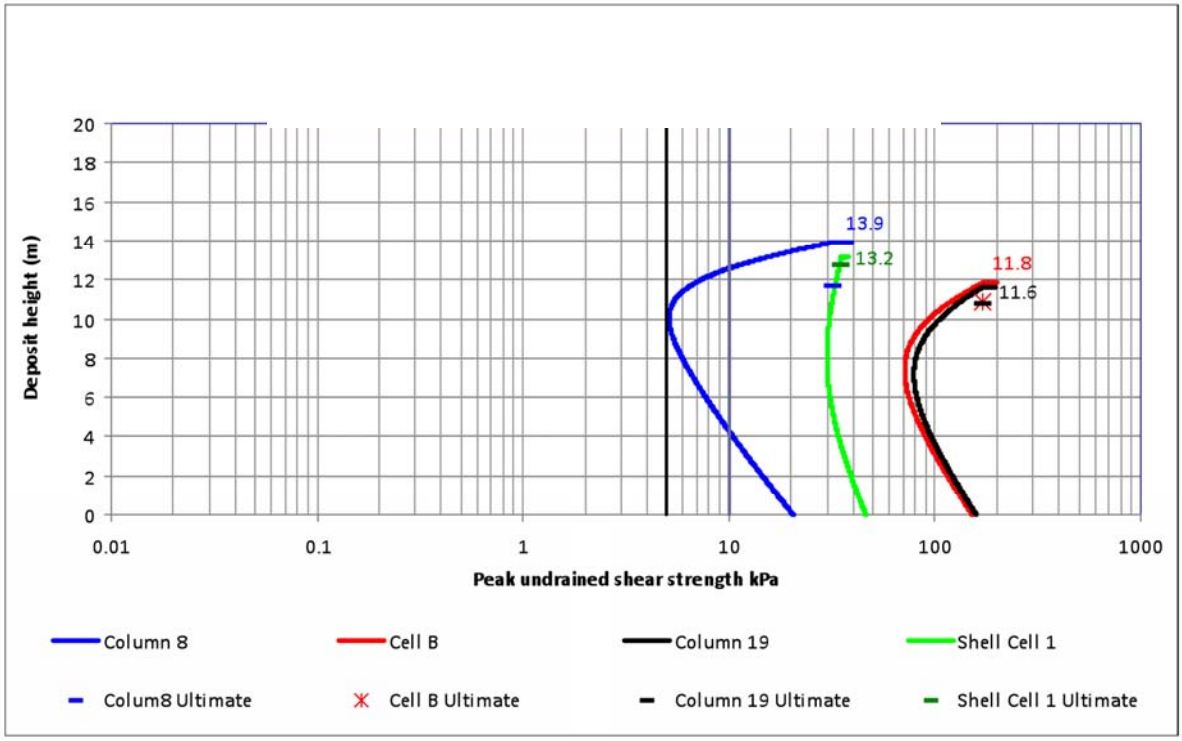

CAPPING AND RECLAMATION

Two important conclusions arise from the preceding analysis and projections. While there is a considerable range in strength attainment projected through the 10-year operational period of the TT deposits, assuming TT deposition rates are managed such that consolidation and strength trajectories remain within the expected range:

- Sand capping of the deposit is expected to be achievable within 5 years of the end of TT deposition, even when using the lower end of consolidation predictions, albeit at greater cost and using soft ground access and capping techniques for the poorer-performing deposits.
- To limit residual subsidence after the establishment of a reclamation surface to about 2 m or less, a time period of one to two years after capping will be required for the better-performing TT deposits and of 5-10 years (or less, if enhanced vertical drainage techniques are applied) for the poorer-performing deposits. A value of 2 m residual subsidence is low enough to allow for design of a durable surface topography that will not be disrupted by future settlement.

Therefore, the thickened tailings process is capable of achieving three important tailings management objectives:

- Fines can be processed in an economical manner through the operating period of the mine, avoiding a continuous buildup of fluid fine tailings.
- Thickened tailings deposited out-of-pit in a dedicated disposal area, with a relatively small footprint, can be capped and surface reclamation commenced within a reasonable period following completion of the TT deposition.
- Consolidation of the TT deposit can be measured throughout the period of deposition and capping, and the performance can be compared against modeled projections. The accuracy of the

consolidation model is much better in a quiescent environment.

DDA Performance Measurement

The key performance measure for a TT deposit will be the rate of initial and ongoing dewatering of the deposit and the resulting solids content and strength attainment throughout the years of operation, after deposition quiescence, sand capping and surface reclamation. The following procedures are recommended to monitor TT deposit performance:

- A representative number of sample and measurement points should be established, appropriate to the size and geometry of the TT deposit area. This coverage will be adjusted through experience depending upon the degree of uniformity or diversity of measurement results.
- Each year, through the depth of the deposit, strength measurements should be made, and samples taken and analyzed to determine the strength gain trajectory.
- The solids content and strength measurements should be compared with the model projections to determine if consolidation is within the range of projected behavior, to ensure that reclamation objectives are attainable, and to identify any areas where remedial measures might be needed.

This management process would ensure that mine reclamation and closure plans remain timely, achievable and durable.

Freeze-Thaw and Drying of TT

The consolidation predictions described in this memorandum do not take into account any benefit from drying and freeze-thaw of the TT. These processes will at a minimum increase the solids content and strength of the upper metre or two of the final TT deposit. For lower rates of annual deposition, (e.g., < 1 to 2 m vertically in the DDA), these processes will also improve the performance of the entire deposit. The magnitude of the benefit (in either case) can be maximized by preventing any accumulation of water on the deposit surface.

Ongoing Work

Methods for fine tailings densification and deposition are in the early stages of development. With the exception of CT, which is based upon maintaining a sand matrix to achieve dewatering and solidification, no deposits of greater than a few metres in depth have been created and measured over years. (For example, the deepest cohesive deposit created thus far is Syncrude's 10 metre deep, accelerated dewatering trial deposit. It has had just one year of consolidation since deposition completion.) Work initiated over the past decade on fines-dominated (or cohesive) deposits, culminating with large-scale field demonstrations and initial commercialization this year, will provide consolidation performance of multiple layer deposits measured over several years.

Recently, industry members have committed to arrangements for increased collaboration and transparency in tailings technology according to the following principles:

- Tailings technical information will be broadly available to the industry members, academia, regulators and others interested in working on tailings solutions, and
- Industry members will collaborate on research, development and commercialization of technology among operators and with other research agencies.

In respect of thickened tailings performance specifically, Shell plans to start-up deposition of TT at the Jackpine Mine (JPM) and has committed to the ERCB to manage the TT deposit sub-aerially and to apply other measures to maximize the rate of consolidation and strength gain. Shell has advised that the industry will have full access to learn from the commercial-scale experience at JPM for application at other operations. Measures that will be evaluated by Shell at JPM will include:

- Wick drain installation and working the deposit with specialized equipment to enhance water release,
- Placing intermediate sand layers over partially desiccated thickened tailings deposit, and

- Diverting some thickened tailings to a separate drying facility to enhance rate of water release and strength gain.

Shell is engaging international experts to support rapid transfer of international experience and best practices in enhanced dewatering of slurry based deposits.

CONCLUSIONS

1. Thickened tailings deposits are projected to consolidate sufficiently for completion of sand capping within five years after the end of deposition to support surface reclamation activities.
2. While TT deposits may take several years to attain sufficient consolidation for final reclamation, they require less area than other methods relying on very low rates of vertical annual deposition. This is an important factor in considering constrained sites and in avoiding area disturbance for the sole purpose of fines management.
3. Performance measurement of the deposits will indicate the projected timing for completion of capping and final surface reclamation, and whether any remedial measures are warranted.
4. Additional field test data is needed to improve the fidelity of modeling projections and to gain a full understanding of the factors influencing consolidation behavior and strength gain.
5. To improve modeling and performance projections for other types of cohesive deposits based upon MFT treatment, (such as thin-lift deposition, centrifugation and accelerated dewatering), it is important to generate and assemble data from large-scale, deep deposits as they become available from commercial-scale field trials.

REFERENCES

Hyndman, A and Sobkowicz, J., 2010. Oil Sands Tailings: Reclamation Goals & the State of Technology. Geo2010, Calgary, Alberta, 10 September, 2010.

Sobkowicz, J. and Morgenstern, N.R., 2009. Oil Sands Tailings Reclamation – Technology Road Map. Tailings and Mine Waste ’09, Banff, Alberta, December 2009.

Attachment 1A

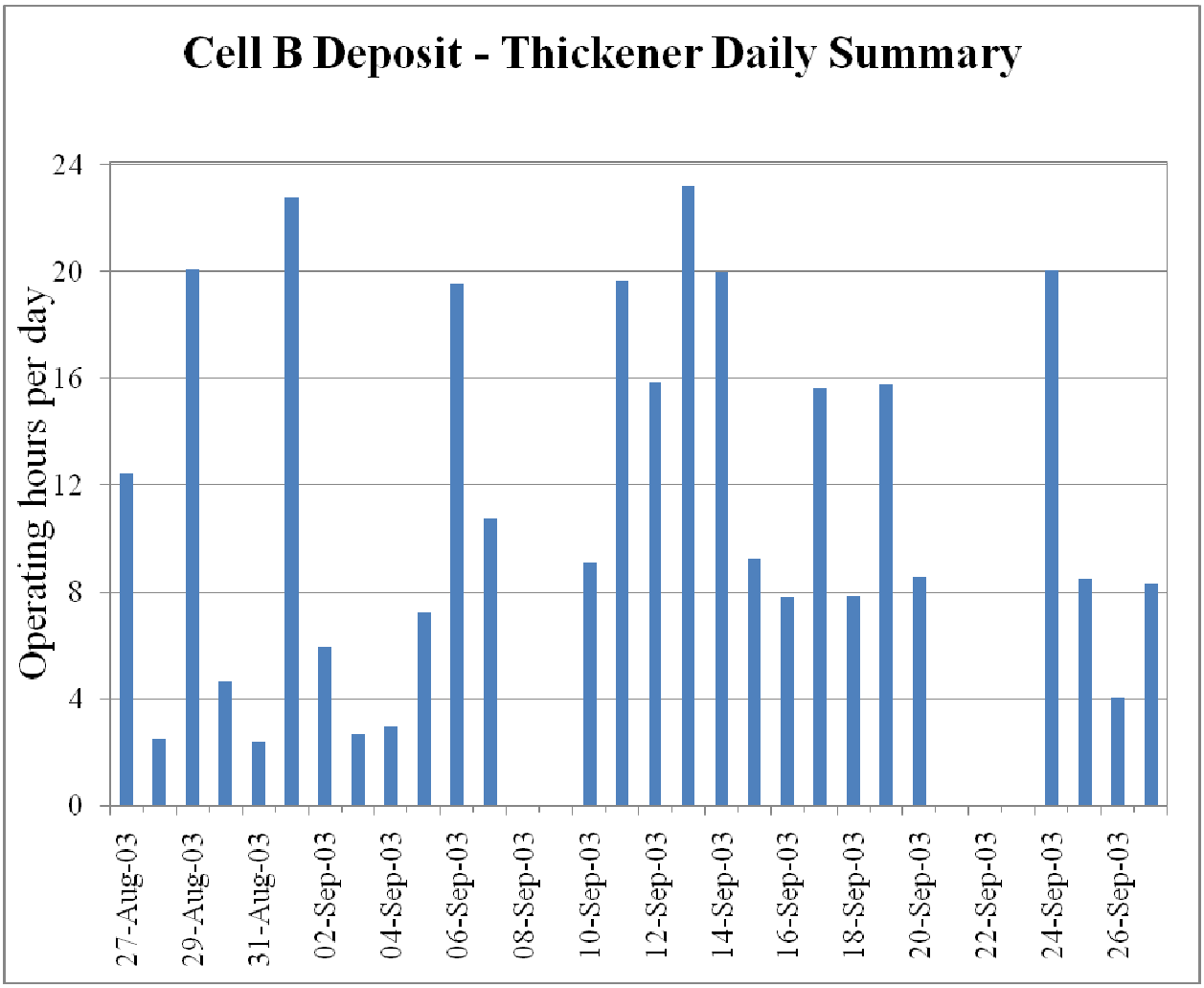

Attachment 1B

Shell Cell 1 Deposition Timeline

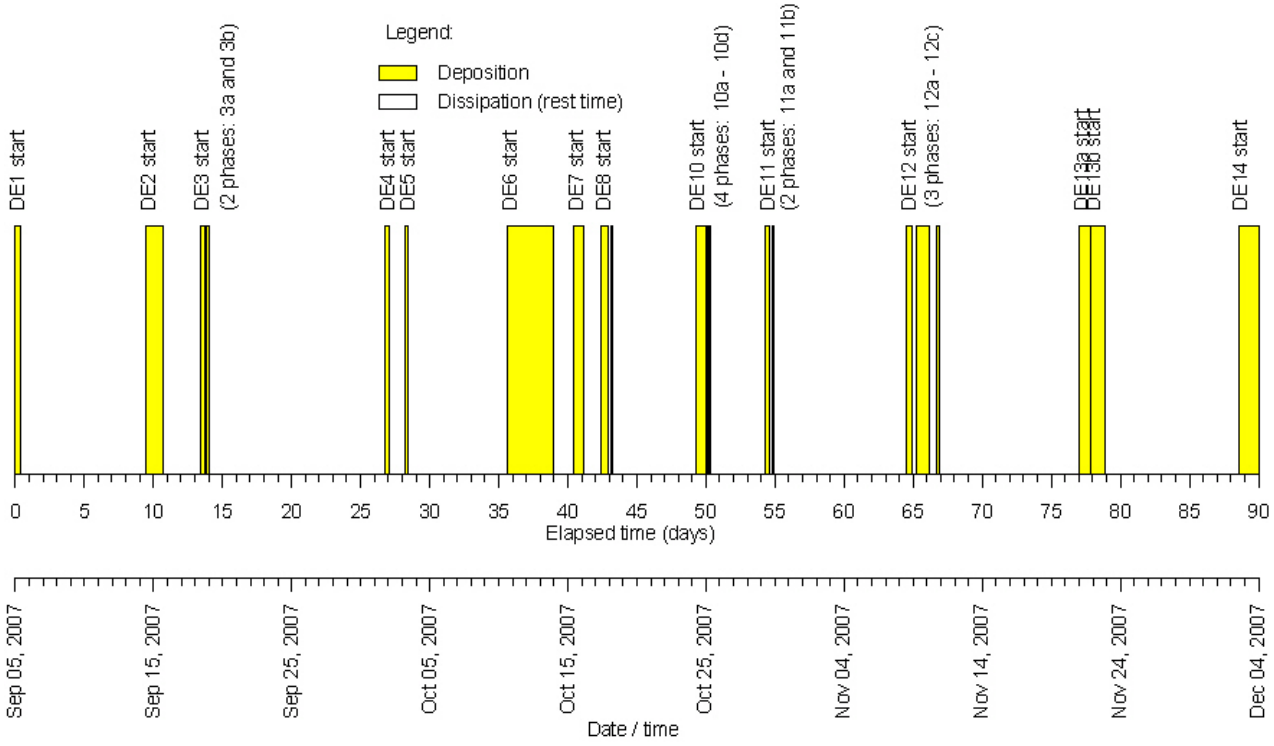

Attachment 2

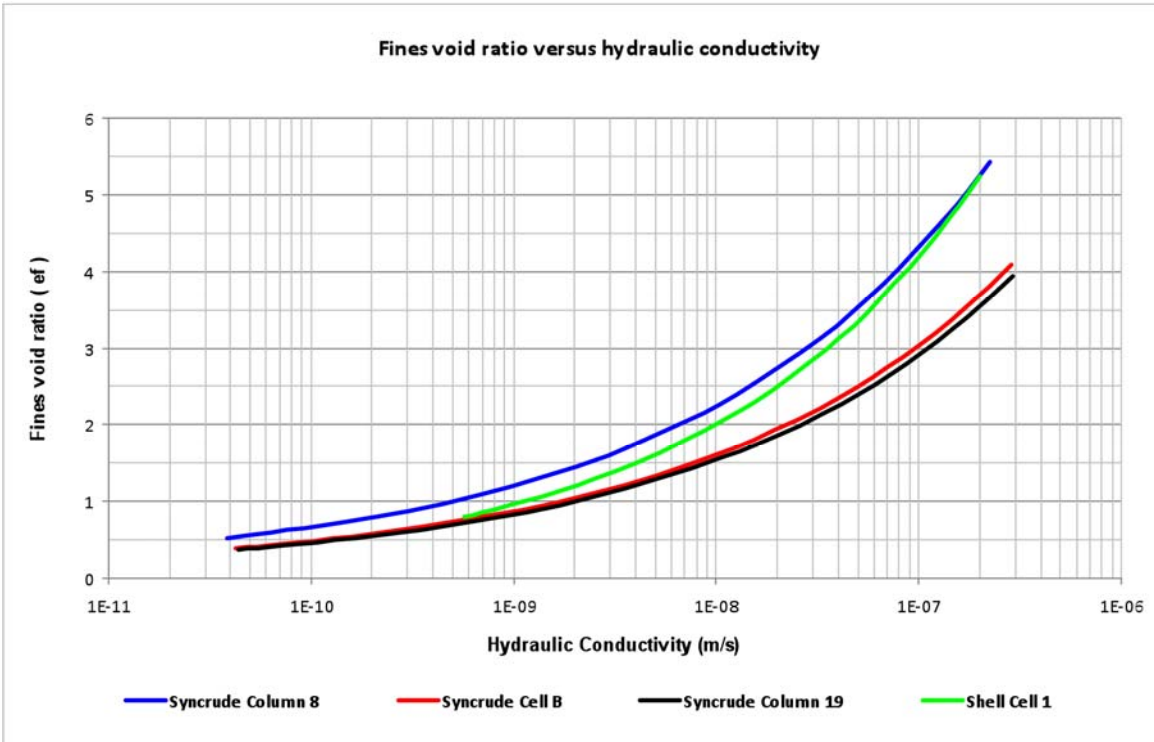

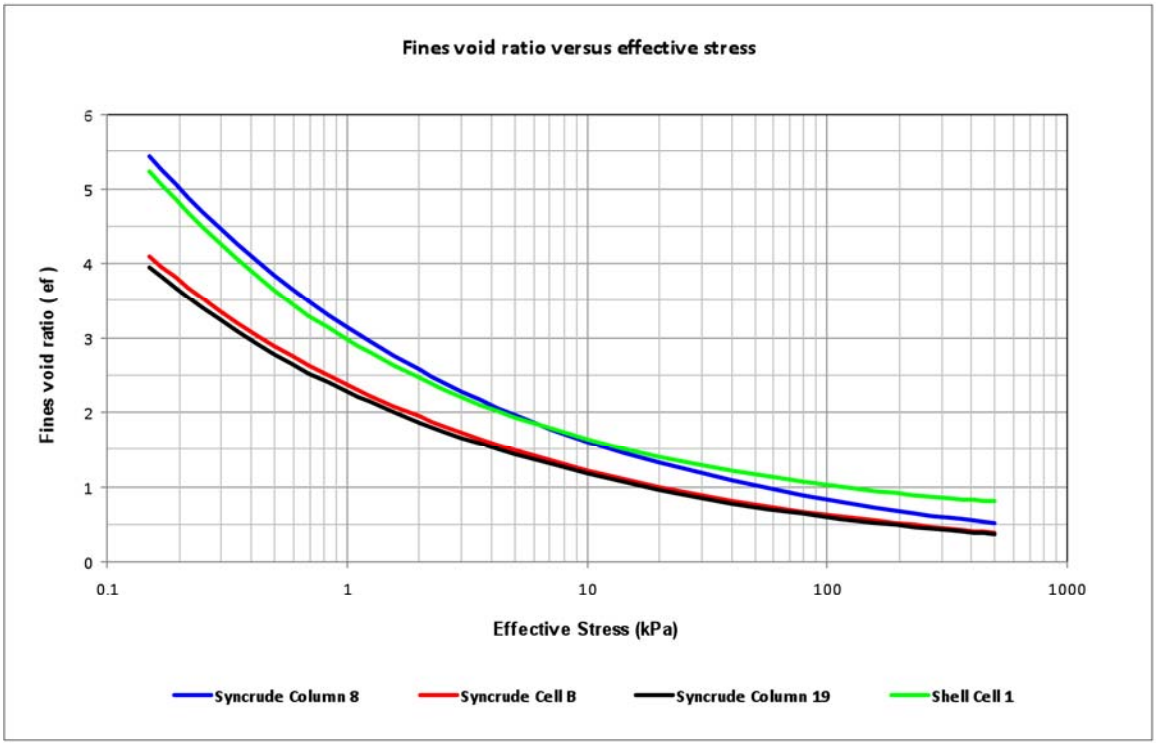

Attachment 3

Figure A-1 – Peak Undrained Strength vs Effective Stress

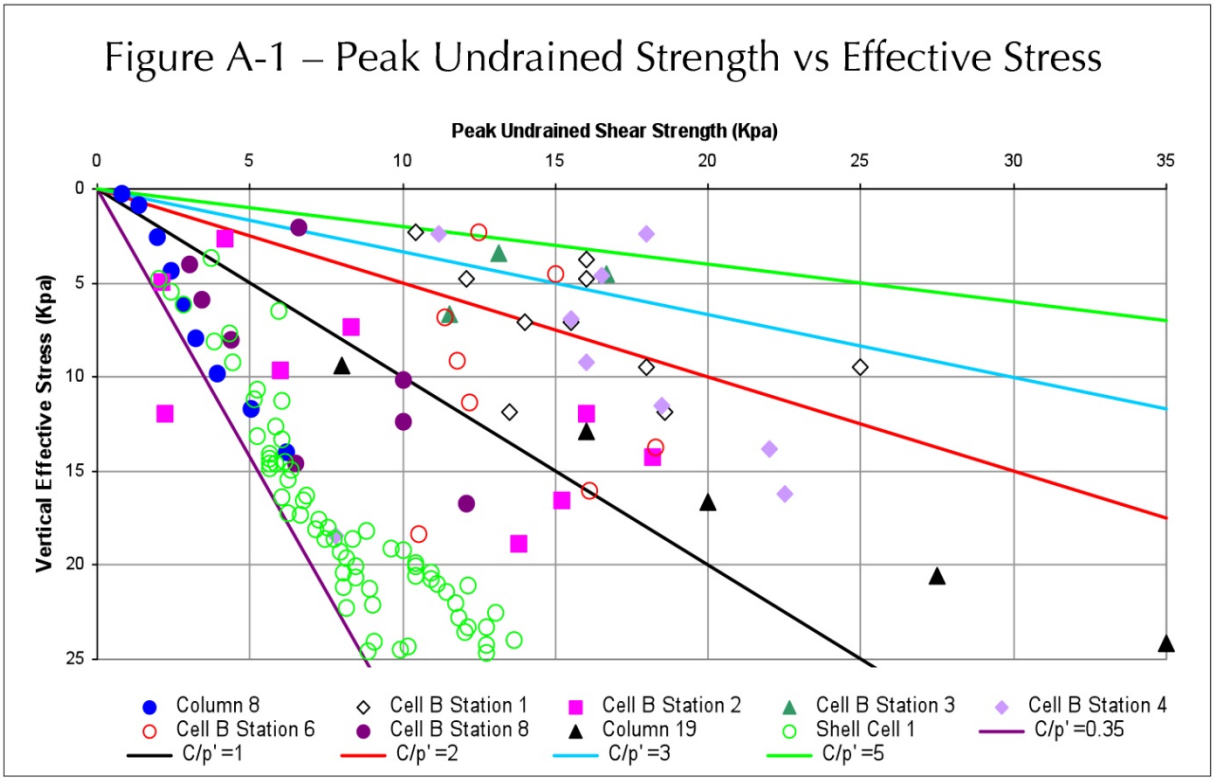

Figure A-2 – Residual Undrained Strength vs Effective Stress

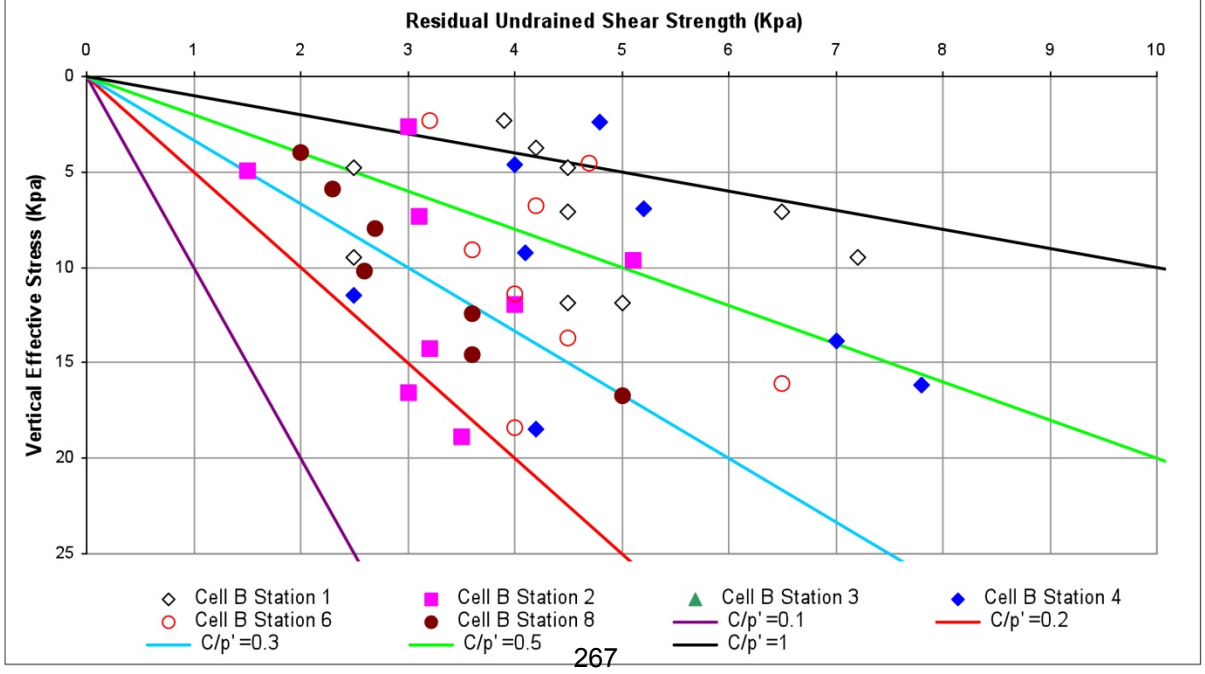

RECLAMATION AND CLOSURE OF AN OIL SANDS TAILINGS FACILITY

J.C. Sobkowicz[1] and N.R. Morgenstern
[1]Thurber Engineering Ltd., Calgary, Canada
[2]University of Alberta, Department of Civil & Environmental Engineering, Edmonton, Canada

ABSTRACT

Considerable attention is being focused on the reclamation and closure of oil sands tailings facilities by all oil sands Mine Operators, as a result of the ERCB Tailings Directive 074. Much of that discussion centers on the means of developing strength with time in a Dedicated Disposal Area (DDA), to meet the minimum strength criteria given in Directive 074. This paper provides a comprehensive geotechnical discussion of the related issues. It begins with a review of the primary objectives of reclamation and closure, classifies the potentially reclaimable tailings streams and their characteristics, elucidates reclamation strategies for these materials, and then proposes a modified approach to assessing the reclamation readiness of a DDA, including means for measuring its performance.

INTRODUCTION

This paper discusses the means by which strength is developed with time in a Dedicated Disposal Area (DDA; as defined in the ERCB Tailings Directive 074) and provides some recommendations on methods of measuring strength gain and progress of consolidation in a DDA. The objective is to propose alternate criteria for monitoring of DDAs compared to the one currently included in ERCB D-074.

BACKGROUND

The ERCB issued a draft Tailings Directive in June of 2008, which after a brief discussion with industry participants was issued in final form in February of 2009 (ERCB, 2009). The Directive was developed in response to direction given to ERCB staff in July of 2004.

The Directive requires operators to reduce fluid tailings through fines captured in dedicated disposal areas (DDAs), and to form and manage DDAs. The operators are further required to submit tailings plans, pond status reports, DDA plans, and annual compliance reports for DDAs, which will allow the ERCB to assess overall compliance with the directive.

The Directive was developed as the "…first component of a larger initiative to regulate tailings management…" (ERCB, 2009), and contains a list of long-term objectives which presumably will govern the development of further regulations on tailings management.

Of relevance to this paper are several "technical" requirements contained in the Directive:

- Certain targets are given for fines capture in DDA's, expressed as a percentage of the mass of dry fines in the oil sands feed (this target is in addition to the fines captured in hydraulically placed dykes and beaches). The target is 20% for mid-2010 to mid-2011, 30% for mid-2011 to mid-2012, and 50% thereafter.

- "DDAs must be formed in a manner that ensures trafficable deposits." The stated criteria to meet this objective is a) to achieve a minimum undrained shear strength of 5 kPa for material deposited in the previous year, b) to be ready for reclamation within five years of end of deposition, and c) when ready for reclamation, the trafficable surface layer must have a minimum undrained shear strength of 10 kPa.

- Once the trafficable surface layer has been achieved, the operator is to file an application to abandon the DDA, (what "abandonment" means is not explicitly stated in the Directive, nor is the need to establish a closure landscape addressed).

In the authors' opinion, D-074 is timely and contains some needed regulatory oversight on the oil sands tailings management process. However, D-074 is not perfect and could be considerably improved. As a case in point, the strength criteria listed in D-074 are too stringent and lack flexibility. In the following sections, the authors will develop concepts for an alternate way of regulating DDA

performance, by a) discussing reasonable objectives for the reclamation of a DDA, b) describing the types of material that might be stored in a DDA and the different reclamation strategies that might be applied to each, and c) discussing alternative performance measures that should be considered by the ERCB to improve the regulatory process.

Other material evaluating the impact of D-074 on the industry (both good and bad), and discussing appropriate roles for the Operators and the Regulators, is found in Sobkowicz (2010).

RECLAIMABILITY OF A DDA

General Reclamation Objectives

The following is a suggested set of general reclamation objectives for DDAs, both during their operating life, and then at and after closure. They are taken from Hyndman and Sobkowicz (2010), and are, in the authors' opinion, equivalent to or compatible with the tailings management objectives given in Directive 074.

Goals for the operating period of the mine (preceding mine closure) include, to the greatest extent practical:

- Reclaim tailings as mining proceeds, avoiding excessive accumulations of contained fluid fines that must be remediated at or near the end of mine life.

- Limit the required containment volumes of MFT (in particular, in out-of-pit dam structures) to that required for effective tailings management.

- Without compromising the essential elements of a closure landform design or the efficiency of tailings operation plans, conduct as much remediation as is practical during the active mine life, when there is operating revenue to cover the costs and while the mine organization and operating infrastructure are in place to efficiently conduct the activity.

The following are general objectives for returning mine site lands to the public without ongoing liabilities:

- Avoid DDAs in the reclaimed landscapes that require ongoing maintenance for decades following active mining.

- Attain landforms with geotechnical stability that are resistant to natural processes and are self-healing after natural erosion, with self-sustaining, native vegetation cover.

- Design productive, self-sustaining land and water features that are integrated into the natural ecosystem without adverse consequences to downstream watercourses.

Reclamation Objectives Specific to the Immediate Reclamation of a DDA

Specific to the immediate reclamation of a DDA, tailings should with time meet several important objectives:

- They should develop strength at a rate sufficient to allow timely capping, in order to meet reclamation and closure requirements.

- They should develop a low compressibility so as to minimize post-closure settlement and not disrupt the closure landscape.

The rate at which these two objectives can be met will be different, and thus reclamation may be a two-stage process: a) capping and constructing an initial reclamation surface, and b) constructing the closure landscape (drainage and flora) when long-term settlements have reduced to manageable values.

CLASSIFICATION OF POTENTIALLY RECLAIMABLE TAILINGS STREAMS

This section will focus on tailings streams with a moderate to high proportion of fines, which are the ones that are potentially problematic from a reclamation perspective. In practice, tailings products have a wide spectrum of gradations and properties. However, it is useful to consider a classification of tailings as deposited in a DDA into three types, as defined in the following sub-sections.

Reference should be made to Sobkowicz and Morgenstern (2009) for a more detailed discussion (and a definition of some terms). Acronyms are defined at the end of this paper. The characteristics of Types 1, 2 and 3 materials are discussed in greater detail in Section 4.3 of Sobkowicz and Morgenstern (2009), and illustrated in the associated Figures 5a and 5b of that paper.

Type 1 – Fines-Dominated Tailings (SFR < ~0.3)

This material consists mostly of fines (< 44 μm), often with a high percentage of clay size particles (e.g., 50% to 60% < 2 μm).

A typical example is TFT/MFT. This material is produced by segregation of other tailings streams and accumulates in a fluid pond. Initially the solids content is relatively small (~15%) and the material is referred to as TFT. With settlement over time, the solids content can increase into the range of 25% to 35% and the material is referred to as MFT.

This type of material has the potential for maximum fines storage efficiency. However, it will have the lowest hydraulic conductivity and highest compressibility, which could, for some treatment processes, result in a long time to achieve reclamation objectives.

Type 2 – Sand-Depleted Tailings (~0.3 < SFR < ~3)

This material consists of a mixture of fines and sand of approximately similar proportions. Some examples are TT, which is a manufactured product, and materials that result from the segregation of other tailings streams.

Thickened tailings have an SFR of ~1, (referred to as TT), and are essentially a sand-depleted whole tailings, with some water removed. The clay portion of the fines in this material typically is lower than it is for MFT. Out of the thickener, the solids content can vary, depending on thickener type. For example, solids content for a High Rate Thickener would be in the range of 40% to 50%, and for a Paste Thickener of 50% to 60%.

Material that results from segregation of other tailings streams typically has a higher range of SFR and of clay content.

Materials in this category have a moderately high fines storage efficiency but still exhibit low hydraulic conductivity and moderately high compressibility, similar to the Type 1 materials.

Type 3 – Sand-Dominated Tailings (SFR > 3)

This material has a solid matrix that is dominated by the sand particles, and which contains a relatively small proportion of fines. The clay fraction in the fines is variable, depending on the feed stock. Examples of this material type are whole tailings (WT) and manufactured products such as CT and NST.

WT has an SFR that is representative of the fines in the combined oil sand ore and associated inter-burden that is delivered to the extraction plant. It can range from 5 to as high as 20 (for high grade ore with little inter-bedded clay layers). CT and NST are artificially created tailings products with a SFR in the range of 3 to 5, an initial solids content of about 60%, and a solids content after deposition in excess of 70%.

This type of material has the lowest potential for storage of fines. The incentive for creating CT or NST is to enhance fines capture compared to WT, consistently reducing the SFR to values in the range of 3 to 5, but still retaining the granular nature of the deposit. When deposited, CT/NST has a loose to compact density, and a relatively high permeability and low compressibility compared to Type 1 or 2 materials. It thus will densify and gain strength quickly under load.

RECLAMATION STRATEGIES

Each of the types of tailings deposits described in the previous section presents its own challenges in regards to reclamation.

Type 1 (Fines-Dominated Tailings)

Reclamation of this type of material will be discussed using the most common example, MFT.

MFT is a mature product that, in a pond, would take a long time to settle and consolidate. Thus, without further treatment, it remains in a fluid state for a long period of time. To achieve strengths suitable for reclamation, the solids content would have to increase to a value in the range of about 65% to 70% (depending on the plasticity characteristics of the fines). Several stages of additional treatment (chemical, mechanical, electrical or environmental; see “road map” in Sobkowicz and Morgenstern, 2009) will likely be required to sufficiently increase the solids content; various methods for doing so are under active research (pilot stage) in the various oil sands mines.

Some treatment strategies to further dewater Type 1 tailings are:

- Centrifuging the MFT (possibly with associated flocculation) to produce a “paste” with about a 60% solids content.

- Thin-lift dewatering – in-line or other flocculation of the MFT and then deposition in thin (~100 mm to 300 mm) lifts to promote dewatering through flocculation-assisted sedimentation and possibly other secondary processes. Again, it is expected that the MFT solids content can be increased to values of about 55% using this method.

- Either of the above supplemented by environmental effects (drying and/or freeze/thaw) or by consolidation in the DDA, to further increase the solids content and develop strength and stiffness.

The reclamation strategy for a DDA with this type of material is relatively straightforward. The surface of the DDA can be accessed using conventional small to medium sized-construction equipment, which will allow placement of a cap, grading of the closure landscape, and placement of reclamation material.

Because this type of tailings is mostly fines, with a high clay content, and because it will be deposited in the DDA at a relatively high solids content, achieving a specified undrained strength within 1 year is a reasonable approach. While the strength gain is quick and occurs as part of the tailings treatment process, one must recognize that an operator’s ability to process MFT or other Type 1 tailings in this manner will be limited by a number of factors, including available area for treatment facilities and consistency of environmental conditions.

The above discussion anticipates that reclamation of the Type 1 deposit will be undertaken by terrestrial-based methods. There is considerable experience in reclaiming fine-grained soft deposits using methods that rely on floating plants. These are not controlled by surface shear strength to the same degree as terrestrial-based methods. The authors are not aware of any proposals employing water-based methods at a commercial scale to reclaim Type 1 tailings in the oil sands industry. However, it would be regrettable if regulations precluded the adoption of such methods given their widespread success elsewhere.

Other treatment processes are being researched to dewater Type 1 tailings, such as filtration, mixing and co-deposition with overburden and/or sand, and electrical treatment. The solids content and properties of material produced by these methods are not yet well defined, and hence neither are suitable reclamation strategies (yet).

Type 2 (Sand-Depleted Tailings)

Type 2 tailings could be produced by a number of processes:

- The leading contender is to separate the fines from the coarse part of the whole tailings stream (using a hydro-cyclone), controlling the SFR of the cyclone overflow to a value around 1, and then passing the overflow through a thickener. The resulting product (TT) has a similar fines makeup to the whole tailings line, but has had much of the coarse particles and some water removed.

- Another possible method is to use in-line thickening of the cyclone overflow, FTT or on some other relatively fines-rich tailings stream.

- In some cases, this material is also produced during the unintentional segregation of other tailings streams.

These materials are likely to be transported to the DDA in a pipeline and possibly also discharged hydraulically into the DDA. Under some circumstances, the material so deposited will settle/consolidate to a moderately high solids content (~65% to 70%) over a time period of a few years. Current research suggests there is some chance of achieving a low to moderate strength in the process. However, this type of tailings is usually placed continuously, resulting in thick lifts, and hence the time required to meet the ERCB strength criteria using this approach alone will be longer than anticipated in ERCB D-074. For any particular DDA, the oil sand operators are able to predict the time-strength trajectory for the tailings deposit.

The final DDA surface will benefit from environmental “treatment” (drying and freeze/thaw), which will enable an easier placement of an initial capping material, which will in turn enhance the consolidation of the deposit. Interim surfaces (i.e., surfaces within the deposit) that are strengthened in this manner might inhibit subsequent consolidation.

One strategy for reclaiming this type of material is:

- Placement of an initial cap to enhance access, increase rate of consolidation, and allow for installation of vertical drains or other features to further enhance rate of consolidation. The placement might be done hydraulically (beaching of sand), using low-pressure ground access equipment, using lightweight fill for capping, and/or using other methods to temporarily enhance surface strength.

- After a suitable time (several years), access with larger equipment to place a thicker cap and to start grading for the closure landscape.

- Once the potential for additional settlement has been reduced to a manageable level, final grading and placement of the closure reclamation surface.

Clearly this approach requires a good knowledge of the consolidation behaviour of the TT, and of the relationship between solids content and strength.

The fines content of TT is still sufficiently high that it will behave as a fines-dominated material, and thus access for grading and capping will still be governed by undrained strength considerations. Using strength-based criteria for assessing reclamation readiness is thus reasonable, but the time frame required for reclamation may be somewhat longer, and the required strengths lower, than anticipated in ERCB D-074. The process can be managed by:

- Operators providing a plan which includes: a) predictions of time-strength trajectory of the deposit, b) monitoring methods, and c) mitigation measures to improve consolidation if necessary.

- The ERCB accepting this plan.

- Operators monitoring performance of the deposit until a suitable solids content, strength and stiffness are achieved, and taking whatever mitigative measures are necessary to meet the plan.

Comments related to water-based access and reclamation for Type 1 deposits given in the previous section apply also to Type 2 deposits.

Type 3 (Sand-dominated Tailings)

CT or NST has in the past been transported to the DDA by pipeline and discharged by beaching. A variety of beaching configurations have been used, in an attempt to minimize segregation. Achieving minimal segregation and maximizing the potential of CT to capture fines in a stable deposit requires a low energy depositional environment. This has been demonstrated at a commercial scale by Syncrude, and is an area of ongoing research and development within the industry. However, no matter how good the end product, there will likely be a small amount of segregated material that needs to be removed from the DDA and reprocessed, or managed in a wetland.

CT/NST is fundamentally a different material than MFT or TT, in that the fines content is low and it behaves under loading essentially as a granular material. Considerations of “undrained” strength are thus misleading, since the strength of the material is frictional and can be increased significantly under modest load. For example, placement of a 2 m (above water table) to 4 m (below water table) thick cap on the surface of the CT/NST will increase the vertical effective stress at the top of the CT/NST by about 80 kPa in a short period of time (weeks). This is a sufficient to create a frictional strength at that point equivalent to the ERCB 5 kPa criterion and allow access for further land forming and reclamation activities. The CT/NST right after deposition would still be in a loose to compact state, and any strength measurement right at the surface of the CT would have no meaning. The projection of the strength trajectory with loading and consolidation history is the most reliable method of evaluating deposit strength.

This has also been demonstrated in practice at a commercial scale. Operators have shown that it is possible to place a cap several meters thick on this material by hydraulic means, as long as the rate of construction is controlled to avoid excessive pore pressure generation in the underlying material. The reclamation strategy would thus be:

- Place a cap on the CT/NST deposit, as described above.

- Create the closure landscape, again controlling rate of construction.

- Carry out reclamation activities.

It is anticipated that these activities can be carried out within a few years of filling of the DDA.

These considerations would not restrict placement of cap (e.g., coke) and/or reclamation material by water-based methods.

PERFORMANCE MEASURES

An Alternative to the 5 kPa Strength Criteria

In the author's opinion, the strength criteria contained in Directive 074 are too restrictive, given the number of technical options being considered and under development by oil sands operators to meet the Directive objectives. A better approach would be to replace the existing strength criteria by a detailed consideration of the following (Sobkowicz and Morgenstern, 2009):

- What are the anticipated properties of the tailings in the DDA?
- How will they be capped?
- What will be the schedule for capping?
- What are the time-strength trajectory and the associated subsidence of the tailings deposit, and how is this addressed in the reclamation plan?

This approach is less "formulaic" than the one advocated in Directive 074, and has the flexibility to adapt tailings management plans to the specifics of each DDA. Application of the approach requires a proper understanding of the different types of oil sands tailings materials and the appropriate reclamation strategy that can be used for each (as discussed in the previous section).

In adopting the approach advocated above, one must recognize that trajectory and demonstration of behaviour are more important than meeting artificial goal posts. For example, what better meets reclamation objectives – a DDA that is capped soon after completion and demonstratively improves (following a predicted trajectory) over a period of say 10 years, to a point where a closure landscape can be constructed, or a DDA that meets all of the Directive 074 criteria but nevertheless takes 50 years or 100 years to reach the same point? The latter scenario is quite possible and reflects the dangers associated with setting the wrong goal posts. Recognizing as well that "consolidation over time" is usually less costly than forcing accelerated dewatering of soft tailings, one should question the economic values associated with too rigid a set of tailings management criteria (some of the pitfalls of adopting arbitrary strength goal posts are discussed in Sobkowicz, 2010).

Improved Performance Measures

The ERCB has chosen as their primary measurement of DDA performance the undrained shear strength of the deposit in various locations and at various times after deposition. This might seem like a preferable approach as it directly measures the property that is perceived to be the most relevant to the performance of the deposit. However, there are a number of issues associated with this approach:

- Inaccuracy and unreliability of measuring low strength values, (which would be further exacerbated in the case where one accepts the use of reclamation strategies at very low surface strengths).
- Applicability of undrained shear strength measurements in granular materials.
- Difficult access for, and high cost of, the moderately large equipment needed to measure strength.
- Needless restriction of reclamation to terrestrial-based methods (other methods do not require the same surface conditions).

There are other types of measurement that can be used to monitor the progress of consolidation/densification in the various DDA deposits, to predict the performance of the deposits at any time, and to assess the readiness of the deposit to accept any particular reclamation strategy. One type of measurement that avoids the disadvantages described above is sampling of the deposit combined with the measurement of solids content and related material index tests, (such as Atterberg Limits). This method allows:

- Easier access (for lighter equipment) and less costly monitoring campaigns.
- Accurate results.
- Clear indication of improving material state (consolidation in the fines-dominated materials and densification in the granular materials).

- Direct measurement of, or correlation to, desired geotechnical characteristics of the deposit.

- A basis for projecting long term behaviour, e.g., to forecast the subsidence of the tailings deposit.

Note that the authors are not advocating the abandonment of undrained strength measurements in a DDA – in situ tests (e.g., vane shear, CPT, BPT) are useful and should be combined with the sampling and testing recommended above. What the authors are advocating is the abandonment of specific undrained strength values as D-074 "acceptance" criteria.

CONCLUSIONS

In the authors' opinion, the strength criteria given in Directive 074 are too restrictive, considering the number of technical options being researched and/or under development by oil sands operators to meet D-074 objectives. Alternative means of assessing and validating DDA deposits will lead to improved regulatory effectiveness and operating latitude, without adversely impacting the regulatory objective of having the operators deliver tailings deposits that can be effectively reclaimed in a timely fashion.

The authors believe that the ERCB should be less prescriptive and focus more on objectives, allowing the operators to develop and then propose solutions to meet reclamation objectives. This approach would still allow effective regulatory oversight on the management process. It might include the following steps:

- Clearly define DDA reclamation objectives, stating those objectives in terms of performance to be met within stated time frames. Temporary goal posts and prescriptive methods for achieving the reclamation objectives should be removed from D-074. The regulatory process should be more flexible and capable of adaptation to a wider range of tailings management plans.

- The operator should still be required to submit a DDA plan, outlining how it will meet the objectives. This would include a detailed prediction of tailings performance, a comprehensive monitoring plan, and a detailed discussion of what mitigation actions would be taken if actual performance did not track predicted performance.

- The operator should be required to implement his monitoring plan and report performance, at a minimum on a yearly basis, but more frequently if the discrepancy between predicted and actual performance is large.

This process would hold the Operator accountable, in a transparent way, to the Regulator (in this case, the ERCB) and to all Stakeholders, for accomplishing the reclamation objectives, without unduly restricting the range of methods employed.

ACRONYMS

The following acronyms have been used for technical terms in this paper. Other acronyms for organizations and locations have been defined where they were first used.

BT - Beached Tailings

CT - "Consolidated" Tailings

DDA - Dedicated Disposal Area

MFT - Mature Fine Tailings

NST - Non-segregated Tailings

TFT - Thin Fine Tailings

TT - Thickened Tailings

WT - Whole Tailings (from extraction plant)

REFERENCES

Energy Resources Conservation Board 2009. Directive 074: Tailings Performance Criteria and Requirements for Oil Sands Mining Schemes, Province of Alberta.

Hyndman, A. & Sobkowicz, J.C., 2010. Oil Sand Tailings: Reclamation Goals & the State of Technology. In *Geo2010*; *Proc. 63rd Canadian Geotechnical Conf., Calgary, Canada, 12-16 September 2010*. Canadian Geotechnical Society.

Morgenstern, N.R., 2010. Improving the Safety of Mine Waste Impoundments. In *Tailings and Mine Waste '10*; *Proc. Intern. Conf., Vail, Colorado, 17˙20 October 2010*. Colorado State University.

Sobkowicz, J.C. & Morgenstern, N.R., 2009. A Geotechnical Perspective on Oil Sand Tailings. In Sego, Alostaz & Beir (eds.), *Tailings and Mine Waste '09*; *Proc. Intern. Conf., Banff, Canada, 1-4 November 2009*. University of Alberta Geotechnical Center / OSTRF.

Sobkowicz, J.C., 2010. History and Developments in the Treatment of Oil Sands Fine Tailings. In *Tailings and Mine Waste '10*; *Proc. Intern. Conf., Vail, Colorado, 17-20 October 2010*. Colorado State University.

Session 6

Water Treatment

METAL REMOVAL FROM TAILINGS POND WATER USING INDIGENOUS MICRO-ALGA

H. Mahdavi, A.C. Ulrich, and Y. Liu
University of Alberta, Edmonton, Alberta, Canada

ABSTRACT

Removal of metals of environmental concern including Co, Ni, As and Ba from oil sands tailings pond water (TPW) was investigated using indigenous micro-alga. Using 23S rDNA gene sequencing, the indigenous micro-alga was identified as *Parachlorella kessleri*. Removal of metals by *P. kessleri* in filtered, sterilized TPW taken from Syncrude Co. (West In-pit pond) as well as Albian Co. (ETF pond) was examined over 14 days. Each TPW was enriched with low and high concentrations of nitrate and phosphate as nutrient supplements. High nutrient concentrations did not affect algal cell numbers, the log phase period nor dry biomass during cultivation. While addition of the nutrient improved the removal percentages of target metals from Syncrude's TPW, it had an adverse effect on metal removal from Albian's TPW. The highest removal percentages of Co, Ni, As and Ba were 30%, 46%, 46% and 67% from Syncrude's TPW and 42%, 50%, 50% and 69% from Albian's TPW, respectively. The majority of removed metals were bioaccumulated inside *P. kessleri* cells. During the stationary phase, bioaccumulated metals were partially released back into the solution leading to a slight decrease in metal removal percentages after eight days of cultivation.

Keywords: *Parachlorella kessleri*, metal removal, bioaccumulation, oil sands tailings pond water.

INTRODUCTION

The world's second largest petroleum reserve (in the form of oil sands) in north-eastern Alberta, Canada, has attracted many oil companies to invest in oil production. In 2005, the rate of oil production was approximately one million barrels, and it has been anticipated to increase five-fold within the next two decades (Siddique et al. 2008). Oil sands contain bitumen – a viscous, tar-like organic material – which is mixed with clay and sand particles (Scott, Young and Fedorak 2008). Every barrel of oil produced is accompanied by 1.25 m^3 of oil sands tailings pond water (TPW) which contains solids (clay and sand), uncovered hydrocarbons and metals of environmental concern. Oil producers work under a zero-discharge policy upheld by the Alberta Environmental Protection and Enhancement Act (1993) which requires all pollutants, including metals of environmental concern, to be removed from the TPW prior to release into the environment (Giesy, Anderson and Wiseman 2010). There are three major companies operating in Alberta's oil sands including Suncor Energy Corp. (Suncor), Syncrude Canada Ltd. (Syncrude) and Albian Sands Inc. (Albian) (Allen 2008). Depending on the ore source and the extraction method used, the various companies' TPW characteristics will vary.

There are several physical-chemical methods to treat metal-contaminated water such as precipitation-filtration, ion exchange, reverse osmosis and oxidation-reduction reactions. These physical-chemical methods usually are inefficient and expensive, especially when applied to large volumes of water with low metal content, such as TPW (Lourie, Patil and Gjengedal 2010).

There has been a variety of research on the removal of metals using algae (Worms et al. 2010; Travieso et al. 1999; Chojnacka 2007; Romera et al. 2007; Wang and Chen 2009). Algae are photosynthetic organisms that can be categorized into unicellular (micro-algae) and multicellular forms. Accumulation of metals in algal cells is achieved through biosorption (passive sorption) or bioaccumulation (sorption via metabolic activity of living cells). A majority of investigations have focused on biosorption or passive types of metal removal. There are fewer studies on bioaccumulation, even though viable organisms have shown promising capabilities in sewage treatment (Kaduková and Virčíková 2005).

Bioaccumulation processes in algal cells can occur in several ways. For example, extracellular accumulation occurs when metals are adsorbed on the cells' wall and bounded with a carboxylic functional group on the surface. Another removal mechanism is intracellular accumulation which involves the uptake of metals inside the cells. It was found that bioaccumulation efficiency varied considerably in a multi-ionic environment, such as

TPW, in comparison to a single ion solution. In a multi-ionic situation, the metal bounding capacity is much lower than a single-ion system and consequently the bioaccumulation rate declines (Chojnacka 2007).

The removal of metals using algae has been proven for various sewages, but no research has been conducted on TPW thus far. Laboratory studies have shown that some algal strains can survive in TPW (Headley et al. 2008), but due to the multi-ionic composition and complexity of TPW, more research is required. The main objective of this research is the removal of Co, Ni, As and Ba as metals of environmental concern from TPW using the indigenous micro-alga, *Parachlorella kessleri* (Figure 1). The effect of different nutrient levels on the metal removal efficiency from TPW taken from Syncrude and Albian ponds has also been studied.

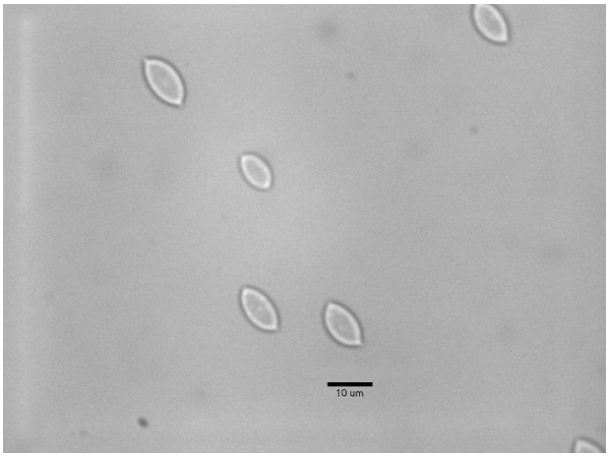

Figure 1. Light transmission microscopy image of *P. kessleri* cells

MATERIALS AND METHODS

All glassware were cleaned (Sparkleen2, Fisher brand), acid washed and finally rinsed three times with deionised water and Milli-Q water, respectively. All chemicals and acid/base reagents were *Certified A.C.S* or trace metal graded, if needed. Unless otherwise specified, cultivations were performed at 28^{o}C, under continuous illumination at 4300 lux (cool light, 44W, Philips, USA) and at a 100 rpm shaking rate.

Strain identification and inoculum preparation

Highly adapted green algae were cultivated, and young cells were used for DNA extraction using the *Qiagen DNeasy Plant Mini Kit*. The extracted algal DNAs were amplified using algal universal primers (23S rDNA plastid marker in eukaryotic algae and cyanobacteria) (Sherwood and Presting 2007) in a polymerase chain reaction (PCR). Amplified DNAs were used for denaturing gradient gel elecrophoresis (DGGE), and the results implied the sample contained a single strain. The amplified DNA was purified (*Qiagen PCR purification kit*), and DNA sequencing data identified the unknown strain to be *P. kessleri* with a max similarity of 99%.

Experimental conditions

P. kessleri cells were cultivated for seven days in artificial TPW (without trace metals), and the resulting young cells were used as inoculum. Two types of TPW (one from Syncrude (West In-pit pond) and one from Albian (ETF pond)) were used for this investigation. The TPWs were filter-sterilized (0.22µm, Stericup® Millipore) and enriched by various concentrations of nitrate and phosphate. Nutrient concentrations were as low as 0.24 mM of NO_3^- and 0.016 mM of PO_4^{-3} as suggested by Levy et al. (2009) and as high as 1.98 mM of $NO_3^-$and 0.201 mM of PO_4^{-3} as suggested in the general purpose medium (GMP) (Andersen 2005). Five 1,000 mL Erlenmeyer flasks were filled with 200 mL of Syncrude's low-nutrient TPW. Three of these flasks were inoculated with *P. kessleri* cells to a final concentration of 10^5 cells mL^{-1} (22.4 mg L^{-1} dry biomass), and the remaining two flasks were left as blanks. The same procedure was performed for Syncrude's high-nutrient TPW as well as for Albian's low- and high-nutrient TPW. Aliquots of 5g (≈5mL) after four hours of inoculation (and after one, four, eight and 14 days) were taken from each flask and assayed for pH, cell count, dry biomass and the amount of metals removed.

Metals measurement analytical methods

To measure metal concentrations in TPW, 5g samples were centrifuged (3700xg), and the supernatant was assayed using Inductively Coupled Plasma Mass Spectrometry (ICP-MS). Algal pellet was digested using concentrated nitric acid (70%, trace-metal grade Fisher Scientific, Canada) (Chojnacka 2007) to measure bioaccumulated metals. The solutions were diluted

with an appropriate ratio of 1.5% nitric acid and were analyzed for the metal concentration by ICP-MS.

Multi-elemental analysis was performed with the use of an ICP-MS instrument (PerkinElmer SCIEX, ELAN 9000). For quality assurance and control, after each 20th TPW sample, a standard sample spiked with a multi-element solution was tested against the same TPW sample without additional multi-element. Both solutions were run through the ICP-MS to see the significance of interfering constituents of TPW with the metal measurement. For all tested samples, the value of the initial metal concentrations in the inoculum was deducted from the bioaccumulated metals concentrations.

RESULTS AND DISCUSSION

Initial metal concentration in both TPW samples

Initial concentrations of Co, Ni, As and Ba in both TPW samples are presented in Table 1. The concentration of As and Co in Syncrude's TPW are higher than Albian's. Further experiments indicated that the concentrations of some metals in Syncrude's TPW, such as Cr, Mn, Co, Mo, Cd and Cs, are two times or more than Albian's TPW (not shown). Alkalinity and total dissolved solids (TDS) in Syncrude's TPW were 526 mg $CaCO_3$ L^{-1} and 2856 mg L^{-1}, respectively, and 353 mg $CaCO_3$ L^{-1} and 1184 mg L^{-1} in Albian's TPW.

Table 1. Initial metal concentration in raw TPWs measured using inductively coupled plasma mass spectrometry (ICP-MS)

Sample (µg L^{-1})	Co	Ni	As	Ba
Syncrude	2.13	9.90	5.11	134.53
Albian	1.43	10.33	3.57	239.54

Growth rate and pH change

By introducing inoculums, the cell number increased until the eighth day and then stayed constant, indicating the beginning of the stationary phase (not shown). Duration of the log phase in algae usually lasts between 7-10 days (Andersen (2005). Higher nutrient concentration in both TPWs did not affect the cell number nor the duration of the log phase. In Figure 2 (a), the high nutrient concentration results show dry biomass stability in both TPWs, whereas there are more fluctuations at low nutrient levels. In this figure, commencement of the stationary phase on day eight is clear; after this point, the dry biomass remained constant or decreased.

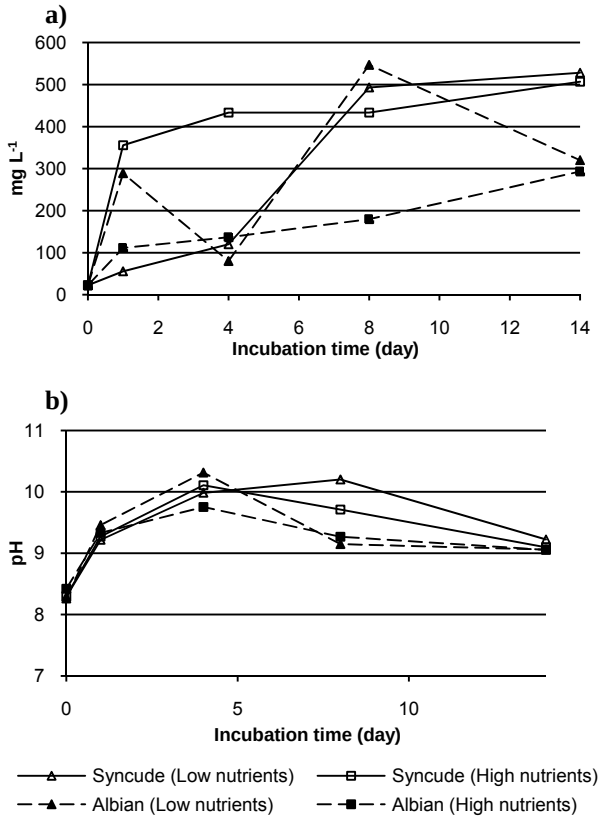

Figure 2. *P. kessleri* dry biomass (a) and pH (b) in low (0.24 mM of NO_3^- and 0.016 mM of PO_4^{-3}) and high (1.98 mM of NO_3^- and 0.201 mM of PO_4^{-3}) nutrient concentrations.

As a result of algal photosynthesis, pH increased. The amount of increase in pH depends on the buffering properties of the solution and the photosynthesis rate. Figure 2(b) illustrates a pH increase in both TPWs. The pH reached approximately 10 in all samples, and after the eighth day, the pH reduced to 9 which indicate a lower photosynthesis rate during the stationary phase. The pH increase was not affected by the high nutrient concentrations in both TPWs.

Metal removal

Figure 3 shows the removal percentages of Co, Ni, As and Ba versus cultivation time. The removal percentages increased until the eighth day, and

when the stationary phase commenced, the percentages decreased or stayed constant for all target metals. The metals can be bound on the cell surface (extracellular accumulation) or accumulated inside the cell. The extracellular mechanism of metal removal is based on physical-chemical interaction between metals and functional groups of the cell wall (Kaduková and Virčíková 2005). The metals may bind with cation-binding functional groups on the cells' surface, such as carboxylic acids, polysaccharides, lipids or proteins (Chojnacka 2007). The second mechanism is the intracellular sorption of metals involving accumulation of metals inside the cells which is a metabolism-dependent process.

By washing the cells with EDTA buffer solution, bound metals can be detached from the cells' surface. Further ICP-MS results indicated that the majority of removed metals were accumulated by intracellular sorption (not shown).

In Figure 3, there is a slight reduction in the removal percentages of some metals during the stationary phase (after the eighth day), which implies the release of metals. This phenomenon has been reported by other researchers (Kaduková and Virčíková 2005) and occurs when algal cells lose their binding capacity, subsequently releasing metals back into solution. In some cases, extremely high concentration of metals may cause the death of cells over long periods of exposure. Since the cell debris resulting from cell death showed higher sorption capability, a fraction of released metals can rebound (Kaduková and Virčíková 2005). A small fraction of metals was accumulated extracellularly, therefore, the amount of released metals during the stationary phase was not considerable, and in most cases, the removal percentages only decreased slightly.

The nutrient effect on the removal efficiency is shown in Figure 3. For all target metals, Syncrude's high-nutrient TPW and Albian's low-nutrient TPW had the highest removal percentages. These results imply that, addition of nitrate and phosphate in Albian's TPW as high concentrations as GMP medium, may lead to poorer metal removal than lower concentrations; however, the opposite was true for Syncrude's TPW. The highest removal percentages for this study came from Syncrude's high-nutrient TPW after 14 days of cultivation for Co, Ni, As, and Ba (30%, 46%, 46% and 67%, respectively), and from Albian's low-nutrient TPW (42%, 50%, 50% and 69%, respectively).

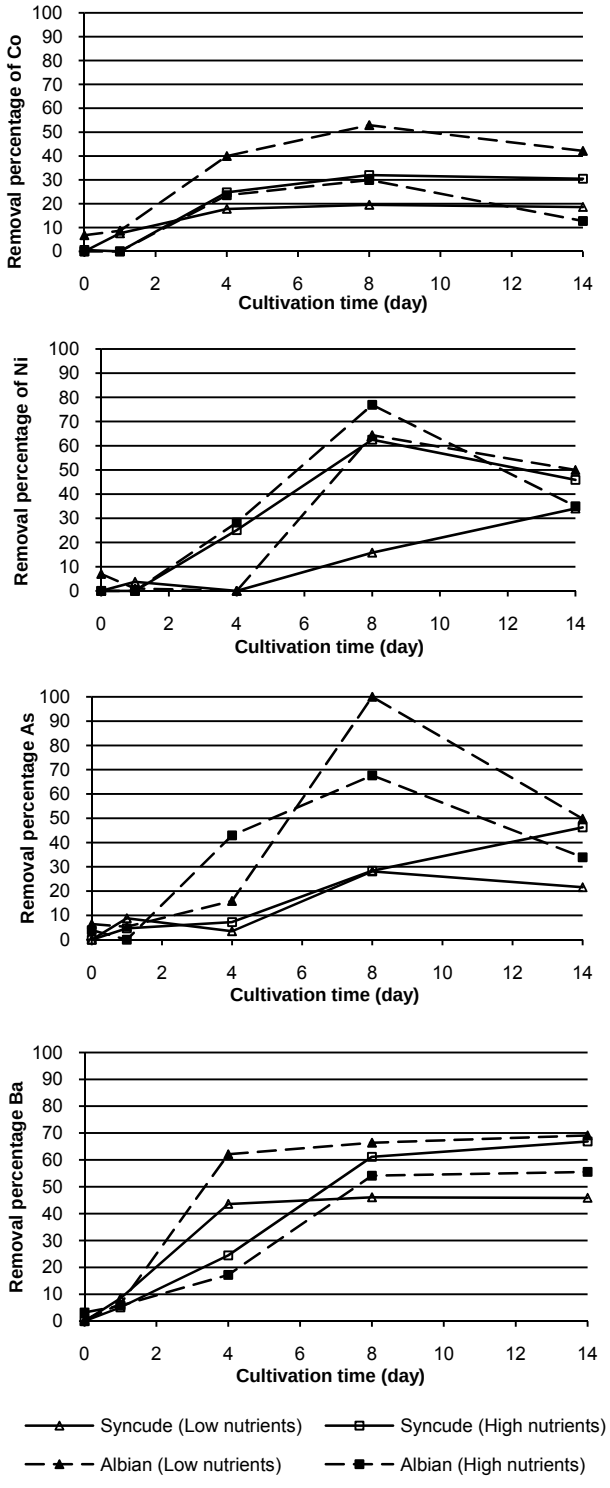

Figure 3. Removal percentages of each metal versus cultivation time for the both TPWs in low and high nutrient levels.

CONCLUSION

Indigenous micro-alga *P. kessleri* was used for the removal of metals of environmental concern including Co, Ni, As and Ba from Syncrude and Albian's TPWs. The TPWs were enriched with low and high concentrations of nitrate and phosphate as nutrients. The cellular growth rate and pH increment did not change considerably with the addition of nutrients. Results indicated a positive effect of higher nutrient concentrations on the removal of target metals from Syncrude's TPW, whereas it may have had a negative effect on the removal rate of metals from Albian's TPW. During the stationary phase, extracellularly-bound metals were partially released which caused a mild reduction in the removal percentages.

REFERENCES

Allen, E. W. (2008) Process water treatment in Canada's oil sands industry: I. Target pollutants and treatment objectives. J. Environ. Eng. Sci. **7**(2), 123-138.

Andersen, R. A. (2005) Algal culturing techniques.

Chojnacka, K. (2007) Biosorption and bioaccumulation of microelements by Riccia fluitans in single and multi-metal system. Bioresour. Technol. **98**(15), 2919-2925.

Giesy, J.P., Anderson, J.C., Wiseman, S. B. (2010) Alberta oil sands development. Proc. Natl. Acad. Sci. U. S. A. **107**(3), 951-952.

Headley, J.V., Du, J.L., Peru, K.M., Gurprasad, N., McMartin, D.W. (2008) Evaluation of algal phytodegradation of petroleum naphthenic acids. J. Environ. Sci. Health Part A-Toxic/Hazard. Subst. Environ. Eng. **43**(3), 227-232.

Kaduková, J. and Virčíková, E. (2005) Comparison of differences between copper bioaccumulation and biosorption. Environ. Int. **31**(2), 227-232.

Levy, J.L., Stauber, J.L., Wakelin, S.A., Jolley, D.F. (2009) The effect of bacteria on the sensitivity of micro-algae to copper in laboratory bioassays. Chemosphere **74**(9), 1266-1274.

Lourie, E., Patil, V., Gjengedal, E. (2010) Efficient Purification of Heavy-Metal-Contaminated Water by Micro-algae-Activated Pine Bark. Water Air Soil Pollut. **210**(1-4), 493-500.

Romera, E., González, F., Ballester, A., Blázquez, M.L., Muñoz, J.A. (2007) Comparative study of biosorption of heavy metals using different types of algae. Bioresour. Technol. **98**(17), 3344-3353.

Scott, A. C., Young, R. F., Fedorak, P. M. (2008) Comparison of GC–MS and FTIR methods for quantifying naphthenic acids in water samples. Chemosphere **73**(8), 1258-1264.

Sherwood, A.R. and Presting, G.G. (2007) Universal primers amplify a 23S rDNA plastid marker in eukaryotic algae and cyanobacteria. J. Phycol. **43**(3), 605-608.

Siddique, T., Gupta, R., Fedorak, P.M., MacKinnon, M. D., Foght, J. M. (2008) A first approximation kinetic model to predict methane generation from an oil sands tailings settling basin. Chemosphere **72**(10), 1573-1580.

Travieso, L., Cañizares, R.O., Borja, R., Benítez, F., Domínguez, A.R., Dupeyrón, R., Valiente, Y.V. (1999) Heavy metal removal by micro-algae. Bull. Environ. Contam. Toxicol. **62**(2), 144-151.

Wang, J. and Chen, C. (2009) Biosorbents for heavy metals removal and their future. Biotechnol. Adv. **27**(2), 195-226.

Worms, I.A.M., Traber, J., Kistler, D., Sigg, L., Slaveykova, V.I. (2010) Uptake of Cd(II) and Pb(II) by micro-algae in presence of colloidal organic matter from wastewater treatment plant effluents. Environmental Pollution **158**(2), 369-374.

THE ADSORPTION OF OIL SANDS NAPHTHENIC ACIDS FROM PROCESS-AFFECTED TAILINGS WATER USING ACTIVATED PETROLEUM COKE

Christina Small, Ania C. Ulrich, and Zaher Hashisho
University of Alberta, Edmonton, Alberta, Canada

ABSTRACT

Oil sands process-affected tailings water is known to be highly concentrated with organic acids, including naphthenic acids. Naphthenic acids are of concern to the oil sands industry due to their toxic and corrosive nature, presenting issues surrounding the oil refining infrastructure as well as the prospect of mine closure. This paper investigates the use of activated oil sands petroleum coke as an available adsorbent for naphthenic acid removal. Physical activation of delayed and fluid coke was completed. In order to generate the most effective adsorbent, the following treatment conditions were tested: temperature (800-900^{o}C); time (2-6 hours); and, activation atmosphere (CO_2 Only, N_2 + steam, and CO_2 + steam). The characterization of the activated products was completed through iodine number as well as BET (N_2) adsorption isotherms. The adsorbent with the greatest surface area and most appropriate pore size distribution for water adsorption was selected for adsorption tests. Batch tests were completed using 0.0625-0.5% of activated coke by weight. The removal efficiency of oil sands naphthenic acids was then observed through the analysis of fluorescence spectrometry. Such analyses provide an understanding of the adsorptive behaviour of petroleum coke.

INTRODUCTION

Bitumen extraction and processing within the Athabasca oil sands region (AOSR), Alberta, Canada, produces significant quantities of both dry and wet wastes. The production of over 1 million barrels of oil per day has resulted in the consumption of an average of 3 barrels of river water per barrel of produced oil (Allen, 2008a). Roughly, 0.1 to 0.2 m^3 of process-affected tailings water is generated per tonne of processed oil sands; where, over $4x10^8$ m^3 of tailings water is currently stored within tailings ponds in the AOSR (Headley et al, 2009). The process-water is known to contain substantial quantities of coarse and fine sediments (sands and clays), dissolved inorganic (metals) and organic by-products, and small fractions of non-recoverable bitumen. The concentrations of the wide variety of pollutants are dependent upon the unique geology of the mining area, and the age of the oil and gas field (Vlasopoulos, 2006). At mine closure, the process-water is required to be reintegrated into a sustainable landscape (Allen, 2008a). As a result, the accumulation of process-affected tailings water represents a challenge for the oil sands industry.

A major dry waste by-product of bitumen upgrading to synthetic crude oil is petroleum coke. It has been estimated that Suncor Energy, Inc., and Syncrude Canada, Ltd., produce about 39.6 and 23 kg of coke per barrel of processed bitumen, respectively, resulting in over 5 million tonnes of produced coke per year (Fedorak and Coy, 2006). Though part of Suncor's coke is burnt in boilers for steam and electricity generation, most of the coke material produced within the AOSR is stockpiled on-site; representing one of the most unique energy reserves in the world (Furimsky, 1998).

Oil Sands Naphthenic Acids (OSNAs)

Common organic compounds found within the oil sands tailings pond water include bitumen, aromatic compounds, and organic acids (of which 80% consist of naphthenic acids) (Allen, 2008a). Oil sands naphthenic acids (OSNAs) collectively represent all of the carboxylic acids present within the crude oil located within the AOSR (Brient, 1995). These OSNAs correspond to a class of alkyl-substituted acyclic and cyclo-aliphatic carboxylic acids, where the unique structures vary depending on the number of hydrogen atoms lost as linear hydrocarbon chains are gained and substituted (Janfada et al, 2006). The presence of pyrroles, thiophenes, and phenols in some OSNAs add to the complexity and uncertainty surrounding the unique class of compounds (Whitby, 2010). The composition and concentration of the OSNAs are variable throughout the AOSR, and differ depending on the geology of the area in which the ores are mined. Typically, OSNAs range from 40 to 120 mg/L in oil sands tailings pond water (Holowenko et al, 2001; Janfada et al, 2006). With

the future expansion and development of the AOSR, it can be expected that the concentrations OSNAs will increase as well. It has been determined that the natural concentrations of OSNAs range from 0.1 to 0.9 mg/L within the Athabasca river (Clemente and Fedorak, 2005).

The literature suggests that the OSNAs are acutely and chronically toxic to a variety of organisms (including plants, fish, mammals, amphibians, and bacteria), especially when concentrations exceed 2.5-5 mg/ L (Clemente and Fedorak, 2005; Allen, 2008a; Whitby, 2010). At the same time, OSNAs have been related to corrosion in petroleum-refining infrastructure since the early 1900s (Brient, 1995). This is caused through the formation of hydrogen gas at typical operating temperatures (220-400^{o}C), promoting chelation of metal ions in the presence of carboxylic acid groups (Clemente and Fedorak, 2005; Whitby, 2010). Steel alloys have been found to be susceptible to OSNA corrosion, leading to issues surrounding equipment failures, safety, and reliability (Whitby, 2010).

Until the OSNAs can be individually and uniquely characterized, remediation techniques which aim to remove the complete range of naphthenic acids should be considered for the treatment of process-affected water.

Adsorption

The use of adsorption principles for the removal of organics from oil sands tailings ponds has been considered to be an emerging technology, due to the low impact on the environment and the minimal production of associated wastes (Allen, 2008b).

The effectiveness of adsorption is dependent upon the nature of the adsorbent and the adsorbate as well as the conditions of the solution in which both the adsorbent and adsorbate reside (Barczak et al, 2005). The adsorption capacity is also dependent upon the surface area and pore size distribution of the adsorbent, as this will affect the amount of adsorbate (or molecule participating in adsorption) that is adsorbed.

Activated carbon has been widely used for the removal of organic contaminants from industrial wastewater (Allen, 2008b). Activated carbon can be generated from a variety of organic precursors including coals, bamboo, wood, corn, coconut shells, etc. Recently, there has been shift towards using waste materials as a precursor for activated carbon due to its wide availability and economic feasibility (Stavropoulos and Zabaniotou, 2009).

Application to Petroleum Coke

Delayed and fluid petroleum cokes are suitable precursors for activated carbon preparation due to their high carbon content ranging from 80 to 85 % by weight (Furimsky, 1998). Research has indicated that once activated, petroleum coke has a higher yield and surface area than most raw materials (Stavropoulos and Zabaniotou, 2009). The availability of coke makes its use a viable option to the oil sands industry.

Activation of the petroleum coke is necessary to produce an enhanced surface area and porosity throughout the material and increase the effectiveness of the adsorbent. Activation typically consists of two phases: carbonization- causing initial pyrolytic decomposition within the pores of a material; and, activation- turning the carbonized product into one with the greatest number of pores (Bansal and Goyal, 2005). During upgrading processes, the thermal treatment differs between delayed and fluid coking techniques where temperatures range between 415-450^{o}C and 480-565^{o}C, respectively (Fedorak and Coy, 2006). These temperatures are consistent with those typical of carbonization sequences; consequently, petroleum coke can be considered to be pre-carbonized.

The activation stage can be completed either physically or chemically. Physical activation generally consists of conventional heating at high temperatures in the presence of steam, carbon dioxide, air, or any mixture. The active oxygen within the gases reacts with the carbon skeleton, releasing CO_2 and CO; where, external heating drives the reactions on the surface of the carbon- resulting in an etching of pores. In contrast, chemical activation requires the carbon material to be initially impregnated with an activating agent such as KOH, $ZnCl_2$, HPO_3, or K_2S before heating (Yang, 2003). These dehydrating reagents allow for lower external heating temperatures as well as shorter activation times to produce a higher yield of active carbon.

Activation conditions can directly influence the following properties of an adsorbent, including its structure and pore development, activation yield, surface functional groups, and surface area. Physical activation has the advantage of using activation agents such as steam and $CO_{2\,(g)}$, which

are readily available at industrial facilities making this technique attractive to the oil sands industry.

This paper will investigate the physical activation of delayed and fluid petroleum coke through the exploration of a range of activation conditions. It will also evaluate the ability of the activated products to remove OSNAs from oil sands process-affected tailings pond water.

EXPERIMENTAL METHODS

Delayed and fluid cokes were obtained from Suncor Energy Inc. and Syncrude Canada Ltd., respectively. The delayed coke was ground and sieved to an approximate sieve size of 75-150 μm. The fluid coke was already in granular form of approximately >300 μm, and was sieved to achieve the same size range of the delayed coke.

Activation and Characterization of Petroleum Coke

Physical activation involved a fixed-bed muffle furnace and a two-stage simultaneous carbonization/ activation sequence, where activation commenced as soon as the desired activation temperature was reached. Steam was generated using a syringe pump and heating tape (180^{o}C). The following parameters were controlled in order to determine the most efficient activation conditions: time (2 to 6 h); temperature (800-900^{o}C); atmosphere ($CO_{2(g)}$, $CO_{2(g)}$ and steam, and $N_{2(g)}$ and steam); and, steam rate (0.3 to 0.5 mL/min).

After activation, the samples were characterized through iodine adsorption tests using ASTM method D 4607 (ASTM, 2006). Liquid-phase adsorption of methylene blue consisted of a 24 h batch test between activated samples (0.05 g) and 25 mL of diluted methylene blue stock solution (1200 mg/L). The methylene blue stock solution was prepared using 5% acetic acid, and a standard calibration curve was generated by diluting the stock solution in 0.25% acetic acid. After 24 h, the samples were filtered in order to separate the coke from the filtrate. Absorbance was measured using a UV-VIS spectrometer (Shimadzu, UV-2401 PC) at 630 nm (the point of maximum absorbance). Results were then compared with the standard calibration curve and used in the following equation to obtain the methylene blue value at equilibrium (Hameed et al, 2007):

$$q_e = \frac{(C_{initial} - C_{equilibrium})V}{M}$$

where C is the concentration of the methylene blue solution; V is the volume of the solution; and, M is the mass of the dry adsorbent. The results describe the amount of methylene blue adsorbed per weight of carbon (mg/g).

N_2 adsorption isotherms were determined at 77.3 K by a surface area analyzer (Quantachrome, Autosorb 1-MP). Approximately 0.1 g of sample was degassed for 3 to 4 h at 250^{o}C under vacuum with a backfill gas of helium. The Brunauer, Emmett, and Teller (BET) model was used to determine the surface area using a pressure range of 0.02 to 0.055 (P/P_o).

Scanning electron micrographs (SEMs) were obtained using a Hitachi S-2500 using an excitation voltage of 10 kV. Samples were initially light sputtered with electrically conductive gold film for 13 s.

Adsorption of Oil Sands Naphthenic Acids

Batch tests were conducted on raw and activated delayed and fluid coke. Process-affected (PA) water was initially centrifuged and filtered with 0.45 μm filters to remove any clays/ colloids that may become competitive during adsorption. For the raw coke samples, batch tests were completed with the filtered PA water in 5, 10, 20, and 30% by weight intervals. The activated coke samples were mixed with the PA water in 0.5, 0.25, 0.125, and 0.0625% by weight intervals. Batch tests followed procedures outlined by ASTM D 4646 (ASTM, 2008). The agitation speed for the mixtures was altered to 160 rpm. Afterwards, the samples were filtered through 0.45 μm filters to collect the coke particles. The filtrates were then analyzed for OSNAs using fluorescence spectrometry and Fourier Transform Infra-red spectrometry (FT-IR).

Fluorescence spectrometry was used as a screening tool for detecting and measuring signatures typical of OSNAs within the treated and non-treated process-water (Mohamed et al, 2008; Brown et al, 2009). This method allows for the monitoring of benzene groups and double bonds thought to be consistent within OSNA structures. Neither sample nor standard preparation was necessary. The filtered samples were excited with wavelengths from 260 to 600 nm on a Varian Cary Eclipse fluorescence spectrometer. Emission wavelengths were obtained from 250 to 600 nm in 1 nm increments. The slit width was set to 10 nm

and 5 nm for excitation and emission collection, respectively. Afterwards, the sample absorbance was collected from 250 to 600 nm using a UV-VIS spectrometer (Shimadzu UV 2401-PC). This data was used to correct for inner and outer filtering artifacts caused by solute self-absorption within the fluorescence emission-intensity data (Tucker et al, 1992).

Naphthenic acids were detected using an FT-IR spectrometer (Perkin Elmer Spectrum 100). Extracted samples were mixed with methylene chloride and absorbance peak heights were observed at 1706 and 1743 cm^{-1} and compared to a standard calibration curve generated through commercially prepared naphthenic acids (Sigma Aldrich). This technique, developed by Syncrude Canada Ltd., is currently used as the standard oil sands industry method for detecting OSNAs (Clemente et al, 2005; Yen et al, 2004; and Holowenko et al, 2001).

RESULTS AND DISCUSSION

Activation Experiments

Activation under CO_2 only did not result in major changes in iodine number; consequently, the technique is not efficient in enhancing the surface area of petroleum coke. When steam was added to CO_2, increased pore development began to positively impact the iodine numbers of both activated delayed and fluid coke samples. Activation under N_2 + steam and CO_2 + steam proved similar results; however, activation under CO_2 + steam is preferred due to a uniform burning of a carbon material resulting in the uniform gasification of carbon and ultimately, a uniform development of pores (Mattson and Mark, 1971; Yang, 2003).

Increasing the activation temperature from 800 to 900^{o}C also improved the iodine numbers for the activated samples. The reactions occurring between the carbon material and the activation atmosphere are endothermic and require higher temperatures to allow for increased pore development. At the same time, increases in temperature can be used to overcome longer activation times.

Table 1 shows the results for the best physically activated delayed and fluid coke samples. For comparison, non-activated delayed and fluid cokes have iodine numbers of approximately 23 and 16 mg/g, respectively.

Table 1: Characterization parameters of activated delayed and fluid coke samples.

Sample	Iodine Number (mg/g)	Methylene Blue Value (mg/g)	BET Surface Area (m^2/g)
DCS9006(0.5)	670	123.9	577.5
DCS9006(0.3)	579.5	122.6	472
FCS9006(0.5)	620	122.6	493.5
FCS9006(0.3)	520	98.4	532.9

** Samples can be described by the following parameters: D: delayed coke; F: fluid coke, CS: CO2 (g) + steam, 6: activation time, and 0.5/ 0.3: steam rate of 0.5 or 0.3 mL/min.*

The results indicate that physical activation of delayed and fluid coke can produce activated carbons comparable to commercially available products. The greatest surface area is achieved when activating delayed coke for 6 h with a steam rate of 0.5 mL/min. The treatment gas composition (in mole %) for H_2O and $CO_{2\ (g)}$ were 86%:14% and 79%:21% for 0.5 and 0.3 mL/min, respectively. Consequently, it is expected that increasing the steam rate will allow for increased moles of H_2O to interact with the carbon surface leading to an enhancement in carbon removal. In contrast, activation of fluid coke for 6 h with a steam rate of 0.5 mL/min produced a lower surface area than activation with a steam rate of 0.3 mL/min. Increased gasification may have lead to the burn-out of carbon material between pores.

Iodine adsorption isotherms are used to assess the adsorption capacity of a material to pollutants of a smaller molecular size (typically used in air pollution studies). In contrast, methylene blue adsorption tests are typically used to help characterize adsorbents used in wastewater treatment, since the molecule is of intermediate size (Sontheimer et al, 1988). The high iodine and methylene blue values for both activated delayed and fluid coke samples indicate that there is the development of a range of micro- and mesopores; and ultimately, a greater pore size distribution.

For comparison purposes, activated delayed and fluid coke physically activated under the following parameters were characterized and used in further adsorption experiments: CO_2 + steam, 6 hours, 900^{o}C, 0.5 mL/min.

Figures 1 and 2 show SEMs of the raw and activated delayed and fluid coke samples. SEMs allow for the observation of physical changes on the surface of materials. These figures do not demonstrate the internal micro-/ mesoporous surface area and porosity responsible for adsorption.

The raw delayed and fluid coke samples are observed to be smoother than the activated samples. The appearance of pores and cracks on the surface of the raw materials is minimal. Once activated, the delayed coke develops erratic cracking and flaking. Due to the build up of the flakes, it is difficult to differentiate between pores and a change in depth on the surface. Though the surface of the activated fluid coke became rougher than its raw counterpart, a wider distribution of pore sizes was observed. The rough surfaces and pore development can be attributed to the irregular loss of carbon due to the gasification reactions during activation.

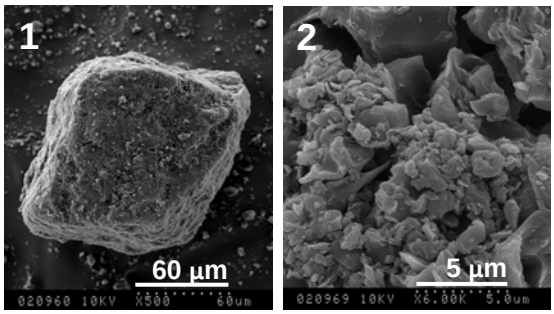

Figure 1. SEMs of raw (1) and activated (2) delayed coke. The activation conditions chosen were 900°C, 6 h, CO_2 + steam (0.5 mL/min).

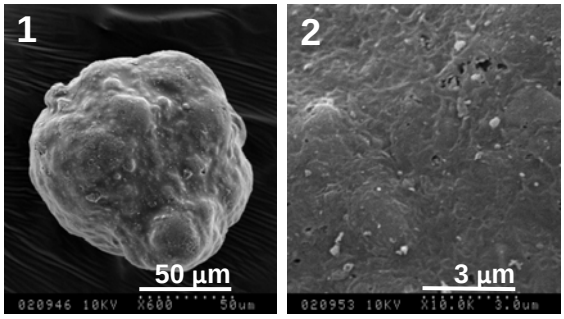

Figure 2. SEMs of raw (1) and activated (2) fluid coke. The activation conditions chosen were 900°C, 6 h, CO_2 + steam (0.5 mL/min).

Adsorption Experiments

Fluorescence spectrometry is typically used as a quick forensics scanning tool to observe characteristic peaks corresponding to benzene groups and double bonds relating to various levels of unsaturation and aromaticity of OSNAs (Headley et al, 2009b). Consequently, OSNAs will produce a unique signature within the process-affected water. Figure 3 shows emission spectra for straight process-affected tailings water obtained from the AOSR. In the production of this figure, the original excitation-emission matrix was corrected for inner and outer filtering effects with the use of UV-VIS absorption results.

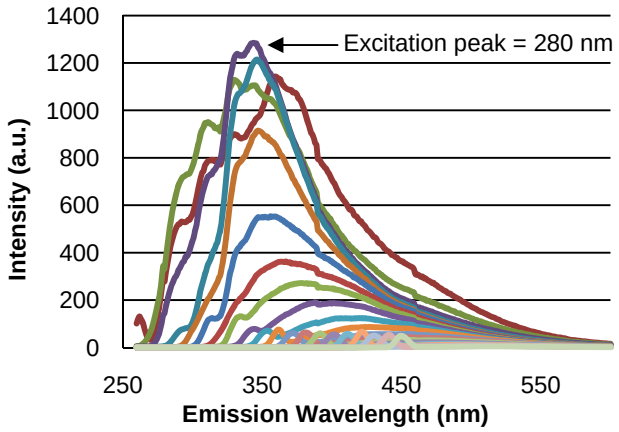

Figure 3. Emission spectra including excitation wavelengths of 260 to 450 nm for straight process-affected tailings pond water.

The peak intensity occurs at excitation peak 280 nm and emission wavelength 350 nm, where the intensity is observed to be exceeding 1200 arbitrary units (a.u.). This signal has been considered to be indicative of OSNAs within process-water (Brown et al, 2009). This peak intensity was observed throughout the process-water samples treated with raw and activated delayed and fluid coke (Figures 4 and 5).

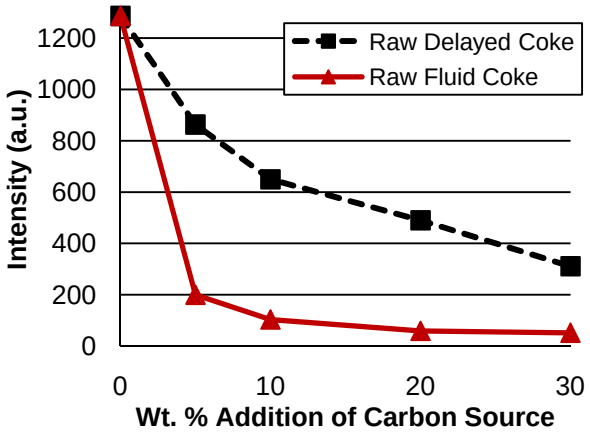

Figure 4. Peak intensities of the 280 nm excitation wavelengths for increasing weight additions of raw delayed and fluid coke.

Figure 4 shows the intensity of the 280 nm peak obtained from the fluorescence data of process-water mixed with increasing weight additions of raw delayed and fluid coke. Both samples indicated decreasing trends in OSNA concentrations where the maximum removal is obtained at 30% wt. addition. Here, the intensity is reduced to 52 and 31 a.u. for fluid and delayed coke, respectively. Consequently, the removal efficiency is greater for the raw fluid coke samples than for the delayed coke. This is may be due to the structural nature of the material. During upgrading, fluid coke undergoes higher temperatures than delayed coke (Fedorak and Coy, 2006). As a result, there are higher quantities of volatile matter caught up within the pores of the delayed coke material, reducing the initial surface area.

Figure 5 shows the intensity of the 280 nm peak obtained from process-water mixed with activated delayed and fluid coke samples. The removal efficiency of OSNA signature is consistent between activated delayed and fluid coke, where the maximum removal (99.8%) occurs at 0.5% wt. addition. In contrast to the raw coke samples, less material is required to adsorb OSNAs. Figure 5 also compares the activated delayed and fluid coke samples to commercially available granular activated carbon (GAC) with a BET surface area of 1050 m^2/g (Jacobi Aquasorb 1500). With 0.0625% wt. addition of GAC to process-water, 99.8% of the OSNA signature is removed. The activated delayed and fluid petroleum cokes show comparable results with commercial GAC starting at 0.25% wt. addition, proving the success of the activated material.

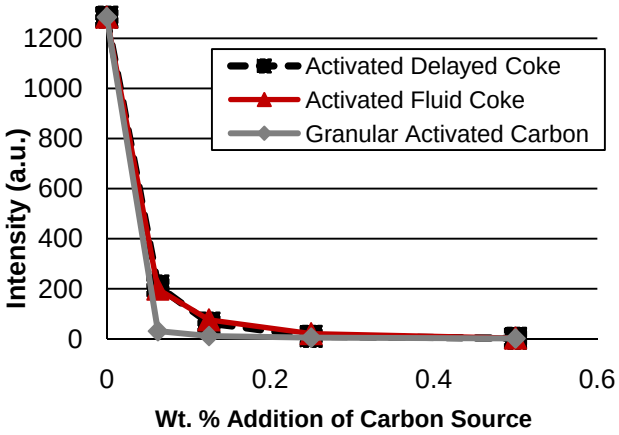

Figure 5. Peak intensities of the 280 nm excitation wavelengths for increasing weight additions of granular activated carbon, and activated delayed and fluid coke.

OSNA concentrations on process-water treated with activated delayed and fluid coke were measured through FT-IR spectrometry in order to compare fluorescence spectrometry removal rates to a quantitative industrial method (Figure 6).

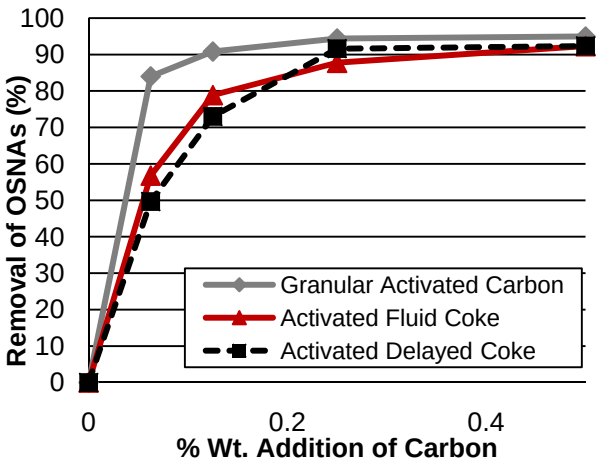

Figure 6. Removal efficiency of OSNAs from process-affected water using granular activated carbon and activated delayed and fluid coke (based on FT-IR spectrometry).

The results indicate a 50-92% and 55-92% removal of OSNA concentrations with the use of

activated delayed and fluid coke, respectively. The GAC showed a greater removal efficiency of the OSNAs; however, this is to be expected due to its greater surface area. The FT-IR results confirm that the fluorescence results over-estimate the actual amount of OSNAs within the process-water. This error may be attributed to difficulties in measuring low level emissions. Nevertheless, the trends in removal rates are consistent with FT-IR results indicating that fluorescence spectrometry may be used as a screening tool for monitoring the adsorption of OSNAs onto carbon-based adsorbents. At the same time, the FT-IR results indicate that over 90% of OSNAs can be removed by adsorption from process-affected water when 0.5 wt. % of activated delayed and fluid coke is used. Therefore, physical activation is a suitable technique for converting oil sands petroleum coke into an activated carbon adsorbent for treatment of PA water.

CONCLUSIONS AND SUMMARY

Activation experiments demonstrated that increased time (6 hours) and temperature (900^{o}C) will generate higher surface areas under CO_2 + steam atmosphere. Though a higher steam rate of 0.5 mL/ min produced a higher iodine number (670 mg/g) and surface area (578 m^2/g) for activated delayed coke, a lower steam rate of 0.3 mL/min was most ideal for activated fluid coke pore development (533 m^2/g). Methylene blue values indicated that both activated delayed and fluid coke samples had a wider pore size distribution including a range of micro- and mesopores.

Petroleum coke (a waste by-product of bitumen upgrading) can be used as an adsorbent to successfully remove OSNAs from oil sands process-water. Preliminary results indicated that raw delayed and fluid coke can reduce OSNA signatures by 76% and 96%, respectively when added to straight process-affected water by 30% wt. Once physically activated, 0.5% wt. addition of activated delayed and fluid coke can efficiently remove approximately 99.8% of the OSNA fluorescence signature. These results correspond to a 92% removal of measured OSNA concentrations obtained through FT-IR spectrometry.

The removal of OSNAs from oil sands process-water would reduce their toxicity and corrosivity, supporting remediation efforts and recycling initiatives.

ACKNOWLEDGEMENTS

The authors would like to acknowledge the University of Alberta; funding from NSERC; and, the delayed and fluid coke samples provided by Suncor Energy Inc. and Syncrude Canada Ltd.

REFERENCES

Allen, E. 2008a. Process water treatment in Canada's oil sands industry: I. Target pollutants and treatment objectives. Journal of Environmental Engineering and Science; **7**: 123-138.

Allen, E. 2008b. Process water treatment in Canada's oil sands industry: II. A review of emerging technologies. Journal of Environmental Engineering and Science; **7**: 499-524.

ASTM. 2006. Standard test method for determination of iodine number of activated carbon. ASTM International. PA, USA; D 4607-94.

ASTM. 2008. Standard test method for 24-h batch-type measurement of contaminant sorption by soils and sediments. ASTM International. PA, USA; D 4646-03.

Bansal, R.C., and Goyal, M. 2005. Activated Carbon Adsorption. Taylor and Francis Group, Florida, 497 pp.

Barczak, M., Dabrowski, A., Hubicki, Z., and Podkoscielny, P. 2005. Adsorption of phenolic compounds by activated carbon- A critical review. Chemosphere; **58**: 1049-1070.

Brient, J.A., Wessner, P.J., Doyler, M.N. 1995. Naphthenic Acids. Kirk-Othmer Encylopedia of Chemical Technology, Fourth Edition. John Wiley and Sons; New York: 1017-1029.

Brown, L.D., Alostaz, M., and Ulrich, A.C. 2009. Characterization of oil sands naphthenic acids in oil sands process-affected water using fluorescence technology. In Proceedings, 62nd Canadian Geotechnical Conference & 10th Joint CGS/ IAH-CNC Groundwater Conference, Halifax, NS; September 20-24, 2009; 659-665.

Clemente, J.S., and Fedorak, P.M. 2005. A review of the occurance, analyses, toxicity, and biodegradation of naphthenic acids. Chemosphere; **60**: 585-600.

Fedorak, P.M., and Coy, D.L. 2006. Oil sands cokes affect microbial activities. Fuel; **85**: 1642-1651.

Furimsky, E. 1998. Gasification of oil sands coke: Review. Fuel Processing Technology; **56**: 263-290.

Gregg, S.J., and Sing, K.S.W. 1982. Adsorption, surface area and porosity. Academic Press Incorporated; London: 1-39.

Hameed, B.H., Ahmad, A.L., and Latiff, K.N.A. 2007. Adsorption of basic dye (methylene blue) onto activated carbon prepared from rattan sawdust. Dyes and Pigments; **75**: 143-149.

Headley, J.V., Hill, G.A., Nemati, M., and Paslawski, J.C. 2009a. Biodegradation kinetics of trans-4-methyl-1-cyclohexane carboxylic acid. Biodegradation; **20**: 125-133.

Headley, J.V., Peru, K.M., and Barrow, M.P. 2009b. Mass spectrometric characterization of naphthenic acids in environmental samples: a review. Mass Spectrometry Reviews; **28**: 121-134.

Holowenko, F.M., Mackinnon, M.D., and Fedorak, P.M. 2001. Naphthenic acids and surrogate naphthenic acids in methanogenic microcosms. Water Resources; **35**: 2595-2606.

Janfada, A., Headley, J.V., Peru, K.M., and Barbour, S.L. 2006. A laboratory evaluation of the sorption of oil sands naphthenic acids on organic rich soils. Journal of Environmental Science and Health Part A; **41**: 985-997.

Mattson, J.S., and Mark, H.B. 1971. Activated carbon: surface chemistry and adsorption from solution. Marcel Dekker, Inc.; New York, USA.

Mohamed, M.H., Wilson, L.D., Headley, J.V., and Peru, K.M. 2008. Screening of oil sands naphthenic acids by UV-Vis absorption and fluorescence emission spectrophotometry. Journal of Environmental Science and Health Part A; **43**: 1700-1705.

Sontheimer, H., Crittenden, J., Summers, R., Fettig, J., Horner, G., Hubele, C., and Zimmer, G. 1988. Activated carbon for wastewater treatment. AWWA Research Foundation, Denver, CO.

Stavropoulos, G.G., and Zabaniotou, A.A. 2009. Minimizing activated carbons production cost. Fuel Processing Technology; **90**: 952-957.

Tucker, S.A., Amszi, V.L., and Acree Jr., W.E. 1992. Primary and secondary inner filtering- effect of $K_2Cr_2O_7$ on fluorescence emission intensities of quinine sulfate. Journal of Chemical Education; **69**: A10-A12.

Vlasopoulos, N., Memon, F.A., Butler, D., and Murphy, R. 2006. Life cycle assessment of wastewater treatment technologies treating petroleum process waters. Science of the Total Environment; **367**: 58-70.

Whitby, C. 2010. Microbial naphthenic acid degradation. Advances in Applied Microbiology; **70**: 93- 125.

Yang, R.T. 2003. Adsorbents: fundamentals and applications. John Wiley and Sons, Inc.; New Jersey, USA: 79-123.

Yen, T., Marsh, W.P., MacKinnon, M.D., and Fedorak, P.M. 2004. Measuring naphthenic acids concentrations in aqueous environmental samples by liquid chromatography. Journal of Chromatography A; **1033**: 83-90.

AN INTEGRATED ENGINEERING SOLUTION IN TREATING TAILINGS POND WATER FROM ALBERTA'S OIL SANDS INDUSTRY

Zhangyi Guo
University of Alberta, Edmonton, Canada

ABSTRACT

Tailings water generated from Alberta's oil sands industry has become a great environmental concern due to its large volume and its acute and chronic toxicity. To comply with the "zero discharge" policy imposed by the government, large tailings ponds have been built to store a large amount of tailings water on oil sands sites. The sustainability of the industry is threatened by the limited water supply. This has forced the industry to look for feasible tailings pond water (TPW) treatment methods in order to increase he reuse of the treated TPW, to reduce the water demand, and/or to make the treated TPW eligible for environmental release to offset the industry's water consumption.

It has been widely recognized that any valid treatment method for treating TPW has to be technically practicable and economically feasible. In this paper, after reviewing recent, published literature related to TPW treatment, and based on knowledge and experiences gained from other industrial water and wastewater treatment, an integrated tailings pond water treatment process is proposed. This engineered treatment process consists of bioadsorption/bioflocculation, sludge-blanket-assisted clarification, ozonation, and a hybrid biological process assisted by petroleum coke. The objective of this proposed treatment process is environmental release and further reuse of the treated TPW. The proposed process reuses two waste materials that are produced from the industry in order to enhance the treatment efficiency, to increase financial feasibility, and to maximize environmental benefits of the treatment. This paper discusses the design and the expected results of the process.

INTRODUCTION

Tailings water generated from Alberta's oil sands industry has become a great environmental concern due to its large volume and its acute and chronic toxicity (Allen 2008a). The current "zero discharge" policy imposed by the government has resulted in the creation of large tailings ponds to store the tailings pond water (TPW) on a given site. Although a portion of tailings water is recovered from the ponds and is reused for extraction of bitumen, a large amount of water is still trapped in the ponds, resulting in a continuously increasing TPW inventory. Moreover, occupying a large area of landscape and hold a large volume of toxic TPW (over 50 km^2 and 5.5 billion m^3, Government of Alberta 2007), the oil sands tailings ponds can result in significant environmental effects. This is well demonstrated by a recent incident that killed hundreds of migrating birds in one of Syncrude's tailings pond. In addition to being a serious threat to wildlife, toxic TPW and sediments in the ponds are also a great potential threat to the ground water due to the possibility of leakage.

The sustainability of Alberta's oil sands industry is threatened by the limited water supply. Due to the large water demand of the industry, which is expected to grow rapidly in the future, the Athabasca River watershed may not be capable of supporting the industry in the long run without significant impacts on its aquatic ecosystems, especially during the Athabasca River's low winter flows (Allen 2008a). Alberta Environment is considering a river water allocation limitation to restrict water withdrawals to up to 30% of the river's total flow during low flow periods (Sawatsky, 2004). More stringent regulations on the conservation and reuse of water are also expected to be imposed on the industry. This has forced the industry to look for treatment methods to increase the reuse of TPW, and in order to make the treated TPW eligible for environmental release; both of these processes would offset the industry's water consumption.

Owing to its toxic and biologically recalcitrant nature, complex water chemistry, high total dissolved salts (TDS), high concentration of slow settling fine particles, significant presence of oil and grease, as well as the large-scale treatment required, treatment of TPW poses a great challenge both technically and economically. Despite the progress in the research that has been made, many potential TPW treatment technologies , such as advanced oxidation, are still

at the development stage and far from application at the required scale, Some others, such as biodegradation, activated carbon adsorption, chemically enhanced sedimentation, and some membrane technologies, though technically feasible, may be hindered by reduced efficiencies, elevated operational costs, increased energy consumption, and intensified maintenance issues. More importantly, no single treatment technology could possibly remove all the target pollutants of concern; it is widely accepted that for industrial wastewaters containing complex toxic compounds that resist biodegradation, a combination of physical, chemical, and biological treatments is normally required. It has also been widely recognized that any valid TWP treatment methods have to be technically practicable and economically feasible. Experience has shown that it is very beneficial reuse waste by- products from the industry in the treatment process to reduce the costs, improve the efficiency, and maximize environmental benefits of the treatment.

This paper proposes an integrated engineering solution based on recent advances in TPW treatment and on innovated technologies that are applied in treating other industrial wastewaters. The proposed treatment process focuses on two fundamental issues associated with TPW management: water reuse and water release.

TARGET POLLUTANTS AND TREATMENT REQUIRMENTS

Allen (2008a) conducted an intensive tailings water quality review based on field data of Syncrude and Suncor, from which a number of target pollutants were identified. They were classified into organic compounds, inorganic compounds, and trace metals (Allen 2008a). Table 1 compares the concentrations of the major target pollutants in TPW and in the Athabasca River to their criteria for industrial reuse and environmental release.

Among organic pollutants, naphthenic acids (NAs) exert the greatest environmental and treatment challenges due to their acute and chronic toxicities to aqatic biota, and their resistance to biological degradation (Allen 2008a, Scott et al. 2007, Del Rio et al. 2006, Clements and Fedorak 2005 Holowenko 2002). Most of the acute aquatic toxicity of the oil sands process affected water (OSPW) is attributed to this group of organic compounds (Allen 2008a, Del Rio et al. 2006), especially those with carbon numbers less than 22 (Holowenko, et al. 2002). NAs have been shown to be toxic to a range of aquatic biota at concentrations in excess of 2.5~5 mg/L (Small et al. 2009). They also account for more than 95% of Dissolved Organic Carbon (DOC) in OSPW (Fu et al. 2008). Considering the concentration of NAs in the Athabasca River (<1 mg/L), a discharge limitation of 1~5 mg/L, or lower may be desired for environmental release of treated TPW, even though a regulatory limit has not been defined. This implies that more than a 95% reduction of NAs would be required to release treated TPW to the environment.

Oil and grease have a significant presence in TPW, mostly in the form of emulsion (Kasperski 1992), and their existence has adverse impacts on some potential TPW treatment technologies, for instance, they cause fouling issues for membrane treatment (Allen 2008a). More than a 90% reduction of oil and grease would be required for both industrial reuse and environmental release. Phenols, PAHs, and BTEX also exist, and their removals by up to 90% have to be considered for any environmental release and industrial reuse, if there is any potential direct human contact. The lower BOD/COD ratio of roughly 0.01~ 0.12 calculated from Table 1 suggests poor biodegradability of the TPW.

Total suspended solids (TSS) and TDS are two of the most important inorganic target pollutants in the TPW. The former contains a significant portion of slow-settling fines, and traps a large amount of water (Kasperski 1992). Its removal is a precondition for more effective applications of many treatment technologies, including ozonation, adsorption, membrane filtration, reversed osmosis (RO) etc. The industrial reuse of treated TPW, such as for once-through steam generation and conventional boiler feed water, also requires highly purified water with very low TSS levels. Elevated TDS levels, which result from the consolidation tailings (CT) process, are a concern for the current bitumen extraction process, as they tend to decrease the extraction efficiency (Allen 2008a).

Table 1 Concentrations of Target Pollutants in TPW and in the Athabasca River relative to the Criteria for Reuse and Release

Pollutant (mg/L)	Tailings[a] pond water	Industrial Reuse Criteria			Athabasaca River[a]	Environment Release Criteria[d]
		Boiler Feed Water[b]	Once Through Steam[b]	Cooling Water[c]		
Inorganic						
Ammonia	14				0.06	1.3-5
Bicarbonate	775–950				115	500
Chloride	80–540				6	150-500
Sulphate	218–290				22	50-80
TDS	1900–2221	100-650	8000	2000	120-230	1340
COND[e]	1506–2400	150-1000		1200	280	150–1000
Alkalinity	600-800	100		400	90-230	
Hardness	90-120	0.05	0.5	500	90-270	
TSS	~7000	0	0	50		25
PH	8.2-8.4	8.5-9.5	9-9.5		8.2	6-9
Organic						
Benzene	<0.01–6.3					0.37
BOD	<10–70				<2	<25
COD	86–973				<40	<200
Cyanide	0.01–0.5				0.004	0.005-0.5
Naphthenic acids	40–120				<1	1-5
Oil and grease	9–92	1	1		<0.5	5~10
Phenols	0.02–1.5				<0.001	0.001-0.004
Toluene	<0.01–3					0.002-1.3
PAHs	0.01					0.00001-0.00006
Trace metals						
Aluminum	0.07–0.5					0.1-0.75
Arsenic	0.006–0.015					0.005-0.15
Chromium	0.003–2					0.074
Copper	0.002–0.9					0.002-0.009
Iron	0.8–3	0.02	0.05			0.3-3.5
Lead	0.04–0.19					0.0025
Nickel	0.006–2.8					0.052
Zinc	0.01–3.2					0.12

[a]From Allen (2008) except Naphthenic acids that is from Fu et al. (2008)
[b]Form Allen (2008)
[c]From Superchill (n.d.)
[d]From CCME guideline for the protection of aquatic life (2005), AENV guideline for wastewater treatment (2006), and USEPA water quality criteria for the protection of aquatic life (1999), except for Naphthenic Acids that is assumed.
[e]In the unit of μS/cm

To make TPW suitable for other industrial purposes, especially as boiler feed water, its TDS concentration must be reduced significantly (>90%), while a moderate level of removal (~50%) could make treated TPW suitable for once-through steam generation, or cooling water.

The removal of trace metals is important for the environmental release of the TPW. Required removal rates for some of the trace metals found in the TPW, such as lead, chromium, copper, and nickel, exceed 90%.

LITERATURE REVIEW AND DISCUSSION

Removal of Naphthenic Acids (NAs) From Oil Sands Process Affected Water (OSPW)

Even though NAs found in OSPW can be partially removed through biodegradation, mostly under

aerobic conditions (Holowenko et al. 2002), studies have shown that NAs present in the tailings ponds are poorly biodegradable (Clements and Fedorak 2005, Del Rio et al. 2006, Scott et al. 2005, and Scott et al. 2007). As a result, other treatment methods are needed for effective removal of the NAs within practical time.

The ozonation of NAs in TPW has been studied intensively. In an experiment conducted by Scott et al. (2007), the ozonation of filtered OSPW with approximately 35 mg/L dissolved ozone in the reactor resulted in a roughly 70% reduction of NAs in the sample, and an essentially non-toxic effluent (based on the Microtox bioassay) was obtained after 50 min. After 130 min of ozonation, more than 95% of the NAs were removed, leaving a residual concentration of 2 mg/L in the sample. The experiment also suggested that complete oxidation of NAs did not occur because there was only a small change to the TOC (total organic carbon) before and after ozonation. This small change in TOC indicated that the NAs were oxidized to other organic compounds, and remained in the water sample. The COD of the sample was reduced by about 50% after 130 min of ozonation, while the BOD value increased from 2 mg/L to 15 mg/L, resulting in the increase of the BOD/COD ratio from 0.01 to 0.15. This resulted in a significant improvement in biodegradability after the treatment. This is in good agreement with the general concept that ozonation increases biodegradability of complex wastewater. The changes in the distribution of the speciation of NAs after ozonation was investigated, and the resulting data revealed a significant shift toward a greater proportion of low carbon number, lower ring number, and low molecular weight products; see Figure 1 (from Scott et al. 2007). This shift in the distribution of speciation after ozonation is of interest as a lower residual level could be achieved by biodegradation following ozonation, though this hypothesis has to be examined experimentally.

Similar results and conclusions were produced by Fu et al. (2008). In their experiments, which used membrane-filtered OSPW samples from one of Syncrude's tailing ponds, after only 1 minute exposure to 50 mg/L ozone, the concentration of NAs in the sample was reduced from the 68.2 mg/L to 18.6 mg/L, a 73% reduction. Fu et al. (2008) also suggested that higher ozone dose results in lower concentrations of NAs, as illustrated by Figure 2. 99% removal of NAs was achieved in 30 minutes when an extremely high ozone dose of 1500 mg/L was used. This experiment reported a 3-fold increase in the BOD/COD ratio and the detoxification of the treated sample.

.

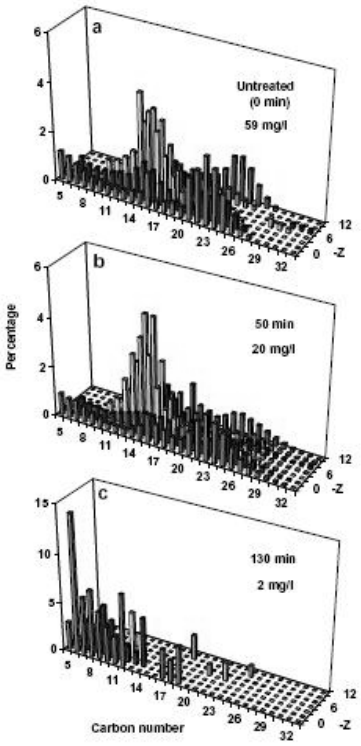

Figure 1. Three-dimensional plots showing changes in the distribution of naphthenic acids in sediment-free OSPW treated with ozone. The sum of the bars in each panel is 100%. (by A.C. Scott et al, 2007. used with permission)

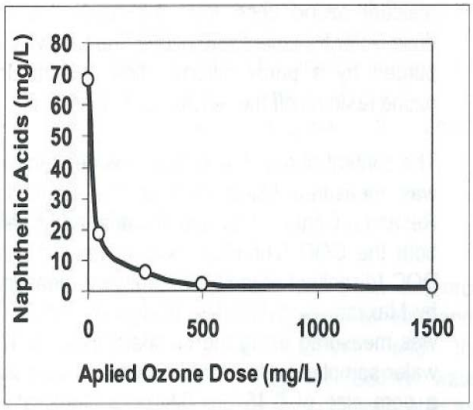

Figure 2. Ozone Dose vs. NAs removal (by H.H. Fu et al, 2008. used with permission.

Ozonation is widely used for disinfection and both taste and odour control of drinking water. The typical dose used in this application is 1~5 mg/L (MWH 2005). Its application in wastewater treatment has also significantly increased in recent years (Reynolds and Richards 1996); this application has been used to target toxicity and recalcitrant organic compounds in industrial wastewater streams, and to enhance the subsequent biological process (Gulyas et al. 1995, Lin and Wang 2002). The typical dose for this application ranges from 5~40 mg/L (Metcalf & Eddy 2004). The City of Montreal is building the largest ozone treatment plant in the world to treat all of its municipal wastewater of more than 2.5 million m^3/day (CBC, 2008), with a proposed ozone dose of 16.5 mg/L (Gehr 2008). Rice (1996) also conducted a detailed review of ozone applications in industrial wastewater treatment, which indicated that ozonation has been successfully employed to treat a variety of industrial wastewaters containing toxic and recalcitrant substances on significant scales, including a German industrial wastewater treatment plant treating 25,000 m^3/d of textile wastewater with an applied ozone dose of 69 mg/L. Therefore, ozonation may be practicable for TPW treatment in terms of the scale of the application and the required dose.

Adsorption of NAs in OSPW by Oil Sands Coke

The use of petroleum coke, a waste by-product from Alberta's oil sands industry, to adsorb NAs in the OSPW was investigated recently. Researchers from Syncrude claimed that the fresh coke generated from a fluid coking operation was effective in removing dissolved organics, including NAs, from OSPW by adsorption. Seventy to ninety percent removal efficiencies of NAs were claimed when a 20-30 wt % slurry of pulverized coke particles in OSPW was mixed and given sufficient contact time (> 20 minutes) (Zubot et al. 2009).

Removal of Oil and Grease

A number of bitumen removal methods currently applied to recover residual bitumen from the tailings ponds have been evaluated by Kasperski (1992). She concluded that any form of tumbling, mixing, aeration, or combinations of these would facilitate dispersion of bitumen and bitumen-mineral agglomerates, resulting in enhanced uprising of oil and grease. As a result, the oil and grease can be removed and recovered from the tailings pond; this was demonstrated by a patented process involving agitation and aeration, which achieved about 70% bitumen recovery from the pond sludge of a Suncor tailings pond.

Studies of oilfield-produced water treatment indicated that biological treatment processes, such as activated sludge and GAC-FBR (fluidized bed reactor), are capable of removing oil and grease by up to 98% (Tellez et al. 2002, Seybold et al. 1997). However, the efficiency was greatly affected by the toxicity of the water (Allen 2008b).

PROPOSED TPW TREATMENT PROCESS

Based on reviews of recent research on TPW and OSPW treatment, and the knowledge and experiences gained from other industries, an integrated treatment process is proposed. This process consists of bioadsorption, bioflocculation, sludge-blanket-assisted clarification, ozonation, and petroleum-coke-assisted hybrid biodegradation. The objective is to treat TPW to the level suitable for both environmental release and reuse by the industry on a much larger scale than is currently practiced. The process is illustrated in Figure 3.

Reuse of two waste materials produced from the same industry was integrated into this process. The first, waste activated sludge (WAS), from domestic wastewater treatment plants operated by the industry, is used as a bio-flocculent/bio-adsorbent to reduce the amount of chemical coagulant and polymer required. The second, petroleum coke produced from oil sands upgrading, is used as a biofilm carrier in the hybrid (activated sludge and biofilm) bioreactor.

Unit Operation and Unit Process

Solids Contact Clarifier with Addition of Waste Activated Sludge

The first process unit is the solid contact clarifier, which has been widely used for water and wastewater treatment, and for lime softening. This type of clarifier features an internal coagulation-flocculation chamber inside its bell-shaped centre column with a column diameter that gradually increases from top to bottom. The influent, after coagulation and flocculation, is re-circulated multiple times by a mechanism, normally a rotor impeller, passing through and contacting with a

suspended sludge blanket formed near the bottom of the settling zone (see Figure 4). This concentrated sludge blanket enhances clarification by promoting flocculation of solids and particle enmeshment (Oasim etal. 2000). It was also pointed out that solids contact clarifiers offer savings in size, construction costs, and mechanical piping, resulting in lower capital costs for a plant (Sanks 1978).

The major drawback of the solids contact clarifiers is the difficulty of maintaining a stable suspended sludge blanket in the clarifier when the particle concentration in the source water is too low, or changes consistently and dramatically (Chen et al. 2002), which is not uncommon when feed water is from a river. However, none of these would occur for TPW treatment.

In addition to chemical coagulants and polymers, bio-adsorbents, such as WAS, have been used with this type of clarifier to improve the settling of fine particles with poor settling characteristics, and to reduce the dose of chemicals required for coagulation and flocculation. In a full scale activated sludge wastewater treatment plant designed by the author for treating pulp and paper mill wastewater (approximately 20,000 m^3/d, including black liquor), the recycling of WAS from the secondary clarifiers to the primary solids contact clarifiers resulted in 15 - 20% savings of PAM. This was attributed to the bio-adsorption and bio-flocculation provided by the recycled WAS.

Bio-adsorption and bio-flocculation contribute to enhanced removal of particles, soluble organic matters, and heavy metals in wastewater. Extracellular polymer substances (EPS), the major constituent of biomass produced from metabolic activities of living cells, enable bio-adsorption and bio-flocculation to take place (Mila and Katja 2007, Galil and Levinsky 2006). Zhao, et al. (2000) conducted an experiment in which the previously settled and re-aerated WAS was directed into the primary clarifier of an activated sludge system. This increased the COD removal rate for conventional primary clarifiers in treating municipal wastewater from typical values of 30-40% to 70-80%. They attributed the high COD removal rate largely to the bio-adsorption and bio-flocculation of small particles, including colloids, and soluble materials, onto the sludge flocs. A few wastewater treatment processes have been developed and implemented to take advantage of bio-flocculation and bio-adsorption to improve efficiencies.

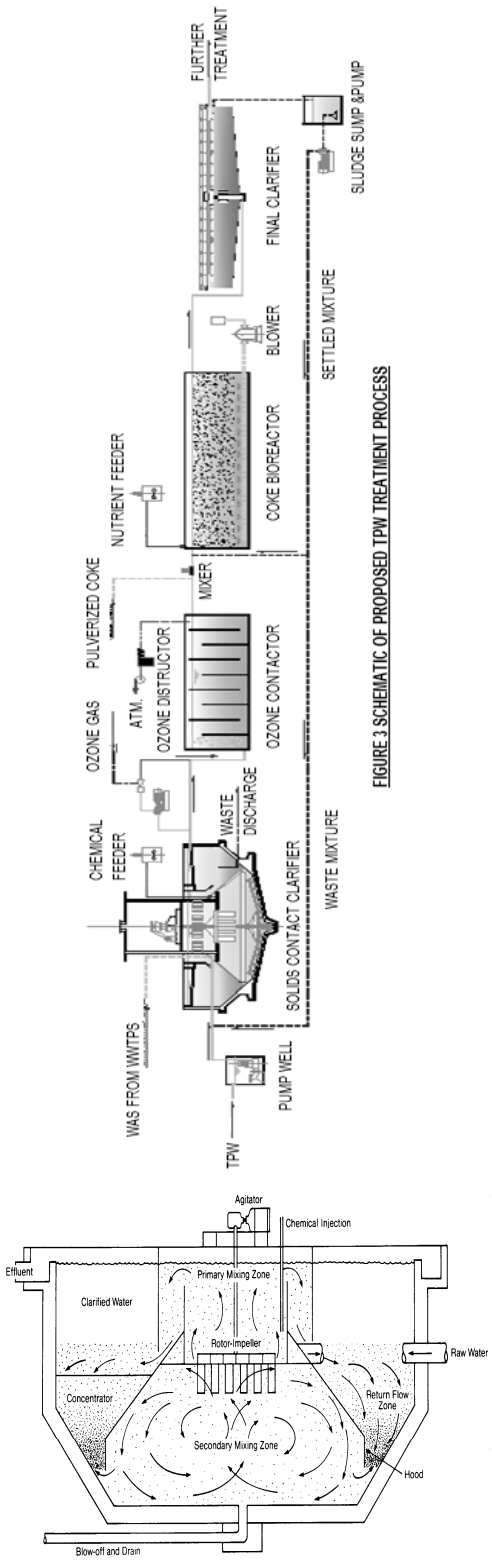

Figure 4. Solids Contact Clarifier. Note the sludge blanket formed on the bottom of the concentrator. (from GC3 Specialty Chemicals, Inc. used with permission

These include the contact stabilization process, the adsorption-bio-oxidation process (Zhao 2000), and the trickling filter/solids contact (TF/SC) process (Boltz et al. 2006), which have been used for a long time, and a newly developed up-flow sludge blanket filtration (USBF) process (Mahvi et al. 2008).

Aksu (2005) concluded that using dead microbial cells, such as WAS, for bio-adsorption offers a few advantages over living microorganisms, including that the bio-sorption capability of dead microbial cells is not affected by the toxicity of wastewater, no nutrients are required, and it is as effective as growing or resting cells. In addition to improving particle removal, enhanced removal of other target pollutants, such as heavy metals and TOC etc., is expected.

Currently, a number of wastewater treatment plants, mostly the activated sludge system and its modifications, such as SBR and MBR, are operated by the industry for domestic wastewater treatment. These treatment plants generate considerable amounts of WAS that need to be further treated before being trucked out to the nearby municipal landfills for final disposal. Owing to the shortage of well-trained operators and the difficulty of sludge handling, sometimes, untreated WAS is taken to the nearby municipal wastewater treatment plant, which is very costly. This WAS can be reused as the bio-adsorbent/bio-flocculent with solids contact clarifiers for TPW treatment.

Inclined plate settlers can be installed in the clarification zone to increase the settling surface area of the clarifier. It is suggested that waste biomass produced from the hybrid biological process should be cycled back to the solids contact clarifier to provide additional biomass. This new process has a single point of discharge of waste solids, which is from the solids contact clarifiers. See Figure 3 for illustration (inclined plates are not shown in Figure 3). Chemical coagulants and polymers may still be needed at a reduced dosage, depending on actual treatment results.

The reuse of WAS for TPW treatment will not only offset the treatment cost and ease the TDS problem, but will also provide an opportunity to have a centralized WAS handling and disposal facility for the industry, which would be more cost effective.

A surface skimming mechanism is recommended to recover the residual bitumen in a concentration range of 25 to 92 mg/L from the pond water (see Table 1), since the thorough mixing that occurs in the solids contact clarifier would facilitate the release of oil and grease previously coated on the surface of particles, as discussed in the review section of this paper. A portion of TOC, including NAs would also be removed from this stage.

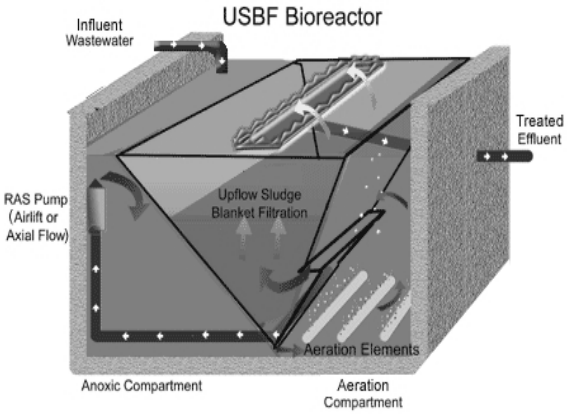

Figure 5. Upflow Sludge Blanket Filtration Process. After aeration, the mixed liquor passes upwards through the sludge blanket at the bottom of the clarifier for better clarification. (from EcoFluid System, Inc., used with permission)

Ozonation

After enhanced sedimentation, a portion of the organic and inorganic substances that would otherwise compete with NAs for consuming ozone in the water stream will have been removed, along with TSS. As a result, the ozonation can be more effective. The purpose of ozonation is to reduce the concentrations of NAs and their associated toxicity, as well as to improve overall biodegradability of the TPW.

Considering the high ozone dose required, as well as the heavy presence of oil and fine particles in TPW, a side-stream ozone system is proposed. Compared with conventional ozone systems that use the bubble diffusion system to introduce ozone-containing gas directly into ozone contactors, it first injects ozone-containing gas into a portion of feed water called a side stream. Then this ozone-rich stream is directed into ozone contactors, a simple, reliable, and effective design. As a result, the intensive maintenance requirement associated with the bubble diffusion system is eliminated.

The high O-content in the ozone-containing gas benefits the subsequent biological process, and it allows one to operate the system at higher gas/liquid ratios, thereby reducing the size and the energy consumption of the side-stream system. Therefore, a degas-vessel should not be used. Two configurations of side-stream ozone systems are illustrated in Figure 6.

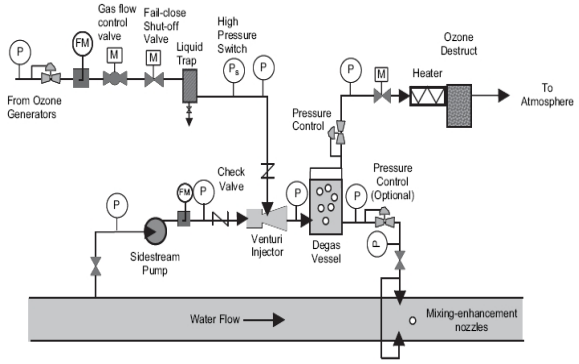

a) Side-stream ozone system with degas vessel

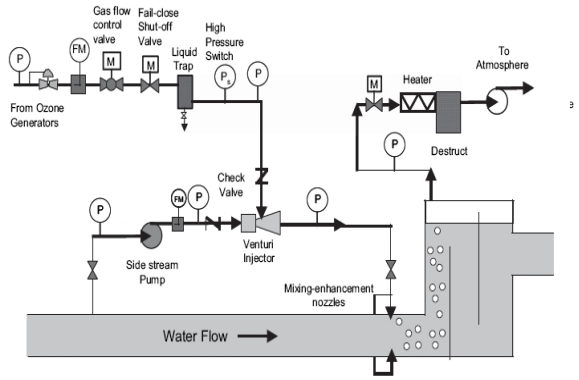

b) Side-stream ozone system without degas vessel

Figure 6. Side stream ozone systems in two configurations (from Raknees, 2007, used with permission)

Because of its physical and chemical properties, ozone cannot be stored, and has to be generated on site. Both air and pure oxygen are used to generate ozone. The ozone gas generated from air typically contains ozone ranging from 1~4 wt %, whereas that from an oxygen feed generation ranges from 8~12 wt %, even as high as 16 wt % in some industrial applications (Raknees 2005). Higher ozone concentration in the ozone-containing gas is very desirable in TPW treatment, because the better ozone transfer rate and kinetics would have positive impacts on the system efficiency and operational costs when the required ozone dose is high. Moreover, generation of ozone from oxygen requires less than half the specific energy for generation of ozone from air (Horn 1996). As a result, ozone generation from pure oxygen should be considered.

Pulverized Petroleum Coke Assisted Biofilm and Activated Sludge Process (Hybrid)

Powdered activated carbon treatment (PACT), is a well-established wastewater treatment process, where powdered activated carbon (PAC) is introduced into the activated sludge system as a biofilm carrier and adsorbent. It is used to treat a wide range of municipal and industrial waste-waters containing toxic and biologically recalcitrant organic compounds and heavy metals. The advantages provided by this hybrid process include system stability during shock load, reduction of refractory priority pollutants, and improved sludge settleability (Metcalf & Eddy, 2004). Research has revealed a synergism between carbon adsorption and biodegradation of organic compounds in this combined treatment process, which leads to a much better overall removal efficiency, more than the sum of that provided by using carbon adsorption and biodegradation independently in the same treatment train. This is attributed to the stimulation of the biological activity of microorganisms attached to the surface of the PAC, and the biological renew of PAC's adsorption capability (Sublette et al. 1982).

It has also been proven that a large quantity of biofilm coated on the carbon surface is effective in the removal of heavy metals from wastewater. Scott et al. (1995) reported that the biofilm of bacteria attached to granular activated carbon enhanced both rate and quantity of metal uptake from wastewater, and concluded that even though activated carbon itself is not an effective adsorbent of heavy metals, the attached biofilm consisting of bacteria held in an expansive excreted polysaccharide coating can significantly increase the rate and quantity of metal uptake.

However, the high operational cost exerted by the expensive PAC would inhibit its application in TPW treatment.

On the other hand, there are large quantities of petroleum coke produced by Alberta's oil sands industry. Suncor reportedly produced over 3000 tonnes/day of oil sands coke (Dipanfilo and

Egiebor 1995). Currently, this oil sands upgrading by-product has to be disposed of as a waste, creating another environmental problem.

It is the author's opinion that it would be more practicable to use pulverized raw oil sands coke, instead of PAC, to form a hybrid biological system as a portion of the proposed treatment process for the following reasons:

1. waste material is readily available in a large quantity with almost no additional cost for reuse;
2. 70~90% removal efficiencies of NAs are claimed for coke adsorption (Zubot et al. 2009);
3. it is ideal for use as a biofilm carrier with a much larger surface area compared with most bio-media currently used in water and wastewater treatment.

Some of the physical and chemical properties of raw oil sands coke, compared with a commercial activated carbon, are listed in Table 6.

Though the surface area of oil sands coke is 2 orders of magnitude smaller than that of activated carbon, it is still approximately 3~5 orders of magnitude larger than most biofilm media currently used in biological wastewater treatment. For the purpose of comparison, the specific surface areas of common biofilm media currently used and that of oil sands coke are tabulated in Table 7, along with the bioreactor types used.

Table 6. Physical properties of delayed petroleum coke vs. a commercial PAC used for PACT process

Parameter	Delayed Petroleum Coke[a]	Hydrodarco-C[b]
Moisture (wt%)	1.8	4
BET-surface area (m^2/g)	9	600
Iodine number	28	500
Bulk density (g/cm^3)	1.0415	0.51

[a]From Shawwa et al. (2001)
[b]Form Norit (2007)

Coke particles should also provide significant adsorption capacity in general as evidenced by its capability of NAs adsorption. When a substrate is low in concentration and is biologically recalcitrant, such as NAs in TPW for example, it is probably adsorbed and concentrated on the surface of biofilm carriers, and is further degraded. This elevated substrate concentration would provide a higher kinetic driving force for the degradation compared to that in a suspended system since biological degradation of organic matters in wastewater is likely a pseudo first order reaction. Moreover, once pollutants are adsorbed on the media, their reaction time will no longer depend on the hydraulic resident time (HRT) in the bioreactor. Instead, it will be the same as that of the microbes that attach to the same media. As a result, sufficient reaction time for the biodegradation, which is crucial for breaking down complex and refractory organic maters, can be achieved without enlarging the size of the bioreactor. The attached microbial community also provides denser and more diversified microbial species than those in suspended microbial communities; thus, they are able to produce more diversified extracellular enzymes to attack complex and refractory organic matter. This provides a better chance for the pollutants to be degraded. The synergism between adsorption and biodegradation is also expected. With enhanced biodegradation of the adsorbed organic pollutants, the adsorption capability of the media will be restored quickly.

Table 7. Specific areas of common biofilm media and oil sands coke

Reactor Applied	Material	Specific surface area, m^2/m^3
Trickling filter	Rock	50~100
	Plastic	100~200
RBC	Plastic	100~200
	Plastic	300
	Porous clay	1,000~1,400
IFAS/MBBR	Porous slate	1,200~1,400
	Polystyrene	1,100
	Anthracite	1,900
	Quartz sand	3,000
	Basalt	3,600
Fluidized bed	Sand or bassalt	3,000~4,000
PACT	PACT	300,000,000
Coke bioreactor	Oil sands coke	~10,000,000

Note: the specific surface areas of oil sands coke and PAC are calculated roughly based on the surface ratios, and bulk densities presented in Table 6. The others are from Henze et al. 2008

As in the PACT process, oil sands coke particles need to be separated from the water stream and to be recycled back to the bioreactor to maintain a desired biomass and coke particle concentration. Membrane filtration may be used as the separation method as long as its higher energy consumption, capital, operational, and replacement costs are justified for the smaller footprint and better effluent quality (especially with respect to TSS).

When gravity sedimentation is considered, the solids loading rate needs to be carefully evaluated in the design because the solid concentration in the water stream will be quite high due to the introduction of oil sands coke.

Fresh oil sands coke needs to be added continuously into the bioreactor, not only to compensate for coke particles removed with biomass, but also to provide additional adsorption capacity. Addition of nutrients needs to be considered since the TPW may not have sufficient nutrients for effective biodegradation

Overall Description of the Proposed Treatment Process

The proposed treatment process is illustrated by Figure 3. The influent is taken from the existing oil sands tailings ponds between the water zone and the fine tailing zone. The influent is pumped into the solids contact clarifiers, mixing with the WAS from domestic wastewater treatment plants in the region and the mixture of waste oil sands coke and biomass from the final solid/liquid separation. Chemical coagulants and polymers may be also added but with reduced dose at this stage. The solids from the clarifiers are discharged for further treatment and disposal.

Subject to field verification, removal rates of 80~90% of TSS and 40~60% of oil & grease may be expected at this stage. Removal of heavy metals and TOC, including NAs, is also expected.

The clarified water is then directed into the ozone contactor. A portion of the water is pumped from the mainstream line to be mixed with ozone-containing gas that is produced in the side-stream ozone system, and subsequentially back to the main stream. Given that a higher ozone dose results in better treatment efficiency as suggested by Fu et al. (2008), and the intention to minimize technical risk, an ozone dose up to 100 mg/L may be used, though further investigation is needed to optimize the dosage. The contact time may be limited up to 2 hours, based on Scott's research (2007). Multiple injections may be required to ensure treatment results, as ozone is an unstable gas with a half-life of about 30 minutes at 15°C.

The expected removal efficiency of NAs at this stage could be ~ 80%, and the acute toxicity of the water should no longer have significant adverse impacts on the later biological process (Fu et al. 2008, Scott et al. 2007). Some other soluble organic pollutants, such as BTEX and phenols, are expected to be reduced by approximately 60% ~ 90%, based on the experiences gained from ozonation of other industrial waters similar to TPW, as reported by Allen (2008b).

After ozonation, the water flows into the bioreactor, where pulverized oil sands coke is added. Subject to field optimization, the dose may maintain the coke concentration in the bioreactor at ~ 30 wt %. Continuous addition of the coke powder should be provided to compensate for the loss due to wastage from the subsequent liquid/solid separation. Nutrients may be added by chemical feeders to facilitate the biodegradation.

The bioreactor is designed as a completely stirred reactor, and mixing is provided by aeration. The aeration also supplies oxygen to facilitate the growth of microbes. Since after ozonation, the water stream is probably saturated with oxygen (Raknees 2005, Raknees 2006) and the BOD level is low, the aeration should be designed focusing on sufficient mixing.

The final clarification may be done by gravity sedimentation or membrane filtration (MF/UF). A portion of settled coke-biomass sludge is wasted by sedimentation to maintain an appropriate sludge resident time (SRT) in the bioreactor, and the rest is recycled to the bioreactor to maintain a desired biomass and coke concentration for biodegradation and adsorption.

The concentration of NAs in the clarified effluent is expected to be 1.5~5 mg/L with a hypothetical removal rate of 70~90. It should be noted that the same NAs removal rate claimed by Zubot et al. (2009) was achieved by coke adsorption only while, the combination of biodegradation and adsorption in this proposed process should produce better results, as discussed earlier.

The other target pollutants, such as BOD, TSS, oil and grease, BTXE, phenol, and heavy metals, are expected to be reduced to the level that is suitable or nearly suitable for environmental release or industrial reuse.

The predicted concentrations of some target pollutants in treated TPW after each treatment stage are listed in Table 8.

Table 8. Calculated TWP quality after each treatment stage with hypothetical removal rate

Pollutant	TPW	Solids Contact Clarifier		Ozonation		Coke Assisted Activated Sludge	
TSS	7000	70~140	80~90%	70~140	-	7~14	90%
BOD	10~70	-	-	<100*	-	<20	90%
NAs	50~120	-45~114	-5~10%	10~25	75%	1.5~5	70~90%
Oil and Greas	9~92	4~38	40~60%	-	-	<5	90%
Phenols	0.02~1.5	-	-	0.005~0.4	75%	<0.004	90%

Note: All the number values in the unit of mg/L. Hypothetical % removal is given for each pollutant after each treatment stage.
* indicates the assumed BOD that is increased after ozonation.

Sludge Handling and Disposal

As previously stated, the waste solids, as a result of sedimentation from the solids contact clarifiers and from the biological process, are expected in a large quantity. It is proposed to disharge all the waste solids from the solids contact clarifiers. Further treatment of the waste solids from the system is required because it would contain considerable amounts of organic matter, toxic substances, and heavy metals

The applications of aerobic or anaerobic digestion of the waste sludge, which are commonly used for treating WAS from municipal wastewater treatment plants, may have to be carefully evaluated prior to making any sludge handling decision, because a large quantity of inorganic material (introduced into the system with petroleum coke) in the waste solids could deteriorate the efficiency of digestion. It may be worth investigating the possibility of direct mechanical dewatering of the waste sludge.

The disposal strategy developed for disposing the bottom sediments of the tailings ponds may be considered for the final disposal of the waste sludge from this proposed TPW treatment process; however, regulatory requirements and environmental impacts of the disposal need to be carefully studied.

FURTHER TREATMENT FOR ENVIRONMENTAL RELEASE AND INDUSTRIAL REUSE

For environmental release, constructed wetlands might be used to polish treated TPW to ensure that the environmental impacts of the released TPW are at a minimal level; ideally, the concentration of NAs in the discharged stream should be below 1 mg/L, the current level in the Athabasca River (Allen 2008a).

Allen (2008b) cited a number of studies, including pilot and full-scale wetland treatment systems, on treatment of oifield-produced water. These studies indicated a variable, but proven performance with reported BOD_5 removal from 55% to 84%, COD removal from 53% to 86%, oil and grease removal from 54% to 94%, and phenols removal from 10% to 94%. It was also pointed out that constructed wetlands have been intensively studied for Alberta's oil sands industry, and have demonstrated modest reductions in organic compounds and incomplete detoxification (reduction of 40% for NAs was reported).

Studies for the treatment of other industrial waste effluents, such as mining tailings, indicated that a properly designed, constructed wetland is capable of removing a number of divalent metals, including zinc, copper, mercury, chromium and lead that are all present in TPW, and contribute to the TDS. The reported removal rate ranged from 50-95% (Kadlec an Knight 1996, Nelson and Gladden 2008).

While simple in design and economically viable, constructed wetlands also possess a number of drawbacks, including slow biodegradation, a large footprint, and poor performance in cold weather (Allen 2008b). As a result, they are more suitable as an "add on" after the proposed TPW treatment process, depending on the actual effluent quality and future regulatory requirement.

In addition to bitumen extraction, the treated TPW may be used directly to control construction dust on the site, depending on treatment results from real applications and Alberta Environment's approval. Other potential reuses include once-through cooling water, grey water for equipment cleaning, and firefighting water. To make the treated TPW suitable for once-through steam generation and conventional boiler feed water, electrodialysis reversal (EDR) may be used to reduce TDS to a required level.

Unlike MF/UF, NF and RO, which are pressure-driven membrane technologies, the electrodialysis (ED) process is driven by an electric potential to remove charged ions. Under a direct current (DC) voltage, anions and cations are driven through anion- and cation-permeable membranes, respectively, leaving purified water between the two selective membranes. ED membranes are also susceptible to fouling and scaling; however, compared with the same problems for pressure driven membrane technologies, it can be eased by intermittent reversals in polarity, called electrondialysis reversal or EDR (AWWA 1999). Allen (2008b) reported several successful bench and pilot scale demonstrations, indicating that EDR is an energy- and cost-efficient technology for TDS reduction in terms of its good removal rates (>90%), lower feed water quality requirements, longer membrane life, and higher water recovery.

CHALLENGES AHEAD

Tailings pond water treatment is definitely a challenge facing Alberta's oil sand industry. Any valid treatment methods have to be technically practicable and financially feasible while handling a large quantity of the TPW in a big scale. Many innovated and conventional technologies have been developed or evaluated to battle this challenge.

In this paper, a TPW treatment process integrated with the reuse of industrial wastes, including WAS and oil sands coke, is proposed. Based on recent research and literature reviews, some design criteria and operating parameters that might be used have been discussed in this paper. The hypothetical removal efficiencies for some important target pollutants were also explored based on those studies and experiments, as well as fundamental theories of water and wastewater treatment, and the author's personal experiences. The ideas and thoughts presented in this paper are very preliminary, and subject to further examination. Final disposal of waste coke-biomass sludge containing residual NAs and heavy metals is another challenge that has to be addressed carefully.

Efforts have been made to use proven technologies that have already been applied in large-scale industrial applications compatible with that which would be applied in Alberta's oil sands industry for treating TPW. However, the author recognizes that a tremendous amount of research and investigation, including thorough economic analysis, financial evaluation, and large scale pilot tests, will be needed before the conclusion can be made.

ACKNOWLEDGMENTS

The author wants to thank Dr. Ian Swainson, Dr. Tamara Yankovich and Dr. Andrew Harwood for their valuable inputs and generous .help.

The author also thanks following people and organizations for their permission to use their figures and pictures in my research report:

Dr. Phillip M. Fedork,
Dr. Hongjing Fu
Mr. Kervin L. Rakness
EcoFluid System, Inc.
GC3 Specialty Chemicals, Inc.

REFERENCES

Aksu, Z., 2005. Application of biosorption for the removal of organic pollutants: a review. Process Biochem. 40: 997–1026. doi: 10.1016./j.procbio.2004.04.008.

Allen, E.W., 2008a. Process water treatment in Canada's oil sands industry: 1. Target pollutants and treatment objectives. J. Environ. Eng. Sci. 7: 123-138. doi: 10.1139/S07-038.

Allen, E.W., 2008b. Process water treatment in Canada's oil sands industry: 2. A review of emerging technologies. J. Environ. Eng. Sci. 7: 499-524. doi: 10.1139/S07-020.

AWWA, 1999. Water quality and treatment: a handbook of community water supplies, 5th edition. McGraw-hill, Inc., New York, N.Y.

Boltz, J.P., Motta, E.J.L., and Madrigal, J.A., 2006. The role of bioflocculation on suspended solids and particulate COD removal in the trickling filter process. J. Environ. Eng. 132: 506-513. doi: 10.1061/(ASCE)0733-9372(2006)132:5(506)

CBC, 2008. Montreal chooses new sewage treatment system. CBC News, 30 Jan. 2008. CBC website. Available online at

www.cbc.ca/canada/montreal/story/2008/01/30/qc-sewagetreatment0130.html [cited 12 April 2009].

Chen, L.C., Sung, S.S., Lin, W.W., Lee, D.J., Huang, C., Juang, R.S., Chang, H.L. 2002. Observation of blanket characteristics in full-scale floc blanket clarifiers. Water Sci. Thechnol., 47: 197-204.

Clements, J.S. and Fedorak, P.M. 2005. A review of the occurrence, analyses, toxicity, and biodegradation of naphthenic acids. Chemosphere 60 (2005) 585-600. Available online at www.sciencedirect.com [cited 12 April 2009].

Dipanfilo, R. and Egiebor, N.O., 1995. Structural features of activated carbon produced from oil sands coke. Development in Chemical Engineering, mineral Processing. 3: 3-13. doi: 10.1002/apj.5500030102

Del Rio, L.F., Hadwin, A.K., Pinto, L.J., MacKinnon, M.D., and Moore, M.M. 2006. Degradation of naphthenic acids by sediment microorganisms. J. Appl Microbiol. 101:1049-1061. doi: 10.111/j.1365-2672.2006.03005.x.

Fu, H., Gamal El-Din, M., Smith, D.W., MacKinnon, M.D. and Zubot, W., 2008. Ozone treatment of naphtenic acids in Athabasca oil sands process-affected water. In Proceedings of First International Oil Sands Tailings Conference, Edmonton, Alberta, Canada, Dec. 7-10, 2010. pp: 228-231.

Gailil, N.I., and Levinsky, Y., 2006. Sustainable reclamation and reuse of industrial wastewater including membrane bioreactor technologies: case studies. Desalination 202: 411-417.

Gehr, R. 2008. Disinfection of Montreal wastewater: brief to the public hearings. Hold in Montreal, Quebec, Canada, 9 April 2008. Available online at http://ville.montreal.qc.ca/pls/portal/docs/PAGE/COMMISSIONS_PERMANENTES_FR/MEDIA/DOCUMENTS/MEMOIRE_GEHR_20080409.PDF. [cited 12 April 2009].

Government of Alberta 2007. Water use in Alberta oil sands. Water innovation in the oil patch forum. PTAC. Available online at http://www.albertacanada.com/documents/AIS-ENVIRO_oilsands07.pdf [cited 12 April 2009].

Gulyas, H., von Bismarck, R., and Hemmerling, L., 1995. Treatment of industrial wastewaters with ozone/hydrogen peroxide. Water Sci. Tech. 32: 127-134.

Henze, M., van Loosdrecht, M.C.M., Ekama, G.A. and Brdjanovic, D., 2008. Biological wastewater treatment: principles, modeling and design, Chapter 18. IWA Publishing, London. doi: 1002/clen.200990037.

Holowenko, F.M., MacKinnon, M.D., and Fedorak, P.M., 2002. Characterization of naphthenic acids in oil sands wastewaters by gas chromatography-mass spectrometry. Water Res. 36: 2843-2855.

Horn, R.J. Straughton, J.B., Dyer-Smith, P. and Lewis, D.R., 1996. Criteria for the selection of the feed gas for ozone generation. Ozone Sci. Eng., 18: 57-71. International Ozone Association, USA.

Kasperski, K. L. 1992. A review of properties and treatment of oil sands tailings. AOSTRA J. Res. 8: 11-5.

Kadlec, R.H. and Knight, R.L. 1996. Treatment Wetland: Boca Raton, New York, Lewis Publishers.

Lin, S.H., Wang, C.H. 2002. Industrial wastewater treatment in a new gas-induced ozone reactor. J. Hazard. Mater. 98: 295-309. doi:10.1016/S0304-3894(03)00003-7.

Mahvi, A.H., Nabizadh, R., Pishrafti, M.H., and Zarei, Th. 2008. Evaluation of single state USBF in removal of nitrogen and phosphorus from wastewater. Euro. J. Sci. Res. 23: 204-211.

Matthews, J.G., Shaw, W.H., Cuddy, R.G., and MacKinnon, M.D. 2002. Development of composite tailings technology at Syncrude. International J. Mining, Reclamation and Environment. 16: 24-39. doi: 10.1076/ijsm.16.1.24.3407.

Metcalf & Eddy 2004. Wastewater Engineering: treatment and reuse, 4th edition. Publishing Mc Graw Hill, New York, N.Y
.
Mila, S. and Katja, H. 2007. Flocculation in paper and pulp mill sludge process. Res. J. Chem. Environ. 11: 97-103.

MWH 2005. Water treatment: principles and design, 2nd edition. John Wiley & Sons, Inc., Hoboken, N.J.

Nelson, E.A. and Gladden, J.B. 2008. Full scale treatment wetlands for metal removal from industrial wastewater. Environ. Geosci. 15: 39-48. doi: 10.1306/eg.09200707005.

Norit 2007. Data sheet: Hydrodarco C powdered activated carbon. Available online at www.norit-americas.com [cited 5 April 2010].

Oasim, S.R., Motley, E.M., and Zhu, G., 2000. Water works engineering: planning, design & operation. Prentice Hall PTR, Prentice-Hall, Inc., Upper Saddle River, N.J.

Raknees, K.L., 2005. Ozone in drinking water treatment: design, operation and optimization. American Water Works Association, Denver, CO.

Raknees, K.L., 2007. Ozone side-stream design options and operating considerations. Ozone Sci. Eng., 29: 231-244. International Ozone Association. USA. doi:10.1080/01919510701450864.

Reynolds, T.D., and Richards, P.A. 1996. Unit operation and processes environmental engineering, 2nd edition. PWS Publishing Company, Boston, MA.

Rice, R.G. 1996. Application of ozone for industrial wastewater treatment: a review. Ozone Sci. Eng., 18: 447-515. International Ozone Association. USA.

Rogers, M.E. 2004. Water management issues in oil sands industry. Canadian Oil Sands Networ for Research and Development (CONRAD) oil sands water usage workshop, 24-25 Feb. 2004. Fort McMurray, Alberta.

Sanks, R.L., 1978. Water treatment plant design for the practicing engineer. ANN Arbor Science. Michigan.

Sawatsky, L. 2004. Water supply security for the oil sands mines by upstream offsite storage. Canadian Oil Sands Networ for Research and Development (CONRAD) oil sands water usage workshop, 24-25 Feb. 2004. Fort McMurray, Alberta.

Scott, A.C., MacKinnon, M.D., Fedorak, P.M., 2005. Naphthenic acids in Athabasca oil sands tailings waters are less biodegradable than commercial naphthenic acids. Environ. Sci. Technol. 39: 8388-8394. doi:10.1021/es051003k.

Scott, C. A; Zubot, W., MacKinnon, MD., Smith, D.W. Fedorak, P.M. 2007. Technical note: Ozonation of oil sands process water removes naphthenic acids toxicity. Chemosphere 71:156-160. doi:10.1016/j.chemosphere.2007.10.051.Available online at www.sciencedirect.com [cited 12 April 2009].

Scott, J.A., Karanjkar, A.M. and Rowe, D.L., 1995. Biofilm covered granular activated carbon for decontamination of streams containing heavy metals and organic chemicals. Minerals. Eng. 8: 221-230. doi: 10.1o16/j.tim2006.07.001.

Seybold, A., Cook, J., Rajan, R.V., Hickey, R., Lawrence, A. and Hayes, T., 1997. Demonstration of dissolved organics removal from produced water. In Proceedings of the Production Operations Symposium, Oklahoma City, OK, 9-11 March, 1997. Pp. 281-287.

Shawwa, A.R., Smith, D.W. and Sego, D.C., 2001. Color and chlorinated organics removal from pulp mills wastewater using activated petroleum coke. Water Res. 35: 745-749. Doi: 10.1016/S0043-1354(00)00322-5.

Small, C.C., Ulrich, A., Hashisho, Z. 2009. Potential use of carbonaceous materials for the treatment of process affected-water. Presentation on Tailings and mine waste conference 2009. Banff, Alberta, Canada. November 3, 2009. Available on line from http://ostrfdownload.civil.ualberta.ca/Tailings%20and%20Mine%20Waste%202009/ [cited 12 June 2010].

Sublette, K.L., Snider, E.H., and Sylvester, N.D. 1982. A review of the mechanism of powdered activated carbon enhancement of activated sludge treatment. Water Res. 16: 1075-1082.

Superchill Australia Pty Ltd. Water quality required for trouble free cooling tower operation. Available on line from www.superchill.com. [cited 12 April 2010].

Syncrude Canada Ltd. n.d. Environmental sustainability: water use. Syncrude's website. Available on line from http://sustainability.syncrude.ca/sustainability2007/enviro/water/. [cited 12 April 2009].

Tellez, G.T., Nirmalakhandan, N., and Gardea-Torresdey, J.L. 2002. Performance evaluation of an activated sludge system for removing petroleum hydrocarbons form oilfield produce water. Adv. Environ. Res. 6: 455-470. Doi: 10.1016/S1093/0191(01)00073-9.

Wang, Y., Pourrezaei, P., and Gamal EL-Din, M. 2008. Coagulation-flocculation pre-treatment of oil sands process affected waters. *In* Proceedings of First International Oil Sands Tailings Conference, December 7-10, 2008, Edmonton, Alberta, Canada. pp: 232-237.

Zhao, W.W., Ting, Y.P., Chen, J.P., Xing, C.H., and Shi, S.Q. 2000. Advanced primary treatment of wastewater using a bio-flocculation-adsorption sedimentation process. Acta Biotechnol. 20:53-64.

Zubot, W., Mackinnon, M., and Chung, K. 2009. United States patent: Method of treating water using petroleum coke. Patent No: 7638057B2.

Session 7

New Concepts

BIG PICTURE THINKING IN OIL SANDS TAILINGS

Jeremy Boswell
Thurber Engineering Ltd., Calgary, Alberta, Canada

ABTRACT

In the areas of tailings engineering, environmental assessment, public accountability and waste management, the author advocates a better way for industry to approach the challenges of sensitive projects to ensure that important issues are addressed and the potential impacts on the public or natural environment are understood from the outset.

This strategy has become known as Big Picture Thinking, and has been successfully demonstrated by the author in a number of international tailings and waste management projects over the past twenty years. In the context of tailings engineering, Big Picture Thinking encompasses five components: technical, operational, environmental, legal and public. It is necessary for the solution to embrace sufficient understanding and detail of each of the sub-components for the wider impacts to be understood. But, the big picture needs to be the priority.

It is critical amongst the technical community to understand the demands in the public arena, and the opportunities for environmental leadership to recognize the simultaneous demands of the five sub-sectors and translate them into big picture solutions.

This new approach to strategic thinking as introduced in projects in Oil Sands tailings over the past two years is presented in this paper.

INTRODUCTION

Background

While working in South Africa, the author witnessed public opposition force the closure of the largest hazardous waste facility servicing Cape Town. His professional team tackled this challenge with Big Picture Thinking. They engaged the public asking them under what conditions the landfill could be allowed to re-open and continue to operate. After a series of workshops, a social contract was drawn up with the community which outlined a way forward for everyone. Big Picture Thinking led the way to the re-opening of the landfill and satisfied stakeholders.

External challenges to the Oil Sands tailings industry

Closer to home, the Oil Sands tailings industry continues to face a number of challenges:

- The challenge of multiple project imperatives, or non-commensurate objectives. In other words, being pulled in more than one direction at the same time.
- Credibility of environmental performance.
- Public image and attacks on the credibility of the industry.
- The ongoing demand for information and public consultation.
- Changing legislation and ever increasingly stringent regulations.
- An over-focus on negative ecological impact while overlooking the benefits of economic and societal growth: a skewing of the triple bottom line by not looking objectively at Sustainable Development.
- Technical issues.

As engineers and scientists we have tended to stick to technology. After all, that is what we do best. But there is a need for us to metaview to a higher level than normal technology, if we are to add our true value to society.

THE BIG PICTURE

It may be asked: “What IS the Big Picture in Oil Sands tailings?”

This paper suggests the view that the Big Picture is managing the interface between:

- Tailings
- The Environment
- The Public

Big Picture Thinking encompasses five components:

- Technical
- Operational
- Environmental
- Legal
- Public

It is necessary for the solution to embrace sufficient understanding and detail of each of the sub-components for the wider impacts to be understood. But, the big picture needs to be the priority.

It is critical amongst the technical community to understand the demands in the public arena, and the opportunities for environmental leadership to recognize the simultaneous demands of the five sub-sectors and translate them into big picture solutions.

TECHNICAL

The technical challenges are well known to us as engineers, and for those challenges we are reasonably well equipped:

- Engineering investigations
- Tailings and mine plans
- Engineering designs
- Material supply
- Reclamation

These aspects are elaborated upon by others at this conference, most eloquently, and are not expanded upon in this paper.

OPERATIONAL

Translation of engineering designs into practice is a little more difficult than in other areas of engineering, party because tailings structures continue to be constructed throughout the operational life. Reliance is placed on other influences and practices, for a successful tailings operation. These include:

- Mining
- Extraction
- Waste disposal
- Tailings
- Reclamation

Longer term planning for future tailings management would benefit from a consideration of the following themes:

- Integration of tailings operational deposition with reclamation so as to develop tailings facilities which facilitate reclamation.
- Systems which are easier to operate, and less likely to fail.
- Energy savings, reducing pipe wear, reducing flushing requirements, pumping of paste.

Innovation, change and new ideas should only be introduced after a careful consideration of all the knock-on effects on all aspects of tailings management.

New proposals and changes should be developed with operational simplicity in mind. Any new idea that makes the complex more difficult to operate should be reconsidered. In other words, in terms of impact on the operation, design and planning should pay careful attention to:

- Constructability.
- Versatility and flexibility.
- Robustness of design.
- Solving more than one problem at a time (killing two birds with one stone).
- Simplifying the day-to-day operations.

ENVIRONMENTAL

It is entry into the environmental domain that presents the greatest difficulty to the practising engineer. However, unless the project can successfully withstand environmental scrutiny, the design is not complete. Aspects requiring consideration include:

- Sustainability
- Environmental Impact Assessment
- Ecology
- Water use
- Land use
- Cumulative impact
- Climate change

In papers delivered in Shanghai, China (Boswell et al, 2002), and in Stellenbosch South Africa, (Boswell et al, 2004), the authors advanced a

wider role for engineers in providing sustainable solutions for society.

Engineers build bridges. We are able to build bridges:

- between politicians and citizens
- between engineers and community
- between first world and third world
- between government and NGO's
- between all environmental professionals
- between big business and small business
- building capacity

Reclamation

Reclamation areas provide a laudable and highly visible message to the public about environmental commitment. However, operators could go further: there needs to be a more direct connection to tailings, to show an environmentally responsible life cycle approach to tailings management and reclamation. The use of scale models and life-size site modelling showing the various phases of tailings reclamation would go a long way to show visitors to the mine what plans are in place. This approach has been successfully used in other high profile industries. This step would hold the following benefits:

- Demonstrating that operators are serious about tailings reclamation.
- Showing what steps are involved, especially since most ponds are still active and few reclamation processes are complete yet.
- Researching and presenting environmentally innovative reclamation solutions, building on valuable research already being conducted on site in regard to tailings, reclamation and wetlands.
- Inviting ongoing public comment and input into reclamation.
- Satisfying the requirements of the regulators.
- Building public trust and boosting corporate image.
- Moving beyond "Tell me" to "Show me".
- Showing progress by narrating "the story so far" (leaving an unreclaimed cross-section to show where we have come from, in terms of progress).

LEGAL

The publication on February 3, 2009 of *Tailings Directive 74: Tailings Performance Criteria and Requirements for Oil Sands Mining Schemes* has ensured that legal considerations remain central to tailings management in the Oil Sands industry. Legal aspects require detailed attention. A recent public hearing by an Oil Sands operator for regulatory approval noticeably depleted the resources of most local legal practices in Alberta. Legal risks requiring attention include:

- Tracking of changes in environmental law and administration
- Licensing and regulatory applications
- Regulatory liaison
- Litigation
- Enviro-legal risk management and due diligence
- Contracts

There have been and continue to be important changes in environmental legislation coupled with requirements to interact with and obtain authorization from the regulators. Operators have substantial responsibilities in dealing with the regulators on a frequent basis: (ERCB, AENV, SRD, AT and DFO). This demands a carefully integrated, proactive and systematic approach to the planning of engagement with the regulators. Aspects bearing risk include:

- Pro-active tracking of changes in legislation.
- Anticipating new requirements and suggesting alternative approaches to tailings legislation by proactively commenting on any new draft legislation, and suggesting alternative wording.
- Jurisdictions and overlaps. It is critical that operators are aware of the jurisdictional limits of each regulator, and of the manner in which inter-regulator liaison and communication takes place.
- Building partnership. At all times operators should be providing proactive leadership and working with the regulators, not against them, in developing reclamation solutions, and in satisfying current

regulatory requirements and anticipating future requirements.

- Careful consideration and presentation of alternative solutions to Directive 074.

PUBLIC

However, in the view of the author, it is in the arena of the public domain, that the greatest unresolved challenges to the Oil Sands challenges remain. The management of tailings according to the principles of Big Picture Thinking is paramount. Each time the industry forges ahead with new initiatives and a renewed sense of diligence and duty of care, further public, environmental and legal scrutiny emerges to batter the industry down further. Public issues include:

- Media & issue management
- Non-governmental organizations(NGOs), community & pressure groups
- Public participation
- Stakeholder management and public accountability
- Engagement with First nations, Métis, and Inuit communities
- Social impact scoping and assessment
- Corporate social responsibility

Public Accountability

High visibility of the tailings operations and the current focus of the media on Oil Sands tailings have meant that every aspect of tailings management must be considered to be under daily public scrutiny. This has critical implications for the management of tailings: There is little or no margin for error in tailings operations, environmental impact and safety.

Operators have the opportunity to present the true facts about tailings to the public, since the operations are visible to anyone driving along Highway 63, in any case. Since the operations are so publicly visible already, proactive communication of the tailings plans would appear to be imperative, and would build public trust.

Invited comment from the public, and incorporating public input into the tailings and reclamation planning would be consistent with industry commitments to public accountability and consultation.

Boswell et al (2000) described the process of communication of engineering risk. Natural risks seem more acceptable than artificial risks. Hence a risk caused by God (a so-called act of God) is more acceptable than one caused by people, since natural risks provide no focus for anger. Here for example, the loss of life as a result of earthquake, flood or fire is seen as an act of God and therefore in some strange way, more acceptable. The loss of life associated with man-made structures such as buildings, dams or bridges is somehow seen to be less acceptable since it is supposedly more foreseeable. The fact that more people are killed through by road accidents or criminal violence does not mitigate the loss of life associated with a civil engineering disaster.

CONCLUSION

That old, old cliché - there is no single “silver bullet” solution to these challenges. However, in order to pursue and successfully resolve challenges for tailings management and reclamation at the workface, there is a key requirement for Big Picture Thinking. In other words, a holistic and integrated consideration of:

- Tailings operations.
- Design and planning.
- Environmental concerns.
- Public image.
- New legislation.

The challenges presented in Oil Sands tailings management are daunting, but can be successfully addressed. Industry efforts to co-operate and share ideas towards forward progress in the management of Oil Sands tailings and improvement in public image of the industry are to be welcomed and encouraged.

The attached two figures attempt to show the interrelationship between the five components of Big Picture Thinking described above, and offer a way forward for those who cannot see the wood for the trees yet.

REFERENCES

Boswell, J.E.S. (1996). 'Public Participation in the Waste Management Industry.' Proceedings of the 2nd National Conference on Environmental Management, Technology and Development, Fourways, South Africa, SA Institution of Civil Engineers, October 1996.

Boswell, J.E.S., De Waal, D. and Hattingh, N. (2000). 'Communication with the public about tailings projects'. 7th International Conference on Tailings and Mine Waste 2000 at Fort Collins, Colorado. January 2000.

Boswell J.E.S. (2002). Sustainable Development in the Consulting Engineering Industry. Keynote address: International Engineering Consulting Forum on Sustainable Development of Shanghai May 2002. Shanghai, China.

Boswell J.E.S., Wallace W., Boswell Dr P., Boyd J., van der Putte Dr I., Walker L. and Rigby S-A (2004) FIDIC Sustainable Development Task Force 'Project Sustainability Management: A Framework to Translate Words into Action' 4th Sustainable Building Conference Stellenbosch, South Africa, September 2004.

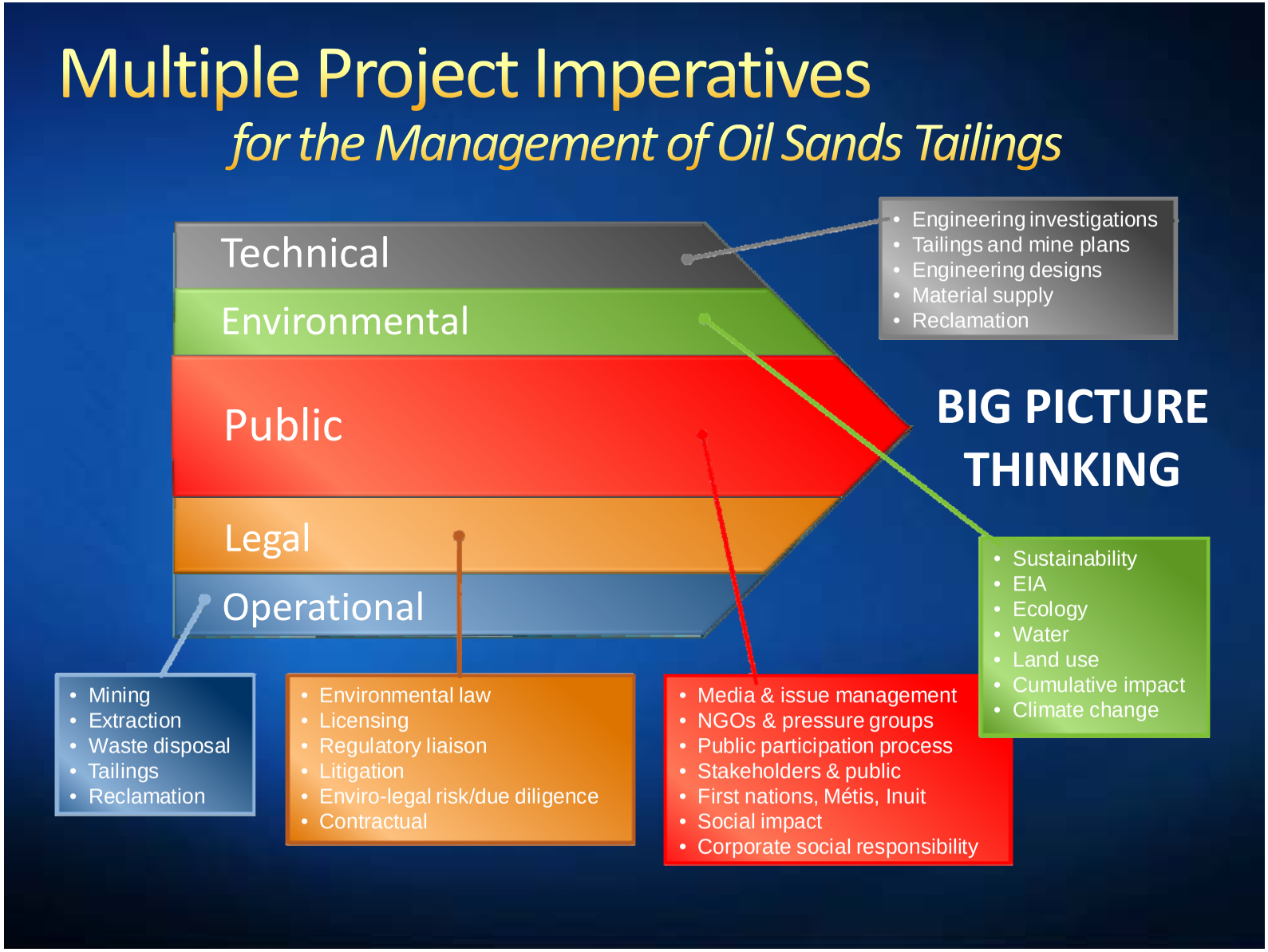

Figure 1. Multiple Project Imperatives For The Management Of Oil Sands Tailings.

Figure 2. So What Solutions Can Be Offered? For The Management Of Oil Sands Tailings.

FLOW BEHAVIOUR AND ROBUSTNESS OF NON-SEGREGATING TAILINGS MADE FROM FILTERED/CENTRIFUGED MFT

Reza M. Nik, David C. Sego, Norbert R. Morgenstern
University of Alberta, Edmonton, Alberta, Canada

ABSTRACT

In a previous study feasibility of using a filtering centrifuge to produce a more concentrated MFT had been presented (Moussavi Nik et al 2008). The resultant concentrated MFT can be used either as a component for making CT/NST, or as a paste backfill. The present study investigates the flow behaviour of CT/NST made from the concentrated MFT. A flume apparatus is used to resemble the CT/NST deposition under laboratory conditions and the depositional profile is determined. Also, for several samples taken along the flume, the ratio of sand (coarse) to fines is calculated in order to determine the level of segregation. A strain-controlled viscometer with vane spindles is used to measure the yield stress of the tailings and correlate it with their depositional angle. Also for a number of NST samples with varying solids content, the results obtained from vane shear tests and slump tests were compared to investigate capability of the slump test for evaluation of shear stress. Results of tests indicate that CT/NST made from concentrated MFT leads to a more robust tailings stream which promises saving in the land required for depositional purposes.

INTRODUCTION

It is more than a decade since the oil sands industry in northern Alberta started production of CT (composite / consolidated tailings) or NST (non-segregating tailings) as a method of tailings management. CT/NST is composed of MFT (mature fine tailings) plus a coagulant (gypsum) and the sand from cyclone underflow (Scott and Cymerman 1984, Morgenstern and Scott 1995). This engineered waste stream is non-segregating when discharged, but in practice it is not particularly robust and partial segregation has been observed resulting in fines release at the surface following deposition. In order to achieve a more robust tailings stream, a CT/NST with higher solids content is desired. The possible approaches to achieve a more concentrated CT/MFT would be either further enhancing the solids content of CT/NST as a whole mixture, or dewatering each of its components (i.e. MFT and Sand) separately before mixing them together. Focus of the present study has been on dewatering MFT.

Review of the literature shows that previously either filtration or centrifugation has been considered as possible methods for dewatering the oil sands fine tailings (Baillie and Malmberg, 1969; Corti and Falcon, 1989; Hepp and Camp, 1970). However, most of the mechanical and physical methods of treatment including centrifugation and filtration have had difficulty to design a feasible and economic process that would be acceptable to the industry (Kasperski, 1992). Specifically for dewatering by means of filtration, presence of the unrecovered bitumen/asphaltene in the oil sands fine tailings has been a challenge due to its tendency to clog the filter pores. In the recent years, solid bowl centrifuging has attracted more attention in the oil sands industry and bench scale and pilot scale tests have been conducted to study the practicability of this dewatering method (Lahaie et al, 2009).

Possibility of using a filtering centrifuge for dewatering of oil sands tailings was studied for the first time by Moussavi Nik et al (2008). Observations from a series of batch centrifugal filtration tests revealed that in this dewatering method the majority of the bitumen/asphaltene formed a separate internal layer close to the centre of rotation. This indicates that in this method of filtration the bitumen has less opportunity to be in touch with the filter medium and blockage of pores in the filter cloth is significantly reduced.

Several filtering centrifuge tests with a variety of test conditions were conducted on the MFT received from Syncrude, Suncor and Albian Sands companies. The test results showed that a significant percentage of the MFT fed into the system could be collected as a cake with solids content ranging from 43%wt to 65%wt, suitable either for making a robust CT/NST or for deposition as paste (Moussavi Nik et al, 2008).

The present paper investigates the flow behaviour and robustness of CT/NST made from the cake obtained from the filtering centrifuge tests.

EXPERIMENTAL PROCEDURE

Materials

The MFT used in this study was collected from tailings ponds of the Suncor, Syncrude and Albian Sands companies. Composition of the MFT received from each company is presented in Table 1. The solids and bitumen contents stated in this table represent the average values for each source of MFT. The fines content values reflect the percentage of solids finer than 44 microns (i.e. passing through sieve #325). It should be noted that in calculation of the geotechnical solids content, the percentage of bitumen remaining in the samples after oven drying is considered as part of the solids.

Table 1. Characteristics of the MFT used for making NST

MFT Source	Geotechnical Solids Content (%)	Solids (%)	Water (%)	Bitumen/Asphaltene (%)	Fines Content (%)
Suncor	27.0	24.62	73.3	2.08	97.2
Syncrude	36.5	34.92	63.33	1.75	97.7
Albian Sands	37	35.13	63.72	1.15	98

For all of the experiments, the sand used for making NST has been sourced from the beach of Suncor tailings pond. The sand solids content and fines content were about 98.8% and 1.2% accordingly. The fines content was determined by washing the sand over sieve #325.

Making NST from concentrated MFT

In the field production of CT/NST, phosphogypsum is added to MFT as a coagulant and the resultant stream is mixed with sand. The sand is sourced from cyclone underflow and has a solids content of about 75%. In this study, the sand used for making NST had a solids content of about 98.8% and was relatively dry. In order to increase water content of the sand similar to its field value, pond water was added to it. The concentrated MFT obtained from the filtering centrifuge tests was added to this mixture of sand and pond water to create Non-Segregating Tailings (NST). Because phosphogypsum had already been used for treatment of MFT during the centrifugation stage, no additional gypsum was added for making the NST. Also for the centrifuged MFT's that were produced without addition of gypsum, no further gypsum was added to the NST mixture. The purpose of these specific tests was to investigate possibility of making NST with no chemical additives. To ensure obtaining a homogenous CT/NST mixture, a dual blade mortar mixer was utilized.

Prior to making NST in the lab, it was necessary to determine the solids content of the centrifuged MFT, also its SFR (Sand to Fines Ratio). The SFR in the centrifuged MFT can be quite different from the SFR in the source MFT. The reason is that due to the centrifugal field that the material experiences inside the filtering centrifuge, segregation of the fine and coarse fractions can occur. As a consequence, percentage of the coarse particles can increase in the MFT cake in comparison to the source MFT. After determining the solids content and SFR of the centrifuged MFT and sand, the required amount of each component for making NST was calculated. For this purpose the multiphase mass-volume relationships developed by Scott and Boratynec (2003) were used.

Tables 2 and 3 present the specifications of some examples of NST samples made from Albian Sands and Syncrude Tailings. In these tables, the source of MFT, solids content of the MFT/Cake, amount of the gypsum used prior to centrifugation, solids content of the produced NST, the SFR and the yield stress obtained from vane shear tests are presented. Findings obtained from studying the

Table 2 - Samples of NST made from Albian Sands MFT/Cake

Test ID	SC of the MFT / Cake (%wt)	Gypsum (ppm)	SC of the NST (%wt)	SFR	Yield Stress (Pa)	Average Slope (%)	Duration of flow (sec)
Albian NST-1	37.05 (MFT)	600	60.91	4.04	20.63	0.57	1.868
Albian NST-2	64.2 (Cake)	600	73.11	4.05	53.30	1.25	1.409

Table 3 - Samples of NST made from Syncrude MFT/Cake

Test ID	SC of the MFT / Cake (%wt)	Gypsum (ppm)	SC of the NST (%wt)	SFR	Yield Stress (Pa)	Average Slope (%)	Duration of flow (sec)
Syncrude NST-1	37.66 (MFT)	600	62.81	4.3	25.06	0.44	2.193
Syncrude NST-2	44.41 (Cake)	300	66.91	4.04	28.34	0.63	1.999
Syncrude NST-3	64.21 (Cake)	No Gypsum	73.72	4.31	33.73	0.69	1.733

flow characteristics of these NST samples are presented in the results section as some typical examples.

Characterization Tests

The flow properties and robustness of the NST's made were studied by means of a flume, a strain-controlled viscometer, and by conducting slump tests.

Flume Tests

Figure 1 illustrates the flume apparatus that was designed to investigate the depositional behaviour of NST under laboratory conditions. Other researchers have used similar flume designs to study the depositional behaviour of tailings. (Sofra and Boger, 2001; Kwak et al. ,2005 and Henriquez and Simms, 2009).

The flume is made of ~12mm thick acrylic sheets with high optical quality. The total length of the flume is about 240cm with an internal width of 18cm. A sliding gate is devised at the closed end of the flume. When this gate is down, it creates a reservoir with about 8 liters of volume. As it is shown in Figure 1, the NST sample is poured into this reservoir up to a certain thickness. Then the gate is quickly lifted upwards, letting the NST to flow along the flume and to come to rest. As depicted in Figure 1, a graph paper covers the back side of the flume wall, which will help measuring the flow runout more precisely. In order to obtain the flow profile in each flume test, thickness of the deposited NST was measured by means of a ruler at 10cm intervals along the flume centre line and at shorter intervals at the front edge of the flow foot print. All deposition tests were videotaped using a digital video camera. The intent was to record duration of the flow for each NST sample. As it will be shown in the results section, duration of the flow can be correlated with shear strength of the material.

To characterize the NST used for each flume deposition experiment, a 300ml snap seal container was filled with a sample of NST and its solids content and SFR were determined. Also a 600ml beaker was filled with a sample of NST and immediately vane shear tests were conducted on it to achieve the yield stress of the material. Details of the vans shear tests are provided in the following sub-section.

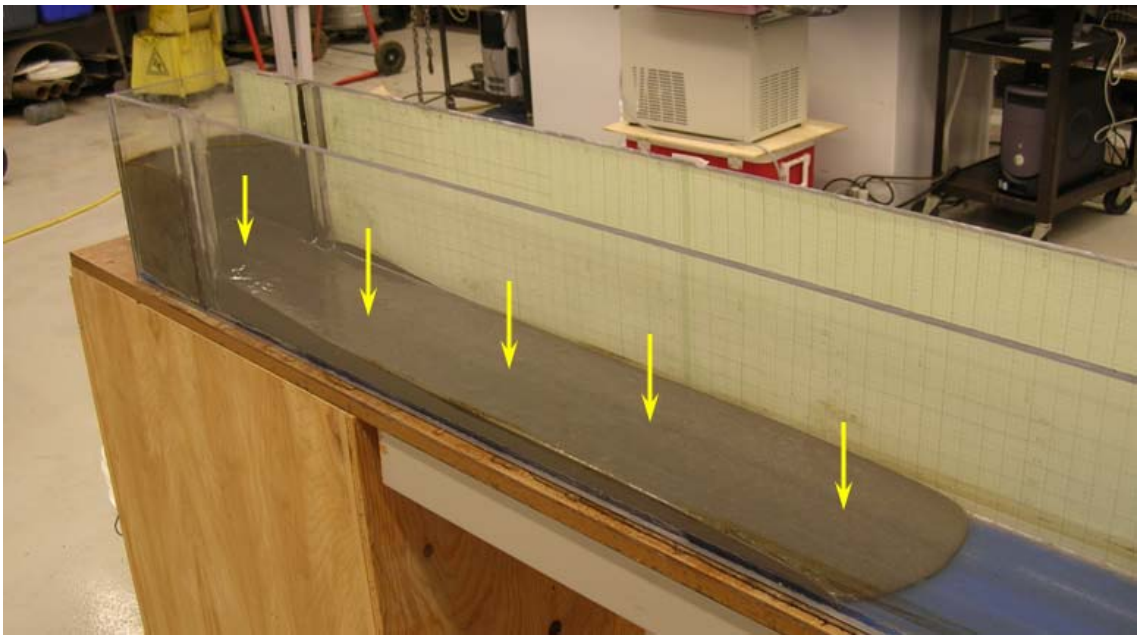

Figure 1. A flume deposition test and location of the samples taken along the flow

To evaluate the level of segregation along the flume, samples of NST were taken at five or six spots along the centre line of the deposited material (Fig. 1). Each sample was placed inside a container and later was characterized. Characterization tests comprised of solids content measurement through oven drying and washing over sieve #325 to measure the sand to fines ratio.

Vane Shear Tests

A strain controlled viscometer (Brookfiled Digital Viscometer - Model DV-II+) with vane spindles was used to measure the shear strength of the NST samples. In order to achieve the yield stress of the NST sample, it was necessary to spin the vane spindle at very low rotational speeds (Dzuy and Boger, 1983). The vane tests were conducted at the rotational speed of 0.1 rpm.

Slump Tests

To investigate capability of the slump test for evaluation of tailings shear strength, a number of NST samples with varying solids contents (ranging from 61%wt to 76%wt) and a SFR equal to 4.0 were made. For each NST sample, both the slump test and the vane shear test were performed and the results were compared. The slump tests were conducted using a cylinder with a height to diameter ratio equal to one (i.e. height = diameter = 76mm). For each test the thickness and radius of the slumped material is measured.

RESULTS AND OBSERVATIONS

Flume Tests

Figure 2.a shows two examples of the flume test flow profiles for NST's made from Albian Sands MFT. Table 2 provides the related information for each test. As stated in this table, Albian NST1 is made by adding 600ppm gypsum to regular MFT at a solids content of 37.05%wt. Solids content of the resultant Albian NST1 is about 60.91% and the vane shear test has resulted a yield shear strength of 20.63 Pa for this material. On the other hand, Albian NST2 is made from filtered/centrifuged MFT. The amount of gypsum used during production of the MFT cake has been 600ppm and the resultant cake has a solids content of 64.2%wt. Solids content of the Albian Sands NST2 made from this cake is about 73.11%wt. From Figure 2.a it can be observed that the deposition angle of the NST has been significantly improved. Figures 2.b and 2.c illustrate the variations of SFR along the profile of each test. Figure 2.b shows a constant decrease in the value of SFR which can be interpreted as dynamic segregation along the flume; i.e. the percentage of coarse particles decreases as the material finds its way towards the end of the flume.

(a)

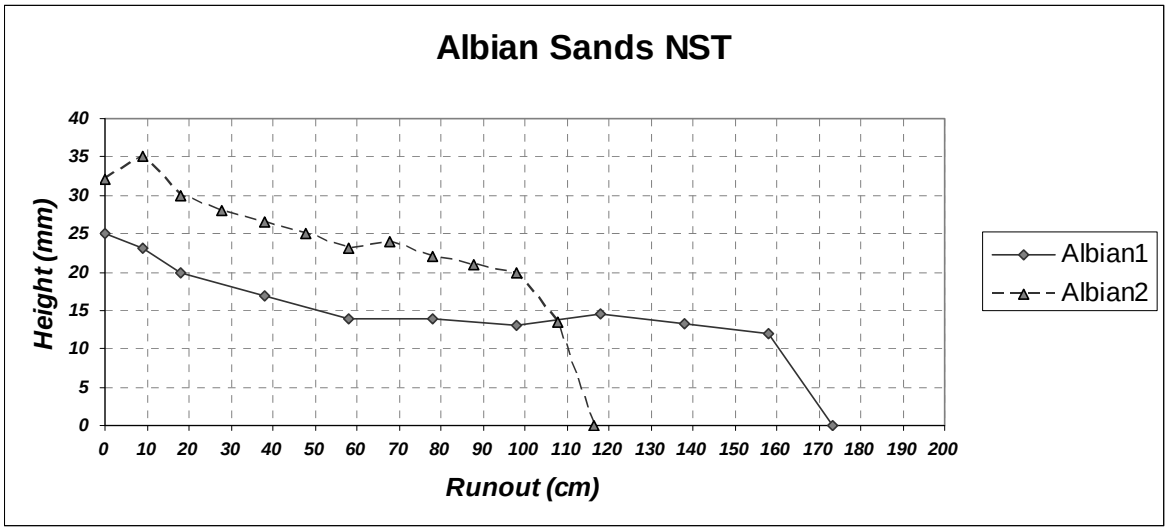

(b)

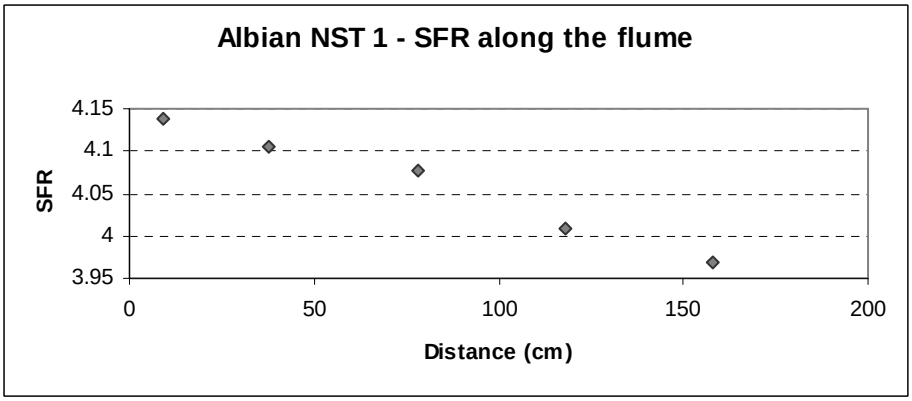

(c)

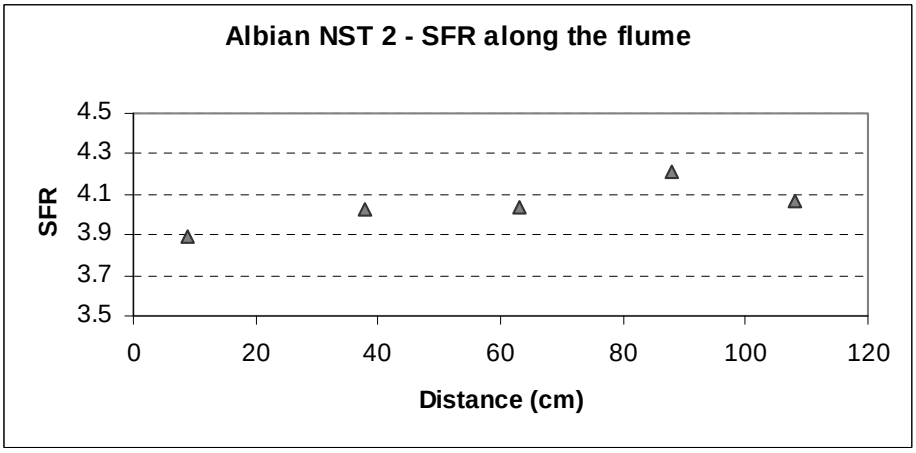

Figure 2. (a) Flow profile of the flume deposition tests Albian-NST1 and Albian-NST (b) and (c): Variations of SFR along the flume for each test

(a)

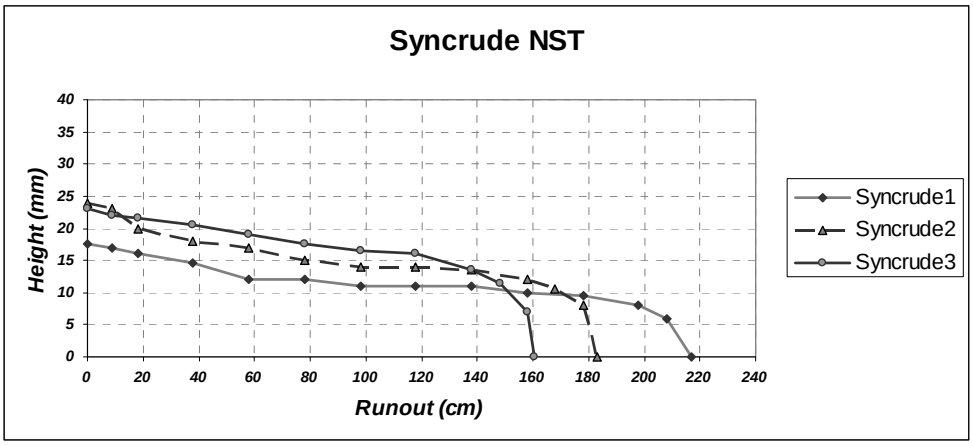

(b)

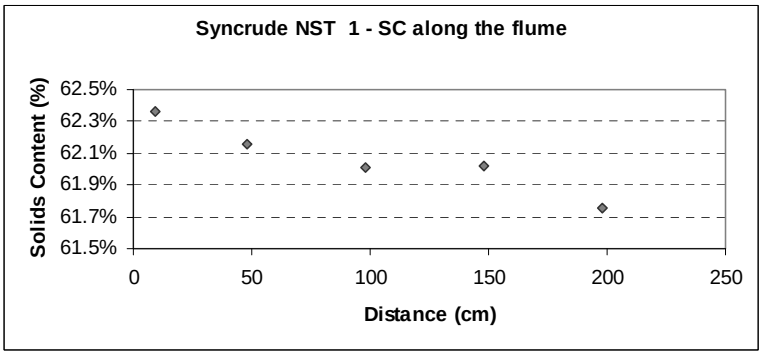

(c)

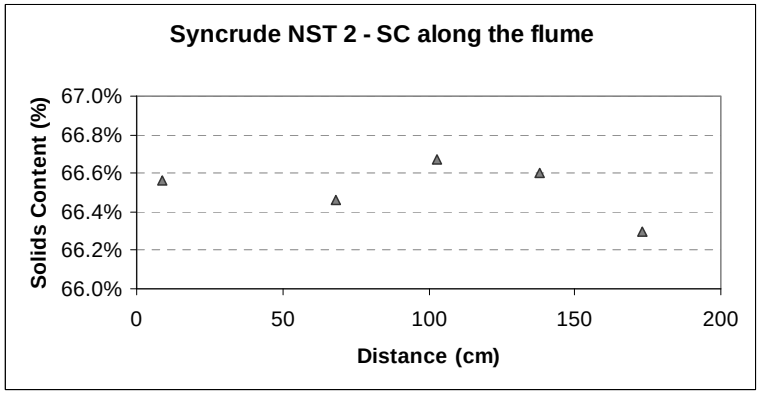

(d)

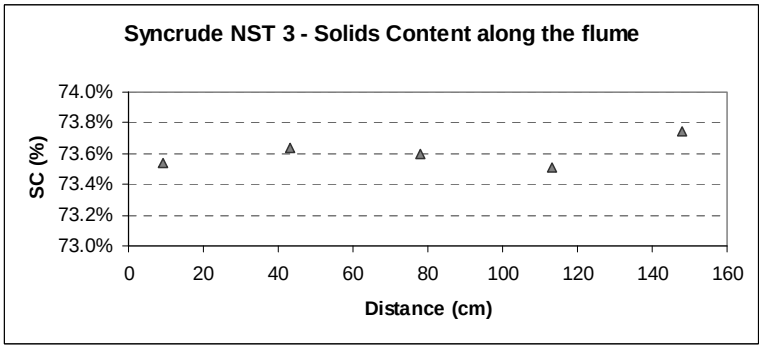

Figure 3. (a) Flow profile of the flume deposition tests Syncrude-NST1, NST2 and NST3 (b), (c) and (d): Variations of solids content along the flume for each test

Figure 3.a illustrates flow profiles of three flume tests conducted on NST's made from Syncrude MFT. Table 3 provides the related information for each test. According to this table, Syncrude-NST1 is made by adding 600ppm gypsum to regular MFT at a solids content of 37.66%wt. Solids content of the resultant Syncrude-NST1 is about 62.81% and the vane shear test has showed yield shear strength of 25.06 Pa. The other two NST samples, Syncrude-NST2 and 3 are made from filtered/centrifuged MFT and have a solids content of 66.91% and 73.72%. The thick MFT used for Syncrude-NST2 has been produced by adding 300ppm gypsum, while the MFT paste used for making Syncrude-NST3 has been produced without addition of any gypsum. The flow profiles illustrated in Figure 3.a indicate that using concentrated MFT as a component of CT/NST leads to significantly higher angles of deposition. In the mean time, it can be observed that by dewatering MFT the amount of coagulant required to create a more robust NST can be reduced. Figures 3.b to 3.d show that as the concentration of the tailings stream is increased, variations of the SC along the flume are reduced, in other words a more robust tailings stream is achieved.

It should be noted that although Syncrude NST-3 has been created with no chemical additive and holds a high angle of deposition, but this material does not completely satisfy the requirements of a successful tailings management plan. The reason is that due to absence of the chemical additives, segregation of the coarse and fine particles occurs within the centrifuge and the resultant paste contains only about 30% of the fine particles (Moussavi Nik et al., 2008). On the other hand, Syncrude NST-2 can be regarded as a suitable blend for tailings management purposes. In comparison to the conventional NST mixtures, robustness and angle of deposition of this NST has been improved, also the amount of the coagulant used in this mixture is reduced resulting in lower amount of the Ca^{2+} ions in the recovered water. Addition of this minimum amount of gypsum to the MFT and the delay time applied to the MFT-Gypsum mixture before centrifuging it results in almost 100% capture of the fines within the cake. This issue was discussed in the previous publication by the present authors (Moussavi Nik et al., 2008)

Correlation between the shear strength and the flow duration

As previously stated, all of the flume tests conducted in this study were videotaped by a digital video camera. The camera was not a high speed model, so in order to measure the flow duration with the highest possible precision, a computer software was used to display the recorded movie at 25% of the original speed. A computer based chronometer was used to calculate the time between opening of the flume gate until the moment the material stops flowing; this measured time was divided by 4 to obtain the real flow time. Figure 4 shows the correlation between the shear strength and flow duration for the NST's made from Albian Sands, Suncor and Syncrude fine tailings. A linear correlation can be observed for the data points obtained for each NST group. Knowing the approximate time that it takes for a tailings stream to cover a certain area, along with its flow profile (i.e. the thickness, the average slope and the flow runout) are essential information for devising a tailings deposition plan.

Correlation between the shear strength and the average angle of deposition

Figure 5 shows the average surface slope of the deposited material with regard to its measured yield stress. The data plotted in this diagram is obtained from eleven flume tests conducted on NST's made from different sources of MFT. According to this diagram, the average angle of deposition almost shows a linear correlation with the yield stress of the deposited material. This finding can be used to approximately predict surface slope of the deposited tailings. More precise prediction of the tailings flow profile is possible through solving a number of equations available in the literature, all involving the yield stress of material as a definitive parameter (Henriques and Simms, 2009).

Comparison of the Vane Shear and Slump tests

Figure 6 illustrates the shear stress diagrams for the vane tests conducted on seven samples of NST with solids content values varying from 61.5%wt to 75.8%wt. All the NST samples have a SFR of 4.0 and are made from the same source

Albian Sands MFT. The yield stress values obtained from these diagrams are plotted with regard to the solids content of the material in Figure 7. According to this diagram the shear strength of the NST can be expressed as an exponential function of its consistency.

Result of the slump tests conducted on each of the above mentioned NST samples are also presented in Figure 7. In this figure, the ratio of thickness to radius of the slumped material is plotted against its measured solids content.

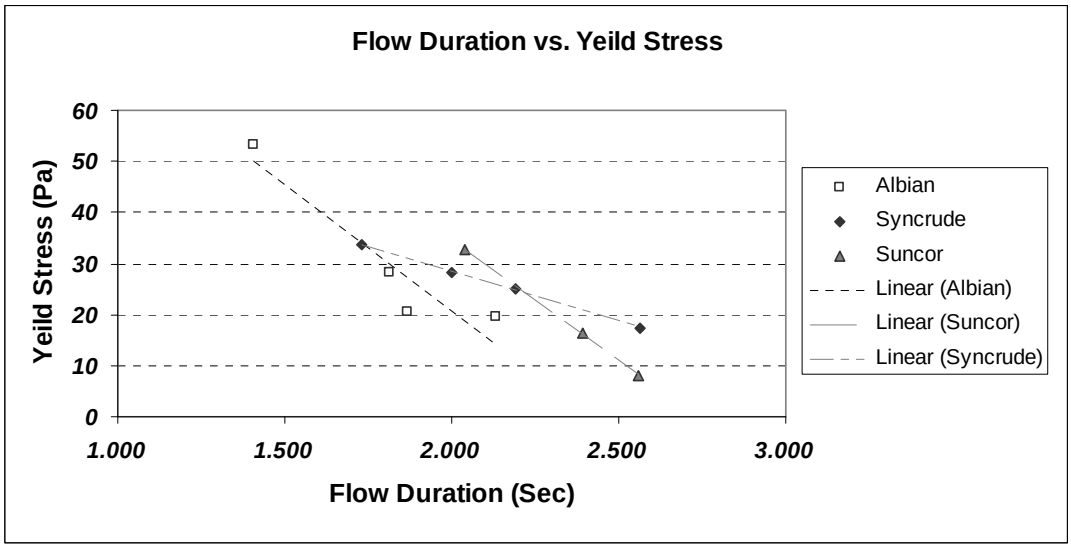

Figure 4. Correlation of flow duration and yield stress for NST samples made from different MFT sources.

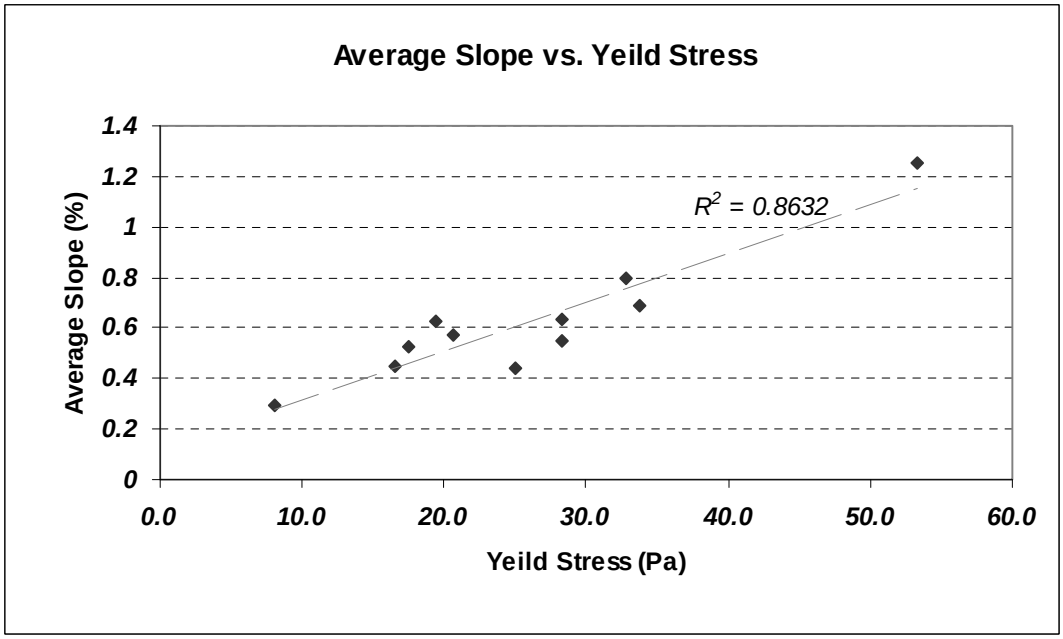

Figure 5. Correlation between the average surface slope of the deposited MST and its yield stress.

A similar exponential relationship can be observed between the two parameters. It can be shown that the value of yield stress divided by pressure of the of material (Equation 1) has a linear correlation with the average ratio of thickness to diameter of the slumped material:

$$\tau_y' = \tau_y / (\rho.g.H) \quad (1)$$

Where τ_y' is the normalized shear strength, τ_y is the measured shear strength, ρ is the density, g is the gravity acceleration and H is the height of the sample. This finding is in accordance with the theory developed by Pashias and Boger (1996). Based on these findings it can be concluded that the modified slump test provides an acceptable indication of yield stress of the material.

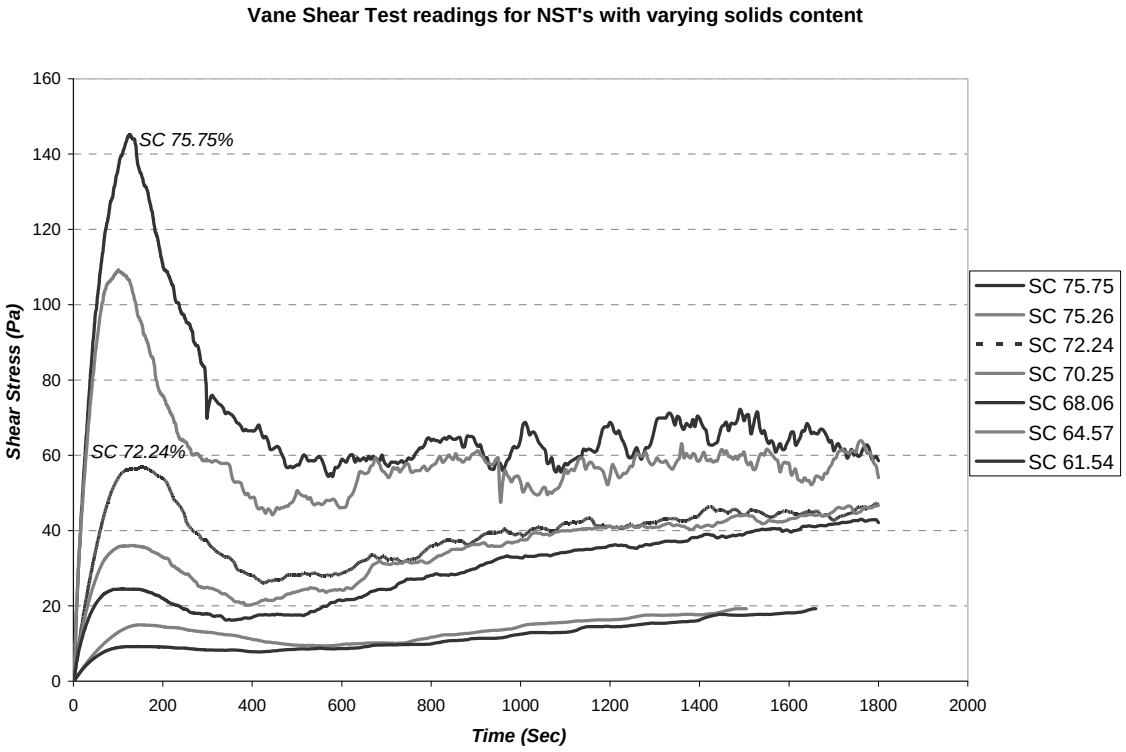

Figure 6. Diagrams of shear stress readings recorded during vane shear tests on seven NST samples with varying solids content and similar SFR

SUMMARY AND CONCLUSION

The cake obtained from several filtering centrifuge tests on MFT was used as a component for making non-segregating tailings (NST). A flume was used to study the flow behaviour of the produced NST samples. For each fume deposition test, the flow profile was recorded and the shear strength of the NST sample was evaluated by means of a strain-controlled viscometer and vane spindles. To assess the dynamic segregation occurring along the flume, a number of samples were taken along the deposited material and the solids content and SFR values of these samples were measured.

Results of the flume tests indicate that using the filtered/centrifuged MFT as a component for making NST results in a robust tailings stream with higher angles of deposition, which promises saving in the land required for depositional purposes and will contribute to rapid drainage to a collection point for water released to the surface. Based on the observations made in this research, dewatering of MFT has the potential to be considered as the initial stage of a multistage tailings management plan. Different solid-liquid separation methods (eg.

thickeners, centrifuges, etc.) may be used for this purpose. The present study shows that proper treatment of the MFT before introducing it into a filtering centrifuge can result in a cake with suitable consistency in which a high percentage of the fine particles can be captured. In the mean time, the filtrate obtained from a filtering centrifuge can be considered as a source of recycle water to be reused in the extraction process. This study showed that dewatering of MFT reduces the amount of coagulants required for production of NST, thus the water drained either during centrifugation or after deposition of the tailings will have lower level of chemical additives. These findings are all promising steps towards solving the environmental issues associated with production of oil sands fine tailings.

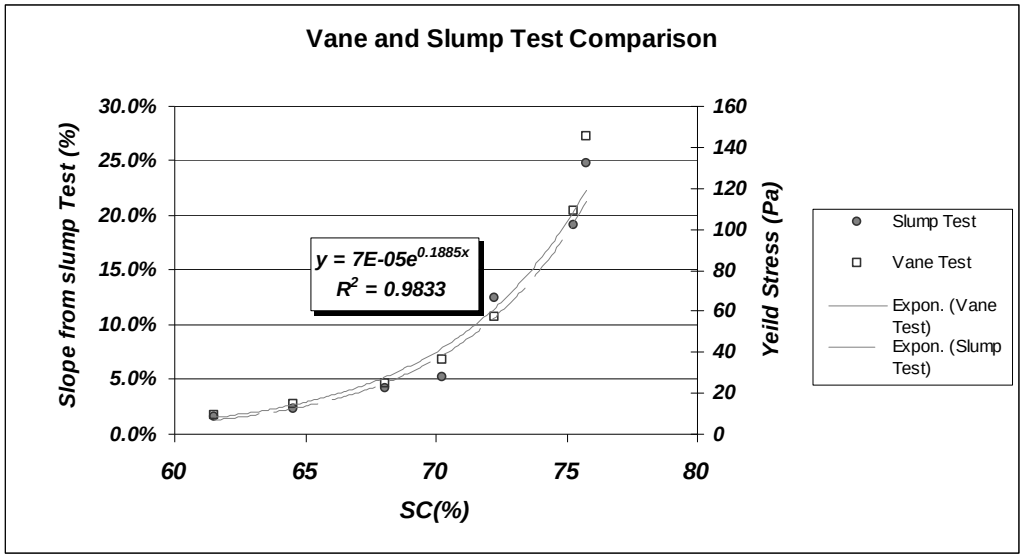

Figure 7. The slope obtained from the slump tests (left vertical axis) shows an exponential correlation with the solids content of NST. Similarly, the yield stress measured by the vane shear tests (right vertical axis) has an exponential correlation with the solids content.

ACKNOWLEDGEMENT

The financial support from the Oil Sands Tailings Research Facility (OSTRF) which made this research possible is appreciated.

REFERENCES

Baillie R.A., and Malmberg, E.W. (1969). “Removal of Clay from the Water Streams of the Hot Water Process by Flocculation”, *U.S.Patent.* No. ,3,487,003.

Corti, A. and Falcon, J.A. (1989) “Method and Treatment for Contaminated Oil Sludge.”, *U.S. Patent* No. 4,812,225.

Henriquez, J. and Simms, P. (2009) “Dynamic imaging and modeling of multilayer deposition of gold paste tailings” *Mineral Engineering*., 22 (2009) pp. 128-139.

Hepp, P.S., and Camp, P.W. (1970). “Treating Hot Water Process Discharge Water by Flocculation and Vacuum Precoat Filtration.”, *U.S. Patent* No. 3,502,575.

Kasperski, K.L. (1992). "A Review of Properties and Treatment of Oil Sands Tailings." *AOSTRA Journal of Research*, 8 11-53.

Kwak, M., James, D.F., and Klein, K.A. (2005). "Flow behaviour of tailings paste for surface disposal." *Int.J.Miner.Process.,* 77(3), 139-153.

Lahaei, R., Ahmeh, I., Labelle, M. and Brown, R. (2009) “Paste Pumping and Deposition Field Trials and Concepts on Syncrude’s Dewatered Mature Fine Tailings (MFT) (Centrifuge Cake)” *Tailings and Mine Waste 2009*, Banff, Canada.

Morgenstern, N.R., and Scott, J.D. (1995). "Geotechnics of fine tailings management." *Geoenvironment 2000, ASCE,* 2 1663-1673.

Moussavi Nik, R., Sego, D.C. and Morgenstern, N.R. (2008) “Possiblity of using Centrifugal Filtration For Production of Non-Segregating Tailings” *First International Oil Sands Tailings Conference*, Edmonton, Canada. pp. 200-209.

Scott, J.D., and Cymerman, G.J. (1984). "Prediction of viable tailings disposal methods." *Symposium on Sedimentation and Consolidation Methods*, American Society of Civil Engineers, 522-544.

Sofra, F., Boger, D.V., 2001. ”Slope prediction for thickened tailings and pastes.” *Tailings and Mine Waste ’01*, Proceedings of the Eightth International Conference on Tailings and Mine Waste, Fort Collins. Balkema, Rotterdam, pp. 75– 83.

CARBON DIOXIDE SEQUESTRATION IN OIL SANDS TAILINGS STREAMS

Randy Mikula, Michael Afara, Behnam Namsechi, Bryan Demko, and Paulina Wong
Natural Resources Canada, CanmetENERGY Research, 1 Oil Patch Drive, Devon, Alberta, T9G 1A8

ABSTRACT

There are many additives available that can be used to modify the behaviour of clays in oil sands tailings in order to create a CT or NST product. Consolidated, composite, or non-segregating tailings all depend upon the development of a certain strength in the fluid tailings. As long as the fluid phase can support the sand grains in the mixture, the sand grains will enhance consolidation of the entire mixture. Field testing in 2004 demonstrated the viability of using carbon dioxide as a CT additive. Since that time, interest has shifted to the quantification and optimization of the amount of carbon dioxide that can be sequestered, while at the same time producing favourable tailings behaviour. This paper discusses the factors that control carbon dioxide sequestration in oil sands tailings, and demonstrates that beneficial tailings behaviour can be achieved. Although these concepts lead to mitigation of the carbon dioxide footprint of oil sands production, further work is required in order to optimize sequestration and process performance.

INTRODUCTION

The water chemistry impacts of gypsum in the CT process have prompted an evaluation of several CT process aid options. In the Suncor application of the CT process, gypsum is available as a byproduct of the flue gas desulphurization of a coke combustion process. The combination of two waste streams or by products (gypsum and fluid fine tailings) to create a solids landscape for reclamation has a certain appeal. Among the CT process aid alternatives tested, carbon dioxide has a similar appeal since carbon dioxide is a byproduct of the hydrogen plant in a typical oil sands bitumen upgrader. Upgrading bitumen to a synthetic crude oil involves increasing the hydrogen to carbon ratio in the hydrocarbon product from the upgrader. This is done in two ways: first by removal of carbon in a coker, which produces a high carbon coke waste stream, and the second is by addition of hydrogen with the help of catalysts. The hydrogen is created by the steam reforming of methane with the overall chemistry according to equation 1.

$$CH_4 + 2H_2O \rightarrow 4H_2 + CO_2 \quad (1)$$

Prior to 2003, the carbon dioxide production from Syncrude and Suncor hydrogen plants combined was about 1.5 Mtonnes per year. Typically these hydrogen plant carbon dioxide streams are better than 90% pure, making them potential candidates as CT/NST additives. Initial investigations of carbon dioxide addition did not focus on sequestration potential, but rather on CT performance.

There are several pathways for sequestration and is useful to compare these to those discussed in geological storage. The main pathways are physical, ionic, and mineral sequestration. In geological storage, physical trapping of the carbon dioxide is the dominant mechanism with ionic and mineral sequestration playing a very minor role. The reverse is true for processes relying on chemical reactions to convert the carbon dioxide into soluble (ionic sequestration) and insoluble (mineral sequestration) chemical constituents. In those cases, physical sequestration is generally insignificant.

This report summarizes some preliminary experimental work designed to estimate the ionic sequestration potential for oil sands tailings, and in particular the clay component in those tailings. In the discussion both laboratory and field results are discussed.

RESULTS AND DISCUSSION

Table 1 outlines the differences between geological sequestration and chemical sequestration. The chemical reactions that lead to ionic and mineral sequestration of carbon dioxide are easily controlled and quantified in industrial processes but very difficult to monitor in geological storage. Sequestration potential, especially in chemical systems can be controlled and monitored, and inevitably the box one puts around the system or process will define the

sequestration. In oil sands applications, one might argue that credit could be taken for neutralization of the sodium hydroxide sometimes used as a process aid. This is reasonable if one only considers the oil sands operation, but perhaps not if one includes the carbon dioxide footprint of the caustic production. This discussion will be limited to the interaction of the oil sands clays with carbon dioxide.

Table 1. Comparison of geological and process or chemical sequestration factors.

Sequestration Mechanism	Geological	Process
Physical	Major component of underground storage	Bubbles trapped in fluid at ambient conditions should not be considered to be sequestered
Ionic	Formation of bicarbonate in solution is limited by the surface area of the gas bubble physically trapped	Conversion of carbon dioxide to carbonate and bicarbonate in solution can be controlled and easily quantified
Mineral	Mineralization to calcium carbonate will depend upon the equilibrium with carbonate, bicarbonate, and calcium	Conversion to calcium carbonate can also be monitored and quantified.

Tables 2 and 3 show the impact of carbon dioxide compared to gypsum on the strength of the clay structure and on the resulting water chemistry. One of the incentives to use carbon dioxide as a CT process additive was to avoid large changes in the release water chemistry, in particular the divalent ions. The data in Table 3 clearly shows that the water chemistry changes are less significant with carbon dioxide than with gypsum.

Table 2. Properties of MFT treated with carbon dioxide or gypsum. The gypsum is noted as g/tonne of solids in the MFT.

Sample	Yield Point (Pa)	Viscosity (mPa.s)
MFT	3.7	17
MFT + air	1.3	18
MFT + CO2	22.8	24
MFT + 1000g/tonne gypsum	8.3	13.8
MFT + 3000g/tonne gypsum	22	28

Table 3. Water chemistry for the carbon dioxide and gypsum additives.

Type of CT	C:W	Ca^{2+}	Mg^{2+}	K^{+}	Na^{+}	HCO_3^{-}	CO_3^{2-}	pH
Gypsum	0.12	62	20	24	1073	934	0	8.25
Carbon Dioxide	0.11	14	15	19	1037	1321	30	8.43

Figure 1 shows the change in pH with carbon dioxide addition to a tailings sample with solids and without solids. Clearly the solids are playing a role in neutralizing the effect of the carbonic acid produced by the addition of carbon dioxide. Without the clays in the tailings, the acidification is much more persistent. The relaxation of the pH back to its original value, coupled with the increase in bicarbonate concentration observed in Table 4, makes it clear that a portion of the added carbon dioxide is ionically sequestered as bicarbonate ion. Table 4 shows the water chemistry changes for a variety of CT samples with the ionic sequestration in the range of 1.0 to 1.7mg carbon dioxide per gram of clay available. The increase in bicarbonate ion appears to be linked to an increase in sodium and calcium and this can be understood in terms of a cation exchange with the clays where the proton from the carbonic acid replaces a sodium ion on the clay. If this were the

case, one could expect an increase in the sodium bicarbonate concentration in the water phase of the tailings slurry after carbon dioxide addition.

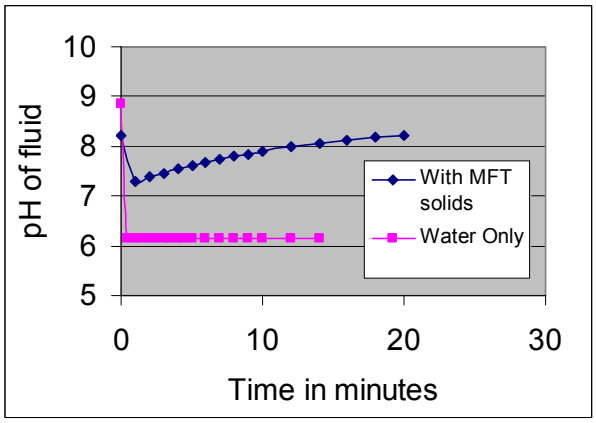

Figure 1. Time dependence of pH in oil sands tailings with and without clay solids.

This is born out with some preliminary work characterizing the solids where after carbon dioxide addition, the water phase was removed from the clays and an increase in the relative amount of sodium bicarbonate to sodium chloride was noted, roughly in proportion to the amount of carbon dioxide added. This data is shown in Table 5.

The ionic sequestration and its link to the clays present is shown in Figure 2 with the increase in bicarbonate concentration proportional to the clay content in a series of tailings samples. The greater the proportion of clays in the sample, the greater is the amount of bicarbonate in the tailings water.

Table 4. Selected carbon dioxide CT mixes and the associated ionic sequestration of carbon dioxide.

Solids wt%	C:W	Ca^{2+}	Mg^{2+}	K^{+}	Na^{+}	HCO_3^{-}	CO_3^{2-}	Cl^{-}	SO_4^{2-}	pH	CO2 t/Mt CT	mg CO_2 per gm Clay
36	0.08	19	14	18	1036	1366	0	689	207	8.06	70	1.4
46	0.12	14	15	19	1037	1321	30	649	245	8.43	66	1.0
50	0.09	22	16	19	1103	1397	4	593	256	8.26	64	1.4
55	0.16	14	16	19	1073	1403	46	719	270	8.53	98	1.4
60	0.13	22	21	21	1151	1520	0	695	332	8.16	89	1.7
MFT pore water		7	7	16	646	978	0					

Table 5. Increase in sodium bicarbonate relative to sodium chloride for a tailings sample set with added carbon dioxide.

Sample	Ca	K	Mg	Na	S	Cl	SO4	HCO3	CO3	pH	IB
Untreated	3	13	1	323	25	167	44	522	12	8.62	1.00
90 ppm CO2	1	12	1	349	25	157	42	619	0	8.21	1.01
140 ppm CO2	1	14	1	463	25	219	49	821	0	8.23	1.00

Previous work has suggested both ionic sequestration of carbon dioxide as sodium bicarbonate increases in the tailings water, and some precipitation of calcium carbonate. The extent of the mineral sequestration has yet to be quantified, but the increase in bicarbonate is clear. Figure 3 shows the relationship between carbon dioxide uptake in the clay tailings slurry and the clay in the slurry for a series of equivalent carbon dioxide additions. The slope of this line is the amount of carbon dioxide sequestered per gram of clay. This is approximately 1.8mg of carbon dioxide per gram of clay in the tailings slurry. Clearly the capacity of the clays for uptake of protons from the carbonic acid and release of cations to balance the resulting bicarbonate ion is not infinite. This limit will depend upon the cations present in the clays and the water phase. Figure 4 shows the increase in bicarbonate even after 300h of bubbling carbon dioxide, illustrating that probing the limits to sequestration will require an approach using pressure vessels.

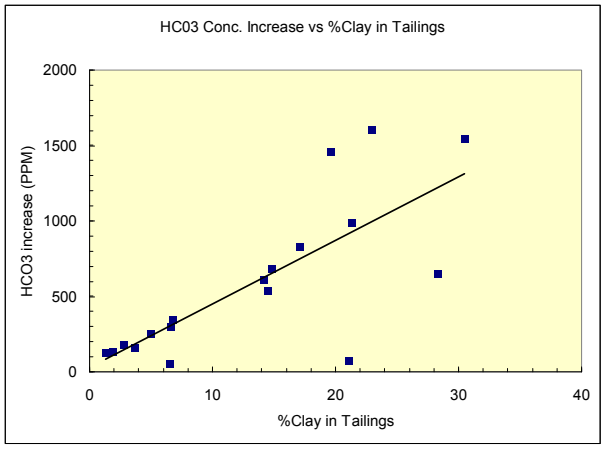

Figure 2. Bicarbonate increase for a variety of carbon dioxide treated tailings samples.

The use of pressure to enhance carbon dioxide uptake will, however, tend to create a non steady state situation that will require some further steps to resolve. In the present set of experiments, a steady state is achieved and we are creating a dense solid tailings and a volume of release water. The release water has an increase in sodium bicarbonate proportional to the carbon dioxide added, indicating that ionic sequestration of carbon dioxide is controllable for oil sands tailings streams.

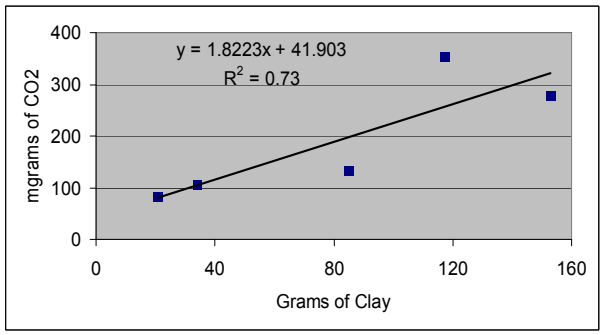

Figure 3. Carbon dioxide sequestration as bicarbonate for a series of maximum carbon dioxide additions.

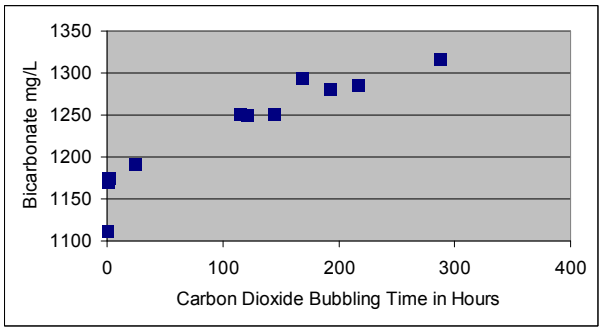

Figure 4. Increase in ionic sequestration of carbon dioxide with increased carbon dioxide addition.

SUMMARY

This preliminary report demonstrated a carbon dioxide uptake on oil sands clays of 1.8mg carbon dioxide per gram of clay. This is equivalent to 2.5mg of bicarbonate per gram of clay. For a 250,000 barrel per day oil sands operation and an with a ore with a fines content of about 20%, the carbon dioxide sequestration potential would be 28,000 tonnes per year. As always there will be tradeoffs between carbon dioxide addition maximization and performance maximization, and further work would be required to optimize this for a given tailings operation.

ACKNOWLEDGMENTS

The authors would like to thank PERD for financial support of this project.

REFERENCE

Mikula, R., Zrobok, R., and Omotoso, O., “The Potential for Carbon Dioxide Sequestration in Oil Sands Processing Streams, Canadian Journal of Petroleum Technology, 2002.

COMPOSITE TAILINGS MADE FROM IN-LINE THICKENED OIL SANDS TAILINGS

S. Jeeravipoolvarn[1], J. D. Scott[2] and R.J. Chalaturnyk[2]
[1]BGC Engineering Inc, Vancouver, BC, Canada
[2]Department of Civil and Environmental Engineering, University of Alberta, Edmonton, AB, Canada

ABSTRACT

An investigation of the use of in-line thickened tailings to create composite tailings at a sand to fines ratio, SFR, of 4:1 without any further chemical amendment is presented in this paper. At this SFR, it was found that the composite tailings made with in-line thickened tailings (ILTT-CT) had a static segregation point at 53% solids content and the composite tailings made with the parent material, cyclone overflow tailings (typical new fine tailings) without any additive, had a static segregation point at 59% solids content. The segregation boundary of the ILTT-CT with no added coagulant is comparable to that of the gypsum treated MFT-CT. It is also at a lower solids content, that is less susceptible to segregation, than the segregation boundary of old MFT-CT. ILTT-CT hydraulic conductivity is found to be controlled by the high hydraulic conductivity of the ILTT fines and the undrained shear strength of the ILTT-CT is considerably higher than that of the ILTT fines at the same fines void ratio. As well, as no coagulant is required, there is no detrimental effect to the reclaim water chemistry. The combination of faster consolidation and higher shear strength means that the ILTT-CT will be able to be reclaimed much earlier than MFT-CT. Judicial deposition techniques may result in it being reclaimed as it is being deposited.

INTRODUCTION

Composite tailings, CT, are produced by mixing and depositing a blend of cyclone underflow and MFT with a coagulant, generally gypsum ($CaSO_4$) to make the mix nonsegregating. The MFT is pumped from the existing tailings ponds where it has accumulated over the years. This procedure is consuming some of the current inventories of MFT and it releases water fairly rapidly for make-up water for the extraction plant (Matthews et al., 2002). Dewatering rates, however, are lower than expected and careful engineering of the CT process is required to prevent segregation during deposition. Another drawback is that the amount of MFT which can be added to the cyclone underflow is limited as too much fines in the CT reduces its hydraulic conductivity and the dewatering rate will be too slow. Generally the sand-fines ratio, SFR, of CT is only 4 or 5, that is, the fines content is from 17% to 20%.

As the oil sands tailings on average contains about 17% fines and the cyclone overflow which contains most of the fines is deposited in a tailings pond and forms more MFT, the CT process which is not continuous cannot keep up with the continuous formation of more MFT and MFT volumes continue to increase. Another problem with the present CT process is that the dosages of gypsum to prevent segregation are quite large resulting in the buildup of Ca^{2+} and SO_4^{2-} ions in the recycle water which in time will negatively affect bitumen extraction.

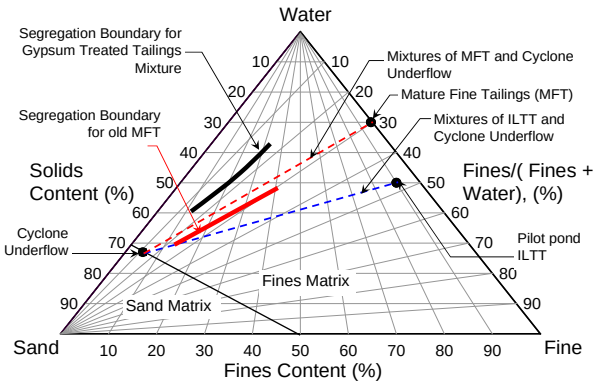

Figure 1. Tailings properties diagram

Figure 1 shows the present CT process. All mixes of MFT and cyclone underflow will lie on the straight line joining the MFT and cyclone underflow materials. The segregation boundary for untreated tailings blends is also shown. All tailings above this segregation boundary will segregate so all untreated mixes of MFT and cyclone underflow will segregate. The segregation boundary for gypsum treated tailings is also shown. All tailings below the gypsum segregation boundary will be nonsegregating so the CT mixes of MFT and cyclone underflow will become nonsegregating with the addition of a coagulant such as gypsum. Figure 1 also shows all possible mixes of ILTT and

cyclone underflow which lie on the line that joins these two materials. It is noted that the ILTT data is obtained from the field pilot pond at a depth of 1 m (Jeeravipoolvarn et al. 2008). Possible CT mixes of ILTT and cyclone underflow lie below the untreated segregation boundary which indicates that these CT mixes would require no or little coagulant addition with a resulting increase in the quality of the recycle water for bitumen extraction.

The greatest advantage of CT made from ILTT and cyclone underflow is the large hydraulic conductivity of the ILTT fines. As shown by Jeeravipoolvarn et al. (2008), at a solids content of 30% (void ratio of about 5.7) the hydraulic conductivity of ILTT is more than 20 times the hydraulic conductivity of new MFT (cyclone overflow) and even greater than that of old MFT. This means the ILTT-CT will release water and consolidate faster than MFT-CT allowing more rapid CT disposal. The greater ILTT hydraulic conductivity will also allow a larger amount of fines in the ILTT-CT than the 20% maximum in the MFT-CT. This would assist in the reduction of fine tails volume stored in tailings ponds.

In order to investigate the production of composite tailings from in-line thickened tailings, a series of static segregation tests and two large strain consolidation tests on composite tailings made from in-line thickened tailings were performed. The sand-fines ratio used in this investigation was limited to 4:1 and no further chemical amendment was used. The hydraulic conductivity behavior of the composite tailings was also obtained from the static segregation tests and these results are combined with large strain consolidation test results for the ILTT-CT to investigate the consolidation characteristics of the ILTT-CT. Also static segregation tests on cyclone overflow and tailings sand mix, COF-CT, were performed to compare with the ILTT-CT results.

This paper begins with composite tailings preparation procedures followed by a full test program including static segregation tests and large strain consolidation tests. Discussion and conclusions on the use of in-line thickened tailings to create composite tailings are then given.

COMPOSITE TAILINGS PREPARATION

In order to create composite tailings, cyclone underflow sand was shipped from Syncrude together with cyclone overflow tailings on 14th April 2008. It is noted that no additive was further processed into in-line thickened tailings and cyclone overflow tailings to create composite tailings in this investigation.

The cyclone underflow sand was characterized for its solids content, fines content, particle size distribution and specific gravity. ILTT was mixed in advance and it was allowed to settle to a solids content of around 30%. ILTT and sand were then mixed together with additional ILTT release water (if required) for 1 minute to obtain the design solids contents. Composite tailings made from the ILTT were immediately poured into different test cells for different tests to proceed. Composite tailings made from cyclone overflow were prepared similarly with an exception that for a high design solids content composite tailings, cyclone overflow tailings was allowed to settle and was consolidated to obtain a higher solids content before mixing.

Non-dispersed particle size distributions of mixtures of cyclone overflow tailings with cyclone underflow sand (COF-CT) and in-line thickened tailings with cyclone underflow sand (ILTT-CT) are shown in Figure 2. Both particle size distributions indicate fines contents (< 45 μm) of about 20% (SFR 4:1). The COF-CT shows 4% clay size material (< 2 μm) while the ILTT-CT shows 0% clay size material. The smaller measured clay size material in the ILTT-CT is an indication of the remaining influence of the in-line thickening process.

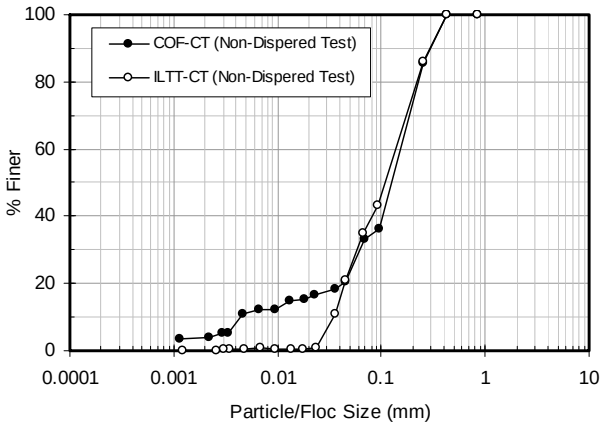

Figure 2. Non-dispersed particle size distributions of COF-CT and ILTT-CT.

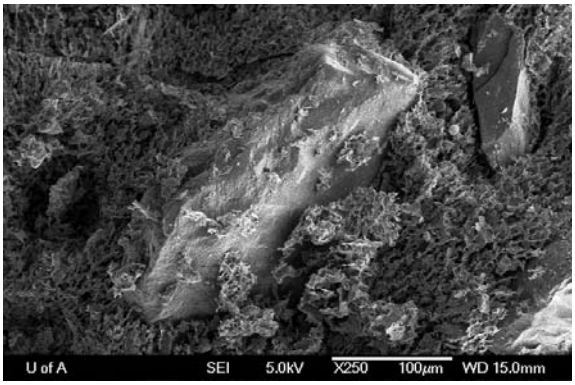

(*a*) ILTT-CT SFR 4:1 ×250

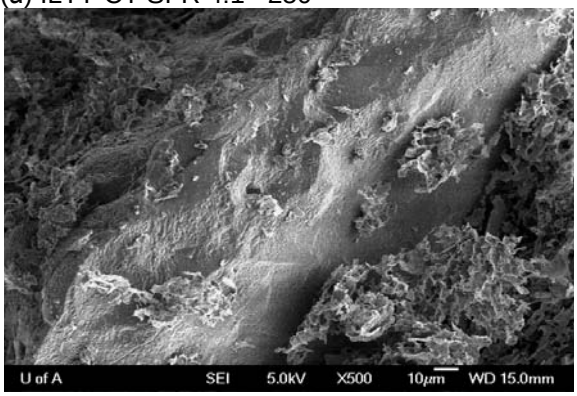

(*b*) ILTT-CT SFR 4:1 ×500

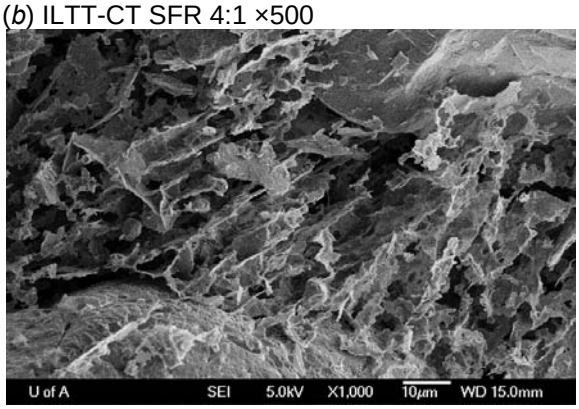

(*c*) ILTT-CT SFR 4:1 ×1000

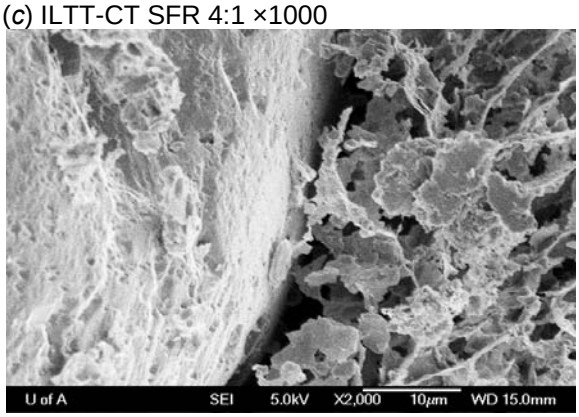

(*d*) ILTT-CT SFR 4:1 ×2000

Figure 3. Scanning electron microscope images of ILTT-CT (55%S, 20%F).

Scanning electron microscope images of composite tailings made from in-line thickened tailings are shown in Figure 3. The composite tailings were prepared at 55% solids content and 20% fines content, this gave a fines-bitumen void ratio of about 9.7. Sand particles can be observed suspended in this high void ratio clay matrix. The clay structure holding the sand can be classified as edge-to-face and edge-to-edge flocculated and aggregated pattern similar to that found in the non-sheared in-line thickened tailings (Jeeravipoolvarn 2010). It can also be seen that at some locations, the ILTT-CT clay structure exhibits a card-house like structure such as found in the cyclone overflow tailings (Figure 3 (*c*)).

STATIC SEGREGATION TEST

A series of static segregation tests on COF-CT and ILTT-CT were performed at a SFR of 4:1 with no further chemical amendment for either tailings. Segregation criterion used to find a segregation boundary in this investigation was 95% fines capture. The results are as follows.

Static segregation tests on composite tailings made from COF

Table 1 shows four static segregation tests on composite tailings made from cyclone overflow. Four solids contents (50.7%, 56.1%, 59.5% and 65.2%) were used with designed fines content of 20% or SFR of 4:1. Figure 4 shows interface settlements of all four tests. The initial settling velocities and hydraulic conductivity corresponding to the initial void ratios were calculated and shown in Table 1.

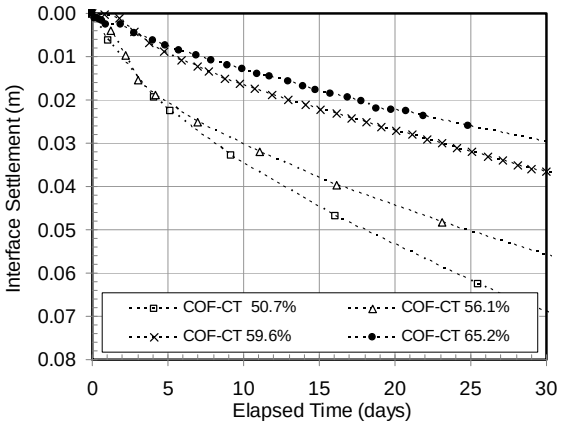

Figure 4. Interface settlement of COF-CT

Table 1. Static segregation tests on COF-CT

Test	Initial solids content (%)	Designed fines content (%)	Void ratio	v_s (m/s)	Hydraulic conductivity (m/s)	Fines capture (%)	Fines-bitumen void ratio
1	50.7	20.0	2.52	4.11E-08	-	49.3	11.57
2	56.1	20.0	2.03	2.33E-08	-	92.2	9.31
3	59.5	20.0	1.76	1.76E-08	3.06E-08	95.6	8.10
4	65.2	20.0	1.38	1.34E-08	2.01E-08	-	6.35

In Figure 5, solids content and fines profiles are shown for COF-CT with solids content of 50.7%, 56.1% and 59.5%. Calculated fines captures in Table 1 show that at initial solids contents of 50.7% and 56.1%, COF-CT segregated and an interpolated static segregation boundary for COF-CT at 95% fines capture is 58.9% solids content (e_{fb} = 8.3, FWR = 22.3%).

A correlation between fines-bitumen void ratio and undrained shear strength of cyclone overflow is given by Jeeravipoolvarn (2010) as Equation 1.

$$e_{fb} = 1.811 \times \tau_u^{-0.278} \quad [1]$$

Where e_{fb} is the fines-bitumen void ratio and τ_u is the undrained shear strength in kPa. The fines-bitumen void ratio which is the volume of voids divided by volumes of fines and bitumen is used to correlate with undrained shear strength as the shear strength has been found to be mainly controlled by the fines matrix and the suspended sand grains generally have little influence at high void ratios.

With Equation 1, the solids content of the COF-CT at the segregation point corresponds to an undrained shear strength of 4.2 Pa before any sedimentation or consolidation takes place.

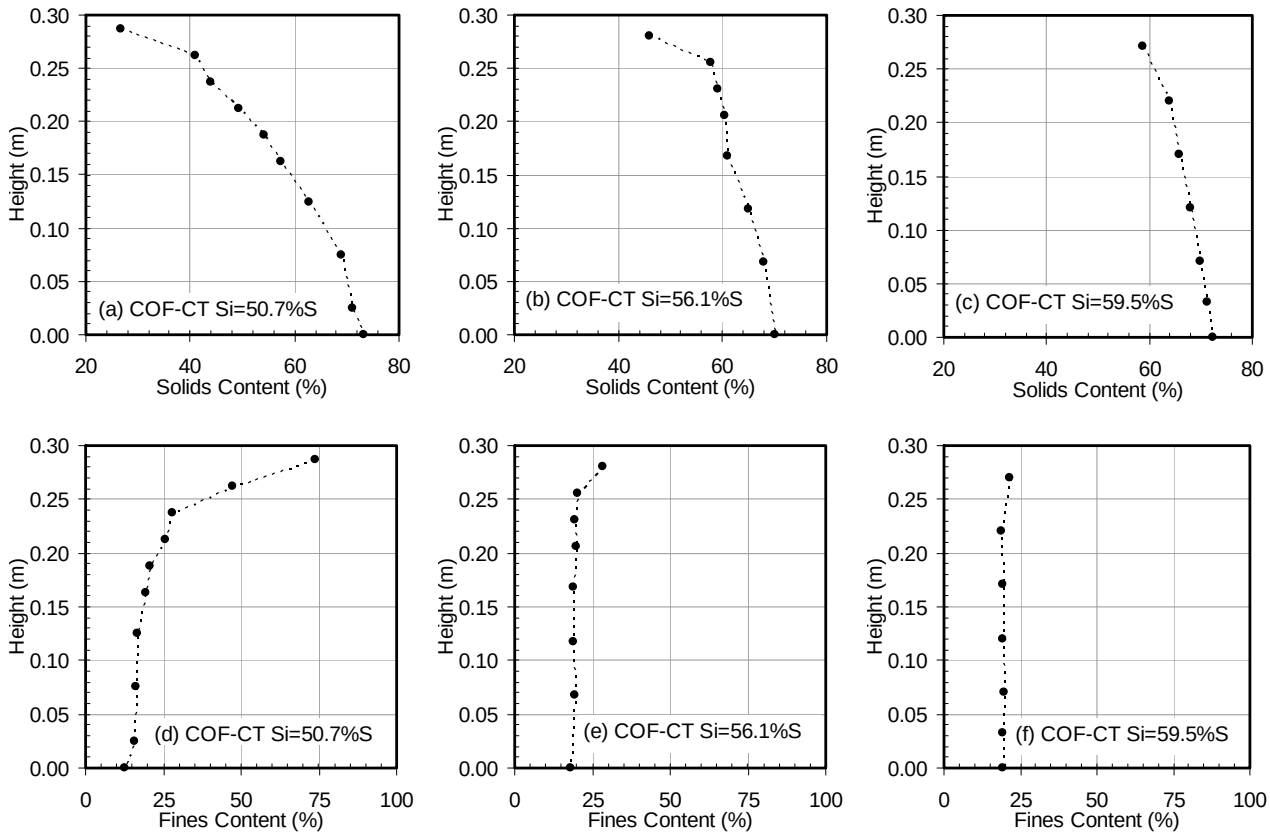

Figure 5. Solids and fines content profiles of COF-CT SFR 4:1

Static segregation tests on composite tailings made from ILTT

Table 2 shows four static segregation tests on composite tailings made from in-line thickened tailings. Four solids contents (50.2%, 52.8%, 61.1% and 65.6%) were used with a designed fines content of 20% or SFR of 4:1. Figure 6 shows interface settlement of all four tests. The initial settling velocities were measured and used to obtain hydraulic conductivities corresponding to the initial void ratios. The results are shown in Table 2.

Figure 7 shows solids content and fines content profiles of ILTT-CT with solids content of 50.2%, 52.8% and 61.1%. It can be seen that the ILTT-CT segregated at 50.2% initial solids content. Fines captures for each test are shown in Table 2 which gives a static segregation boundary of ILTT-CT at 52.6% solids content (e_{fb} = 10.7, FWR = 18%).

Undrained shear strength correlation for sheared in-line thickened tailings is given by Jeeravipoolvarn (2010) in Equation 2.

$$e_{fb} = 3.014 \times \tau_u^{-0.300} \quad [2]$$

Where e_{fb} is fines-bitumen void ratio and τ_u is undrained shear strength in kPa.

From the undrained shear strength correlation in Equation 2, the solids content at the segregation point corresponds to an undrained shear strength of 14.5 Pa. It is noted that these undrained shear strength values are extrapolated. Even though it does not appear that the undrained shear strength of the fines correlates well with the segregation behavior because COF-CT and ILTT-CT segregate at different undrained shear strengths (4.2 Pa and 14.5 Pa respectively), a trend of higher undrained shear strength material and lower solids content at a segregation boundary is achieved. It is noted that the influence of the ions in the cyclone underflow sand was not taken into account in this experiment therefore the correlation between undrained shear strength and fines-bitumen void ratio used in the undrained shear strength extrapolation may not hold for these composite tailings.

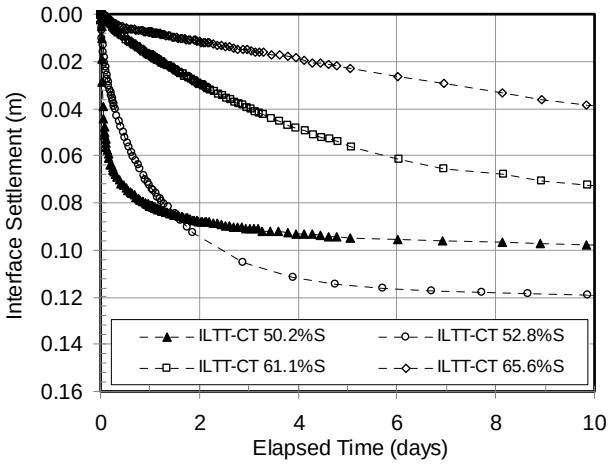

Figure 6. Interface settlement of ILTT-CT.

Table 2. Static segregation tests on ILTT-CT

Test	Initial solids content (%)	Designed fines content (%)	Void ratio	v_s (m/s)	Hydraulic conductivity (m/s)	Fines capture (%)	Fines-bitumen void ratio
1	50.2	20.0	2.57	1.07E-05	-	64.8*	11.81
2	52.8	20.0	2.32	1.65E-06	3.44E-06	97.0	10.64
3	61.1	20.0	1.65	2.31E-07	3.85E-07	96.5	7.58
4	65.6	20.0	1.36	1.82E-07	1.82E-07	-	6.24

* calculated from solids content profile

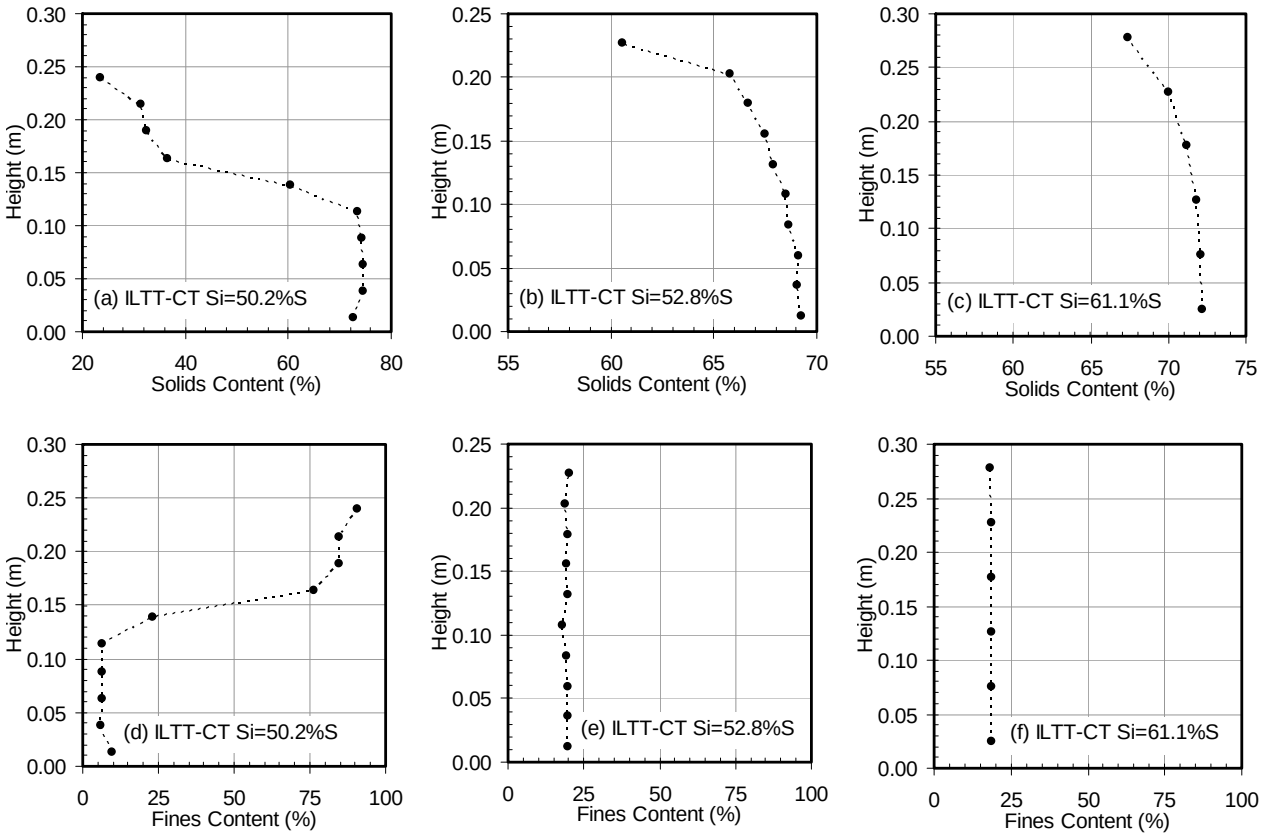

Figure 7. Solids and fines content profiles of ILTT-CT SFR 4:1

LARGE STRAIN CONSOLIDATION TEST

Two large strain consolidation tests with and without vane shear strength tests were performed on ILTT-CT. Initial solids contents of the composite tailings used in this test were 55.4% and 55.2% for tests 1 and 2 respectively. Figures 8, 9 and 10 show combined compressibility, hydraulic conductivity and undrained shear strength measurements of the tailings respectively.

In Figure 8, compressibility of the ILTT-CT shows an apparent pre-consolidation stress. The pre-consolidation behavior occurs at a void ratio of about 1.3 or fines-bitumen void ratio of about 5.8 and an effective stress of about 1 kPa. Compressibility of the ILTT-CT can be expressed as Equation 3.

$$e = \begin{cases} 1.250 \times \sigma'^{-0.0478} & ;1.35 \geq e \geq 1.25 \\ 1.250 \times \sigma'^{-0.308} & ;1.25 \geq e \geq 0.85 \\ 0.962 \times \sigma'^{-0.099} & ;0.85 \geq e \geq 0.5 \end{cases} \quad [3]$$

Where e is void ratio and σ' is vertical effective stress in kPa.

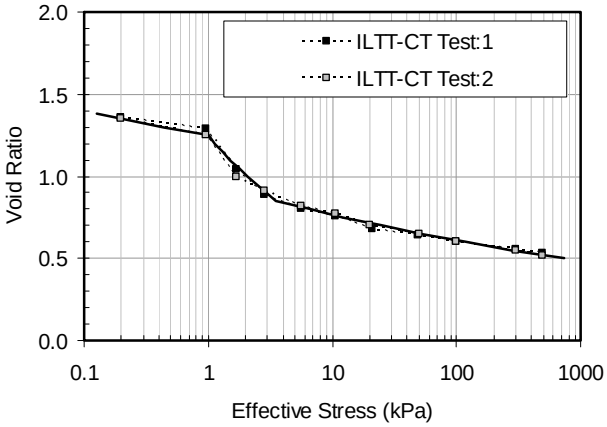

Figure 8. Compressibility of ILTT-CT SFR 4:1 from a large strain consolidation test.

Hydraulic conductivity of the ILTT-CT in Figure 9 can be expressed as Equation 4.

$$k = 4.05 \times 10^{-8} \times e^{4.0} \quad [4]$$

Where *e* is void ratio and *k* is hydraulic conductivity in m/s.

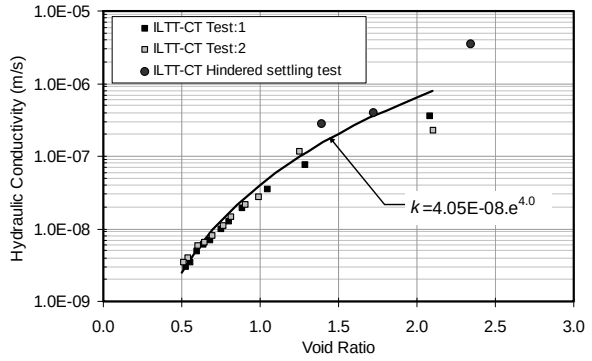

Figure 9. Hydraulic conductivity of ILTT-CT SFR 4:1 from large strain consolidation tests.

Undrained shear strength measurement for ILTT-CT is shown in Figure 10 and a correlation between undrained shear strength and void ratio for the ILTT-CT can be expressed as Equation 5.

$$e = 0.920 \times \tau_u^{-0.159} \quad [5]$$

Where *e* is void ratio and τ_u is undrained shear strength in kPa.

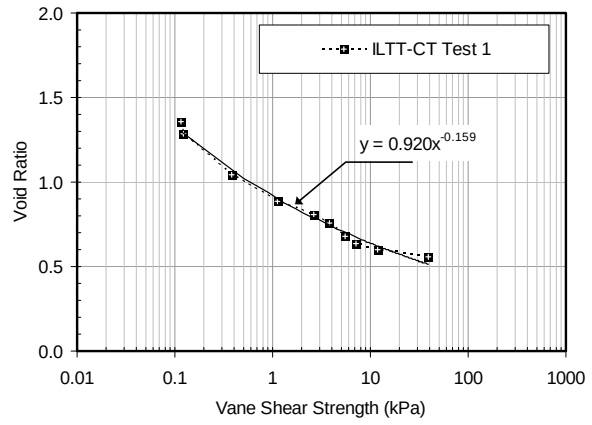

Figure 10. Undrained shear strength of ILTT-CT SFR 4:1 from a large strain consolidation test.

DISCUSSION ON ILTT-CT

In order to perform a comparative study of hydraulic conductivity of COF-CT and ILTT-CT, hydraulic conductivity of both tailings are plotted in Figure 11 against fines-bitumen void ratio with hydraulic conductivity constitutive relationships for in-line thickened tailings, sheared in-line thickened tailings and cyclone overflow given by Jeeravipoolvarn (2010). Fines-bitumen void ratio, defined as volume of voids divided by volume of fines solids and bitumen, is used to normalize hydraulic conductivity data for tailings that have different fines contents.

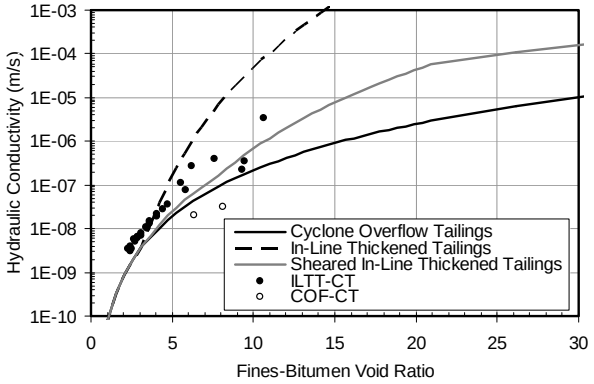

Figure 11. Hydraulic conductivity of ILTT-CT and COF-CT

Hydraulic conductivity measurements of the ILTT-CT are located between the hydraulic conductivities of non-sheared and sheared in-line thickened tailings. The COF-CT's hydraulic conductivity is slightly lower than the fitted hydraulic conductivity function for the cyclone overflow tailings. The trends of the results suggest that the hydraulic conductivities of both composite tailings are controlled by the fines used to create the composite tailings. It can also be seen that at a solids content of about 60% (e_{fb} of about 8) where nonsegregating mixes can be obtained for both tailings, ILTT-CT hydraulic conductivity is about 10 times more permeable compared to that of the COF-CT (Tables 1 and 2).

To perform a comparative study of the ILTT-CT undrained shear strength, correlations of undrained shear strength for sheared and non shear in-line thickened tailings, given by Jeeravipoolvarn (2010), are plotted with the undrained shear strength measurement of ILTT-CT with fines-bitumen void ratio in Figure 12. The undrained shear strength measurements on ILTT-

CT are similar to the sheared in-line thickened tailings at a fines-bitumen void ratio of about 6. At the lower fines-bitumen void ratios, the undrained shear strength of the ILTT-CT diverges from that of sheared in-line thickened tailings and is considerably larger. The higher measured undrained shear strength of the ILTT-CT at lower void ratios is likely caused by the coarse sand particles starting to touch one another. It is noted that the sand matrix is in a loose sand state at a void ratio of about 0.65 or a fines-bitumen void ratio of about 3.0 (for 20% fines content) as indicated by the sand-fines matrix boundary in Figure 1. The measurements show that the undrained shear strength of the ILTT-CT becomes significantly larger than that of ILTT fines starting at a fines-bitumen void ratio of about 4.5 possibly indicating a significant contribution of the coarse particles in this range of void ratios. The interactions of the coarse particles likely occur at a fines-bitumen void ratio higher than 3 possibly due to bridging of various particles' shapes and sizes in a soil. Previous testing of MFT-CT has shown a similar trend of high shear strength in this range of void ratios. It is postulated that the mix of the large flocs of ILTT with sand has a synergistic effect on shear strength.

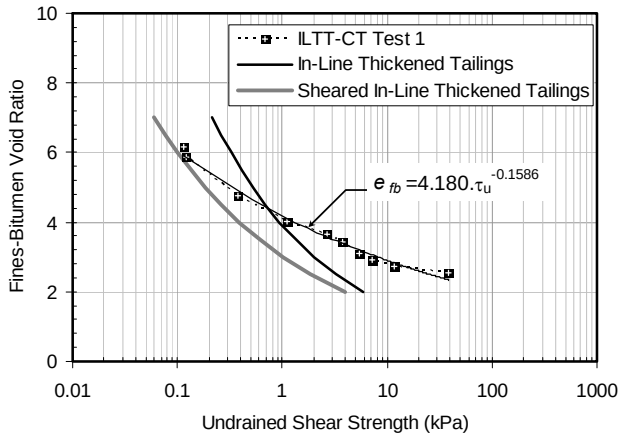

Figure 12. Comparison of undrained shear strength of ILTT and ILTT-CT

Static segregation points of both COF-CT and ILTT-CT at a SFR of 4:1 are shown in Figure 13. In Figure 13, the MFT-CT segregation boundary at a SFR of 4:1 is at a solids content of 65% which is significantly greater than the 59% solids content for the COF-CT found in this experimental program. According to Jeeravipoolvarn (2010), most cation concentrations in this 2008 cyclone overflow have increased significantly compared to that of old MFT. A divalent cation such as calcium is more than double the concentration in the old MFT indicating the possibility of a double layer compression which may potentially lead to particle coagulation. It is then postulated that the possible decrease of the double layer thickness due to the changes in water chemistry contributes to the lower solids content at the segregation point of the COF-CT.

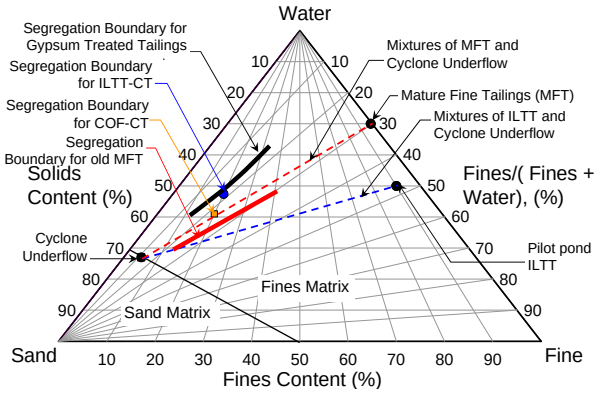

Figure 13. Segregation boundaries of COF-CT and ILTT-CT at SFR 4:1

The results in this composite tailings investigation confirm that composite tailings made from in-line thickened tailings will have a high hydraulic conductivity behavior inherited from the flocculated fines. The shearing of the ILTT during mixing with the sand did not disrupt the floc structure significantly and only reduced the ILTT hydraulic conductivity by a small amount. Composite tailings made with in-line thickened tailings can be deposited at a similar solids content as that of gypsum treated MFT-CT as their static segregation boundaries are essentially comparable at a SFR of 4:1.

COMPARISON OF ILTT-CT AND TYPICAL MFT-CT

Comparing CT made from ILTT and CT made from MFT shows the superior properties of ILTT-CT. Figures 14 and 15 compare compressibility and hydraulic conductivity between ILTT-CT and MFT-CT respectively. For this specific comparison, available data is used for MFT-CT with an initial solids content of 61% made by mixing tailing sand, MFT and gypsum at a dosage of 1000 mg/L as a coagulant.

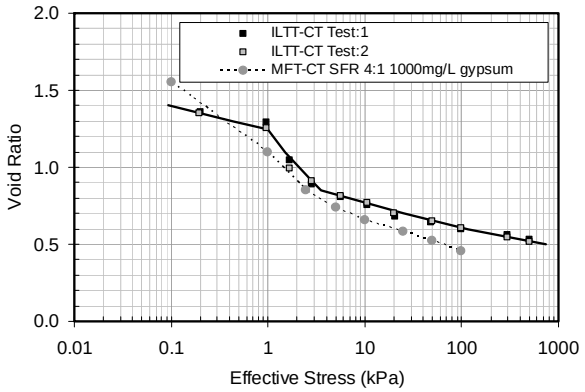

Figure 14. Compressibility comparison between ILTT-CT SFR 4:1 and MFT-CT SFR 4:1.

Comparison between ILTT-CT and MFT-CT in Figure 14 shows that at SFR=4:1, the ILTT-CT requires slightly higher effective stress to compress to the same void ratios compared to the MFT-CT. This is hypothesized to be caused by the stronger inter-particle bonds in the ILTT-CT material. This hypothesis is supported by a comparative study between ILTT and COF by Jeeravipoolvarn (2010) that ILTT fines material requires larger effective stress to compress compared to the COF but that compressibility convergent between the two materials occurs at higher effective stresses.

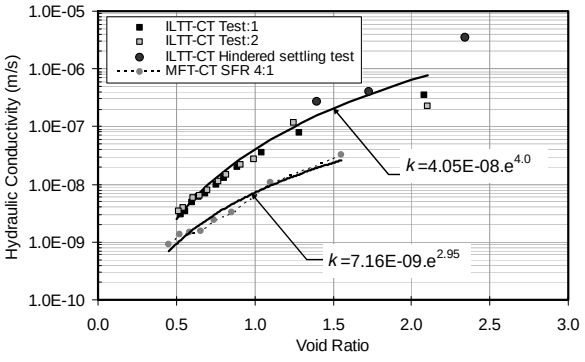

Figure 15. Hydraulic conductivity comparison between ILTT-CT SFR 4:1 and MFT-CT SFR 4:1.

A comparison of hydraulic conductivity between ILTT-CT and MFT-CT in Figure 15 shows that at high initial void ratios the ILTT–CT is 10 times more permeable than gypsum MFT-CT. The difference between hydraulic conductivities of both materials become smaller as the void ratio reduces but that a void ratio of 0.5 the ILTT-CT is still three times more permeable.

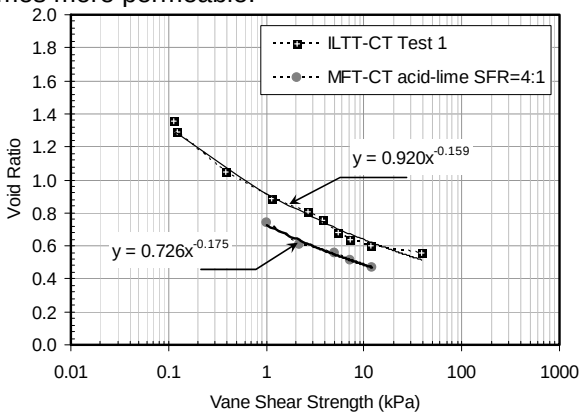

Figure 16. Undrained shear strength comparison between ILTT-CT SFR 4:1 and MFT-CT SFR 4:1

Figure 16 compares undrained shear strengths of ILTT-CT and MFT-CT made with acid-lime. It shows that at the same void ratios, the ILTT-CT is 3 to 4 times stronger than the MFT-CT. This suggests that there are stronger inter-particle bonds present in ILTT-CT.

These favourable material properties of the ILTT-CT imply that that ILTT-CT can settle much more quickly and is able to develop higher undrained shear strength more rapidly. These available material properties can be used in conjunction with a finite strain consolidation theory (Gibson et al. 1967) to investigate different deposition schemes and optimize a deposition strategy for oil sands tailings management. An example of such investigation following ERCB Directive 074 was presented by Jeeravipoolvarn et al. (2010) and it was concluded that the possibility of reclaiming the land can be achieved by combining good tailings, good deposition techniques, external stresses, environmental conditions and good strategy. Further information regarding this investigation can be found in Jeeravipoolvarn et al. (2010).

CONCLUSIONS

An investigation of the use of in-line thickened tailings to create a composite tailings at a SFR of 4:1 without any further coagulant chemical amendment was presented in this paper. At this SFR, it was found that the composite tailings made with in-line thickened tailings (ILTT-CT) had a static segregation point at 52.6% solids content

and the cyclone overflow tailings sand mix (COF-CT) had a static segregation point of 58.9% solids content. The segregation boundary of the ILTT-CT is comparable to that of the gypsum treated CT and is much higher than the segregation boundary of the old mature fine tailings. Therefore under a static condition, nonsegregating behavior of ILTT-CT can be achieved by mixing in-line thickened tailings with cyclone underflow sand at a FWR higher than 18%.

Compressibility, hydraulic conductivity and undrained shear strength of the ILTT-CT were measured. Undrained shear strength measurements indicate that the ILTT-CT has undrained shear strength similar to that of the sheared in-line thickened tailings at fines-bitumen void ratio of about 6. At lower fines-bitumen void ratios, the undrained shear strength of the ILTT-CT diverges from that of sheared in-line thickened tailings and is significantly larger. The higher measured undrained shear strength of the ILTT-CT at lower fines-bitumen void ratios is believed to be caused by the synergistic contribution of the large flocs of ILTT and the sand particles. This greater shear strength of ILTT-CT is very important as it allows the CT to reach a shear strength of 5 kPa at a higher void ratio or a lower solids content to meet the ERCB definition of a solid deposit (ERCB, 2009).

It was found that hydraulic conductivity measurements of the ILTT-CT at large void ratios locate in between the hydraulic conductivities of non-sheared and sheared in-line thickened tailings; while the COF-CT's hydraulic conductivity is slightly lower than that of the cyclone overflow tailings. The trends of the results suggest that the hydraulic conductivities of both composite tailings are controlled by the fines used to create the tailings. The ILTT-CT thus will have a high hydraulic conductivity property inherited from the ILTT fines. Composite tailings at a solids content of about 60% therefore can be made from in-line thickened tailings with an advantage of having a hydraulic conductivity about 10 times greater than that of the composite tailings made from cyclone overflow. Therefore ILTT-CT will consolidate about 10 times faster than the COF-CT.

Comparison between ILTT-CT and coagulant treated MFT-CTs was also presented and it was found that ILTT-CT's hydraulic conductivity and undrained shear strength properties are more favourable. At initial deposition solids contents or void ratios, the ILTT-CT is 10 times more permeable than MFT-CT. This high initial water release rate may overcome the problem of initial surface trafficability of CT deposits.

Also, the combination of faster consolidation and higher shear strength means that the ILTT-CT will be able to be reclaimed much earlier than MFT-CT. Judicial deposition techniques may result in it being reclaimed as it is being deposited.

ACKNOWLEDGEMENTS

The authors are grateful for the financial support from the University of Alberta and Syncrude Canada Ltd. The continued support of Warren Zubot, Geoff Halferdahl and Ron Lewko of Syncrude Canada Ltd. is greatly appreciated especially for procuring large amounts of field cyclone overflow which enabled the laboratory research program to be performed. The authors also appreciate the laboratory support from Steve Gamble and Christine Hereygers, Department of Civil and Environmental Engineering, University of Alberta.

REFERENCES

ERCB 2009. Directive 074 Tailings Performance Criteria and Requirements for Oil Sands Mining Schemes. The Energy Resources Conservation Board of Alberta (ERCB), Calgary, Alberta, pp. 5-10.

Gibson, R.E., England, G.L. and Hussey M.J.L. 1967. The Theory of One-dimensional Consolidation of Saturated Clays. I. Finite Non-linear Consolidation of Thin Homogeneous Layers. Géotechnique, **17**(3): 261-273.

Jeeravipoolvarn, S. 2010. Geotechnical Behavior of In-Line Thickened Oil Sands Tailings. PhD thesis, University of Alberta, Edmonton.

Jeeravipoolvarn, S., Scott, J.D., Chalaturnyk, R.J., Shaw, W., and Wang, N., 2008. "Sedimentation and Consolidation of In-Line Thickened Fine Tailings", Proceedings of International Oil Sands Tailings Conference, December 7-10, Edmonton, AB, pp. 209-223.

Jeeravipoolvarn, S., Scott, J.D., Chalaturnyk, R.J., 2010. "Simulation of Oil Sands in-Line Thickened Tailings Deposition", Proceedings 63rd Canadian

Geotechnical Conference, September 12-16, Calgary, AB.

Matthews, J.G., Shaw, W.H., MacKinnon, M.D., and Cuddy, R.G. 2002. Development of composite tailings technology at Syncrude. International Journal of Surface Mining, Reclamation, and Environment, 16(1): 24-39.

THE USE OF GEOTUBE® BAGS FOR DEWATERING THE RESTIGOUCHE OPEN PIT ZINC MINE AND SETTLING POND BASIN IN, NEW BRUNSWICK, CANADA.

Jocelyn Douhéret[1], Ed Trainer[2], Andy Lister[3] and Stephen Authier[4]
[1]Terratube Inc., Saint-Denis-de-Brompton, Qc, Canada
[2]Ten Cate, Commerce, Georgia
[3]Ten Cate, Oakville, Ont., Canada
[4]ASDR Environment inc., Malartic, Qc, Canada

ABSTRACT

Blue Note Mining in New-Brunswick, Canada had been using an open pit mine as a tailings pond up until 1997. In 2007 they decided to reopen the open pit to extract Zinc. The first challenge was to remove 300,000 m3 of Zinc contaminated water and 32,000 m3 of sludge. Since discharge water would be pumped into a salmon river, environmental regulations originally limited the maximum level of Zinc at 90 ppb but raised the limit to 250 ppb considering the situation. Sludge Zinc concentrations were 2,500 ppb. In total, 17 geotextile containers 60ft (18.29m) circumference x 100 ft (30m) long each were used. Sludge was pumped 24 hours a day during 18 days at an average rate of 75 m3/h. Leachate analysis showed an average level of Zinc of 125 ppb. With that success, the mine decided to start using geotextile containers in their wastewater treatment flow process in

September 2007. The process is now replacing a conventional settling pond.

INTRODUCTION

Restigouche Mine, owned by Blue Note Mining, is located 80 km from the city of Bathurst (in North West New Brunswick, Canada). It was a Zinc and Pb mine.

That site was closed in 1996 and the open pit was used as a tailings pond for the site. As the price of Zinc rose at the stock exchange, Blue Note Mining decided to reopen the open pit to extract the Zinc. 300 000 m³ of water were accumulated into the open pit. Water was mostly contaminated by Zinc (2100 µg/l). There was also more than 32 000 m³ of sludge accumulated at the bottom of the tailings pond.

The mine site is located in a mountainous area with a reputation as being windy with high amounts of precipitation. There is no impermeable soil and water has to be discharged into a salmon river, a federal law protected area, where environmental discharge regulations limit Zinc level at 90 ppb. As the existing WWTP of the mine is old, it couldn't be used to handle such volumes.

Mine schedule was also very short to re-start the operation. Works couldn't start before the end of April 2007 after snow and ice melt down. Mine operation was scheduled to start as early as July 2007.

An engineering company did a review of methods and solution to take care of water and sludge removal on time and in the respect of environmental regulations, mostly due to the discharge into a salmon river. They also had to work on solutions to refresh the old WWTP that had to keep its pollution control performances even at temperatures reaching -45°C.

OPEN PIT CLEANING

Phase 1 – Water management

Water was highly contaminated by Zinc (2100 µg/l). So it was first decided to precipitate Zinc by adding lime. As lime addition raised the pH, they had to balance pH with CO2 injection.

Works were done by batch. After lime injection a "mud cat" type of dredge was used to pump water to the surface to agitate the deep water. A settling time of 4 days was then allowed and surface water was pumped for discharge. A total of 140 metric tons of lime was used. It took 20 days to pump the 300 000 m³ of water at a flow rate of 550 m³ per hour.

Considering that particular situation, environmental authorities raised the discharge criteria to 250 ppb of Zinc. The same criteria applied for sludge leachate.

Phase 2 – Sludge Management

After phase 1, there was 32 000 m3 of sludge corresponding to sludge accumulated within the last 10 years and by sludge produced by lime addition into contaminated water.

Sludge was heterogeneous at the bottom of the open pit. There was a first layer of light sludge (0.5m thick, 2% to 5% solids) above a deep layer of sludge (3m to 6m, 6% to 11% solids).

The engineering company evaluated and tested different ways to take care of that sludge. Their conclusions were the following.

Mechanical dewatering (filter-press, centrifuge, etc.) was not adapted considering the chemical and physical parameters of sludge. Leachate concentration in Zinc was high and the existing WWTP was not able to treat it. Also, that solution proposed dewatered sludge to be transported by trucks to the Caribou site (1000 truckloads @ 34 km) in a relatively short time.

The other solution was to build an onsite storage area with an impermeable membrane. This solution would solve the problem temporary however; sludge and leachate would have to be removed in the future.

Finally, after a local test of sludge dewatering by geotextile containers it was proven that leachate quality was acceptable. Also, as dewatered sludge would be stored, it could be transported out of the site in the dead season without pressure on transport companies and local roads. Also, that solution dramatically reduced the quantity of sludge to be removed compared to other dewatering technologies.

Dewatering and fine particles filtration requires chemical conditioning with flocculants. Flocculants combine with charged particles in order to create larger particles or flocs. Those flocs are retained into the geotextile bags.

Geotextile containers installation and use

Taking care of 32 000 m3 of such sludge required 17 geotextile containers. Each container was 60ft (18.29m) in circumference x 100 ft (30m) in length. A lay down area of 34 100 ft2 (3170 m2) was build for 12 Geotube® bags. 5 additional Geotube® bags were stacked on the 12 Geotube® bags. That site was prepared 500 ft from the open pit. (Table 1 details the fabric characteristics of the Geotube® bags used).

Sludge was pumped at an average flow rate of 75 m³ / hour, 24 hours a day, during 18 days. Sludge was pumped by a “mud cat” type of dredge.

Picture 1: Pad with geotextile containers.

Geotextile containers performances

A sample of leachate was taken and analyzed every day by a representative of the environmental authorities. (Figure 1 shows the results obtained).17 out of 18 days, leachate concentration in Zinc was below the discharge objective of 250 ppb determined by environmental authorities. Zinc concentration was below 125 ppb most of the time.

Compared to an initial concentration of 2100 ppb, results show that the geotextile container, with the proper chemical conditioning, retained more than 95% of Zinc. The process used a small amount of flocculent. Around 1 kg of dry polymer was used per BDT of tailings handled. This consumption rate was also observed in other similar tailings lagoon cleaning projects.

WASTE WATER TREATMENT PLANT REFURBISHMENT

Initial WWTP process

WWTP is composed by 4 steps.

The first step of the process is a sedimentation pond collecting water coming from mining operation and the mine site (hot piles etc.). The second step, supernatant from that pond is treated at the plant itself by adding lime, coagulant (Ferric Chloride) and polymers to collect most of Zinc, other minerals and particles. Lime has two functions: it elevates the pH to make the particles and ions less soluble (when less soluble they will tend to separate from the water). The lime also aggregates to these particles and ions, and thus starts to separate itself from the water. To help the coagulation that the lime started, a solution of ferric chloride is added to the water. Basically, the polymer will cause all gathered particles and ions to be caught and joined together in a chemically inactivated form (the floc). That effluent (treated water and sludge) is then discharged into a settling pond which is the third step of the treatment. During the fourth step, the supernatant from the settling pond is treated by CO2 injection in order to balance the pH while being pumped into a polishing pond.

Finally, supernatant from the polishing pond is discharged into a water stream that is released into a salmon river.

The existing settling pond was not large enough to handle the new expected volumes that would come from mining operation. Also, WWTP performances had to be improved to meet environmental regulation discharge criteria.

To be environmentally legal, the site's discharge must be within the legal requirements of federal and provincial environment departments. (Table 2 identifies these daily sample limits for the metal and solids being released).

Considering geotextile container performances to collect Zinc, the engineering company decided to install geotextile container to take care of sludge produced by the plant itself.

Geotextile containers infrastructure and operation

Geotextile containers are replacing the settling pond. Treated water (mixed with sludge) is pumped into the containers. Leachate goes by gravity to the polishing pond.

Flow rate of the plant is between 100 to 500 gallons per minute.

A new lay-down area, close to the plant, was built for 4 Geotube® containers 60ft (18.29m) circumference x 100 ft (30m) long each.

Two (2) geotextile containers are filled while another one is dewatering. One container is only on site in case of any incident.

One geocontainer is changed once every two months. During the summer period, two containers are changed at the same time.

Similar projects where realized since then in the mining sector following the same principles and the same infrastructure and operating conditions.

Picture 2: Geotextile container set up for filtration in a flow process.

Geotextile containers performances

Geotextile containers proved to be efficient in collecting Zinc. Raw effluent Zinc concentration ranges from 25 000 ppb to 200 000 ppb with an average at 70 000 ppb. Zinc concentration in geocontainer leachate presents an average of 90 ppb on an 8 months survey.

(Figure 2 shows detailed performances of geotextile containers during the period).

Higher concentrations of Zinc in leachate are observed when pumping starts into a new geotextile container. The geotextile containers are usually pumped for 10 hours before a filtration cake is thick enough to retain fine particles. A filtration cake is built by solids and flocs accumulation at the bottom of the geosynthetic bag. That accumulation acts as a filtration media that collect fine particles. That filtration cake improves filtration performances of the whole process.

Geotextile containers are also used during winter months even when temperatures are as low as -45C. During filling process the high level of salinity in the material prevents freezing and does not reduce the filtration capabilities of the geotextile container. Filtration performances are even improved by cold temperature as fabric shrinks. Pores of the filtration fabric are then smaller and retain more particles.

Picture 3: Geotube® containers in operation during winter.

Dewatered tailings management

Tailings management using geosynthetic containers permit both dewatering and storage simultaneously. Improved dewatering resulted in less volume to handle. Storage, without additional infrastructure, allows time for improved logistics and potential reduction of final disposal costs.

Sediments into bags were more concentrated in Zinc than the mine itself. It was possible to recover Zinc from the residues.

Cost savings

Compared to the conventional way the WWTP was organized, using Geotubes® lead to a dramatic reduction of chemical consumption evaluated around $600,000 a year.

CONCLUSION

Both projects at the mine site proved that geotextile containers are efficient, cost effective and safe for contaminated sludge dewatering and containment.

Geotextile containers are commonly used for lagoon clean out. In this case it was proven that geotextile containers used in the flow process could replace settling ponds and improve the overall performance of the mine Waste Water Treatment Plant.

This project showed the most critical parameters to master in order to efficiently use geosynthetic bags to take care of fine tailings: geotextile bag design, polymerization, polymer consumption, and pumping rates.

The knowledge gained during this project has been incorporated into other similar mining projects to take care of mine fine tailings. The same methodology was applied and is continually being improved.

ACKNOWLEDGEMENTS

A special acknowledgement to the WWTP team of the Restigouche Mine and to their collaborators from the engineering company Genivar for the data collections and the pictures of the site.

REFERENCES

Genivar (2008) – Traitement des eaux contaminées – Mine de Restigouche - Maintenance, Engineering and Mining Operators conference, February 24 to 28, 2008, Val d'Or, Québec, CANADA

Table 1: Fabric Characteristics of the Geotube® Bags:

Mechanical Properties	Test Method	Unit	Minimum Average Roll Value	
			Machine Direction	Cross Direction
Wide Width Tensile Strength (at ultimate)	ASTM D 4595	kN/m (lbs/in)	70 (400)	96.3 (550)
Wide Width Tensile Elongation	ASTM D 4595	%	20 (max.)	20 (max.)
Factory Seam Strength	ASTM D 4884	kN/m (lbs/in)	70.1 (400)	
Apparent Opening Size (AOS)	ASTM D 4751	mm (U.S. Sieve #)	0.425 (40)	
Water Flow Rate	ASTM D 4491	$l/m/m^2$ (gpm/ft^2)	813 (20)	
Mass/Unit Area	ASTM D 5261	g/m^2 (oz/yd^2)	585 (17.3) (Typical Value)	
UV Resistance (% strength retained after 500 hrs)	ASTM D 4355	%	80	

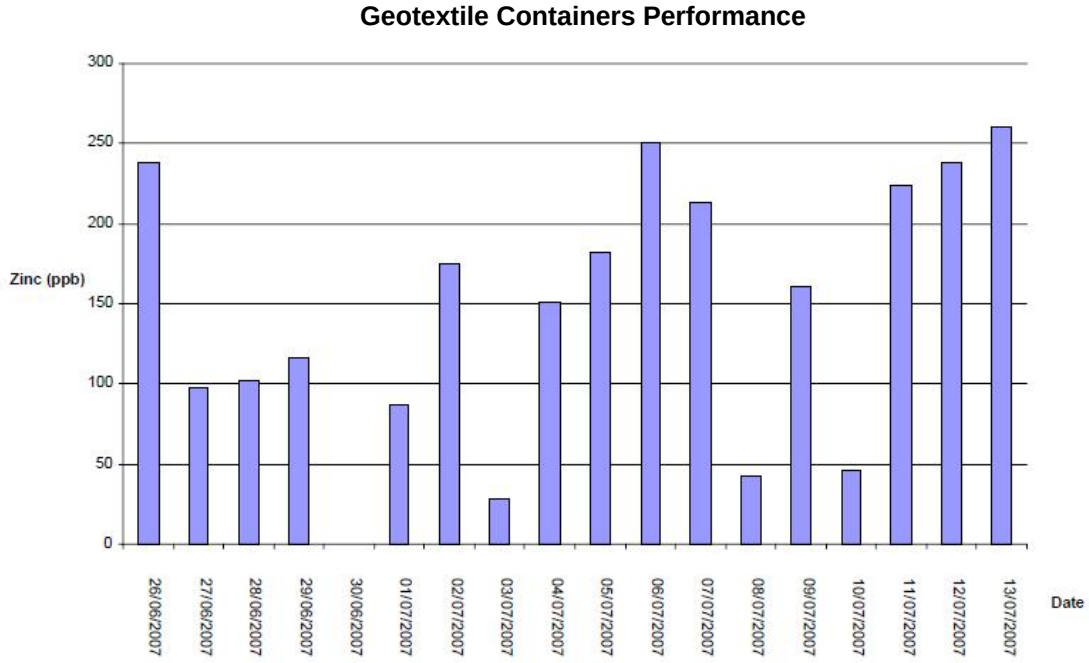

Figure 1: Leachate Concentrations in Zinc (ppb) during the 18 Days of Pumping.

Table 2: Metal and Solids Limits of the Daily Samples:

Type of sample	pH	Cu (µg/L)	Pb (µg/L)	Zn (µg/L)	TSS (mg/L)
Minimum in any grab sample	6,5	-	-	-	-
Maximum in any grab sample	9	30	60	250	25
Monthly mean	-	20	30	-	12

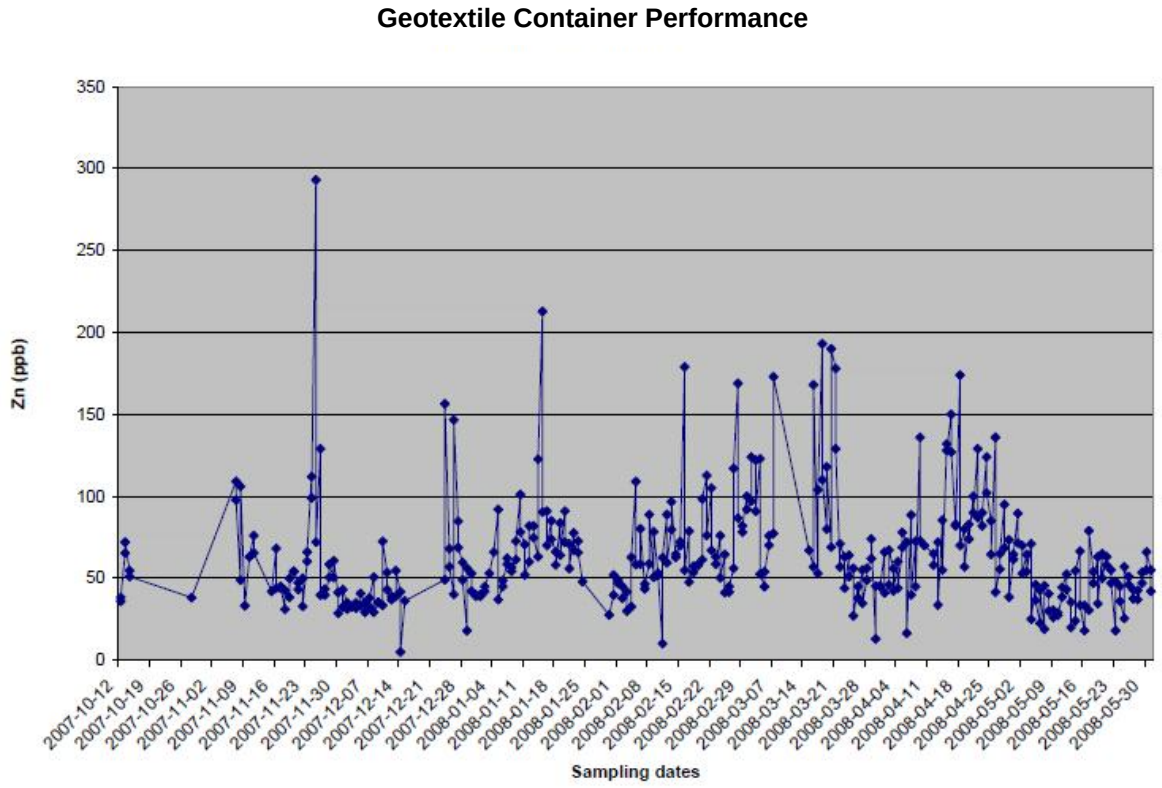

Figure 2: Geotextile Container Performances – Zinc Concentration in Geotextile Container Leachate.

A REVIEW OF METHODS DEVELOPED TO SOLVE THE ISSUE OF WEAK MATURE FINE TAILINGS

M.R. Long, A.C. Ulrich, and D.C. Sego
University of Alberta, Department of Civil and Environmental Engineering

ABSTRACT

The mining industry in the Athabasca Oil Sands has long known the difficulties of managing and storing the mature fine tailings (MFT) produced in their ore processing operations. MFT is made up of very fine, colloidal particles which results in very slow consolidation rates and delays the development of suitable shear strength for the material to be placed outside of impoundment structures (i.e.: use in land reclamation). The high void ratio of these materials gives rise to a high demand for impoundment volume and this presents ongoing challenges for tailings engineers in maintaining satisfactory material balances. Recently, a number of technologies have been evaluated in hopes of solving the issues related to these undesirable properties of MFT. This paper seeks to describe some of these technologies, outline the physical and theoretical basis for their operation and describe the difficulties and advantages in their implementation. Techniques to be discussed include freeze-thaw consolidation, evaporation desiccation, chemical amendment to form non-segregating tailings, and dewatering using vegetation.

INTRODUCTION

The oil sands of northern Alberta contain the equivalent of approximately 170 billion barrels of oil and therefore represent a significant oil resource for Canada and the world (Government of Alberta 2010a). Although only about 20% of the oil sand is located at shallow enough depth for mining to be feasible, at present, most of the oil extracted from the oil sands deposit is via large-scale mining operations (Government of Alberta 2010a). Currently, four companies actively mine the oil sands resource: Suncor, Syncrude, Shell and Canadian Natural Resources Limited (CNRL). While some differences exist in the oil extraction methods used by each of these companies, they generally involve the excavation, crushing and chemical treatment of the oil sands ore in a hydrotransport line to separate the bitumen from the mineral solids (Chalaturnyk et al 2002, Beier et al 2009). The bitumen froth is collected for further processing into synthetic crude oil. For each barrel of oil produced, approximately 3 m^3 of slurry tailings are by-produced (Qiu 2000) and further handling of the slurry results in the segregation and deposition of 1 m^3 of loose sand and 0.25 m^3 fine sludge (Dawson 1999). Combined production output for these companies exceeds 1 million barrels of oil per day (Wu 2009), which roughly results in the production of over 3 million m^3 of slurry tailings per day.

The slurry tailings by-product is composed of water, mineral solids (approximately 50%w/w) and traces of residual bitumen (Beier et al 2009). Historically, these tailings have been disposed of in above-ground tailings impoundments (colloquially termed “tailings ponds”) to serve two purposes: first, to satisfy the “no-discharge” policy imposed by the regulations of the Alberta Government, which disallows discharge of process waters to the environment (Kasperski 1992) and; second, by discharging tailings to a reservoir, time is allowed for the mineral solids to settle out so that the water can be recovered and recycled for use in the extraction process (Government of Alberta 2010b).

Traditionally, when slurry tailings were deposited in the tailings ponds, the coarse- and fine-fractions of tailings segregate: the coarse particles are deposited on the “beach” of the upstream side of the tailings dyke and much of the fines remain suspended in the tailings water, destined for slow sedimentation in the interior of the impoundment (Matthews et al 2002). Two to three years after deposition, the fines eventually settle and accumulate to form “Mature Fine Tails” (MFT) of approximately 30%wt solids content (Liu et al 1994). Due to their clay content and small particle size, the fine tailings take substantial amounts of time to settle and even at the MFT stage they still contain a significant amount of potentially-recyclable water. This slow-settling characteristic results in the need for increasingly large tailings pond capacity to satisfy the extraction plant’s demand for clarified water and to provide storage space for the fine tailings. Over time, the combined tailings inventory for the oil sands mines has resulted in the development of over 130 km^2

of tailings ponds (Government of Alberta 2010b) containing hundreds of millions of cubic metres of tailings (Beier et al 2009).

In response to this vast amount of land being used for tailings storage, the Alberta Energy Resources Conservation Board (ERCB) released Directive 074 in 2009. The goals of Directive 074 include the reduction of tailings pond development and the introduction of more aggressive tailings dewatering in order to "create a trafficable landscape at the earliest opportunity to facilitate progressive reclamation" (ERCB 2009). However, the tendency for MFT to behave unsatisfactorily from a geotechnical perspective (i.e.: slow sedimentation and consolidation rates, low shear strength and bearing capacity) has presented a significant obstacle in readily achieving these goals. Much research over the past few decades has been devoted to improving techniques of managing MFT and tailings and many potential solutions have been proposed. This paper will provide a review of some of the methods developed by research in attempts to solve the issues presented by MFT in environmentally and economically sensible ways.

OBJECTIVES

MFT and the formation thereof have been identified as major obstacles in achieving the goals of ERCB Directive 074. The objective of this paper are two-fold: 1) to provide background on the behaviour and characteristics of MFT and; 2) to highlight some technologies that have been used, or have the potential to be used, in oil sands tailings management schemes to aid in diminishing the current inventory or future rate of production of MFT.

Technologies to be presented include non-segregating tailings, evaporative desiccation (or atmospheric drying), vegetative dewatering, and freeze-thaw consolidation.

CHARACTERISTICS OF TAILINGS

At the outset, it is prudent to note that each oil sands operation produces tailings that vary slightly from one to the next. Indeed, MacKinnon and Sethi (1993) have written that "there is no such thing as a single representative oil sand, whose properties could be considered indicative of what tailings or waste components to expect." With this in mind, the author strives to provide general information on the characteristics of tailings found across the Alberta oil sands industry.

Whole tailings are composed of water, mineral solids (sand-, silt- and clay-sized particles), and residual bitumen (Government of Alberta 2010b). Typical mineralogy of the solid fraction is 85%w/w quartz, 9%w/w clay minerals, 8%w/w feldspars (Kasperski 1992). The clay portion is made up of 40-70%w/w kaolinite, 28-45%w/w illite and 1-15%w/w montmorillonite (Chalaturnyk et al 2002). The particle size distribution of whole tailings is such that approximately 12-25%w/w of the solids are "fines", which are particles passing 44 μm (Liu et al 1994). Traditional oil sands tailings deposition on beaches causes approximately 30-50% of the fine particles to become trapped in the voids among the coarse particles and deposited in the beaches, whereas the remainder stays in suspension and settles out in the settling basin to become MFT (Matthews et al 2002).

MFT is a material of 30%w/w solids, of which 20-50%w/w particles passing 2 μm (i.e.: "clay-sized") almost all of which are phyllosilicate clay-minerals such as kaolinite, illite and montmorillonites (Kasperski 1992). It is this high clay content along with the confounding factor of residual bitumen that produce the poor geotechnical characteristics of MFT. Namely, the most troublesome characteristics are its high compressibility, low shear strength (bearing capacity) and slow consolidation rates.

Suthaker and Scott (1994) indicate that, under external loads, MFT is a highly compressible, large-strain material and that exhibits extremely large void ratio changes with slight increases of effective stress. Their numerical model indicates that, depending on it hydraulic conductivity, it can take several decades to hundreds of years for MFT (initially at 30%w/w solids) to consolidate to half of its original volume if consolidation occurs underwater by self-weight consolidation, which are the conditions experienced at the bottom of tailings ponds. This equates to a void ratio change from greater than 6 to approximately 2.5, which is still very high and indicative of extremely soft soils. Unfortunately, due to its low bearing capacity, surcharging MFT with other materials (sand, for example) to expedite consolidation have not proven practicable at the field scale (Kasperski 1992, Dereniwski and Mimura 1993).

Indeed, MFT is a troublesome material and has deserved the attention that it has received in research over the past few decades. There have been many techniques proposed to mitigate the issues presented by MFT and some of these will be explored in the following sections. However, as a result of the challenging behaviour of MFT and oil sands tailings in general, it is probable that multiple technologies will need to be employed to produce a satisfactory tailings product. Although sought-after, there may be no single, standalone technology that will be a "silver bullet", able to meet dewatering demands of Directive 074 and still remain economical. Indeed, Sobkowicz and Morgenstern (2009) present the perspective that a train of dewatering processes may be required to ensure ease of tailings handling and achievement of dewatering targets. The tailings management technologies that will be presented in this paper are amenable to being combined with one another in a process train, but more research will be required to develop means of optimizing such process trains to meet the needs of industry.

NON-SEGREGATING TAILINGS

Non-Segregating Tailings (NST) is a technology that can be applied in multiple ways but essentially strives toward one goal: preventing the segregation of tailings on the basis of particle-size. As mentioned before, it is the segregation of whole tailings into coarse and fine fractions that allows for the evolution of MFT. Therefore, the theory of the success of NST is that if segregation can be prevented, the production of MFT is avoided and the tailings stream will retain better geotechnical properties such as increased sedimentation and consolidation rates.

Many methods for producing a NST stream have been proposed and in order to visualize the factors involved in a successful NST mixture, the Slurry Properties Diagram has been used (Morgenstern and Scott 1995, Mikula et al 1998). Figure 1 presents the Slurry Properties Diagram upon which the solids content, water content and fines content of the slurry can be plotted. For a given tailings type, a "segregation line" can be determined by testing a variety of tailings mixtures and determining whether or not they segregate upon deposition. Mixtures that plot below the segregation line will resist segregation and so the goal is to produce a tailings stream that falls within this range. It is important to recognize that slurry water chemistry has a significant impact on the location of the segregation line and can be manipulated to decrease the difficulty in producing a mixture of coarse and fine tailings that will resist segregation (Morgenstern and Scott 1995). Mikula et al (1998) and Matthews et al (2002) identify the geochemical interactions between chemical amendments and the clay particles in MFT can diminish the Gouy-Chapman double-diffuse layer of the clays and reduce the repulsive forces between them. This enables the aggregation of fines and allows formation of a fines matrix which will resist separation from the coarse particles.

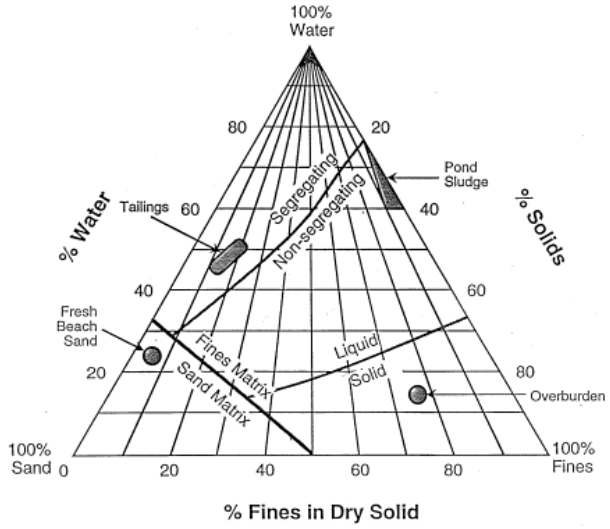

Figure 1. Slurry Properties Ternary Diagram.

% Solids is the Solids Content (by weight) of the slurry mixture. % Water is the water content (by weight) of the slurry mixture. % Fines in Dry Solid is the content (by weight) of the particles finer than 44 µm in the dry solid material. (Diagram from Mikula et al 1998).

Many research projects have endeavoured to find ways of economically adjusting the tailings mixtures to produce NST. Cuddy et al (1993) attempted to produce NST by discharging whole tailings into pre-constructed pools containing MFT and by adding MFT in-line to the whole tailings mixture. Dereniwski and Mimura (1993) also describe field testing at Syncrude involving whole tailings discharged into pools of MFT in order to increase fines capture on the beaches. Their findings were that these methods did help to entrain more fines within the matrix of the coarse particles, however a significant amount of fines were still found to segregate.

Other lines of research focussed on the role of chemistry in determining non-segregating mixtures. By the mid 1990s many researchers had investigated these relationships. Kasperski (1992) describes a number of salts, organic polymer flocculents and acid treatments whose use had been investigated in the preceding decades in attempts to promote flocculation and increase sedimentation and consolidation rates of MFT. Many of these techniques proved either unwieldy or ineffective in producing a satisfactory final material.

Eventually, researchers began to experiment with the addition of these chemical amendments to whole tailings, MFT and mixtures of the two. Caughill et al (1993) conducted a series of standpipe settling tests on Syncrude MFT to which various doses of sulphuric acid (H_2SO_4) and lime (CaO) were added. Their findings demonstrated that optimum doses of either of these chemicals enabled the MFT to reach a void ratio of less than one in a matter of several days to a few weeks of settling in the standpipe. Caughill et al (1994) explored more of the practical aspects of NST technology by conducting field tests at Suncor in the summer of 1993. Whole tailings were run through a hydrocyclone and the coarse cyclone underflow was mixed with MFT and various chemical amendments (H_2SO_4, CaO, and flyash). Results from a test involving subaerial deposition of NST with 53.5%w/w initial solids (21.9%w/w fines) and acid and lime treatment were presented. They showed that from an initial thickness of 3 m, the NST consolidated to 2.5 m and that the lower 2 m had solids content between 75-80%w/w. It is of interest to note that this test involved the drainage of accumulated supernatant water. Caughill et al (1994) also investigated the quality of the NST supernatant water and concluded that the fluid was not acutely toxic.

Before long, NST technology was introduced in full-scale, commercial usage at Suncor in 1995 (Mikula et al 1998). Eventually, Syncrude (Matthews et al 2002) and Shell (Albian Sands) followed suit. The NST processes at Suncor and Syncrude are similar as described by Mikula et al (1998) and Matthews et al (2002): cyclone underflow of whole tailings is mixed with MFT treated with chemical amendments (primarily gypsum). In their tailings management plan for the Horizon mine, Canadian Natural Resources Ltd. (2009) proposed that it will attempt to use carbon dioxide and organic polymers as chemical amendments for the NST process.

In recent years, however, oil sands operators have noted that the NST technology is not performing as well as was expected (Beier et al 2009). In their proposed tailings management plan (issued in response to Directive 074), Suncor (2009) mentioned that it would be phasing out its consolidated tailings (CT) in 2011 in favour of pursuing other technologies. Among reasons for the change, Suncor (2009) cited that it has proven difficult to consistently produce the specified non-segregating mixture and that, even with the use of CT technology, the inventory of MFT continues to increase. Beier et al (2009) also mention that NST production is sensitive to the clay content in the tailings, which is difficult to evaluate accurately on such a large scale but closely dictates the necessary amount of chemical amendment. Other oil sands operators continue to include NST technology in their tailings management plans (CNRL 2009, Syncrude 2009, Shell 2009), although Syncrude (2009) has mentioned that it plans to supplement its fine tailings management by introducing centrifugal dewatering of MFT. With this in mind, it is apparent that industry has not fully settled on NST as being the best technology to apply to the soft tailings issue. However, it is noted that the lessons learned from developing the concepts behind NST are very valuable to the progress of tailings management technology. As will be discussed later in this paper, there is promise for NST, or related concepts, to be complemented by other dewatering techniques as part of a more effective tailings management scheme.

ATMOSPHERIC DRYING

The mining operations in the Alberta Oil Sands take place north of Fort McMurray and occupy an area which experiences net evaporation (Morgenstern and Scott 1995). At first glance, this suggests that dewatering of tailings can proceed simply by exposing the tailings to the air. These dewatering techniques will be referred to as “evaporative desiccation” or “atmospheric drying” in this paper and these approaches have been used on projects in Florida, Jamaica and in the Netherlands (Burns et al 1993) and so are worthy of investigation as a tailings solutions for the oil sands.

There are two main approaches to atmospheric drying: thick layer deposition and thin layer deposition (Burns et al 1993). Thick layer

deposition involves the deposition of tailings in lifts on the order of metres thick. Ditches are excavated around the tailings deposit to remove decant water and precipitation. As tailings dry and a crust of sufficient strength is developed, the drainage ditches are excavated further to encourage dewatering of the tailings at depth. Approaches similar to this are practiced in harbour dredging operations in the Netherlands and in the Florida phosphate mining industry. However, studies by Burns et al (1993) at Suncor have shown via field tests that thick-layer deposition yields unsatisfactory results, primarily due to the confounding factor of bitumen. Their observations showed that bitumen would accumulate at the surface and form a seal, thus impeding water loss by evaporation and preventing improvement of the tailings beneath. The lack of dewatering also precluded the use of vehicles to mix the tailings to break up the bituminous seal or enhance evaporation by exposing wet tailings to the surface.

Thin layer deposition, wherein tailings are deposited in lifts of 10-20 cm thickness, is used to dewater tailings in the Jamaican bauxite mining industry (Burns et al 1993). Tailings are spread in thin lifts over the land surface and allowed to dry to a crust before a new lift is applied. Burns et al (1993) documents a field study carried out at Syncrude in which thin layer drying of MFT was investigated. The results were promising: tailings that had been placed at approximately 35%w/w solids in lifts of the order of 20-50 cm dried over the summer to solids content of around 60-70%w/w. These tests were also conducted such that some of the test deposition pads were underlain by plastic liners and some were deposited on tailings sand. Burns et al (1993) reported that there was no statistical difference between the lined and unlined pads on the basis of dewatering effectiveness and so it was understood that evaporation served as the primary dewatering mechanism.

The difference in effectiveness between the thick and thin layer deposition tests clearly highlighted the need for a rational method of predicting the performance of atmospheric drying of tailings. More recently, numerical models have been developed in an attempt to predict the performance of atmospheric drying and to aid in optimizing the design of their facilities. Qiu (2006a) took into account the processes of cracking, diminished evaporation rates and changes in hydraulic conductivity and developed a model that predicts the optimum depositional design for various types of tailings, oil sands non-segregating tailings included. The effectiveness of Qiu's model (2006b, 2007) and verifying experiments show that the parameters governing evaporative desiccation are relatively well-understood and that thin-layer deposition is the optimal method for oil sands applications.

Further demonstration of the effectiveness of thin-layer deposition has been provided by Wells and Riley (2007) from experiments at Suncor. Evolution of these tests was gradual, progressing from bench-scale tests with MFT in pans dried by sun exposure to field-tests involving thin-lift deposition on shallow slopes of MFT treated with hydrated lime and gypsum (Wells and Riley 2007). Ultimately, they demonstrated that, in spite of periodic spells of inclement weather, atmospheric drying of chemically-treated MFT deposited in thin-lifts (8-10 cm) on shallow slopes (2-4%) is an effective means of dewatering: in their 2005/2006 field trials, the MFT reached solids content of approximately 80%w/w within 14 days of deposition. In addition to these findings, a great deal of information regarding the industrial application of this technology (e.g.: MFT bulking by dredging, piping and mixer configurations, foam control) was developed by Wells and Riley (2007). This prior research has undoubtedly led to the plans of Suncor (2009) to phase out NST technology in favour of atmospheric drying of MFT amended by organic polymer flocculents. It appears that, with these developments, evaporative desiccation is a promising technology for future use in the oil sands industry.

However, difficulties in applying atmospheric drying in the oil sands do still exist. Of perhaps greatest concern is the amount of space that is required. For example, spreading MFT at thicknesses of 10 cm would require an incredible amount of land area: 250 000 m^3 of MFT, approximately one day's production for the entire oil sands mining industry, would take up 250 ha. Multiplying this by an optimistic drying time of 7 days gives a space requirement of 1750 ha, not including the footprint of peripheral berms and infrastructure. Also, Qiu (2000) noted that, at least for atmospheric drying of chemically-treated NST, the accurate prediction of performance depends on reliable measurement of tailings clay content. Unfortunately, inability to properly evaluate clay content has been one of the downfalls in the application of NST. Lastly, atmospheric drying only works during the warm months: in the winter,

the water in the tailings will freeze before evaporating. It is clear that atmospheric drying cannot be a standalone technology in tailings management but could be used to supplement other methods. In spite of these obstacles, it is recognized that atmospheric drying is still a promising technology and that further research and use of the method can improve mine operators' confidence in its application.

FREEZE-THAW CONSOLIDATION

The effects of freezing and thawing of soils has long been of interest to permafrost and cold regions engineers and has been the subject of much research. It is well known that freeze-thaw can cause fine-grained soils to exhibit fissure patterns and can cause the formation of an overconsolidated "crust" in surficial soils. Situated in Northern Alberta, the mining operations in the Athabasca Oil Sands experience average daily temperatures below 0°C five months of the year (Environment Canada 2010). As a result, it is intuitive that dewatering of oil sands tailings may be achieved by optimally placing the tailings and exposing them to natural freeze-thaw cycles. When considering the dewatering of soils (or tailings) subjected to freeze-thaw cycles, two concepts of utmost importance are thermal contraction and cryosuction.

Water expands as it freezes, but mineral grains themselves, like most other solid materials, contract as they cool (Vidstrand 2003). If saturated soil cools rapidly to a sufficiently low temperature, macroscopic patterns of vertical and horizontal fractures can form. These fractures remain after thawing and can significantly increase the hydraulic conductivity through the affected portion of the soil deposit. Therefore, thermal contraction is an important concept: it can help develop drainage paths throughout a tailings deposit.

Cryosuction is a more complicated concept and its action has been described in a variety of ways (Ryckborst 1975, Harlan 1974, Vidstand 2003, Sego et al 1993). The fundamental action of cryosuction is the attraction of liquid water to the freezing front. As the soil freezes, ice crystals that have already begun forming in the larger soil pores draw water from the smaller soil pores, effectively dewatering (or consolidating) the soil matrix while forming a "reticulated ice structure" (Dawson et al 1999). Proskin (1998) notes that the formation of this reticulated ice structure and aggregation of fine-grained particles into consolidated peds results in an increase of hydraulic conductivity and a reduced moisture content once the soil thaws again.

As Dawson et al (1999) note, the potential for dewatering slurries of fine-grained minerals has been recognized for decades. As a result, some research has been conducted to evaluate the effectiveness of a freeze-thaw dewatering strategy implemented in the Athabasca Oil Sands. In general, the procedure is to place tailings in a series of lifts during the winter such that each lift is placed after the previous lift has been fully frozen (Dawson et al 1999). Dawson et al (1999) also indicate that a freeze-thaw facility would benefit from an underdrain to collect water released by freeze-thaw consolidation and recycle it back to the plant. In the Fort McMurray area, the optimum total thickness of lifts placed during the winter is thaw-controlled (Proskin 1998): that is, there is a particular thickness which, if surpassed, will result in a tailings deposit that will not fully thaw the following summer. The implication here is that some of the tailings, unless they are excavated and redistributed (as suggested by Sego et al 1993), will remain frozen, which can be satisfactory from a strength standpoint but is not ideal for volume reduction or water recovery because water will not be released from the frozen soil. Sego et al (1993) conducted tests on MFT generated by the Clark Hot Water Process and found that approximately 50% volume reduction could be achieved by treating it with quicklime and sulphuric acid and then subjecting it to consolidation by one cycle of freeze-thaw. Dawson et al (1999) note that the first two cycles of freeze-thaw produce the most marked reduction in MFT volume, which may be up to 65% (void ratio of ~1.5) in some cases. Dawson et al (1999) conducted a numerical analysis of freeze-thaw scenarios and found that placing a lift of sand as a drainage material between freeze-thaw deposition seasons does not significantly aid in reducing the volume.

Contrary to the notion that optimum deposition of tailings for freeze-thaw consolidation is the thaw-controlled maximum thickness, Wells and Riley (2007) suggest that the optimum method of applying freeze-thaw consolidation involves the placement of frozen tailings to a thickness that will not require the entire summer to fully thaw. Rather, they indicate it may be more effective to instead place the tailings at thicknesses that will

allow early thaw and subsequent deposition of fresh tailings for atmospheric drying during the summer months. Indeed, this strategy fully embraces the concept that multiple dewatering techniques may be required to optimize the tailings management scheme.

Therefore, while it is effective, simplistic in nature, and has apparently low energy requirements, freeze-thaw consolidation may not be feasible to use freeze-thaw as a primary dewatering method (Dawson et al 1999). But, as part of a year-round strategy involving atmospheric drying in the summer and/or additional pre-deposition dewatering technologies, freeze-thaw consolidation may be used in an efficient tailings management scheme.

PLANT DEWATERING

The use of plants to solve problems in geotechnical engineering is not a new or novel concept. For example, constructed embankments and natural slopes benefit from the stabilizing effect of trees and other vegetation. Another potential application of vegetation may be the dewatering and stabilization of oil sands tailings.

Silva (1999) notes that vascular plants have two primary effects that increase soil stability. The first is the mechanical improvement contributed by the tensile strength of the root mass. However, the second and more important is that of their ability to selectively remove water from the soil in order to support their biological processes. This process has the potential to desaturate and progressively dewater the soil medium. The implication for decreasing the saturation of the soil is that the matric suction is increased and the soil achieves increasingly higher shear strengths and bearing capacities (Oloo et al 1997). Clearly there is justified curiosity in the use of plants for the improvement of oil sands tailings.

Two studies have been carried out at the University of Alberta to investigate the effectiveness of vegetative dewatering of oil sands tailings. Silva (1999) performed a greenhouse study in which four-week old grass seedlings of various species were transplanted into a non-segregating tailings mixture (composite tailings from Syncrude). The plants were exposed to sunlight and precipitation in appropriate amounts to simulate the conditions north of Fort McMurray. The successful growth of many of the species was evidence that the composite tailings were not phytotoxic. After 77 days, two plant species, Creeping Foxtail and Reed Canarygrass, were found to have dewatered 70 cm-thick deposits of NST to the point where they exhibited bearing capacities of 600 kPa as measured by plate bearing tests. It is noted that Creeping Foxtail and Reed Canarygrass are commonly used in pastures and hay crops throughout Alberta (Agriculture and Rural Development Alberta 2010). Silva (1999) also developed a numerical model which effectively predicted the change in bearing capacity realized by plant dewatering. However, applying the model to a predict a situation involving vegetative dewatering of a 5 m-thick lift of tailings, Silva (1999) shows that one season of growth is only enough to significantly increase the solids content of the upper 1 m and bearing capacities below this depth remain very small.

A similar study, performed by Wu (2009), addressed the usage of grass species native to the Athabasca oil sands region, indicating that there is an ecological preference to use native species because introduced species may proliferate aggressively and damage the vegetative habitat off-site. Wu (2009) also addressed the practical question as to how the non-segregating tailings can be effectively seeded by investigating in-line injection of seeds, hydroseeding and broadcast seeding onto tailings deposits, each of which proved to be effective methods of seeding. For a 70 cm-thick deposit of NST (initial soilds content approximately 65%w/w) seeded with Northern Wheatgrass, the solids content ranged near-linearly from 95% to 88% (from top to bottom) within 3.5 months of seeding. The use of Slender Wheatgrass showed similar results.

Renault et al (2004) note the potential usefulness of plants for use in initial stages of reclamation of oil sands non-segregating tailings (Syncrude composite tailings). Their study investigated the impact of the use of peat as a soil amendment to benefit vegetative dewatering of tailings. They concluded that peat increased the germination rate (i.e.: the proportion of seeds that germinated) of Altai Wildrye and Slender Wheatgrass as compared to their germination rates in Syncrude composite tailings alone.

While the concept of plant dewatering has been proven to work, it is readily noted that aforementioned studies have all been performed on chemically-amended non-segregating tailings.

By these findings, it is likely that vegetative dewatering would have to be coupled with NST technology in a tailings management scheme, which could greatly improve the dewatering rates of the tailings beyond those realized by use of NST alone.

The application of vegetative dewatering is not without its challenges. One drawback is the amount of time that it takes for dewatering to occur: it may take several weeks for grasses to satisfactorily dewater a lift of tailings on the order of 0.5-1.0 m thick and long retention times require larger areas if the dewatering scheme is meant to keep up with tailings production. Also, Silva (1999) points out that dewatering is less effective in situations where water is available from depth, and as a result there may be diminishing returns if a new lift of tailings is placed prematurely on a previous lift that has not been sufficiently dewatered. It is also noted that the effectiveness of plant dewatering is dependent upon the weather of the growing season and that it cannot be implemented year round.

Even with these challenges, it may yet be worth further investigation to assess the effectiveness of a tailings management scheme involving vegetative dewatering of NST in the summer supplemented by freeze-thaw consolidation in the winter. A potential scenario is one in which seeds are dispersed with the final frozen lift of the winter, sprout in the early spring as the upper layers begin to thaw, and have become mature plants by the time a thin lift of tailings is placed for drying. If the plants adapt well under these conditions, this scenario may help to expedite the drying process of these subsequent lifts. It is clear that there remain a number of research questions in the assessment and application of vegetative dewatering and that there is potential for this method to be incorporated into tailings schemes as a cost-effective supplemental dewatering method.

CONCLUSION

This paper has provided a review of a number of innovative approaches to fine tailings management that have been studied for application in the Athabasca Oil Sands mining industry. Management approaches discussed were non-segregating tailings technology, atmospheric drying, vegetative dewatering and freeze-thaw consolidation. A brief description on theoretical working concepts and a summary description of some research initiatives that investigated these management approaches were given in this paper. In summary, it appears that industry has realized the shortcomings of non-segregating tailings technology and continues to search for economical, effective methods of dewatering and improving the geotechnical properties of the fine tailings produced in bitumen extraction from oil sands. While it is evident that the alternative technologies that have been considered also carry their own challenges, it is understood that combining technologies into a multi-stage approach to tailings dewatering is probably required. The techniques of vegetative dewatering, freeze-thaw consolidation and atmospheric drying each require large-area facilities for effective execution and are season-dependent, but may be of increased effectiveness if they are employed together. Therefore, while continued research is sought to develop new, more effective tailings dewatering techniques, it is clear that ways to optimize the integration of a number of tailings technologies into a robust system for reliable dewatering may also provide the industry with the ability to meet government regulations and achieve environmental expectations.

ACKNOWLEDGEMENTS

Special thanks are due to NSERC and Alberta Innovates – Alberta Ingenuity Awards for their support of Mr. Long in his graduate research. Mr. Long would also like to thank Ms. Marlie DeMontigny for her help and discussion in the early stages of this literature review.

REFERENCES

Agriculture and Rural Development Alberta. 2010. Crop Information Portal: Grasses. [Accessed Online 2 August at http://www.agric.gov.ab.ca/app95/seedinginfo]

Beier, N., Alostaz, M., and Sego, D. 2009. Natural Dewatering Strategies for Oil Sands Fine Tailings. *In* Proceedings from 2009 Tailings and Mine Waste Conference, 4 November 2009.

Burns, R., Cuddy, G and Lahaie, R. 1993. Dewatering of fine tails by natural evaporation.

Proc. Fine Tailings Symposium, Environment Canada, Paper F16, 36p.
Canadian Natural Resources (CNRL). 2009. 2009 Horizon Tailings Management Plan. September 2009.

Caughill, D.L., Scott, J.D., Liu, Y., Burns, R., and Shaw, W.H. 1994. 1993 Field Program on Nonsegregating Tailings at Suncor Inc. Proceedings from 47th Canadian Geotechnical Conference, 21-23 September 1994, Canadian Geotechnical Society. pp. 524-533.

Caughill, D.L., Morgenstern, N.R., and Scott, J.D. 1993. Geotechnics of Nonsegregating Oil Sand Tailings. Canadian Geotechnical Journal, 30: 801-811.

Chalaturnyk, R., Scott, J.D., and Ozum, B. 2002. Management of Oil Sands Tailings. Petroleum Science and Technology. 20(9):1025-1046.

Cuddy, G., Mimura, W. and Lahaie, R. 1993. Spiking tailings as a method to increase fines retention in beach deposits. Proc. Fine Tailings Symposium, Environment Canada, Paper F21, 21p.

Dawson, R.F., Sego, D.C., Pollock, G.W., 1999. Freeze–thaw dewatering of oil sands fine tails. Canadian Geotechnical Journal 36 (4): 587–598.

Dereniwski, T. and Mimura, W. 1993. Sand Layering and Enrichment to Dispose of Fine Tails. Proc. Fine Tailings Symposium, Environment Canada, Paper F20, 42p.

Energy Resources Conservation Board (ERCB). 2009. Directive 074: Tailings Performance Criteria and Requirements for Oil Sands Mining Schemes. Government of Alberta ERCB, Calgary, Canada. [Accessed Online 12 July at http://www.ercb.ca/docs/documents/directives/Directive074.pdf]

Environment Canada. 2010. Canadian Climate Normals: Fort McMurray. Government of Canada. [Accessed Online 21 July 2010 at http://climate.weatheroffice.gc.ca/climate_normals/results_e.html?Province=ALL&StationName=Fort%20McMurray&SearchType=BeginsWith&LocateBy=Province&Proximity=25&ProximityFrom=City&StationNumber=&IDType=MSC&CityName=&ParkName=&LatitudeDegrees=&LatitudeMinutes=&LongitudeDegrees=&LongitudeMinutes=&NormalsClass=A&SelNormals=&StnId=2519&start=1&end=13&autofwd=1]

Government of Alberta. 2010a. Alberta's oil sands: Facts about the resource. [Accessed Online 12 July 2010 at http://www.oilsands.alberta.ca/documents/The_resource.pdf]

Government of Alberta. 2010b. Alberta's oil sands: Facts about tailings management. [Accessed Online 12 July 2010 at http://www.oilsands.alberta.ca/documents/The_resource.pdf]

Harlan, R.L. 1974. Dynamics of Water Movement in Permafrost. Proceedings of workshop seminar 1974. Canadian National Committee the International Hydrological Decade.

Kasperski, K.L. 1992. A Review of Properties and Treatment of Oil Sands Tailings. Alberta Oil Sands Technology and Research Authority Journal of Research, 8(1):11-53.

Liu, Y., Caughill, D., Scott, J.D., and Burns, R. 1994. Consolidation of Suncor Nonsegregating Tailings. In Proceedings from 47th Canadian Geotechnical Conference, 21-23 September 1994, Canadian Geotechnical Society. pp. 504-513.

Matthews, J. G., Shaw, W. H. , MacKinnon, M. D. and Cuddy, R. G. 2002. Development of Composite Tailings Technology at Syncrude. International Journal of Mining, Reclamation and Environment 16(1):4 - 39

MacKinnon, M. and Sethi, A. 1993. Comparison of the Physical and Chemical Properties of the Tailings Ponds at Syncrude and Suncor Oil Sands Plants. Proc. Fine Tailings Symposium, Environment Canada, Paper F2, 33p.

Mikula, R.J., Munoz, V.A., Kasperski, K.L., and Omotoso, O.E. 1998. Commercial Implementation of a Dry Landscape Oil Sands Tailings Reclamation Option: Consolidated Tailings. Proceedings from the 7th UNITAR Conference o Heavy Crude and Tar Sands, 27-30 October 1998.

Morgenstern, N.R. and Scott, J.D. 1995. Geotechnics of Fine Tailings Management. In Geotechnical Special Publication No. 46, Geoenvironment 2000 vol.2: 1663-1683. ASCE. New Orleans, Louisiana.

Oloo, S.Y., Fredlund, D.G., and Gan, J.K-M. 1997. Bearing Capacity of Unpaved Roads. Canadian Geotechnical Journal 34:398-407.

Proskin, S.A. 1998. A Geotechnical Investigation of Freeze-Thaw Dewatering of Oil Sands Fine Tailings. Ph.D. Thesis. University of Alberta.

Qiu, Y. and Sego, D.C. 2007. Optimum Deposition for Sub-Aerial Tailings Disposal Applications. International Journal of Mining, Reclamation and Environment 21(1): 65-74.

Qiu, Y. and Sego, D.C. 2006a. Optimum Deposition for Sub-Aerial Tailings Disposal: Concepts and Theories. International Journal of Mining, Reclamation and Environment 20(4):272-285.

Qiu, Y. and Sego, D.C. 2006b. Optimum Deposition for Sub-Aerial Tailings Disposal: Modeling and Model Validation. International Journal of Mining, Reclamation and Environment 20(4): 286-308.

Qiu, Y. and Sego, D.C. 2000. Optimum Deposition for Sub-Aerial Tailings Disposal. Ph.D. Thesis. University of Alberta.

Renault, S., Qualizza, C., and MacKinnon, M. 2004. Suitability of altai wildrye (*Elymus angustus*) and slender wheatgrass *(Agropyron, trachycaulum*) for initial reclamation of saline composite tailings of oil sands. Environmental Pollution 128(3):339-349.

Ryckborst, H. 1975. On the Origin of Pingos. Journal of Hydrology 26(1975):303-314.

Sego, D., Burns, R., Dawson, R., Dereniwski, T., Johnson, R. and Lowe, L. 1993. Dewatering of fine tails utilizing freeze-thaw process. Proc. Fine Tailings Symposium, Environment Canada, Paper F17, 25p.

Shell Canada Ltd. 2009. Muskeg River Mine: ERCB Directive 074 Submission. September 2009.

Silva, M.J. 1999. Plant Dewatering and Strengthening of Mine Waste Tailings. Ph.D. Thesis. University of Alberta. Edmonton, Canada.

Sobkowicz, J.C. and Morgenstern, N.R. 2009. A Geotechnical Perspective on Oil Sands Tailings. Proceedings from Tailings and Mine Waste 2009. 1-4 November 2009. Banff, Canada.

Suncor Energy Inc. 2009. ERCB Directive 074 Annual Tailings Management Plan. September 2009.

Suthaker, N.N. and Scott, J.D. 1994. Large Strain Consolidation of Oil Sand Fine Tails in a Wet Landscape. Proceedings from 47th Canadian Geotechnical Conference, 21-23 September 1994, Canadian Geotechnical Society. Pp. 514-523.

Syncrude Canada Ltd. 2009. 2009 Annual Tailings Management Plan Submission: Syncrude Mildred Lake (Leases 17 and 21). September 30, 2009.

Vidstrand, P. 2003. Surface and Subsurface Conditions in Permafrost Areas – a Literature Review. Technical Report TR-03-06. Swedish Nuclear Fuel and Waste Management Co.

Wells, P.S. and Riley, D.A. 2007. MFT Drying – Case Study in the Use of Rheological Modification and Dewatering of Fine Tailings Through Thin Lift Deposition in the Oil Sands of Alberta. *In* Paste 2007. Australian Centre for Geomechanics, Perth. Pp. 271-284.

Wu, S. 2009. A Greenhouse Study of Native Plant Species for Dewatering CT. M.Sc. Thesis. University of Alberta. Edmonton, Canada.

SUB-STRATUM INJECTION OF FINE TAILINGS

Walther Van Kesteren[1], John Cornelisse[2], Michael Costello[2] and Eric Hedblom[2]
[1]Deltares, Delft, The Netherlands
[2]Barr Engineering Company, Minneapolis, MN, USA

ABSTRACT

The waste material from oil sand production results in a large volume of fine tailings that have very low settling rates and high consolidation times. At present, a large number of solutions are being researched, like treating with flocculants, drying beds and composite tailings of fines, sand and gypsum. All these solutions require large areas for storage, treatment, and disposal. In the Netherlands, The authors are working on a new innovative method for land lifting by injection. This same method can be used for the disposal of untreated fine tailings and mature fine tailings below the oil sand stratum. This paper will present the theory behind the method (see Figure 1), experimental results on a pilot scale, and the feasibility for application to the oil sand tailings.

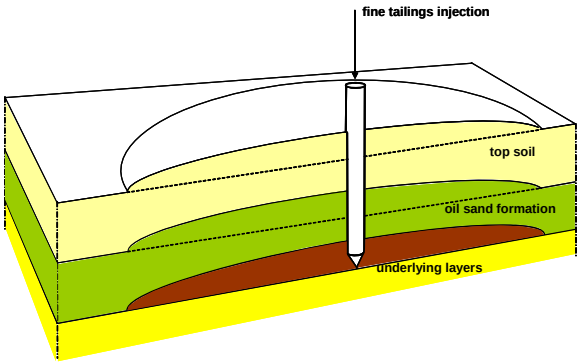

Figure 1. Disposal of fine tailings below oil sand stratum by injection

BACKGROUND

The Netherlands is facing a sea level rise and subsidence of land due to the last glacial rebound. About one third of the country is below the present sea level. To protect these low lands from flooding, higher dikes are needed. For local areas where no dikes are present yet, like wetlands, it is an option to raise the land instead of building dikes. Methods were invented to inject mud through vertical pipes creating mud spheres, and horizontal drains by directional drilling or deep ploughs. These methods were not further considered due to the risk of blow outs and leakage to the surface through small mud volcanoes. The hydraulic fracturing and blow out failure in directional drilling was thoroughly studied by Deltares (Huisman, Talmon etc). An example of hydraulic fracture during directional drilling is shown in Figure 2a, where colored water is injected into transparent gel. The fractal-like crack propagation is upward due to the lowest principal stress being horizontal. In Figure 2b a forced blow out was created in a field test showing upward channels of drilling mud.

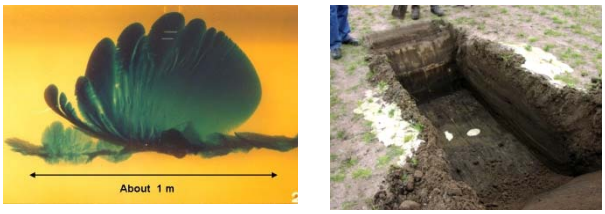

a hydraulic fracturing b blow out

Figure 2. Processes in directional drilling

A new innovative concept of mud injection was presented by Deltares in 2007. The method is based on creating a hydraulic fracture between two different strata with different elasto-plastic parameters and different permeability. The idea of a horizontal hydraulic fracture between two different strata was born by a serendipity experience. In a pilot test with subsurface dredging of sand from beneath a clay layer, a hydraulic fracture was created by excess water pressure in the cavity and resulted in a flow of process water towards ditches about 100 m away. The new concept of mud injection was tested in the Water Soil Flume at Deltares (see Figure 4) as part of the innovation project WINN.

HYDRAULIC FRACTURING IN OIL SANDS

Hydraulic fracturing is a common process in extraction of oil and gas from reservoirs to increase the permeability towards the well. By

pressurizing the borehole the diameter of the borehole increases and horizontal tensile stresses occur at the wall. Vertical cracks will appear when sufficient elastic energy can be released to overcome the fracture energy at the crack tip. Depending on the initial stress state of the formation, vertical crack propagation can turn into horizontal cracks. In general crack propagation will turn towards the lowest principle stress. These conditions can occur in shallow, over-consolidated formations. Due to unloading, f.i. by uplifting and erosion or after a glacial period, the horizontal stresses will be higher than the vertical stresses. Horizontal cracks are reported in rock at shallow depths (Veatch et al, 1989), but at depths below 600 m mainly vertical cracks will appear due to the change in primary stress field orientation.

Figure 3. Subsurface dredging pilot test

Figure 4. Water Soil Flume at Deltares

Crack propagation in rock, clay and sand is basically the same process, but with different constitutive behavior with respect to the stress-strain relations, heat and liquid transport. In Figure 5a the vertical elastic stress near the crack tip of a penny shaped crack is depicted (dashed line) with a singularity of the vertical stress at the crack tip given by (Broek, 1982):

$$\sigma_y = \frac{K_I}{\sqrt{2\pi r}} \qquad K_I = \frac{2}{\pi}\sigma\sqrt{\pi a} \tag{1}$$

In which K_I is the stress intensity factor in mode I (tensile stress loading), a is the radius of the crack and σ the external tensile stress.

The infinite stress at the crack tip will be reduced by plastic yielding of the soil around the crack tip with a maximum stress of about 3 times the yield strength (plane strain condition). The plastic zone is depicted by the two vertically orientated oval-hooped loops, and is independent of the size of the crack. The loading of the crack tip by an external tensile stress σ is equivalent with an internal pressure σ inside the crack (see Figure 5b).

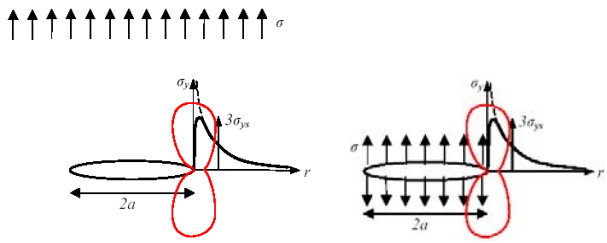

a external b internal

Figure 5. Stresses near crack tip

The crack will grow by failure in the plastic zone around the crack tip. This failure is initiated by the opening of micro cracks followed by an increase in size until they approach their neighbors. They never touch their neighbor and try to overlap resulting in shear failure between two micro cracks (see Figure 6). This process of brittle crack propagation is typical for granular soils like sand, clay and sedimentary rock (Winterwerp & Van Kesteren, 2004). Figure 7 shows an example of the crack propagation of a clay sample in tensile loading with a constant strain rate. From the initial flaw at the boundary (black dot in Figure 7) a radial pattern is created during the crack propagation due to the shear failure between cracks.

The brittle crack propagation will only occur when the strain rate is sufficiently low to assure a drained condition in the plastic zone around the crack tip. The opening of micro cracks depends on the flow of pore water towards the micro cracks. When higher strain rates are applied, there is less

time for pore water movement and the pressure in the micro crack will drop. When the pressure is dropped to the level of tensile stresses in the plastic zone (see Figure 5), micro cracks do not grow and large strains will occur at undrained conditions in the plastic zone around the crack tip. In Figure 8 an example is shown of tensile tests with a high strain rate on the same type of clay sample as in

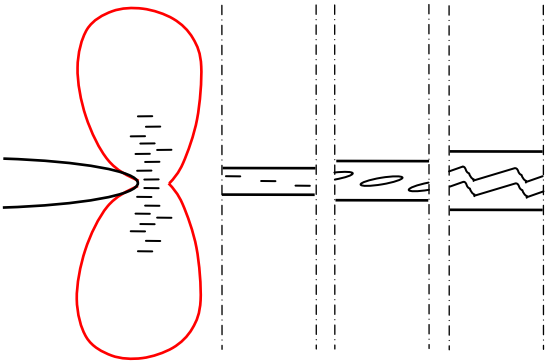

cross sectional crack tip opening and failure

Figure 6. Failure in plastic zone crack tip

Figure 7. The large strains are visible with necking in the middle (Figure 8a).

The final rupture occurs by shearing in the necking area and large voids will be formed as shown with the failure surface in Figure 8b. This is the ductile failure mode in tension with tensile failure stresses at about the undrained shear strength of the clay (see Winterwerp & Van Kesteren, 2004).

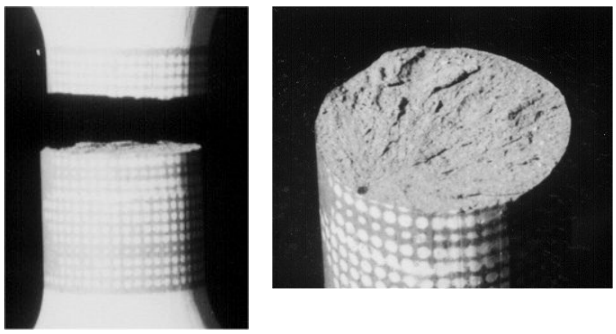

Figure 7. Brittle crack propagation in clay (low strain rate)

As shown above, it is important to acknowledge that crack propagation in porous materials will change from brittle to ductile behavior depending on the drainage in the deformation area at the crack tip. The drainage is determined by the permeability, skeleton compressibility, pore fluid compressibility and the propagation velocity. In clay, the permeability is low (10^{-12} m/s) and skeleton compressibility is high (10^{-8} to 10^{-7} m^2/N) which results in a transition from brittle to ductile crack propagation at low propagation velocities. The same holds also for the oil sands, where the viscosity of the bitumen is about 10^6 times that of water. The intrinsic permeability of the sand is on the order of 10^{-10} m^2 to 10^{-11} m^2, which translates into a hydraulic permeability of 10^{-11} m/s to 10^{-12} m/s, the same level as clay. The skeleton of dense sand has a skeleton compressibility of 10^{-8} m^2/N, which is similar to stiff clay. Given the same range of permeability and compressibility, the clay analog can be applied for hydraulic fracturing in oil sands, with ductile behavior at the crack tip and larger crack opening displacement (see Fig. 8) compared to the brittle crack in Figure 7. The oil sands are densely packed, which results in tendency to dilate when shear is applied. Dilation will only occur when pore fluid is flowing into the dilation area. Due to the low permeability the pore pressure drops in the deformation area at the crack tip and isotropic effective stress increases. When this stress reaches the critical state level, where shear deformation is possible without volume change, undrained conditions apply and the crack propagation will be ductile as shown in Figure 8b. Experimental hydraulic fracturing on oil sands (Pak et al., 2008) shows a quite different cracking process than normally occcurs in rock. And might confirm the ductile crack propagation in oil sands.

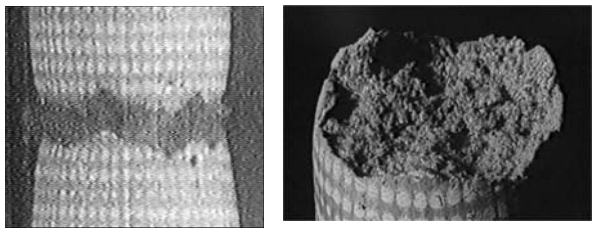

a large strains b ductile crack surface

Figure 8. Ductile crack propagation in clay (high strain rate)

The pore pressure drop in the deformation area at the crack tip may create gas bubbles in the pore system which increases the pore fluid compressibility tremendously, in which case crack propagation will be brittle. The formation of gas bubbles depends on the initial saturation level of gasses in the pore water or bitumen, and the initial pore pressure at depth.

CONCEPT OF INJECTION BY HYDRAULIC FRACTURE

When from a single point, fluid is injected into a soil formation, different failure modes can appear: a spherical cavity, a cylindrical channel upward and horizontal hydraulic fracturing. (see Figure 9). The spherical cavity requires an injection pressure equal to the sum of the isotropic pressure in the soil at depth and the excess pressure necessary to create the cavity. Given the low permeability for the bitumen in the oil sand an undrained deformation of a cavity or channel is expected. The limit pressure P_L is given by (Vesic, 1972):

$$P_L = p + \xi c_u \left[1 + \ln\left(\frac{E}{2(1+\nu)c_u} \right) \right] \qquad (2)$$

In which p is isotropic pressure at depth, c_u the undrained shear strength, E the Youngs modulus, ν the Poisson ratio (0.25) and ξ is 4/3 for spherical cavity and 1 for channels.

A typical ratio of E/c_u is about 100 to 500, which yields for the excess pressure (P_L- p) a range of 6 to nine times the undrained shear strength for the cavity. The excess pressure for a channel is always ¾ smaller than for the cavity and therefore a cavity can bifurcate into a vertical channel, especially when the vertical stress is lower than the horizontal stress.

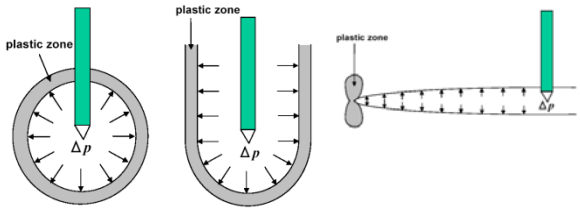

spherical cavity channel hydraulic fracturing

Figure 9. Failure modes at injection point

For hydraulic fracturing an initial crack must be present, which can be defined by the diameter of the injection well. In order to extend the inital crack, horizontal jets can be applied before the mud is injected. Growth of the initial crack occurs when the fracture threshold energy is achieved. The fracture energy will be much less for brittle crack propagation than for ductile crack propagation. Assuming a ductile process, the fracture energy R_f can be estimated with:

$$R_f \approx 2c_u \; pcf \; \delta_f \;\; \text{[N/m]} \qquad (3)$$

In which δ_f is the tensile failure distance for a free fracture surface and pcf is the plastic constraint factor that is related to the stress condition in the plastic zone of the crack tip and Poison ratio. The plane strain condition applies for a penny-shaped crack and the pcf is given as a function of the Poison ratio:

$$pcf = 1 - 4\upsilon + 4\upsilon^2 \qquad (4)$$

The Poison ratio ν is for oil sands about 0.25, which results in a pcf of 2.
The excess pressure for crack growth can be determined with Eq.(1), including the plastic zone in the crack tip:

$$K_I = \frac{2}{\pi}\sigma\sqrt{\pi(a + r_p)} \qquad (5)$$

Where r_p is the size of the plastic zone given by:

$$r_p = \frac{K_I^2}{2\pi(2c_u pcf)^2} \qquad (6)$$

Eq.(5) and (6) combined gives a relation between the excess pressure in the crack and the stress intensity factor K_I. Due to the elastic energy outside the plastic zone in the crack tip, energy will be released when crack growth occurs. The energy release must be sufficient to overcome the fracture energy R_f. The energy release rate G_I in N/m is for the plane strain condition given by:

$$G_I = (1 - \nu^2)\frac{K_I^2}{E} \qquad (7)$$

In Figure 10 the energy release rate is shown as a function of the excess pressure for crack growth for an initial radius of 0.2 m and 1 m. The computation is done with c_u = 100 kPa and E = 10 MPa. The maximum excess pressure, where no crack growth occurs, with only ductile deformation, is given by (see dashed line in Fig.10):

$$\sigma_{\max} = \pi\sqrt{2}c_u pfc \approx 900 \text{ kPa} \qquad (8)$$

The maximum excess pressure is about 9 times the undrained shear strength, which is the same level as the limit pressure for a spherical cavity.

In Figure 10 also four values of fracture energy R_f are shown: 3, 10, 30 and 100 kN/m. The crossing of these levels with the solid lines yields the minimum excess pressure for crack growth under those conditions.

These crossings are shown in Figure 11, where the excess pressure in the crack is given as function of the radius of the crack for these same four values of fracture energy. When the crack starts growing the required excess pressure is dropping.

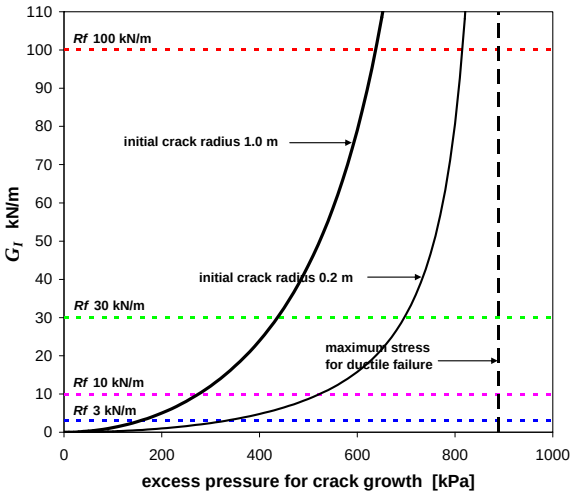

Figure 10. Energy release rate as function of excess pressure

When the injection is done at the interface of oil sands and the base rock (Devonian Limestone, Flach, 1984), the amount of fracture energy could be reduced by a maximum factor of 2. In Figure 12 the interface is shown assuming a much higher Young's modulus for the Devonian Limestone than for the oil sands. During crack propagation the limestone will release elastic energy, but does not consume plastic deformation energy. Therefore the plastic zones are mainly in the oil sands, which reduce the fracture energy by a factor 2.

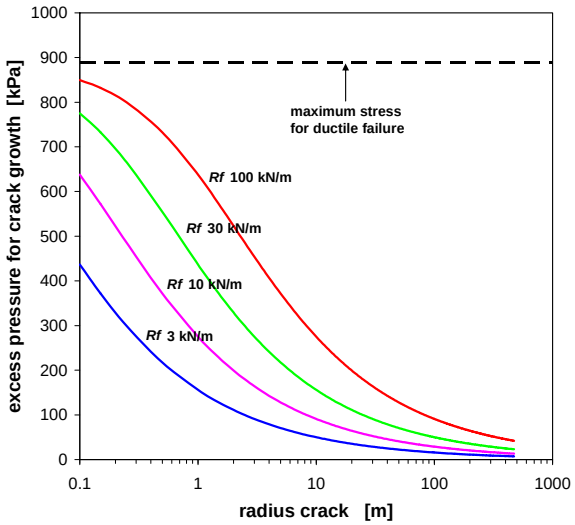

Figure 11. Excess pressure for crack growth

Besides the excess pressure for crack growth, there is also excess pressure required for the flow of mud into the crack. For MFT with yield strength of 10 Pa and viscosity of 50 mPas the excess flow pressure is about 500 Pa and therefore orders of magnitude less than the excess pressure for the crack propagation.

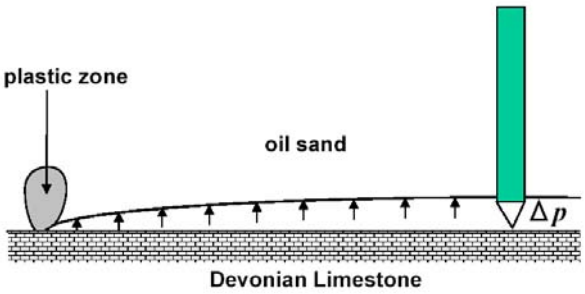

Figure 12. Hydraulic fracturing at interface

From these theoretical considerations the following can be concluded:

- Hydraulic fracturing will occur when the excess pressure for crack propagation is much less than the pressure needed for spherical cavity or channels.

- The undrained condition applies for crack propagation in oil sands, given the very low permeability and ductile cracks are expected.

- When the fracture energy of oil sands is known the radius of the initial crack can be determined by limiting the excess pressure with the undrained shear strength of the oil sand.

EXPERIMENT IN WATER SOIL FLUME

Within the WINN innovation program an experimental study was granted to perform a proof of concept for lifting land by injection of mud through hydraulic fracturing between strata. This test was executed in the Water Soil Flume at Deltares.

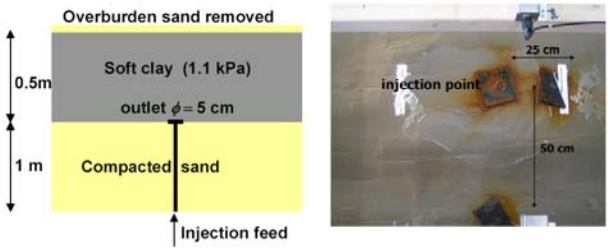

a soil layers b elevation probes

Figure 13. Test set-up in Water Soil Flume

The set-up is shown in Figure 13, in which a soft illite clay layer of 0.5 m is overlaying a dense sand layer of 1 m. A temporarily overburden of 0.5 m of sand has been applied to consolidate the soft clay layer to a thickness of 0.4 m. After removal of the overburden a shallow layer of 10 cm sand remained. The injection system was feeding from below to prevent leakage to the surface. The elevation of the surface was measured at three locations as indicated in Figure 13b: at the injection point, 25 cm from the injection point lateral and 50 cm from the injection point in flume direction. The elevation results are shown in Figure 14 as function of time and as function of distance from the injection point. Within the first 2 minutes (see Fig.14a) an increase in elevation was measured in all locations, showing the initiation of a horizontal crack up to at least 0.5 m. After 2 minutes the elevations were increasing differently with the highest level at the injection point, forming a conical shaped dome with a slope of 7% resulting in a total volume of 90 to 100 liters (see Fig. 14b). In Figure 15 the elevations are shown in time and distance.

The outlet diameter was 5 cm with a horizontal flow of kaolin mud (yield strength 20 Pa) with a constant discharge of 5 l/min.

The relatively steep slope of 7% is due to the low strength of the soft clay (1.1 kPa). The undrained shear strength of oil sand is much higher and about 100 to 1000 kPa. It is expected that the slope in oil sand could vary between 0.5% to 2%.

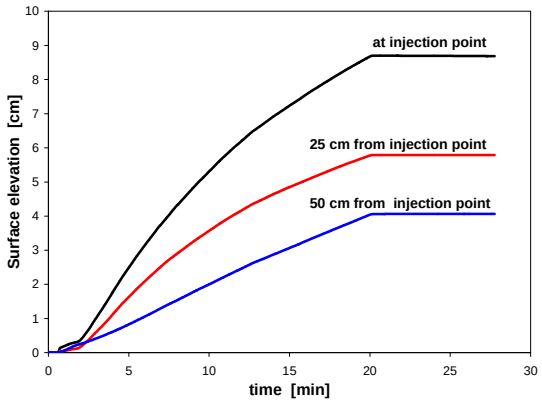

a elevation in time

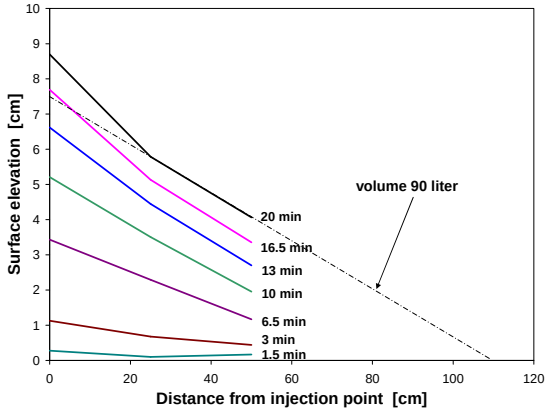

b elevation with distance from injection point

Figure 14. Elevation measurements

After the test, the formed dome was penetrated with a conductivity probe on 4 locations. The injected kaolin mud was treated with salt (NaCL) and had a salinity of 13.4 ppt (w); the soft clay layer had salinity less than 4 ppt (w). Measuring the conductivity allows to determine where the

injected mud was going. In Figure 16 the profiles are shown with depth of the top surface of the sand layer at the same positions of the elevation measurements (see Fig. 14a).

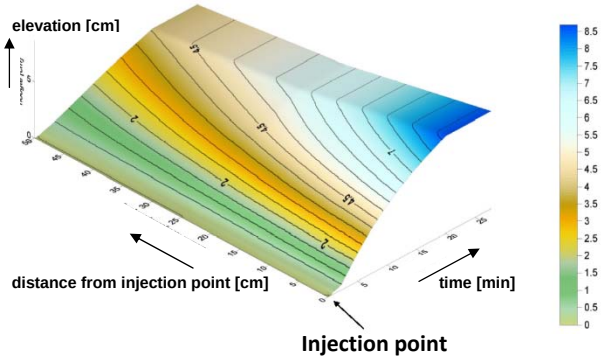

Figure 15. Elevation measurements

The forth location was 90 cm away from the injection point. The profiles show that in the soft clay layer no increase of salinity occurs and that only a higher salinity was measured in the mud layer. Fifty centimeters from the injection point the salinity is dropping and at ninety centimeters from the injection point no mud was detected.

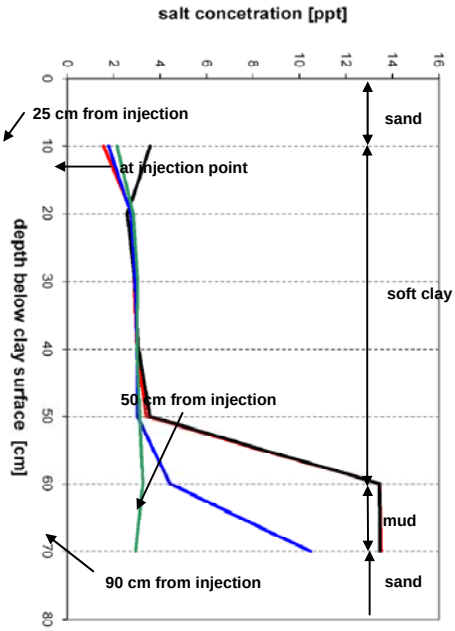

Figure 16. Salinity profiles

CONCLUSIONS

Hydraulic fracturing will occur when the excess pressure for crack propagation is much less than the pressure needed for spherical cavity or channels.

The undrained condition applies for crack propagation in oil sands, given the very low permeability and ductile cracks are expected.

It is important to control the pressure near the injection point to prevent channel formation.

When the fracture energy of oil sands is known the radius of the initial crack can be determined by limiting the excess pressure with the undrained shear strength of the oil sand.

From the experiment in the Water Soil Flume it can be concluded that hydraulic fracturing occurred at the initial stage of mud injection, followed by filling a conical dome below the soft clay that expanded radially with a slope of 7%..

For the oil sand the undrained strength is much higher (about a factor 100 – 1000) than the soft clay in the experiment, and slopes between 0.4% to 2 % are expected..

REFERENCES

Flach, P.D., 1984, “Oil sands geology –Athabasca deposit north”, Geological Survey Department, Alberta Research Council. Edmonton, Alberta, Canada.

Pak, A and Chan, D.H., 2008, “Numerical modeling of hydraulic fracturing in oil sands”, Scientia Iranica, Vol.15, No.5, pp 516-535.

Veatch, R.W., Moshovidis, Z.A. and Fast, C.R., 1989, “An overview of hydraulic fracturing”, in Recent Advances in Hydraulic Fracturing, SPE Monograph, 12, pp 2-38

Vesic, A.S., 1972, “Expansion of cavities in infinite soil mass”, Jnl. Soil Mechanics Foundation Div., Proc. ASCE, vol. 98, nr. SM 3, pp 265-290.

Winterwerp, J.C. and Van Kesteren, W.G.M., 2004, “Introduction to the physics of cohesive sediment in the marine environment”, Developments in Sedimentology 56, Elsevier.

METHODS TO REDUCE PRODUCTION OF OIL SANDS FLUID FINE TAILINGS

Baki Ozum[1] and J. Don Scott[2]
[1]Apex Engineering Inc., Edmonton, Alberta, Canada
[2]University of Alberta, Edmonton, Alberta, Canada

ABSTRACT

The Clark Hot Water Extraction process uses caustic *NaOH* as an extraction process aid which disperses the clay-shale seams and layers in the oil sands and results in the formation of fluid fine tailings. These fluid fine tailings have poor settling and consolidation properties. The process also increases the salinity, specifically Na^+ concentration, of the recycled release water. In Alberta, the oil sands toxic mature fine tailings inventory exceeds 800,000,000 cubic metres and its volume is steadily growing as the present mines are expanded and new ones opened. To manage the environmental impact of the oil sands tailings the Energy Resources Conservation Board has issued Directive 074 which requires that oil sands mining companies develop measures to reduce the amount of fluid fine tailings being produced by 50% by 2013. One alternative to reduce the amount of fluid fine tailings being produced is to use an extraction process that would reduce the amount of dispersion of the clay-shale materials. The oil sands industry previously has implemented non-caustic extraction processes which cause less dispersion and produce tailings with improved settling and consolidation characteristics. These processes; however, were later modified to some version of the Clark Hot Water Bitumen Extraction process.

The performance of alternative extraction process aids which cause less dispersion has been evaluated in our laboratories. In these tests *CaO* and ozone were used to adjust the *pH* of the ore-water slurry and produce surfactants from bitumen asphaltenes respectively. Increasing the *pH* of the ore-water slurry with *CaO* instead of *NaOH* eliminates Na^+ accumulation in the process water and reduces the clay dispersion. The performance of biodiesel, such as fatty acids methyl esters, as a surfactant additive in the extraction process after conditioning the ore-water slurry with *CaO* was also investigated. It was observed that *CaO* and ozone as well as *CaO* and biodiesel could be used as extraction process aids replacing *NaOH*; by which the salinity of the recycled release water and the production of fluid fine tailings could be reduced.

INTRODUCTION

Conventional Bitumen Extraction, Froth Treatment and Tailings Disposal Practices

In northern Alberta, bitumen is produced from surface mineable oil sands by using some version of the Clark Hot Water Extraction (CHWE) process which was discovered by Dr. Karl A. Clark and his coworkers at the Alberta Research Council (Clark and Pasternack, 1932; Clark 1939); a schematic of which is depicted in Figure 1.

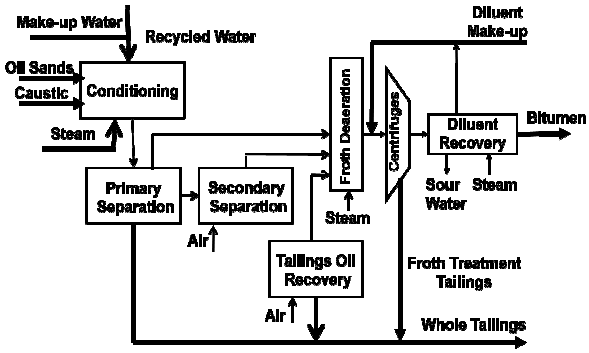

Figure 1. Process flow diagram for a typical CHWE process.

A typical oil sands bitumen extraction plant is composed of: (i) ore-water slurry preparation and extraction; (ii) froth treatment; and (iii) tailings disposal plants. In the ore-water slurry preparation and extraction plant, bitumen is separated from the oil sands and floated forming a froth composed of about 60% bitumen, 30% water and 10% solids. In the froth treatment plant bitumen is separated from the froth using naphthenic or paraffinic solvents depending on the downstream method for the processing of the bitumen (Long et al. 2002; Romanova et al. 2003; Shelfantook, 2004). Bitumen produced using naphthenic solvents has a higher asphaltenes content (about 18%) in

comparison to those produced using paraffinic solvents (about 8%). Bitumen with a higher asphaltenes content has a high viscosity and for pipeline transportation requires separation of asphaltenes or viscosity reducing treatments. Also, bitumen with higher asphaltenes content is suitable for coking, producing coker gas oil which is upgraded to synthetic crude oil by hydrotreating processes. Bitumen produced using paraffinic (i.e. *i-*C_5, C_5 and C_6) solvents in froth treatment is of lower asphaltenes content and of lower viscosity; which is suitable for pipeline transportation and more acceptable for further upgrading to refined products. Tailings produced at the froth treatment plant are about 10% of the total tailings; with a composition which depends on the type of solvent used in the froth treatment plant (about 10% hydrocarbons by paraffinic and <4% hydrocarbons by naphthenic solvents). Regardless of the type of solvent used for froth treatment, bitumen with minimum clay and water contents is desired for further upgrading.

Production of Mature Fine Tailings

Oil sand contains minor amounts of clay particles in the water layer surrounding the quartz sand grains. The great majority of clay minerals in the tailings come from the indurated clay-shale discontinuous seams and layers in the oil sands ore bodies. These dense but weak clay-shale materials are broken up during the mining process and the larger more indurated pieces are screened out as reject materials. In the bitumen extraction process, the clay-shale pieces are further broken down into clay aggregates and lumps and some clay lumps are dispersed into small clay booklets and flakes. The extent of clay dispersion in the extraction process depends on the additives used to promote bitumen extraction efficiency. Some additives used in the extraction process effectively disperse much of the clay aggregates into clay flakes smaller than 2 μm which have large active clay surfaces.

Almost all of the oil sands plants are using caustic *NaOH* or sodium salts of weak acids as extraction process aids to maintain the *pH* of the ore-water slurry at about 9.0-10.5. At elevated *pH* the asphaltic acids, which are partly aromatic, contain oxygen functional groups such as phenolic, carboxylic and sulphonic types, become water soluble and act as surfactants reducing the surface and interfacial tensions and promote the efficiency of the bitumen extraction process (Moschopedis et al. 1977 and 1980). The use of *NaOH* or sodium salts of weak acids in the extraction process provides the most optimum conditions to maintain high bitumen extraction efficiency; however, it produces tailings with poor settling and consolidation properties and increases the salinity, specifically the Na^+ concentration, of the release water (Allan, 2008a, 2008b; MacKinnon, 2001; MacKinnon and Sethi, 1993).

Existing ore-water slurry based bitumen extraction processes produce about 1.5 m^3 of tailings per barrel of bitumen, which tailings is composed of sand, silt, clay, water and residual bitumen. Tailings discharged from the extraction plant segregate during deposition because of low solids contents. When the tailings are discharged into tailings ponds the sand particles segregate and settle out to form dykes and beaches, while the fine particles (<45 μm size) are carried with the run-off water into the ponds. Over a two year period the fine particles settle and form Mature Fine Tailings (MFT), which is a stable suspension of fluid fine tailings that has undergone settlement and compression to about 33% solids content by mass. Further densification of the MFT is a very slow process; as a result of which all tailings produced and discharged into tailings ponds without any treatment contribute to the accumulation of MFT.

ERCB Directive 074 and Oil Sands Industry's Tailings Management Plans

Accumulation of MFT is considered as an environmental liability; both the oil sands industry and government regulatory agencies have committed to reduce the production of MFT as outlined in the ERCB Directive 074 (ERCB, 2009).

Oil sands operators have submitted their plans to comply with the Directive 074. Production of Nonsegregating Tailings (NST), also called Composite or Consolidated Tailings (CT), with $CaSO_4$ or CO_2 additives to prevent segregation remains one of the major technologies to reduce MFT accumulation. Shell Energy Canada is planning the implementation of nonsegregating tailings at a commercial scale. The timing of which recognizes the needs for testing, compilation, data analysis and detailed design for a commercial facility. Syncrude Canada Ltd. is proposing the implementation of MFT centrifuging technology to complement CT as a fines management technology to reduce the MFT inventory. Centrifuging MFT accelerates the release of water from the MFT and produces a soft, clay-rich soil

termed “centrifuge cake”. Syncrude proposes to sand cap the resulting centrifuge cake deposit for reclamation as a dry landscape feature. The implementation of MFT centrifuging technology is proposed to be executed in three stages, commencing in 2012 and in increased capacity in 2018. Suncor Energy Inc. is proposing a Tailings Reduction Operations (TRO) to reduce MFT accumulation as an alternative to CT production. The TRO process is based on the addition of a polymeric flocculent to MFT and spreading it in a thin layer to dry. The product of the Tailings Reduction Operation is a clay material that may be reclaimed in-place or rehandled to mine dumps. Canadian Natural Resources Ltd. is in the start-up phase of operations and has proposed to develop and implement fines capture technology with a target of 2015. Two technology options are being investigated; the use of thickeners to make NST and dewatering MFT by treating it with an organic polymer and CO_2.

The technologies proposed by the oil sands players have appeared as novel and ambitious processes for the management of their MFT inventory; cost effectiveness and practicality of which appear to be the foremost constraints.

All oil sands operators envision the use of end pit lakes at mine closure. Any fluid tailings remaining at this time will be returned to the mined pits and capped with water. It is planned that these lakes will, with time, become viable ecosystems that will sustain plant and aquatic life. Environmental concerns exist with this concept and end pit lakes have not yet been approved by the ERCB. Syncrude has been conducting long-term field tests to develop and prove out this technology.

Previous Effort to Reduce MFT Production

During the last five decades significant research and development efforts have been devoted for altering the bitumen extraction and the tailings disposal practices. Non-caustic, low temperature (or low energy) extraction (LTE) processes were developed and implemented commercially at two oil sands plants. In both plants thickeners were also used for the thickening of Cyclone Overflow to improve the thermal efficiency of oil sands plants (Burns et al. 1998). However, commercial operations of the LTE processes attained lower than expected bitumen extraction efficiency. Both temperature and *pH* were increased to boost the extraction efficiency, by which the LTE processes have been reduced to some version of the CHWE process which is the process developed in the 1930s.

Another remarkable effort to reduce MFT inventory was the development of the nonsegregating tailings (NST) process also called Composite or Consolidated Tailings (CT) which was implemented commercially at two oil sands plants (Caughill, Morgenstern and Scott, 1993; Chalaturnyk, Scott and Ozum, 2002; Matthews et al. 2002); a schematic of which is depicted in Figure 2. Production of CT requires sufficiently high solids and fines contents, which is accomplished by the use of cyclones separating the whole tailings into Cyclone Underflow composed of high solids contents and low fines content (>55% solids and <7% fines) and Cyclone Overflow composed of low solids content with a high fines content (<30% solids and >50% fines). A nonsegregating CT mixture is produced by blending Cyclone Underflow and existing MFT, usually at a sand-fines ratios (SFR) of 4 to 5, with the addition of gypsum ($CaSO_4$) as a coagulant additive to prevent segregation.

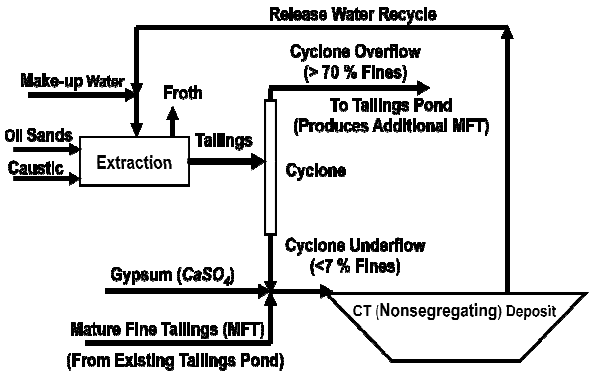

Figure 2. CT production process.

CT production technology accelerates tailings densification and reclamation, however, the continuous accumulation of Ca^{2+} and SO_4^{2-} ions detrimentally affects recycled release water chemistry (Allan 2008a, 2008b; MacKinnon, 2001). Implementation of the CT production process doesn’t significantly reduce the MFT inventory since additional MFT is produced from the Cyclone Overflow effluent. Also, the CT process doesn’t improve the thermal energy efficiency of the oil sands plants because of the discharge of warm Cyclone Overflow into the tailings ponds. Furthermore, CT production using gypsum as a coagulent may cause H_2S emissions from the tailings ponds by anaerobic reduction of SO_4^{2-} by the residual bitumen in the tailings.

In summary, after five decades of effort the oil sands industry is still using the CHWE process which operates at elevated *pH*, causes an increase in the salinity of the recycled release water and produces tailings with poor settling and consolidation properties. Novel bitumen extraction and tailings disposal processes are needed to attain high bitumen extraction efficiency, especially for the processing of low grade ores with low bitumen and high fines contents.

REDUCTION OF MFT PRDUCTION

Methods to Reduce Production of Mature Fine Tailings

MFT production could be reduced by:

(i) reducing the extent of clay dispersion in the extraction process by which the tailings produced at the extraction plant would posses improved geotechnical properties and reduce the formation of MFT; and,

(ii) disposing the fines fraction of the tailings as nonsegregating tailings (NST); this could be done by adding sand into the fines fraction and using a chemical additive to promote nonsegregating behaviour of the NST product.

In other words, reduction of MFT production would be possible by producing tailings with fewer fines and with improved settling and consolidation properties in the first place; and then disposing the tailings as a NST mixture. Therefore, reduction of MFT production would be possible by developing novel bitumen extraction and NST production processes as well as satisfying release water chemistry constraints.

Bitumen Extraction Processes Using *CaO* & Ozone (O_3) or *CaO* & Biodiesel (*BD*) and NST Production Processes using *CaO* or *CaO* & CO_2 to Reduce MFT Production

Bitumen extraction involves disintegration of the oil sands ore matrix into an ore-water slurry followed by the liberation/mobilization and aeration of bitumen to form an oil rich froth. Extraction temperature, hydrodynamics and process water chemistry are the major factors affecting the performance of the extraction process. Reduction of the surface and bitumen-water interfacial tensions increases the bitumen recovery efficiency by promoting disintegration of the oil sands ore structure, detachment of bitumen from the sand and attachment of bitumen to air bubbles (Masliyah et al. 2004; Kasperski, 2001).

As an alternative to the CHWE process, our research was focused on the use of *CaO* as a *pH* adjusting additive replacing caustic *NaOH*. Furthermore, to promote bitumen extraction efficiency especially for the processing of low grade (low bitumen and high fines contents) ores, the production of additional surfactants by oxidation of asphaltenes with O_3 and the use of Biodiesel (*BD*) as surfactant additive were also investigated (Moschopedis and Speight, 1974; Babadagli and Ozum, 2010; Ozum and Scott, 2010; Babadagli et al. 2008).

In these tests *BD* derived from fatty acids, such as canola and tall oil fatty acids methyl esters (C_nH_m-$COOCH_3$; $m<2n+1$), were used. Tall oil is a by-product of the pulp & paper mills using the bleached Kraft process. *BD* possesses both hydrophobic hydrocarbon (C_nH_m) and hydrophilic ester (-$COOCH_3$) functional groups, by which they perform as a surfactant (reducing the bitumen-water interfacial tension) promoting bitumen recovery efficiency.

It is known that the ion exchange reaction between Ca^{2+} and clay reduces the swelling of clay in water and causes the formation of a yield stress in the fines-water matrix by flocculating clay particles which aids in preventing segregation of fines from sands (Rogers, 1953; Speight and Moschopedis, 1977/78):

$$2Clay-Na+Ca^{2+} \leftrightarrow (Clay)_2 Ca+2Na^{+} \quad [1]$$

Formation of the yield stress however requires greater than a critical fines-water ratio (more correctly the clay-water ratio) which is defined as the ratio of *fines*/(*fines*+*wate*r) on mass basis (or *clay*/(*clay*+*water*)). This known fact was probably the discouraging factor in considering *CaO* (*Ca(OH)*$_2$ in an aqueous environment) as an extraction process additive.

When *CaO* is used as an additive as an extraction process additive to adjust the *pH* of oil sands-ore water slurry, at about 100 to 300 mg-*CaO*/kg-ore dosages, it works similar to the caustic *NaOH* additive used in the CHWE process. The advantages of using *CaO* are that it reduces Ca^{2+} concentration in the process water by the ion exchange reaction with *Clay-Na* as expressed in Equation 1 and converts water soluble calcium and

magnesium bicarbonates to calcium and magnesium carbonates with limited solubility in water:

$$Ca,Mg(HCO_3)_2 + Ca(OH)_2 \leftrightarrow 2Ca,MgCO_3 + 2H_20 \quad [2]$$

When *CaO* is used as an extraction process additive at 150 mg-*CaO*/kg-ore dosage into an ore-water slurry made of equal amounts of ore and water, the amount of Ca^{2+} addition is about 120 gm-Ca^{2+}/L-process water. Experiments performed using oil sands ores of different grades showed that release water Ca^{2+} concentrations were in the range of 10 to 20 mg\L. Because of the chemical reactions expressed in Equations [1] and [2], the use of *CaO* as an extraction process additive at 50 to 300 mg-*CaO*/kg-ore dosages decreases the Ca^{2+} concentration in the release water. The final composition of the release water is determined by the chemical equilibrium (thermodynamics) of the system which would be influenced by the initial compositions of the process water and oil sands mixture. When *CaO* is used at 50 to 300 mg-*CaO*/kg-ore dosages acceptable bitumen extraction efficiencies are attained. Furthermore, bitumen extraction efficiency could be increased by slight modifications in the hydrodynamics of the primary and the secondary extraction processes. The advantages of using *CaO* as an additive in the extraction process would be improved release water chemistry and reduced clay dispersion; which would produce tailings with improved geotechnical characteristics reducing MFT production (Scott et al. 2007) and potentially produce bitumen froth with lesser clay content (Jiang et al. 2010)

Comparison of Extraction Process Aids; a Case Study

Bitumen extraction tests were performed using a Denver D-12 Flotation Cell apparatus (operating at 800 rpm) to compare the performance of *CaO*, *NaOH* and *Na*-Citrate additives as bitumen extraction process aids. In all tests artificial process water (APW) was used; the composition of which is presented in Table 1.

Extraction Tests Using High Grade Ore

A high grade ore of 11.6% bitumen, 4.5% water, 83.7% solids, MBI = 136mL 0.006N/100g, D_{50} = 140μm, 20.3% <44μm (fines) was used in these tests. Extraction tests were performed by *CaO* addition at 150 ppm, *NaOH* addition at 300 ppm and *Na*-Citrate addition at 500 ppm on an ore mass basis (ppm is equivalent to mg/kg).

Table 1. Artificial process water chemistry.

	Total Alkalinity		Cations			Anions				
	(mg CaCO3/L)		(mg/L)			(mg/L)				
pH	Alkal	Hard	Na	Ca	Mg	Cl	HCO3	SO4	CO3	OH
8.4	324	130	332	30	14	214	375	255	10	0

Bitumen extraction tests were performed at 50°C temperature by conditioning (10 minutes digesting of 500 g ore in 150 g water with process additive and air intake), primary extraction (450 mL additional water, 10 minutes digestion, no air intake) and secondary extraction (350 mL additional water, 5 minutes digestion, with air intake) extraction steps. The air intake was caused by the vacuum created by the rotor which was presumed to be the same in all tests. Bitumen, water and solids contents of the froths produced by the primary and the secondary extractions were analyzed using the Dean-Stark extraction method. The residual material in the cell was transferred to jars (middling and tailings fractions) and the release water recovered from these jars was submitted to water chemistry analysis.

Extraction test results for the high grade ore are presented in Table 2 and the release water chemistry corresponding to these tests is presented in Table 3. Data presented in these tables show that *NaOH* additive provides higher extraction efficiency in the primary extraction. However, all additives provide similar overall extraction (primary plus secondary) efficiencies and solids/bitumen (S/B) ratios. Water chemistry data suggest that *CaO* dosage could be increased beyond 150 ppm. The *CaO* additive produces release water with the lowest Na^+ and $HCO3^-$ concentrations, which indicates that *CaO* addition reduces the extent of clay dispersion and improves the release water chemistry. The photographic images of the middling (upper jars) and the tailings (lower jars) presented in Figures 3 and 4 support the water chemistry results.

Similar tests were performed allowing air intake in the primary extraction step. Extraction test results and the corresponding release water chemistry data are presented in Tables 4 and 5. Comparison

of the data presented in Tables 2 to 4 suggest that if air intake is allowed in the primary extraction step the difference between the performance of *CaO* and *NaOH* additives becomes insignificant.

Table 2. Extraction test results, high grade ore.

		Primary Froth		Secondary Froth		Bitumen	Total
		Bitumen		Bitumen		Toluene	Bitumen
Test		Recovery	S/B	Recovery	S/B	Wash	Recovery
ID	Additive	(%)	Ratio	(%)	Ratio	(g)	(%)
A-8	Blank	41.38	0.27	53.20	0.85	1.46	94.6
A-9	CaO	46.34	0.27	48.51	1.07	1.28	94.8
A-12	CaO(*)	64.91	0.27	30.11	1.11	0.95	95.0
A-10	NaOH	61.88	0.22	35.81	0.73	1.06	97.7
A-11	Na Citrate	62.19	0.25	33.99	0.98	1.17	96.2

(*) Longer retension (10 minutes) time.
S/B: Solids to bitumen ratio.

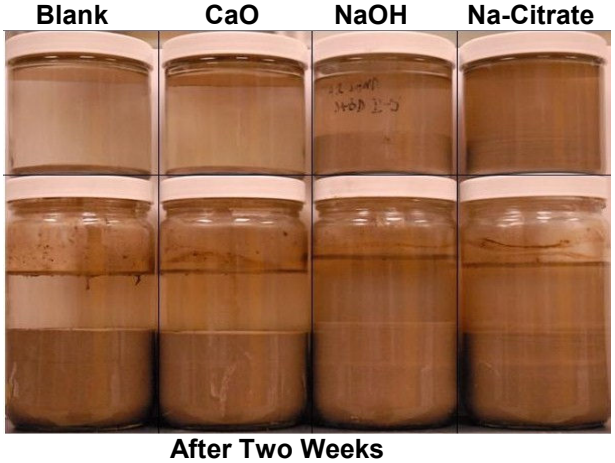

Figure 3. Middlings (top) and tailings produced with different process additives, low grade ore.

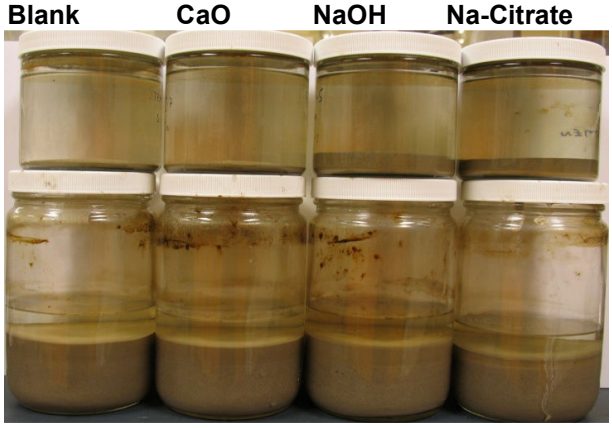

Figure 4. Middlings (top) and tailings produced with different process additives, low grade ore.

Extraction Tests Using the Low Grade Ore

A low grade ore of 10.4% bitumen, 4.72% water, 84.9% solids, MBI = 148mL 0.006N/100g, D_{50} = 86µm, 24.9% <44µm was used in these tests. Extraction tests were performed by *CaO* addition at 150 ppm, *NaOH* and *Na*-Citrate addition both at 600 ppm on an ore mass basis. In these tests the experimental procedure described in the extraction tests using high grade ore was also followed.

Table 3. Release water chemistry (for the tests presented in Table 2).

Test			Conduc.	Alkalinity (*mg CaCO3/L*)			Cations *(mg/L)*			Anions *(mg/L)*	
ID	Additive	pH	*(mS)*	Total	CO3	HCO3	Na	Mg	Ca	Cl	SO4
APW	-	8.7	1.797	288	14	274	340	13	17	179	229
A-8	Blank	8.4	1.788	242	4	238	333	11	19	186	248
A-9	CaO	8.4	1.769	229	2	227	334	10	17	187	251
A-12	CaO(*)	8.5	1.755	241	8	233	338	11	20	185	255
A-10	NaOH	8.8	1.900	298	26	272	384	5	6	184	247
A-11	Na Citrate	8.0	1.871	349	0	349	372	13	22	183	247
(*) Longer residence (10 minutes) time.											
AWP: Artifical process water.											

Extraction test results for the low grade ore are presented in Table 6 and the corresponding release water chemistry is presented in Table 7.

Data presented in Table 6 show that extraction efficiency with the use of *CaO* at 150 ppm dosage is approximately 2.0% less than that of the *NaOH* or *Na* citrate additions at 600 ppm. The difference in extraction efficiencies could be reduced by allowing air intake into the primary extraction, increasing CaO dosage (increasing pH) or using O_3 or *BD* additives after conditioning the ore-water slurry with *CaO* (Ozum and Scott, 2010).

Table 4. Extraction test results with high grade ore, air intake in primary extraction.

		Primary Froth		Secondary Froth		Bitumen	Total
		Bitumen		Bitumen		Toluene	Bitumen
Test		Recovery	S/B	Recovery	S/B	Wash	Recovery
ID	Additive	(%)	Ratio	(%)	Ratio	(g)	(%)
A-7	Blank	57.95	0.41	36.81	0.64	1.35	94.8
A-4	CaO	62.12	0.27	35.25	0.57	1.08	97.4
A-5	NaOH	71.04	0.36	24.46	0.34	3.47	95.5
A-6	Na-Citrate	70.06	0.43	22.67	0.32	3.32	92.7

S/B: Solids to bitumen ratio.

Release water chemistry data presented in Table 7 also show the use of *NaOH* significantly increases Na^+ concentration. Lowest Na^+ and HCO_3^-

concentrations in the release water were observed when *CaO* is used as an additive for the extraction process. Relatively low *pH* and high Ca^{2+} and Mg^{2+} concentrations in the release water with the use of *CaO* at 150 ppm suggests that the *CaO* dosage should be increased when low grade ores with high fines contents are processed. In fact, in these tests, *CaO* dosage was 150 ppm and *NaOH* dosage was 600 ppm. It is believed that higher dosages of *CaO* addition when low grade ores are processed would have beneficial effects on the bitumen recovery efficiency and the release water chemistry.

Table 5. Release water chemistry for the tests presented in Table 4.

Test			Conduc.	Alkalinity (mg CaCO3/L)			Cations (mg/L)			Anions (mg/L)	
ID	Additive	pH	(mS)	Total	CO3	HCO3	Na	Mg	Ca	Cl	SO4
APW	-	8.7	1.797	288	14	274	340	13	17	179	229
A-7	Blank	8.4	1.769	245	0	245	330	11	19	179	243
A-4	CaO	8.4	1.766	243	4	239	331	11	19	180	245
A-5	NaOH	8.8	1.912	313	24	289	390	6	8	183	251
A-6	Na-Ct	8.0	1.977	339	0	339	381	14	25	181	243

AWP: Artificial process water

The advantages of using *CaO* as an extraction additive are that it improves the release water chemistry by eliminating Na^{+} accumulation and reducing HCO_3^{-} concentrations which are essential for the reduction of MFT production.

PRODUCTION OF NONSEGREGATING TAILINGS

For the disposal of oil sands tailings we have investigated production of NST (nonsegregating tailings) from the blend of course cyclone underflow, fine thickener underflow (that is, thickened cyclone overflow) and optionally fine MFT; which could be an alternative to the conventional NST or CT process. We recommend using *CaO* or *CaO* and CO_2 as additives to prevent segregation, instead of $CaSO_4$, which also simultaneously improves the release water chemistry (Ozum and Scott, 2009).

The geotechnical properties of oil sands tailings are controlled by the ore characteristics as well as by the additives used in the extraction process. Conditions favouring dispersion of clay in the extraction process promotes bitumen extraction efficiency; however, it produces tailings with poor settling and consolidation properties. Hydrometer-sieve tests were performed on middling tailings using two different methods: (i) following ASTM Designation: D422-63 (Reapproved 1998) and ASTM Designation: D4221-99 by using sodium hexametaphosphate ($(NaPO_3)_6$) as a dispersant; and, (ii) without using any dispersant or mixing in a blender. The second method measures the grain size distribution of the tailings in its natural state while the first method, using a dispersant and blending the tailings, disperses the tailings in the test procedure. Hydrometer-sieve test results using these two methods were almost similar for the middling tailings produced with the CHWE process; which indicates that the extent of clay dispersion caused by the CHWE process is very high. Hydrometer-sieve test results on a typical middling tailings, produced at a commercial plant operating with a non-additive extraction process, are presented in Figure 5 which shows that the non-additive extraction process produces middling tailings with much less clay dispersion. Almost no clay sized fraction (<0.002 mm) is in these middling tailings in its natural state but the dispersed test has about 30% clay size. These hydrometer-sieve test data support the relations between the extent of clay dispersion and extraction efficiency as well as the poor settling and consolidation characteristics of the tailings with a higher clay size content.

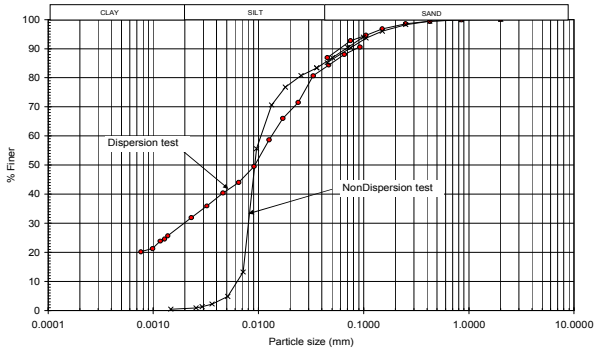

Figure 5. Dispersed and nondispersed PSD.

As previously discussed, the modification of the bitumen extraction process to reduce clay dispersion would result in a major reduction in the production of MFT compared to the existing MFT output. Regardless of the extraction process being used, oil sands tailings must have acceptable settling, consolidation and nonsegregating properties for their safe disposal. Generally, oil sands tailings have to be cycloned or centrifuged with a chemical additive to improve their

geotechnical properties without harming the release water chemistry and environment.

Table 6. Extraction test results, low grade ore.

		Primary Froth		Secondary Froth		Bitumen	Total
		Bitumen		Bitumen		Toluene	Bitumen
Test		Recovery	S/B	Recovery	S/B	Wash	Recovery
ID	Additive	(%)	Ratio	(%)	Ratio	(g)	(%)
ALG-4	Blank	20.52	0.61	60.46	0.91	0.49	81.0
ALG-3	CaO	14.16	0.63	71.73	0.77	0.57	85.9
ALG-1	NaOH	55.11	0.27	33.20	0.79	0.52	88.3
ALG-2	Na-Citrate	39.23	0.31	48.73	0.83	0.51	88.0

S/B: Solids to bitumen ratio.

We have tested the performance of *CaO* (lime) as an additive to prevent segregation, that is, to produce a nonsegregating tailings product (Scott et al, 2007). A segregation boundary line for the *CaO* additive was established and plotted with the segregation lines for other additives as depicted in Figure 6. As can be deduced from Figure 6, there are three options to produce a nonsegregating tailings if the whole tailings stream composition is not suitable to produce a nonsegregating tailings stream:

(i) increase the solids content, preferably using cyclones and thickening the cyclone overflow to above 40% solids content using high performance thickeners, as depicted in Figure 6.

(ii) increase the fines content; which is not practical beyond a critical fines content due to the reduction in permeability and water dewatering rate; and,

(iii) use additives such as *CaO* to prevent segregation.

Table 7. Release water chemistry for the tests presented in Table 6.

Test			Conduc.	Alkalinity (mg CaCO3/L)			Cations (mg/L)			Anions (mg/L)	
ID	Additive	pH	(mS)	Total	CO3	HCO3	Na	Mg	Ca	Cl	SO4
APW	-	8.7	1.797	288	14	274	340	13	17	179	229
ALG-4	Blank	8.3	1.790	222	0	222	327	19	25	189	286
ALG-3	CaO	8.3	1.789	227	0	227	324	19	27	184	285
ALG-1	NaOH	9.1	2.030	340	57	283	432	3	5	184	287
ALG-2	Na-Ct	8.2	1.941	325	0	325	384	21	29	181	276

AWP: Artificial process water

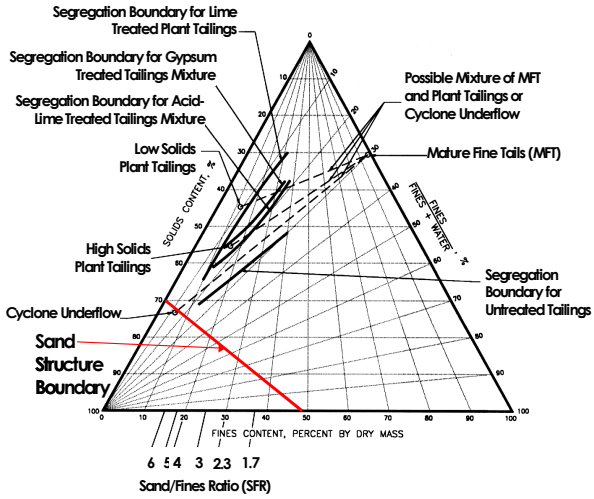

Figure 6. Segregation boundary diagram.

Laboratory scale tests showed that *CaO* addition as low as 0.6 kg-*CaO*/m^3-NST would be sufficient to prevent segregation. However, higher dosages around 0.8 kg-*CaO*/m^3-NST could be needed for high fines NST mixtures. Excess amounts of *CaO* would not cause any harm; it could be utilized to reduce bicarbonate hardness of the make-up water with the chemical reaction expressed in Equation [1]. Also, atmospheric CO_2 would consume excess $Ca(OH)_2$ which would precipitate in the form of $CaCO_3$ by the following reaction:

$$Ca(OH)_2 + CO_2 \leftrightarrow CaCO_3 + H_2O \qquad [3]$$

The use of *CaO* as an additive to produce NST therefore reduces Ca^{2+} and Mg^{2+} concentrations in the release water to be recycled to the extraction process. The reduction in Mg^{2+} concentration is due to the co-precipitation with calcium carbonate minerals and at a higher *pH* (*pH*>10.5) by the precipitation of Brucite ($Mg(OH)_2$) (Donahue at al, 2008).

Similar to CT production, a NST mix could be prepared from the blend of cyclone underflow, thickener underflow and existing MFT, as depicted in Figure 7. Addition of MFT into an NST mix would be optional depending on the desired sand to fines ratio (SFR). The advantage of using *CaO* or *CaO* & CO_2 as additives is that settling, consolidation and nonsegregating properties of the NST mix are improved and the salinity of the release water in terms of Ca^{2+}, Mg^{2+} and Na^{+} concentrations are reduced simultaneously. The simultaneous use of *CaO* as an additive for both the bitumen extraction and NST production

processes would provide an additional advantage since the tailings to be handled would have different characteristics. Our visual observations suggest that the settling, consolidation and nonsegregating properties of the tailings would be improved by using *CaO* and O_3, or *CaO* and *BD* as extraction process additives.

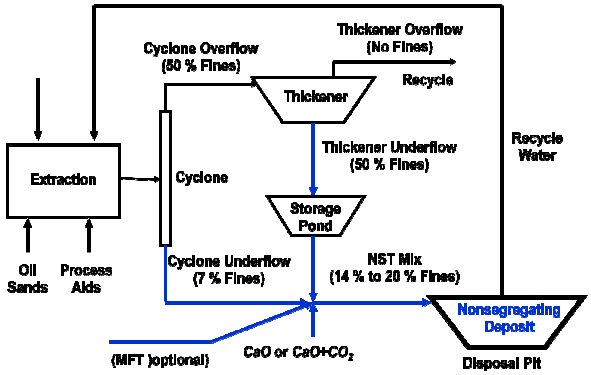

Figure 7. NST production process.

CONCLUSIONS

The conclusions of the above review are that neither the LTE nor the CT production processes are the solutions for the accumulation of the MFT and the release water salinity problems. Bitumen extraction using *CaO* and O_3 or *CaO* and *BD* and NST production using *CaO* or *CaO* and CO_2 could provide simple, cost effective and environmentally friendly solutions. Further testing of the laboratory findings is needed at a larger scale.

ACKNOWLEDGEMENTS

Funding provided by the Alberta Energy Research Institute and the Industrial Research Assistance Program-National Research Council are appreciated. NST production work was partially sponsored by Shell Energy Canada and Canadian Natural Resources Limited.

REFERENCES

Allan, E.W. 2008a. Process water treatment in Canada's oil sands industry: Part I. Target pollutants and treatment objectives, J. Environ. Eng. Sci. 7, 123-138.

Allan, E.W. 2008b. Process water treatment in Canada's oil sands industry: Part II. A review of emerging technologies, J. Environ. Eng. Sci. 7, 499-524.

Babadagli, T. and Ozum, B. 2010. Biodiesel as Surfactant Additive in Steam Assisted Recovery of Heavy-Oil and Bitumen, SPE 133376, SPE Western Regional Meeting, May 27-29, Anaheim, California, USA.

Babadagli, T., Burkus, T., Moschopedis, S.E. and B. Ozum. 2008. Bitumen Extraction from Oil Sands Ore-Water Slurry Using CaO (Lime) and/or Ozone, SPE 117677, SPE/PS/CHOA International Thermal Operations and Heavy Oil Symposium, October 20-23, Calgary, Alberta, Canada.

Burns, R., Tipman, R., Firmin, K. Mikula, R.J., Munoz, V.A., Kasperski, K.L. and Omotoso, O.E. 1998. Bitumen Release Mechanisms and New Process Development, Seventh UNITAR International Conference on Heavy Crude and Tar Sands, Paper No. 1998.226, October 27-30, 1998, Beijing, China.

Caughill, D.L., Morgenstern, N.R., and Scott, J.D. 1993. Geotechnics of Nonsegregating Oil Sand Tailings. Canadian Geotechnical Journal, 30: 801-811.

Chalaturnyk, R.J., Scott, J.D., and Ozum, B. 2002. Management of Oil Sands Tailings. Petroleum Science and Technology, 20(9&10): 1025-1046.

Clark, K.A. 1939. The Hot Water Method for Recovering Bitumen from Bituminous Sand, Report on Sullivan Concentrator, Alberta Research Council, Alberta Canada.

Clark, K.A. and Pasternack, D.S. 1932. Hot Water Separation of Bituminous Sand, Ind. Eng. Chem. 24, 1410.

ERCB 2009. Directive 074 Tailings Performance Criteria and Requirements for Oil Sands Mining Schemes. The Energy Resources Conservation Board of Alberta (ERCB), Calgary, Alberta, pp. 5-10.

Jiang, T., Hirasaki, G.J. and Miller, C.A. 2010. Characterization of Kaolinite ζ Potential for Interpretation of Wettability Alteration in Diluted Bitumen Emulsion Separation, *Energy Fuels*, *24* (4), 2350–2360.

Kasperski, K.L. 2001. Review of Research on Aqueous Extraction of Bitumen from Mined Oil Sands, Natural Resources Canada, Western Research Centre, Division Report May 2001, CWRC 01-17.

Long, Y., Dabros, T. And Hamza, H. 2002. Stability and settling characteristics of solvent-diluted bitumen emulsions, Fuel, 81(15), 1945-1952.

MacKinnon, M. and Sethi, A. 1993. A comparison of the physical and chemical prpperties of the Tailings ponds at the Syncrude and Suncor oil sands plants, Proceedings of Fine Tailings Symposium, Oil Sands-Our Petroleum Future Conference, April 4-7, Edmonton, Alberta, Canada.

MacKinnon, M. 2001. Process Affected Waters: Impact of Operating Factors On Recycle Water Quality, CONRAD Extraction Fundamentals and Process Water Workshop, May 7-8, Fort McMurray, Alberta, Canada.

Masliyah, J., Zhou, Z., Xu, Z, Czarnecki, J. and Hamza, H. 2004. Understanding Water-Based Bitumen Extraction from Athabasca Oil Sands, Can. J. Chem. Eng., 82, 628-654.

Matthews, J.G., Shaw, W.H., MacKinnon, M.D., and Cuddy, R.G. 2002. Development of composite tailings technology at Syncrude. International Journal of Surface Mining, Reclamation, and Environment, 16(1): 24-39.

Moschopedis, S.E., Schulz, K.F., Speight, J.G. and Morrison, D.N. 1980. Surface-Active Materials from Athabasca Oil Sands, Fuel Processing Technology, 3: 55-61.

Moschopedis, S.E., Fryer, J.F. and Speight, J.G. 1977. Water-soluble constituents of Athabasca bitumen, Fuel, 56: 109-110.

Moschopedis, S.E. and Speight, J.G. 1974. Oxidation of bitumen in relation to its recovery from tar-sand formations. Fuel, 53, 21-25.

Ozum, B. and Scott, J. D. 2010. Methods to Reduce Production of Oil Sands Mature Fine Tailings. GEO2010 Calgary Conference, September 12-16, Calgary, Alberta, Canada.

Rogers, W.F. 1953. Composition and Properties of Oil Well Drilling Fluids, Gulf Publication, Co., Houston, TX, USA.

Romanova, U.G. Yarranton, H.W., Schramm, L.L. 2003. Towards the Improvement of the Efficiency of Oil Sands Froth Treatment, Paper No. 2003-010, Can. Int. Petroleum Conference.

Scott, J.D., Donahue, R., Blum, J.G. Paradis, T. G., Komishke, B. and Ozum, B. 2007. Production of Nonsegregating Tailings with CaO or CaO and CO_2 for Improved Recycle Water Quality, CONRAD's Water Usage Workshop, November 21 & 22, Calgary, Alberta, Canada.

Shelfantook, W.E. 2004. A Perspective on the Selection of Froth Treatment Processes, Can. J. Chem. Eng., 82,704-709.

Speight, J. G. and S.E. Moschopedis. 1977/78. "Factors Affecting Bitumen Recovery by the Hot Water Process", Fuel Technology, 1: 261-268.

TREATMENT OF OIL SANDS MATURE FINE TAILINGS WITH SILICA

Robert H. Moffett
DuPont Chemicals and FluoroProducts, Wilmington, DE, USA

ABSTRACT

Bitumen extraction from Canadian oil sands generates vast quantities of fine tailings suspended in water. Historically, these fluid fine tailings have been impounded and allowed to consolidate into what is known as mature fine tailings (MFT). Recently enacted ERCB directive 074 requires fine tailings to be treated to generate a trafficable surface. The ERCB directive dictates the minimum undrained shear strength of the deposited fines shall be 5 kPa at 1 year after treatment and 10 kPa after 5 years. Untreated MFT has essentially no mechanical strength and represents a continuing environmental challenge to the oil sands industry.

Yield stress of MFT can be increased an order of magnitude within minutes by the in-situ polymerization of silica within the water phase of the MFT. With minimal dewatering the treated MFT can exceed the one and five year ERCB shear strength requirements. Dewatering of the treated MFT can be accomplished by a number of different techniques. The in-situ silica polymerization treatment has been demonstrated to work with flocculent thickened tailings as well as MFT.

This paper will discuss rheology modification of oil sands MFT using silica and the subsequent dewatering of the tailings.

INTRODUCTION

Management of fluid fine tailings remains an environmental challenge to the oil sands industry. Newly enacted ERCB directive 074 requires oil sands operators to reduce fluid tailings through fines capture in dedicated disposal areas in a manner that creates trafficable deposits. These deposits must have minimum undrained shear strength of 5 kPa within one year of deposition and 10 kPa within 5 years. Deposition of oil sands tailings into holding ponds creates what the industry terms MFT (mature fines tailings). It is estimated it will take centuries for the tailings in these ponds to reach the consistency of soft clay (Lord 1998). Even if the MFT consolidates to 60 wt% solids the yield stress is only about 0.5 kPa which is far short of the ERCB 1 year requirement (Wells 1997).

Since the 1990's oil sands operators have sought to create geotechnically stable fine tailings through the use of NST or CT technology (Non Segregating Tailings and Consolidated Tailings respectively). Although variations exist for these processes they basically require a specific blend of fine tailings and coarse sand tailings along with a chemical coagulant to prevent separation of the fines from the sand after deposition. A number of chemical coagulants have been proposed and tested for producing CT and NST. At this time gypsum (Omotoso 1999) and carbon dioxide (Mikula 2006) have found the most commercial success for this purpose. Reported drawbacks to the CT and NST process are the necessity for large volumes of sand which is preferentially used to create dikes, the creation of ponds and lack of robustness (MacKinnon 2007).

Another approach to fine tailings management has been the use of high molecular weight flocculants to facilitate solid/liquid separation. Anionic polyacrylamide (APAM) is generally the polymer of choice in this application. APAM can be used in conjunction with mechanical thickeners to generate a more highly concentrated tailings stream to avoid creation of tailings ponds and MFT. Underflows from thickeners are reported to be as high as about 50 wt% solids. However at 50 wt% solids, the thickened tailings have a yield strength of only about 50 Pa and will not meet ERCB yield stress requirements without further drying (Lord 1998). The polymer thickened tailings must have a solids concentration of nearly 75 wt % to achieve a yield stress approaching 5 kPa.

Flocculation of MFT with APAM followed by subsequent drainage and drying in thin lifts has been also trialed. Reportedly this approach will allow MFT to self dewater to about 55 wt % solids. However, this treatment technique suffers from requiring very specific mixing conditions to achieve good drainage of the flocculated MFT. APAM flocculated tailings are reported to be very susceptible to shear thinning (Mikula 2006). Mikula also notes that dried polymer treated MFT

will more easily reabsorb rain water than lime/gypsum treated MFT (Mikula 2008a).

Mechanical assisted dewatering of APAM flocculated fine tails has also been evaluated. Centrifugation has been reported to require less high molecular weight polymer compared to thin lift drying, however the chemical cost savings is offset by the large capital expense of the centrifuges. What's more the solids from the centrifuge need to be conveyed or trucked to the disposal area rather than being simply pumped as the solids cake discharged from the centrifuge is reported to be quite susceptible to shear thinning. Mikula states the yield stress decreases from approximately 6 kPa to about 0.3 kPa after shearing (Mikula 2008b).

SILICA FOR TREATMENT OF MFT

Silica (SiO2) in the form of sand is the major constituent in the mined oil sands ore. Silica may however take numerous other forms, some of which are water soluble while others are water dispersible. Many of these silica sources can be made to polymerize into three dimensional chained networks at relatively low SiO2 concentrations. We have found these silica networks can also be formed in-situ within the water present in fluid fine tailings (Moffett 2010). The networks are capable of making major changes in the rheology of oil sands fine tailings at relatively low silica concentrations. Upon dewatering and/or drying the yield stress of the silica treated tailings increases.

In-situ silica polymerization and network formation can be initiated by the addition of small amounts of various chemicals along with the silica source. Totally inorganic treatment systems can be practiced by initiating silica polymerization by the addition of bi or tri-valent metal salts such as calcium chloride, magnesium sulfate or sodium aluminate. Alternatively, acids or organic esters can also be used to initiate silica polymerization. Silica network formation can be accomplished in seconds or over days depending upon the choice of initiator, dose and silica source and optional use of accelerants. Perhaps the simplest and safest initiator is carbon dioxide.

The silica network provides strength to the treated MFT while encompassing the water and solids until dewatering is desired. A small applied pressure will cause the water contained within the network to exude. The solids however remain trapped within the silica matrix. Water can also be removed from the network through evaporative drying. The ease of water release allows for multiple potential methods to dewater the treated tailings. Some dewatering methods that could be potentially utilized include; in-pit self-weight consolidation, centrifugation, pipe-line dewatering, belt pressing, and thin lift deposition. Upon loss of water the silica treated tailings consolidate with significant reduction in volume

EXPERIMENTAL

Yield Strength Development and Evaporative Drying

Samples of MFT were obtained from a major oil sands producer. The MFT was found to contain 73 wt% water and 27 wt% solids. Particle size distribution was determined by static light scattering using a Malvern Instruments Mastersizer 2000. Results indicate > 90% of the particles are smaller than 44 micron (Figure 1). Yield stress of the MFT was measured with a Brookfield DV-III+ HB rheometer equipped with a vane spindle rotating at 0.1 rpm. The Brookfield rheometer can measure yield strength up to 8.8 kPa. Yield stress of the untreated MFT at 27 wt% solids was found to be approximately 5 Pa. A 2000 gram sample of the untreated MFT was allowed to evaporate while solids concentration and yield stress were being measured (see Figure 2). Results show this untreated MFT would need to concentrate to over 70% solids to meet the one year ERCB yield strength requirement.

Samples of the MFT were dosed with various amounts of silica in the form of sodium silicate solution. Silica polymerization was initiated within the MFT by addition of gaseous carbon dioxide. After treatment the MFT samples were stored in sealed containers to prevent evaporation. Yield stress was measured approximately 24 hours later. The treated samples were then exposed to the environment to allow water evaporation. Yield stress and solids concentration of the samples was measured over time as the water evaporated. As can be seen in Figure 3 creation of the silica networks significantly increases yield stress compared to untreated MFT. Yield stress of the silica treated samples rapidly increases with limited drying. Yield stress values meeting the ERCB 1-year requirement of 5 kPa are achievable at MFT solids concentrations of < 50 wt%.

Thin lift deposition and evaporative drying of MFT has been discussed by Wells (Wells 2007). To assess the evaporative drying potential and strength gains of silica treated MFT, 5 and 10 cm thick lifts were poured onto sand beds in 4 liter plastic beakers and allowed to dry. As a comparison, a 10 cm thick lift of MFT treated with gypsum and lime following the recipe disclosed by Wells was also prepared. Full depth core samples of the MFT for moisture analysis and yield stress measurements were taken over a 9 day period. The drying rate for the silica treated MFT was found to be similar to that of the gypsum/lime treated material (see Figure 4). However, the yield stress of the silica treated MFT was approximately an order of magnitude higher than the gypsum/lime treated MFT. For example, after 7 days of drying the gypsum/lime treated MFT had a moisture content of 50 wt% and a yield stress of 1414 Pa. Comparatively after the same 7 days of drying the 5 cm silica treated lift moisture content was 48.2 wt% and the yield stress of >8800 Pa. The 10 cm silica treated lift moisture content was 43.7 wt% and the yield stress 8520 Pa.

Thin lift deposition of APAM treated MFT has been investigated by many researchers. To compare strength development and dewatering/drying rates, MFT was treated with APAM (Magnafloc® 1011) and in-situ polymerized silica. The APAM dose rate tested was 1000 grams of Magnafloc® 1011 per dry tonne of MFT solids. The Magnafloc® 1011 was prepared and added to the MFT as a 0.3 wt% solution. Preliminary tests indicated that maximum flocculation (as noted visually) of the APAM treated MFT occurred 35 seconds after addition of the Magnafloc® 1011. Additional mixing was observed to reduce the floc size. Shorter mix times resulted in a non-flocculated slurry.

Silica treatment used for a comparison was 12.3 kg SiO2 (as sodium silicate solution) per dry tonne of MFT solids. Silica polymerization was initiated with sulfuric acid and magnesium sulfate. Onset of visual thickening with silica treatment was noted at 35 seconds after pH adjustment. The silica treated MFT continued to thicken until mixing was stopped at 68 seconds.

Ten cm thick lifts of the treated MFT were poured onto sand beds. The material was exposed to the atmosphere to allow for evaporative drying. Any free water present on the surface of the MFT was removed daily. Yield stress measurements and solids concentration were measured over a 7 day period. Drying rate of the APAM treated MFT with optimal mix conditions was found to be slightly better than the silica treated MFT. However, the yield stress of the silica treated MFT was much higher. For example, after six days of drying the yield stress of the silica treated MFT was approximately 4 times higher than the APAM treated MFT (see Figure 5).

One of the difficulties often attributed to the use of APAM for MFT flocculation and dewatering is sensitivity to mixing conditions. Over or under mixing does not provide dewatering to nearly the same degree as that seen with optimal mixing. In our laboratory tests 35 seconds from APAM addition to cessation of mixing was believed to provide optimum flocculation when using 1000 gram Magnafloc® 1011 per dry tonne of MFT. Two additional MFT samples were treated with 1000 grams Magnafloc® 1011 per tonne having mix times of 17 and 60 seconds from APAM addition to cessation of mixing. These samples were again poured 10 cm thick onto a sand bed to allow for dewatering and drying. Yield strength and solids concentration were monitored over a seven day period. As a comparison, three silica treated MFT samples were also tested in a similar manner with mix times of 34, 51, and 68 seconds. On-set of thickening was observed at 34 seconds. Optimal mix time was assumed to be approximately 50 seconds. Figure 6 shows a quite large variation in dewatering occurs when the APAM is under or over mixed. This decrease in dewatering results in lower MFT yield strengths. Comparatively the silica treated MFT shows little variation in dewatering or yield strength as a function of mixing time.

Dewatering via Pressure

Tailings treated by the CT process dewater through self consolidation. To investigate the potential of silica treated MFT to dewater via self-weight consolidation a pressure cell was employed. MFT was treated with sodium silicate at 6.8 kg SiO2/tonne of MFT solids. Silica network formation was initiated by CO_2 addition and addition of 5.4 kg of gypsum/tonne of MFT solids. The cell was equipped with a perforated metal plate and coarse filter paper through which water exuded from the treated MFT could pass (Figure 7). The cell was filled with 7.4 cm of silica treated MFT on top of the filter paper. A load of 17.9 kPa was then applied and maintained to the top surface of the MFT while the water passing through the filter paper was collected and weighed. When essentially no further water was being

exuded, the applied load was increased to 38.6 kPa and then finally to a maximum of 73.1 kPa. MFT solids concentration within the cell at various intervals was estimated based upon the mass of water collected (Figure 8). Upon completion of the test the pressure cell was disassembled and the consolidated solids removed. The solids thickness had been reduced by 55% from 7.4 to 3.4 cm. Some free water was found to have drained from the MFT but was trapped within the pressure cell. This water was not included in the estimated MFT solids calculations. As a result, the solids concentration of the MFT left within the pressure cell was found to be somewhat higher than what was estimated based upon the captured water (Figure 8). These results demonstrate that with a small amount of head pressure the same amount of dewatering can be achieved in hours as would require days to achieve when the MFT is deposited in thin lifts.

Recycle Water Quality

Oil sands operators attempt to recycle as much water from the tailings as possible. Consolidation of the tailings in the ponds allows up to about 80% of the water added into the ponds to be recycled (Mikula, 1996). It would be desirable to also recycle any water released from the treated tailings. High cation concentrations in the recycled water can have a negative impact on the bitumen extraction process and must be evaluated. Fortunately the interstitial water associated with the MFT represents less than about 15% of the water volume released into the pond during consolidation of the tailings. Therefore, any changes in the soluble ion concentration in the MFT interstitial water as the result of chemical treatment should have only minor effects on the quality of the total recycled water stream.

To gauge the effect of various MFT treatment chemistries water samples were collected in the manner described below and submitted for ICP analysis. Prior to ICP all samples were filtered with a 0.45 micron syringe filter:

1. Untreated MFT interstitial water collected by vacuum filtration using a coarse filter paper followed by filtration through a 0.45 micron syringe filter.

2. APAM treated MFT. Sample collected from free water generated by addition of 1000 gram Magnafloc® 1011 per tonne of MFT solids.

3. Silica treated MFT. MFT treated with 13.5 kg SiO2 (as sodium silicate) per tonne. Silica polymerization initiated with sulfuric acid and gypsum. Sample collected from water discharged from pressure cell.

4. MFT saturated with gaseous CO_2, pH ~ 6.5. Water sample expressed from the MFT using pressure cell.

Results of the ICP analysis are shown in Table 1. As expected, the sodium ion concentration for the silica treated MFT is nearly double that of the untreated MFT. This corresponds to the sodium introduced from the sodium silicate. The Ca, Mg and K ion concentration of the silica treated and CO_2 treated MFT are essentially the same. Compared to untreated MFT the Ca, Mg, and K concentrations are approximately 2 to 4 times higher. This increase is likely from displacement of these ions from the clay's surface by either H^+ or Na^+ ions.

Table 1. ICP Analysis

	Ion Concentration (ppm)					
	Al	Ca	K	Mg	Na	Si
Untreated MFT	1	28	19	13	950	5
APAM Treated MFT	4	9	18	8	920	9
CO2 Saturated MFT	<1	105	30	36	1050	6
Silica Treated MFT	<1	145	31	42	1920	55

CONCLUSIONS

In-situ polymerization of silica offers a unique method to treat oil sand fine tailings streams. Formation of silica networks within the water phase of fluid fine tailings can significantly increase the yield stress. Laboratory tests indicate silica treated MFT can achieve 5 kPa yield strength at solids concentrations of less than 50 wt%. This is a far lower solids concentration than what is needed to achieve 5 kPa with either APAM or gypsum/lime treated MFT. Silica treated MFT can be easily dewatered by a number of methods including self weight consolidation and

evaporation. Soluble cation concentration in the water released from the silica treated MFT is similar to water released from CO_2 saturated MFT with the exception of sodium.

REFERENCES

Lord, E.; Liu, Y. 1998. Depositional and Geotechnical Characteristics of Paste Produced from Oil Sand Tailings, Fifth International Conference on Tailings and Mine Waste '98, Fort Collins Co, 1998: 147-157.

MacKinnon, M. 2007. Surface Oil Sands Operations Will Affect Water Quality and Impact Options for Water Management, Part II: Process Effects, Conrad Water Usage Workshop, November 2007

Mikula, R., Kasperski, K., Burns, R., and MacKinnon, M. 1996. Nature and Fate of Oil Sands Fine Tailings, Solutions: ACS; Fundamentals & Applications in Petroleum Industry, 1996: 677-723.

Mikula, R. Omotoso, O. 2006. Role of Clays in Controlling Tailings Behavior in Oil Sands Processing, Clay Science, 2006, 12 Supplement 2: 177-182.

Mikula, R.J., Munoz, V.A., Omotoso, O. 2008. Water Use in Bitumen Production: Tailings Management in Surface Mined Oil Sands, Canadian International Petroleum Conference, 2008: 1-8.

Mikula, R.J., Munoz, V.A., Omotoso, O. 2008. Centrifuge options for production of "Dry stackable tailings" in surface mined oil sands tailings management, Canadian International Petroleum Conference, 2008: 1-8.

Moffett, Robert H. 2010. U.S. patent application publication 2010/0104744 A1.

Omotoso, O.E., Mikula, R.J. 1999. Alternative Consolidated Tailings Chemicals, Canmet division report WRC 99-23, May 1999

Wells, P.S., Riley, D.A. 2007, MFT Drying – Case Study in the Use of Rheological Modification and Dewatering of Fine Tailings through Thin Lift Deposition in the Oil Sands of Alberta, 10th International Seminar on Paste and Thickened Tailings, March 2007

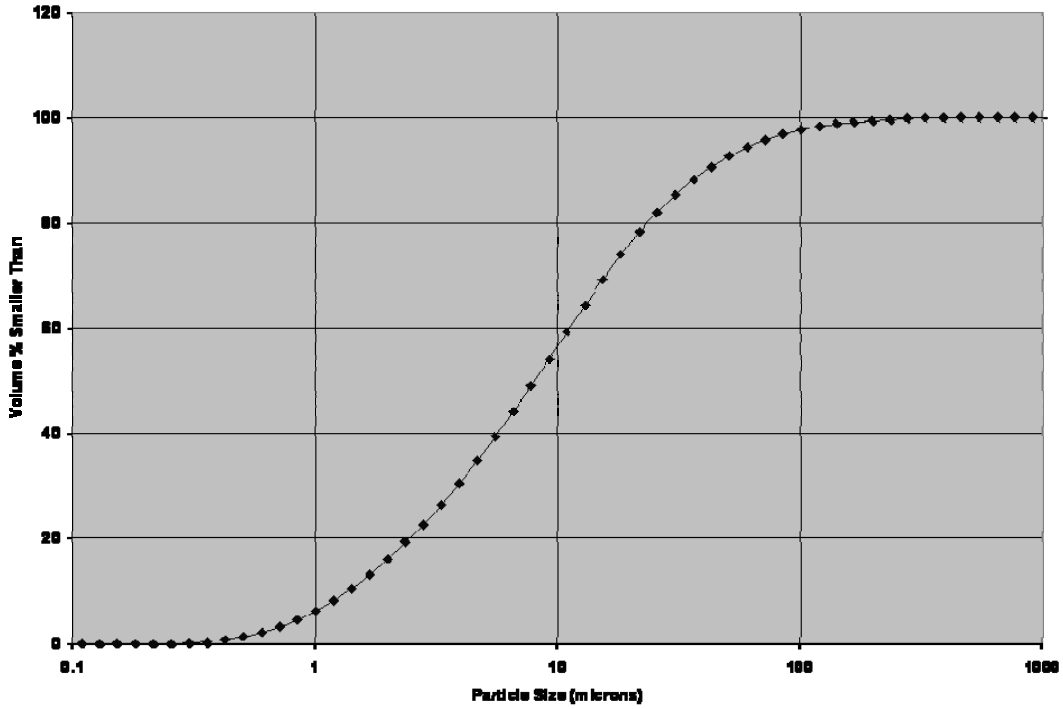

Figure 1. Untreated MFT Particle Size by Static Light Scattering

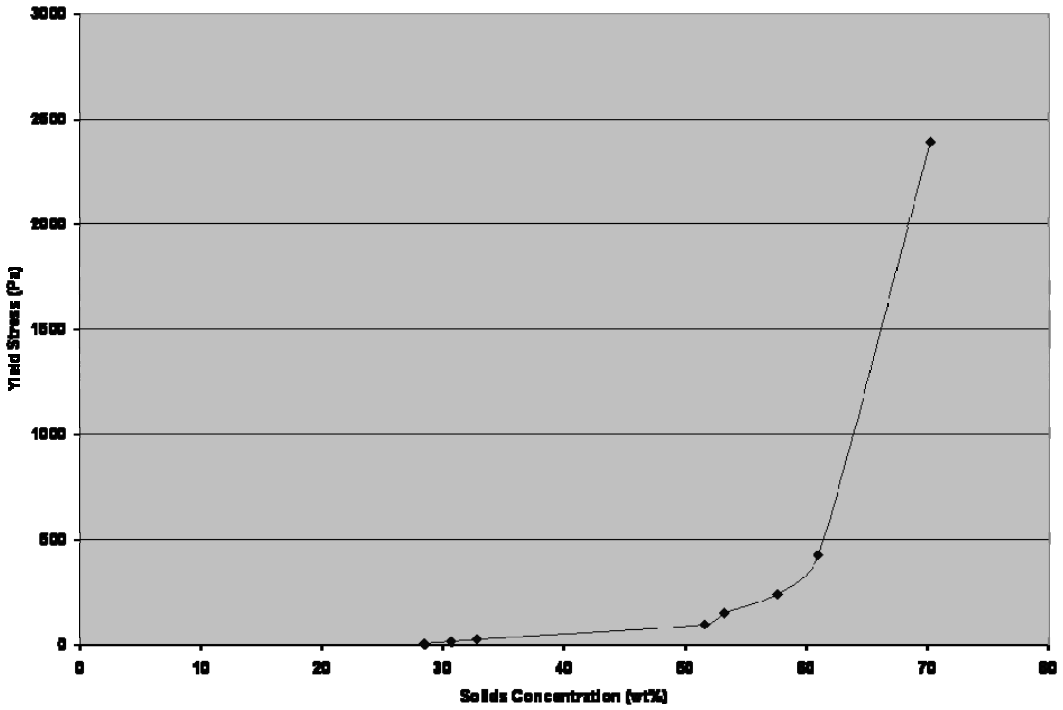

Figure 2. Yield Strength of Untreated MFT vs. Solids Concentration

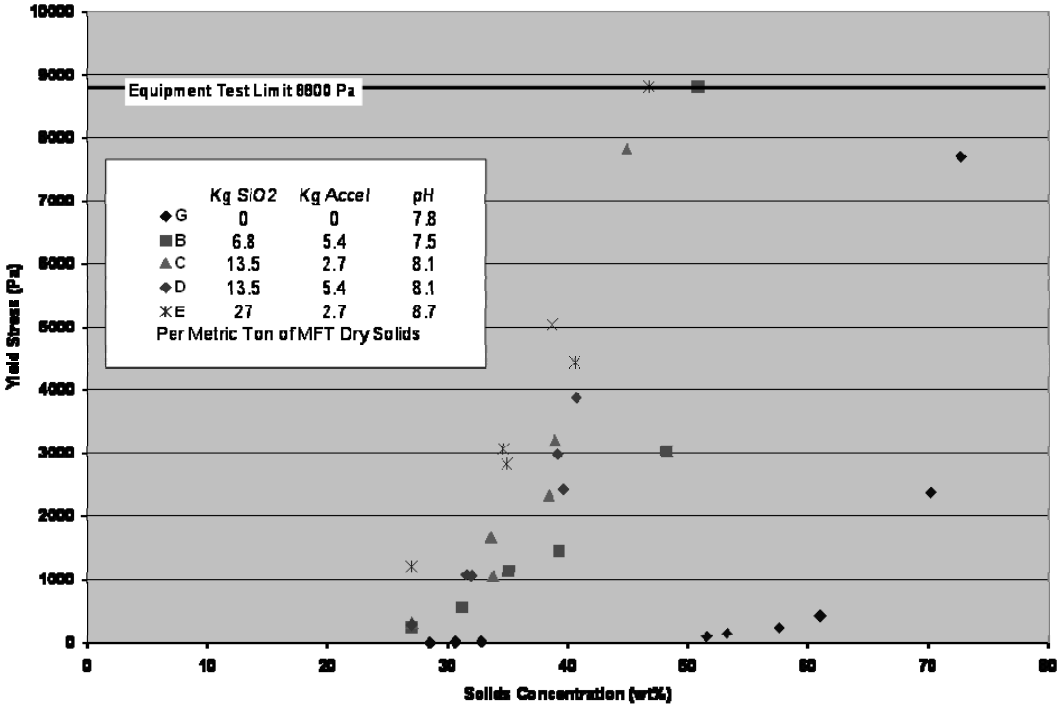

Figure 3. Yield Strength of Silica Treated MFT as a Function of Silica Dose and Solids Concentration

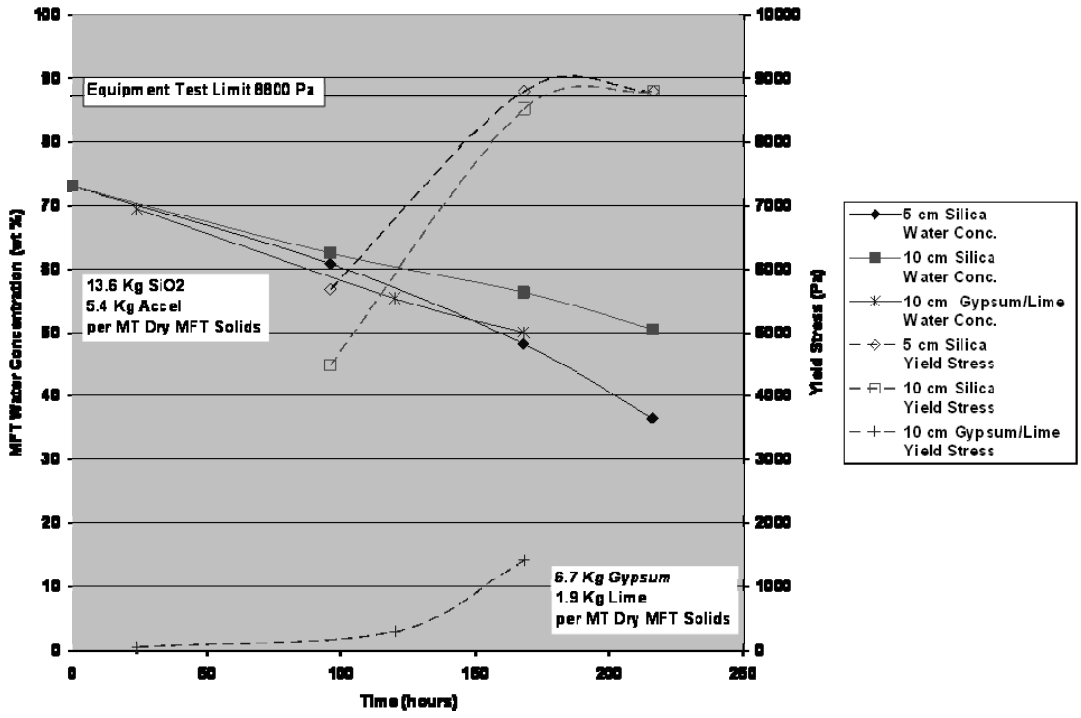

Figure 4. Yield Strength and Drying Rate of MFT Treated with Silica as Compared to Gypsum/Lime

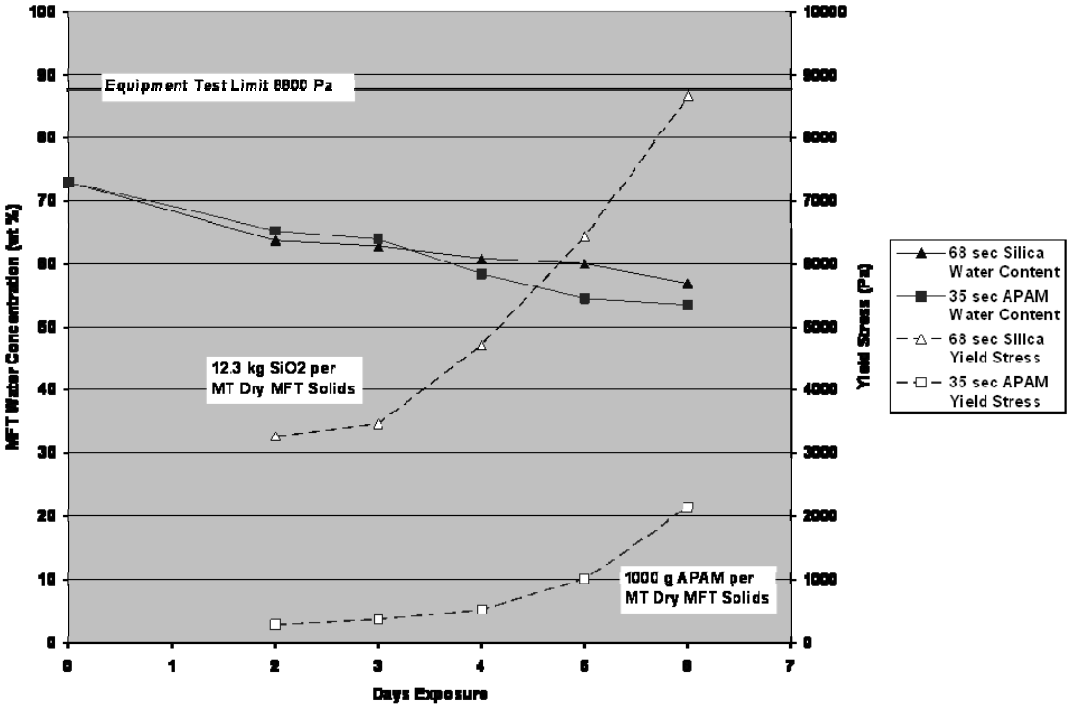

Figure 5. Yield Strength and Drying Rate of MFT Treated with Silica Compared to APAM

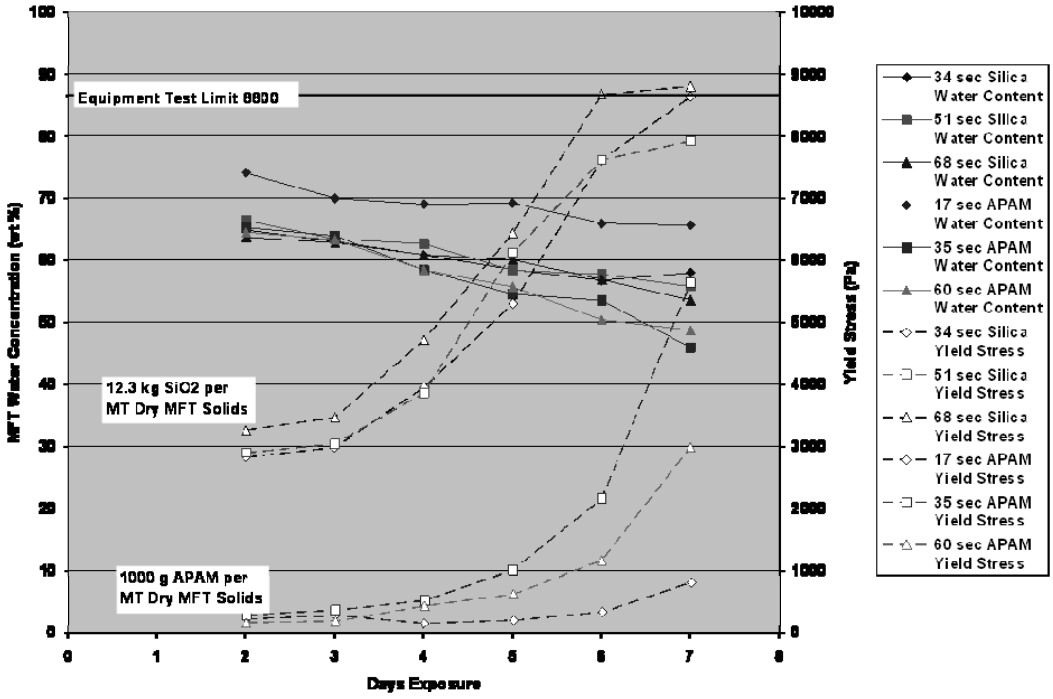

Figure 6. Yield Strength and Drying Rate of Under and Over-Mixed MFT Treated with Silica Compared to APAM

Figure 7. Pressure Cell Apparatus

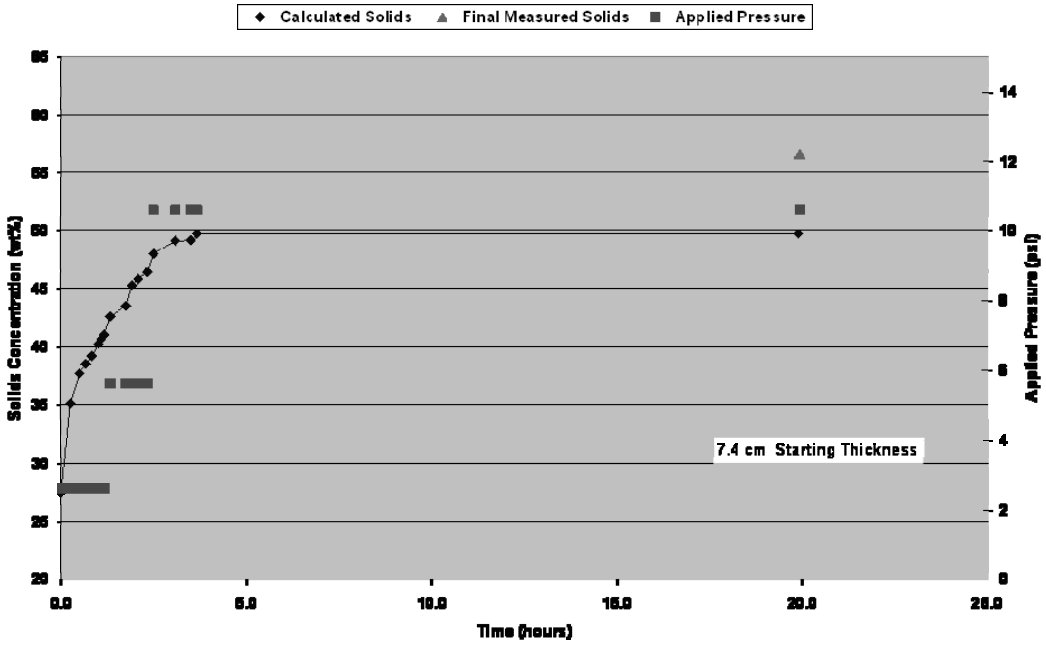

Figure 8. Dewatering of MFT Treated with Silica as a Function of Applied Pressure

MICROORGANISMS IN OIL SANDS TAILINGS PONDS INFLUENCE THE PROPERTIES AND BEHAVIOUR OF MATURE FINE TAILINGS (MFT)

D. Bressler, M. Cardenas, P.M. Fedorak, S. Guigard, R. Gupta, T. Siddique and J. Foght
University of Alberta, Edmonton AB Canada

ABSTRACT

Natural communities of microorganisms in oil sands tailings ponds affect the behaviour of mature fine tailings (MFT) and produce methane and carbon dioxide gases in tailings ponds. By as-yet-unknown mechanism(s), the microbes influence gravitational settling of fine clay particles in MFT and de-watering (recovery of pore water). Thus, microbes can have detrimental environmental effects by producing greenhouse gases but also beneficial effects for management of tailings ponds by increasing the rate of densification and accelerating the recovery of water for process re-use. We are examining the effects of microbes on MFT when they are stimulated by adding readily fermented organic supplements. Increased microbial activity resulted in greater production of methane (a potential on-site fuel source) and increased pore water recovery.

INTRODUCTION

Oil sands tailings ponds naturally develop and sustain complex communities of microorganisms that are active in situ and that reflect the chemical composition of the tailings. Because these ponds are predominantly anaerobic, many of the naturally occurring microbes are anaerobes: nitrate-, sulfate- and iron-reducers, fermenters or methanogens (methane-producers). These microbial groups have been detected in numbers as high as 10^8 per mL MFT (10^{11} cells per L) but more commonly around 10^4–10^5 per mL. The microbes consume solvent components (preferentially the straight-chain alkanes and some monoaromatics like toluene and xylenes) and/or chemical additives (e.g. trisodium citrate) that are present in the tailings after extraction, and generate end-products that include substantial volumes of carbon dioxide and methane gas. These gases create voids in the settling MFT and intermittently escape to the atmosphere as bubbles of greenhouse gases. One of the tailings ponds is estimated to produce a methane flux of ≥40 million L (≥28 tonnes) of methane per day [Holowenko et al. 2000].

Through unknown mechanism(s), microbial methanogenesis accelerates settling (biodensification) of the fines in MFT and concomitant recovery of pore water at the surface (de-watering) [Fedorak et al. 2002]. This phenomenon is industrially and environmentally significant because faster pore water recovery provides water for re-use and decreases the need for fresh make-up water; also, accelerated densification decreases MFT inventory volumes more quickly, thus allowing longer use of the tailings ponds. Therefore, it is important to understand the factors controlling formation and release of biogenic gases in MFT because of the opposing detrimental (greenhouse gas emission) and beneficial (biodensification) effects. An additional potential benefit is that microbially produced methane would be a clean-burning on-site fuel if it could be trapped economically in situ.

Supported by funding from the Alberta Water Research Institute, our group is investigating the effects of biogenic methane and carbon dioxide on MFT properties in the laboratory, particularly rates of biodensification and de-watering, as well as measuring the physical effects of stimulating microbial activity by amending MFT with fermentable agricultural and industrial by-products. Cutting edge DNA-based research supported by Genome Canada/Genome Alberta is helping identify the myriad of microbial species present and to infer their metabolic roles in MFT. These results will be incorporated into a general model to predict the consequences of microbial activity in situ and to provide guidance for tailings management and reclamation strategies.

METHODS

Microbial activity (particularly methanogenesis) in MFT accelerates tailings densification and pore water recovery, but it is slow because it is driven by anaerobic hydrocarbon biodegradation, which is a slow process. Therefore, we hypothesized that stimulating microbial activity by supplementing MFT with substrates that could be readily fermented to methane would accelerate beneficial effects. We chose to test several agricultural and bioindustrial

by-products, some of which have negative commercial value (i.e., their disposal incurs a cost to the producer). The substrates and the rationale for their selection for study are shown in Table 1. We selected substrates that were available regionally but were non-bulking and non-pathogenic; the latter considerations eliminated potential substrates like chopped straw, wood chips or feedlot manure. Complex test substrates were analyzed for elemental composition to determine carbon content, and were added to MFT on the basis of 40 mg carbon per litre MTF; i.e., they were added on a carbon-normalized basis rather than by total weight of substrate.

Microbial activity was measured in two ways: methane production was quantified in triplicate sealed anaerobic microcosm bottles (Fig. 1A) that were mixed intermittently to release gas into the headspace for analysis; biodensification was measured in single static open glass cylinders (Fig. 1B). During preparation of columns and bottles, the anaerobic condition of the MFT was maintained so that all measured effects were due to anaerobic activity. Methane was quantified using a gas chromatograph and biodensification was measured as the incremental change in solids volume and overlying pore water. Microcosms and cylinders were incubated in the dark at room temperature (~20°C, similar to in situ temperature).

RESULTS

MFT samples amended with agricultural and bio-industrial by-products generally produced more methane faster than parallel unamended control microcosms (Table 2). Some supplements were poor substrates and some (e.g. stearic acid) initially inhibited methanogenesis. The complex supplements (canola, distillers' grains, hydrolyzed blood or bone meal) that were a source of carbon, nitrogen and phosphorus were generally more successful at stimulating methane production.

Biodensification followed the same trends as methane production, with faster onset of solids settling (Fig. 1B) and faster recovery of pore water (Fig. 2) in MFT amended with by-products. However, the final volume of recovered water was not necessarily greater than the baseline (unsupplemented) control condition: de-watering simply was achieved at a greater rate or with a shorter lag time. Notably, in some cases the total volume of solids plus recovered pore water was actually greater than the original volume dispensed to the cylinder (Fig. 1B,C): the increase represented the volume of gas voids trapped in the MFT. On occasion the gas escaped to the surface, staining the inner surface of the cylinder with released bitumen from the MFT.

These effects are biological rather than chemical because the addition of bromoethane-sulfonate (BES), a specific methanogen inhibitor, reduced the settling effect to background levels (Fig. 2)

DISCUSSION

The results obtained by stimulating microbial activity in MFT are encouraging, namely enhanced production of methane gas (a potential on-site fuel) and accelerated biodensification and de-watering of MFT. However, the mechanism(s) by which this is achieved are still unknown and are under study in our laboratories. We have several hypotheses, including localized pH and cation exchange effects on the clay particles; physical or biosurfactant effects on hydrophobic surfaces of fines that have an undefined organic coating; and physical channels caused by the formation and coalescence of microbubbles of biogenic gas. However, the full range of microbial effects on MFT settling remains to be elucidated, and the potential for manipulating microbial activity to achieve beneficial effects in situ remains to be determined.

ACKNOWLEDGEMENTS

The authors thank the Alberta Water Research Institute and Genome Canada–Genome Alberta for funding; Syncrude Canada Ltd., Suncor Ltd. and Albian Sands Energy (Shell Canada) for providing samples and in kind support; and D. Coy, E. Underwood and K. Semple for technical support.

REFERENCES

Fedorak PM, Coy DL, Dudas MJ, Simpson MJ, Renneberg AJ, MacKinnon MD. 2003. Microbially-mediated fugitive gas production from oil sands tailings and increased tailings densification rates. *J Environ Eng Sci* **2**: 199-211.

Holowenko FM, MacKinnon MD, Fedorak PM. 2000. Methanogens and sulfate-reducing bacteria in oil sands fine tailings waste. *Can J Microbiol* **46**(10): 927-937.

Table 1: Agricultural and bioindustrial by-products added to MFT as methanogenic substrates, and chemicals used as positive or negative 'control' substrates.

By-product	Source or rationale for use
No amendment	Baseline control for endogenous substrates in MFT
Canola meal	Post-pressing by-product
Corn-based dry distillers' grains	Source of nitrogen and fermentable carbohydrates
Bone meal*	Contains phosphorus, which can be a limiting element
Blood and meat meal*	Contains amino acids that are readily fermented
Stearic acid	Pure chemical; model for tallow (rendering by-product)
Whey powder	Dairy by-product; contains protein as source of nitrogen
Glycerol	By-product of biodiesel production
Trisodium Citrate	Water conditioning agent used by Albian Sands Energy
Acetate	Known methanogenic substrate
Bromoethane sulfonate (BES)	Specific inhibitor of methanogenesis; negative control

* Before use, bone meal and blood/meat meal were hydrolyzed to Canadian Food Inspection Agency (CFIA) standards to ensure safety

Table 2: Methane production from microcosms containing MFT and methanogenic medium with or without substrates after 114 days incubation at room temperature.

Treatment	Methane (mmol)	Fold increase above baseline control
No amendment (baseline control)	0.17	1
Canola meal	1.6	9
Corn-based dry distillers' grains	2.1	12
Bone meal	2.0	12
Blood/meat meal	2.3	14
Stearic acid	0.39	2
Glycerol	1.9	1
Whey powder	2.1	12
Acetate + Nitrate	1.1	6
Acetate+BES (negative control)	0.12	0.7

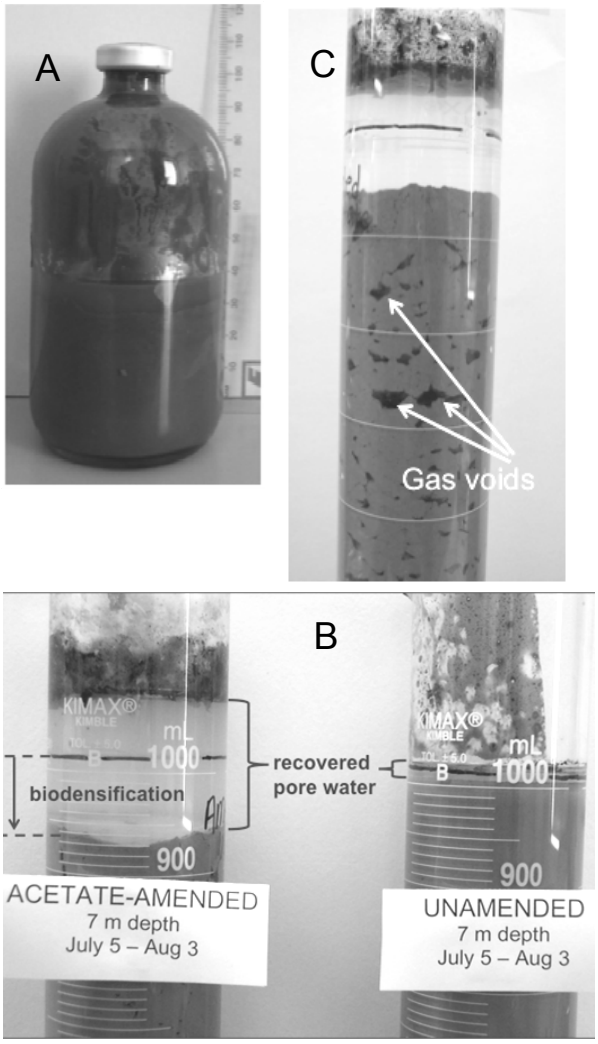

Figure 1: (A) Sealed glass microcosm used to measure methane production. The 158-mL microcosm contains 75 mL MFT, 25 mL mineral plus vitamin medium, an organic supplement added at the rate of 40 mg carbon per litre of MFT, and an anaerobic headspace of 10% CO_2, balance N_2 gas; (B and C) Static glass cylinders used to measure biodensification and pore water recovery, initially containing exactly 1L MFT. In (B), the MFT in the cylinder on the left received a supplement of acetate (positive control substrate) whereas the one on the right received no supplement (baseline control condition). After incubation for 4 weeks the volume of recovered pore water was significantly greater in the amended MFT than in the baseline control and the volume of settled solid was smaller (i.e., biodensification had occurred). Note that the total volume of solids and water in (C) is greater than the initial volume due to trapped gas creating voids in the MFT.

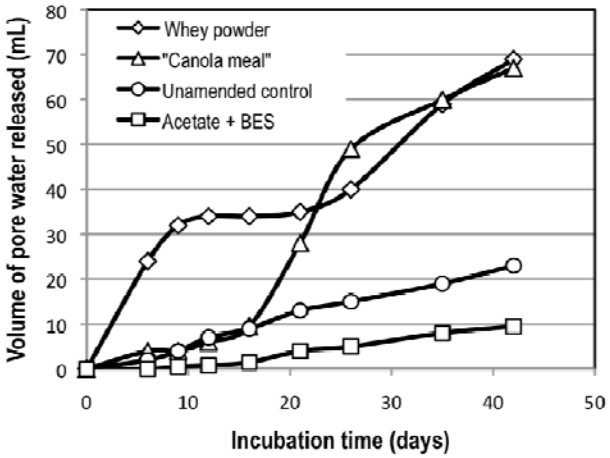

Figure 2: Pore water recovery in static settling columns settling for 6 weeks at room temperature (representative results from one producer's MFT). Initial volume of MFT was 1800 mL.